

# ACTA CHIMICA ACADEMIAE SCIENTIARUM HUNGARICAE

ADIUVANTIBUS

M. T. BECK, R. BOGNÁR, GY. HARDY,  
K. LEMPERT, B. LENGYEL, K. POLINSZKY,  
E. PUNGOR, G. SCHAY,  
Z. G. SZABÓ, P. TÉTÉNYI

REDIGUNT

F. MÁRTA et GY. DEÁK

TOMUS 110

FASCICULUS 1



AKADÉMIAI KIADÓ, BUDAPEST

1982

ACTA CHIM. ACAD. SCI. HUNG.

ACASA2 110 (1) 1-110 (1982)

# ACTA CHIMICA

A MAGYAR TUDOMÁNYOS AKADÉMIA  
KÉMIAI TUDOMÁNYOK OSZTÁLYÁNAK  
IDEGEN NYELVŰ KÖZLEMÉNYEI

FŐSZERKESZTŐ  
MÁRTA FERENC

SZERKESZTŐ  
DEÁK GYULA

TECHNIKAI SZERKESZTŐ  
HAZAI LÁSZLÓ

SZERKESZTŐ BIZOTTSÁG  
BECK T. MIHÁLY, BOGNÁR REZSŐ, HARDY GYULA,  
LEMPERT KÁROLY, LENGYEL BÉLA, POLINSZKY KÁROLY,  
PUNGOR ERNŐ, SCHAY GÉZA, SZABÓ ZOLTÁN,  
TÉTÉNYI PÁL

Acta Chimica is a journal for the publication of papers on all aspects of chemistry in English, German, French and Russian.

Acta Chimica is published in 3 volumes per year. Each volume consists of 4 issues of varying size.

Manuscripts should be sent to

*Acta Chimica*  
Budapest, P.O. Box 67, H-1450, Hungary

Correspondence with the editors should be sent to the same address. Manuscripts are not returned to the authors.

Hungarian subscribers should order from Akadémiai Kiadó, 1363 Budapest, P.O. Box 24. Account No. 215 11488.

Orders from other countries are to be sent to "Kultura" Foreign Trading Company (H-1389 Budapest 62, P.O. Box 149. Account No. 218 10990) or its representatives abroad.

# ACTA CHIMICA

## ACADEMIAE SCIENTIARUM HUNGARICAE

ADIUVANTIBUS

M. T. BECK, R. BOGNÁR, GY. HARDY,  
K. LEMPERT, B. LENGYEL, K. POLINSZKY,  
E. PUNGOR, G. SCHAY,  
Z. G. SZABÓ, P. TÉTÉNYI

REDIGUNT

F. MÁRTA et GY. DEÁK

TOMUS 110



AKADÉMIAI KIADÓ, BUDAPEST

1982

ACTA CHIM. ACAD. SCI. HUNG.



# ACTA CHIMICA

TOMUS 110

Fasciculus 1  
 Fasciculus 2  
 Fasciculus 3  
 Fasciculus 4

## INDEX

ÁGAI, B., BITTER, I., CSONGOR, É., TÓKE, L.: Modified Crown Ethers, I. Carbonic Acid Derivatives Containing One Crown Ether unit (Preliminary Communication) . . . .	25
ÁGAI, B., BITTER, I., CSONGOR, É., TÓKE, L.: Modified Crown Ethers, II. Carbonic Acid Derivatives of Bis-Crown Ethers (Preliminary communication) . . . . .	29
AGÓCS, P. M., MOTIKA, G., ZSÉDENYI, P.: Liquid Crystals, IV. Correlation between the Thermal Stability and Molecular Structure in Cholesteryl 2-Ethoxyethyl-carbonate and its Sulfur-Containing Analogues . . . . .	357
AMETA, S. C., GUPTA, H. L., PANDE, P. N., CHOWDHRY, H. C.: Kinetics of Oxidative Decarboxylation of L-Cysteine by Permanganate . . . . .	7
ANTUS, S. s. MÁRVÁNYOS, E.	
ARAMENDIA, M. A., BORAU, V., JIMENEZ, C., MARINAS, J. M.: New Metallic Catalysts Obtained by Supporting Platinum on $AlPO_4-Al_2O_3$ and $AlPO_4-SiO_2$ Systems . . . .	97
ARANYOSI, K. s. SZABÓ, G. T.	
AROCA, R., ROBINSON, E. A., PANCHENKO, YU. N., PUPYSHEV, V. I.: On the Torsional Internal Coordinate in Molecular Vibrations . . . . .	471
BAIJAL, J. S. s. RANI, I.	
BALOGH, S., FARSANG, GY., MAROS, L.: Voltammetric Determination of the Dissociation Constant of Glycolaldehyde and DL-Glyceraldehyde Bisulphites . . . . .	191
BARCZA, L. s. BUVÁRI, Á.	
BARCZA, L. s. DARUHÁZI, L.	
BAR-ELI, K., GEISELER, W.: Multiple Steady States and Hysteresis During Stirred Flow Oxidation of Cerous Ion by Bromate. Experiments and Models . . . . .	239
BAZSA, GY. s. PÓTA, GY.	
BECK, M. T. s. GÁSPÁR, V.	
BECK, M. T. s. PÓTA, GY.	
BEG, M. N., SHYAM, R., KHANDELWAL, R. P.: Studies with Inorganic Precipitate Membrane. Membrane Selectivity from Multiionic Potential and Conductivity Measurements . . . . .	65
BÉRCES, T. s. HUNYADI-ZOLTÁN, Zs.	
BERÉNYI, S., HOSZTAFI, S., MAKLEIT, S., SZEIFERT, I.: A New Route for the Preparation of N-Substituted N-Demethylapocodeine Derivatives . . . . .	363
BERNDT, K.-G., GLOYNA, D.: Electronic Interactions in $\omega$ -Diphenylphosphinyl-trans-styrenes Substituted in Position 4 and in their Derivatives (in German) . . . . .	145
BHATTACHARYA, B. K., SINGH, H., YADAV, L. D. S., HOORNAERT, G.: Synthesis of some New 2-Aryl-5-aryl/aryloxymethyl-1,3,4-oxadiazolo[3,2-a]-s-triazine-7-thiones and their Parent Thioureas as Potential Pesticides . . . . .	133
BITTER, I. s. ÁGAI, B.	
BORAU, V. s. ARAMENDIA, M. A.	
BURGER, K., DOMOKOS, L., PETHÓ, G., PUNGOR, E.: Error Analysis of a New Potentiometric Evaluation Method Based on the Measurement of the Bound Reagent Concentration . . . . .	85
BURGER, M., RÁCZ, K.: On the Preoscillatory Period of the Belousov-Zhabotinsky Reaction. A Search for Intermediates . . . . .	315
BUVÁRI, Á., SZEJTLI, J., BARCZA, L.: The 1 : 1 and 1 : 2 Complex Formation between $\beta$ -Cyclodextrin and Benzoic Acid . . . . .	51

CHOWDHRY, H. C. s. AMETA, S. C.	
CONNICK, R. E. s. NAGYPÁL, I.	
CSONGOR, É. s. ÁGAI, B.	
CZERWIEC, Z. s. MANDECKI, Z.: X-Ray Study of the Lattice Parameters of the Four Dichloro- <i>N</i> -sulfinylaniline Isomers .....	183
DARUHÁZI, L., SZEJTLI, J., BARCZA, L.: Polarographic Determination of Potential Guest Molecules in the Presence of Cyclodextrin .....	127
DEÁK, GY. s. GÁLL-ISTÓK, K.	
DOMBI, GY. s. SCHNEIDER, GY.	
DOMOKOS, L. s. BURGER, K.	
DRÁTOVSKÝ, M., DVOŘÁKOVÁ, E., RYTÍŘ, Z.: Oxidation of Alkali Metal Iodates in Molten Alkali Metal Nitrates .....	175
DVOŘÁKOVÁ, E. s. DRÁTOVSKÝ, M.	
FÁBLÁN, I. s. NAGYPÁL, I.	
FARSANG, GY. s. BALOGH, S.	
FELLER, A. s. NOSZTICZIUS, Z.	
FÖLDESI, A. s. LÓRÁND, T.	
FÖRSTERLING, H. D., LAMBERZ, H. J., SCHREIBER, H., ZITTLAU, W.: BrO <sub>2</sub> as an Intermediate in the Belousov-Zhabotinsky Reaction .....	251
FÜLEP-POSZMIK, A. s. NÉMETH, S.	
GÁLL-ISTÓK, K., ZÁRA-KACZLÁN, E., KISFALUDY, L., DEÁK, GY.: Synthesis of Peptides Containing <i>D</i> -Glucosaminic Acid, III. Sulfation of Peptides .....	441
GARAI, T. s. MÉSZÁROS, L.	
GARG, G. P. s. PATHAK, V. P.	
GÁSPÁR, V., BECK, M. T.: The Influence of the Ionic Strength on the Dissociation Constant of Hydrogen Cyanide (Short Communication) .....	425
GEISELER, W. s. BAR-ELI, K.	
GIRI, S., NIZAMUDDIN, MISHRA, A. K.: Synthesis of some 3-Aroylflavones as Potential Fungicides .....	117
GLOYNA, D. s. BERNDT, K.-G.	
GODSIL, C. D., GUTMAN, I.: Contributions to the Theory of Topological Resonance Energy	415
GROSSMANN, G. s. POHLE, U.	
GUNDA, E. T. s. JÁSZBERÉNYI, J. Cs.	
GUPTA, H. L. s. AMETA, S. C.	
GUTMAN, I. s. GODSIL, C. D.	
HACKLER, L. s. SCHNEIDER, GY.	
HADŽIJA, O. s. TONKOVIĆ, M.	
HOORNAERT, G. s. BHATTACHARYA, B. K.	
HORVÁTH-TORÓ, Cs. s. KAJTÁR, M.	
HOSZTAFI, S. s. BERÉNYI, S.	
HOSZTAFI, S. s. JÁSZBERÉNYI, Cs.	
HUNYADI-ZOLTÁN, Zs., ZALOTAI, L., BÉRCES, T., MÁRTA, F.: Thermal Decomposition of Oxetane and Oxetane- <i>d</i> <sub>2</sub> in the Pressure Independent Range .....	371
JÁSZBERÉNYI, J. Cs., PETRIKOVICS, I., GUNDA, E. T., HOSZTAFI, S.: The Mannich Reaction of Cephalosporin Sulfoxides and Sulfones .....	81
JIMENEZ, C. s. ARAMENDIA, M. A.	
KAJTÁR, M., HORVÁTH-TORÓ, Cs., KUTHI, É., SZEJTLI, J.: A Simple Rule for Predicting Circular Dichroism Induced in Aromatic Guests by Cyclodextrin Hosts in Inclusion Complexes .....	327
KHANDELWAL, R. P. s. BEG, M. N.	
KHANNA, R. N. s. PATHAK, V. P.	
KISFALUDY, L. s. GÁLL-ISTÓK, K.	
KÖRÖS, E., PUTIRSKAYA, G., VARGA, M.: Perturbation of Bromate Oscillators, I. Perturbation by $\gamma$ -Irradiation .....	295
KUTHI, É. s. KAJTÁR, M.	
LAMBERZ, H. J. s. FÖRSTERLING, H. D.	
LENGYEL, B., MÉSZÁROS, L.: Simulation of the Instabilities Observed in Potentiostatic Studies of Active-Passive Transition .....	397
LENGYEL, B. s. MÉSZÁROS, L.	
LÓRÁND, T., SZABÓ, D., FÖLDESI, A., NESZMÉLYI, A.: Reactions of Mono- and Diarylidene-cycloalkanones with Thiourea and Ammonium Thiocyanate, VI. <i>Z-E</i> -Isomerization of 2-Alkylmercapto-4-phenyl-8-benzylidene-5,6,7,8-tetrahydroquinazolines ...	231
MAKLEIT, S. s. BERÉNYI, S.	

MANDECKI, Z. s. CZERWIEC, Z.	
MARINAS, J. M. s. ARAMENDIA, M. A.	
MAROS, L. s. BALOGH, S.	
MÁRTA, F. s. HUNYADI-ZOLTÁN, Zs.	
MÁRVÁNYOS, E., ANTUS, S., NÓGRÁDI, M.: Oxidation of some Cyclic $\alpha$ -Benzylidene Ketones with Thallium(III) Nitrate in Methanol .....	93
MÉSZÁROS, L., LENGYEL, B., GARAI, T.: Study of Inhibitors by Electrode Impedance Measurements .....	57
MÉSZÁROS, L. s. LENGYEL, B.	
MISHRA, A. K. s. GIRI, S.	
MOTIKA, G. s. AGÓCS, P. M.	
MUSIĆ, S. s. TONKOVIĆ, M.	
NAGY-CZAKÓ, I. s. TONKOVIĆ, M.	
NAGYPÁL, I., FÁBIÁN, I., CONNICK, R. E.: NMR Relaxation Studies in Solution of Transition Metal Complexes, VII. Protonation of the Vanadyl Ion in Aqueous Solution	447
NÉMETH, S., FÜLEP-POSZMIK, A., SIMÁNDI, L. I.: Mechanistic Features of Cobaloxime(II) Catalyzed Oxidations with Dioxygen .....	461
NESZMÉLYI, A. s. LÓRÁND, T.	
NIZAMUDDIN s. GIRI, S.	
NÓGRÁDI, M. s. MÁRVÁNYOS, M.	
NOZTICZIUS, Z., FELLER, A.: On the Applicability of the Lotka—Volterra Scheme for Different Types of the Belousov—Zhabotinskii Reaction .....	261
PANCHENKO, YU. N. s. AROCA, R.	
PANDE, P. N. s. AMETA, S. C.	
PANDEYA, K. B. s. RANI, I.	
PANDEY, B. D., RUPAINWAR, D. C.: The Extraction of Iron(III)-Salicylate with an Indigenous Solvent Tri-isoamyl Phosphate (TAP) .....	1
PANDEY, S. s. PATEL, P. N.	
PAPP, S. s. VINCZE, L.	
PATEL, P. N., PANDEY, S.: Preparation, Infrared Absorption Spectra and X-Ray Powder Diffraction Patterns of Mixed (Ca + Sr + Pb) Hydroxylapatites .....	13
PATHAK, V. P., GARG, G. P., KHANNA, R. N.: Synthesis of 5-Methoxy-2-(3,4-methylenedioxyphenyl)-4 <i>H</i> -furo[2,3- <i>h</i> ]-[1]-benzopyran-4-one and 5-Methoxy-2-phenyl-4 <i>H</i> -furo[2,3- <i>h</i> ][1]-benzopyran-4-one .....	123
PETHŐ, G. s. BURGER, K.	
PETRIKOVICS, I. s. JÁSZBERÉNYI, J. Cs.	
POHLE, U., GROSSMANN, G.: Effect of Dispersion Interactions on NMR Shielding Constants (in German) .....	381
PÓTA, Gy., BAZSA, Gy., BECK, M. T.: Study of Pseudo—Waves in Periodic Reactions ....	277
PUNGOR, E. s. BURGER, K.	
PUPYSHEV, V. I. s. AROCA, R.	
PUTIRSKAYA, G. s. KÖRÖS, E.	
RÁCZ, K. s. BURGER, M.	
RANA, V. B. s. SANGAL, S. K.	
RANI, I., PANDEYA, K. B., SAWHNEY, G. L., BAIJAL, J. S.: Mössbauer and Magnetic Studies on Hydroxo—Bridged Iron(III) Complexes of some Oximes .....	75
ROBINSON, E. A. s. AROCA, R.	
RUPAINVAR, D. C. s. PANDEY, B. D.	
RYTÍŘ, Z. s. DRÁTOVSKÝ, M.	
SAHNI, S. K. s. SANGAL, S. K.	
SANGAL, S. K., SAHNI, S. K., RANA, V. B.: FIVE-Coordinate Manganese(II) and Iron(II) Complexes of [2,6-( <i>N,N'</i> -Diacetyl and <i>N,N'</i> -Dibenzoyl)]-diaminopyridine .....	19
SAWHNEY, G. L. s. RANI, I.	
SCHNEIDER, Gy., VINCZE, I., HACKLER, L., SZABÓ, J. A., DOMBI, Gy.: Steroids, XXVIII. Neighbouring Group Participation, V. (0 <sup>-</sup> —4) Neighbouring Group Participation and Fragmentation in the 16-Hydroxymethylandroster-5-ene-3,17-diol Series ....	429
SCHREIBER, H. s. FÖRSTERLING, H. D.	
SERES, L.: Molecular Decomposition Reactions of Dialkyl Ethers. The Estimation of Pre-exponential Factors .....	39
SHYAM, R. s. BEG, M. N.	
SIMÁNDI, L. I. s. NÉMETH, S.	
SINGH, C. P.: Synthesis of <i>N</i> <sup>1</sup> -Isonicotinoyl-3,5-diphenyl-4-(sulfamoylphenylazo)-1,2-diazoles as Antimalarial Agents .....	35

SINGH, H. s. BHATTACHARYA, B. K.	
SZABÓ, D. s. LÓRÁND, T.	
SZABÓ, G. T., ARANYOSI, K., TÓKE, L.: Polyethylene Glycol Derivatives as Complexing Agents and Phase—Transfer Catalysts, IV. Behaviour of Phase—Transfer Catalysts in Solid—Liquid Phase Equilibria .....	215
SZABÓ, G. T., ARANYOSI, K., TÓKE, L.: Polyethylene Glycols as Complexing Agents and Phase-Transfer Catalysts, V. Reaction Rates in the Organic Phase .....	225
SZABÓ, J. A. s. SCHNEIDER, Gy.	
SZEIFERT, I. s. BERÉNYI, S.	
SZEJTLI, J. s. BUVÁRI, Á.	
SZEJTLI, J. s. DARUHÁZI, L.	
SZEJTLI, J. s. KAJTÁR, M.	
TONKOVIĆ, M., MUSIĆ, R., HADŽIJA, O., NAGY-CZAKÓ, I., VÉRTES, A.: Mössbauer Study of Iron-Sugar Complexes .....	197
TÓKE, L. s. ÁGAI, B.	
TÓKE, L. s. SZABÓ, G. T.	
TURCSÁNYI, B.: Oscillatory Reactions: Model Construction and Possibilities of Realization .....	305
VARGA, M. s. KÓRÓS, E.	
VÉRTES, A. s. TONKOVIĆ, M.	
VÉRTES, Gy.: Electrochemistry of Stainless Steels, I. Potentiodynamic Polarization Curves	203
VINCZE, I. s. SCHNEIDER, Gy.	
VINCZE, L., PAPP, S.: Calculation of Association Constants and Distribution of Contact and Dipolar Interactions for $[R_3P^+R']-[FeCl_4]^-$ Ion Pairs .....	163
VINCZE, L., PAPP, S.: $^1H$ -NMR- and Mössbauer Investigations on the Ion Pairs of Tetrachloroferrate(III) Anion with Quaternary Phosphonium Cations .....	153
YADAV, L. D. S. s. BHATTACHARYA, B. K.	
ZALOTAI, L. s. HUNYADI-ZOLTÁN, Zs.	
ZÁRA-KACZIÁN, E. s. GÁLL-ISTÓK, K.	
ZHABOTINSKII, A. M.: Self-Oscillating Chemical Reactions. Mechanism of Oscillating Oxidations with Bromate .....	183
ZITTLAU, W. s. FÖRSTERLING, H. D.	
ZSÉDENYI, P. s. AGÓCS, P. M.	

## THE EXTRACTION OF IRON(III)-SALICYLATE WITH AN INDIGENOUS SOLVENT TRI-ISOAMYL PHOSPHATE (TAP)

B. D. PANDEY and D. C. RUPAINWAR\*

(*Applied Chemistry Section, School of Applied Sciences, Institute of Technology, Banaras Hindu University, Varanasi-221005, India*)

Received November 25, 1980

Accepted for publication March 12, 1981\*\*

The extraction of iron(III) from its aqueous perchlorate solutions in presence of salicylic acid into the new and indigenous solvent tri-isoamyl phosphate (TAP) diluted with carbon tetrachloride has been studied using spectrophotometric technique. The higher values for the distribution coefficient for iron(III) are obtained at an initial pH of 3.15 for the aqueous phase and  $[H_2sal] = 0.1 \text{ mol dm}^{-3}$ . A dynamic equilibrium, in the aqueous phase, exists between a number of species containing iron(III) and salicylate anion. The composition of the extracted species is  $FeSal \cdot Hsal \cdot 2TAP$ .

### Introduction

The formation of iron(III)-salicylic acid complexes is rather well known and the concept has been used to develop methods for the quantitative determination of iron(III), the salicylic acid and even some of its derivatives [1-3]. Salicylic acid ( $H_2sal$ ), a dibasic acid, may function as a doubly charged bidentate ligand ( $sal^{-2}$ ) or a singly charged monodentate ligand ( $Hsal^{-}$ ). It forms complexes with iron(III) having Fe: ligand ratios of 1:1, 1:2 and 1:3 [4]. In the extraction of uranium(VI) [5] into methyl *iso*-butyl ketone (MIBK) in the presence of salicylic acid the species extracted were found to be  $UO_2(Hsal)_2$  and  $UO_2(Hsal)_2 \cdot H_2sal$ . However, for Th(IV) the molecular formula of the extracted moiety was  $Th(Hsal)_4 \cdot H_2sal$  [6]. The species formed with beryllium(II) when it is extracted into amyl alcohol has been reported as neutral  $Be(Sal)$  [7]. Ternary lanthanide complexes of the type  $M^{III}(Hsal)_3 \cdot (TBP)_2$  following extraction methods have been prepared and characterised [9]. During the partition of cobalt(II) between its aqueous solution containing salicylic acid and TBP, it has been suggested that the extracted species is  $Co(Hsal)_2 \cdot 2TBP$  [8].

We have prepared the new solvent tri-isoamyl phosphate (TAP) by an indigenous process and the solvent is much cheaper than TBP. The potentialities of this new solvent have already been established for the extraction of trivalent metals, e.g. Ga(III), In(III), Tl(III) [10] and Fe(III) [11] from their

\* To whom correspondence should be addressed

\*\* In final form accepted September 14, 1981

hydrohalic acid solutions. The studies were extended to investigate the chelate extraction system for iron(III) in the presence of salicylic acid, and the results are reported in this communication.

## Experimental

### Tri-isoamyl phosphate (TAP)

It has been prepared from fusel oil, a by-product of Indian Alcohol Industry [10] and was diluted with carbon tetrachloride.

### Stock solution of iron(III)

Ferric hydroxide was freshly precipitated by the addition of aqueous ammonia into a solution of ferric nitrate (AR, BDH). The hydrated oxide was thoroughly washed to remove any adsorbed ions and then dissolved in perchloric acid (60% AR) to get a stock solution of ferric perchlorate. The iron content of this solution was determined spectrophotometrically by the conventional thiocyanate method [12].

All the other reagents and solutions were prepared from the AnalaR grade chemicals.

### Extraction procedure

15 mL of the diluted TAP was pre-equilibrated with an equal volume of the solution containing the desired amounts of salicylic acid at an appropriate pH but not iron(III). It is observed that extraction of small amounts of salicylic acid takes place and it is pH dependent. Nevertheless, the distribution curve for salicylic acid is independent of initial  $[\text{H}_2\text{Sal}]_{\text{total}}$  provided it is maintained as  $< 10^{-1} M$  ( $M = \text{mol dm}^{-3}$  and the notation is used in all the figures and the text). Consequently, for all the subsequent extractions of iron(III) the  $[\text{H}_2\text{Sal}]_{\text{total}}$  was taken to be  $< 10^{-1} M$ . 10 mL of this pre-equilibrated solvent was then added to an aqueous layer having identical conditions and desired amounts of iron(III). The layers were shaken vigorously for 15 minutes (which is sufficient to attain equilibrium) and allowed to stand and then the layers were separated.

5 mL aliquots from both layers were withdrawn, the organic acid decomposed by treatment with *conc.*  $\text{HNO}_3$  and finally their iron(III) content was estimated spectrophotometrically. The salicylate concentration was evaluated from the spectral data by a method reported earlier [8] which utilized the formation of mono salicylate iron(III) species showing strong absorption at 530 nm in the aqueous phase. However, in some cases, the analysis of salicylic acid was also checked by independent method, *i.e.* by the volumetric bromometric method reported earlier [4]. The mass balance for the iron(III) content of the aqueous and organic layer has been checked.

The pH of the solutions were measured accurately with a standard pH meter (ECIL, Hyderabad, India). The ionic strength was maintained at 0.5 *M* throughout these experiments by the addition of calculated amounts of concentrated solution of sodium perchlorate. It was further assumed that under these conditions the activity factors are constant and hence concentrations can be used instead of activities in the system. All the equilibrations were done in glass stoppered measuring cylinders in a thermostatic bath maintained at  $25 \pm 1^\circ \text{C}$ .

## Results and Discussion

The distribution ratio (*D*) for iron(III) was evaluated at a constant  $[\text{H}_2\text{Sal}]_{\text{total}}$  while the initial metal concentration was in the range of  $10^{-2} - 10^{-5} M$ . The results (given in Table I) show that at an initial iron(III)

**Table I***Effect of the iron(III) concentration on the distribution ratio at pH = 3.15*[H<sub>2</sub>sal]<sub>total</sub> = 10<sup>-1</sup> M, vol. of aq. layer = vol. of org. layer = 10 mL,[TAP] = 10% vol/vol in CCl<sub>4</sub>, μ = 0.5 M

S. No.	1	2	3	4
Fe(III) conc. in mol dm <sup>-3</sup>	1.0 × 10 <sup>-5</sup>	4.0 × 10 <sup>-4</sup>	1.0 × 10 <sup>-3</sup>	5.0 × 10 <sup>-3</sup>
Distribution ratio ( <i>D</i> )	8.49	8.49	8.49	9.55
	5	6	7	8
Fe(III) conc. in mol dm <sup>-3</sup>	8.0 × 10 <sup>-3</sup>	1.0 × 10 <sup>-2</sup>	2.0 × 10 <sup>-2</sup>	5.0 × 10 <sup>-2</sup>
Distribution ratio ( <i>D</i> )	10.18	10.61	11.04	11.67

concentration of less than 10<sup>-3</sup> M the distribution ratio is independent of the iron(III) concentration. At higher metal concentration the values of *D* show slight and gradual increase and the colour of the organic layer changes from purple to pink. When the spectra of the two layers were taken, the extracts at low iron(III) concentrations showed maximum absorption at 530 nm while for those with Fe(III) > 10<sup>-3</sup> M the λ<sub>max</sub> is shifted towards lower wavelengths. Also the increasing iron(III) concentration would bring the equilibrium pH to a lower value than that of the initial and this should give decreased value of *D* but on the contrary the *D* values are increased. Hence it is quite evident that another species is formed at higher concentrations of iron(III). The fact that the *D* values at lower [Fe(III)] up to 10<sup>-3</sup> M are independent of the metal concentration suggests the extraction of only mononuclear species.

Figure 1 shows the plots of log *D* vs. pH at different [H<sub>2</sub>Sal]<sub>total</sub> and it can be seen that at an initial pH of 3.15 for [Fe(III)] = 10<sup>-4</sup> M maximum extraction is observed at [H<sub>2</sub>Sal]<sub>total</sub> = 10<sup>-1</sup> M. The figure also indicates that the *D* values show a gradual increase as the initial pH increases, attain a maxima and then decrease. However, when the salicylic acid concentration decreases the maxima are shifted towards higher pH values.

From the already reported values of the equilibrium constants [4, 13, 14] for this extraction system involving other extractants it appears that below pH 2.0 the predominant species present in the aqueous phase is Fe(III) whereas in the pH range of 2.0–5.0 FeSal<sup>+</sup> and FeSal<sub>2</sub><sup>-</sup> have been found to be the main species. However, as expected, the extraction of iron(III) at varying pH values depends on the salicylate available in the system concerned. The equilibria, in the aqueous phase, can be represented as follows:



Therefore, it can be suggested that at low pH the equilibrium shown by equation (1) is maintained which is followed by the second equation at higher salicylate concentrations. However, at considerably higher pH, *i.e.* 6.0 and above the equilibrium shown in (3) seems to be more predominant in the aqueous phase.

The increasing trend of the distribution ratios with an increase in pH (Fig. 1) may be attributed to the fact that at lower pH values the equilibrium

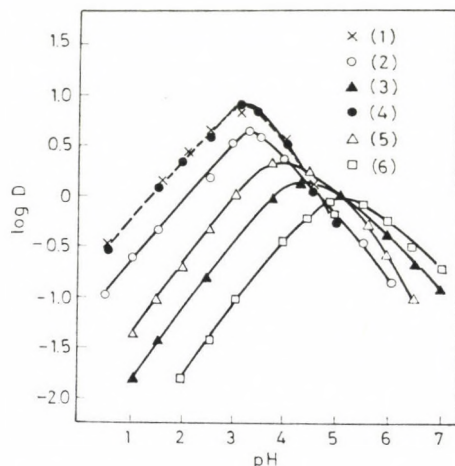


Fig. 1. Fe(III) extraction as a function of total salicylic acid concentration;  $[Fe^{3+}] = 10^{-4} M$ . (1)  $H_2sal = 2 \times 10^{-1} M$ ; (2)  $H_2sal = 3.3 \times 10^{-2} M$ ; (3)  $H_2sal = 4 \times 10^{-3} M$ ; (4)  $H_2sal = 10^{-1} M$ ; (5)  $H_2sal = 10^{-2} M$ ; (6)  $H_2sal = 10^{-3} M$ .  $[TAP] = 10\%$  vol/vol in  $CCl_4$

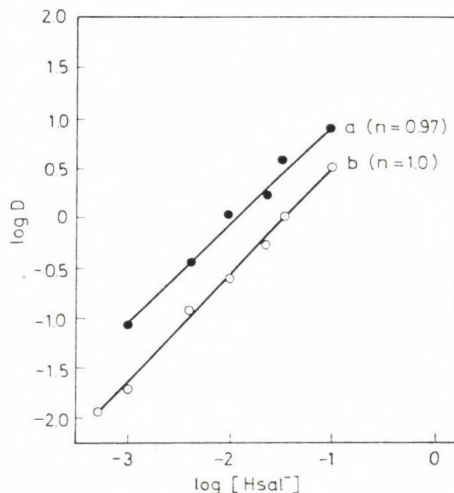


Fig. 2. Extraction of Fe(III) as a function of  $\log [Hsal^-]_{aq}$ , at constant pH. (a) pH = 3.15, (b) pH = 4.0;  $[Fe^{3+}] = 10^{-4} M$ .  $[TAP] = 10\%$  vol/vol in  $CCl_4$ ,  $n =$  solvation number

of Eq. (1) is shifted to the left. As the pH rises  $\text{Hsal}^-$  participates in the equilibrium process and allows an increased extraction by giving uncharged species. However, increasing the pH value still further the  $D$  values decrease and this can be attributed to the hydrolysis of iron(III) species. The possibility of the formation of inextractable polynuclear species also cannot be ruled out. Further detailed evidence described below indicates that in the pH range of 2.0–5.0 the anionic species ( $\text{FeSal}_2^-$ ) though exists in the aqueous phase is not extracted.

Plots of  $\log D$  vs.  $\log [\text{Hsal}^-]_{\text{aq}}$  are shown in Fig. 2. Thus we may conclude that the extracted species contains one  $\text{Hsal}^-$  ion per iron atom and considering that the uncharged species are comparatively more easily extracted into the organic layer another molecule of  $\text{Sal}^{2-}$  is associated and hence the molecular formula of the species can be speculated to be  $\text{FeSal} \cdot \text{Hsal}$ .

The extraction of neutral species *viz.*  $\text{FeSal} \cdot \text{Hsal}$  is substantiated by the absorption spectra of the organic layer which shows a sharp peak at 530 nm. This peak has been reported [4] to correspond with the  $\text{FeSal}^+$  cation in the aqueous solution whereas the other species formed, *viz.*  $\text{FeSal}_2^-$  and the  $\text{FeSal}_3^{3-}$ , show absorptions respectively, at 490 and 430 nm. All these absorptions are related to the charge transfer transition from the phenolic oxygen of the salicylate group to the metal atom and since there is no shift in the absorption maxima at 530 nm it may be inferred that the phenolic oxygen of the  $\text{Hsal}^-$  anion does not coordinate to iron(III).

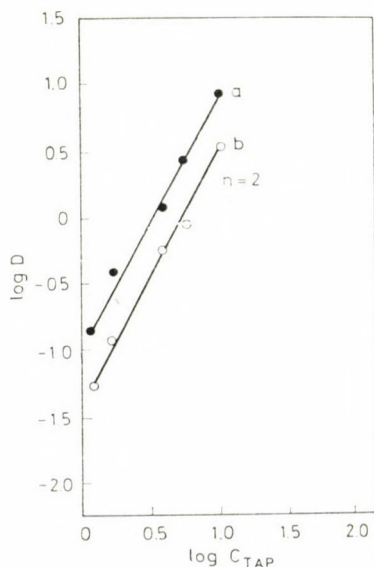


Fig. 3. Variation of  $\log D$  with  $\log C_{\text{TAP}}$  using carbon tetrachloride as a diluent at (a)  $\text{pH} = 3.15$ , (b)  $\text{pH} = 4.0$ .  $[\text{Fe}^{3+}] = 10^{-4} \text{ M}$ ,  $C_{\text{TAP}} = \%$  concentration of TAP in  $\text{CCl}_4$  vol/vol;  $n =$  solvation number

Generally, in such chelate extraction systems the behaviour of the metal depends on its tendency to react with the doubly charged salicylate anion which in turn depends on the size of the cation. Thus beryllium(II) which has small ion radius (0.31 Å) and large formation constant [7] is extracted into amyl alcohol as  $\text{Be-Sal}\cdot 2\text{H}_2\text{O}$  whereas the Mn(II) a larger cation (0.80 Å) with a small formation constant is extracted into TBP as  $\text{Mn(Hsal)}_2\cdot 2\text{TBP}$ . The formation constant of iron(III) (ion radius = 0.64 Å) shows clearly that it readily forms salicylate complexes and the system is very similar to those for the divalent metals. The formula of the extracted species evaluated in the system under investigation is further supported by extraction of Fe(III) into the TBP where the formation of similar type of species has been established [15].

The effect of varying the TAP concentration (in carbon tetrachloride) on the distribution ratio is shown in Figure 3, which shows the plots of  $\log D$  vs.  $\log C_{\text{TAP}}$  at the two pH values of 3.15 and 4.00. The slope for both the straight lines shown in Figure 3 is nearly two indicating thereby that the extracted species is invariably dissolvated and has the formula  $\text{FeSal}\cdot\text{Hsal}\cdot 2\text{TAP}$ . Similar results are obtained when TAP is diluted with benzene instead of carbon tetrachloride.

\*

We are thankful to the Director, I. T., B. H. U., for providing laboratory facilities. One of us (B. D. P.) is thankful to the C. S. I. R., New Delhi for the award of a Post-doctoral Fellowship.

#### REFERENCES

- [1] MEHLING, J. P.: *Ind. Eng. Chem. Anal. Ed.*, **10**, 136 (1938)
- [2] SCOTT, R. O.: *Analyst.*, **66**, 142 (1941)
- [3] PANKRATZ, R. E., BANDELIN, F. J.: *J. Am. Pharm. Assoc. Sci. Ed.*, **41**, 267 (1952)
- [4] ÅGREN, A.: *Acta Chem. Scand.*, **8**, 1059 (1954)
- [5] HOK-BERNSTROM, B.: *Acta Chem. Scand.*, **10**, 163 (1956)
- [6] HOK-BERNSTROM, B.: *Acta Chem. Scand.*, **10**, 174 (1956)
- [7] DE BRUIN, H. J., KAIRAITIS, D., SZIGO, L.: *Austr. J. Chem.*, **15**, 218 (1962)
- [8] AGGETT, J., CROSSLEY, P. J.: *J. Inorg. Nucl. Chem.*, **29**, 1113 (1967)
- [9] SINHA, S. P.: *J. Inorg. Nucl. Chem.*, **33**, 2205 (1971)
- [10] KAKKAR, K. K., RUPAINWAR, D. C.: *Acta Chim. Acad. Sci. Hung.*, **95**, 373 (1977)
- [11] PANDEY, B. D., RUPAINWAR, D. C.: *J. Inorg. Nucl. Chem.*, **41**, 337 (1979)
- [12] VOGEL, A. I.: *A Text Book of Quantitative Inorganic Analysis*, ELBS and Longmans, Green and Co. Ltd., London, 785 (1964)
- [13] AGGETT, J., EVANTS, D., HANCOCK, R.: *J. Inorg. Nucl. Chem.*, **30**, 2529 (1968)
- [14] MARTELL, A., SILLEN, L. G.: *Stability Constants*, Spl. Publ. No. **17**, The Chem. Soc. London (1964)
- [15] AGGETT, J., CROSSLEY, P., HANCOCK, R.: *J. Inorg. Nucl. Chem.*, **31**, 3241 (1969)

B. D. PANDEY }  
 D. C. RUPAINWAR } Banaras Hindu University, Varanasi-221005, India

## KINETICS OF OXIDATIVE DECARBOXYLATION OF L-CYSTEINE BY PERMANGANATE

S. C. AMETA\*, H. L. GUPTA, P. N. PANDE and H. C. CHOWDHRY

(*School of Studies in Chemistry, Vikram University, Ujjain, M. P., 456010 India*)

Received May 22, 1980

In revised form March 16, 1981

Accepted for publication April 7, 1981

Oxidative decarboxylation of L-cysteine by permanganate in sulfuric acid medium has been found to be first order in both oxidant and substrate concentrations. Various hypotheses for the mechanism of acid catalysis have been tested. The energy and entropy of activation have been calculated as 52.7 and 56.5 kJ mol<sup>-1</sup> and -101.7 and -94.9 J mol<sup>-1</sup> K<sup>-1</sup> for two stages of the reaction, respectively. A mechanism is proposed, which is in agreement with the experimental data.

Potassium permanganate has been found to be a good oxidising agent and the kinetics of oxidation of various organic compounds have been studied by previous workers [1–5]. However, careful survey of the literature reveals that oxidative decarboxylation of amino acids by permanganate has received little attention [6–8]. The present paper deals with the kinetic studies of the oxidative decarboxylation of L-cysteine by potassium permanganate in sulfuric acid medium.

L-Cysteine has an -SH group, which is rapidly oxidized by potassium permanganate to an -SO<sub>3</sub>H [9–10]. The object of the present investigation was to study the oxidative decarboxylation, which is a relatively much slower process as compared to the oxidation of -SH group to -SO<sub>3</sub>H group. The amount of potassium permanganate required for the oxidation of the thiol group to sulfonic acid group was determined by adding permanganate solution to a solution of L-cysteine to give a pink colour (in excess) and titrating the excess of permanganate against previously standardized hypo solution.

### Experimental

L-Cysteine, potassium permanganate and other chemicals used were BDH'AR'/SM'GR' grade. Doubly distilled water was used to prepare all solutions. The reaction vessels were coated with black paint to exclude any photochemical effect.

Solutions of sulfuric acid were standardized against previously standardized sodium hydroxide solution. Potassium permanganate solution was prepared by the method of VOGEL [11].

The requisite amounts of L-cysteine and sulfuric acid were taken in the reaction flask and kept in a thermostat at the desired temperature within  $\pm 0.1$  °C. The flask of potassium

\* To whom correspondence should be addressed. Present address: 15, Radhey Skyam Street, Bramh Pole Gate, UDAIPUR (Raj.), 313001 INDIA.

permanganate was also kept in the thermostat. Requisite volume of permanganate was then rapidly mixed. The kinetics of the reaction was followed by estimating unreacted permanganate iodometrically.

## Results and Discussion

Stoichiometry of the reaction was studied. It was observed that two equivalents of permanganate were consumed by five equivalents of L-cysteine. Formation of ammonium ions and carbon dioxide was confirmed by usual tests. 2-Sulfoacetaldehyde was detected as the reaction product. The induced reduction of mercuric chloride by the reaction mixture indicates the participation of free radicals [12].

When the concentrations of L-cysteine and sulfuric acid were in excess, the fading of permanganate followed a first order rate law. The pseudo-first order rate constants,  $k_1$  and  $k_2$ , are listed in Table I.

**Table I**  
*Variation of L-cysteine and permanganate concentrations*

$c(\text{H}_2\text{SO}_4) = 2.0 \text{ mol dm}^{-3}$		Temperature = 303 °K	
$c(\text{KMnO}_4) \times 10^4$ (mol dm <sup>-3</sup> )	$c(\text{L-cysteine})$ $\times 10^4$ (mol dm <sup>-3</sup> )	$k_1(10^{-4} \text{ s}^{-1})$	$k_2(10^{-4} \text{ s}^{-1})$
4.0	10.0	6.13	3.13
6.0	10.0	6.40	3.06
8.0	10.0	6.13	2.95
10.0	10.0	6.06	2.96
10.0	15.0	9.03	4.80
10.0	20.0	12.80	6.40
10.0	25.0	17.06	8.53

**Table II**  
*Variation of sulfuric acid concentration*

$c(\text{L-cysteine}) =$ $= 10^{-2} \text{ mol dm}^{-3};$	$c(\text{KMnO}_4) =$ $= 10^{-3} \text{ mol dm}^{-3};$	Temperature = 303 °K
$c(\text{H}_2\text{SO}_4) \text{ mol dm}^{-3}$	$k_1(10^{-4} \text{ s}^{-1})$	$k_2(10^{-4} \text{ s}^{-1})$
2.0	6.06	2.96
2.5	8.08	3.93
3.0	10.18	4.95
3.5	12.80	6.40
4.0	17.05	8.83

The variation of permanganate concentration has practically no effect on the rate constants, confirming that the order with respect to permanganate is unity.

The plot of  $\log k$  vs.  $\log [\text{L-cysteine}]$  was found to be linear and the slope was unity, indicating that the order of the reaction with respect to the substrate L-cysteine is one. There is no kinetic evidence for intermediate complex formation between substrate and permanganate [13]. The rate has been found to increase with the increasing concentration of sulfuric acid. The pseudo-first order rate constants are listed in Table II.

Further in an attempt to correlate the rate of oxidation with acid concentration, various hypotheses for the mechanism of acid catalysis were tested. In this case, either of two ZUCKER—HAMMETT plots [14], are linear, indicating that the reaction is acid catalyzed, however, none of these plots produces the ideal slope of unity. In view of these departures of ideal slope values, applicability of BUNNETT's hypothesis [15] and the BUNNETT—OLSEN l.f.e.r. [16], were tested. The values of  $-H_0$  and  $\log a_{\text{H}_2\text{O}}$  corresponding to acid concentrations have been taken from PAUL and LONG [17] and BUNNETT [18] respectively.

The values of BUNNETT parameters  $\omega$ ,  $\omega^*$  and  $\Phi$  were found to be  $-6.9$ ,  $1.16$  and  $0.85$  for the first stage and  $-6.6$ ,  $1.25$  and  $0.83$  for the second stage, respectively.

Primary salt effect was not observed, but a linear plot of  $\log k$  against ionic strength was obtained at higher concentrations of added neutral salts. This indicated that the reaction involves at least a neutral molecule in the rate determining step.

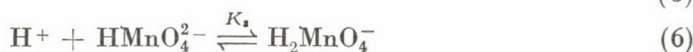
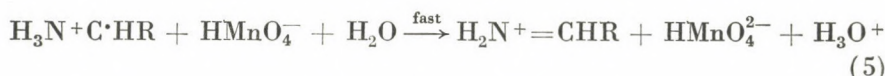
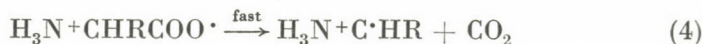
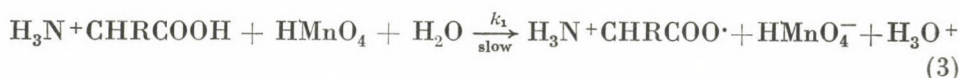
### Activation parameters

The reaction was studied at different temperatures to evaluate the activation parameters. The results are summarized in Table III.

Table III  
Activation parameters

$c(\text{L-cysteine}) = 10^{-3} \text{ mol dm}^{-3}$ ; $c(\text{KMnO}_4) = 10^{-4} \text{ mol dm}^{-3}$ ; $c(\text{H}_2\text{SO}_4) = 2.0 \text{ mol dm}^{-3}$			
Stage	$\Delta E^\ddagger$ (kJ mol <sup>-1</sup> )	$\Delta S^\ddagger$ (J mol <sup>-1</sup> K <sup>-1</sup> )	$pZ$ (dm <sup>3</sup> mol <sup>-1</sup> s <sup>-1</sup> )
First	52.7	-101.7	$7.995 \times 10^5$
Second	56.5	-94.9	$1.750 \times 10^6$

The information gained from the experimental data leads to the following probable mechanism, which explains the observed results well.



where R = -SH (or -SO<sub>3</sub>H) for L-cysteine (or L-cysteic acid).

The concentration of HMnO<sub>4</sub> was determined from the equation (9) as

$$K_2 = \frac{[\text{HMnO}_4]}{[\text{H}^+][\text{MnO}_4^-]_{\text{free}}} \quad (9)$$

Free [MnO<sub>4</sub><sup>-</sup>] can be calculated as

$$\text{Free } [\text{MnO}_4^-] = \text{initial } [\text{MnO}_4^-] - [\text{HMnO}_4] \text{ formed} \quad (10)$$

It will lead to the inclusion of a K<sub>2</sub> term in the numerator of the rate law. The rate expression for this mechanism has been derived as

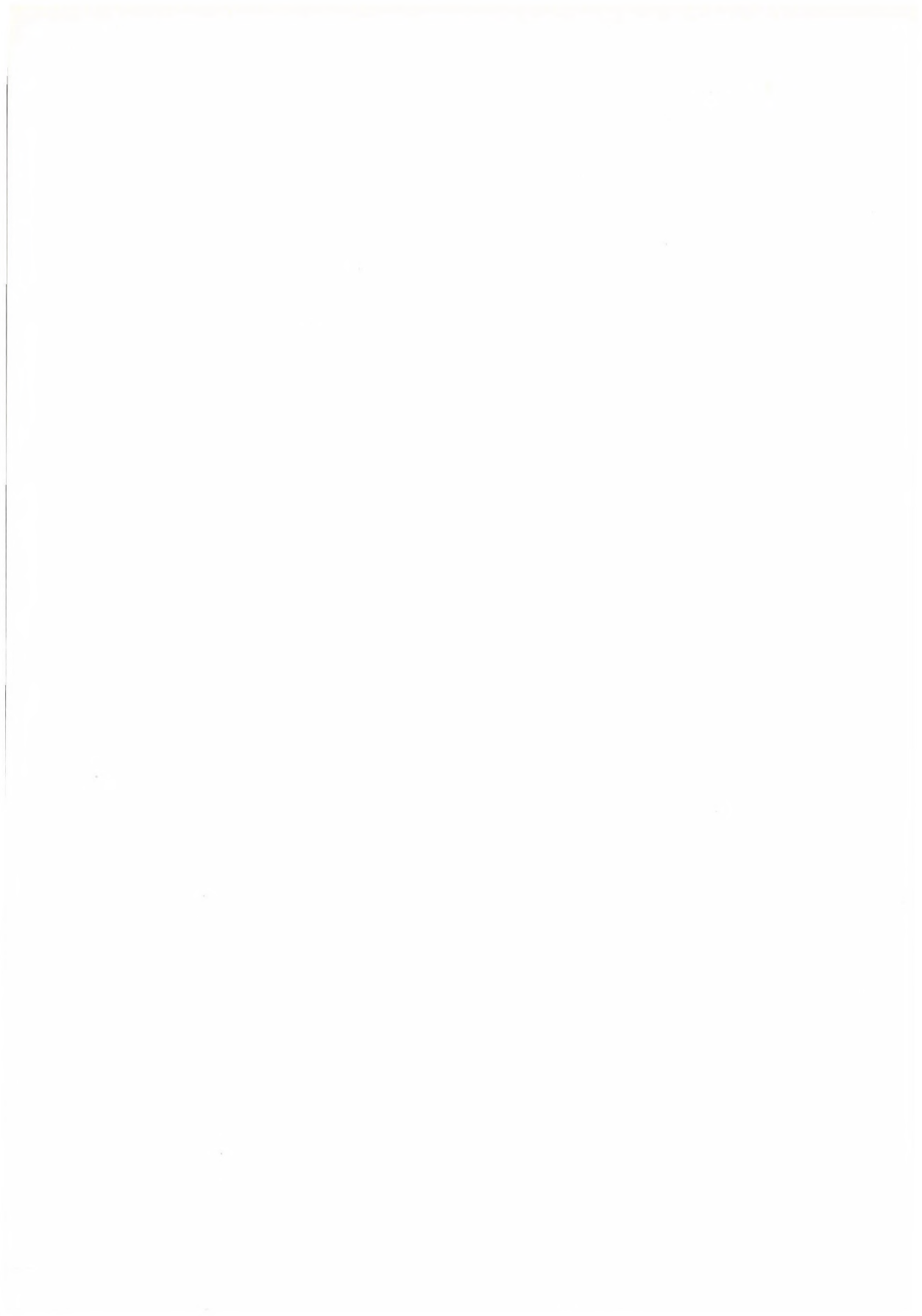
$$\frac{d[\text{MnO}_4^-]}{dt} = \frac{k_1 K_2 K_3 [\text{H}_3\text{N}+\text{CHRCOO}^-] [\text{H}^+]^2 [\text{MnO}_4^-] [\text{H}_2\text{O}]}{1 + K_2 [\text{H}^+]} \quad (11)$$

#### REFERENCES

- [1] LADBURY, J. W., CULLIS, C. F.: Chem. Rev., **58**, 403 (1958)
- [2] WATERS, W. A.: Quart. Rev., **12**, 277 (1958)
- [3] CARRINGTON, A., SYMONS, M. C. R.: Chem. Rev., **63**, 443 (1963)
- [4] STEWART, R.: in "Oxidation in Organic Chemistry", Ed. by K. B. WIBERG, Part A, pp. 1-68, Academic Press, New York 1965
- [5] AMETA, S. C., PANDE, P. N., GUPTA, H. L.: Rasayan Sammeksha (Communicated)

- [6] AMETA, S. C., GUPTA, H. L., PANDE, P. N., CHOWDHRY, H. C.: Z. phys. Chem. (Leipzig), **261**, 802 (1980)
- [7] AMETA, S. C., PANDE, P. N., GUPTA, H. L., CHOWDHRY, H. C.: Z. phys. Chem. (Leipzig), **261**, 1222 (1980)
- [8] VERMA, R. S., REDDY, J. M., SHASTRY, V. R.: J. Chem. Soc. Perkin II, **1976**, 469
- [9] HOLLEMAN, A. F., CALAND, P.: Ber., **44**, 2504 (1911)
- [10] WYNNE, W. P., BRUCE, J.: J. Chem. Soc., **1898**, 731
- [11] VOGEL, A. I.: "A Text Book of Quantitative Inorganic Analysis", pp. 282, Longman Green, London 1964
- [12] DRUMMOND, A. Y., WATERS, W. A.: J. Chem. Soc., **1953**, 2836
- [13] MEHROTRA, R. N.: J. Chem. Soc. (B) **1968**, 1123
- [14] ZUCKER, L., HAMMETT, L. P.: J. Am. Chem. Soc., **61**, 2791 (1939)
- [15] BUNNETT, J. F.: J. Am. Chem. Soc., **83**, 4968 (1961)
- [16] BUNNETT, J. F., OLSEN, F. P.: Can. J. Chem., **44**, 1899, 1917 (1966)
- [17] PAUL, M. A., LONG, F. A.: Chem. Rev., **57**, 1 (1957)
- [18] BUNNETT, J. F.: J. Am. Chem. Soc., **83**, 4956 (1961)

Suresh C. AMETA	}	Department of Chemistry, Madhav Vigyan Mahavidya-	
H. L. GUPTA			laya, Ujjain (M. P.), India
P. N. PANDE			
H. C. CHOWDHRY			



# PREPARATION, INFRARED ABSORPTION SPECTRA AND X-RAY POWDER DIFFRACTION PATTERNS OF MIXED (Ca + Sr + Pb) HYDROXYLAPATITES

P. N. PATEL<sup>1\*</sup> and S. PANDEY<sup>2</sup>

<sup>1</sup> *Post-Graduate Department of Chemistry, G. M. College, Sambalpur, India,*

<sup>2</sup> *Department of Zoology, Women's College, Sambalpur, India)*

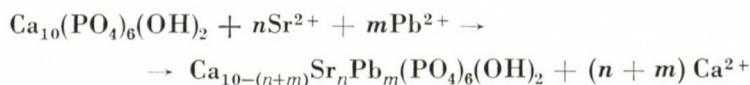
Received February 6, 1981

Accepted for publication April 7, 1981

Homogeneous solid solutions of calcium, strontium and lead hydroxylapatite have been prepared over the entire compositional range by the method of co-precipitation in aqueous media. Frequencies and assignments for the infrared absorption and the lattice constants of the solid solutions have been measured and found to vary linearly with composition between those of the pure and members.

## Introduction

Calcium hydroxylapatite (CaHA),  $\text{Ca}_{10}(\text{PO}_4)_6(\text{OH})_2$ , the principal inorganic constituent of human bones and teeth [1, 2] belongs to an isomorphous series of compounds known as apatites. Calcium hydroxylapatite (CaHA) also exists in nature as the mineral hydroxylapatite, which is similar if not identical to that in bone material, it can be prepared in aqueous solutions [3, 4]. The ionic radii [5] of calcium ( $0.099 \mu\text{m}$ ), strontium ( $0.113 \mu\text{m}$ ) and lead ( $0.120 \mu\text{m}$ ) are close to each other to enable solid solutions to be formed between isomorphous substances containing these ions [5]. Apatite undergoes a series of cationic and anionic replacement reactions [6]. The  $\text{Ca}^{2+} \rightarrow \text{Sr}^{2+}$  and/or  $\text{Pb}^{2+}$  replacement reactions in CaHA are of extreme biological significance and in view of its action on calcified tissue is interesting. They form the basis of incorporation of  $\text{Sr}^{2+}$  and  $\text{Pb}^{2+}$  into human skeletal system according to the following equation:



Solid solutions of calcium, strontium and lead hydroxylapatites were prepared separately earlier [7] by firing mixtures containing various proportions of calcium, strontium and lead hydroxylapatite at about  $1300^\circ\text{C}$ . These samples

\* To whom correspondence should be addressed

prepared by the solid state reaction were, however, found to be discontinuous and non-homogeneous.

Now an attempt has been made by the method of co-precipitation [8–10] to prepare the homogeneous solid solutions of mixed (Ca + Sr + Pb) hydroxylapatite over the entire compositional range.

## Experimental

### Materials

All chemicals used for the preparation of these samples were either AR (BDH) or E. MERCK extra pure grade. Water used in the preparation and for washing was boiled to remove  $\text{CO}_2$ , and then used immediately.

### Preparation

Stoichiometric quantities of ammonium dihydrogen phosphate (Solution A) and a solution containing  $\text{Ca}^{2+}$ ,  $\text{Sr}^{2+}$  and  $\text{Pb}^{2+}$  ions in the proportion desired for the solid solutions (Solution B) were prepared separately in carbon dioxide free doubly distilled water. The pH of these Solutions was adjusted above 11 by the addition of ethylenediamine. Then a part of solution B was put in a flask (2 dm<sup>3</sup>) fitted with two separating funnels and a delivery tube. Solution A and Solution B were poured individually into the separating funnels and added dropwise to the content of the flask simultaneously. Precipitation was carried out in carbon dioxide free atmosphere and the mixture was stirred vigorously by bubbling  $\text{CO}_2$  free air to prevent the formation of carbonato-apatites.

The precipitate and mother liquor were aged by boiling under reflux for 30 min to improve the homogeneity and crystallinity of the precipitate, and the maintenance of the desired pH during precipitation was ensured by testing the filtrate after separation of the precipitate, since any alternation of pH of the medium during precipitation leads to the formation of calcium deficient apatites [11]. The precipitate was washed thoroughly with doubly distilled water to free it from ammonium salts. Samples dried at 100 °C for few hours were analysed colorimetrically [12] and their molar volumes were determined by density method using toluene [13] as a solvent.

### Infrared absorption techniques

Sample used for infrared studies were acetone washed and air dried. All the bands were recorded on a Granting Infrared Spectrophotometer model 577 (Perkin-Elmer) in KBr. A few milligrams of the sample was ground with two drops of Nujol in an agate mortar. About 50 mg of a fine polyethylene powder (VESTOLENA 6016 Chem. Werke Huels, Germany) was added. The resulting paste was melted rapidly at about 140° and pressed between glass plates to a slightly wedged-shaped film of an average thickness of 0.1 mm.

### X-ray diffraction techniques

Samples dried at 110° for few hours were used for X-ray diffraction. The X-ray diffraction pattern of the samples were obtained with Siemens Powder diffractometer with NaCl(Tl) counter employing  $\text{CuK}_\alpha$  (Nickel filtered) radiation with a scanning speed of 1 degree ( $2\theta$ ) per min (using tube voltage of 30 kV and 24 mA, respectively).

### Lattice constant measurements

$\text{CaHA}$ ,  $\text{SrHA}$  and  $\text{PbHA}$  are hexagonal with two lattice constants  $a_0$  and  $c_0$ . These were determined [14, 15] for all the samples by measuring the diffraction angle  $2\theta$  of the three planes (312), (213) and (321). Each sample was thoroughly mixed with 25% NaCl (recrystallized from HCl) which served as a standard. So that the observed values of  $\sin \theta$  for the solid solution lines could be corrected directly for absorption and instrumental errors. The lattice constant of NaCl at 26° was taken to be 0.56403  $\mu\text{m}$  [16]. A least squares calcula-

tion on the corrected values of  $\sin \theta$  for the three reflections then gave the two parameters,  $a_0$  and  $c_0$ , for each sample. The diffraction lines were quite sharp and the diffraction angle was read by counting over the top of the peak with the scaling unit and estimating the position of maximum intensity from a plot of intensity against  $2\theta$ . The average probable error in unit cell parameters is less than  $\pm 0.005 \mu\text{m}$ .

### Results and Discussion

The results of chemical analysis of the samples are given in Table I. Based on the fact that a mole of each sample has a total 10 g-atoms of calcium and/or strontium and/or lead the molecular formula of the samples was calculated from the results of column 2–4 and included in column 6 of the Table I. The g-atom ratio  $\frac{(\text{Ca} + \text{Sr} + \text{Pb})}{\text{P}}$  in a mole of each sample was calculated from the results of columns 2–5 and given in column 8 of the table. The fact that the observed value of molar g-atom ratio of  $\frac{\text{Ca}}{\text{P}}, \frac{\text{Sr}}{\text{P}}, \frac{\text{Pb}}{\text{P}}$  for the end members and  $\frac{\text{Ca} + \text{Sr} + \text{Pb}}{\text{P}}$  were found to be equal to 1.658 (theoretical 1.67) is consistent with the formation of homogeneous solid solution [13]. This was further supported by the closeness of the values of molar volume of the members and those of the intermediate samples which lie within the range of end members.

The formation of solid solutions can be further confirmed by the X-ray diffraction analysis. It is well established that all the members of the apatite series exhibit hexagonal-bipyramidal class  $-6/m$  (space group  $P_{63/m}$ ) [17, 18]. Lattice parameters showed unit cell dilation consequent upon the introduction of bigger ions  $\text{Sr}^{2+}$  ( $0.115 \mu\text{m}$ ) and  $\text{Pb}^{2+}$  ( $0.120 \mu\text{m}$ ) in place of  $\text{Ca}^{2+}$  ( $0.099 \mu\text{m}$ ) ion in the apatite lattice. Such dilation with the proportion of Ca–Sr–PbHA was evident that the unit cell volume of the samples calculated on the basis of the experimentally determined lattice constant increased with the proportion of strontium and lead content in Ca–Sr–PbHA. This, of course, is the real evidence for solid solution in this series and clearly shows that these preparations are not mixtures of two components or one component with absorbed material.

The CaHA and its solid solutions with strontium and lead have hexagonal crystalline structure and are interesting examples of solid state of fairly simple molecules of tetrahedral symmetry where bands become allowed due to relation of the molecular symmetry [19] selection rules due to the influence of site symmetry. The ideal symmetry of tribasic phosphate ion in the free or undistorted state is tetrahedral — a member of  $Td$  point group. In this ideal symmetry condition only a few absorption bands corresponding to  $\nu_4$  ( $570 \text{ cm}^{-1}$ ) and  $\nu_3$  ( $1075 \text{ cm}^{-1}$ ) of  $\text{PO}_4^{3-}$  and  $\nu_1$  ( $630 \text{ cm}^{-1}$ ) and  $\nu_3$  ( $3450 \text{ cm}^{-1}$ ) of  $\text{OH}^-$

Table I  
Chemical analysis of calcium, strontium and lead hydroxylapatites and their solid solutions

Sample No.	Wt %				Molecular formula	Mol. vol.	G-atom ratio Ca+Sr+Pb P	Lattice parameter ( $\mu\text{m}$ )		Unit cell volume $\frac{\sqrt{3}}{2} a^2 c \times 10^3$	Frequency ( $\text{cm}^{-1}$ )		
	Ca	Sr	Pb	P				a	c		$\text{PO}_4^{2-}$ $\nu_1$	$\text{PO}_4^{2-}$ $\nu_2$	OH- $\nu_3$
1	39.88	—	—	18.51	$\text{Ca}_{10}(\text{PO}_4)_6(\text{OH})_2$	338.32	1.665	0.932	0.686	0.523	570	1075	3450
2	25.19	7.77	18.37	14.99	$\text{Ca}_{7.8}\text{Sr}_{1.1}\text{Pb}_{1.1}(\text{PO}_4)_6(\text{OH})_2$	336.42	1.664	0.943	0.690	0.531	565	1072	3450
3	21.99	6.91	25.70	13.98	$\text{Ca}_{7.3}\text{Sr}_{1.05}\text{Pb}_{1.65}(\text{PO}_4)_6(\text{OH})_2$	335.98	1.666						
4	22.86	14.44	14.25	14.95	$\text{Ca}_{7.2}\text{Sr}_{2.05}\text{Pb}_{0.85}(\text{PO}_4)_6(\text{OH})_2$	336.18	1.658						
5	16.10	13.35	28.71	12.88	$\text{Ca}_{5.8}\text{Sr}_{2.2}\text{Pb}_2(\text{PO}_4)_6(\text{OH})_2$	332.72	1.664	0.949	0.698	0.544	562	1070	3445
6	13.91	12.62	33.92	12.18	$\text{Ca}_{5.3}\text{Sr}_{2.2}\text{Pb}_{2.5}(\text{PO}_4)_6(\text{OH})_2$	340.12	1.662						
7	14.67	18.64	24.57	12.97	$\text{Ca}_{5.25}\text{Sr}_{3.05}\text{Pb}_{1.7}(\text{PO}_4)_6(\text{OH})_2$	336.84	1.660						
8	10.07	16.11	36.82	11.40	$\text{Ca}_{4.1}\text{Sr}_{3.0}\text{Pb}_{2.9}(\text{PO}_4)_6(\text{OH})_2$	337.57	1.658	0.955	0.707	0.558	560	1070	3442
9	6.62	14.48	45.64	10.24	$\text{Ca}_2\text{Sr}_3\text{Pb}_4(\text{PO}_4)_6(\text{OH})_2$	339.88	1.666						
10	7.40	20.87	35.78	11.07	$\text{Ca}_{3.1}\text{Sr}_4\text{Pb}_{2.9}(\text{PO}_4)_6(\text{OH})_2$	331.32	1.664						
11	4.85	19.76	42.17	10.23	$\text{Ca}_{2.2}\text{Sr}_{4.1}\text{Pb}_{3.7}(\text{PO}_4)_6(\text{OH})_2$	342.16	1.665	0.962	0.714	0.572	558	1065	3440
12	2.31	17.75	49.74	9.30	$\text{Ca}_{1.15}\text{Sr}_{4.05}\text{Pb}_{4.8}(\text{PO}_4)_6(\text{OH})_2$	344.40	1.665						
13	2.11	23.53	42.55	9.79	$\text{Ca}_1\text{Sr}_{5.1}\text{Pb}_{3.9}(\text{PO}_4)_6(\text{OH})_2$	342.56	1.665						
14	—	22.42	48.42	9.05	$\text{Sr}_{5.2}\text{Pb}_{4.8}(\text{PO}_4)_6(\text{OH})_2$	348.12	1.666	0.968	0.774	0.587	555	1062	3435
15	—	59.20	—	12.57	$\text{Sr}_{10}(\text{PO}_4)_6(\text{OH})_2$	364.61	1.665	0.974	0.726	0.596	550	1060	3425
16	—	—	77.74	6.95	$\text{Pb}_{10}(\text{PO}_4)_6(\text{OH})_2$	348.96	1.664	0.986	0.738	0.621	545	1055	3430

were observed clearly. From the spectra of the samples, it could be seen that the  $\nu_3$  and  $\nu_4$  frequencies corresponding to  $\text{PO}_4^{3-}$  ion and  $\nu_1$  and  $\nu_3$  corresponding to  $\text{OH}^-$  ion are shifted to lower frequencies and the shape of the peaks was affected by the introduction of strontium and lead ion into the samples. The shift of the  $\nu_3$  and  $\nu_4$  of  $\text{PO}_4^{3-}$  vibrations to lower frequencies may be due to the effect of binding energy and atomic mass. The lowering of frequency of  $\nu_3$  of  $\text{OH}^-$  indicates the presence of hydroxyl group in the apatite [20]. This hydroxyl group in hydroxylapatite lies in the internuclear axis coincident with sixfold screw axis. In BARNES expression [21].

$$\nu = \frac{1}{2\pi c} \frac{\sqrt{K}}{\mu}$$

which gives a relationship between frequency, atomic mass and force constant. The vibrational frequencies are dependent on the reduction mass  $\mu$  of the participating atoms and restoring forces  $K$  between atoms, all other terms remaining constant. When the equilibrium distance between the positive and the negative atoms of the molecule is decreased  $K$  generally increases in the above equation. This equilibrium distance depends on the ionic radii of the participating atoms in the molecule. Substitution of  $\text{Ca}^{2+}$  with a  $\mu$  ion like  $\text{Sr}^{2+}$  and/or  $\text{Pb}^{2+}$  gives rise to stronger coordination of the  $\text{PO}_4^{3-}$  group through oxygen. This in turn weakens the P—O bond, lowering  $K$  (increasing P—O bond length) and the frequency is lowered. The  $\text{PO}_4^{3-}$  bonding is normally around  $520 \text{ cm}^{-1}$  and bending modes do not shift very much under these conditions. But here the substitution is more complex, presumably because of the splitting of the triply degenerate mode at  $600 \text{ cm}^{-1}$  and thus there is an increase in the frequency from  $520 \text{ cm}^{-1}$  to  $570 \text{ cm}^{-1}$ . This theoretical explanation agrees well with the experimental data.

\*

The authors are highly grateful to Prof. G. FERRARIS of University of Torino (Italy) for X-ray data and Dr. M. M. DHAR, F. N. A., C. D. R. I., Lucknow for Infrared spectra, and the financial support to the authors by the University Grants Commission is gratefully acknowledged.

#### REFERENCES

- [1] NEUMAN, W. F., NEUMAN, M. W.: *Chem. Rev.*, **53**, 1 (1953)
- [2] ROBINSON, R. A.: *J. Bone and Joint Surg.*, **34**, 389 (1952)
- [3] WALLACYS, R., CHAUDRON, G.: *Compt. rend.*, **231**, 355 (1950)
- [4] HAYEK, E., STADLMANN, P.: *Angew. Chem.*, **67**, 327 (1955)
- [5] WELLS, A. F.: "Structural Inorganic Chemistry", p. 70, Oxford University Press, London, 1950
- [6] VAN WAZER, J. R.: "Phosphorus and its Compounds" Vol. 1, p. 530, New York, Interscience Publishers, Inc.
- [7] VAN WAZER, J. R.: "Phosphorus and its Compounds" Vol. 2, p. 1429, New York Interscience Publishers, 1966

- [8] PATEL, P. N.: *J. Chem. Ind. (London)*, **20**, 804—805 (1978)
- [9] PATEL, P. N.: *J. Ind. Chem. Soc. Vol. LVI*, **4**, 410—411 (1979)
- [10] PATEL, P. N.: *J. Chem. Ind. (London)* (in Press)
- [11] BERRY, E. E.: *J. Inorg. Nucl. Chem.*, **29**, 1585 (1967)
- [12] PATEL, P. N.: *Z. Anal. Chem.* (in Press)
- [13] PARTINGTON, J. R.: "An Advanced Treatise on Physical Chemistry" Vol. **3**, p. 121, Longman Green and Co. 1952
- [14] AZAROFF, L. C.: "Elements of X-ray Crystallography" Chapter **18**, London, McGraw Hill Book Co., 1968
- [15] CULLITY: "Elements of X-ray Diffraction" pp. 309—313.
- [16] STRAUMANIS, M., LEVINS, A. Z.: *Phys.*, **109**, 728 (1938)
- [17] MEHREL, M. Z.: *Krist.*, **75**, 323 (1930); NÁRAY-SZABÓ, I.: *ibid.*, **75**, 387 (1930)
- [18] HENTSCHEL, H.: *Z. Mineral Geol.*, **1923**, 609
- [19] NAKAMOTO, K.: "Infrared Spectra of Inorganic and Co-ordination Compounds" p. 103, New York, John Wiley Sons, Inc., 1966
- [20] ENGLE, G., KLEE, W. E.: *J. Solid State Chem.*, **6**, 28 (1972)
- [21] BARNES, R. B., GORE, R. C., LIDDEL, V., WILLIAMS, V. Z.: "Infrared Spectroscopy" Reinhold, New York, 1944

Prema N. PATEL Post-Graduate Department of Chemistry, G. M. College  
Sambalpur 768004, India

S. PANDEY Department of Zoology, Women's College, Sambalpur, India

## FIVE-COORDINATE MANGANESE(II) AND IRON(II) COMPLEXES OF [2,6-(*N,N'*-DIACETYL AND *N,N'*-DIBENZOYL)]-DIAMINOPYRIDINE

S. K. SANGAL\*, S. K. SAHNI and V. B. RANA

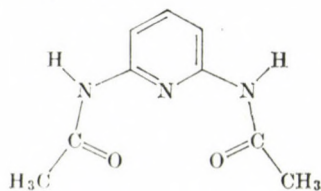
(Department of Chemistry, Meerut College, Meerut-250001, India)

Received January 13, 1981

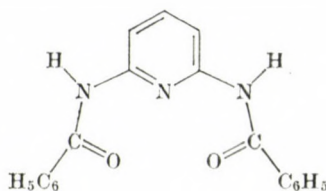
Accepted for publication April 16, 1981

The five-coordinate manganese(II) and iron(II) complexes of two new ligands 2,6-(*N,N'*-diacetyl) diaminopyridine, (DAP) and 2,6-(*N,N'*-dibenzoyl) diaminopyridine (DBP) have the formula (MLX<sub>2</sub>) where M = Mn(II) or Fe(II), L = DAP or DBP; X = Cl<sup>-</sup>, Br<sup>-</sup>, NO<sub>3</sub><sup>-</sup> or NCS<sup>-</sup>. The complexes have been characterised on the basis of elemental analysis, electrical conductance, spectral (infrared and electronic) and magnetic susceptibility data. All the complexes are high-spin and appear to have trigonal bipyramidal stereochemistry. Both DAP and DBP act as *N,O,O*-tridentate chelating agents.

In recent years, a large number of five-coordinate complexes of the first transition metal ions have been reported and their thermodynamic, magnetic and spectroscopic aspects have been dealt with at length [1–9]. However, relatively a few five-coordinate manganese(II) and iron(II) complexes have been studied [2–6]. It is now well established that the formation of a five-coordinate complex depends upon the shape and size of the metal ion besides the ionic radii and nature of the counter ion [2]. Five-coordination can be achieved successfully by the use of sufficiently bulky ligands in which inter-donor atom distances and angles closely match the edges of the coordination polyhedra [1, 2]. Two such ligands conforming to this criteria have been synthesised by acetylation and benzylation of 2,6-diaminopyridine. One of these ligands (DAP) has been found to form five-coordinate complexes with divalent cobalt, nickel and copper [7]. These studies are now extended to manganese(II) and iron(II) complexes with 2,6-(*N,N'*-diacetyl) diaminopyridine, (DAP) and 2,6-(*N,N'*-dibenzoyl) diaminopyridine, (DBP) whose structures are depicted below:



(DAP)



(DBP)

\* To whom correspondence should be addressed

## Experimental

All the chemicals used were of analytical grade and solvents were dried before use. The ligands were synthesised by a method described earlier [10]. The ligands DAP and DBP melt at 203 °C and 176 °C, respectively.

### Preparation of complexes

A general procedure was adopted to synthesise the complexes; the iron(II) complexes were prepared under a stream of nitrogen.

The appropriate metal salt (0.01 mole), dissolved in sufficient quantity of a mixture of ethanol and acetone (1 : 1), was mixed with the hot solution of the ligand (0.01 mole) in acetone (50 mL). The mixture was refluxed for 2 hr on a water bath and cooled. The crystals separated on cooling were washed with acetone and dried. Yield ~70%.

### Analytical procedures and physical measurements

The methods used for the determination of C, H and N are the same as described earlier [7]. The metal contents were determined by EDTA titration using Eriochrome Black-T and sulphosalicylic acid, respectively as an indicator. The electrical conductance in dimethyl formamide were determined on an Elico conductivity bridge type CM82T. The details of physical measurements are the same as described earlier [10, 11].

## Results and Discussion

The analytical data (Table I) reveal 1 : 1 metal to ligand stoichiometry for all these complexes. The complexes are partially soluble in common organic solvents, but highly soluble in dimethyl formamide and these complexes are

**Table I**  
*Analytical and magnetic data*

Complex	Calculated %			Found, %			$\mu$ eff. BM
	Metal	Nitrogen	Halogen	Metal	Nitrogen	Halogen	
[Mn(C <sub>9</sub> H <sub>11</sub> N <sub>3</sub> O <sub>2</sub> )Cl <sub>2</sub> ]	17.24	13.16	22.25	16.58	14.10	22.80	5.84
[Mn(C <sub>9</sub> H <sub>11</sub> N <sub>3</sub> O <sub>2</sub> )Br <sub>2</sub> ]	13.48	10.29	39.21	14.00	10.05	40.00	5.88
[Mn(C <sub>9</sub> H <sub>11</sub> N <sub>3</sub> O <sub>2</sub> )(NO <sub>3</sub> ) <sub>2</sub> ]	14.78	18.81	—	15.15	18.25	—	5.80
[Mn(C <sub>9</sub> H <sub>11</sub> N <sub>3</sub> O <sub>2</sub> )(NCS) <sub>2</sub> ]	15.06	19.17	—	15.20	19.52	—	5.86
[Fe(C <sub>9</sub> H <sub>11</sub> N <sub>3</sub> O <sub>2</sub> )Cl <sub>2</sub> ]	17.50	13.12	22.18	17.65	13.20	21.88	5.25
[Fe(C <sub>9</sub> H <sub>11</sub> N <sub>3</sub> O <sub>2</sub> )Br <sub>2</sub> ]	13.69	10.26	39.11	10.42	10.85	38.65	5.12
[Fe(C <sub>9</sub> H <sub>11</sub> N <sub>3</sub> O <sub>2</sub> )(NO <sub>3</sub> ) <sub>2</sub> ]	15.01	18.76	—	14.85	19.02	—	5.18
[Fe(C <sub>9</sub> H <sub>11</sub> N <sub>3</sub> O <sub>2</sub> )(NCS) <sub>2</sub> ]	15.30	19.12	—	15.05	19.15	—	5.20
[Mn(C <sub>19</sub> H <sub>13</sub> N <sub>3</sub> O <sub>2</sub> )Cl <sub>2</sub> ]	12.47	9.52	16.09	12.52	10.00	16.05	5.82
[Mn(C <sub>19</sub> H <sub>13</sub> N <sub>3</sub> O <sub>2</sub> )Br <sub>2</sub> ]	10.37	7.92	30.12	8.02	8.00	30.20	5.84
[Mn(C <sub>19</sub> H <sub>13</sub> N <sub>3</sub> O <sub>2</sub> )(NO <sub>3</sub> ) <sub>2</sub> ]	11.13	14.16	—	11.80	14.50	—	5.83
[Mn(C <sub>19</sub> H <sub>13</sub> N <sub>3</sub> O <sub>2</sub> )(NCS) <sub>2</sub> ]	11.31	14.40	—	11.50	15.00	—	5.87
[Fe(C <sub>19</sub> H <sub>13</sub> N <sub>3</sub> O <sub>2</sub> )Cl <sub>2</sub> ]	12.67	9.50	16.06	13.00	9.20	16.00	5.10
[Fe(C <sub>19</sub> H <sub>13</sub> N <sub>3</sub> O <sub>2</sub> )Br <sub>2</sub> ]	10.54	7.90	30.13	10.84	7.95	30.00	5.18
[Fe(C <sub>19</sub> H <sub>13</sub> N <sub>3</sub> O <sub>2</sub> )(NO <sub>3</sub> ) <sub>2</sub> ]	11.11	14.14	—	11.00	14.82	—	5.25
[Fe(C <sub>19</sub> H <sub>13</sub> N <sub>3</sub> O <sub>2</sub> )(NCS) <sub>2</sub> ]	11.49	14.35	—	11.50	14.52	—	5.24

non-conducting in this solvent. Accordingly, the complexes may be formulated as  $[MLX_2]$ , where L = DAP or DBP and X =  $Cl^-$ ,  $Br^-$ ,  $NCS^-$  or  $NO_3^-$ . These formulations are further supported by the infrared and electronic spectra of the complexes.

### Infrared spectra

The infrared spectra of 2,6-(*N,N'*-diacetyl) diaminopyridine has been recently reported [7]. The present assignments are based on i.r. study of DAP and other related compounds [12–14] and their complexes. The infrared spectra of DAP and DBP show bands at 1690, 1520, 1230, 650 and 550  $cm^{-1}$  attributable to amide-I ( $\nu C=O$ ), amide-II ( $\nu CN + \delta NH$ ), amide-III ( $\delta NH$ ), amide-IV (C=O in-plane deformation) and amide-VI (C=O out-of-plane deformation) vibrations, [12–15], respectively. These bands appear in the 1640–1650, 1550–1560, 1250–1265, 655, and 580–585  $cm^{-1}$  regions, respectively. In the spectra of the complexes, the downward shift in amide-I band (40  $cm^{-1}$ ) and upward shift in the amide-II and amide-VI bands are compatible with the amide-oxygen coordination to the metal atom [14–16]. The bands occurring at *ca.* 370  $cm^{-1}$  assigned to  $\nu(M-O)$  vibrations, substantiate the amide-oxygen coordination. The band at *ca.* 3250  $cm^{-1}$  occurring in the spectra of ligands, assigned to  $\nu NH$ , appear in the spectra of complexes as broad bands at  $\sim 3250-3000$   $cm^{-1}$ , confirm the amide oxygen coordination in ketonic form and rule out the possibility of keto  $\rightleftharpoons$  enol  $RCONHR' \rightleftharpoons RC(OH)=NR'$  tautomerisation.

The pyridine ring vibrations most affected on its coordination to a metal atom include 8a (pyridine ring deformation), 6a (in-plane ring deformation) and 16b (out-of-plane ring deformation) vibrations. In the spectra of free ligands these vibrations occur at 1585, 610, and 400  $cm^{-1}$ , respectively. In the spectra of complexes, these bands appear at higher frequencies  $\sim 1605$ , 630 and 425  $cm^{-1}$ , respectively. The upward shift in 8a, 6a and 16b vibrations indicates the coordination of pyridine nitrogen to the metal atom. This contention finds support by the appearance of  $\nu(Mn-py)$  and  $\nu(Fe-py)$  bands *ca.* 240 and 250  $cm^{-1}$ , respectively.

The chloro complexes of Mn(II) and Fe(II) show medium intensity bands *ca.* 260  $cm^{-1}$  and in bromo complexes new bands are observed  $\sim 210$   $cm^{-1}$ . These bands may be assigned to  $\nu(M-Cl)$  and  $\nu(M-Br)$  vibrations [18], respectively. The metal-halogen frequencies observed in the spectra of these complexes are lower than those observed for four-coordinate complexes and are much higher than those for high-spin six-coordinate complexes of these metal ions involving both bridged or terminal halogen atoms [18, 19]. The intermediate, values of  $\nu(M-X)$  vibrations suggest that the present complexes are five-coordinate. The ratio  $\frac{\nu(M-Cl)}{\nu(M-Br)}$  in the present complexes comes out

to be 0.78–0.81 and is comparable to other five-coordinate complexes reported earlier [20].

The thiocyanato complexes show three characteristic bands at 2050, 815 and  $485\text{ cm}^{-1}$  assignable to  $\nu(\text{CN})$ ,  $\nu(\text{CS})$  and  $\delta(\text{NCS})$  vibrations and are consistent with monodentate N-bonded thiocyanate group [18, 21]. This mode of coordination is supported by the appearance of new bands at *ca.* 270 and  $275\text{ cm}^{-1}$  characteristic of  $\nu\text{Fe}-\text{NCS}$  and  $\nu\text{Mn}-\text{NCS}$  vibrations, respectively. The nitrate complexes show new bands in the 1460–1475, 1255–1260 and 890–900  $\text{cm}^{-1}$  regions attributable to different NO stretching vibrations [18]. An additional band at *ca.* 1750 with a shoulder on the low energy side at *ca.*  $1740\text{ cm}^{-1}$  is also observed in the spectra of nitrate complexes. The presence of two bands with small splitting ( $\sim 10\text{ cm}^{-1}$ ) also indicates that the nitrate groups are coordinated monodentately [22]. The presence of weak bands at *ca.*  $265\text{ cm}^{-1}$  in these complexes may be assigned to  $\nu(\text{M}-\text{ONO}_2)$  vibrations.

#### *Magnetic moments and electronic spectra*

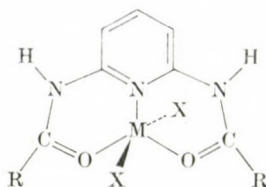
The magnetic moments (Table I) at room temperature of manganese and iron complexes lie between 5.80 and 5.88 and 5.10 and 5.25 BM, respectively. These values are well in the range of high-spin complexes of these metal ions. The  $\mu_{\text{eff}}$  values of iron(II) complexes are, however, slightly lower than the predicted (5.1–5.5 BM) values [23].

The electronic spectra of manganese complexes recorded in nujol mull and dimethyl formamide show bands at *ca.* 16 500, 19 200 and 22 000  $\text{cm}^{-1}$ . The positions of these bands are comparable to those five-coordinate complexes for which a trigonal bipyramidal geometry has been established by X-ray measurement [5, 25]. The weak intensity bands can be attributed to the spin-forbidden transitions from the ground sextet to the first excited quartet levels [5].

The iron(II) complexes show one band in the visible region at *ca.* 12 000  $\text{cm}^{-1}$  and another in the near i.r. region at *ca.*  $4000\text{ cm}^{-1}$ . The nature of the latter bands is not certain due to the possibility of absorption by the ligands in this region. However, the band observed  $\sim 12\,000\text{ cm}^{-1}$  indicates that iron(II) complexes are also five-coordinated [24]. On the basis of simple crystal field calculations CIAMPOLINI *et al.* [5] predicted two spin-allowed-bands for trigonal bipyramidal complexes. Accordingly, the band  $\sim 12\,000\text{ cm}^{-1}$  can be assigned to  $5_A \rightarrow 5_{E(1)}$  and the possible assignment of the band  $\sim 4000\text{ cm}^{-1}$  can be  $5_{E(2)} \rightarrow 5_{E(2)}$  in trigonal bipyramidal field. The spectra in nujol mull and in coordinating dimethyl formamide solution are almost similar indicating penta-coordination in solid state and in solution.

On the basis of magnetic, i.r. and electronic spectral studies it appears that these complexes are five-coordinate and have trigonal bipyramidal geom-

etry with the tridentate ligand forming a trigonal base and anions being present in axial positions. The structure of these complexes may be proposed as follows:



\*

The authors are thankful to U. G. C. and C. S. I. R., New Delhi for financial assistance, to C. D. R. I. Lucknow for elemental analyses and to R. S. I. C., I. I. T. Madras for recording i. r. spectra.

#### REFERENCES

- [1] MUETTERTIES, E. L., SCHUNN, R. A.: *Quart. Rev.*, **20**, 245 (1966); CIAMPOLINI, M., NARDI, N., SPERONI, G. P.: *Coord. Chem. Rev.*, **1**, 222 (1966)
- [2] WOOD, J. S.: *Progr. Inorg. Chem.*, **16**, 227 (1972); FURLANI, C.: *Coord. Chem. Rev.*, **3**, 141 (1968)
- [3] SACCONI, L.: *Pure and Appl. Chem.*, **17**, 95 (1968), **27**, 161 (1977); *Trans. Metal Chem. Ed. CARLIN, R. L.*: **4**, 210 (1968); *Coord. Chem. Rev.*, **8**, 351 (1972)
- [4] BERTINI, I., MORASSI, R., SACCONI, L.: *Coord. Chem. Rev.*, **11**, 343 (1973)
- [5] CIAMPOLINI, M., NARDI, N.: *Inorg. Chem.*, **5**, 1150 (1966)
- [6] CIAMPOLINI, M., SPERONI, G. P.: *Inorg. Chem.*, **5**, 45 (1966); ORIOLI, P. L., VAIRA, M. Di., SACCONI, L.: *Inorg. Chem.*, **5**, 400 (1966)
- [7] RANA, V. B., SANGAL, S. K.: *Acta Chim. Acad. Sci. Hung.*, **104**, 29 (1980)
- [8] TSCHITSCHIBABIN, Z.: *Russ. J. Chem. Soc.*, **50**, 522 (1920); *Chem. Abst.*, **18**, 1496 (1924)
- [9] MEYER, A., TROSH, C.: *Montash*, **35**, 207 (1914)
- [10] RANA, V. B., SANGAL, S. K., SAHNI, S. K.: *Acta Chim. Acad. Sci. Hung.*, **101**, 405 (1979)
- [11] RANA, V. B., SAHNI, S. K., SANGAL, S. K.: *J. Inorg. Nucl. Chem.*, **41**, 1498 (1979)
- [12] BOULD, J., BRIDON, B. R.: *Inorg. Chim. Acta*, **19**, 159 (1976)
- [13] NONOYAMA, M., TOMITA, S., YAMASAKI, K.: *Inorg. Chim. Acta*, **12**, 33 (1975)
- [14] NONOYAMA, M., TOMOMOTO, Y., YAMASAKI, K.: *Nippon Kagaku Zasshi*, **93**, 562 (1972)
- [15] SAHNI, S. K., GUPTA, S. P., SANGAL, S. K., RANA, V. B.: *J. Inorg. Nucl. Chem.*, **39**, 1098 (1977); *J. Indian Chem. Soc.*, **54**, 200 (1977)
- [16] BROWN, D. H., MAC SWEEN, D. R., MERCER, M., SHARP, D. W. A.: *J. Chem. Soc. (A)*, **1971**, 1575; REEDIZK, J.: *Inorg. Chim. Acta*, **5**, 687 (1971)
- [17] CLARK, R. J. H., WILLIAMS, C. S.: *Inorg. Chem.*, **4**, 350 (1965); MADDEN, D. P., DAMOTA, M. M., NELSON, S. M.: *J. Chem. Soc. (A)*, **1970**, 790; MADDEN, D. P., NELSON, S. M.: *J. Chem. Soc. (A)*, **1968**, 2342
- [18] NAKAMOTO, K.: *Infrared spectra of inorganic and coordination compounds*. Wiley-Interscience, New York 1978
- [19] FERRARO, J. R.: *Low frequency vibrations of inorganic and coordination compounds*. Plenum, New York 1971
- [20] KEETON, M., LEVER, A. B. P.: *Inorg. Chem.*, **10**, 47 (1971); BEECROFT, B., CAMPBELL, M. J. M., GRAZESKOVIAK, R.: *Inorg. Nucl. Chem. Lett.*, **8**, 1087 (1972)
- [21] BURMEISTER, J. L.: *Coord. Chem. Rev.*, **1**, 205 (1966), **3**, 225 (1968)
- [22] CURTIS, N. F., CURTIS, Y. M.: *Inorg. Chem.*, **4**, 804 (1965)
- [23] BAREFIELD, E. K., BUSCH, D. H., NELSON, S. M.: *Quart. Rev.*, **22**, 457 (1968); LEWIS, J., FIGGIS, B. N.: *Progr. Inorg. Chem.*, **6**, 37 (1964)
- [24] LIONS, F., DANCE, I. G., LEWIS, J.: *J. Chem. Soc. (A)*, **1967**, 565

Sudhir Kumar SANGAL	}	‘Prakashika’, 184 Abu Lane, Meerut-250001, India
Suresh Kumar SAHNI		
Vidya Bhushan RANA		



## MODIFIED CROWN ETHERS, I

### CARBONIC ACID DERIVATIVES CONTAINING ONE CROWN ETHER UNIT (PRELIMINARY COMMUNICATION)

B. ÁGAI, I. BITTER, É. CSONGOR and L. TÓKE \*

(Department of Organic Chemical Technology, Technical University, Budapest)

Received December 16, 1981

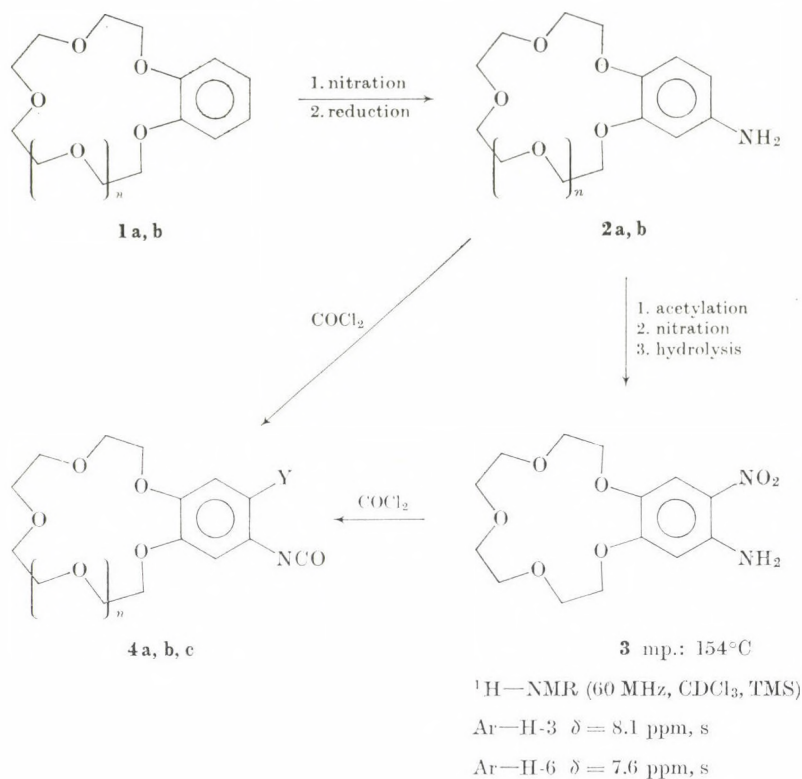
Accepted for publication February 3, 1982

Although crown ethers are widely used in chemical reactions as phase transfer catalysts by virtue of their cation complexing ability, relatively few examples are published on their application for effecting transport processes of cations in biological systems [1]. In this respect crown ethers of selective  $\text{Na}^+$ ,  $\text{K}^+$  and  $\text{Ca}^{2+}$  complexing ability and with stability constants of about  $\log K \sim 5$  are regarded to be the most interesting compounds [2]. On the other hand, the solubility of crowns in water and lipoids seems to be a very important factor besides stability constants and selectivity. Ligands of ion-selective membrane electrodes are expected to possess the same features as mentioned above. In an attempt to satisfy all these demands, we aimed at preparing new crown derivatives the solubility of which in water and apolar solvents can be altered over a wide range without considerable decrease of the stability constant. For this purpose the readily available benzo-15-crown-5 (**1a**) and benzo-18-crown-6 (**1b**) were used as starting materials [3]. Nitration of **1a**, **b** and catalytic hydrogenation of the nitro compounds by known methods [4]\*\* led to **2a**, **b** [5], which were transformed into **4a**, **b** crown isocyanates with excess phosgene in boiling chlorobenzene. The isocyanate **4c** was prepared from **2a** in four steps. The yields of phosgenation were excellent (87–94%); compounds **4a**, **b**, **c** were purified by vacuum distillation or recrystallization.

The crown isocyanates **4a**, **b**, **c** readily reacted with alcohols and amines affording the ureas and urethans **5–25** which had different solubilities and partition coefficients between water and apolar media (*e.g.* **14** is soluble in water, while **24** is dissolved by *n*-heptane). Additions were effected in dioxane or methylene chloride solution at room temperature, using 1:1 molar ratios.

\* To whom correspondence should be addressed.

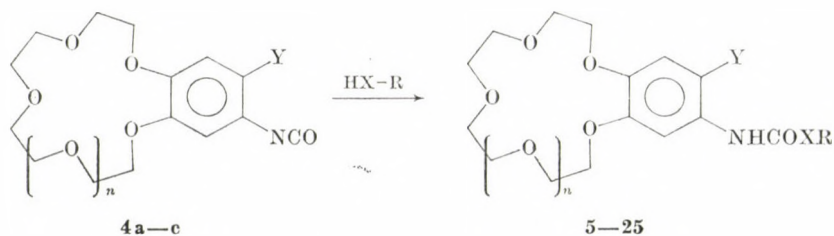
\*\* Instead of Pd/C in DMF, described in the literature, we used Raney-Ni in MeOH-H<sub>2</sub>O solvent.



4	n	Y	%	M.p. (B.p.), °C	IR $\nu_{\text{N}=\text{C}=\text{O}}$ , $\text{cm}^{-1}$	$M^+$	(%)
a	1	H	87.0	150—152/0.1	2280	309	(35)
b	2	H	87.4	168—180/0.1	2290	353	(3.7)
c	1	NO <sub>2</sub>	94.0	116 (petroleum spirit)	2270	354	(32)

The pure products were obtained after recrystallization in yields of 90—93%. In the preparation of the urethans **16—25** a few drops of triethylamine catalyst was used.

All new compounds have been identified by correct elemental analysis and spectral data. The IR spectra have two very intense bands at 1230—1220  $\text{cm}^{-1}$  (C—O—C<sub>as</sub>) and 1130—1115  $\text{cm}^{-1}$  (C—O—C<sub>s</sub>), characteristic of the polyether ring. For the derivatives containing NO<sub>2</sub> group, the corresponding regions are 1280—1220  $\text{cm}^{-1}$  and 1170—1110  $\text{cm}^{-1}$ . In the spectra of the



	n	Y	X-R	M.p., °C	IR $\nu_{\text{N-C-X}}$ , $\text{cm}^{-1}$ $\parallel$ O
5	1	H	NH-CH <sub>2</sub> CH <sub>2</sub> CHPh <sub>2</sub>	125	1660*/1630
6	2	H	NH-CH <sub>2</sub> CH <sub>2</sub> CHPh <sub>2</sub>	129	1680*/1635
7	1	NO <sub>2</sub>	NH-CH <sub>2</sub> CH <sub>2</sub> CHPh <sub>2</sub>	185	1695 /1640*
8	1	H	NH-CH <sub>2</sub> CH <sub>2</sub> C <sub>6</sub> H <sub>3</sub> (OCH <sub>3</sub> ) <sub>2</sub> -3,4	152	1680*/1640
9	2	H	NH-CH <sub>2</sub> CH <sub>2</sub> C <sub>6</sub> H <sub>3</sub> (OCH <sub>3</sub> ) <sub>2</sub> -3,4	148	1670*/1630
10	1	NO <sub>2</sub>	NH-CH <sub>2</sub> CH <sub>2</sub> C <sub>6</sub> H <sub>3</sub> (OCH <sub>3</sub> ) <sub>2</sub> 3,4	165	1695 /1640*
11	1	H	NH-CH <sub>2</sub> -CH <sub>2</sub> -N	130	1640
12	1	H	NH-CH <sub>2</sub> -CH <sub>2</sub> -N	117	1640
13	1	H	NH-CH <sub>2</sub> CH <sub>2</sub> N[CH(CH <sub>3</sub> ) <sub>2</sub> ] <sub>2</sub>	88	1640
14	1	H	NH-CH <sub>2</sub> CH <sub>2</sub> -OH	122	1635
15	2	H	NH-CH <sub>2</sub> CH <sub>3</sub>	78	1640
16	1	H	OCH <sub>3</sub>	128	1720 /1700*
17	2	H	OCH <sub>3</sub>	83	1720 /1700*
18	1	NO <sub>2</sub>	OCH <sub>3</sub>	147	1740 /1725*
19	1	H	OCH(CH <sub>3</sub> ) <sub>2</sub>	139	1700*/1685
20	2	H	OCH(CH <sub>3</sub> ) <sub>2</sub>	104	1690
21	1	NO <sub>2</sub>	OCH(CH <sub>3</sub> ) <sub>2</sub>	138	1720
22	1	H	O-CH <sub>2</sub> -CH <sub>2</sub> -N	83	1685
23	1	H	OCH <sub>2</sub> CH <sub>2</sub> N(CH <sub>2</sub> CH <sub>3</sub> ) <sub>2</sub>	75	1685
24	1	H	OCH <sub>2</sub> CH <sub>2</sub> OCH <sub>2</sub> CH <sub>2</sub> N(CH <sub>2</sub> CH <sub>3</sub> ) <sub>2</sub>	69	1690
25	1	H	OCH <sub>2</sub> CH <sub>2</sub> OCH <sub>2</sub> CH <sub>2</sub> OCH <sub>3</sub>	53	1690

\* Shoulder

urethans **16**–**25** the respective pair of bands can be recognized at 1195–1180  $\text{cm}^{-1}$  and 1110–1090  $\text{cm}^{-1}$ . The  $\nu\text{CO}$  bonds of the ureas **5**–**15** appear at 1630–1690  $\text{cm}^{-1}$ , while those of the urethans at 1685–1740  $\text{cm}^{-1}$ , mostly with shoulder. In the  $^1\text{H}$ –NMR spectra the  $\text{O}-\text{CH}_2$  groups of the ring and the chain exhibit a broad multiplet at  $\delta = 3.4$ – $4.5$  ppm. Only the signals of  $\text{CH}_2$  groups attached to nitrogen atom can be distinguished in the spectra of the ureas **5**–**15** at 2.8–3.2 ppm.

The complex stability constants were measured in alcohol and, as expected, the magnitudes were found to be independent of the side chain. The  $\log K$  values for  $\text{Na}^+$  ion were found to be 3.4–4.2, depending on the number of the ring members. Unfortunately, none of the compounds had any selectivity in the complexation of alkaline and alkaline earth metal cations. Since bis-crown compounds have been reported to exhibit increased selectivity [6], we decided to prepare carbonic acid derivatives of that type. This will be the subject of a forthcoming paper.

\*

Support of this research by the Chinoin Pharmaceutical and Chemical Works is gratefully acknowledged.

#### REFERENCES

- [1] VÖGTLE, F., WEBER, E., ELBEN, V.: Kontakte, **1978**, and **1979**, 1
- [2] BERNARD, D., LEHN, J. M., SAUVAGE, J. P.: Chemie in unserer Zeit, **7**, 120 (1973)
- [3] PEDERSEN, C. J.: J. Am. Chem. Soc., **89**, 7017 (1967)
- [4] UNGARO, R., EL HAJ, B., SMID, J.: J. Am. Chem. Soc., **98**, 5198 (1976)
- [5] KIKUKAWA, K., NAGIRA, K., MATSUDA, T.: Bull. Chem. Soc. Jpn., **50**, 2207 (1977)
- [6] KIMURA, K., MAEDA, T., SHONO, T.: J. Electroanal. Chem., **95**, 91 (1979)

Béla ÁGAI	}	H-1111 Budapest, Műgyetem rkp. 3.
István BITTER		
Éva CSONGOR		
László TÓKE		

## MODIFIED CROWN ETHERS, II<sup>+</sup>

### CARBONIC ACID DERIVATIVES OF BIS-CROWN ETHERS (PRELIMINARY COMMUNICATION)

B. ÁGAI, I. BITTER, É. CSONGOR and L. TÓKE\*

(Department of Organic Chemical Technology, Technical University, Budapest)

Received December 19, 1981

Accepted for publication February 13, 1982

In our previous paper [1] we reported on the preparation of urethan and urea derivatives containing one crown ether unit. These compounds can advantageously be used for effecting  $\text{Na}^+$ ,  $\text{K}^+$  ion transport through artificial and biological membranes.\*\* Owing to the lack of selectivity of complexation, however, the compounds are not suitable ligands for membranes of ion-selective electrodes. Recently, bis-benzo-15-crown-5 [2] and 12-crown-4 derivatives [3] have been reported to exhibit selective complexation of  $\text{K}^+$  and  $\text{Na}^+$  ions, respectively. In these ligands the two crown units are linked with a flexible chain so that the optimal conformation can be achieved during complexation. SMID *et al.* have found [4] that the stability constant of bis [3,4-(1', 4', 7', 10', 13'-pentaoxacyclopentadeca-2-ene)-phenylcarboxy] ether in THF for potassium picrate is much greater than that of the corresponding monocyclic benzo-15-crown-5 derivative. Japanese researchers have published the synthesis of bis-crown ethers containing amide and ester moieties in the chain and their application as ligands of membranes in ion-selective electrodes [5].

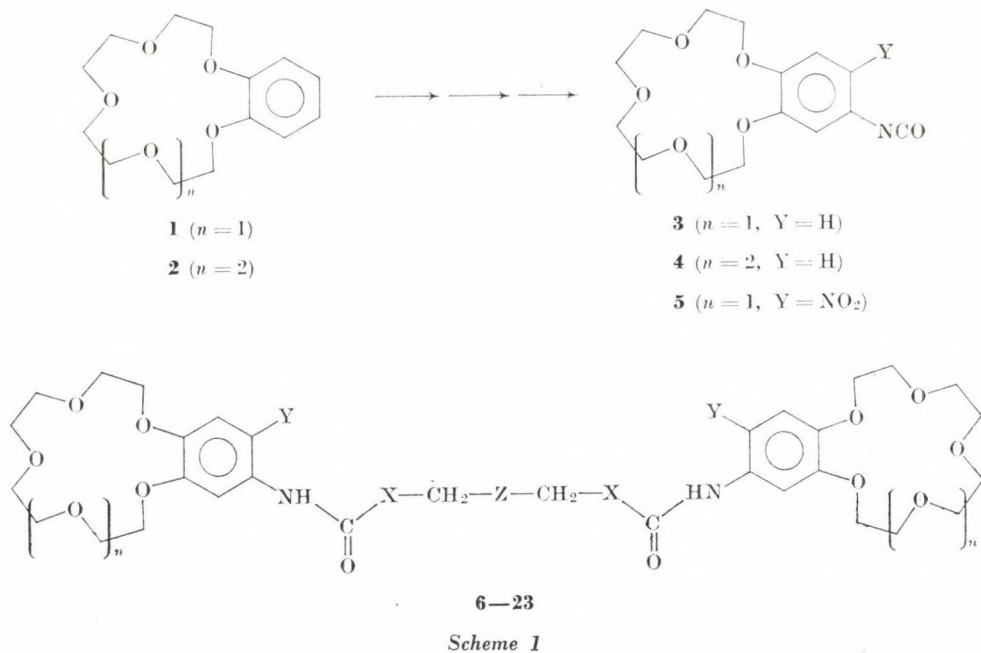
We supposed that the complexing ability and particularly the selectivity of bis-crown ethers should depend on the length, the number and quality of the heteroatoms and on the steric orientation of the chain linking the crown units. Besides these factors we wanted to investigate the effect of substituents in the aromatic ring, which may influence the selectivity of complexation by fixing a unique conformation in the complex by means of strong intramolecular hydrogen bonds. For this purpose the nitro group in *ortho* position to the chain seemed to be suitable.

+ For Part I, see Ref. [1]

\* To whom correspondence should be addressed

\*\* Measurements have been carried out in a Sartorius apparatus using an artificial stomach wall membrane. We measured the rate of sodium dinitrophenolate (DNP) transport in water in the presence of crown ether urethans and ureas. DNP concentrations on both sides of the membrane were measured by UV spectroscopy.

The crown ether isocyanates **3**, **4**, **5**, prepared by the phosgenation of the corresponding amines [1], proved to be excellent starting materials, because they add bifunctional alcohols and amines very readily, affording the urethans and ureas **6—23** (Scheme 1). The  $\alpha,\omega$ -diamines or glycols were allowed to react with two equivalents of crown isocyanate in dioxane or chloroform at ambient temperature (with glycols, triethylamine catalyst was used).

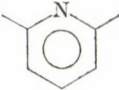
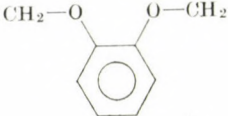
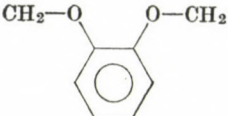


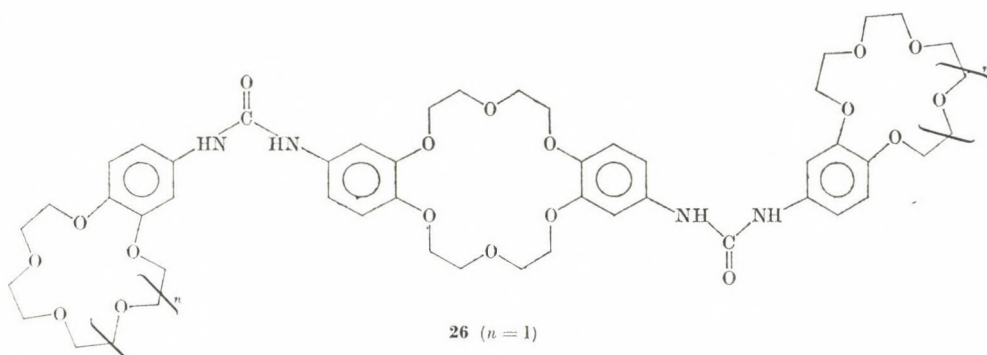
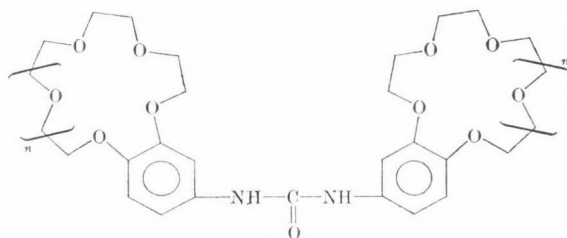
Yields are 60—80%. According to POPOVA's method [6], we have prepared *trans*-4,4'-diaminodibenzo-18-crown-6 and treated it with the isocyanates **3** and **5** to obtain the tris-crown ethers **26** and **27** (Scheme 2).

All compounds were characterized by correct elemental analysis, IR, UV and  $^1\text{H}$ -NMR spectroscopic data.\* The latter are in accordance with those of the similar mono-crown ether derivatives [1]. Electrochemical measurements have been carried out in order to establish the selectivities of these compounds for a number of cations. Details will be reported elsewhere; here we mention that compounds **17**, among the other nitro derivatives, exhibits

\* IR(KBr): urea 1620/1680 sh (**6**, **8**, **10**); 1690 (**7**, **9**) urethan 1735 (**11**, **14**, **17**); 1715/1690 sh (**12**, **13**, **15**, **16**, **18—21**)

$^1\text{H}$ -NMR (60 MHz,  $\text{CDCl}_3$ , TMS):  $\text{NO}_2$  derivatives Ar—H-3  $\delta$ (ppm) 8.0—8.1 s, Ar—H-6 7.6—7.7, s; derivatives without  $\text{NO}_2$  Ar—H-3  $\delta$ (ppm) 7.1—7.2 d; Ar—H-5,6 6.7—6.8 dd; O— $\text{CH}_2$  3.5—4.5 m.

	Y	n	X	Z	M.p °C
6	H	1	CH <sub>2</sub>	CH <sub>2</sub>	183
7	NO <sub>2</sub>	1	NH	CH <sub>2</sub>	235
8	H	1	NH	(CH <sub>2</sub> ) <sub>4</sub>	180
9	NO <sub>2</sub>	1	NH	(CH <sub>2</sub> ) <sub>4</sub>	230
10	H	1	NH	(CH <sub>2</sub> -O-CH <sub>2</sub> ) <sub>2</sub>	134
11	NO <sub>2</sub>	1	O	—	172
12	H	2	O	—	132
13	H	1	O	CH <sub>2</sub> -O-CH <sub>2</sub>	84
14	NO <sub>2</sub>	1	O	CH <sub>2</sub> -O-CH <sub>2</sub>	120
15	H	2	O	CH <sub>2</sub> -O-CH <sub>2</sub>	64
16	H	1	O	CH <sub>2</sub> -S-CH <sub>2</sub>	135
17	NO <sub>2</sub>	1	O	CH <sub>2</sub> -S-CH <sub>2</sub>	100
18	H	2	O	CH <sub>2</sub> -S-CH <sub>2</sub>	87
19	H	1	O		134
20	H	1	O		150
21	H	2	O		109
22	NO <sub>2</sub>	1	O		119
23	NO <sub>2</sub>	1	O		192

26 ( $n = 1$ )27 ( $n = 2$ )24 ( $n = 1$ )25 ( $n = 2$ )

Scheme 2

very remarkable  $K^+$ -ion selectivity  $\left(\log \frac{K_{Na^+}}{K_{K^+}} = -3.0\right)$ . This value is of the same order of magnitude as that of valinomycin  $\left(\log \frac{K_{Na^+}}{K_{K^+}} = -3.4\right)$ , but our ligand is more selective towards  $NH_4^+$ ,  $Rb^+$  and  $Cs^+$  ions. The lack of the nitro group (e.g. **16**) dramatically decreased the selectivity. These observations support our hypothesis on the important role of the nitro group in the formation of selective complexes.

\*

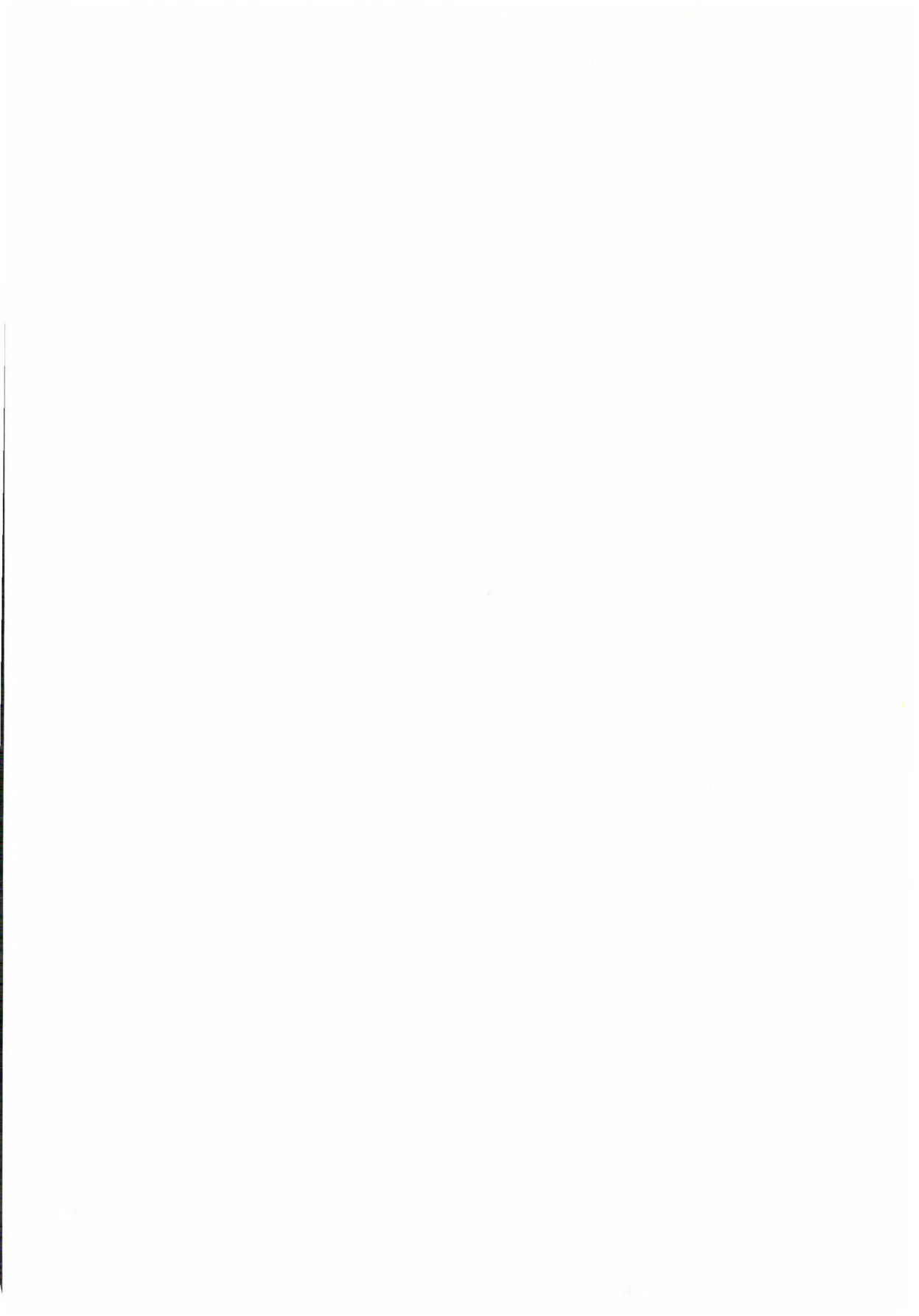
Support of this research by the Chinoin Pharmaceutical and Chemical Works is gratefully acknowledged.

## REFERENCES

- [1] ÁGAI, B., BITTER, I., CSONGOR, É., TÓKE, L.: Acta Chim. Acad. Sci. Hung. (In the press)  
[2] WADA, F., WADA, Y., GOTO, T., KIKUKAWA, K.: Chemistry Letters, **1980**, 1189  
[3] IKEDA, I., KATAYAMA, T., OKAHARA, M., SHONO, T.: Tetrahedron Lett., **1981**, 3651  
[4] BOURGOIN, M., WONG, K. H., HUI, L. Y., SMID, I.: J. Am. Chem. Soc., **97**, 3462 (1975)  
[5] KIMURA, K., MAEDA, T., TAMURA, H., SHONO, T.: J. Electroanal. Chem., **95**, 91 (1979)  
[6] POPOVA, V. A., PODGORNYAYA, I. V., POSTOVSKII, I. Y., FROLOVA, N. N.: Khim. Pharm., **10**, 66 (1976)

Béla ÁGAI  
István BITTER  
Éva CSONGOR  
László TÓKE

} H-1111 Budapest, Műegyetem rkp. 3.



## SYNTHESIS OF *N*<sup>1</sup>-ISONICOTINOYL-3,5-DIPHENYL-4-(SULFAMOYLPHENYLAZO)-1,2-DIAZOLES AS ANTIMALARIAL AGENTS

C. P. SINGH

*(Chemical Laboratories, Sahu Jain College, Najibabad-246763 U. P. India)*

Received February 23, 1981  
Accepted for publication May 1, 1981

A series of *N*<sup>1</sup>-isonicotinoyl-3,5-diphenyl-4-(sulfamoylphenylazo)-1,2-diazoles have been synthesized by the condensation of sulfamoylphenylazo-1,3-diphenyl-1,3-propanedione with isonicotinic acid hydrazide, using glacial acetic acid as the condensing agent. Some of the products showed significant antimalarial activity against *Plasmodium berghei* KBG 173 in swiss mice.

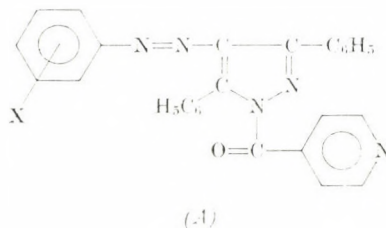
### Introduction

A survey of the literature reveals that diazole derivatives possess various types of biological activities, *viz.*, potential antituberculous [1], antineoplastic [2], antidiabetic [3], antifertility [4], antirheumatic, anti-inflammatory, analgetic, antipyretic, adrenolytic, narcosis-potentiating [5] and antitumor [6, 7] actions, *etc.* Isonicotinic acid hydrazide (INH) is used as an antituberculous [8] and antitumor [9] agent. In view of these observations, it was thought desirable to synthesize some new diazole derivatives having the sulfonamide moiety attached through an azo linkage at position 4 and an isonicotinoyl moiety at position 1 in the hope that the resulting compounds may prove to possess valuable pharmacological properties.

The present communication describes the synthesis of *N*<sup>1</sup>-isonicotinoyl-3,5-diphenyl-4-(sulfamoylphenylazo)-1,2-diazoles of type (A) by the condensation of sulfamoylphenylazo-1,3-diphenyl-1,3-propanediones [10] with INH, using glacial acetic acid as the condensing agent, and the study of the biological activity of the products. The homogeneity and purity of the compounds were checked by TLC and their structures established by IR, NMR spectral studies and elemental analyses (Scheme 1).

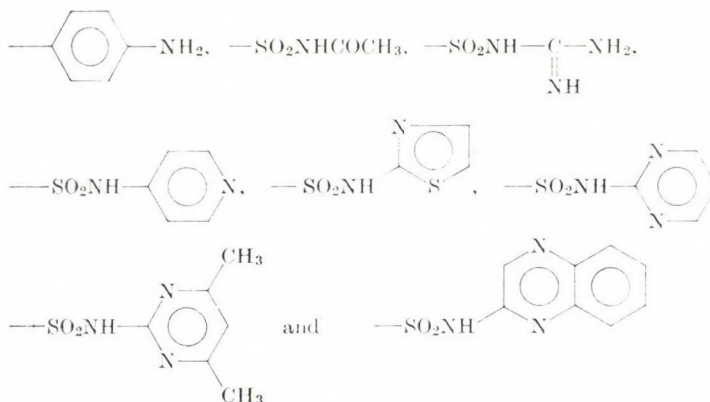
### Experimental

All the chemicals used were either BDH or E. Merck products of Analar grade, except INH (C. C. P. Najibabad).



where:

X = -Cl, -Br, -F, -NO<sub>2</sub>, -CH<sub>3</sub>, -OCH<sub>3</sub>, -CO<sub>2</sub>H,



Scheme 1

#### Synthesis of *N*<sup>1</sup>-isonicotinoyl-3,5-diphenyl-4-(X)-azo-1,2-diazoles

A mixture of the appropriate sulfamoylphenylazo-1,3-diphenyl-1,3-propanedione (0.1 g) and isonicotinic acid hydrazide (0.5 g) in glacial acetic acid was refluxed on an oil bath at 160–170 °C for 6 h and then allowed to stand overnight. The coloured compound which separated was filtered off, washed well with water, dried and recrystallized from a mixture of glacial acetic acid and DMF.

By analogous procedures, several substituted 1,2-diazoles have been synthesized, their characteristics are recorded in Table I. The yields were between 70 and 80%.

#### IR and NMR spectra

IR spectra in KBr were recorded on a Perkin-Elmer grating IR spectrophotometer. The spectra had characteristic peaks at 780 cm<sup>-1</sup> (aromatic ring), 1580 cm<sup>-1</sup> (-N=N-) 1600 cm<sup>-1</sup> (C=N); 1740 cm<sup>-1</sup> (C=O of *tert.* amide having N in diazole ring) which helped in establishing the structures of the compounds.

The structures of the substituted diazoles were also confirmed by <sup>1</sup>H-NMR spectra studies. In CDCl<sub>3</sub> solution, the following δ (ppm) values were obtained: 7.47–7.50 (2s, 10, -C(C<sub>6</sub>H<sub>5</sub>)<sub>2</sub>); 7.35 (dd, 2, meta to -N=N-C<sub>6</sub>H<sub>4</sub>X, J = 6 Hz); 7.12 (dd, 2, 4-pyridinecarbonyl, *ortho* to C=O, J = 9 and 2 Hz); 7.93 (dd, 2, *ortho* to X, J = 9 and 3 Hz); 8.04 (dd, 2, 4-pyridinecarbonyl, *meta* to C=O, J = 9 and 2 Hz).

Where X = substituent group.

**Table I**  
 Characteristics of  $N^1$ -isonicotinoyl-3,5-diphenyl-4-(X)azo-1,2-diazoles

S	X	M.P.°C	Colour	Molecular formula	Nitrogen		$R_f$ Value
					Found	Calcd.	
1	2	3	4	5	6	7	8
1.	Phenyl	146	dark yellow	$C_{27}H_{19}N_5O$	16.29	16.31	0.8457
2.	2-Chlorophenyl	165	pale yellow	$C_{27}H_{18}N_5OCl$	15.10	15.12	0.7079
3.	3-Chlorophenyl	203	light brown	$C_{27}H_{18}N_5OCl$	15.10	15.12	0.6954
4.	4-Chlorophenyl	156	brown	$C_{27}H_{18}N_5OCl$	15.09	15.12	0.7234
5.	4-Bromophenyl	245	dark yellow	$C_{27}H_{18}N_5OBr$	13.76	13.78	0.7534
6.	2,4,6-Tribromophenyl	249	yellow	$C_{27}H_{16}N_5OBr_3$	10.47	10.51	0.9856
7.	3-Fluorophenyl	289	pale yellow	$C_{27}H_{18}N_5OF$	15.63	15.66	0.8499
8.	2-Chloro-4-nitrophenyl	211	pale yellow	$C_{27}H_{17}N_6O_3Cl$	16.51	16.54	0.5683
9.	2-Nitrophenyl	274	light yellow	$C_{27}H_{18}N_6O_3$	17.63	17.72	0.7943
10.	3-Nitrophenyl	267	brown	$C_{27}H_{18}N_6O_3$	17.69	17.72	0.8682
11.	2-Methylphenyl	133	pale yellow needles	$C_{28}H_{21}N_5O$	15.78	15.81	0.9160
12.	4-Methylphenyl	173	white needles	$C_{28}H_{21}N_5O$	15.79	15.81	0.9237
13.	2-Methoxyphenyl	221	pale yellow	$C_{28}H_{21}N_5O_2$	15.21	15.25	0.8360
14.	4-Methoxyphenyl	188	dark brown	$C_{28}H_{21}N_5O_2$	15.21	15.25	0.8860
15.	4-Aminodiphenyl	265	dark yellow	$C_{23}H_{24}N_6O$	16.14	16.15	0.8239
16.	1-Naphthyl	240	red	$C_{31}H_{21}N_5O$	14.59	14.62	0.5909
17.	2-Naphthyl	235	yellow needles	$C_{31}H_{21}N_5O$	14.56	14.62	0.5448
18.	4-Carboxyphenyl	275	dark yellow	$C_{28}H_{19}N_5O_3$	14.78	14.80	0.7665
19.	4-Hydroxyphenyl	199	pale yellow	$C_{27}H_{19}N_5O_2$	15.69	15.73	0.7099
20.	2,3-Dimethyl-1-phenylpyrazolone	282	brown	$C_{32}H_{25}N_7O_2$	18.15	18.18	0.8091
21.	2-Sulfonamidobenzene	191	dark yellow	$C_{27}H_{20}N_6O_3S$	16.52	16.54	0.5023
22.	$N^1$ -2-pyridylsulfonamidobenzene	285	dark yellow	$C_{32}H_{23}N_7O_3S$	16.70	16.75	0.6988
23.	$N^1$ -2-pyrimidylsulfonamidobenzene	262	red	$C_{31}H_{22}N_8O_3S$	19.07	19.11	0.5838
24.	$N^1$ -2-thiazolylsulfonamidobenzene	215	pale yellow needles	$C_{30}H_{21}N_7O_3S_2$	16.51	16.58	0.9084
25.	$N^1$ -2-guanylsulfonamidobenzene	295	pale yellow	$C_{28}H_{22}N_8O_3S$	20.31	20.36	0.6284
26.	$N^1$ -2(4,6-dimethyl)pyrimidylsulfonamidobenzene	321	pale yellow	$C_{33}H_{26}N_8O_3S$	18.21	18.24	0.4511
27.	$N^1$ -2-acetylsulfonamidobenzene	278	brown	$C_{29}H_{22}N_6O_4S$	15.21	15.27	0.6924

### Biological assay

All compounds were screened for their antimalarial activity against *Plasmodium berghei* KBG 173 malaria in Swiss mice by the OSDENE and RUSSELL method [11]. Some of the products, namely, *N*<sup>1</sup>-isonicotinoyl-3,5-diphenyl-4-(*N*<sup>1</sup>-sulfonamidobenzeneazo)-, -4-(*N*<sup>1</sup>-2-thiazolylsulfonamidobenzeneazo)-, -4-(*N*<sup>1</sup>-2-pyrimidylsulfonamidobenzeneazo)-, -4-(*N*<sup>1</sup>-2-(4,6-dimethyl)-pyrimidylsulfonamidobenzeneazo)-, and 4-(*N*<sup>1</sup>-2-pyridylsulfonamidobenzeneazo)-1,2-diazoles showed significant antimalarial activity.

\*

The author wishes to express their cordial thanks to the Sahu Jain College, Najibabad for laboratory facilities and to Dr. Shyam SINGH, CDRI, Lucknow for spectral data and elemental analyses.

The author is also indebted to Dr. T. R. SWEENEY, Director, W. A. R. I., Washington (D. C.), for testing the compounds as antimalarial agents and to CSIR, New Delhi, for financial assistance.

### REFERENCES

- [1] BEHNISCHI, R., MIETZCH, F., SCHMIDT, H.: *Am. Rev. Tuber.*, **61**, 1 (1950)
- [2] GARG, H. G., SHARMA, R. A.: *J. Pharm. Sci.*, **59**, 350 (1970)
- [3] GARG, H. G., SINGH, P. P.: *J. Med. Chem.*, **13**, 1250 (1970)
- [4] TIWARI, S. S., SHARMA, A.: *J. Indian Chem. Soc.*, **52**, 153 (1975)
- [5] JUCKER, E., LINDEMANN, A. J., RISSI, E.: *U. S. Pat.*, **342**, 3041 (1962)
- [6] WILSON, W., BOTTIGLIERE, N.: *Cancer Chemotherapy*, **21**, 137 (1962)
- [7] NOELL, C. W., CHENG, C. C.: *J. Med. Chem.*, **12**, 545 (1969)
- [8] *Dictionary of Organic Compounds*, Vol. 5, p. 2317 Oxford, New York, 1965
- [9] WOODBURG, E. C., KOPPAKA, V.: *Cancer Chemotherapy Rept.*, **6**, 58 (1974)
- [10] SINGH, C. P.: Ph. D. Thesis, "Synthesis and Studies of 1,2-Diazoles and Diazolones", Rohilkhand University, Bareilly, 1980
- [11] OSDENE, T. S., RUSSELL, P. B., RANE, L.: *J. Med. Chem.*, **10**, 431 (1967)

C. P. SINGH Chemical Laboratories, Sahu Jain College, Najibabad-246763  
(U. P.) India

## MOLECULAR DECOMPOSITION REACTIONS OF DIALKYL ETHERS

### THE ESTIMATION OF PREEXPONENTIAL FACTORS

L. SERES

(*Institute of General and Physical Chemistry, A. József University, Szeged*)

Received January 19, 1981  
In revised form April 27, 1981  
Accepted for publication May 14, 1981

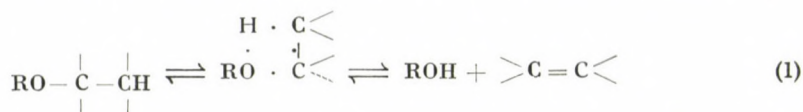
Calculations based on statistical thermodynamic methods have been performed to estimate the preexponential factors of four-center molecular elimination reactions of dialkyl ethers. The changes in overall symmetry, the number of optical isomers, the three main moments of inertia and the hindered internal rotations frozen in the activation process make comparable contributions to the activation entropy. Thus neglect of the role of the change in overall rotation can only be justified in the differential method of estimation of activation entropies when the structure of the activated complex is tight.

Calculations were made for the following ethers (in parentheses are the  $\lg(A_{800}/s^{-1})$  values): methyl ethyl ether (12.6), methyl isobutyl ether (11.7), methyl *tert*-butyl ether (13.6), diethyl ether (13.2), di-*n*-propyl ether (12.4), di-*n*-butyl ether (12.1). The estimated preexponential factors are in reasonable agreement with the data available in the literature.

### Introduction

The thermal decompositions of dialkyl ethers are complicated processes characterized by the competition of radical and molecular reactions [1–3]. Modelling of the reaction systems is a major method in the establishment of the relative kinetic roles of the competing processes and in the elucidation of the possible mechanisms of the reactions. To set up a model, the rate constants of the elementary reactions of the assumed mechanism, if possible, characterized by the Arrhenius parameters, must be known. Since only a limited number of rate constants are available for the elementary reactions involved in the mechanisms of dialkyl ether decompositions, studies to estimate the Arrhenius parameters are of importance.

The thermochemical calculations outlined below are aimed at obtaining the estimated activation entropies ( $\Delta S_T^{\circ\ddagger}$ ) and, consequently, the preexponential factors of the reactions characterized by the general equation



for the customary temperatures of thermal decompositions.

The preexponential factors of unimolecular reactions are generally estimated *via* transition-state theory by a differential method (see *e.g.* [4, 5]). In the application of the method the rotational entropy change ( $\Delta S_{\text{rot}}^{\circ\ddagger}$ ) is usually left out of consideration, since the latter is normally negligible for small molecules [6, 7]. Since the molecules studied here are of considerable size and the products of the three principal moments of inertia increase considerably in the activation process, the omission of  $\Delta S_{\text{rot}}^{\circ\ddagger}$  results in an error no longer negligible. To avoid this source of error, the overall entropies of the models of the reactant molecules and activated complexes were calculated. This procedure made it possible to check the probable errors of the calculations by comparison of the calculated and experimental data for the molecules.

### Calculation of $\Delta S_T^{\circ\ddagger}$ by a statistical mechanical method\*

It has been shown by BENSON [4] that  $S^\circ$  and  $C_{p,T}^\circ$  can be estimated with sufficient precision using characteristic frequencies for the individual internal degrees of freedom, provided the pertinent molecular structure data needed in the calculation of the contributions of other degrees of freedom are known. The reliability of the estimation is enhanced by the fact that the contributions of vibrational degrees of freedom are relatively small in molecules not involving hindered internal rotations.

The  $S^\circ$  and  $C_{p,T}^\circ$  functions of hindered internal rotations can also be calculated with high precision, provided the rotors are symmetrical and the frame they are attached to is rigid.

Although theoretically unjustified, reliable estimations have also been made for asymmetric, rigid rotors using the equations valid for symmetrical rigid rotors [4].

In the case of molecules containing non-rigid rotors, the calculation of  $S^\circ$  and  $C_{p,T}^\circ$  for the rotors is theoretically unfounded. If the calculation is made by using the equations valid for rigid rotors, the thermodynamic functions are overestimated, since the reduced moment of inertia is also overestimated. The difference is not important in most cases, however. In the present paper the  $S^\circ$  and  $C_{p,T}^\circ$  functions of hindered rotors are also calculated for rotors having a loose structure, by using the equations valid for symmetrical, rigid, coaxial rotors. The method applied gives results with errors not exceeding  $\pm 1 \text{ cal mol}^{-1} \text{ K}^{-1}$ .

The preexponential factor of a unimolecular rate constant can be calculated from the activation entropy [4, 8] *via* the equation

\* Units of  $S^\circ$  and  $C_p^\circ$  are:  $\text{cal mol}^{-1} \text{ K}^{-1}$  (e.u.);  $1 \text{ cal} = 4.184 \text{ J}$ .

$$A = \frac{ekT}{h} \frac{l^\ddagger \sigma^\ddagger n}{\sigma n^\ddagger} e^{\Delta S_T^{\circ\ddagger}/R} \quad (2)$$

( $l^\ddagger$  is the reaction path degeneracy,  $\sigma^\ddagger$  and  $\sigma$  are the overall symmetry numbers, while  $n^\ddagger$  and  $n$  are the numbers of optical isomers of the activated complex and the reactant molecule, respectively).

$\Delta S_T^{\circ\ddagger}$  was estimated by using identical calculation procedures for the activated complexes and the reactant molecules. The translational entropy change is zero; however, important changes occur in the vibrational entropy, the entropies of external and internal rotations, the symmetry and the number of optical isomers.

In the calculations made for the molecules, some of the rotational barriers of the heavier rotations have been changed slightly to obtain a better agreement between experimental and calculated overall entropies and molar heat capacities [1, 13]. Although this procedure may result in sizeable errors in the calculation of the contributions of individual rotors, it is suitable for the calculation of the sum of the contributions of heavy rotors. Since the degrees of freedom of the rotors in the  $\alpha$  and  $\beta$  positions to the ether oxygen are changed in the activation process, even a considerable error in the calculated contributions of the individual rotors is expected to give merely a negligible error in  $\Delta S_T^{\circ\ddagger}$ , because in all the ethers considered here (with the exception of DNBE) heavy rotors are only present in the  $\alpha$  and  $\beta$  positions to the ether oxygens. In the alkyl group not involved in the activation process, the change in the contribution of the rotor in the  $\alpha$  position to the ether oxygen is small and can be estimated with reasonable precision.

The accuracy of the estimation of  $\Delta S_T^{\circ\ddagger}$  depends upon the fulfilment of the following assumptions:

a) Using the characteristic frequencies given by BENSON instead of the actual values, no major error is committed.

b) Application of the equations valid for symmetrical, coaxial, rigid rotors for the calculation of the contributions of non-coaxial, asymmetric, loose rotors of molecules and activated complexes gives a good approximation, or at least the errors committed are compensated in the calculation of  $\Delta S_T^{\circ\ddagger}$ . The models chosen are correct; the calculated quantities do not depend much on the bond distances and angles assigned.

The fulfilment of the above conditions is illustrated in the cases of the ether molecules, where the agreement between the calculated and experimental data is reasonable (see below). Hopefully, calculations of the  $S^\circ$  and  $C_{p,T}^\circ$  functions of the models describing the activated complexes give results of similar accuracy.

The contributions of translational, rotational and vibrational degrees of freedom were calculated by using the following equations of statistical mechan-

ics [9]:

$$S_{\text{tr}}^{\circ} = R(1.5 \ln M + 2.5 \ln T) - 2.315, \quad (3)$$

$$C_{p,\text{tr}}^{\circ} = 2.5 R, \quad (4)$$

$$S_{\text{rot}}^{\circ} = 2.2878 \lg(I_A I_B I_C 10^{120}) + 6.8634 \lg T - 4.5756 \lg \sigma_{\text{ex}} - 6.8966, \quad (5)$$

$$C_{p,\text{rot}}^{\circ} = 1.5 R, \quad (6)$$

$$S_{\text{vib}}^{\circ} = R \left[ \frac{U}{eU-1} - \ln(1 - eU) \right], \text{ and} \quad (7)$$

$$C_{p,\text{vib}}^{\circ} = \frac{RU^2 eU}{(eU-1)^2} \quad (8)$$

where  $M$  is the molecular mass,  $R$  is the molar gas constant ( $1.987 \text{ cal mol}^{-1} \text{ K}^{-1}$ ),  $I_A I_B I_C$  is the product of the three main moments of inertia,  $\sigma_{\text{ex}}$  is the external symmetry number and  $U = h\nu/kT$ . The product  $I_A I_B I_C$  was calculated by the method of HIRSCHFELDER from the masses and the CARTESIAN coordinates of the atoms [10]. The bond distances and bond angles were the average values suggested for dimethyl ether and paraffins:  $r(\text{C}-\text{H}) = 109.4$ ,  $r(\text{C}-\text{O}) = 141.6$ ,  $r(\text{C}-\text{C}) = 153.7 \text{ pm}$ ;  $\angle(\text{COC}) = 3.897$ ,  $\angle(\text{HCC}) = 3.823$ ,  $\angle(\text{CCC}) = 3.821 \text{ rad}$  [11].

For the calculation of the  $S^{\circ}$  and  $C_{p,T}^{\circ}$  functions of internal rotations, the rotational barriers were taken from the literature or estimated. Corrections were made in the rotational barriers of some heavy rotors, but these never exceeded  $0.5 \text{ kcal mol}^{-1}$ . The calculations were performed with a digital computer [12].

The assumptions made regarding the structure of the activated complex, and the calculations performed, are illustrated on the example of DEE (Table I).

In the molecular decomposition of DEE, a four-membered activated complex is formed [Eq. (1)].

Rotation around the C-C and C-O bonds involved in the reaction is hindered by interaction between the ether oxygen and the hydrogen atom of one of the methyl groups.

The decomposition of internal degrees of freedom into normal coordinates was performed according to standard procedures [4]. Characteristic frequencies estimated on the basis of bond length — bond distance correlations (ref. [4], Table A 13) were used in the calculations. The missing frequencies were calculated *via* the equation

$$\frac{\bar{\nu}_1}{\bar{\nu}_2} = \sqrt{\frac{\mu_2}{\mu_1}}. \quad (9)$$

Table I

Estimation of the preexponential factor of molecular decomposition of diethyl ether\*

DEE				DEE <sup>‡</sup>			
Degrees of freedom	g <sup>**</sup>	$\bar{\nu}(\text{cm}^{-1})$	$S_{298}^{\circ}$	Degrees of freedom	g <sup>**</sup>	$\bar{\nu}/\text{cm}^{-1}$	$S_{298}^{\circ}$
<i>Bond stretches</i>				<i>Bond stretches</i>			
C—H	1	3100	0.00	C · H	1	2200	0.00
C—O	1	1100	0.06	O · H	1	2200	0.00
C—C	1	1100	0.09	C · O	1	r. c.	—
				C—C	1	1300	0.03
<i>Deformations</i>				<i>Deformations</i>			
(H—C—C) <sub>t,w</sub>	3	1150	0.16	H—C—C	3	800	0.62
(H—C—O) <sub>t,w</sub>	1	1150	0.05	H—C · O	1	800	0.21
H—C—H	2	1450	0.03	H · C—H	2	1100	0.12
C—O—C	1	400	0.96	C—O · C	1	280	1.53
C—C—O	1	400	0.96	C—C · O	1	280	1.53
(CH <sub>2</sub> ) <sub>r</sub>	1	700	0.31	H · O—C	1	800	0.21
				(C · O—C) <sub>o,p</sub>	1	170	2.44
<i>Hindered rotations</i>				<i>Hindered rotations</i>			
CH <sub>3</sub> $\diagdown$ CH <sub>2</sub> OEt	2		4.16	CH <sub>3</sub> $\diagdown$ CH <sub>2</sub> OEt <sup>‡</sup>	1		2.08
$V_0 = 3400 \text{ cal mol}^{-1}$				$V_0 = 3400 \text{ cal mol}^{-1}$			
$I_r = 5.2 \times 10^{-40} \text{ g cm}^2$				$I_r = 5.2 \times 10^{-40} \text{ g cm}^2$			
Et $\diagdown$ OEt	2		11.01	Et $\diagdown$ OEt <sup>‡</sup>	1		5.69
$V_0 = 5000 \text{ cal mol}^{-1}$				$V_0 = 5500 \text{ cal mol}^{-1}$			
$I_r = 3.3 \times 10^{-39} \text{ g cm}^2$				$I_r = 4.5 \times 10^{-39} \text{ g cm}^2$			
<i>Opt. isomers</i>				<i>Opt. isomers</i>			
$\Delta S_{\text{rot}}^{\circ \ddagger'}$			—	$R \ln 2$			1.38
			17.79				2.02
							17.86

$$\Delta S_{298}^{\circ \ddagger'} = 0.7; \Delta S_{800}^{\circ \ddagger'} = -0.75; A_{800} = 10^{13.2} \text{ s}^{-1}$$

$$* S^{\circ} = S^{\circ}/\text{cal mol}^{-1} \text{ K}^{-1}$$

\*\* Degeneration

The distances between atoms involved in the ring of the activated complex are  $r(\text{O} \cdot \text{H}) = 138$ ,  $r(\text{O} \cdot \text{C}) = 223$ ,  $r(\text{C} \cdot \text{C}) = 140$ ,  $r(\text{C} \cdot \text{H}) = 209$  pm,\* in agreement with those suggested in the literature [14]. The changing of the assumed bond angles within reasonable limits results in a negligible change in the computed  $S^{\circ}$  and  $C_p^{\circ}$  functions.

$$* r = r_0 + 80 \text{ pm, for the breaking bonds; } \langle \text{H} \cdot \text{O} \cdot \text{C} \rangle = 3.142 \text{ rad.}$$

In the calculations outlined above, the number of different atoms present in the molecule, the Cartesian coordinates of the atoms,  $\sigma_{\text{ex}}$ , and the characteristic frequencies of the normal internal degrees of freedom were used as input data. In the calculation of the contributions of hindered internal rotations, the reduced moments of inertia of the rotors, the rotational barriers and the symmetries of rotations served as input data. The errors caused by the overestimation of the  $S^\circ$  and  $C_{p,T}^\circ$  functions of the bulky loose rotors and by the application of the characteristic frequencies of the normal degrees of freedom are of comparable magnitude for the molecule and the activated complex (with the exception of the two rotors frozen in the activated complex). Hence, the error committed in the estimation of the activation entropy is considerably reduced.

In order to decrease the relative error caused by the assignment of the rotational barrier of the hindered internal rotations, identical barrier heights were assumed for identical rotors in similar positions.

## Results

An examination of the thermochemical feasibility of the molecular elimination in the chosen group of dialkyl ethers shows (Table II) that the free energy changes in these reactions are considerable in most cases. Since the similar reaction of dimethyl ether is unfavourable because of its large positive  $\Delta G^\circ$  value, the preexponential factor for this compound was not estimated.

With the calculation procedure outlined above, the entropies and molar heat capacities of the following dialkyl ethers and activated complexes formed from them were calculated: dimethyl ether (DME), methyl ethyl ether (MEE), methyl *n*-propyl ether (MNPE), methyl isopropyl ether (MIPE), methyl isobutyl ether (MIBE), diethyl ether (DEE), di-*n*-propyl ether (DNPE) and di-*n*-butyl ether (DNBE).

The rotational barriers assumed for the individual rotors on the basis of literature data [15] are listed in Tables III and IV for the molecules and activated complexes, respectively.

The calculated entropy and molar heat capacity contributions of the various degrees of freedom are shown in Tables V and VI. A comparison of the calculated and experimental data demonstrates the reliability of the calculations.

It is to be noted that the contributions of various methyl rotors in different ether molecules can be calculated with high precision for all the compounds studied. Since the calculation for the methyl rotors present in the activated complexes gives results of similar precision and (with the exception of a few rotors) only methyl rotors are present in these species, the sum of the

**Table II**  
*Examination of the thermochemical feasibilities of molecular eliminations\**

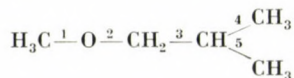
Ether	ROH	Olefin	$\Delta H_{800}^{\circ'}$	$\Delta S_{800}^{\circ'}$	$\Delta G_{800}^{\circ'}$	$K_{c,800}$
Dimethyl ether (DME)**	CH <sub>3</sub> OH	: CH <sub>2</sub>	88.9	40.0	56.9	$4 \times 10^{-18}$
Methyl ethyl ether (MEE)	CH <sub>3</sub> OH	C <sub>2</sub> H <sub>4</sub>	15.5	34.3	-12.0	28
Methyl <i>n</i> -propyl ether (MNPE)	CH <sub>3</sub> OH	C <sub>3</sub> H <sub>6</sub>	12.6	35.7	-16.0	$3.5 \times 10^2$
Methyl isopropyl ether (MIPE)	CH <sub>3</sub> OH	C <sub>3</sub> H <sub>6</sub>	16.0	38.3	-14.7	$1.5 \times 10^2$
Methyl <i>t</i> -butyl ether (MTBE)	CH <sub>3</sub> OH	<i>i</i> -C <sub>4</sub> H <sub>8</sub>	16.7	41.0	-16.1	$3.9 \times 10^2$
Methyl isobutyl ether (MIBE)	CH <sub>3</sub> OH	<i>i</i> -C <sub>4</sub> H <sub>8</sub>	11.0	34.7	-16.8	$6.1 \times 10^2$
Diethyl ether (DEE)	C <sub>2</sub> H <sub>5</sub> OH	C <sub>2</sub> H <sub>4</sub>	16.1	37.1	-13.6	77
Di- <i>n</i> -propyl ether (DNPE)	C <sub>3</sub> H <sub>7</sub> OH	C <sub>3</sub> H <sub>6</sub>	12.2	38.3	-18.5	$1.7 \times 10^3$
Di- <i>n</i> -butyl ether (DNBE)	C <sub>4</sub> H <sub>9</sub> OH	1-C <sub>4</sub> H <sub>8</sub>	13.1	38.1	-17.4	$8.8 \times 10^2$

\*  $\Delta H_{800}^{\circ'} = \Delta H_{800}^{\circ}/\text{kcal mol}^{-1}$ ;  $\Delta S_{800}^{\circ'} = \Delta S_{800}^{\circ}/\text{e.u.}$ ;  $\Delta G_{800}^{\circ'} = \Delta G_{800}^{\circ}/\text{kcal mol}^{-1}$   
 \*\*  $\Delta G_{800}^{\circ'}$  estimated from  $\Delta H_{298}^{\circ}$  and  $\Delta S_{298}^{\circ}$

**Table III**  
*Calculation of thermodynamic functions of hindered internal rotations;  
 barriers to rotations and reduced moments of inertia for different ethers\**

	$V'_{0,1}$	$I'_{r,1}$	$V'_{0,2}$	$I'_{r,2}$	$V'_{0,3}$	$I'_{r,3}$	$V'_{0,4}$	$I'_{r,4}$	$V'_{0,5}$	$I'_{r,5}$
DME	2800	4.82								
MEE	3100	5.05	5000	26.8	3400	5.06				
MNPE	3100	5.25	5000	34.3	7200	37.6	3400	5.25		
MIPE	3400	5.23	5000	34.3	3600	5.20	3600	5.20		
MIBE	3100	5.27	5000	42.0	8000	55.3	3600	5.29	3600	5.29
MTBUE	3400	5.27	2500	38.4	4000	5.21	4000	5.25	4000	5.25
DEE	3400	5.24	5000	33.4						
DNPE	3400	5.31	5300	52.1	7200	75.8				
DNBE	3400	5.33	5300	56.1	7500	95.6	6500	184.4		

\*  $V'_{0,i} = V_{0,i}/\text{cal mol}^{-1}$ ;  $I'_{r,i} = I_{r,i}/10^{-40} \text{ g cm}^2$ ;  
 enumeration of hindered rotations, illustrated on the example of MIBE:



contributions of the rotors frozen in the activation process can also be estimated with reasonable precision.

As the data obtained are used for the calculation of  $\Delta S_T^{\circ+}$ , the error committed is further reduced, for the contributions of the degrees of freedom not involved in the activation process cancel out.

Table IV

Calculation of thermodynamic functions of hindered internal rotations; barriers to rotations and reduced moments of inertia for different cyclic activated complexes\*

	$V'_{0,1}$	$I'_{r,1}$	$V'_{0,2}$	$I'_{r,2}$	$V'_{0,3}$	$I'_{r,3}$	$V'_{0,4}$	$I'_{r,4}$	$V'_{0,5}$	$I'_{r,5}$	$V'_{0,6}$
MEE	3600	5.18									
MNPE	3600	5.23	3900	5.29							
MIPE	3900	5.26	3900	5.27							
MIBE	3600	5.26	3600	5.29	3600	5.29					
MTBUE	4000	5.29	4700	5.28	4700	5.28					
DEE	3400	5.24	5500	45.2							
DNPE	3400	5.31	5300	56.0	7700	78.9	3600	5.33			
DNBE	3400	5.33	5399	60.4	7500	104.1	7000	155.1	5800	60.4	3400

\*  $V'_{0,i} = V_{0,i}/\text{cal} \cdot \text{mol}^{-1}$ ;  $I'_{r,i} = I_{r,i}/10^{-40} \text{ g cm}^2$ ;  
enumeration of hindered rotations,  
illustrated on the example of MIBE:

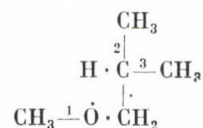


Table V

Calculation of entropies and molar heat capacities of different ethers\* (298 K)

	$S_{\text{tr}}^{\circ}$	$S_r^{\circ}$	$S_p^{\circ}$	$S_{r,\text{rot}}^{\circ}$	$S_{\text{calc.}}^{\circ}$	$S_{\text{exp.}}^{\circ}$	$C_{p,t}^{\circ}$	$C_{p,r}^{\circ}$	$C_{p,v}^{\circ}$	$C_{p,t,\text{rot}}^{\circ}$	$C_{p,\text{calc.}}^{\circ}$	$C_{p,\text{exp.}}^{\circ}$
DME	37.41	20.95	1.34	4.48	64.18	63.83	4.97	2.98	3.51	4.30	15.75	15.73
MEE	38.2	24.03	3.37	9.50	75.08	74.24	4.97	2.98	7.95	6.48	22.33	21.45
MNPE	38.82	25.65	4.26	15.00	83.74	83.52	4.97	2.98	9.97	8.54	26.46	26.89
MIPE	38.82	25.70	4.63	11.61	80.76	80.86	4.97	2.98	9.87	8.49	26.31	26.55
MIBE	39.34	27.10	5.96	15.41	89.83	91.09	4.97	2.98	13.03	10.51	31.58	31.50
MTBE	39.34	26.04	6.55	12.08	84.01	84.36	4.97	2.98	13.37	10.54	31.86	32.07
DEE	38.82	24.13	4.33	15.17	82.45	81.90	4.97	2.98	10.00	8.61	26.56	26.89
DNPE	39.78	26.55	7.18	28.01	101.22	100.98	4.97	2.98	16.50	12.96	37.41	37.83
DNBE	40.50	28.39	9.96	42.06	120.90	119.60	4.97	2.98	22.80	17.00	47.77	48.76

\*  $S_i^{\circ} = S_i^{\circ}/\text{cal mol}^{-1} \text{ K}^{-1}$ ;  $C_{p,i}^{\circ} = C_{p,i}^{\circ}/\text{cal mol}^{-1} \text{ K}^{-1}$

From the calculated  $C_p^\circ$  values the parameters of the equation

$$C_p^\circ = a + bT + cT^2 + dT^3 \quad (10)$$

were calculated for the individual molecules and activated complexes by using non-linear least squares [16]. These values were used to calculate  $\Delta S_T^{\circ\ddagger}$  from the equation

$$\Delta S_T^{\circ\ddagger} = \Delta S_{298}^{\circ\ddagger} + \int_{298}^T \frac{\Delta C_p^{\circ\ddagger}}{T} dT \quad (11)$$

and the preexponential factor from equation (2) at different temperatures (Table VII).

The insensitivity of the activation entropy to the structure of the ring in the activated complex is reflected in the relatively small change in the intrinsic entropy of overall rotation ( $0.8 \pm 0.2 \text{ cal mol}^{-1} \text{ K}^{-1}$ ). The absolute entropy increment is greater by  $1.38 \text{ cal mol}^{-1} \text{ K}^{-1}$  for the last three compounds (Table VII), reflecting an external symmetry change of 2.

Since two internal rotations are lost in the activation process, a substantial loss in the internal rotation entropy occurs, especially when both rotors are heavy.

On the other hand, an increase in the vibrational entropy is observed mostly due to the two new vibrations replacing the frozen rotors. The entropies of these degrees of freedom depend on whether or not low frequency vibrations appear. Substitution in  $\alpha$ -position to the O-atom in the ring seems to be very favourable in this respect owing to the presence of C—C·O low frequency bendings in the activated complex.

On the basis of these considerations the nearly two order of magnitude difference in the  $A$ -factors of MIBE and MTBE molecular decompositions is easily explained: the decrease in the entropy due to the freezing of two rotors is smaller, the increase in the vibrational contributions and the reaction path degeneracy are greater in the latter case.

The calculated  $A$ -factors can be checked against those reported in the literature in only a few cases. The  $A$ -factor calculated for the molecular decomposition of DEE ( $\lg A/s^{-1}$ ) =  $13.2 \pm 0.3$ ) is in reasonable agreement with those determined experimentally [SERES and HUHN [2] (13.9), FOUCAUT and MARTIN [3] (13)], but it is considerably lower than that determined experimentally by LAIDLER and MCKENNEY [17] (18) and that estimated by HAUGEN and BENSON [14] (14.4).

The value now estimated for MTBE (13.6) is lower than both the experimental value of DALY and WENTRUP [18] (14.4) and the estimated value of BENSON and coworkers [14] (13.9).

Table VI

Calculation of entropies and molar heat capacities of cyclic activated complexes\* (298 K)

	$S_{tr}^{\circ'}$	$S_r^{\circ'}$	$S_r^{\circ'}$	$S_{i,rot}^{\circ'}$	$S_{opt,i}^{\circ'}$	$S_{calc}^{\circ'}$	$C_{p,tr}^{\circ'}$	$C_{p,r}^{\circ'}$	$C_{p,v}^{\circ'}$	$C_{p,i,rot}^{\circ'}$	$C_{p,calc}^{\circ'}$
MEE*	38.20	24.81	6.31	1.99	1.377	73.31	3.97	2.98	10.48	2.09	20.52
MNPE*	38.82	26.73	8.30	3.92	1.377	79.15	4.97	2.98	13.44	4.20	25.59
MIPE*	38.82	26.35	8.28	3.84	1.377	78.67	4.97	2.98	13.48	4.11	25.52
MIBE*	39.34	27.83	9.36	6.03	1.377	83.94	4.97	2.98	15.76	6.29	3.000
MTBE*	39.34	26.89	12.45	5.29	1.377	85.35	4.97	2.98	18.11	5.93	31.99
DEE*	38.82	26.15	8.40	7.77	1.377	82.52	4.97	2.98	13.72	4.27	25.95
DNPE*	39.78	28.54	11.10	15.92	1.377	96.72	4.97	2.98	19.89	8.47	36.31
DNBE*	40.50	30.51	13.98	28.93	1.377	115.30	4.97	2.98	26.33	12.75	47.03

\*  $S_i^{\circ'} = S_i^{\circ}/\text{cal mol}^{-1} \text{K}^{-1}$ ;  $C_{p,i,rot}^{\circ'} = C_{p,i,rot}^{\circ}/\text{cal mol}^{-1} \text{K}^{-1}$ 

Table VII

Activation entropies and preexponential factors of molecular elimination reactions\*

Ether	$\Delta S_T^{\circ \ddagger'}$	$\Delta S_B^{\circ \ddagger'}$	$\Delta S_{i,rot}^{\circ \ddagger'}$	$\Delta S_{298,int}^{\circ \ddagger'}$	$\Delta S_{673}^{\circ \ddagger'}$	$\Delta S_{800}^{\circ \ddagger'}$	$\frac{l^{\ddagger} \sigma^{\ddagger} n}{\sigma n^{\ddagger}}$	$10^{-12} \times A_{673}(\text{s}^{-1})$	$10^{-12} \times A_{800}(\text{s}^{-1})$
MEE	0.78	3.56	-7.51	-5.33	-3.33	-3.60	0.5	3.6	3.7
MNPE	1.08	4.04	-11.08	-5.97	-5.53	-5.79	1	2.4	2.5
MIPE	0.65	3.65	-7.77	-5.65	-2.65	-2.76	1	10	11
MIBE	0.73	3.40	-9.38	-4.51	-7.37	-7.72	0.5	0.47	0.47
MTBE	0.85	5.90	-6.79	-4.39	1.29	1.30	0.5	36	44
DEE	2.02	4.07	-7.40	-4.87	-0.60	-0.75	0.5	14	15
DNPE	1.99	3.92	-12.09	-7.25	-5.63	-5.95	1	2.2	2.3
DNBE	2.12	4.02	-13.13	-8.35	-6.57	-6.89	1	1.4	1.4

\*  $\Delta S_T^{\circ \ddagger'} = \Delta S_T^{\circ \ddagger}/\text{cal mol}^{-1} \text{K}^{-1}$

On the basis of the above results, the following conclusions are drawn:

a) The estimated values of the  $A$  factors are influenced to similar extents by the number of H atoms present in  $\beta$  position to the ether oxygen, the number of internal rotations changing appreciably in the activation process,\* the reduced moments of inertia of the frozen rotors, and the change in the product of the three principal moments of inertia.

b) The activation entropies decrease with increasing temperature. On the other hand, the  $A$  factors are proportional to the temperature [Eq. (2)]. The resulting compensation effect renders the preexponential factors nearly independent of temperature.

c) Of the 8 reactions studied, the reaction path degenerations calculated from the symmetry numbers and by simple counting are identical in only 4 cases.

One of the referees\*\* called the author's attention to the good linear correlation between the calculated  $\Delta H_{800}^{\circ}$  and  $\ln A_{800}$  (i.e.  $\Delta S^{\circ \neq}$ ) values ( $r^2 = 0.84$ ); on the other hand, no such correlations were found between either  $\Delta S_{800}^{\circ}$  and  $\ln A_{800}$  ( $r^2 = 0.43$ ) or  $\Delta G_{800}^{\circ}$  and  $\ln A_{800}$  ( $r^2 = 0.15$ ).

The first observation is probably a consequence of the double effect of chain branching at the C-atom in  $\alpha$ -position to the other oxygen:

a)  $\Delta H^{\circ}$  increases because of the pronounced stabilizing effect of the O-atom. (The enthalpy of formation is considerably greater in the case of  $n$ -dialkyl ethers.)

b) The  $A$ -factor increases for the reasons discussed above.

Since most of the effects influencing the magnitude of  $\Delta S^{\circ \neq}$  have little effect on  $\Delta S^{\circ}$ , the absence of a good linear correlation between  $\Delta S_{800}^{\circ}$  and  $\ln A_{800}$  is understandable. The same applies to the possible correlation of  $\Delta G_{800}^{\circ}$  and  $\ln A_{800}$ , since the former is considerably dependent on  $\Delta S_{800}^{\circ}$ .

From a comparison of the estimated data and the few experimental data available, the possibility of the presence of a low-frequency pseudo-rotation in the activated complex cannot be excluded. The reality of this assumption cannot be judged without further experimental investigations.

#### REFERENCES

- [1] CHOO, K. Y., GOLDEN, D. M., BENSON, S. W.: *Int. J. Chem. Kinet.*, **6**, 631 (1974)
- [2] SERES, I., HUHN, P.: *Magy. Kém. Folyóirat*, **81**, 120 (1975)
- [3] FOUCAUT, J. F., MARTIN, R.: *J. Chim. Phys.*, **75**, 132 (1978)
- [4] BENSON, S. W.: *Thermochemical Kinetics*, 2nd Ed. John Wiley and Sons, New York 1976
- [5] COLUSSI, A. J., BENSON, S. W.: *Int. J. Chem. Kinet.*, **9**, 295 (1977)

\* Internal rotations frozen in the activated complex and rotors attached to the ring formed

\*\* M. SIMONYI, Central Research Institute for Chemistry of the Hungarian Academy of Sciences, Budapest, Hungary

- [6] O'NEAL, H. E., BENSON, S. W.: *J. Phys. Chem.*, **71**, 2903 (1967)
- [7] BLADES, A. T., SANDHU, H. S.: *Int. J. Chem. Kinet.*, **3**, 187 (1971)
- [8] MURREL, J. N., LAIDLER, K. J.: *Trans. Faraday Soc.*, **64**, 371 (1968)
- [9] BLINDER, S. M.: *Advanced Physical Chemistry*, p. 438. The Macmillan Co., London 1969
- [10] HIRSCHFELDER, J. O.: *J. Chem. Phys.*, **8**, 431 (1942)
- [11] *Tables of Interatomic Distances and Configuration in Molecules and Ions*, Special Publication No. 18, The Chemical Society, London 1965
- [12] ZALOTAI, L., SERES, L., FEJES, P.: FORTRAN programs for the solution of physico-chemical problems. Műszaki Könyvkiadó, Budapest 1978 (in Hungarian)
- [13] PERONA, M. J., BEADLE, P. C., GOLDEN, D. M.: *Int. J. Chem. Kinet.*, **5**, 495 (1973)
- [14] HAUGEN, G. R., BENSON, S. W.: *Int. J. Chem. Kinet.*, **2**, 235 (1970)
- [15] *Internal Rotation in Molecules*, Ed. W. J. ORVILLE—THOMAS. John Wiley and Sons, New York, 1974
- [16] SERES, L., ZALOTAI, L., MÁRTA, F.: *Acta Phys. Chem.*, **23**, 433 (1977)
- [17] LAIDLER, K. J., MCKENNEY, D. J.: *Proc. Roy. Soc.*, **A278**, 505 (1964)
- [18] DALY, N. J., WENTRUP, C.: *Aust. J. Chem.*, **21**, 2711 (1968)

László SERES H-6701 Szeged, P. O. Box 105.

## THE 1 : 1 AND 1 : 2 COMPLEX FORMATION BETWEEN $\beta$ -CYCLODEXTRIN AND BENZOIC ACID

Á. BUVÁRI<sup>1</sup>, J. SZEJTLI<sup>2</sup> and L. BARCZA<sup>1\*</sup>

<sup>1</sup> *Department of Inorganic and Analytical Chemistry, L. Eötvös University, Budapest and*  
<sup>2</sup> *Biochemical Research Laboratory of Chinoin Chem.-Pharm. Works, Budapest)*

Received March 26, 1981  
Accepted for publication May 25, 1981

Based on solubility measurements the existence of a complex containing two molecules of benzoic acid for one molecule of cyclodextrin has been proved in which the second acid is assumed to be bound by hydrogen bridge. The formation constants of the 1 : 1 and 1 : 2 complexes have been determined.

The solubility properties of several organic compounds are often essentially modified by complex formation with cyclodextrins. The solubility increasing effect may be an important point for the application of cyclodextrins in the pharmaceutical industry. In most cases only the formation of simple 1 : 1 complexes is assumed unless the guest molecules are so small that two or more of them can penetrate into the cyclodextrin cavity at the same time (*e.g.* HCl) [1].

It has been observed [2, 3] that the slopes of the solubility *vs.* cyclodextrin concentration plots are often greater than unity, suggesting that not only simple binary but also ternary complexes are formed. This suggestion was supported also by our (preliminary) experiments: complexes of benzoic acid and cycloheptaamylose ( $\beta$ -cyclodextrin,  $\beta$ -CD) were prepared and then heated at 150 °C for 2 hours in a vessel covered with a cooled lid. A minor but strict amount of benzoic acid could always be detected on the lid even if the analytical composition of the sample was 1 : 1, in spite of the fact that benzoic acid was not released from the inclusion complex until very close to the decomposition temperature of the  $\beta$ -CD ( $\sim$ 190 °C) as it has been proved in other experiments.

Our aim was to interpret these phenomena in terms of complex formation and to determine the stability of the complexes.

Three independent series of experiments were carried out:  
the solubility of benzoic acid was measured

- 1) in solutions of  $\beta$ -CD and
- 2) in solutions of carefully prepared  $\beta$ -CD—benzoic acid complex;
- 3) the solubility of the  $\beta$ -CD—benzoic acid complex was measured in solutions of benzoic acid.

\* To whom correspondence should be addressed

### Results and Discussion

The saturation concentration of benzoic acid as the function of the concentration of  $\beta$ -CD or  $\beta$ -CD—benzoic acid complex (series 1 and 2, resp.) is shown on Fig. 1, while Fig. 2 shows the solubility of the 1 : 1 complex in the function of the initial benzoic acid concentration.

As it can be seen on Fig. 1 the  $c_{\text{HB}}$  vs.  $c_{\text{CD}}$  plots give practically a straight line but the slope is 1.05, in accordance with the results of COHEN and LACH [2].

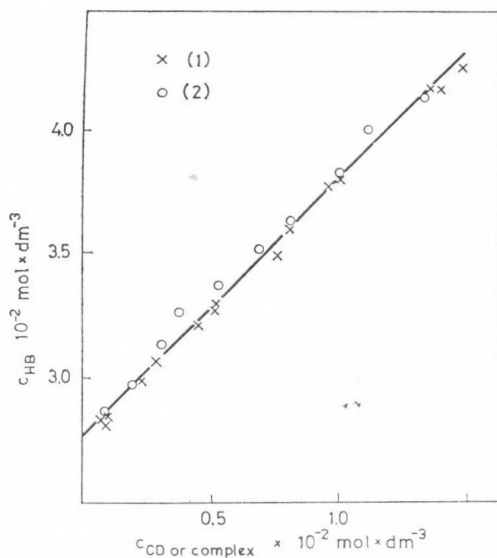


Fig. 1. The solubility of benzoic acid plotted against the concentration of  $\beta$ -CD (1) or  $\beta$ -CD—benzoic acid complex (2), respectively.  $c_{\text{HB}}$  is the total concentration of the benzoic acid, including also the acid content of the complex

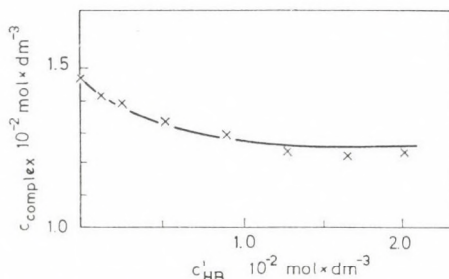
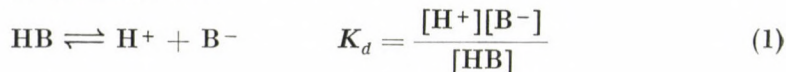


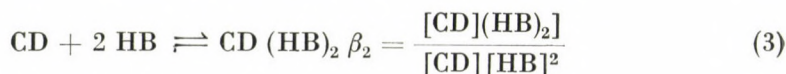
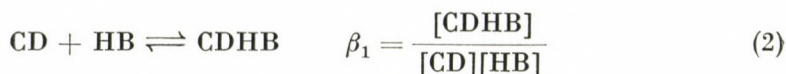
Fig. 2. The solubility of the  $\beta$ -CD—benzoic acid complex in the function of the initial benzoic acid concentration

To evaluate the experimental data the following equilibria (with the correspondent equilibrium constants) were assumed:

dissociation of the benzoic acid



the formations of 1 : 1 and 1 : 2 complexes:



where the square-brackets denote the equilibrium concentrations of the different species. So the total concentrations of benzoic acid and  $\beta$ -cyclodextrin can be written as follows:

$$c_{\text{HB}} = k_d^{1/2}[\text{HB}]^{1/2} + [\text{HB}] + \beta_1[\text{CD}][\text{HB}] + 2\beta_2[\text{CD}][\text{HB}]^2 \quad (4)$$

$$c_{\text{CD}} = [\text{CD}] + \beta_1[\text{CD}][\text{HB}] + \beta_2[\text{CD}][\text{HB}]^2 \quad (5)$$

For  $K_d$  a value of  $6 \times 10^{-5}$  was accepted from the literature [4]. For the other equilibrium constants the following values could be calculated (with the given standard deviations):

$$\log \beta_1 = 2.9 \pm 0.15$$

$$\log \beta_2 = 3.5 \pm 0.2$$

The agreement with the experimental data is fairly good for all the three series as it can be seen on Figs 1 and 2 where the calculated curves are drawn in continuous lines. [For the solutions saturated with the complex (series 3) the solubility product

$$K_{\text{SO}} = [\text{CD}][\text{HB}]$$

had to be taken into account as well, and its value has been found to be  $\text{p}K_{\text{SO}} = 4.85$ . Some slight deviation may arise from the fact that minor phenomena (as complex formation with the benzoate anion and the solubility of the 1 : 2 complex) were neglected.] The distribution of  $\beta$ -CD among the different species is shown on Fig. 3 as the function of the excess benzoic acid concentration.

Summarizing the results, beside the simple binary complex the existence of a complex containing one molecule of  $\beta$ -CD and two molecules of benzoic acid has been proved. Since two molecules of benzoic acid can not penetrate into the  $\beta$ -cyclodextrin cavity [5] and the second acid molecule is bound rather weakly as reflected by the low equilibrium constant of the second

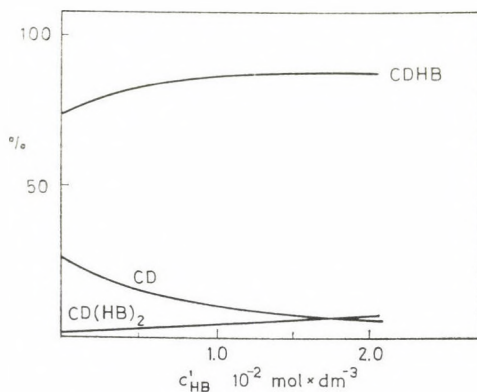


Fig. 3. Percentage of the different species containing  $\beta$ -CD as the function of the excess benzoic acid concentration

complex formation step ( $\log \beta_2 - \log \beta_1 = 0.6$ ), the second molecule must be attached to the cyclodextrin surface by hydrogen bonds. (Bonding to the included benzoic acid is unlikely because its  $-\text{COOH}$  is hydrogen bonded to the cyclodextrin OH-groups and so — as it has been shown by potentiometric measurements [6] — the acidic strength as well as the tendency to dimerize is decreased.) This structure gives explanation for the sublimation of small but strict amount of benzoic acid below the decomposition temperature. So in all other cases when the guest molecule is capable of hydrogen bonding, an “outer sphere” complex with the composition of 1 : 2 can be formed as well and the properties of such complexes must be highly different from those of real inclusion complexes.

### Experimental

The concentration of  $\beta$ -CD in the first series of experiments was  $0-1.5 \times 10^{-5} \text{ mol dm}^{-3}$ , and that of the benzoic acid in series 3, was  $0-2 \times 10^{-2} \text{ mol dm}^{-3}$ .

The  $\beta$ -CD—benzoic acid complex was prepared by dissolving equimolar amounts of  $\beta$ -CD and benzoic acid in hot water and then crystallized by cooling. The composition was proved to be 1 : 1. Its concentration in series 2 was  $0-1.33 \times 10^{-2} \text{ mol dm}^{-3}$ .

The temperature was always kept at  $25 \pm 0.1^\circ \text{C}$ .

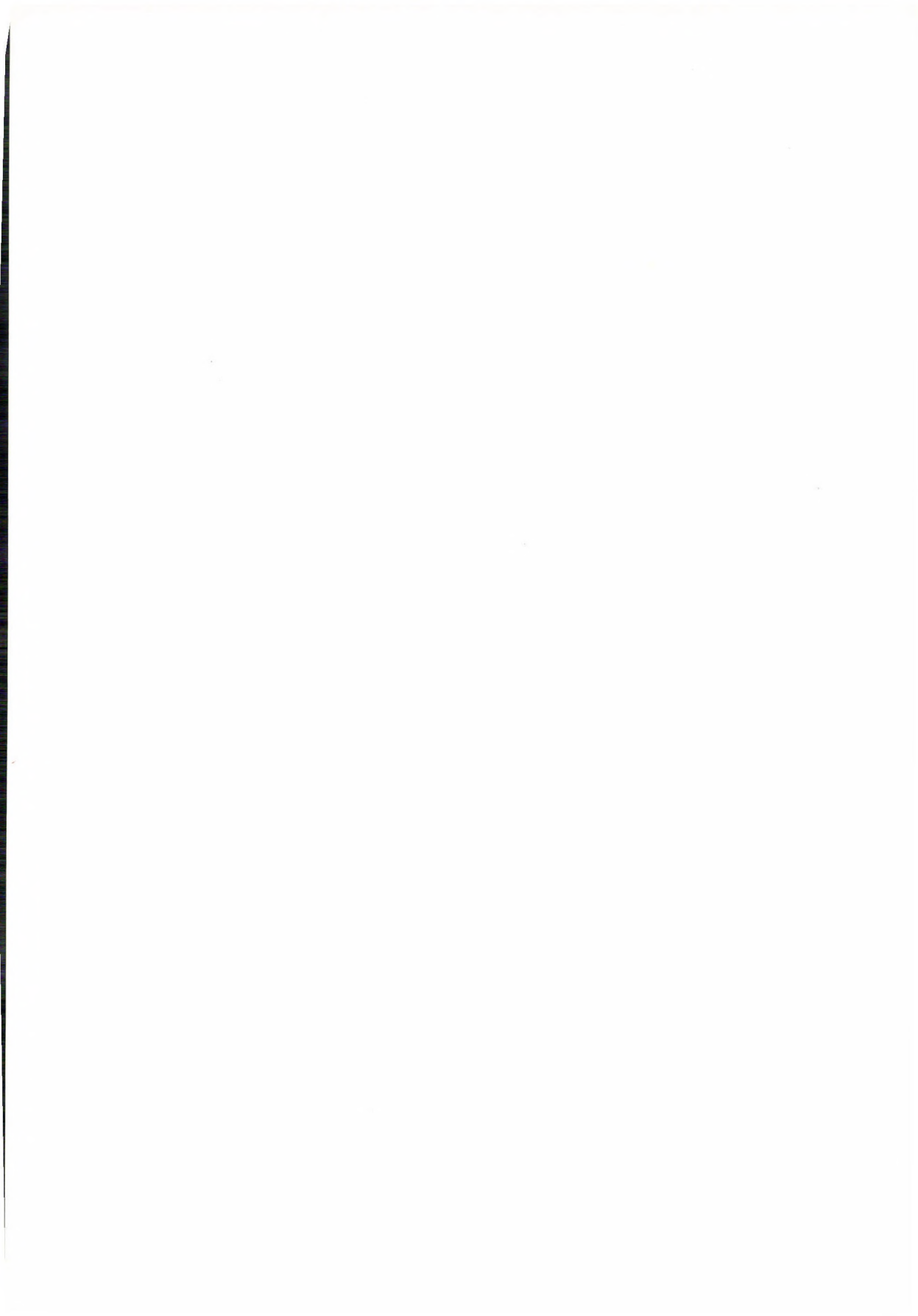
After the solubility equilibrium had been reached (at least 12 hours) the concentration of benzoic acid was determined by alkalimetric titration and that of the  $\beta$ -CD by optical rotatory measurement. (First it was proved that in solution the optical rotatory of  $\beta$ -CD was not modified by the presence of the benzoic acid.)

## REFERENCES

- [1] SZEJTLI, J., BUDAI, Zs.: *Acta Chim. Acad. Sci. Hung.*, **94**, 383 (1977)  
[2] COHEN, J., LACH, J. L.: *J. Pharm. Sci.*, **52**, 132 (1963)  
[3] PAULI, W. A., LACH, J. L.: *J. Pharm. Sci.*, **54**, 1745 (1965)  
[4] KORTÜM, G., VOGEL, W., ANDRUSSOW, K.: *Dissociation Constants of Organic Acids in Aqueous Solution*. Butterworths, London, 1961  
[5] BENDER, M. L., KOMIYAMA, M.: *Cyclodextrin Chemistry*. Springer Verl., Berlin—Heidelberg—New York, 1978  
[6] CONNORS, K. A., LIPARI, J. M.: *J. Pharm. Sci.*, **65**, 379 (1976)

Lajos BARCZA }  
Ágnes BUVÁRI } H-1443 Budapest, P. O. Box 123.

József SZEJTLI H-1045 Budapest, Tó u. 1—5.



## STUDY OF INHIBITORS BY ELECTRODE IMPEDANCE MEASUREMENTS<sup>+</sup>

L. MÉSZÁROS\*, B. LENGYEL and T. GARAI

*(Research Laboratory for Inorganic Chemistry of the Hungarian Academy of Sciences,  
Budapest)*

Received March 30, 1981

Accepted for publication May 25, 1981

On the basis of theoretical considerations a relationship was established between the polarization resistance and the corrosion-current density for the case of metal dissolution inhibited by an adsorption-type inhibitor. The corrosion-current density can be evaluated when the potential dependence of the electrode coverage is known in addition to the polarization resistance and the Tafel slopes.

### Introduction

The technique of electrode impedance measurement has become widespread in electrochemical and corrosion studies during the last decades. Impedance diagrams recorded in a wide frequency range are especially useful for the separation of consecutive and/or parallel processes of different relaxation times. The analysis of electrode impedance was employed by GERISCHER and MEHL [1] for the study of adsorbed intermediates in the hydrogen evolution reaction. EPELBOIN and his co-workers [2 to 8] investigated the metal dissolution and metal deposition processes using impedance diagrams. ARMSTRONG and his co-workers [9 to 18] employed this method for the study of various electrode reactions. An excellent account of this technique is found in the monograph of MACDONALD [19] on perturbation methods.

ARMSTRONG [9] assumed in his study of the impedance relations of active to passive transition that the metal dissolution is a simple single-step reaction which is inhibited only by the geometric effect of oxygen adsorbed on the surface. The author applied the method of FRUMKIN and GAIKAZYAN [20] in the determination of adsorption impedance.

In this paper the application of the impedance method for the study of inhibitors is presented basically in accordance with ARMSTRONG's treatment assuming the adsorption of neutral molecules and a simple charge transfer reaction energetically independent of the latter.

<sup>+</sup> This paper was presented at the 5th European Symposium on Corrosion Inhibitors at Ferrara (Italy), 15–19. September 1980.

\* To whom correspondence should be addressed.

### The electrode admittance

The current density of the adsorption process and that of the charge-transfer reaction assumed to be energetically independent one from another are given by the following formulas:

$$\mathbf{j}_F = \mathbf{j}_{\text{corr}} \left( \frac{1 - \Theta}{1 - \Theta_{\text{corr}}} e^{\frac{\Delta E}{\beta_a}} - e^{-\frac{\Delta E}{\beta_c}} \right) \quad (1)$$

the current density of the faradaic process (charge transfer reaction) and

$$\mathbf{j}_A = \frac{d\sigma_{\text{Me}}}{dt} = \frac{d}{dt} [(\sigma_1(1 - \Theta) + \sigma_2\Theta)] \quad (2)$$

the current density of the adsorption transient, where  $\mathbf{j}_{\text{corr}}$  is the corrosion-current density,  $\beta_c$  and  $\beta_a$  are the Tafel slopes of the anodic partial process (metal dissolution) and of the cathodic reaction ( $\text{H}^+$  reduction), respectively,  $\Theta$  is the coverage of the inhibitor,  $\sigma_{\text{Me}}$  is the charge density of the electrode having  $\Theta$  coverage while  $\sigma_1$  and  $\sigma_2$  are the charge densities of the uncovered electrode ( $\Theta = 0$ ) and of the completely covered ( $\Theta = 1$ ) electrode, respectively.  $\Delta E = E - E_{\text{corr}}$  is the polarization.

The admittance of the faradaic reaction is given by

$$Y_F = \frac{d\mathbf{j}_F}{d\Delta E} = \left( \frac{\partial \mathbf{j}_F}{\partial \Delta E} \right)_{\Theta} + \left( \frac{\partial \mathbf{j}_F}{\partial \Theta} \right)_{\Delta E} \left( \frac{\partial \Theta}{\partial \Delta E} \right) \quad (3)$$

Employing the treatment of FRUMKIN and GAIKAZYAN [19] for the case of sinusoidal perturbation

$$\Delta E = \overline{\Delta E} + U_0 e^{j\omega t}$$

we obtain

$$\frac{\partial \Theta}{\partial \Delta E} = \left( \frac{\partial \Theta}{\partial \Delta E} \right)_{\omega=0} \frac{1}{1 + i\omega\tau} \quad (4)$$

where  $\left( \frac{\partial \Theta}{\partial \Delta E} \right)_{\omega=0}$

is the derivative of the stationary  $\Theta$  vs.  $\Delta E$  function,  $\omega$  is the angular frequency,  $U_0$  is the amplitude while  $\tau = 1/k$  is the time constant, where  $k$  is the rate constant defined by the equation of a first order kinetic reaction:

$$\frac{d\Theta}{dt} = -k(\Theta - \Theta_e) \quad (5)$$

where  $\Theta_e$  is the equilibrium coverage corresponding to the instantaneous potential.

The faradaic admittance at the corrosion potential  $\Delta E = 0$  is given by the following formula taking into account equations (1), (3) and (4)

$$Y_F = \mathbf{j}_{\text{corr}} \left\{ \left( \frac{1}{\beta_a} + \frac{1}{\beta_c} \right) - \frac{1}{1 - \Theta_{\text{corr}}} \left( \frac{\partial \Theta}{\partial \Delta E} \right)_{\omega=0} \frac{1}{1 + i\omega\tau} \right\}. \quad (6)$$

The current density [equation (2)] corresponding to the perturbation of the adsorption process is given by the following equation

$$\mathbf{j}_A = \left[ \left( \frac{d\sigma_1}{d\Delta E} (1 - \Theta) + \frac{d\sigma_2}{d\Delta E} \Theta \right) - (\sigma_1 - \sigma_2) \frac{\partial \Theta}{\partial \Delta E} \right] \frac{d\Delta E}{dt} \quad (7)$$

and the admittance corresponding to the adsorption process when a sinusoidal perturbation

$$\Delta E = \overline{\Delta E} + U_0 e^{i\omega t}$$

is applied reads

$$Y_A = i\omega \left\{ C_{dl} - \frac{\sigma_1 - \sigma_2}{1 + i\omega\tau} \left( \frac{\partial \Theta}{\partial \Delta E} \right)_{\omega=0} \right\} \quad (8)$$

where  $C_{dl}$  is the capacity of the double layer:

$$C_{dl} = \frac{d\sigma_1}{d\Delta E} (1 - \Theta) + \frac{d\sigma_2}{d\Delta E} \Theta \quad (9)$$

where  $\frac{d\sigma_1}{d\Delta E}$  and  $\frac{d\sigma_2}{d\Delta E}$

are the specific double layer capacities of the uncovered and completely covered electrode, respectively.

Separating the real and imaginary parts of faradaic admittance (6) and of adsorption admittance (8) the real and imaginary parts of the electrode impedance are obtained

$$Y'_e = \mathbf{j}_{\text{corr}} \left\{ \left( \frac{1}{\beta_a} + \frac{1}{\beta_c} \right) - \frac{1}{1 - \Theta_{\text{corr}}} \left( \frac{\partial \Theta}{\partial \Delta E} \right)_{\omega=0} \frac{1}{1 + \omega^2 \tau^2} \right\} - \quad (10)$$

$$- (\sigma_1 - \sigma_2) \frac{\omega^2 \tau}{1 + \omega^2 \tau^2} \left( \frac{\partial \Theta}{\partial \Delta E} \right)_{\omega=0}$$

$$Y''_e = \omega C_{dl} - (\sigma_1 - \sigma_2) \frac{\omega}{1 + \omega^2 \tau^2} \left( \frac{\partial \Theta}{\partial \Delta E} \right)_{\omega=0} + \quad (11)$$

$$+ \frac{\mathbf{j}_{\text{corr}}}{1 - \Theta_{\text{corr}}} \frac{\omega\tau}{1 + \omega^2 \tau^2} \left( \frac{\partial \Theta}{\partial \Delta E} \right)_{\omega=0}$$

or by simplifying the notations

$$Y'_e = \frac{1}{R_t} + \frac{1}{R_{t0}} \frac{1}{1 + \omega^2 \tau^2} + \frac{1}{R_{A\infty}} \frac{\omega^2 \tau^2}{1 + \omega^2 \tau^2} = \quad (12)$$

$$= \frac{1}{R_t} + \frac{1}{R_{A\infty}} - \left( \frac{1}{R_{t0}} - \frac{1}{R_{A\infty}} \right) \frac{1}{1 + \omega^2 \tau^2}$$

$$Y''_e = \omega \left\{ C_{dl} + [C_{A0} + C_{t0}] \frac{1}{1 + \omega^2 \tau^2} \right\}. \quad (13)$$

The notations of equations (12) and (13) are the following:

$$\frac{1}{R_t} = \mathbf{j}_{\text{corr}} \left( \frac{1}{\beta_a} + \frac{1}{\beta_c} \right) \quad (14)$$

the charge-transfer resistance of the faradaic process,

$$\frac{1}{R_{t0}} = - \mathbf{j}_{\text{corr}} \frac{1}{1 - \Theta_{\text{corr}}} \left( \frac{\partial \Theta}{\partial \Delta E} \right)_{\omega=0} \quad (15)$$

the additional charge-transfer resistance connected parallelly to the latter at low frequencies and

$$\frac{1}{R_{A\infty}} = - \frac{\sigma_1 - \sigma_2}{\tau} \left( \frac{\partial \Theta}{\partial \Delta E} \right)_{\omega=0} \quad (16)$$

another additional charge-transfer resistance due to the effect of the adsorption process at very high frequencies ( $\omega\tau \gg 1$ ) which can be regarded from an electrical point of view as the loss resistance of the adsorption pseudocapacity. The latter is given by

$$C_{A0} = - (\sigma_1 - \sigma_2) \left( \frac{\partial \Theta}{\partial \Delta E} \right)_{\omega=0} = \frac{\tau}{R_{A\infty}} \quad (17)$$

while the pseudocapacity of the faradaic process reads

$$C_{t0} = \mathbf{j}_{\text{corr}} \frac{\tau}{1 - \Theta_{\text{corr}}} \left( \frac{\partial \Theta}{\partial \Delta E} \right)_{\omega=0} = - \frac{\tau}{R_{t0}}. \quad (18)$$

The latter are effective when  $\omega\tau \ll 1$ . In addition formulas

$$\frac{1}{R_\infty} = \left( \frac{1}{R_t} + \frac{1}{R_{A\infty}} \right), \quad (19)$$

$$\frac{1}{R_0} = \left( \frac{1}{R_{t0}} - \frac{1}{R_{A\infty}} \right) \quad (20)$$

and

$$C_0 = (C_{t0} + C_{A0}) = -\frac{\tau}{R_0} \quad (21)$$

are introduced, whence the real and imaginary parts of the electrode impedance are obtained

$$Y'_e = \frac{1}{R_\infty} + \frac{1}{R_0} \frac{1}{1 + \omega^2 \tau^2} \quad (22)$$

$$Y''_e = \omega C_{dl} - \frac{1}{R_0} \frac{\omega \tau}{1 + \omega^2 \tau^2} \quad (23)$$

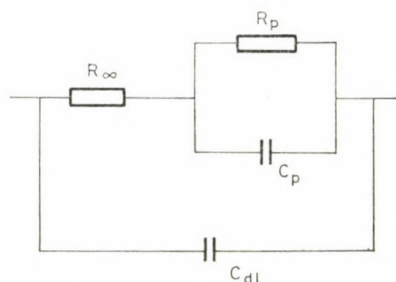


Fig. 1. Equivalent circuit of the electrode impedance for the case of a charge-transfer reaction coupled with adsorption

Equations (22) and (23) are identical to the admittances derived by ARMSTRONG and HENDERSON [10] for adsorbed intermediates. The electrode impedance according to the latter authors can be represented by the equivalent circuit shown in Fig. 1 where

$$R_p = -\frac{R_\infty^2}{R_0 + R_\infty} \quad (24)$$

$$C_p = -\frac{R_0 \tau}{R_\infty^2} \quad (25)$$

$$Z_e = Z'_e + iZ''_e = \frac{1}{Y'_e + iY''_e} \quad (26)$$

The complex plane display of the electrode impedance is shown in Fig. 2 for some typical cases.

The diagrams generally consist of two fairly well separated semi-circles if the time constants of the  $R_\infty - C_{dl}$  and  $R_p - C_p$  circuits, respectively, differ to a sufficient extent.

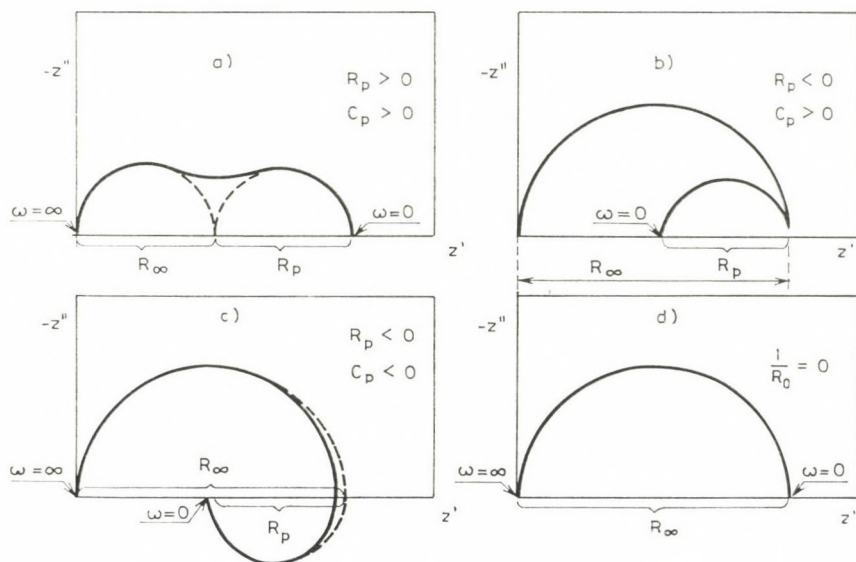


Fig. 2. Typical impedance plots of a charge-transfer reaction coupled with adsorption

The point of the diagram corresponding to frequency  $\omega = 0$  permits the determination of the polarization resistance using equations (19), (20) and (24). Hence

$$R_{\pi} = R_{\infty} + R_p = \left( \frac{1}{R_t} + \frac{1}{R_{t0}} \right)^{-1} \quad (27)$$

and taking into account equations (14) and (15) we obtain

$$\frac{1}{R_{\pi}} = \frac{1}{R_t} + \frac{1}{|R_{t0}|} = \mathbf{j}_{\text{corr}} \left[ \frac{1}{\beta_a} + \frac{1}{\beta_c} - \frac{1}{1 - \Theta_{\text{corr}}} \left( \frac{\partial \Theta}{\partial \Delta E} \right)_{\omega=0} \right]. \quad (28)$$

Thus the corrosion-current density can be calculated if Tafel slopes  $\beta_a$  and  $\beta_c$  are known as well as the potential dependence of the coverage with the inhibitors.

The determination of the corrosion-current density can be considerably simplified if the adsorption of the inhibitor does not depend on the potential. This is the case when e.g. a neutral molecule dissociates in the double layer and an organic cation is formed which can be contact-adsorbed on the surface. Thus the repelling effect of water molecules is balanced by chemical binding forces when the metal surface is positively charged and by electrostatic forces if the surface is negatively charged. In such cases  $\left( \frac{\partial \Theta}{\partial \Delta E} \right)_{\omega=0} = 0$  and thus equation (28) becomes

$$R_{\pi} = R_t, \quad (29)$$

*i.e.* resistances  $R_\infty + R_p$  correspond to the charge-transfer resistance (Fig. 2d). (In this case the slope of the polarization curve obtained under stationary conditions by using the so-called linear polarization method yields a correct value for the corrosion current.)

A similar consideration is valid when the corrosion potential is very nearly equal to or identical with the potential corresponding to maximum coverage as in this case  $\left(\frac{\partial\Theta}{\partial\Delta E}\right)_{\omega=0} \cong 0$  at the corrosion potential or in its vicinity.

The determination of the corrosion-current density can be simple also, when the adsorption process is slow. In fact,  $\frac{1}{R_{A\infty}}$  [equation (16)] may be negligible as compared to  $\frac{1}{R_t}$  [equation (19)] if rate constant  $k$  defined by equation (5) is small, *i.e.* time constant  $\tau = \frac{1}{k}$  is large. In this case  $R_\infty$  determined on the basis of the high frequency semi-circle is equal to the charge-transfer resistance [*c.f.* equation (19)]:

$$R_\infty = R_t \quad (30)$$

Apart from the above special cases, the knowledge of  $\left(\frac{\partial\Theta}{\partial\Delta E}\right)_{\omega=0}$  and  $\Theta_{\text{corr}}$  is indispensable for the determination of the corrosion-current density. The coverage prevailing at potential  $\Delta E$  can be evaluated on the basis of the double layer capacity  $C_{\text{dl}}$  obtained from the high frequency semi-circle. The double layer capacity of the electrode of coverage  $\Theta$  is given by the following formula in accordance with equation (9)

$$C_{\text{dl}} = C_1(1 - \Theta) + C_2\Theta \quad (31)$$

where  $C_1$  and  $C_2$  are the capacities of the uncovered and completely covered electrodes, respectively. Hence coverage  $\Theta$  is

$$\Theta = \frac{C_{\text{dl}} - C_1}{C_2 - C_1} \quad (32)$$

$\left(\frac{\partial\Theta}{\partial\Delta E}\right)_{\omega=0}$  can be evaluated by a graphical or numerical method using the value of coverage ( $\Theta_{\text{corr}}$ ) determined at the corrosion potential and in its vicinity according to the above formulas. The corrosion-current density can be obtained from equation (28) if  $\beta_a$  and  $\beta_c$  are known in addition to the above

mentioned data

$$j_{\text{corr}} = \frac{1}{R_{\pi}} \frac{1}{\frac{1}{\beta_a} + \frac{1}{\beta_c} - \frac{1}{1 - \Theta_{\text{corr}}} \left( \frac{\partial \Theta}{\partial \Delta E} \right)_{\substack{\omega=0 \\ \Delta E=0}}} \quad (33)$$

Thus it can be concluded that the knowledge of the polarization resistance and the Tafel slopes is not sufficient for the determination of the corrosion-current density (except in some special cases), since neither  $R_{\pi}$  [equation (27)] nor  $R_{\infty}$  [equation (19)] can be assumed to correspond to the charge-transfer resistance ( $R_t$ ). Except some special cases the results can only be satisfactory if the adsorption isotherm is known and taken into consideration.

The experimental study of the above theoretical considerations will be presented in a subsequent communication.

#### REFERENCES

- [1] GERISCHER, H., MEHL, W.: *Z. Elektrochem.*, **59**, 1049 (1955)
- [2] EPELBOIN, I., KEDDAM, M., LESTRADE, J. C.: *Disc. Faraday Soc.*, **56**, 264 (1973)
- [3] EPELBOIN, I., KEDDAM, M.: *J. Electrochem. Soc.*, **117**, 1052 (1971)
- [4] EPELBOIN, I., WIART, R.: *J. Electrochem. Soc.*, **118**, 1577 (1971)
- [5] EPELBOIN, I., KEDDAM, M.: *Electrochim. Acta*, **17**, 177 (1972)
- [6] EPELBOIN, I., KSOURI, M., WIART, R.: *J. Electrochem. Soc.*, **122**, 1206 (1975)
- [7] EPELBOIN, I., GABRIELLI, C., KEDDAM, M., TAKENOUTI, H.: *Electrochim. Acta*, **20**, 913 (1975)
- [8] EPELBOIN, I., KSOURI, M., WIART, R.: *J. Electroanal. Chem.*, **65**, 373 (1975)
- [9] ARMSTRONG, R. D.: *J. Electroanal. Chem.*, **34**, 387 (1972)
- [10] ARMSTRONG, R. D., HENDERSON, M.: *J. Electroanal. Chem.*, **39**, 81 (1972)
- [11] ARMSTRONG, T. F., FIRMAN, R. E., THIRSK, H. R.: *Disc. Faraday Soc.*, **56**, 244 (1973)
- [12] ARMSTRONG, R. D., THIRSK, H. R.: *Electrochim. Acta*, **17**, 171 (1972)
- [13] ARMSTRONG, R. D., DICKINSON, T., WILLIS, P. M.: *J. Electroanal. Chem.*, **48**, 47 (1973)
- [14] ARMSTRONG, R. D., EDMONDSON, K.: *Electrochim. Acta*, **18**, 937 (1973)
- [15] ARMSTRONG, R. D., BELL, M. F., FIRMAN, R. E.: *J. Electroanal. Chem.*, **48**, 150 (1973)
- [16] ARMSTRONG, R. D., EDMONDSON, K.: *J. Electroanal. Chem.*, **53**, 371 (1974)
- [17] ARMSTRONG, R. D., BELL, M. F.: *J. Electroanal. Chem.*, **55**, 201 (1974)
- [18] ARMSTRONG, R. D., METCALFE, A. A.: *J. Electroanal. Chem.*, **71**, 5 (1976)
- [19] MACDONALD, D. D.: *Transient Techniques in Electrochemistry*, Plenum Press (New York), 1977
- [20] FRUMKIN, A. N., MELIK-GAIKAZYAN: *Dokl. Akad. Nauk. SSSR*, **77**, 855 (1951)

Lajos MÉSZÁROS Béla LENGYEL Tibor GARAI	}	H-1112 Budapest, Budaörsi út 45.
---	---	----------------------------------

## STUDIES WITH INORGANIC PRECIPITATE MEMBRANE

MEMBRANE SELECTIVITY FROM MULTIIONIC POTENTIAL AND  
CONDUCTIVITY MEASUREMENTS

M. N. BEG<sup>1</sup>, R. SHYAM<sup>2\*</sup> and R. P. KHANDELWAL<sup>2</sup>

<sup>1</sup> *Department of Chemistry, Aligarh Muslim University, Aligarh-202001,*

<sup>2</sup> *Department of Chemistry, Bipin Bihari Post-Graduate College, Jhansi-284001, India)*

Received April 3, 1981

Accepted for publication May 25, 1981

Biionic and multiionic potentials using various combinations of 1 : 1 electrolytes at different concentrations across cobalt-sulphide membrane have been measured. Membrane conductivity values in contact with single electrolyte have been experimentally determined in order to evaluate membrane selectivity using the predetermined values of intramembrane mobility ratio. The selectivity sequence of the membrane has been found as  $K^+ > Na^+ > Li^+$ , which on the basis of EISENMAN–SHERRY model of membrane selectivity indicates the weak field strength of the charged groups attached to the membrane matrix. Three different methods based on various integrated forms of NERNST–PLANCK flux equation have been used in order to derive the potentiometric selectivity constant  $K_{ij}^{Pot}$  of the membrane. The values of  $K_{ij}^{Pot}$  derived from three methods were closer to each other.

### Introduction

In a series [1–8] of communications on the basis of EISENMAN–SHERRY model [9, 10] of membrane selectivity and by using theories for membrane potential based on thermodynamic considerations, we have demonstrated the small fixed charge density at the skeleton of parchment supported inorganic precipitate membranes. In this paper the biionic and multiionic potential measurements for cobalt-sulphide membrane are described for the evaluation of membrane selectivity for ions. Membrane conductance in contact with various 1 : 1 electrolyte solutions have also been experimentally determined in order to substantiate our findings.

### Experimental

The membrane was prepared by the method of interaction suggested by BEG and SHYAM [2]. To precipitate these substances in the interstices of the parchment paper, 0.2 M solution of sodium sulphide was kept inside the glass tube, to one end of which was tied the parchment paper previously soaked in water. This was suspended for 72 h in a 0.2 M solution

\* To whom correspondence should be addressed.

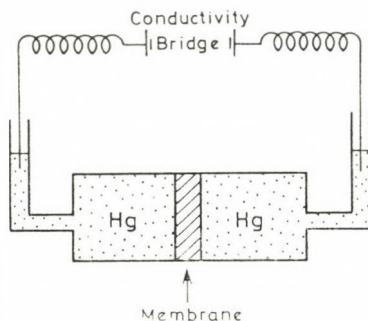
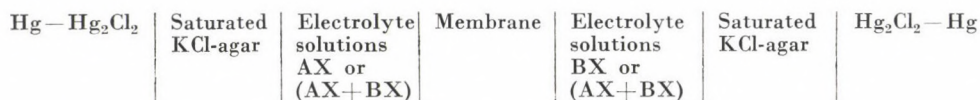


Fig. 1. Cell for measuring electrical conductivity of membrane

of cobalt chloride. The two solutions were interchanged later and kept for another 72 h. The membrane was washed with deionized water for the removal of free electrolyte. The biionic and multiionic potentials were measured by constructing an electrochemical cell of the following type using a Pye-precision vernier potentiometer



The solutions on both sides of the membrane were vigorously stirred by electrically operated magnetic stirrer to remove completely or to minimize the effect of film controlled diffusion [11].

Electrical conductivity of the membrane was determined by setting up a cell of the type shown in (Fig. 1) using a conductivity bridge (Cambridge Instrument Co. Ltd., England). All measurements were carried out at  $25 \pm 0.1$  °C. The error in measurement of membrane potential was within  $\pm 1.0\%$  whereas the electrical conductance could be measured to better than 99.5% accuracy.

## Results and Discussion

When an ion-exchange membrane is interposed between two solutions of an electrolyte at different concentrations the mobile species penetrate the membrane and various transport phenomena are induced in the system [12]. An electrical potential across the membrane is generated which is called concentration potential or membrane potential. The sign and magnitude of the emf give the selectivity of the membrane towards the ions of electrolyte. If the membrane is used for two separate electrolyte solutions of the type AX and BX (or AX and AY), the steady potential developed is called biionic potential  $E_{BIP}$  [13]. The BIP has been considered by HELFFERICH [14] in accordance with the concepts of the TMS theory [15, 16] as being the algebraic sum of two interfacial potentials and an internal diffusion potential. A complete mathematical discussion under conditions of (a) membrane diffusion control, (b) film diffusion control and (c) coupled membrane film diffusion control has been presented. For a general case involving complete membrane diffusion

control, the total biionic potential for ions of equal valence is given by

$$E = \frac{RT}{ZF} \ln \bar{D}_i a'_i \bar{\gamma}_j / \bar{D}_j a''_i \bar{\gamma}_i \quad (1)$$

where  $a'_i/a''_i$ ,  $\bar{D}_i/\bar{D}_j$ ,  $\bar{\gamma}_i/\bar{\gamma}_j$  are the activity ratios of solutions, diffusion coefficient of ions in membrane phase and the ratio of the activity coefficient of ions;  $R$ ,  $T$ ,  $Z$  and  $F$  have their usual meaning. Equation (1) reduces to the form (eq. 2) by WYLLIE and KANAAN [17, 18].

$$E = \frac{RT}{F} \ln a_i \bar{U}_i / a_j \bar{U}_j \quad (2)$$

provided  $\bar{\gamma}_i = \bar{\gamma}_j$  and diffusion coefficients are replaced by mobilities [17]. WYLLIE [18] expressed the intramembrane mobility ratio as

$$\bar{U}_i / \bar{U}_j = \bar{t}_i / \bar{t}_j = \bar{m}_i \bar{\lambda}_i / \bar{m}_j \bar{\lambda}_j \quad (3)$$

where  $\bar{t}_i/\bar{t}_j$  is the intramembrane transference ratio,  $\bar{m}_i$  and  $\bar{m}_j$  are the steady state equilibrium concentration of  $i$  and  $j$  in the respective junction zone.  $\bar{\lambda}_i$  is the conductivity of the membrane when it is wholly in  $i$  form and  $\bar{\lambda}_j$  is the conductivity of the membrane when it is wholly in  $j$  form. Further more, it was shown that  $\bar{m}_i/\bar{m}_j = K_{ji} \cdot K_{ji}$  is the selectivity. This on substitution into equation (3) gives

$$\bar{U}_i / \bar{U}_j = K_{ji} (\bar{\lambda}_i / \bar{\lambda}_j) \quad (4)$$

Thus the ratio of mobilities was related to the chemical and electrical properties of the membrane.

Biionic potential measurements were also carried out by interposing the membrane between two different electrolyte solutions at the same concentration. The values of biionic potentials across parchment supported cobalt-sulphide membrane with various 1:1 electrolyte combinations at different concentrations are given in Table I. Equation (2) was used to evaluate the intramembrane mobility ratio  $\bar{U}_i/\bar{U}_j$ , given in Table II. An interesting point with the values of  $\bar{U}_i/\bar{U}_j$  is the fact that the mobility ratio goes through a considerable change with the concentration of the external electrolyte solution.

In order to have a knowledge of selectivity  $K_{ij}$  from the predetermined values of  $\bar{U}_i/\bar{U}_j$ , the ratio of electrical conductivities  $\lambda_i/\lambda_j$  as demanded by equation (4), must be known. Membrane conductance measurements were carried out when it was wholly in the form  $i$  or wholly in the form  $j$ . The values of membrane conductances at various electrolyte concentrations are given in Table III. The values of membrane conductances are relatively more dependent

**Table I**

*Experimentally observed values of biionic potentials E (mV) across parchment supported cobalt-sulphide membrane*

Concentration (M)	Electrolyte pair		
	KCl—NaCl	KCl—LiCl	NaCl—LiCl
0.1/0.1	2.4	7.6	6.5
0.05/0.05	3.5	8.5	7.2
0.02/0.02	4.8	10.1	8.5
0.01/0.01	6.5	15.5	10.4
0.005/0.005	7.2	17.6	11.5
0.002/0.002	8.3	21.6	12.2
0.001/0.001	9.8	23.5	15.4

**Table II**

*Values of the intramembrane mobility ratios of various 1 : 1 electrolyte ion pairs*

Concentration (M)	Electrolyte ion pair		
	$\bar{U}_{K^+}/\bar{U}_{Na^+}$	$\bar{U}_{K^+}/\bar{U}_{Li^+}$	$\bar{U}_{Na^+}/\bar{U}_{Li^+}$
0.1/0.1	1.09	1.34	1.28
0.05/0.05	1.13	1.39	1.32
0.02/0.02	1.20	1.48	1.39
0.01/0.01	1.28	1.82	1.49
0.005/0.005	1.32	1.98	1.56
0.002/0.002	1.38	2.31	1.60
0.001/0.001	1.46	2.42	1.82

**Table III**

*Experimentally observed values of membrane conductance (MHOS) for monovalent electrolytes at various concentrations at  $25^\circ \pm 0.1^\circ \text{C}$*

Concentration (M)	Electrolytes		
	KCl	NaCl	LiCl
0.1/0.1	$0.88 \times 10^{-2}$	$0.77 \times 10^{-2}$	$0.67 \times 10^{-2}$
0.05/0.05	$0.64 \times 10^{-2}$	$0.48 \times 10^{-2}$	$0.40 \times 10^{-2}$
0.02/0.02	$0.34 \times 10^{-2}$	$0.25 \times 10^{-2}$	$0.20 \times 10^{-2}$
0.01/0.01	$2.30 \times 10^{-3}$	$1.50 \times 10^{-3}$	$1.55 \times 10^{-3}$
0.005/0.005	$2.00 \times 10^{-3}$	$1.35 \times 10^{-3}$	$1.30 \times 10^{-3}$
0.002/0.002	$1.60 \times 10^{-3}$	$0.90 \times 10^{-3}$	$0.85 \times 10^{-3}$
0.001/0.001	$1.18 \times 10^{-3}$	$0.60 \times 10^{-3}$	$0.55 \times 10^{-3}$

upon the concentration of electrolyte within the membrane as depicted in Fig. 2. This implies that the membrane has a relatively high DONNAN uptake of anion and a low selectivity constant value. The values of selectivity  $K_{ij}$  evaluated from the ratio of electrical conductivity and intramembrane mobility ratio using the data from Table II and III are given in Table IV. The intramembrane mobility ratio values also refer to the selectivity sequence of the membrane for the cations as follows;



This order of selectivity on the basis of the EISENMAN—SHERRY model of membrane selectivity [9, 10] point towards the weak field strength of the charged groups attached to the membrane matrix. This is in accordance with

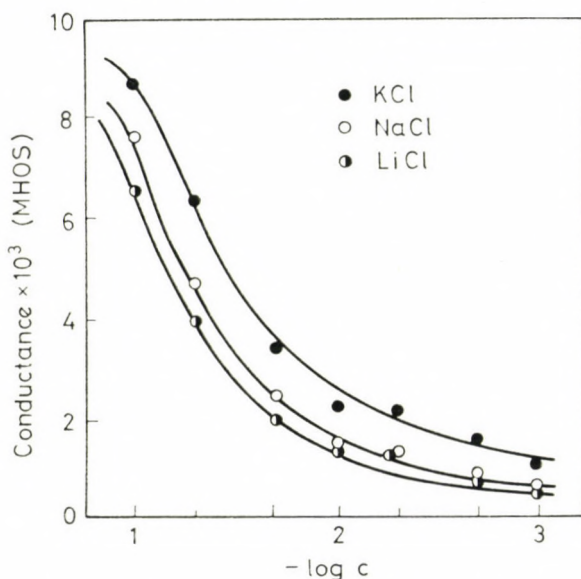


Fig. 2. Plots of conductance  $\times 10^3$  (MHOS) vs.  $\log C$  for cobalt-sulphide membrane

Table IV

Values of the selectivity  $K_{ji}$  ( $K_{ij} \approx 1/K_{ji}$ ) evaluated from intramembrane mobility ratio and the ratio of electrical conductivities at various electrolyte concentrations

Selectivity	Concentration (M)						
	0.1/0.1	0.05/0.05	0.02/0.02	0.01/0.01	0.005/0.005	0.002/0.002	0.001/0.001
$K_{Na, K}$	0.95	0.84	0.88	0.83	0.78	0.77	0.79
$K_{Li, K}$	1.02	0.86	0.87	1.22	1.29	1.22	1.21
$K_{Li, Na}$	1.12	0.82	0.81	1.01	1.02	0.85	0.97

an earlier finding of charge density determinations of cobalt-sulphide membrane [2].

A number of methods [19–24] have been suggested for the determination of potentiometric selectivity constant  $K_{ij}^{\text{Pot}}$  using a mixture of electrolytes on the two sides of the membrane and measuring the potential developed across it. The general equation for membrane potential (eq. 5) in an electrochemical cell of the type



has been derived following the tenets of the fixed charge theory of membrane potential and by integrating the NERNST–PLANCK flux equation for diffusion [16].

$$B = \frac{nRT}{F} \ln [(a'_i)^{1/n} + (K_{ij}^{\text{Pot}} a'_j)^{1/n}] [(a''_i)^{1/n} + (K_{ij}^{\text{Pot}} a''_j)^{1/n}] \quad (5)$$

where  $K_{ij}^{\text{Pot}} = K(\bar{U}_j/\bar{U}_i)$

If  $n = 1$  and the concentrations on side (") are held constant, eq. (5) can be written as

$$E = \text{Const} + \frac{RT}{F} \ln [a_i + (K_{ij}^{\text{Pot}} a_j)] \quad (6)$$

Various aspects of eq. (5) and (6) have been discussed and reviewed by LAKSHMINARAYANAIAH [25, 26]. Equation (6) has been used in three different ways for the evaluation of potentiometric selectivity constant  $K_{ij}^{\text{Pot}}$ . In the first procedure electrical potential across the electrochemical cell, containing both the primary ions (*i.e.*,  $i$  and  $j$ ) on the side (') and only one type of ion on the other side (")<sup>1</sup> (*i.e.*,  $a_j = 0$  and  $i = 1$ ), is measured. For this condition eq. (6) reduces to

$$E_1 = E^\circ + \frac{RT}{F} \ln a_1 \quad (7)$$

In another experiment the other ion (*i.e.*,  $j = 2$ ) is taken on the side (") (*i.e.*,  $i = 0$ ). Then eq. (6) reduces to

$$E_2 = E^\circ + \frac{RT}{F} \ln K_{ij}^{\text{Pot}} a_2 \quad (8)$$

For the condition  $a_1 = a_2$ , eqs (7) and (8) give at 25 °C, the relation

$$\log K_{ij}^{\text{Pot}} = E_2 - E_1/59.2 \quad (9)$$

Table V

Values of selectivity constant ( $K_{ij}^{\text{Pot}}$ ) for parchment supported membrane obtained employing various methods

Selectivity constant	Method		
	I	II	III
Selectivity constant			
$K_{K-Na}$	1.18	1.30	1.15
$K_{K-Li}$	1.28	1.60	1.17
$K_{Na-Li}$	1.13	1.50	1.10

The values of  $K_{ij}^{\text{Pot}}$  derived by this method [23, 24] using eq. (9) for cobalt-sulphide membrane are given in Table V. In the second procedure [21–25]

the potentials are measured as in the first procedure but the concentration of the solutions of ion  $i$  as well as that of ion  $j$  on the side (") is varied and the successive potentials  $E_1 \dots$ , and  $E_2 \dots$  are measured. A pair of plots (Fig. 3) between  $E_1$  vs.  $a_1$  as well as  $E_2$  vs.  $a_2$  are drawn. Now the concentration of the solution containing ion  $i$  and of ion  $j$  are so chosen that  $E_1 = E_2$ , then eqs (7) and (8) give

$$K_{ij}^{\text{Pot}} = a_1/a_2 \quad (10)$$

The values of  $K_{ij}^{\text{Pot}}$  thus derived for the membrane using various 1 : 1 electrolyte combinations are given in Table V. In the third method [21–24]

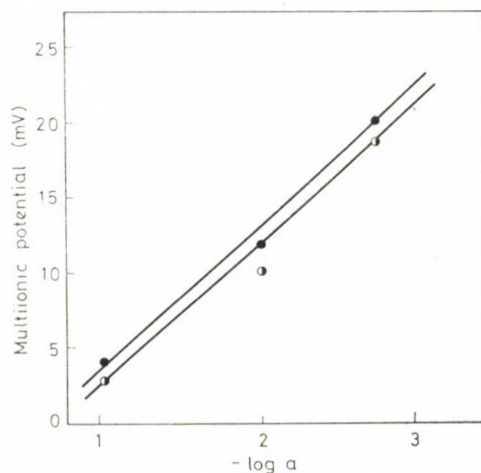


Fig. 3. Plots of multiionic potentials (mV) vs. logarithm of activity using cobalt-sulphide membrane

both the primary ions on the side (") are utilized in the test solution instead of only one ion used in procedures I and II. The potential  $E^*$  developed across the cell for this type of system, according to eq. (6) is given by

$$E^* = E^\circ + \frac{RT}{F} \ln (a_1 + K_{ij}^{\text{Pot}} a_2). \quad (11)$$

Combining eqs (7) and (11) we have

$$E^* - E_1 = \frac{RT}{F} \ln \frac{(a_1 + K_{ij}^{\text{Pot}} a_2)}{a_1} \quad (12)$$

which on rearrangement gives an explicit expression for  $K_{ij}^{\text{Pot}}$  i.e.,

$$\left[ \exp \left\{ \frac{(E^* - E_1) F}{RT} \right\} a_1 - a_1 \right] = K_{ij}^{\text{Pot}} a_2 \quad (13)$$

Equation (13) predicts a linear relationship between  $\exp \left\{ \frac{(E^* - E_1) F}{RT} \right\} a_1 - a_1$  and  $a_2$ , the slope of which gives the value of  $K_{ij}^{\text{Pot}}$ . The straight line plots from the experimental data, depicted in Fig. 3, are in full agreement with the prediction of eq. (13). The values of  $K_{ij}^{\text{Pot}}$  (Table V) derived from the slopes of the lines are comparable to those derived by the previous procedures. A little difference may be attributed to the graphical procedure adopted for the evaluation of the data. It may be concluded that the membrane is weakly selective and the methods developed recently from the theoretical considerations may be utilized for the determination of potentiometric selectivity of the membrane-electrolyte systems under investigation and such other systems.

#### REFERENCES

- [1] SIDDI, I., F. A., LAKSHMINARAYANAIAH, N., BEG, M. N.: *J. Polymer Sci.*, **9**, 2853, 2869 (1971)
- [2] BEG, M. N., SIDDIQI, F. A., SHYAM, R.: *Can. J. Chem.*, **55**, 1680 (1977)
- [3] BEG, M. N., SIDDIQI, F. A., SHYAM, R., ALTA, I.: *J. Electroanal. Chem.*, **98**, 140 (1979)
- [4] BEG, M. N., SIDDIQI, F. A., SHYAM, R., ARSHAD, M.: *J. Membrane Sci.*, **2**, 365 (1977)
- [5] SIDDIQI, F. A., BEG, M. N., PRAKASH, P.: *J. Electroanal. Chem.*, **80**, 223 (1977)
- [6] BEG, M. N., SIDDIQI, F. A., SHYAM, R., ARSHAD, M.: *Proc. Indian J. INSA*, **45A** (6), 543—557 (1979)
- [7] SIDDIQI, F. A., BEG, M. N., SINGH, S. P., HAQ, A.: *Bull. Chem. Soc. Japan*, **49**, 2858, 2864 (1976)
- [8] BEG, M. N., SHYAM, R., BEG, M. M.: *J. Polymer Sci.* (1979)
- [9] EISENMAN, G.: *Membrane Transport and Metabolism*, Editor KLEINZER, A., KOTYK, A., Academic Press, New York, 163 (1961); *Biophys. J. suppl.*, **2**, 259 (1962)
- [10] SHERRY, H.: "Ion Exchange", Editor, MARINSKY, J. A.: Dekker New York, 2 (1968)
- [11] SCATCHARD, G., HELFFERICH, F.: *Disc. Faraday Soc.*, **21**, 70 (1956)
- [12] KOBATAKE, Y., KAMO, N.: *Prog. Sci. Japan*, **5**, 257 (1973)

- [13] WILSON, J. R.: "Deminalisation by electrolysis", Butterworth, London and Washington, D. C. 84 (1960)
- [14] HELFFERICH, F.: "Ion Exchange", Mc Graw Hill, New York, 1962
- [15] TEORELL, T.: Proc. Soc. Expt. Biol. Med., **33**, 282 (1935); Proc. Natl. Acad. Sci., (USA), **21**, 152 (1935); Z. Electrochem., **55**, 460 (1951); Prog. Biophys. Chem., **3**, 385 (1953)
- [16] MEYER, K. H., SIEVERS, J. F.: Helv. Chim. Acta, **19**, 649, 665, 987 (1936)
- [17] WYLLIE, M. R. J., KANAAN, S. L.: J. Phys. Chem., **58**, 73 (1954)
- [18] WYLLIE, M. R. J.: J. Phys. Chem., **58**, 67 (1954)
- [19] BUCK, R. P.: J. Anal. Chem., **48**, 2312 (1976)
- [20] BUCK, R. P.: Electroanalytical Chemistry of Membrane, March, 323 (1976)
- [21] SRINIVASAN, K., RECHNITZ, G. A.: Anal. Chem., **41**, 1203 (1969)
- [22] LAKSHMINARAYANAIHAH, N.: "Membrane Electrode". Academic Press, New York, 124 (1976)
- [23] RECHNITZ, G. A.: Chem. Eng. News, **45** (25), 146 (1967)
- [24] LIGHT, T. S., SWARTZ, J. L.: Anal. Lett., **1**, 825 (1968)
- [25] LAKSHMINARAYANAIHAH, N.: "Transport Phenomena in Membrane", Academic Press, New York 1969
- [26] LAKSHMINARAYANAIHAH, N.: Chem. Rev., **65**, 491 (1965)

Mohd. Nasim BEG

Department of Chemistry, University of Calabar 1115, Nigeria

Radhey SHYAM

Rameshwer Prasad KHANDELWAL

} Department of Chemistry, Bipin Bihari P. G. College, Jhansi-284001, India



## MÖSSBAUER AND MAGNETIC STUDIES ON HYDROXO-BRIDGED IRON(III) COMPLEXES OF SOME OXIMES

I. RANI<sup>1</sup>, K. B. PANDEYA<sup>1\*</sup>, G. L. SAWHNEY<sup>2</sup> and J. S. BAIJAL<sup>2</sup>

<sup>1</sup> *Department of Chemistry, University of Delhi, Delhi-110007,*

<sup>2</sup> *Department of Physics and Astrophysics, University of Delhi, Delhi-110007, India)*

Received November 17, 1980

In revised form May 13, 1981

Accepted for publication May 26, 1981

Iron(III) forms complexes of general composition  $\text{FeL}_2\text{OH}$  with dimethylglyoxime and salicylaldoxime and  $\text{FeL}_2\text{OH}$  and  $\text{FeL}(\text{OH})_2$  with 2-hydroxy-3-methoxybenzaldoxime (all ligands abbreviated as HL). Magnetic moments, infrared spectra and Mössbauer spectra of the complexes have been reported and discussed for iron(III).

### Introduction

Considerable interest has been shown in the study of bridged hydroxo complexes during the last decade because of polynuclear iron clusters having been recognized as important entities in the metal bonding sites of a number of proteins and enzymes. The present paper describes hydroxo-bridged iron(III) complexes of dimethylglyoxime (Hdmg), salicylaldoxime (Hsal) and 2-hydroxy-3-methoxybenzaldoxime (Hhmb). Dimethylglyoxime (Hdmg) has been the first selective organic reagent used in inorganic analysis. Structural studies of metal complexes of this ligand have also been performed in detail. BURGER *et al.* have reported [1] a low-spin octahedral iron(III) complex of dimethylglyoxime  $\text{Na}[\text{Fe}(\text{dmg})_2(\text{OH})_2]$  and made also its Mössbauer study [10]. We have prepared the complex  $\text{Fe}(\text{dmg})_2\text{OH}$  which shows magnetic and Mössbauer properties of a hydroxo-bridged high-spin iron(III) complex. Reactions of salicylaldoxime (Hsal) with iron(III) have earlier been studied [2] in solution and the existence of three different complex species  $[\text{Fe}(\text{HL})]^{3+}$ ,  $[\text{FeLH}(\text{OH})_2]^+$  and  $[\text{FeLH}(\text{OH})_3]^-$  at different pH values have been suggested. In the present studies we have isolated the complex  $\text{Fe}(\text{sal})_2\text{OH}$ . With 2-hydroxy-3-methoxybenzaldoxime (Hhmb), two complexes, viz.,  $\text{Fe}(\text{hmb})_2\text{OH}$  and  $\text{Fe}(\text{hmb})(\text{OH})_2$ , have been prepared under different experimental conditions.

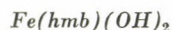
\* To whom correspondence should be addressed

## Experimental

### Preparation of complexes



Solutions of iron(III) perchlorate (aqueous) and the ligand (ethanolic) were mixed together in 1 : 2 metal-ligand ratio. Sodium hydroxide solution was added dropwise until a dark brown complex separated. It was filtered, washed with water and finally with 50% ethanol. The complexes were dried in an electric oven at  $\sim 70^\circ\text{C}$ .



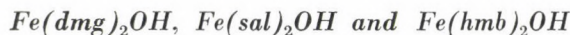
Solution of iron(III) perchlorate (aqueous) and the ligand (ethanolic) was mixed in 1 : 1 ratio and sodium acetate solution was added dropwise until a reddish brown complex separated. It was filtered, washed with water and finally with dilute ethanol.

The  $FeL_2(OH)$ -type complexes are insoluble in water and soluble in alcohol and other common organic solvents while the complex  $Fe(hmb)(OH)_2$  is insoluble in water as well as in chloroform and benzene but partially soluble in alcohol. The elemental analysis data are presented in Table I.

### Physical measurements

Magnetic susceptibility measurements on powdered solid complexes were made at room temperature ( $300^\circ\text{K} \pm 1^\circ\text{K}$ ) on a Gouy balance using mercury tetrathiocyanato cobaltate(II) ( $\chi_g = 16.44 \times 10^{-6}$  c.g.s. units). Infrared spectra were recorded on a Perkin-Elmer 137 spectrophotometer in KBr medium. Mössbauer studies were carried out by using a 15 mCi  $Co^{57}$  source (in Pd) held at room temperature. The samples were finely powdered and cooled to liquid nitrogen temperature in a cryostat. The Mössbauer absorption spectra were obtained using a spectrometer in MCS mode in conjunction with a 512 multichannel analyser. The velocity calibration was done, using an enriched iron absorber (NEN). Sufficient counts were stored in each channel and the data from multichannel analyser were reduced by means of a least square fitting programme run on an IBM 360 computer.

## Results and Discussion



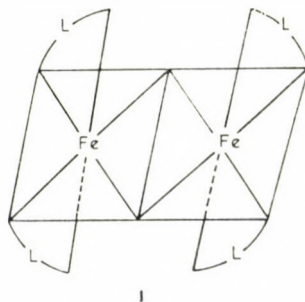
These complexes show magnetic moments in the range 4.0–4.3 B. M. in contrast to the magnetic moments of BURGER *et al.* [10] for Fe(III) dm $\bar{g}$ . Iron(III) ion has five d-electrons so that the possible ground states are  $(t_{2g})^3(e_g)^2$  ( $S = 5/2$ ),  $(t_{2g})^4(e_g)^1$  ( $S = 3/2$ ) and  $(t_{2g})^5$  ( $S = 1/2$ ). Magnetic moments in all the cases are much higher for the doublet ground state. Quartet ground state in iron(III) complexes is not very common and is usually observed for a specific class of compounds [9], which show Mössbauer properties quite different from those of the complexes under study. Mössbauer parameters of our complexes are clearly suggestive of high-spin iron(III). The observed lower magnetic moments than 5.92 B. M. may arise due to antiferromagnetic interaction between iron(III) centres of  $S = 5/2$ . The alternative possibility of spin-state equilibrium should lead to temperature dependent Mössbauer quadrupole splitting [3b], while the complexes under study show remarkably temperature independent Q. S. values.

**Table I**  
*Colour, composition and magnetic moment of the complexes*

Complex	Colour	Elemental analysis, found (calculated)				$\mu_{\text{eff}}$ B.M.
		M%	C%	H%	N%	
Fe(dmg) <sub>2</sub> OH	Dark brown	17.97 (18.48)	31.02 (31.68)	4.55 (4.92)	18.33 (18.48)	4.28 (2.1) <sup>a</sup>
Fe(sal) <sub>2</sub> OH	Dark brown	16.85 (16.23)	48.59 (48.69)	3.59 (3.76)	8.23 (8.11)	4.13 (4.9) <sup>a</sup>
Fe(hmb) <sub>2</sub> OH	Dark brown	13.44 (13.82)	47.23 (47.40)	4.20 (4.19)	6.82 (6.91)	4.03
Fe(hmb)(OH) <sub>2</sub>	Dark reddish brown	20.80 (21.87)	37.80 (37.50)	3.84 (3.90)	5.39 (5.47)	3.04

<sup>a</sup> Data of BURGER *et al.* [10]

Keeping in view the composition of the complexes and the bidentate nature of the ligands the following dihydroxo-bridged structure may be considered. Such a structure is quite common in iron(III) chemistry and is in



line with the existence of the dimer  $[\text{Fe}(\text{H}_2\text{O})_4(\text{OH})_2\text{Fe}(\text{H}_2\text{O})_4]^{4+}$  in aqueous solution. Dihydroxo-bridging of this type may give rise to moderate antiferromagnetic exchange interaction causing only small lowering in the magnetic moment value as observed in these complexes. This may be further confirmed by susceptibility data. The characteristic Fe—O—Fe antisymmetric vibrations in such complexes are known to absorb at  $\sim 950 \text{ cm}^{-1}$  in the infrared spectra. Fe(sal)<sub>2</sub>OH and Fe(dmg)<sub>2</sub>OH, both show medium non-ligand bands at  $960 \text{ cm}^{-1}$ . The spectrum of Fe(hmb)<sub>2</sub>OH contains strong ligand bands at this position.

Mössbauer parameters for these complexes are given in Table II. The isomer shift values lie in the range  $0.54\text{--}0.69 \text{ mm sec}^{-1}$  ( $300 \text{ }^\circ\text{K}$ ), which is indicative of an  $S = 5/2$  iron(III) state [3a]. Quadrupole splitting values

**Table II**  
*Mössbauer parameters*

Complex	Temp. (°K)	I. S. <sup>a</sup> (mm sec <sup>-1</sup> )	Q. S. <sup>b</sup> (mm sec <sup>-1</sup> )	HW <sub>h</sub> <sup>c</sup> (mm sec <sup>-1</sup> )	HW <sub>l</sub> <sup>d</sup> (mm sec <sup>-1</sup> )	$\frac{HW_h^e}{HW_l}$
Fe(dmg) <sub>2</sub> OH	300	0.54 (0.17) <sup>f</sup>	0.70 (0.72) <sup>f</sup>	0.59	0.70	0.84
	78	0.84 (0.28) <sup>f</sup>	0.68 (0.70) <sup>f</sup>	0.48	0.94	0.51
Fe(sal) <sub>2</sub> OH	300	0.63	0.97	0.64	0.57	1.12
	78	0.77 (0.77) <sup>g</sup>	0.94 (0.9) <sup>g</sup>	0.94	0.77	1.22
Fe(hmb) <sub>2</sub> OH	300	0.69	0.72	0.40	0.50	0.80
	78	0.78	0.78	0.46	0.42	1.09
Fe(hmb)(OH) <sub>2</sub>	300	0.62	1.33	0.31	0.41	0.76
	78	0.78	1.34	0.44	0.38	1.16

<sup>a</sup> Values are relative to sodium nitroprusside absorber

<sup>b</sup> I. S. and Q. S. accurate upto  $\pm 0.04$  mm sec<sup>-1</sup>

<sup>c</sup> HW = full width at half height HW<sub>h</sub> and HW<sub>l</sub> refer to peaks at high and low energy, respectively

<sup>d</sup> Error is generally less than 0.04 mm sec<sup>-1</sup>

<sup>e</sup> Error is less than 0.1

<sup>f</sup> Data of BURGER *et al.* [10]

<sup>g</sup> Data of BURGER *et al.* [11] (relative to sodium nitroprusside)

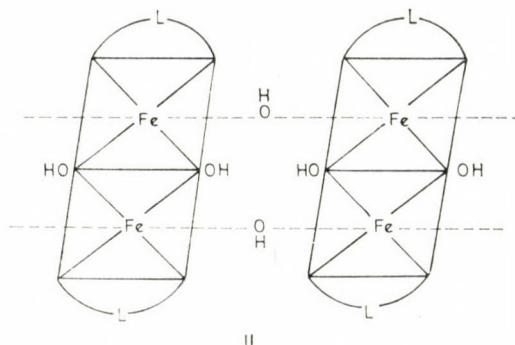
(0.70—0.97 mm sec<sup>-1</sup>) lie in the range for high-spin iron(III) complexes [4, 5]. In iron(III) complexes there is no valence contribution to the Q. S. The only source of Q. S., therefore, remains the lattice contribution arising mainly from the asymmetry of the ligand field, which is further supported by the temperature independence of the Q. S. values.

All the three complexes show asymmetry effect in the spectra as expected for dimeric iron(III) compounds [6]. The half width ratios are temperature dependent for Fe(dmg)<sub>2</sub>OH and Fe(hmb)<sub>2</sub>OH and temperature independent for Fe(sal)<sub>2</sub>OH. The asymmetry of the quadrupole doublet may be attributed to the interaction of the nucleus with fluctuating electric and magnetic field. Fluctuations due to spin-lattice relaxations cause a temperature dependent and concentration independent asymmetry and those due to spin-spin relaxation give temperature independent and concentration dependent asymmetry [7, 8]. Fe(dmg)<sub>2</sub>OH and Fe(hmb)<sub>2</sub>OH for which asymmetry is temperature dependent, involve spin-lattice relaxation. Since concentration dependence has not been studied, spin-spin relaxation can also not be ruled out. Fe(sal)<sub>2</sub>OH shows temperature independent asymmetry and hence involves spin-spin and not spin-lattice relaxation.

These investigations strongly support the suggestion that dmg can form high-spin iron(III) complexes besides the low-spin ones reported by BURGER *et al.* [10].

$Fe(hmb)(OH)_2$ 

When sodium acetate instead of sodium hydroxide is added to the reaction mixture, a complex of composition  $FeL(OH)_2$  is obtained in the case of Hhmb. With Hdmg and Hsal complexes of such composition can not be prepared. For  $Fe(hmb)(OH)_2$  a polymeric structure of the type (II) may be proposed.



Additional antiferromagnetic exchange interaction *via* hydrogen bridging between two adjacent planar  $Fe(hmb)(OH)_2$  units may account for the lower magnetic moment value of the complex (Table I).

Mössbauer parameters for the complex are given in Table II. The isomer shift value of  $0.62 \text{ mm sec}^{-1}$  ( $300^\circ\text{K}$ ) is in the range characteristic for high-spin iron(III) compounds [3a]. The quadrupole splitting value is larger than those for  $Fe(\text{ligand})_2(OH)$ -type complexes. Comparatively larger asymmetry of the ligand field is obvious with structure (II). This complex also shows asymmetry of the quadrupole doublet, which is temperature dependent. The observation is suggestive of spin-lattice relaxation of the magnetic hyperfine interaction in addition to the possible spin-spin relaxation.

\*

Thanks are due to University Grants Commission, New Delhi for awarding J. R. F. to one of us (Indra RANI).

## REFERENCES

- [1] BURGER, K., RUFF, I., RUFF, F.: *J. Inorg. Nucl. Chem.*, **27**, 179 (1965)
- [2] MONOLOV, K. R.: *Russ. J. Inorg. Chem.*, **12**, 1431 (1967)
- [3] GREENWOOD, N. N., GIBB, T. C.: "Mössbauer Spectroscopy", Chapman and Hall, London, 1971 (a) p. 162 (b) p. 206.
- [4] BERRETT, R. R., FITZSIMMONS, B. W., OWUSU, A.: *J. Chem. Soc. (A)*, **1968**, 1575

- [5] REIFF, W. M., BAKER, W. A. JR., ERICKSON, N. E.: J. Amer. Chem. Soc., **90**, 4794 (1968)  
[6] BANCROFT, G. M., MADDOCK, A. G., RANDL, R. P.: J. Chem. Soc. (A), **1968**, 2939  
[7] BLUME, M., JON, J. A.: Phys. Rev., **165** (2), 446 (1968) and references therein  
[8] WIGNALL, J. W. G.: J. Chem. Phys., **44**, 2461 (1966)  
[9] NAIRCTIOS, D., KOSTIKAS, A., SIMPOULOS, A., COUCOUVANIS, D., PILTINGSRUD, D.,  
COFFMAN, R. E.: J. Chem. Phys., **69**, 4411 (1978) and references therein  
[10] BURGER, K., KORECZ, L., MANUABER, I. B. A., MAC, P.: J. Inorg. Nucl. Chem., **28**, 1673  
(1966)  
[11] BURGER, K., KORECZ, L., VÉRTES, A.: Proc. Conf. Appl. Mössbauer Effect, Tihany 1969,  
Akadémiai Kiadó, Budapest, 721, 1971

I. RANI  
K. B. PANDEYA  
G. L. SAWHNEY  
J. S. BAIJAL

} University of Delhi, Delhi-110007, India

## THE MANNICH REACTION OF CEPHALOSPORIN SULFOXIDES AND SULFONES<sup>+</sup>

J. Cs. JÁSZBERÉNYI\*, I. PETRIKOVICS, E. T. GUNDA and S. HOSZTAFI

(*Research Group of Antibiotics, Hungarian Academy of Sciences, Debrecen, and Institute of Organic Chemistry, Kossuth Lajos University, Debrecen*)

Received April 29, 1979  
In revised form May 29, 1981  
Accepted for publication June 9, 1981

Cephalosporin *S*-sulfoxides and sulfones give 2-exomethylene derivatives under Mannich conditions, but the corresponding *R*-sulfoxides fail to react.

It is known that cephalosporin sulfoxides undergo a reaction under Mannich conditions to give 2-exomethylene cephalosporin derivatives [1, 2]. However, the *R* ( $\alpha$ )-sulfoxides (**1e**, **f**, **q**, **k**)\*\* (Scheme 1) remained unchanged [3]<sup>†</sup> if a mixture of cephalosporin *S*- and *R*-sulfoxides, or pure *R*-sulfoxide was heated in the presence of formaldehyde or paraformaldehyde and a secondary amine hydrochloride or trifluoroacetate [4, 5]<sup>×</sup> (1 day, in *t*-butyl alcohol-dichloromethane 7 : 1 at 65 °C inner temperature).

At a higher temperature both *R*- and *S*-sulfoxides are transformed (TLC). Using *R*/*S*-sulfoxide mixtures, the *S*( $\beta$ )-sulfoxides are converted to 2-exomethylene-cephalosporin sulfoxides (**2a–d**) within 5 hours (in *t*-butyl alcohol-dichloromethane-dioxane 4 : 1 : 6, inner temperature 85 °C). The corresponding *R*( $\alpha$ )-sulfoxides react slowly and required 24 hours of heating at this temperature. However, this reaction gave only the corresponding 2-exomethylene-cephem- $\beta$ -sulfoxides (**2a–d**) and some oily decomposition products, containing no  $\beta$ -lactam. The question arises, therefore, as to whether an *R*  $\rightarrow$  *S*-sulfoxide isomerization takes place first [6–8], followed by the known Mannich reaction of the *S*( $\beta$ )-sulfoxides. Heating of the sulfoxide mixture without a secondary amine salt and formaldehyde in a refluxing mixture of *t*-butyl alcohol-dichloromethane-dioxane (4 : 1 : 6) (inner temperature 85 °C) for 3 days resulted neither in changes of the *R*/*S* ratio, nor in decomposition

<sup>+</sup> Presented in part at the IUPAC International Symposium on Low Molecular Weight Sulfur Containing Natural Products, Jablonna/Warsaw, July 6–10, 1976

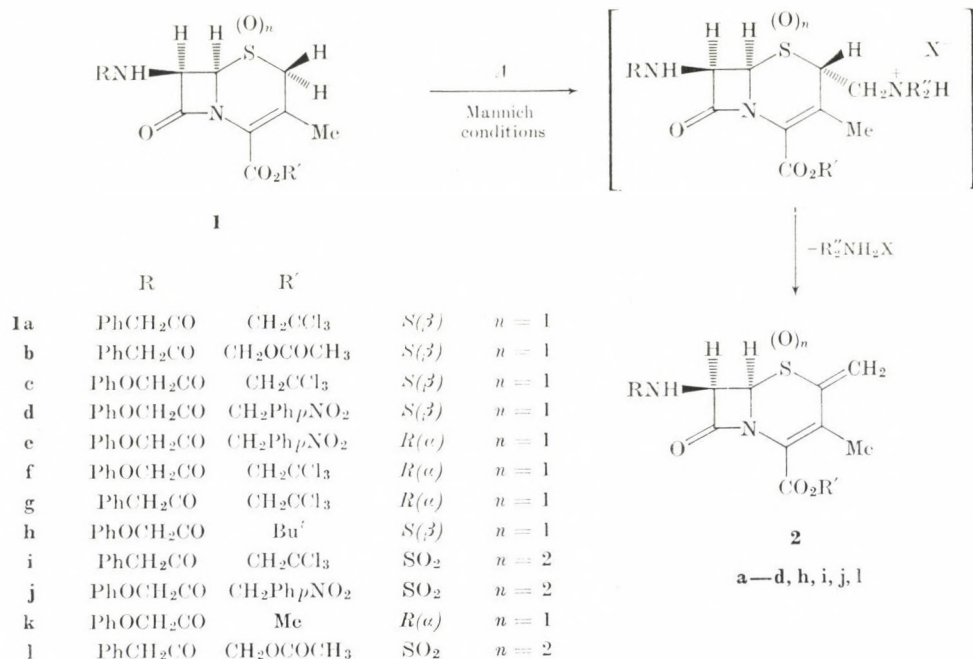
\* To whom correspondence should be addressed

\*\* All the compounds described here gave satisfactory elemental analysis and mass spectroscopy data; the IR and NMR data are consistent with the proposed structures

† BREMNER and CAMPBELL described similar reactivity differences of cephalosporin *S*( $\beta$ ) and *R*( $\alpha$ ) sulfoxides in attempted diazotransfer reactions [3]

× A similar trifluoroacetate (*N*-methylanilinium trifluoroacetate, TAMA) has recently been described as a useful reagent for the direct synthesis of  $\alpha$ -methylene ketones [5]

of the starting material. No changes were observed either in the attempted isomerization of pure *R*-sulfoxides under the above conditions. This shows that the non-cleavable cephalosporin sulfoxides do not undergo thermal iso-



Scheme 1

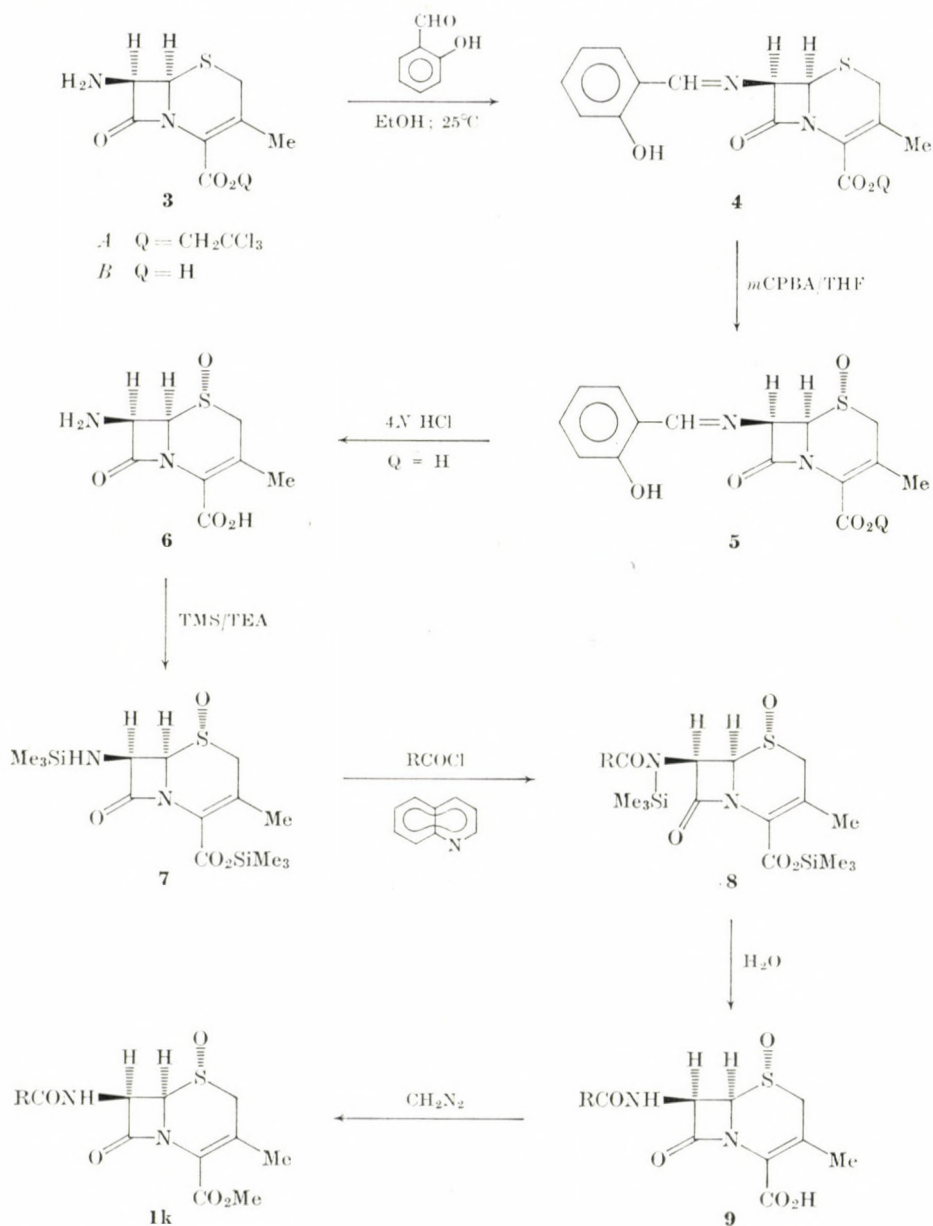
merization. In the presence of a secondary amine salt (diethylamine hydrochloride, dibenzylamine trifluoroacetate, dicyclohexylamine trifluoroacetate etc.) both *S*- and *R*-sulfoxides are decomposed upon heating in refluxing *t*-butyl alcohol-dichloromethane-dioxane (4 : 1 : 6) (inner temperature 85 °C) for one day.

Having prepared the corresponding pure *R*(α)-sulfoxides (*N,N*-dichlorourethane oxidation for the preparation of **1e** [9], Scheme 2 for **1f** [10]) the attempted Mannich reaction (*t*-butyl alcohol-dichloromethane-dioxane (4 : 1 : 6), 85 °C inner temperature, one day) gave only a dark oily complex mixture of β-lactam-free decomposition products.

The corresponding sulfones (**1i**, **j**, **l**) undergo a reaction of the Mannich type in dioxane-*t*-butyl alcohol-dichloromethane (4 : 3 : 2, inner temperature, 64 °C) to give the elimination products (**2i**, **j**, **l**), similarly to the cephalosporin *S*-sulfoxides, and sulfones of other types [12–15].\*

\* The authors are indebted to Dr. J. VERWEIJ for the unpublished experimental data concerning the preparation of cephalosporin *R*(α)-sulfoxides [11]

Since the 2-exomethylene-cephalosporin derivatives (**2a—d, h**) are formed from the corresponding *S*-( $\beta$ )-sulfoxides only, these findings indicate that the attack of the Mannich reagents presumably takes place from the less hindered



Scheme 2

$\alpha$ -face of the cephalosporin sulfoxides. Because of the steric sensitivity of the Mannich reaction, the oxidation needed for activation of the methylene  $\alpha$  to the sulphur prevents the formation of the Mannich base in the case of *R*-sulfoxides. Under more severe conditions an alternative pathway also exists, leading to decomposition products instead the desired 2-exomethylene cephalosporins.

This reaction is, therefore, not generally applicable to oxidized cephalosporins: 2-exomethylene cephalosporins can be prepared from *S*-sulfoxides and sulfones.

## REFERENCES

- [1] WRIGHT, I. G., ASHBROOK, C. W., GOODSON, T., KAISER, G. V., VAN HEYNINGEN, E. M. *J. Med. Chem.*, **14**, 420 (1971)
- [2] MURPHY, C. F., WEBBER, J. A.: in *Cephalosporins and Penicillins, Chemistry and Biology* (E. H. FLYNN, Ed.), Chapter 4, p. 138, Academic Press, New York and London 1972
- [3] BREMNER, D. H., CAMPBELL, M. M.: *J. Chem. Soc. Perkin Trans. I*, **1977**, 2298
- [4] HOSZTAFI, S.: Thesis, Debrecen, 1976
- [5] GRAS, J. L.: *Tetrahedron Lett.*, **1978**, 2111
- [6] CIONI, M., CIUFFARIN, E., GAMBAROTTA, S., ISOLA, M., SENATORE, L.: *J. Chem. Research (S)*, **1978**, 270
- [7] CIONI, M., CIUFFARIN, E., GAMBAROTTA, S., ISOLA, M., SENATORE, L.: *J. Chem. Research (M)*, **1978**, 3429
- [8] JOHNSON, C. R.: *J. Am. Chem. Soc.*, **85**, 1020 (1963)
- [9] JÁSZBERÉNYI, J. Cs., FARKAS, E. R., GUNDA, E. T., TAMÁS, J., MÁK, M., HOSZTAFI, S., SZILÁGYI, L., BOGNÁR, R.: *Acta Chim. Acad. Sci. Hung.*, **98**, 103 (1978)
- [10] DE KONING, J. J., MARX, A. F., POOT, M. M., SMID, P. M., VERWEIJ, J.: in "Recent Advances in the Chemistry of  $\beta$ -Lactam Antibiotics" (J. ELKS, Ed.), The Chemical Society, London, 1977, Chapter 17, p. 161
- [11] VERWEIJ, J. (Gist-Brocades, Delft): Personal Communication
- [12] BALIAH, V., SESHAPATHIRAO, M.: *J. Org. Chem.*, **24**, 867 (1959)
- [13] NOBLES, W. L., THOMPSON, B. B.: *J. Pharm. Sci.*, **54**, 576 (1965)
- [14] NOBLES, W. L., THOMPSON, B. B.: *J. Pharm. Sci.*, **54**, 709 (1965)
- [15] SPRY, D. O.: *Tetrahedron Lett.*, **1978**, 4751

Csaba J. JÁSZBERÉNYI  
 Ilona PETRIKOVICS  
 Tamás E. GUNDA  
 Sándor HOSZTAFI

H-4010 Debrecen, P. O. B. 22

## ERROR ANALYSIS OF A NEW POTENTIOMETRIC EVALUATION METHOD BASED ON THE MEASUREMENT OF THE BOUND REAGENT CONCENTRATION

K. BURGER<sup>1\*</sup>, L. DOMOKOS<sup>2</sup>, G. PETHŐ<sup>1</sup> and E. PUNGOR<sup>2</sup>

<sup>(1)</sup> *Institute of Inorganic and Analytical Chemistry, L. Eötvös University of Budapest,*

<sup>(2)</sup> *Institute for General and Analytical Chemistry, Technical University, Budapest)*

Received May 6, 1981

Accepted for publication June 9, 1981

Authors studied the conditions of the applicability of an earlier proposed potentiometric evaluation method [1].

The relationship between the stability constants of equilibrium reactions and the errors of the determination was shown for cases based on the formation of compounds of the composition 1 : 1 and 2 : 1. Authors examined also the influence of the individual experimental parameters exerted upon the error of the determination.

A new potentiometric evaluation method [1] is based on the fact that reactions characterized by low equilibrium constants can also be used in potentiometric analysis if the concentration of the bound titrant (and not the free one) is recorded as a function of the volume of the titrant. Saturation type curves are obtained in this way and the reaction reaches its saturation section when the reaction becomes quantitative as defined by the chemical equilibrium. The saturation value of this curve is equivalent to the concentration of the substance to be determined. The bound reagent concentration is obtained as the difference between the total concentration added during titration and the concentration of the free reagent measured potentiometrically. Naturally, it has to be corrected also for dilution. Thus the following formula is used for the calculation of the bound reagent concentration:

$$C_i - [X_i] = \frac{\left( \frac{V_i C_X}{V_0 + V_i} - 10^{\frac{E_i - E_0}{S}} \right) \frac{V_i + V_0}{V_0}}{n} \quad (1)$$

- where  $C_X$  is the concentration of the standard titrant solution;  
 $C_i$  is the actual total concentration of the titrant;  
 $[X_i]$  the free concentration of the titrant;  
 $V_i$  the actual consumption of titrant and  
 $E_i$  the actual electromotive force value in each titration point;

\* To whom correspondence should be addressed

- $E_0$  is the formal potential of the system;  
 $S$  the slope of the indicator electrode response;  
 $n$  the number of the reagent's molecules or ions X bound by the material (A) to be determined (mostly 1 or 2).

The  $C_i - [X_i]$  value at the saturation part of the curve represents  $C_A$ , the concentration to be determined.

The method is to be used when a reagent excess is needed to make the reaction proceed with analytical accuracy.

On the basis of equilibrium calculations [2] the lower limit of  $K$  equilibrium constant (e.g. protonation or complex stability constant) and the corresponding  $C_R$  reagent concentration in the titrated solution can be computed which makes still possible a determination of satisfying accuracy. For the analytical procedure based on the equilibrium



with an error of  $\Delta$  relative % due to the state of the equilibrium,  $C_R$  can be calculated by the equation

$$C_R = (100 - \Delta) \left( \frac{1}{\Delta \cdot K} + \frac{C_A}{100} \right) \quad (3)$$

where  $C_A$  is the total concentration to be determined and

$$\Delta = \frac{[A]}{C_A} \cdot 100 \quad (4)$$

Equation (3) defines the magnitude of the reagent concentration needed to ensure the required  $\Delta$  accuracy ( $K$  and  $C_A$  are given). It can be seen that with decreasing  $K$  the concentration of the substance to be determined must increase in order to keep the error at the same value. So, e.g. if we permit a 1% error in a system characterized by an equilibrium constant  $K = 10^3$ , the measurement can be performed in 0.1 M concentration, while in the case of  $K = 10^6$  it can be carried out even in a solution of  $10^{-4}$  M concentration.

Due to practical causes the determination may in general be performed if the saturation value of the bound reagent concentration can be attained with a reagent excess below 100%. If e.g. we have to determine a compound in 0.01 M concentration with a relative error below 0.5% with the help of a reaction having a  $K$  value of  $10^4$  (in the case of  $V_0 = 10 \text{ cm}^3$ ) the minimal  $C_R$  concentration necessary for the quantitative performance of the reaction is [on the basis of eq. (3)] 0.029 M. If we perform the titration with a 0.1 M

titrant, we attain even with a 100% excess only a concentration of 0.0167 *M*. A 408.5% excess of the titrant would be needed to assure the necessary 0.029 *M* titrant concentration. This would make the error in  $C_i - [X]_i$  very large. In contrast, if the value of  $K$  is  $10^5$  then the necessary  $C_R = 0.0119$  *M*. This can be attained with the 30–40% excess of the titrant, accordingly the measurement can be performed.

The lower concentration limit of the determination can be characterized also with  $Y$ , the concentration ratio of the species formed in the reaction and that of the free reagent:

$$Y = \frac{[AX]}{[X]} = \frac{C_R - [X]}{[X]} \quad (5)$$

The value of  $Y$  is  $\geq 1$  if the analytical error got by the use of this evaluation method is equal or lower than that of the potentiometric measurement. In this case from equations (4) and (5) considering that  $C_R - [X] = [AX]$

$$\Delta = \frac{100}{KC_A} \quad (6)$$

representing the dependence of  $\Delta$  from  $K$  and  $C_A$ .

For analytical procedures based on the two step equilibria



and using the quantitative formation of  $AX_2$  for the determination, the values  $C_R$  and  $Y$  can be derived in a similar way leading to

$$C_R = [X] + \frac{100 - \Delta}{100} \cdot C_A \left( \frac{1}{K_2[X]} + 2 \right) \quad (9)$$

and

$$Y = \frac{[AX] + 2[AX_2]}{[X]} = \frac{C_R - [X]}{[X]} \quad (10)$$

It is to be seen from (9) that  $\Delta$  depends only on  $K_2$  but not on  $K_1$ , thus  $\Delta$  can be calculated by eq. (6) from the value of former one.

To show the practical applicability of the procedure for such two-step equilibria the acidimetric determination of the disodium salts of (L)-malic acid, (D-L)-camphoric acid, succinic acid, and of potassium-sodium tartrate have been performed using hydrochloric acid standard solutions. The saturation value of  $C_H - [H^+]$  vs.  $\text{cm}^3$  standard solution curve appeared after the

coordination of the second proton in each system. As a typical example the primary titration curve and the derived  $C_H - [H^+] vs. cm^3$  titrant curve of the determination of disodium malate is shown on Fig. 1. The protonation constants of the compounds are shown in Table I. The analytical errors and standard deviations of the measurements are summarized in Table II.

It is to be seen, that the results of the determinations are independent of  $K_1$ . Every compound could be determined with a good accuracy in 0.1 M concentration since their  $\lg K_2 > 3$ ; the salts of camphoric and succinic acids also in 0.01 M concentration having  $\lg K_2 > 4$ ; none of the compounds in 0.001 M concentration. A similar correlation was shown for one-step equilibria in publication [1] presenting the principles of this procedure.

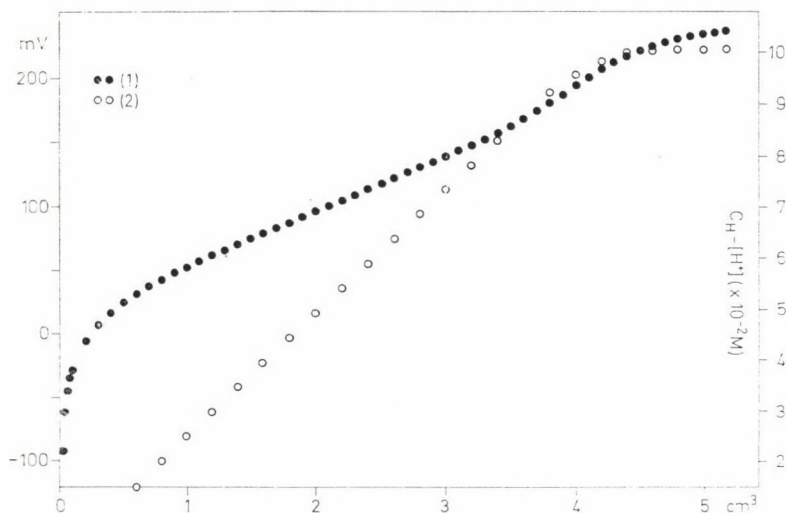


Fig. 1. The primary potentiometric titration curve of 10.00 cm<sup>3</sup> 0.1 M disodium malate in aqueous solution with a 0.5 M hydrochloric acid standard solution (1) and the derived curve  $C_H - [H^+] vs. cm^3$  titrant (2)

Table I

The protonation constants of the dicarboxylate compounds examined [5]  
(in  $\lg K$  values)

Compound	$\lg K_1$	$\lg K_2$
Disodium malate	5.05	3.46
Potassium-sodium tartrate	4.44	2.95
Disodium succinate	5.48	4.19
Disodium camphorate	5.10	4.57

The effect of the experimental error in the individual parameters on the final analytical result can be approached, in the case of small errors, with the differentiation of equation (1) according to the examined parameter [3, 4]. These equations are the following:

$$\frac{\partial C_A}{\partial C_X} = \frac{V_i}{V_0} \cdot \frac{1}{n} \quad (11)$$

$$\frac{\partial C_A}{\partial V_i} = \frac{1}{V_0 \cdot n} \left[ C_X - 10^{\frac{E_i - E_0}{S}} \right] \quad (12)$$

$$\frac{\partial C_A}{\partial V_0} = \frac{1}{n \cdot V_0^2} \left[ V_i \cdot 10^{\frac{E_i - E_0}{S}} - C_X V_i \right] \quad (13)$$

$$\frac{\partial C_A}{\partial E_i} = \frac{1}{n \cdot V_0 \cdot S} \left[ -10^{\frac{E_i - E_0}{S}} \cdot (V_i + V_0) (\ln 10) \right] \quad (14)$$

$$\frac{\partial C_A}{\partial E_0} = - \frac{\partial C_A}{\partial E_i} \quad (15)$$

$$\frac{\partial C_A}{\partial S} = \frac{1}{n \cdot V_0} \cdot 10^{\frac{E_i - E_0}{S}} \cdot (V_i + V_0) (\ln 10) \frac{E_i - E_0}{S^2} \quad (16)$$

where  $V_0$  is the original volume of the solution to be analysed.

With the help of these equations the effect of the error in  $C_X$  (concentration of the titrant),  $V_i$  (volume of the titrant added),  $V_0$  (starting volume of titration),  $E_i$  (electromotive force),  $E_0$  (formal potential of the system) and  $S$  (slope of electrode response) could be calculated. The results of such calculations are presented in Figs 2 and 3 for two model systems (of equilibrium constants  $10^5$  and  $10^6$ ). It is to be seen that identical changes in  $C_X$ ,  $V_i$  and  $V_0$

**Table II**  
The analytical results of the measurements

Compound	Calculated concentration, M	Determined concentration, M	Relative error %	Standard deviation of error %
Disodium malate	$9.82 \cdot 10^{-2}$	$9.67 \cdot 10^{-2}$	-1.61	$\pm 0.62$
Potassium-sodium tartrate	$1.02 \cdot 10^{-1}$	$1.00 \cdot 10^{-1}$	-1.82	$\pm 1.48$
Disodium succinate	$9.87 \cdot 10^{-2}$	$9.94 \cdot 10^{-2}$	+0.69	$\pm 0.68$
	$9.88 \cdot 10^{-3}$	$9.73 \cdot 10^{-3}$	-1.57	$\pm 1.23$
Disodium camphorate	$9.96 \cdot 10^{-2}$	$9.86 \cdot 10^{-2}$	-0.98	$\pm 0.81$
	$9.97 \cdot 10^{-3}$	$9.75 \cdot 10^{-3}$	-2.23	$\pm 1.03$

caused errors of similar magnitude in  $C_A$  (the analytical result), the effect of the error in  $E_i$  and  $E_0$  are the mirror images of each other, the effect in the error of  $S$  has a greater influence than those of  $E_i$  and  $E_0$ .

For a better characterization of the effect of the error in the single experimental data on the final analytical result the magnitude of the experi-

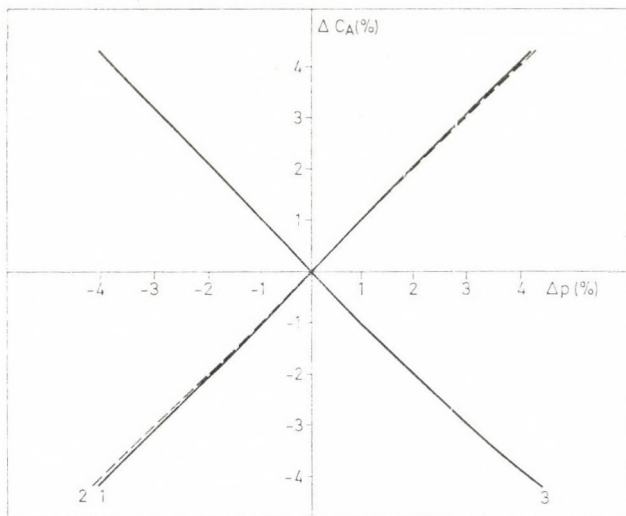


Fig. 2. The effect of the experimental error (1.  $C_X$ , 2.  $V_i$ , 3.  $V_0$ ) on the final result of the analysis  $C_A$  (in %) )

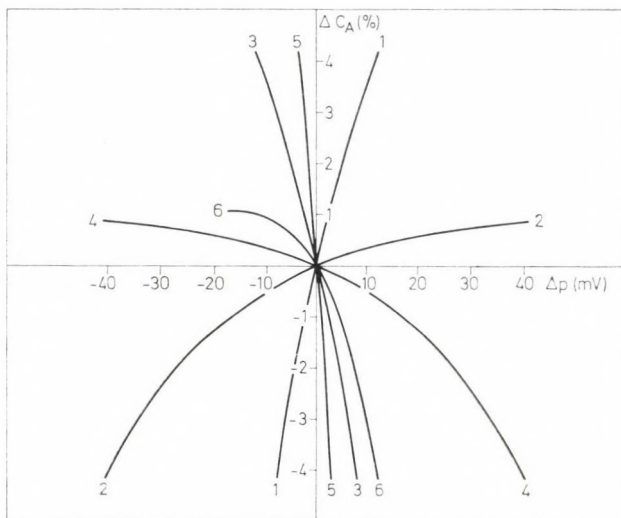


Fig. 3. The effect of the experimental error on the final result of the analysis  $C_A$  (in %) •  
 $\Delta p$ : 1.  $E_0$ , 3.  $E_i$ , 5.  $S$  ( $K = 10^5$ ); 2.  $E_0$ , 4.  $E_i$ , 6.  $S$  ( $K = 10^6$ )

Table III

The effect of the experimental error causing  $\pm 1$  rel % change in the concentration  $C_A$  to be determined

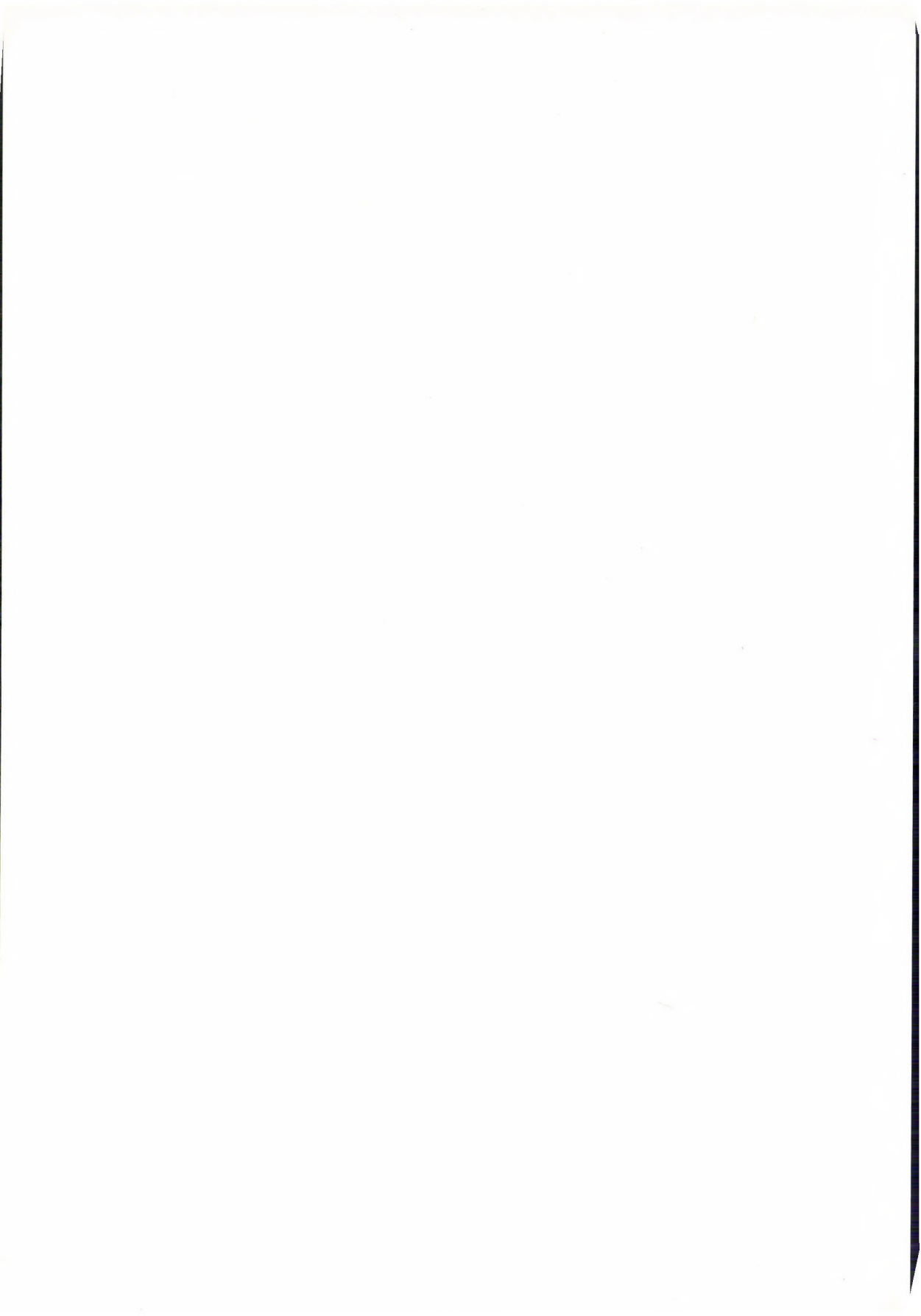
$K$	$C_A$ mol dm <sup>-3</sup>	$C_X$ %	$V_i$ %	$V_o$ %	$E_i$ mV	$E_o$ mV	$S$ mV
$10^3$	0.1	$\pm 0.45$	$\pm 0.51$	$\mp 0.51$	$\mp 0.3$	$\pm 0.3$	$\mp 0.2$
$10^4$	0.1	$\pm 0.90$	$\pm 0.91$	$\mp 0.91$	$\mp 2.5$	$\pm 2.5$	$\mp 1.2$
	0.01	$\pm 0.45$	$\pm 0.51$	$\mp 0.51$	$\mp 0.3$	$\pm 0.3$	$\mp 0.2$
$10^5$	0.1	$\pm 0.99$	$\pm 0.99$	$\mp 1.00$	-67 +17	+67 -17	-16 +6.2
	0.01	$\pm 0.90$	$\pm 0.91$	$\mp 0.91$	$\mp 2.4$	$\pm 2.4$	$\mp 0.8$
	0.001	$\pm 0.45$	$\pm 0.51$	$\mp 0.51$	$\mp 0.3$	$\pm 0.3$	$\mp 0.2$
$10^6$	0.1	$\pm 1.00$	$\pm 1.00$	$\mp 1.00$	$-\infty$ +40	$+\infty$ -40	$-\infty$ +20
	0.01	$\pm 0.99$	$\pm 0.99$	$\mp 1.00$	-63 +17	+63 -17	-14 +4
	0.001	$\pm 0.90$	$\pm 0.90$	$\mp 0.91$	$\mp 2.4$	$\pm 2.4$	$\mp 0.61$

mental errors which caused a  $\pm 1$  relative % error in the final result is presented in Table III. These data reflect clearly the limits of applicability of the new evaluation method.

## REFERENCES

- [1] BURGER, K., PETHŐ, G., NOSZÁL, B.: *Anal. Chim. Acta*, **118**, 93—100 (1980)  
 [2] INCZÉDY, J.: *Analytical Applications of Complex Equilibria*, Ellis Horwood, Chichester 1976  
 [3] *Mathematical Handbook for Scientists and Engineers*. 2. Ed. McGraw-Hill, New York—Toronto—London, 1961  
 [4] STILL, E.: *Talanta*, **27**, 573 (1980)  
 [5] *Stability Constants*, Special Publication No. 17, London, The Chemical Society, 1964

Kálmán BURGER }  
 Gábor PETHŐ } H-1088 Budapest, Múzeum krt. 4/b.  
 László DOMOKOS }  
 Ernő PUNGOR } H-1521 Budapest, Gellért tér 4.



## OXIDATION OF SOME CYCLIC $\alpha$ -BENZYLIDENE KETONES WITH THALLIUM(III) NITRATE IN METHANOL

E. MÁRVÁNYOS<sup>1</sup>, S. ANTUS<sup>2</sup> and M. NÓGRÁDI<sup>2\*</sup>

<sup>1</sup> *Chinoin Pharmaceutical and Chemical Works, Budapest, and*

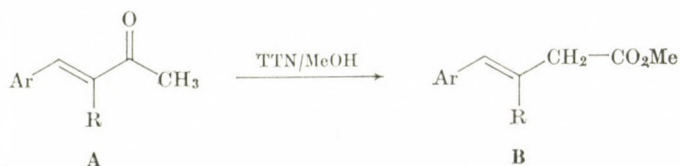
<sup>2</sup> *Research Group for Alkaloid Chemistry, Hungarian Academy of Sciences, Budapest)*

Received May 11, 1981

Accepted for publication June 9, 1981

With  $\text{Tl}(\text{NO}_3)_3 \cdot 3 \text{H}_2\text{O}$  in MeOH the title compounds undergo slow oxidation to give either, as expected, acetals by aryl migration or other oxidation products.

Recently we reported [1] some examples of a novel oxidative transformation (**A**  $\rightarrow$  **B**) and postulated a mechanism for it involving a cyclopropanone-type intermediate.

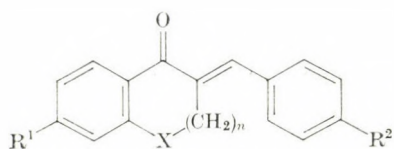


In order to explore the scope of this reaction, some analogues, in which the carbonyl group was part of a ring, were subjected to oxidation by TTN/MeOH. However, none of the compounds **1**–**7** showed the expected behaviour.

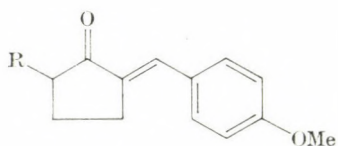
The tetralone **1** and the benzofuranone **5** gave the acetals **9** and **10**, respectively, in a low yield, by the well-known aryl migration process [1, 2]. Exchange of the *p*-methoxyl group in **1** for chlorine (**2**) rendered the molecule completely resistant to TTN/MeOH. Replacement of the ring-oxygen by methylene had the same effect: the indanone **4** also failed to react with TTN/MeOH. This latter phenomenon was not due to the presence of the fused benzene ring, since the cyclopentanone **7**, though it was oxidized rapidly, did not undergo rearrangement either, but only  $\alpha$ -methoxylation to give **8**.

Activation of **4** by a second carbonyl group, as in the indandione **6**, made possible the oxidative rearrangement, which was followed by oxidation of the acetal group to yield the ester **11** as the final product.

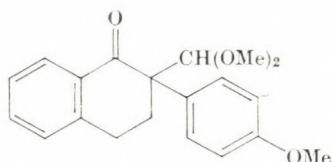
\* To whom correspondence should be addressed.



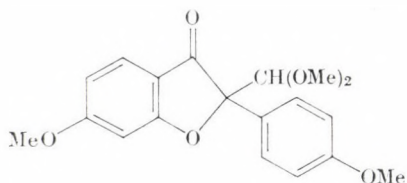
	R <sup>1</sup>	R <sup>2</sup>	X	n
1	H	OMe	CH <sub>2</sub>	1
2	H	Cl	CH <sub>2</sub>	1
3	OMe	OMe	O	1
4	H	OMe	CH <sub>2</sub>	0
5	OMe	OMe	O	0
6	H	OMe	CO	0



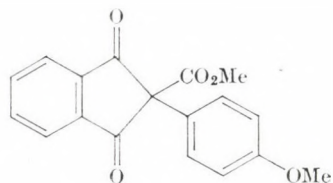
- 7 R = H  
8 R = OMe



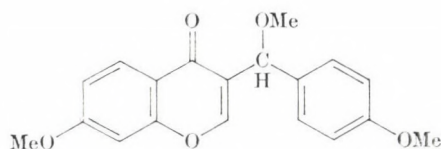
9



10



11



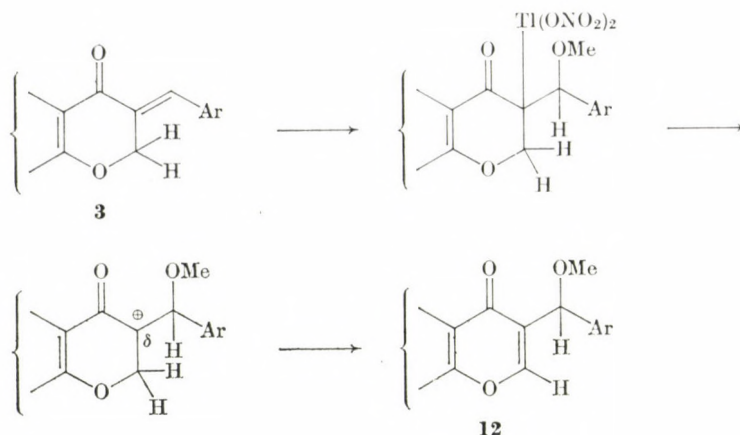
12

Oxidation of the chromanone **3** gave the chromone **12**. The formation of **12** can be readily explained by the mechanism postulated for the oxidative rearrangement of chalcones [3]. The carbonium ion generated by cleavage of the primary methoxy-thalliated intermediate is stabilized, not as usual, by aryl migration, but by the loss of an  $\alpha$ -proton (*cf.* scheme on p. 95).

The structures of all new compounds have been verified by spectroscopic methods (*cf.* Experimental).

### Experimental

Substances 1 [4], 2 [5], 3 [6], 4 [7], 5 [8], 6 [9], and 7 [10] are known compounds, and were identified by their m.p.'s and <sup>1</sup>H-NMR spectra.



### General method

The substrate (1.0 mmol) was dissolved or suspended in dry methanol (25 mL),  $\text{Tl}(\text{NO}_3)_3 \cdot 3 \text{H}_2\text{O}$  (1.2 mmol) was added and the mixture refluxed with stirring. The reaction was monitored by TLC and, if necessary, more TTN (0.2 mmol) was added after 1 h. After completion of the reaction, saturated sodium chloride solution (2 mL) was added, the precipitate was filtered off and the filtrate diluted with water. The precipitate was extracted with dichloromethane, the extract dried, evaporated and the residue, if necessary, purified by chromatography.

#### 5-Methoxy-2-(4-methoxybenzylidene)-cyclopentanone (8)

M. p. 78.5–80.5 °C (from MeOH), yield 44%.

$^1\text{H-NMR}$  ( $\text{CDCl}_3$ ):  $\delta$  = 1.80 (mc, 1H,  $4_{\text{trans}}\text{-H}$ ), 2.37 (mc, 1H,  $4_{\text{cis}}\text{-H}$ ), 2.87 (mc, 2H, 3- $\text{CH}_2$ ), 3.52 (s, 3H, 5-OMe), 3.82 (s, 3H, Ar-OMe), 3.8 (q (overlapped), 1H, 5-H), 6.90 (d,  $J$  = 8 Hz, 2H, 3',5'-H), 7.47 (d,  $J$  = 8 Hz, 2H, 2', 6'-H), 7.45 (mc, 1H, =CH-).

$\text{C}_{14}\text{H}_{16}\text{O}_3$  (232.3). Calcd. C 72.39; H 6.94. Found C 72.50; H 6.71%.

$M^+$  232.

#### 2-(Dimethoxymethyl)-2-(4-methoxyphenyl)-1,2,3,4-tetrahydronaphthalene-1-one (9)

M.p. 114–115 °C (from MeOH), yield 20%.

$^1\text{H-NMR}$  ( $\text{CDCl}_3$ ):  $\delta$  = 2.65 (m, 4H,  $\text{CH}_2$ ), 3.02 and 3.40 [2xs, 6H,  $\text{CH}(\text{OMe})_2$ ], 3.60 (s, 3H, ArOMe), 4.67 (s, 1H, CH), 6.6–7.3 (m, 7H, aromatic-H), 7.95 (mc, 1H, 8-H).

$\text{C}_{20}\text{H}_{22}\text{O}_4$  (326.4). Calcd. C 73.60; H 6.79. Found C 73.74; H 6.71%.

#### 2-Dimethoxymethyl-6-methoxy-2-(4-methoxyphenyl)-2H-3-benzofuranone (10)

M.p. 142–143.5 °C (from MeOH), yield 9.3%.

$^1\text{H-NMR}$  ( $\text{CDCl}_3$ ):  $\delta$  = 3.10 and 3.16 [2xs, 6H,  $\text{CH}(\text{OMe})_2$ ], 3.82 and 3.89 (2xs, 6H, ArOMe), 4.52 (s, 1H, CH), 6.55–6.70 (m, 2H, 5,7-H), 6.95 (d,  $J$  = 9 Hz, 2H, 3',5'-H), 7.45 (d,  $J$  = 9 Hz, 2H, 2',6'-H), 7.60 (d,  $J$  = 8.5 Hz, 1H, 4-H).

$\text{C}_{19}\text{H}_{20}\text{O}_6$  (344.4). Calcd. C 66.26; H 5.85. Found C 66.38; H 5.70%.

#### 2-Methoxycarbonyl-2-(4-methoxyphenyl)-indan-1,3-dione (11)

M.p. 110–112 °C (from MeOH), yield 61%.

$^1\text{H-NMR}$  ( $\text{CDCl}_3$ ):  $\delta$  = 3.43 (s, 3H,  $\text{CO}_2\text{Me}$ ), 3.72 (s, 3H, ArOMe), 6.80 (d,  $J$  = 9 Hz, 2H, 3',5'-H), 7.34 (d,  $J$  = 9 Hz, 2H, 2',6'-H), 7.9 (mc, 4H, 4,5,6,7-H).

$\text{C}_{18}\text{H}_{14}\text{O}_5$  (310.3). Calcd. C 69.67; H 4.55. Found C 69.43; H 4.63%.

**7-Methoxy-3-[methoxy-(4-methoxyphenyl)-methyl]-4H-1-benzopyran-4-one (12)**

M.p. 92–94 °C (from MeOH), yield 9%.

<sup>1</sup>H-NMR (CDCl<sub>3</sub>): δ = 3.37 (s, 3H, CHOMe), 3.78 and 3.87 (2xs, 6H, ArOMe), 5.49 (s, 1H, CH), 6.88 (d, J = 9 Hz, 2H, 2',6'-H), 7.97 (d, J = 0.9 Hz, 1H, 2-H), 8.06 (d, J = 9 Hz, 1H, 5-H).<sup>13</sup>C-NMR (CDCl<sub>3</sub>): δ = 55.16 (q, OMe), 55.69 (q, OMe), 56.89 (q, OMe), 76.76 (d, CH), 100.04 (d, 8-C), 113.72 (d, 3',5'-C), 114.40 (d, 6-C), 117.92 (s, 4a-C), 125.70 (s, 3-C), 127.08 (d, 5-C), 128.37 (d, 2',6'-C), 131.86 (s, 1'-C), 152.56 (d, 2-C), 157.95 (s, 4'-C), 159.13 (s, 8a-C), 163.85 (s, 7-C), 175.51 (s, 4-C).C<sub>19</sub>H<sub>18</sub>O<sub>5</sub> (326.4). Calcd. C 69.92; H 5.56. Found C 69.77; H 5.62%.

\*

The authors are indebted to Dr. D. KORBONITS for helpful discussion, and to Dr. P. KOLONITS and Dr. K. HORVÁTH for the analyses of NMR spectra.

## REFERENCES

- [1] ANTUS, S., BOROSS, F., KAJTÁR-PEREDY, M., NÓGRÁDI, M.: *Ann.*, **1980**, 1283
- [2] MCKILLOP, A., SWAN, B. P., FORD, M. E., TAYLOR, E. C.: *J. Am. Chem. Soc.*, **95**, 3641 (1973)
- [3] MCKILLOP, A., HUNT, J. D., KIENZLE, F., BIGHAM, E., TAYLOR, E. C.: *J. Am. Chem. Soc.*, **95**, 3635 (1973)
- [4] MOLHO, D.: *Bull. Soc. Chim. France*, **1948**, 1042
- [5] CROMWELL, N. H., BAMBURY, R. E., BARLEY, R. P.: *J. Am. Chem. Soc.*, **81**, 4294 (1959)
- [6] EVANS, D., LOCKHARDT, I. M.: *J. Chem. Soc.*, **1966**, 711
- [7] IMBACH, J. L., POHLAND, A. E., WEILER, E. D., CROMWELL, N. H.: *Tetrahedron*, **23**, 3931 (1967)
- [8] GOWAN, J. E., HAYDEN, P. M., WHEELER, T. S.: *J. Chem. Soc.*, **1955**, 862
- [9] IONESCU, M. V.: *Bull. Soc. Chim. France*, **47**, 210 (1930)
- [10] ELPHIMOFF-FELKIN, I., SARDA, P.: *Tetrahedron*, **31**, 2781 (1975)

Ede MÁRVÁNYOS H-1077 Budapest, Wesselényi utca 69.

Sándor ANTUS	}	H-1111 Budapest, Gellért tér 4.
Mihály NÓGRÁDI		

## NEW METALLIC CATALYSTS OBTAINED BY SUPPORTING PLATINUM ON $\text{AlPO}_4\text{--Al}_2\text{O}_3$ AND $\text{AlPO}_4\text{--SiO}_2$ SYSTEMS

M. A. ARAMENDIA, V. BORAU, C. JIMENEZ and J. M. MARINAS\*

*(Departamento de Química Orgánica, Facultad de Ciencias,  
Universidad de Córdoba, Córdoba, Spain)*

Received February 6, 1981  
In revised form April 17, 1981  
Accepted for publication June 16, 1981

The synthesis of metallic catalysts obtained by supporting platinum on  $\text{AlPO}_4/\gamma\text{-Al}_2\text{O}_3$  and  $\text{AlPO}_4/\text{SiO}_2$  systems is described. Their performance in the reduction of alkenes at low hydrogen pressure (1–5 bar) is reported.

### Introduction

Colloidal aluminium orthophosphates [1–2],  $\text{AlPO}_4/\gamma\text{-Al}_2\text{O}_3$  [3] and  $\text{AlPO}_4/\text{SiO}_2$  [4] have been widely used as catalysts in Friedel–Crafts-type processes in different media. In the present paper, the synthesis and catalytic performance of metallic systems obtained by supporting platinum on  $\text{AlPO}_4/\gamma\text{-Al}_2\text{O}_3$  and  $\text{AlPO}_4/\text{SiO}_2$  at low metallic loading is reported.

### Experimental

#### *Catalysts*

The catalysts have been obtained by impregnation of  $\text{AlPO}_4/\text{SiO}_2$  (E) or  $\text{AlPO}_4/\text{Al}_2\text{O}_3$  (CB) with an aqueous solution ( $3.86 \times 10^{-5} M$ ) of hexachloroplatinic acid. The synthesis of the supports has been described elsewhere [5], and only particles with sizes between 70–200 mesh  $\text{cm}^{-2}$  were used. The catalysts thus obtained contained 1% (*w/w*) platinum, as determined by atomic absorption, and have been named Pt1E and Pt1CB, according to the nature of the support.

The procedure to support the metallic phase was as follows. After standing at room temperature for 24 h, a suspension consisting of 0.99 g support and 13.27 mL of an aqueous solution ( $3.86 \times 10^{-5} M$ ) of hexachloroplatinic acid was evaporated to dryness at 40 °C and a reduced pressure of 33 mbar. The solid material thus obtained was kept in air at 120 °C for 72 h and then reduced in flowing hydrogen ( $50 \text{ mL min}^{-1}$ ) at 250 °C for 2 h. In order to stabilize the catalysts, and prior to the kinetic studies, they were used to catalyze the reduction of cyclohexene with hydrogen at 5 bar and 25 °C for 2 h. Surface characterization data are summarized in Table I.

#### *Chemicals*

Linear and cyclic alkenes from Merck or Fluka (99.9%) with boiling points between 37 and 90 °C were used in the reduction experiments, and the solvents were distilled twice before use.

\* To whom correspondence should be addressed

**Table I**  
*Surface characterization data of the synthesized metallic catalyst*

Catalyst	Metallic surface (m <sup>2</sup> g <sup>-1</sup> )	Average metallic diameter (nm)*	Dispersity
PtIE	58	4.8	0.08
PtICB	65	4.3	0.09

\* As measured by TEM using a Philips EM-300 instrument working at 100 kV

### *Reaction System*

The reduction runs were carried out in a Parr-type system from GERHARDT, which allows to control the temperature and the shaking velocity, with a total reaction volume of 500 mL. A built-in burette permits introduction of the reactants once the pressure in the reaction vessel drops to 0.33 mbar. The reaction temperature was controlled by means of a water-jacket system connected to an external thermostat and changes of the pressure in the reaction vessel were monitored (0.1 bar) with a manometer.

### *Procedure*

0.05 g catalyst is introduced in the reaction vessel and, after standing at 0.33 mbar for 5 min, a pressure of 5 bar of hydrogen is adjusted and the system shaken (300 min<sup>-1</sup>) for 10 min; with this shaking velocity, no diffusion effect is observed. Hydrogen is then pumped off and the alkene, dissolved in methanol, is admitted in the reaction vessel from the burette. Hydrogen (5 bar) is again introduced and after raising the temperature to the desired value, a period of 20 min is left for stabilization (no change in the pressure is observed during this period). Shaking is then started ( $t = 0$ ) and changes in the gas pressure are monitored at regular time intervals.

### *Analysis of products*

Analysis of the reaction products has been carried out using a Hewlett—Packard 5830-A gas chromatograph with an incorporated integrator-computer unit. In some of the experiments, simultaneous GC-MS has also been performed using a Hewlett—Packard 5552 system. In all the cases studied, the alkane corresponding to the hydrogenation of the double C=C bond in the original alkene has been detected as the only reaction product. On the other hand, the proportion of saturated hydrocarbons, as determined by GC, agrees with that estimated from the change in hydrogen pressure.

## **Results and Discussion**

Blank experiments carried out without catalyst or with the pure supports, did not yield any reaction product, even 5 h reaction.

Table II collects the initial reduction rate of cyclohexene using various amounts of catalyst, PtIE, and methanol as a solvent.

In Table III, the initial reduction rate of cyclohexene is given using, in the same experimental conditions, catalysts PtIE and PtICB and the commercial catalysts Pt/Al<sub>2</sub>O<sub>3</sub> and Pt/C (Fluka, ref. 80992 and 80982, respectively). Similar experiments have been carried out with other olefins studied in this paper. It can be observed that catalyst PtIE shows a larger activity than that of the commercial catalysts.

**Table II***Initial reduction rate of cyclohexene*Catalyst: Pt1E, solvent: methanol, initial concentration: 2.47 mol L<sup>-1</sup>, hydrogen pressure: 5 bar, reaction temperature: 27 °C

Weight of catalyst (g)	Initial rate, $r_0$ (mol/min gPt)
0.15	0.94
0.10	0.93
0.05	0.93

**Table III***Initial reduction rate of cyclohexene*Solvent: methanol, initial concentration: 2.47 mol L<sup>-1</sup>, hydrogen pressure: 5 bar, reaction temperature: 27 °C

Catalyst	Initial rate $r_0$ (mol/min gPt)
Pt1E	0.93
Pt1CB	0.37
Pt/Al <sub>2</sub> O <sub>3</sub> *	0.20
Pt/C*	0.85

\* From "Fluka" Ref. 80992 and 80982

**Table IV***Dependence of the initial reduction rate of cyclohexene on the nature of solvent*Initial concentration: 2.47 mol L<sup>-1</sup>, hydrogen pressure: 5 bar, reaction temperature: 27 °C

Solvent	Solubility at 20 °C (mol L <sup>-1</sup> ) × 10 <sup>4</sup>	$r_0$ (mol/min gPt)	
		Pt1E	Pt1CB
<i>n</i> -Hexane	12.50	1.45	0.63
<i>iso</i> -Octane	7.80	1.23	0.55
<i>n</i> -Heptane	6.90	1.07	0.47
Cyclohexane	3.80	0.85	0.42
Benzene	2.60	0.50	0.21
Methanol	1.60	0.93	—
Acetone	2.30	0.81	—
Tetrahydrofurane	—	0.54	—
<i>N,N</i> -Dimethylformamide	—	—	—

Table V

*Initial reduction rate of various alkenes*Catalyst: Pt1E, initial reactant concentration: 2.47 mol L<sup>-1</sup>, solvent: methanol, initial hydrogen pressure: 5 bar, reaction temperature: 27 °C

Reactant	Product	$r_0$ (mol/min gPt)
Cyclopentene	cyclopentane	0.99
Cyclohexene	cyclohexane	0.93
Cycloheptene	cycloheptane	0.16
Cyclooctene	cyclooctane	0.00
1-Methylcyclohexene	methylcyclohexane	0.25
4-Methylcyclohexene	methylcyclohexane	0.50
3-Methylcyclohexene	methylcyclohexane	0.57
Styrene	ethylbenzene	0.46
$\alpha$ -Methylstyrene	isopropylbenzene	0.09
<i>E</i> -1-Phenylpropene	propylbenzene	0.03
2-Methylphenylpropene	isobutylbenzene	0.01
1-Pentene	<i>n</i> -pentane	0.16
1-Hexene	<i>n</i> -hexane	0.27
1-Heptene	<i>n</i> -heptane	1.20
1-Octene	<i>n</i> -octane	1.08

In Table IV, the initial reduction rates of cyclohexene in several solvents using both 1% Pt catalysts, are collected.

As can be seen in Table IV, when nearly nonpolar hydrocarbons are used as solvents, the reduction rate changes with the solubility of hydrogen in these solvents at 20 °C [6]. On the contrary, when highly polar solvents are used, this relationship is no longer observed, probably because of the strong structural differences among these solvents.

In Table V, the initial reduction rate of several alkenes using an initial hydrogen pressure of 5 bar and catalyst Pt1E are given.

The results obtained agree with those reported previously by HUSSEY *et al.* [7] for the reduction of alkenes on a Pt/Al<sub>2</sub>O<sub>3</sub> catalyst, using cyclohexane, methylcyclohexane and *n*-octane as solvents.

Under the same experimental conditions, the initial reduction rate for cycloalkenes decreases on increasing the size of the ring. On the contrary, for linear alkenes, the initial reduction rate increases with the chain length, except for 1-octene, which exhibits a peculiar behaviour.

The possible steric hindrance due to the presence of substituents on the ethylenic carbon atoms has been studied in the cyclohexene and styrene series. The results obtained can be explained if co-planar adsorption of the olefin on

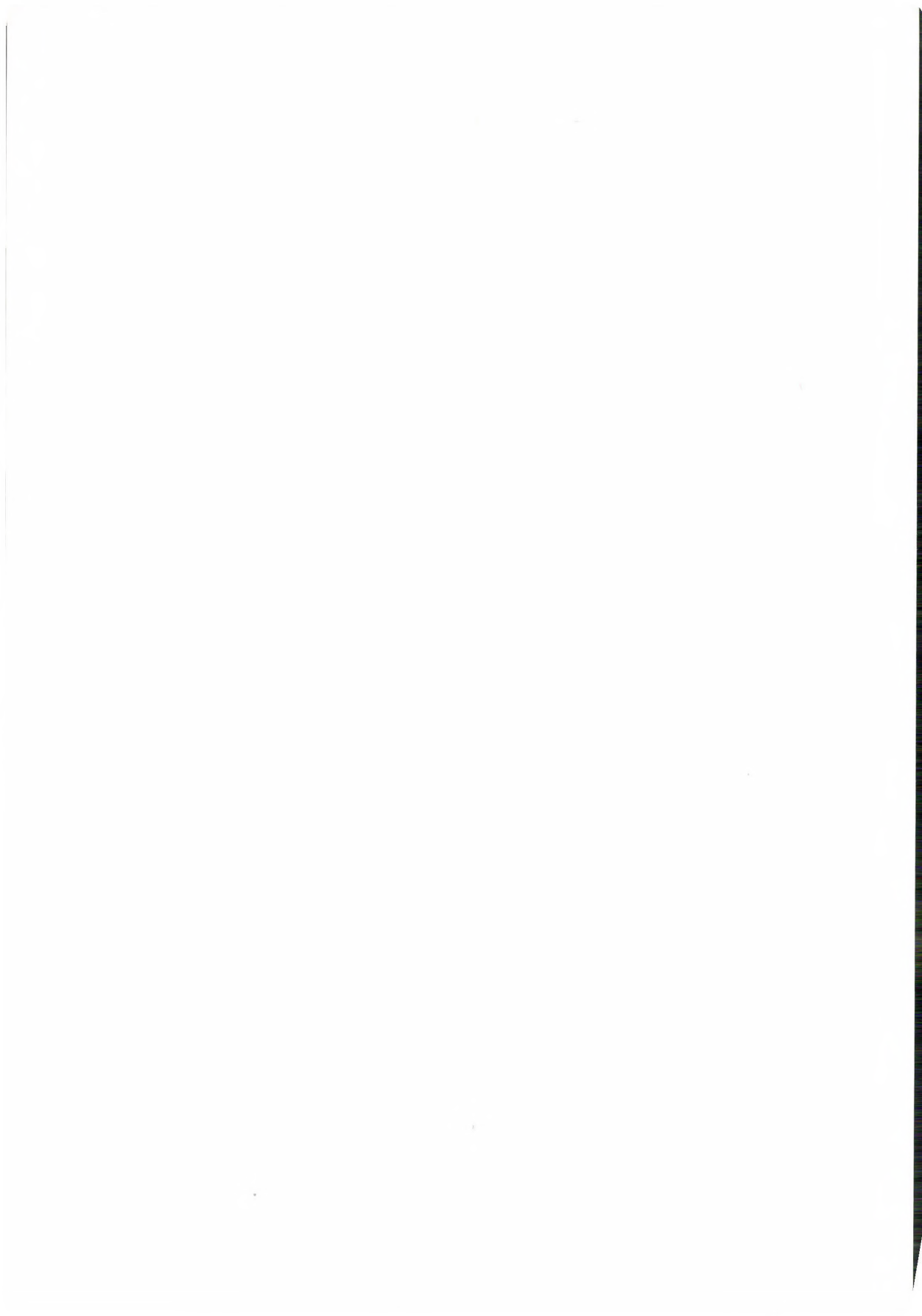
the metallic surface is assumed. For 1-methyl-1-cyclohexene, the neighbouring presence of methyl groups prevents adsorption of the olefin, thus leading to a lower reduction rate than that observed for cyclohexene in the same conditions. However, if substrates with a methyl group in positions 3 or 4 are reduced, this effect is less pronounced, and the reduction rates are slightly lower than that of cyclohexene.

On the other hand, in styrene series it is observed that increasing substitution at the ethylenic carbon atoms markedly decreases the reduction rate of the hydrocarbon.

## REFERENCES

- [1] JIMENEZ, C., MARINAS, J. M., PEREZ-OSSORIO, R., SINISTERRA, J. V.: *An. Quim.*, **70**, 860 (1974)
- [2] JIMENEZ, C., MARINAS, J. M., PEREZ-OSSORIO, R., SINISTERRA, J. V.: *An. Quim.*, **72**, 254 (1976)
- [3] CAMPELO, J. M., MARINAS, J. M., PEREZ-OSSORIO, R.: *V<sup>o</sup> Simposio Iberoamericano de Catálisis, Lisboa, 1976. Vol. 1, pag. 84 (1978)*
- [4] JIMENEZ, C., MARINAS, J. M., PEREZ-OSSORIO, R., SINISTERRA, J. V.: *An. Quim.*, **73**, 64 (1977)
- [5] SINISTERRA, J. V., JIMENEZ, C., BORAU, V., MARINAS, J. M.: *V<sup>o</sup> Simposio Iberoamericano de Catálisis, Lisboa, 1976. Vol. 2, pag. 359 (1978)*
- [6] GUERASIMOV, Ya., DREVING, V., ERIOMIN, E., KISELION, A., LEBEDEV, V., PANCHENKOV, G., SHLIGUIN, A.: *Ed. Mir, Moscú, 1, 227 (1977)*
- [7] HUSSEY, A. S., KEULKS, G. W., NOWACK, G. P., BAKER, R. H.: *J. Org. Chem.*, **33**, 610 (1968)

M. Angeles ARAMENDIA Victoriano BORAU Cesar JIMENEZ J. Maria MARINAS	}	Avda. Medina Azahara S. N. Córdoba, Spain
---	---	---



# RECENSIONES

## *Inorganic Pigments Manufacturing Processes*

Edited by M. H. GUTCHO

Noyes Data Corporation, Park Ridge, New Jersey, U.S.A. 1980

The book, appearing as the 166th volume of the series Chemical Technology Review, includes the part on inorganic pigments from 1975 to 1980 of the American Patent Literature, the world's largest collection of this kind.

Inorganic pigments are finely distributed colourless or coloured solid particles (of micrometer order) of various geometry.

Man has used since several thousand years inorganic pigments for the colouring of other substances, either by admixing the pigments in uniform distribution, or as paint, mixed with a suitable vehicle, for the coating of surfaces.

Inorganic pigments are primarily used in the paint, printing ink, plastic, paper, ceramic and fired email industries, but they find application in all the fields of technology.

Owing to their favourable properties, such as high thermal resistance, tinting strength, hiding power, colour fastness, chemical resistance, absence of dullness, and last but not least to their weathering resistance, the importance and field of application of inorganic pigments steadily increases in the industrial branches mentioned above.

Organized in 12 chapters, the book covers over 487 pages 281 patent specifications concerning the manufacture of novel types and improved varieties of inorganic pigments, and the realization of more economic manufacturing and application technologies.

Processes described in the book reflect more and more the endeavour to manufacture with more economic technologies new inorganic pigments of improved quality, while meeting the more and more rigorous stipulations of environmental protection and labour safety.

### *1. Titanium dioxide pigments*

Titanium dioxide pigment is considered today as the most important white pigment<sup>1</sup> used in steadily increasing quantities by the paint, paper, fired enamel industries, in synthetic fibre manufacture, titanium metallurgy, steel production, *etc.*

As inorganic pigment preferably the rutile type is used, because this is photochemically less active than the anatase form.

Photochemical activity is manifested in the very rapid surface degradation by sunlight of organic substances pigmented with titanium dioxide.

The rapid degradation of the organic substance by light is caused by the catalytic action of titanium dioxide. Titanium dioxide catalytically activates air oxygen, which oxidizes then gradually the organic substance in the environment of the pigment particle. After the degradation of the organic vehicle at the surface, titanium dioxide pigment particles which were embedded are set free, and like chalk, can be wiped off from the surface.

The photostability, hiding power, weathering stability, dispersibility and tinting strength of titanium dioxide pigments can be improved, their photochemical activity reduced by the surface treatment of the pigments. From an aqueous suspension silica, Al-phosphate, Al-silicate, insoluble Zn, Zr, Mg compounds, organophilizing and hydrophobizing agents are precipitated in a very thin layer at the surface, or rubbed in by dry milling and mixing.

The chapter comprises 34 patent specifications in the following grouping:

Beneficiation of Titaniferous Ores.

Techniques for Improving Photostability of Titanium Dioxide.

TiO<sub>2</sub> of Reduced Photosensitivity.

TiO<sub>2</sub> Pigment of Improved Hiding Power.

Coating TiO<sub>2</sub> to Enhance Durability.

Modifying Surface Properties of TiO<sub>2</sub> Pigments.

Other Processes.

## 2. Yellow and green pigments

Of the inorganic pigments of both shades compounds containing chromium are the most important. Chromates containing hexavalent chromium are of yellow-orange colour, while trivalent chromium compounds are green.

Chromium oxide green pigments are valuable colouring agents of good thermal and chemical resistance and durability, in spite of the fact that their tint, particularly that of  $\text{Cr}_2\text{O}_3$ , is somewhat dull.

Chromium oxide green can be most simply prepared from ammonium bichromate by heating:



The processes described start also from ammonium bichromate or from a mixture of alkali bichromates and ammonium salts, which are calcined at about  $950^\circ\text{C}$ , then leached with water and dried.

Alkali bichromates heated at  $600^\circ\text{C}$  with carbon, sulfur or other reducing agents and leached with water yield also chromium oxide green:



Patent specifications described in the chapter are aimed at the preparation of chromium oxide green pigments of more vivid colour and higher tinting strength.

Of the inorganic yellow pigments the most widely used are lead chromate pigments, such as lead sulfochromate, lead silicochromate, orange basic lead chromate, *etc.* Lead chromate pigments have very good tinting strength, hiding power and full colour, but they have the disadvantage of being toxic, and moreover, their weather resistance is limited, particularly in industrial environment. Relevant patent specifications described several processes, according to which the surface of yellow and green pigments is coated with a thin layer of silica, zirconia, various insoluble phosphates, synthetic resins, oxides or organic organophilic compounds, to improve their quality parameters. In addition, yellow pigments, various titanates, bismuth compounds, *etc.*, manufactures in smaller quantities for special purposes, are discussed.

The chapter contains 28 patents concerned with the development of yellow and green pigments:

- Chromium Oxide Green Pigment.
- Bright Primrose Yellow Monoclinic Bismuth Vanadate Pigment.
- Lead Chromate Pigment of Improved Thermal Stability.
- Lead Chromate Pigments of Improved Abrasion Resistance.
- Other Lead Chromate Pigment Processes.
- Additional Inorganic Yellow Pigments.

## 3. Iron Oxide Pigments

Iron oxide pigments, various kinds of red iron oxide, yellow iron oxides and black iron oxides are nontoxic, inexpensive pigments with excellent properties, the use of which steadily gains ground.

Pure, special iron oxides of definite structure are manufactured as paints and plastic colouring agents, applied in telecommunication and electronics, and to satisfy other special industrial demands.

Increasing use in a wide field and trends of development of iron oxide pigments are well reflected by the grouping of the 19 patent specifications, discussed in this chapter of the book:

- Iron Oxide Pigments from Industrial Wastes.
- Iron Oxide Pigments *via* Reduction of Aromatic Nitro Compounds by Ferrous Salts.
- Yellow Iron Oxide Pigments.
- Red Iron(III) Oxide (Hematite).
- Black Iron Oxide.
- Acicular Magnetic Iron Oxide Pigments.

## 4. Carbon black

Of the black pigments, various kinds of carbon black are the most valuable. Carbon blacks are in general apolar microcrystalline carbon particles of high specific surface ( $100 - 170 \text{ m}^2/\text{g}$ ) and very fine distribution, contaminated by high molecular, multiply unsaturated hydrocarbons of complicated structure.

According to their manufacturing technology and the raw materials used channel black, carbon black and lamp black, furnace black are distinguished.

The 13 patents contained in this chapter concern the improvement of the quality of furnace black to that of channel black, the modification of the surface of carbon blacks, the improvement of their dispersibility, the enhancement of the bluish tint and the development of manufacturing technology according to the following grouping:

- Carbon Black from Oil Feedstock for Xerographic Toner Compositions.
- Carbon Black Pigments for Waxless Carbon Paper and Printing Inks.
- Carbon Black Reinforcing Agents for Rubber.
- Other Processes.

### 5. Lustrous Pigments

Lustrous pigments increasingly command the interest in several industrial sectors, as, e.g. paint, plastic, cosmetic and other industries.

Typical representatives of lustrous and nacreous pigments are micaceous pigments and all those pigments which are transparent or translucent and have a planar structure. The iridescence of mica flakes is caused by the interference of composite light, but thin coloured metal oxid formed at the surface of the sheets or other insoluble additives with a refractive index different from that of the base play also a role. Iridescent pigments introduced in recent years in this special field belong into this group of pigments. The base is generally mica or a micaceous substance (cryst. alpha iron oxide, lead thiosulfate, bismuth oxychloride *etc.*), while the applied very thin layer is usually  $TiO_2$  or  $ZrO_2$ . Finally, this thin surface layer is dyed with a dye dissolved in water, oil or organic solvents to the required tint. The dye is bound by adsorption.

The 21 patent specifications in this chapter reflect the most recent developments of lustrous, nacreous and iridescent pigments in the following grouping:

- Mica Flake-Based Pigments Suitable for Cosmetic Use.
- Lustrous Pigments for Plastics.
- Iridescent Pigments.
- Other Similar Pigments.

### 6. Clay pigments

Typical representatives of hydrosilicates with laminar lattice structure, occurring in nature, are kaolinite, dickite, nacrite and halloysite. In these minerals the layers are separated by lattice-held water.

In clay minerals, thus in montmorillonites the single inter-lattice ions can be easily exchanged or fixed within wide limits.

The 10 patent specifications composed in this chapter deal with the purification separation and possible transformations of clay minerals according to the following grouping:

- Improving Properties of Kaolin Clay.
- Clay Pigments for Pressure Sensitive Record Material.
- Other Clay Pigments.

### 7. Pigment dispersion

Inorganic colouring pigments or fillers can be used in paints, enamel varnishes or printing inks only if the pigments particles are uniformly distributed in aqueous or organic liquids' in vehicles. The originally dry pigment agglomerates must be comminuted, and the surface of the single elementary pigment particles must be wetted and coated with a vehicle. This is the essence of paint manufacture. To wet an inorganic pigment of strongly polar surface with an organic vehicle of apolar character and to distribute uniformly the pigment in the vehicle requires relatively high mechanical work. The situation is the same in the opposite case, if a pigment of apolar character, e.g. carbon black must be distributed in a vehicle of polar (aqueous) character. The difficulty is caused by the interfacial tension between the pigment particle and the vehicle. The problem can be solved by the reduction or elimination of interfacial tension.

Another method is the predispersing of the pigment. The surface of the pigments or fillers is precoated with a thin layer of synthetic resins or substances, which are soluble in most of the solvents, or are simply miscible, i.e. compatible with most of the vehicles or the selected one.

The chapter contains 20 patent specifications dealing with this theme in the following grouping:

## Facilitating Dispersion of Titanium Dioxide and Iron Oxide by Treatment with Organic compounds.

- Dispersing Agents.
- Dispersants for High Solids Suspension.
- Dry Water Dispersible Pigment Compositions.
- Predispersed Pigments.
- Dispersion Stabilizers.

### 8. Anticorrosion pigments

Of the active corrosion-inhibiting pigments used in practice the most important are red lead, zinc chromate, strontium chromate, zinc dust, *etc.*

Owing to their toxicity anticorrosive pigments containing lead or chromate are more and more banned by environmental protection. The non-toxic, relatively cheap Ca, Mg, Ba and Zn ferrites with active anticorrosive properties have been developed in recent years. Certain (Zn, Sr, Ca) molybdates are similarly anticorrosive. The other new non-toxic anticorrosion pigments are basic zinc phosphate, Ca-Zn phosphate, Mg phosphate, Ti phosphate, Zr phosphate, Ca silicofluoride, *etc.*

- The chapter on anticorrosive pigments discusses 18 patents in the following grouping:
  - Iron Oxide Based Anticorrosion Pigments.
  - Molybdate Corrosion-Inhibiting Pigments.
  - Other Anticorrosion Pigments.
  - Corrosion-Inhibiting Primers.

### 9. Pigments for synthetic materials

In the pigmentation of apolar thermoplastics, which can be considered as liquids of extremely high viscosity, similarly as in paint manufacture, the inorganic pigment particles with polar surface must be wetted, coated with the plastic as vehicle. This operation requires already such high energy input that the plastics themselves are degraded in most of the cases by shear force and heat produced in the operation. Owing to all this the reduction or elimination of the interfacial tension between the synthetic material and the pigment is a task of particular importance in this case. Here too, surface-treated organophilic pigments, predispersed pigments coated with resin and special plastics-coated pigment concentrates represent the best solutions.

- Grouping of the pertinent patents:
  - Colouring Plastics.
  - Pigment Composition for Plastics in Bead Form.
  - Pigmentation of Synthetic Fibers.
  - Decreasing Photosensitivity of  $\text{TiO}_2$  to be used in Artificial Fibers.

### 10. Improving optical properties of paint and paper

To improve surface whiteness, smoothness and brightness, pigments and fillers are used in the paper industry. Most frequently, the pigment is  $\text{TiO}_2$ , the filler  $\text{CaCO}_3$ ,  $\text{BaSO}_4$ , talc, caolin, *etc.*

A long-standing wish of the paper industry is a pigment or a filler, which surpasses in quality clay minerals,  $\text{CaCO}_3$  and  $\text{BaSO}_4$ , but is cheaper than  $\text{TiO}_2$ .

Substances of this kind are, *e.g.*  $\text{CaCO}_3 \cdot \text{Mg}(\text{OH})_2$ , ultrafine  $\text{CaCO}_3$ , clay mineral-silicate compositions,  $\text{TiO}_2$ -containing chalk, aluminosilicates, Al-monohydrate and several other combinations, discussed in 17 patent descriptions in this chapter in the following grouping:

- Paper Pigments.
  - Titanium Dioxide-Containing Composites as Paper Opacifiers.
  - Titanium Dioxide-Composites as Paper Opacifiers.
  - Aluminosilicate Pigments.
  - Pigmented Microporous Silicate Microsphere Opacifiers.
  - Other Paint and Paper Pigments.

### 11. Pigments for other specific needs

The chapter discusses the possibilities to meet the special demands of modern scientific technical development concerning inorganic pigments.

Protecting coatings applicable to supersonic and space vehicles, rockets, detector paint

for toxic chemical warfare agents, coatings for the collectors of solar energy utilization request the development and application of inorganic pigments of newer and newer kind.

The chapter covers then the development of new easily dispersible pigments, the mode of manufacture of pigment coatings prepared from their components "in situ" at the surface to be coated, the elaboration of annealed pigments of spinell structure, the safe manufacture of toxic pigments and the manufacture of ceramic pigment components.

For the varnishing of wood and furniture, varnishes originally glossy-drying, are modified by the adding of flattening agents.

The chapter closes with patent descriptions concerning the preparation of pigments for the painting of concrete structures, for cosmetic-sanitary purposes, for conducting layers, magnetic layers, photoreceptors in telecommunication, and for other special purposes.

The grouping of the 52 patent descriptions is the following:

Specialized Protective Coatings.

Silica Pigments For Rubber.

Ceramic Pigments.

Flattening Pigments for Use in Nitrocellulose Coating Compositions.

Construction Elements.

Amorphous Precipitated Siliceous Pigments for Dentrifices.

Other processes.

## 12. Other processes

The 26 patent descriptions comprised in this chapter deal with special pigments and fillers, which are not manufactured on industrial scale, but require individual technologies.

These include Berlin blue, and in general hexacyanoferrate pigments, antimony pigments, white crystalline  $\text{CaTiZr}_3\text{O}_9$  and  $\text{CaTiHf}_3\text{O}_9$  oxide pigments, metal pigments, hydrophobized pigments, and other specific surface treated pigments and fillers.

The specialized grouping of the patents in this chapter is the following:

Berlin Blue.

Antimony Pigments.

White Crystalline Compounds Useful as Pigments.

Metal Pigments.

Refractive Index Pigments.

Hydrophobized Pigments and Fillers.

Modifying Rheological Properties.

## Company Index

Companies, institutions named in the patent descriptions contained in the book, in alphabetic order, with page number.

## Inventor Index and U.S. Patent Number Index

The book, discussing 281 patents, gives a vast number of new informations, not only for specialists and researchers of pigments and fillers, but for all those engaged in industrial research, development and production in the fields to which the patents pertain.

The book gives a realistic picture of the present state and future trends of the scientific-technical development of pigments and fillers and fields concerned.

The style of the book is the language of patent literature, technically and juridically simple and clear.

J. SZERECZ

## J. S. ROBINSON: *Spinning, Extruding and Processing of Fibres. Recent Advances*

Chemical Technology Review No. 159.

Noyes Data Corp. Park Ridge, N. J., U.S.A., 1980, pp. 436

This is the middle volume in a smaller series of three within the overall one, which is about the manufacture and application of polymer fibres, yarns and fabrics. The first volume of the shorter series has been issued under the title "Fibre-Forming Polymers, Recent Ad-

vances" the forthcoming third will have the title "Manufacture of Yarns and Fabrics from Synthetic Fibres".

The volume under review is a survey of 250 patents granted in the U.S.A., from January 1977 on, for the formation, extrusion, and manufacture of synthetic fibres, including stretching, heat setting, and dyeing operations, with discussion of the wide range of applications open to these fibres and yarns.

The patent specifications are grouped in 12 chapters in agreement with the grouping to be found in technical monographs on the manufacture of fibres. Accordingly, the first three chapters deal with the formation of fibres from solutions or from melts by means of wet or dry spinning. The next chapter brings the extrusion of filaments, films and specially shaped fibres. A separate chapter is devoted to the spinning and extrusion of hollow fibres, glass fibres, carbon and metal carbide fibres, core yarns and other composite fibres, together with the production of fibrils and microfibrils. A separate chapter again deals with drawing, stretching, heatsetting, and with dyeing. The last chapter is about methods of how to recover the polymer substance from fibre waste.

Even this simple enumeration of the chapters suggests that every technical novelty that is important in the field of chemical fibres and of those produced for specific technological purposes will be found in this book. This initial impression will be reinforced by the perusal of these chapters.

Though limits of space prevent a detailed review and appreciation of the several chapters, it seems to be expedient to point out the most important technological novelties.

In the first chapter dry spinning of acrylics and modified varieties of these, and the production of celluloses, and fibres of other polymers, are discussed. Among the technological novelties the reader finds new compositions of solvents, descriptions of acrylic fibres with permanent crimp, of modacrylics with improved coloristic properties, of the novel fibres made of polypyrrolidone, together with the description of the apparatus and machinery suitable for the manufacture of these.

The second chapter deals with the wet spinning of acrylics and modacrylics, cellulose and starch fibres, polyamides and other nitrogen containing polymers and vinyls. The processes by means of which quite a number of properties of acrylics can be improved deserve special attention, as do the processes owing to which it became possible to produce wholly aromatic polyamide fibres of ever increasing importance.

The third chapter about melt-spinning, is not only the most extensive but also the most abundant in technological novelties. Most of the processes mentioned serve the production of polyester fibres, among them the high-speed production of pre-oriented yarns, then here are discussed further methods for the production of copolymers to reduce pilling, for that of antistatic fibres, and for that of fibres easier to dye, and more resistant to the effects of heat. A number of novel features concerning the polyamide fibres, non-woven webs, and the finishing of fibres are to be found in this chapter, together with new machinery put into the service of these new technologies.

The fourth chapter, on the extrusion of filaments, films, and shaped articles, offers a survey of the methods of up-to-date production of fibres. Here we find multilayer extrusion, preparation of semipermeable membranes, fibrillated polyester fibres, anionic polymerization of lactams in an extruder, and some more technological novelties.

Many technological novelties concerning the production of hollow fibres are described in the fifth chapter. Among these novelties we find hollow fibres for ion-exchange, reverse osmosis, ultra-filtration, and the separation of gases by selective permeability, and high-crimp and high-strength hollow rayon fibres.

A voluminous chapter, the sixth, treats of both the types, staple and filament, of glass fibres. These technical novelties are important because glass fibres are used in ever increasing quantities for the reinforcing of plastics. Not only the various general techniques of production of glass fibres are mentioned in this chapter but also those which serve the production of particular sorts of these fibres, e.g. that of glass fibres textured in analogy to other textile fibres, that of optical fibres, then of new adhesives which effect stable adhesion of polymers to glass fibres.

Chapter 7 is about carbon and metal carbide fibres. Carbon fibres are widely applied because they are elastic and show good tensile strength. In this chapter are discussed electrically conductive fibres, heat-conducting polytetrafluoroethylene, reinforcing yarns, and fabrics made of metal carbides.

Chapter 8 quotes patents for core yarns and composite fibres. The majority of these patents utilizes the possibilities inherent in the combination of filaments of various characters into a composite cord, provided that these characters successfully blend to be able to serve the specific purpose in mind, e.g. for the re-inforcing of tyres. Another method mentioned, of

manufacturing fibre with specific properties is based upon the principle of bicomponent fibres. A number of new apparatus for the realization of these novelties is also described.

Products partly applied in the textile industry, e.g. electrostatic spinning, and partly in other fields, are mentioned in Chapter 9. Several technologies serve the production of fibrils for paper industry. Hydrophilic fibrils made of polyolefines must be pointed out because these are noteworthy due to their containing inorganic pigments, on the one hand, and are not produced by known techniques of fibre formation, on the other. This chapter mentions patent specifications which describe, in contrast to usual fibre formation techniques, fibre formation from emulsion.

Some important technological operations relevant to man-made fibres, viz. drawing, stretching, and heatsetting, constitute the subject matter of the tenth chapter. Not only special technical processes are presented but also some which achieve the imparting of specific properties to the fibres by the appropriate selection of the chemical composition of the substances used for their formation, such as a fibre which is a spontaneously crimping composite of polyacrylonitrile.

Novel methods for improving dyeability of synthetic fibres are mentioned in the eleventh chapter. Such efforts can be realized in part by the alteration of the morphology of the fibres to favour their acceptance of the dyestuff, and in part by synthesis of specific dyestuffs, e.g. ones that are soluble in the spinning fluid. Six patent specifications deal with dyeing of polyester fibres. There are cases in which apparatus particularly associated to the method makes dyeing feasible at all.

Recovery of polymer substance is the topic of the twelfth chapter. First of all, regeneration of cellulose and of polyester are mentioned. Increase of the prices of the staple substances makes these methods important: these offer a way of how to utilize fibre waste.

This volume, like its fellows, is completed with the characteristic triple index, i.e. for company names, patent register numbers, and inventors.

In summary, it can be stated that this volume deserves perhaps more attention than even the other volumes in this series that already has become, and is becoming ever more, popular with professional people in Hungary. It offers a rich variety of knowledge in the field of the manufacture, processing, and application of synthetic fibres. These applications of the novel products are not confined to the textile industry but penetrate a wider domain, from the paper industry to the manufacture of artificial leather, of technical applications of all sorts. The new ideas highlighted in this volume may give new impetus to a somewhat slackened progress of synthetic fibre manufacture in recent years.

Gy. BERTALAN

*Topics in Current Chemistry, Vols 89 and 90*  
*Plasma Chemistry I—II*

Editors: S. VEPREK and M. VENUGOPALAN

Springer-Verlag, Berlin, Heidelberg, New York 1980, 143 and 121 pp.

The two volumes contain five review articles in different fields of plasma chemistry. David SMITH and Nigel G. ADAMS: *Elementary Plasma Reactions of Environmental Interest* (43 pages with 8 figures and 219 references).

The progress made in the last 10–15 years in the field of chemistry of the upper reaches of the atmosphere is reviewed. Data obtained from *in-situ* ion composition measurements as well as from appropriate laboratory experiments are summarized. In this review emphasis is placed on the detailed elementary ionic processes. Individual interactions as binary and tertiary ion-molecule reactions, electron-ion dissociative recombinations, ion-ion recombinations are discussed separately.

Dieter M. GRUEN, Stanislav VEPREK and Randy B. WRIGHT: *Plasma-Materials Interactions and Impurity Control in Magnetically Confined Thermonuclear Fusion Machines* (60 pages with 23 figures, 5 tables and 211 references).

This review deals with one of the problems that have to be solved if controlled thermonuclear fusion is to become an economically and environmentally acceptable energy source and summarizes the status of this field at the beginning of 1979.

After a short introduction, this review consists of the following sections:

The physics and technology of controlled thermonuclear fusion.

The role of impurities in TOKAMAKS.

Hydrogen Isotope Recycling.

Impurity release mechanisms.

Impurity control.

In this paper emphasis is placed on the importance of impurity problems, which constitute one of the limiting factors in the performance of present day TOKAMAKS.

This review will be of interest not only for chemists but also for physicists and for materials scientists.

D. KÜPPERS and H. LYDTIN: *Preparation of optical waveguides with the aid of plasma-activated Chemical Vapour Deposition at Low Pressures* (23 pages with 21 figures and 24 references).

This review gives an introduction into the preparation of optical fibers by means of the plasma-activated chemical vapour deposition (PCVD) method.

Deposition of silica, germania, boron oxide from their halides via a microwave oxygen discharge is discussed. High quality optical fibers have been obtained using the PCVD method. The PCVD process has now been in operation under pilot plant conditions.

Thus, this review will be important for those engaged in research on this or related areas and for those who want to obtain up-to-date information on this field of materials science.

Mundiyath VENUGOPALAN, Uptal K. RAYCHOWDHURY, Katherina CHAN and Marion L. POOL: *Plasma Chemistry of Fossil Fuels* (57 pages with 23 figures, 21 tables and 313 references).

In this review an attempt is made to summarize the results obtained in the field of plasma chemistry of fossil fuels between the period from the first efforts till 1978.

Following the introduction, in Section 2 thermodynamic and kinetic aspects of fossil fuel chemistry are discussed.

Section 3 deals with natural gas and methane gas plasmas. Reaction in low frequency, triboelectric and high frequency discharges, in electric arcs and plasma jets are discussed separately.

Section 4 is concerned with petroleum and petroleum by-product plasmas. The following topics are discussed: low and high frequency discharges, electrical arcs and plasma jets, submerged arcs in liquid petroleum, laser irradiation, plasma desulfurization of petroleum.

Section 5 gives a survey on the use of plasmas in coal treatment. Low and high frequency discharges, electrical and arc jets, flash and laser radiation of coal, plasma gasification of coal and plasma desulfurization of coal are discussed separately.

Section 6 deals with other fossil fuel plasmas. This section covers work on tar, heavy oil sands, oil shales and gilsonite.

In their concluding remarks the authors underline the diversity of results obtained in the systems considered. According to their conclusion, "further experimental work and theoretical modelling under more carefully controlled conditions are required for comprehensive understanding of the behaviour of fossil fuel plasmas".

Nevertheless, this review offers useful information for those who are working in the field of hydrocarbon and coal chemistry.

Mario CAPITELLI and Ettore MOLINARI: *Kinetics of dissociation processes in plasmas in the low and intermediate pressure range* (50 pages with 44 figures, 4 tables and 71 references).

In this review attention is focused on processes of molecular dissociation under non-equilibrium plasma conditions.

After introduction, Section 2 is devoted to a case study: the dissociation of molecular hydrogen. Evaluations of the electron energy distribution function (EDF), the pure vibrational mechanism (PVM), the joint vibroelectronic mechanism (JVE), the direct electronic mechanism (DEM) have been made and recombination processes discussed.

Section 3 deals with the dissociation of different diatomic molecules as  $N_2$ ,  $O_2$ , CO and HF.

Section 4 is devoted to polyatomic molecules. Three cases are examined: dissociation of carbon dioxide cracking of hydrocarbons, and ammonia decomposition.

In these sections an attempt has been made to compare the rates of selected plasmachemical reactions with predictions by mechanisms (PVM, DEM, JVE) based on the existence of electronic and vibrational non-equilibrium in the plasma.

In summary the 89th and 90th volumes of "Topics in Current Chemistry" contain five reviews covering different fields of plasma chemistry. These volumes can give plenty of new information to a broad spectrum of readers and will be important to those who want to be up to date in this rapidly advancing field.

J. MARGITFALVI

L. PATAKI and E. ZAPP: *Basic Analytical Chemistry*

Akadémiai Kiadó, Budapest 1980

This book gives a good survey of analytical chemistry in six chapters.

The first chapter deals with chemical equilibria, the concept of acids and bases the formation of complexes, precipitation, redox reactions, and the theory of partition equilibria. Qualitative analysis is the subject matter of Chapter 2. Classification according to FRESSENIUS is discussed in detail, but other possibilities of classification are also mentioned.

In the third chapter various fields of quantitative analysis, *viz.* gravimetry and titrimetry, are treated on the common theoretical grounds to be found in the theory of BRÖNSTED and LAWRY and in the principle of protonacceptors. Thus the fundamentals of the various methods are easy to retain in memory.

Instrumental methods of analysis are discussed in the fourth chapter. Progress in this field in recent years has been very rapid, thus it was a rather difficult task for the authors to acquaint the reader, within this small space at their disposal, with the fundamental principles at least, of every important method. Perhaps they had to keep in view the interest of non-chemists who study chemical analysis. Very little place could be allotted to the discussion of NMR or mass-spectrometry.

Chapter 5 is about methods of separation, with principal emphasis, quite correctly, on the techniques of chromatography.

The sixth chapter contains analytical methods relevant to organic compounds: this is a good review of the field.

This book, by L. PATAKI and E. ZAPP, certainly will be very useful for students of chemical analysis, and will offer valuable data to those engaged in analytical practice, considering that this concise volume exposes most clearly every important branch of chemical analysis.

T. MEISEL

Giulio MILAZZO: *Elektrochemie: Grundlagen und Anwendungen*

Zweite neubearbeitete und erweiterte Auflage, Band I

Birkhäuser Verlag, Basel—Boston—Stuttgart, 1980, 529 Seiten, 111 Abbildungen

Elektrochemische Methoden werden in sehr vielen und verschiedentlichen Gebieten des praktischen Lebens verwendet. Dies folgt aus dem interdisziplinären Charakter der Elektrochemie. Deshalb kann ein jedes in diesem Gebiet erscheinende Werk auf das Interesse eines weiten Kreises von Fachmännern rechnen.

Das Ziel des Autors war laut Vorwort des Buches eine möglichst einfache Zusammenfassung der Grundlagen der Elektrochemie zu geben, die auch von nicht-elektrochemischen Fachmännern gut verwendet werden kann. Dementsprechend behandelt der erste Abschnitt des Buches die Grundlagen der Thermodynamik und leitet jene Grundbegriffe ein, deren Kenntnis der Leser im weiteren unbedingt benötigt.

Die Diskussion der eigentlichen Elektrochemie beginnt mit dem zweiten Abschnitt. Hier beschreibt der Verfasser in der konventionellen Weise die Leitung der Elektrolytlösungen sowie die Eigenschaften der schwachen, starken und Schmelzelektrolyten. Der dritte Abschnitt befasst sich mit den in den Galvanzellen und an den Elektroden von heterogenen elektrochemischen Systemen sich einstellenden Gleichgewichten. Der vierte Abschnitt behandelt die Probleme der Elektrolyse sowie die wichtigsten kinetischen Gesetzmässigkeiten der Elektrolyseprozesse. Der fünfte Abschnitt des Buches befasst sich mit einem wichtigen Anwendungsgebiet der Elektrochemie: mit den elektrochemischen Methoden der analytischen Chemie. Der letzte Abschnitt diskutiert die elektrochemischen Beziehungen der kolloiden Systeme.

Wie aus obigem ersichtlich, folgt der Aufbau des Buches im wesentlichen den Aufbau früherer elektrochemischer Werke. Die Diskussion der einzelnen Fragen ist klar und logisch, wobei auch die verhältnismässig viele Tabellen behilflich sind. In der Bearbeitung der einzelnen Abschnitte wurden auch die berühmten Fachmänner des gegebenen Gebietes einbezogen.

Dies ist offensichtlich vom Gesichtspunkt der Diskussion des betroffenen Themenkreises vorteilhaft, doch verursacht es Schwierigkeiten bei der Vereinheitlichung und Abfassung des Werkes. So ist z. B. die Bearbeitung der Transporterscheinungen in Verbindung mit den Schmelzelektrolyten verhältnismässig eingehender und anspruchsvoller, als die Behandlung der selben Eigenschaften von Wässrigen Elektrolytlösungen. In dem mit Übertritt-Überspannung sich beschäftigenden Abschnitt steht überall Stromstärke  $I$ , während im nächsten Abschnitt, wo die Diffusions-Überspannung behandelt wird, Stromdichte  $j$  verwendet wird. Laut der wenigen Hinweise im ersten Band beschäftigt sich der zweite Band mit den Fragen der praktischen Anwendung der Elektrochemie. Sicher werden dann dort z. B. die Passivierung der Metalle sowie Verfahren in Verbindung mit der elektrolytischen Abscheidung der Metalle beschrieben. Es wäre daher vielleicht richtiger gewesen, die Fragen der Stromverteilung und der Energieausnutzung dort zu behandeln. Hingegen hätten bereits in diesem Band, in der Beschreibung der experimentellen Methoden die galvanostatische und die potentiostatische Untersuchungsmethoden behandelt werden sollen. (Gewisse Anwendungsgebiete dieser Methoden sind bereits im ersten Band erwähnt, s. Seiten 285 und 286.)

Es ist schade, dass Fragen in Verbindung mit der Struktur der elektrischen Doppelschicht im Buch nicht diskutiert werden. (Elektrokapillarkurve, Ladungs-Nullpunktpotential usw.) Ich glaube es wäre nützlich gewesen in Verbindung mit der elektrochemischen Kinetik auch solche Fälle kurz zu diskutieren, in denen die Kinetik durch verschiedene Prozesse gemeinsam beeinflusst wird (Ladungsübertritt, Diffusion, chemische Reaktion), oder in denen sich an der Elektrode parallele Prozesse abspielen. Wenn man nämlich die in der Praxis sich abspielenden Elektrodprozesse betrachtet, handelt es sich stets um verwickelte oder mehrere parallel verlaufende Prozesse.

Mann kann wohl sagen, dass der Verfasser sein grundlegendes Ziel erreichte, denn auch nicht-elektrochemische Fachmänner können mit Hilfe des Buches die Gesetze der Elektrochemie kennenlernen. Ausser den theoretischen Zusammenhängen werden auch die wichtigeren konventionellen Messmethoden der Elektrochemie beschrieben.

Es ist bedauernd, dass der Verfasser nicht die von der IUPAC empfohlene elektrochemische Nomenklatur verwendet hat. Die im Buch enthaltenen Definitionen, Konventionen und Bezeichnungen weichen an sehr vielen Stellen und in wesentlichen Fragen von der IUPAC-Empfehlung ab.

L. KISS

### J. K. PAUL: *Large and Small Scale Ethyl Alcohol Manufacturing Processes from Agricultural Raw Materials*

Chemical Technology Review No. 169, Energy Technology Review No. 58

Noyes Data Corporation, Park Ridge, New Jersey, U.S.A., 1980. p. 576

This volume provides the reader with process descriptions and economic evaluations for ethyl alcohol manufacturing plants with capacities ranging from 25 gallons per hour to 100 million gallons per year. Most fully described are the 50 million gallon/year and 25 gallon/hour facilities. The book is divided into four parts. Each part details a specific sized system from a particular starting material, with possible excursions on additional sized systems.

*Part 1.* Alcohol manufacture from corn on a 50 million gallons per year scale, with excursions to 10 and 100 million gallons per year pp. 1–345. The detailed analysis covers various raw materials, economic evaluation of the procedure, documentation of detailed design overall material and energy flow, equipment lists, etc., and bibliography 24 references.

*Part 2.* Wheat straw conversion *via* enzymatic hydrolysis for a 25 million gallon/year facility pp. 346–380. The compilation contains detailed technological descriptions, flow charts, economic analysis and 41 references.

*Part 3.* Molasses fermentation to produce 14 million gallons per year pp. 381–427. The chapter gives only a rough outline of the technology; the economic analysis is, however, detailed.

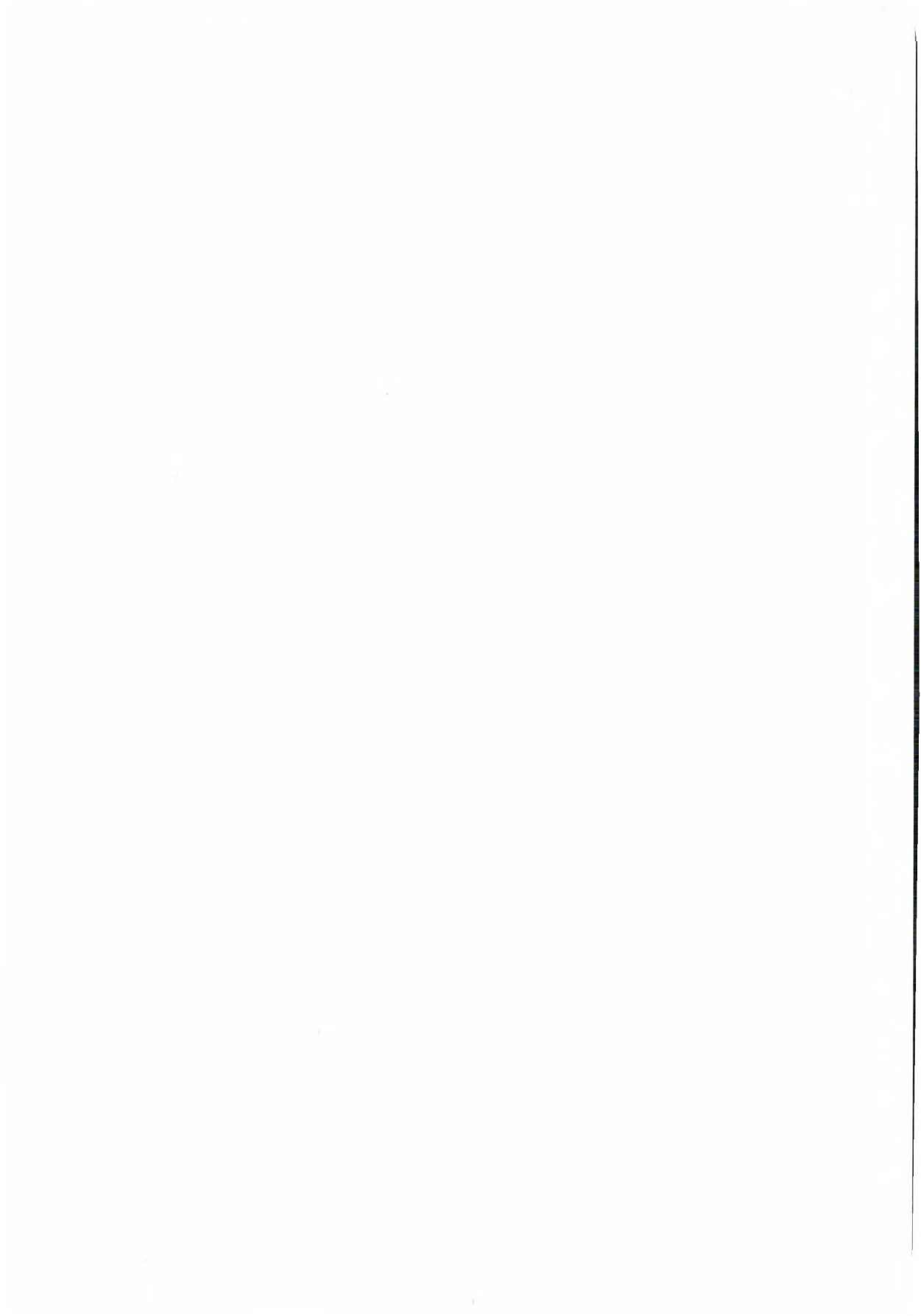
*Part 4.* A guide to small 25 gallons per hour production pp. 428–509, 14 references. This section contains technological and economic analysis for small-scale production.

The book includes discussions of legislation and permit information pertinent to alcohol plant operation, environmental considerations, plus lists of resources, people and organisations involved in alcohol promotion. At the end of the volume there are 78 fundamental literature references.

Interest in the manufacture of ethyl alcohol from agricultural raw materials has increased during the last few years. The use of ethanol as a gasoline extender gasohol has focussed attention on methods for both large- and small-scale ethyl alcohol production. A by-product of alcohol production is distillers dried grain, which could be sold as a protein-rich feed, thus dispelling fears that alcohol production from agricultural raw materials might be a threat to the world food supply.

The current volume is a logical supplement to a previous volume of the series which appeared in 1979 Ethyl Alcohol Production and Use as a Motor Fuel. Energy Technology Review No. 51. The successive publication of the two volumes also points to the timeliness and need for the discussion of the problem.

L. NYESTE



## INDEX

### PHYSICAL AND INORGANIC CHEMISTRY

The Extraction of Iron(III)-salicylate with an Indigenous Solvent Tri-isoamyl Phosphate (TAP), B. D. PANDEY, D. C. RUPAINWAR .....	1
Kinetics of Oxidative Decarboxylation of L-Cysteine by Permanganate, S. C. AMETA, H. L. GUPTA, P. N. PANDE, H. C. CHOWDHRY .....	7
Preparation, Infrared Absorption Spectra and X-Ray Powder Diffraction Patterns of Mixed (Ca+Sr+Pb) Hydroxylapatites, P. N. PATEL, S. PANDEY .....	13
Five-Coordinate Manganese(II) and Iron(II) Complexes of [2,6-( <i>N,N'</i> -Diacetyl and <i>N,N'</i> -Dibenzoyl)]-diaminopyridine, S. K. SANGAL, S. K. SAHNI, V. B. RANA .....	19
Molecular Decomposition Reactions of Dialkyl Ethers. The Estimation of Preexponential Factors, L. SERES .....	39
Study of Inhibitors by Electrode Impedance Measurements, L. MÉSZÁROS, B. LENGYEL, T. GARAI .....	57
Studies with Inorganic Precipitate Membrane. Membrane Selectivity from Multiionic Potential and Conductivity Measurements, M. N. BEG, R. SHYAM, R. P. KHANDELWAL .....	65
Mössbauer and Magnetic Studies on Hydroxo-Bridged Iron(III) Complexes of some Oximes, I. RANI, K. B. PANDEYA, G. L. SAWHNEY, J. S. BAIJAL .....	75
New Metallic Catalysts Obtained by Supporting Platinum on $AlPO_4-Al_2O_3$ and $AlPO_4-SiO_2$ Systems, M. A. ARAMENDIA, V. BORAU, C. JIMENEZ, J. M. MARINAS ..	97

### ORGANIC CHEMISTRY

Modified Crown Ethers, I. Carbonic Acid Derivatives Containing One Crown Ether Unit (Preliminary Communication), B. ÁGAI, I. BITTER, É. CSONGOR, L. TÓKE .....	25
Modified Crown Ethers, II. Carbonic Acid Derivatives of Bis-Crown Ethers (Preliminary Communication), B. ÁGAI, I. BITTER, É. CSONGOR, L. TÓKE .....	29
Synthesis of <i>N</i> <sup>1</sup> -Isonicotinoyl-3,5-diphenyl-4-(sulfamoylphenylazo)-1,2-diazoles as Antimalarial Agents, C. P. SINGH .....	35
The 1:1 and 1:2 Complex Formation between $\beta$ -Cyclodextrin and Benzoic Acid, Á. BUVÁRI, J. SZEJTLI, L. BARCZA .....	51
The Mannich Reaction of Cephalosporin Sulfoxides and Sulfones, J. Cs. JÁSZBERÉNYI, I. PETRIKOVICS, E. T. GUNDA, S. HOSZTAFI .....	81
Oxidation of some Cyclic $\alpha$ -Benzylidene Ketones with Thallium(III) Nitrate in Methanol, E. MÁRVÁNYOS, S. ANTUS, M. NÓGRÁDI .....	93

### ANALYTICAL CHEMISTRY

Error Analysis of a New Potentiometric Evaluation Method Based on the Measurement of the Bound Reagent Concentration, K. BURGER, L. DOMOKOS, G. PETHÓ, E. PUNGOR .....	85
--	----

RECENSIONES .....	103
-------------------	-----

PRINTED IN HUNGARY  
Akadémiai Nyomda, Budapest

Les Acta Chimica paraissent en français, allemand, anglais et russe et publient des mémoires du domaine des sciences chimiques.

Les Acta Chimica sont publiés sous forme de fascicules. Quatre fascicules seront réunis en un volume (3 volumes par an).

On est prié d'envoyer les manuscrits destinés à la rédaction à l'adresse suivante:

*Acta Chimica*  
Budapest, P.O.B. 67, H-1450, Hongrie

Toute correspondance doit être envoyée à cette même adresse.

La rédaction ne rend pas de manuscrit.

Abonnement en Hongrie à l'Akadémiai Kiadó (1363 Budapest, P.O.B. 24, C. C. B. 215 11488), à l'étranger à l'Entreprise du Commerce Extérieur « Kultura » (H-1389 Budapest 62, P.O.B. 149 Compte-courant No. 218 10990) ou chez représentants à l'étranger.

---

Die Acta Chimica veröffentlichen Abhandlungen aus dem Bereich der chemischen Wissenschaften in deutscher, englischer, französischer und russischer Sprache.

Die Acta Chimica erscheinen in Heften wechselnden Umfangs. Vier Hefte bilden einen Band. Jährlich erscheinen 3 Bände.

Die zur Veröffentlichung bestimmten Manuskripte sind an folgende Adresse zu senden

*Acta Chimica*  
Budapest, Postfach 67, H-1450, Ungarn

An die gleiche Anschrift ist jede für die Redaktion bestimmte Korrespondenz zu richten. Manuskripte werden nicht zurückerstattet.

Bestellbar für das Inland bei Akadémiai Kiadó (1363 Budapest, Postfach 24, Bankkonto Nr. 215 11488), für das Ausland bei «Kultura» Außenhandelsunternehmen (H-1389 Budapest 62, P.O.B. 149. Bankkonto Nr. 218 10990) oder seinen Auslandsvertretungen.

---

«Acta Chimica» издают статьи по химии на русском, английском, французском и немецком языках.

«Acta Chimica» выходит отдельными выпусками разного объема, 4 выпуска составляют один том и за год выходят 3 тома.

Предназначенные для публикации рукописи следует направлять по адресу:

*Acta Chimica*  
Budapest, P.O.B. 67, H-1450, ВНР

Всякую корреспонденцию в редакцию направляйте по этому же адресу.

Редакция рукописей не возвращает.

Отечественные подписчики направляйте свои заявки по адресу Издательства Академии Наук (1363 Budapest, P.O.B. 24. Текущий счет 215 11488), а иностранные подписчики через организацию по внешней торговле «Kultura» (H-1389 Budapest 62, P.O.B. 149. Текущий счет 218 10990) или через ее заграничные представительства и уполномоченных.

Reviews of the Hungarian Academy of Sciences are obtainable  
at the following addresses:

**AUSTRALIA**

C.B.D. LIBRARY AND SUBSCRIPTION SERVICE,  
Box 4886, G.P.O., Sydney N.S.W. 2001

COSMOS BOOKSHOP, 145 Ackland Street, St.  
Kilda (Melbourne), Victoria 3182

**AUSTRIA**

GLOBUS, Höchstädtplatz 3, 1200 Wien XX

**BELGIUM**

OFFICE INTERNATIONAL DE LIBRAIRIE, 30  
Avenue Marnix, 1050 Bruxelles  
LIBRAIRIE DU MONDE ENTIER, 162 Rue du  
Midi, 1000 Bruxelles

**BULGARIA**

HEMUS, Bulvar Ruski 6, Sofia

**CANADA**

PANNONIA BOOKS, P.O. Box 1017, Postal Sta-  
tion "B", Toronto, Ontario M5T 2T

**CHINA**

CNPICOR, Periodical Department, P.O. Box 50,  
Peking

**CZECHOSLOVAKIA**

MAD'ARSKÁ KULTURA, Národní třída 22,  
115 33 Praha

PNS DOVOZ TISKU, Vinohradská 46, Praha 2

PNS DOVOZ TLACE, Bratislava 2

**DENMARK**

EJNAR MUNKSGAARD, Norregade 6, 1165  
Copenhagen

**FINLAND**

AKATEEMINEN KIRJAKAUPPA, P.O. Box 128,  
SF-00101 Helsinki 10

**FRANCE**

EUROPERIODIQUES S. A., 31 Avenue de Ver-  
sailles, 78170 La Celle St.-Cloud

LIBRAIRIE LAVOISIER, 11 rue Lavoisier, 75008  
Paris

OFFICE INTERNATIONAL DE DOCUMENTA-  
TION ET LIBRAIRIE, 48 rue Gay-Lussac, 75240  
Paris Cedex 05

**GERMAN DEMOCRATIC REPUBLIC**

HAUS DER UNGARISCHEN KULTUR, Karl-  
Liebknecht-Strasse 9, DDR-102 Berlin

DEUTSCHE POST ZEITUNGSVERTRIEBSAMT,  
Strasse der Pariser Kommüne 3-4, DDR-104 Berlin

**GERMAN FEDERAL REPUBLIC**

KUNST UND WISSEN ERICH BIEBER, Postfach  
46, 7000 Stuttgart 1

**GREAT BRITAIN**

BLACKWELL'S PERIODICALS DIVISION, Hythe  
Bridge Street, Oxford OX1 2ET

BUMPUS, HALDANE AND MAXWELL LTD.,  
Cowper Works, Olney, Bucks MK46 4BN

COLLET'S HOLDINGS LTD., Denington Estate,  
Wellingborough, Northants NN8 2QT

WM. DAWSON AND SONS LTD., Cannon House,  
Folkestone, Kent CT19 5EE

H. K. LEWIS AND CO., 136 Gower Street, London  
WC1E 3BS

**GREECE**

KOSTARAKIS BROTHERS, International Book-  
sellers, 2 Hippokratous Street, Athens-143

**HOLLAND**

MEULENHOF-F-BRUNA B.V., Beulingstraat 2,  
Amsterdam

MARTINUS NIJHOFF B.V., Lange Voorhout 9-11,  
Den Haag

SWETS SUBSCRIPTION SERVICE, 347b Heere-  
weg, Lisse

**INDIA**

ALLIED PUBLISHING PRIVATE LTD., 13/14  
Asaf Ali Road, New Delhi 110001

150 B-6 Mount Road, Madras 600002

INTERNATIONAL BOOK HOUSE PVT. LTD.,  
Madame Cama Road, Bombay 400039

THE STATE TRADING CORPORATION OF  
INDIA LTD., Books Import Division, Chandralok,  
36 Janpath, New Delhi 110001

**ITALY**

EUGENIO CARLUCCI, P.O. Box 252, 70100 Bari

INTERSCIENTIA, Via Mazzè 28, 10149 Torino

LIBRERIA COMMISSIONARIA SANSONI, Via

Lamarmora 45, 50121 Firenze

SANTO VANASIA, Via M. Macchi 58, 20124

Milano

D. E. A., Via Lima 28, 00198 Roma

**JAPAN**

KINOKUNIYA BOOK-STORE CO. LTD., 17-7  
Shinjuku-ku 3 chome, Shinjuku-ku, Tokyo 160-91

MARUZEN COMPANY LTD., Book Department,  
P.O. Box 5050 Tokyo International, Tokyo 100-31

NAUKA LTD. IMPORT DEPARTMENT, 2-30-19  
Minami Ikebukuro, Toshima-ku, Tokyo 171

**KOREA**

CHULPANMUL, Phenjan

**NORWAY**

TANUM-CAMMERMEYER, Karl Johansgatan  
41-43, 1000 Oslo

**POLAND**

WĘGIERSKI INSTYTUT KULTURY, Marszał-  
kowska 80, Warszawa

CKP 1 W ul. Towarowa 28 00-95 Warszawa

**ROUMANIA**

D. E. P., București

ROMLIBRI, Str. Biserica Amzei 7, București

**SOVIET UNION**

SOJUZPETCHATJ — IMPORT, Moscow

and the post offices in each town

MEZHDUNARODNAYA KNIGA, Moscow G-200

**SPAIN**

DIAZ DE SANTOS, Lagasca 95, Madrid 6

**SWEDEN**

ALMQVIST AND WIKSELL, Gamla Brogatan 26,  
101-20 Stockholm

GUMPERTS UNIVERSITETSBOKHANDEL AB,  
Box 346, 401 25 Göteborg 1

**SWITZERLAND**

KARGER LIBRI AG, Petersgraben 31, 4071 Basel

**USA**

EBSCO SUBSCRIPTION SERVICES, P.O. Box  
1943, Birmingham, Alabama 35201

F. W. FAXON COMPANY, INC., 15 Southwest  
Park, Westwood, Mass. 02090

THE MOORE-COTTRELL SUBSCRIPTION

AGENCIES, North Cohocton, N.Y. 14868

READ-MORE PUBLICATIONS, INC., 140 Cedar  
Street, New York, N.Y. 10006

STECHERT-MACMILLAN, INC., 7250 Westfield  
Avenue, Pennsauken N.J. 08110

**VIETNAM**

XUNHASABA, 32, Hai Ba Trung, Hanoi

**YUGOSLAVIA**

JUGOSLAVENSKA KNJIGA, Terazije 27, Beograd  
FORUM, Vojvode Mišića 1, 21000 Novi Sad

# ACTA CHIMICA

ACADEMIAE SCIENTIARUM  
HUNGARICAE

ADIUVANTIBUS

M. T. BECK, R. BOGNÁR, GY. HARDY,  
K. LEMPERT, B. LENGYEL, K. POLINSZKY,  
E. PUNGOR, G. SCHAY,  
Z. G. SZABÓ, P. TÉTÉNYI

REDIGUNT

F. MÁRTA et GY. DEÁK

TOMUS 110

FASCICULUS 2



AKADÉMIAI KIADÓ, BUDAPEST

1982

ACTA CHIM. ACAD. SCI. HUNG.

ACASA2 110 (2) 117-237 (1982)

# ACTA CHIMICA

A MAGYAR TUDOMÁNYOS AKADÉMIA  
KÉMIAI TUDOMÁNYOK OSZTÁLYÁNAK  
IDEGEN NYELVŰ KÖZLEMÉNYEI

FŐSZERKESZTŐ

MÁRTA FERENC

SZERKESZTŐ

DEÁK GYULA

TECHNIKAI SZERKESZTŐ

HAZAI LÁSZLÓ

SZERKESZTŐ BIZOTTSÁG

BECK T. MIHÁLY, BOGNÁR REZSŐ, HARDY GYULA,  
LEMPERT KÁROLY, LENGYEL BÉLA, POLINSZKY KÁROLY,  
PUNGOR ERNŐ, SCHAY GÉZA, SZABÓ ZOLTÁN,  
TÉTÉNYI PÁL

Acta Chimica is a journal for the publication of papers on all aspects of chemistry in English, German, French and Russian.

Acta Chimica is published in 3 volumes per year. Each volume consists of 4 issues of varying size.

Manuscripts should be sent to

*Acta Chimica*

*Budapest, P.O. Box 67, H-1450, Hungary*

Correspondence with the editors should be sent to the same address. Manuscripts are not returned to the authors.

Hungarian subscribers should order from Akadémiai Kiadó, 1363 Budapest, P.O.B. 24. Account No. 215 11488.

Orders from other countries are to be sent to "Kultura" Foreign Trading Company (H-1389 Budapest 62, P.O.B. 149. Account No. 218 10990) or its representatives abroad.

## SYNTHESIS OF SOME 3-AROYLFLAVONES AS POTENTIAL FUNGICIDES

S. GIRI, NIZAMUDDIN and A. K. MISHRA\*

(Department of Chemistry, University of Gorakhpur, Gorakhpur, U.P., India)

Received August 7, 1980

In revised form February 9, 1981

Accepted for publication June 2, 1981

3-Aroylflavones have been prepared by oxidative cyclization of  $\alpha$ -aroylchalcones with selenium dioxide. The required chalcones have been synthesized by the base-catalyzed condensation reaction between  $\omega$ -aroyl-2-hydroxyacetophenones and aldehydes. The fungicidal activity of all these flavones have been evaluated against *Alternaria brassicae* and *Helminthosporium oryzae*.

### Introduction

Flavonoids are invariably present in the heartwood of several plants [1–3]. The durability and resistance towards the attack of pests of these woods is perhaps due to the presence of such flavonoid components or compounds related to them. It is significant that most of these compounds contain the  $-\text{CO}-\text{C}=\text{C}-\text{O}-$  moiety [4], and the pesticidal power is perhaps due to this very feature. This assumption is supported by the observation that natural pesticides like rotenone, chrysin and galangin [5–7] have this structural feature, characteristic of flavonoids and isoflavonoids.

Despite these observations, data on the pesticidal properties of synthetic flavonoid compounds are apparently lacking in the literature. In view of these facts, it appeared worthwhile to undertake the synthesis and investigation of the fungicidal properties of the title flavones reported herein.

The required  $\omega$ -aroyl-2-hydroxyacetophenones (**I**) were prepared by standard methods [8]. The chalcones (**II**) were synthesized by the Knoevenagel reaction [9] and the 3-aroylflavones were obtained by oxidative cyclization of the chalcones (**II**) with  $\text{SeO}_2$  in isoamyl alcohol [10]. The purity of the flavones was checked by TLC and the  $R_f$  values of the individual compounds were also noted.

The  $\omega$ -aroyl-2-hydroxyacetophenones (**I**) were characterized by their elemental analysis and IR absorption spectra. Significant peaks in the IR spectrum are  $3225 \text{ cm}^{-1}$  ( $-\text{O}-\text{H}$  stretching),  $1670 \text{ cm}^{-1}$  (saturated  $\beta$ -diketone

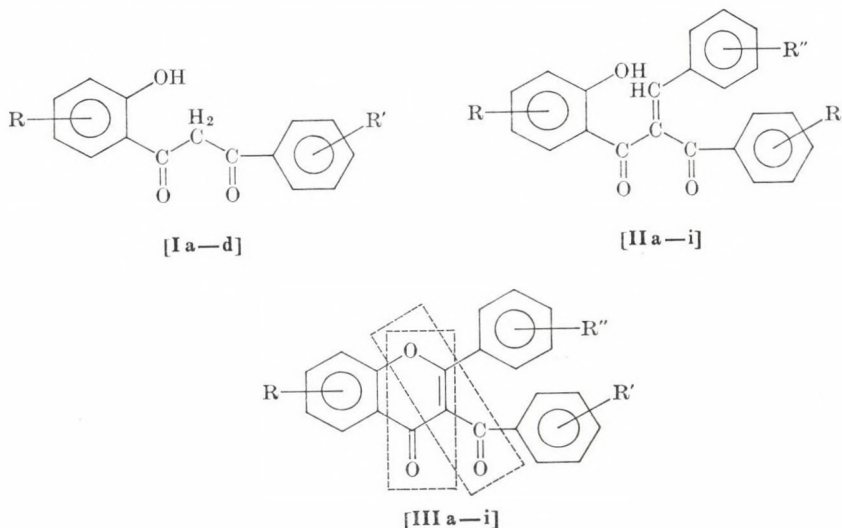
\* To whom correspondence should be addressed

stretching),  $1450\text{ cm}^{-1}$  ( $-\text{CH}_2-$  bending), and  $1600\text{ cm}^{-1}$ ,  $1590\text{ cm}^{-1}$ ,  $1370\text{ cm}^{-1}$  (aromaticity).

The chalcones (**II**) could be recognized by significant peaks in the IR spectra, *viz.*  $3115\text{ cm}^{-1}$  ( $-\text{O}-\text{H}$  stretching),  $1680\text{ cm}^{-1}$  ( $\alpha$ - $\beta$ -unsaturated acyclic ketone),  $1600$ ,  $1585$ ,  $1450\text{ cm}^{-1}$  (aromatic ring). The presence of the  $\gamma$ -pyrone ring in the IR spectrum of the flavones (**III**) affords evidence for the cyclization of the chalcones (**II**). The IR spectra of the flavones reveal characteristic absorption at  $1690\text{ cm}^{-1}$  ( $\gamma$ -pyrone ring);  $1710\text{ cm}^{-1}$  ( $>\text{C}=\text{O}$  stretching),  $1600$ ,  $1580$ ,  $1445\text{ cm}^{-1}$  (aromaticity) and  $1020\text{ cm}^{-1}$  ( $\text{C}-\text{O}-\text{C}$  sym. bond stretching).

The flavones listed in Table III have been screened for their fungicidal activity against two species of fungi, *Helminthosporium oryzae* and *Alternaria brassicae*. It has been found that almost all aroylflavones under investigation are very active against *A. brassicae* at all concentrations, but only few compounds are toxic to *H. oryzae*.

At the same time, the commercial fungicides Bavistin and Dithane M-45 were found to be quite toxic to both these fungal species when tested under identical conditions.



## Experimental

### Substituted 2-hydroxyacetophenones

2-Hydroxyacetophenone, b.p.  $210-212^\circ\text{C}$ , 2-hydroxy-4-methylacetophenone, b.p.  $244-246^\circ\text{C}$ , 2-hydroxy-5-chloroacetophenone, m.p.  $53^\circ\text{C}$  and 2-hydroxy-3-chloroacetophenone, m.p.  $76^\circ\text{C}$  were prepared by the Fries rearrangement of the corresponding esters by a known method [11]. The b.p.'s or m.p.'s of these compounds were consistent with those reported in the literature [12].

***ω*-Aroyl-2-hydroxyacetophenone (I)**

These compounds were prepared by Claisen condensation using the appropriate 2-hydroxyacetophenones (1.0 mol) and the different aryl esters (1 mol) in the presence of sodium ethoxide. The reaction mixtures were refluxed for 5–8 h. It is significant to note that the yield of product was greatly lowered (**Ic** and **Id**) when the starting ester also incorporated a

**Table I**  
*ω*-Aroyl-2-hydroxyacetophenones (I)

Compound No.	R	R'	Yield, %	M.P., °C.	Formula	C, %		H, %	
						Found	Calcd.	Found	Calcd.
<b>Ia</b>	5-Cl	H	65	87–8	C <sub>15</sub> H <sub>11</sub> O <sub>3</sub> Cl	65.57	65.69	3.93	4.01
<b>Ib</b>	4-CH <sub>3</sub>	H	71	119	C <sub>16</sub> H <sub>14</sub> O <sub>3</sub>	75.42	75.59	5.38	5.51
<b>Ic</b>	H	4-OH	51	109	C <sub>16</sub> H <sub>12</sub> O <sub>4</sub>	70.22	70.31	4.58	4.69
<b>Id</b>	3-Cl	4-OH	46	105	C <sub>15</sub> H <sub>11</sub> O <sub>4</sub> Cl	61.93	62.07	3.66	3.79

hydroxyl group. Attempts to improve the yield by allowing longer reaction times were of little avail. The compounds prepared were crystallized from aqueous ethanol and are listed in Table I.

***α*-Aroylchalcones (II)**

The *ω*-aroyl-2-hydroxyacetophenone (1 mol) and appropriate aromatic aldehyde (1 mol) dissolved in absolute alcohol were condensed under the condition of the Knoevenagel reaction, using a few drops of pyridine, for 10–12 h. After removal of the solvent, the residue was treated with dilute hydrochloric acid and then taken up in ether. The ethereal layer was washed with water and dried over anhydrous MgSO<sub>4</sub>. Removal of the ether gave the desired products, which were recrystallized from ethanol. The compounds prepared are recorded in Table II.

**Table II**  
*α*-Aroylchalcones (II)

Compound No.	R	R'	R''	Yield, %	M.p., °C.	Formula	C, %		H, %	
							Found	Calcd.	Found	Calcd.
<b>IIa</b>	5-Cl	H	4-NO <sub>2</sub>	62	86	C <sub>22</sub> H <sub>14</sub> NO <sub>5</sub> Cl	64.02	64.86	3.28	3.44
<b>IIb</b>	4-CH <sub>3</sub>	H	4-NO <sub>2</sub>	65	89	C <sub>23</sub> H <sub>17</sub> NO <sub>5</sub>	69.85	71.31	4.32	4.41
<b>IIc</b>	H	4-OH	4-OCH <sub>3</sub>	58	108	C <sub>23</sub> H <sub>18</sub> O <sub>5</sub>	75.81	76.52	4.66	4.80
<b>IId</b>	H	4-OH	4-NO <sub>2</sub>	60	91	C <sub>22</sub> H <sub>15</sub> NO <sub>6</sub>	67.62	67.86	3.69	3.85
<b>IIf</b>	H	4-OH	4-Cl	55	105	C <sub>22</sub> H <sub>16</sub> O <sub>4</sub> Cl	69.41	69.84	3.81	3.96
<b>IIg</b>	H	4-OH	2-OH	45	108–9	C <sub>22</sub> H <sub>16</sub> O <sub>5</sub>	72.84	73.33	4.00	4.17
<b>IIh</b>	3-Cl	4-OH	4-OH	42	106	C <sub>22</sub> H <sub>16</sub> O <sub>5</sub> Cl	66.62	67.01	3.71	3.81
<b>IIi</b>	3-Cl	4-OH	2-OH	40	118	C <sub>22</sub> H <sub>16</sub> O <sub>5</sub> Cl	66.58	67.01	3.65	3.81
<b>IIj</b>	3-Cl	4-OH	4-NO <sub>2</sub>	56	78	C <sub>22</sub> H <sub>14</sub> NO <sub>6</sub> Cl	62.14	62.41	3.12	3.31

Table III  
3-Aroylflavones (III)

Compd. No.	R	R'	R''	Yield, %	M.p., °C	Formula	R <sub>f</sub>	C, %		H, %	
								Found	Calcd.	Found	Calcd.
IIIa	6-Cl	H	4-NO <sub>2</sub>	56	97	C <sub>22</sub> H <sub>12</sub> NO <sub>5</sub> Cl	0.81 <sup>I</sup>	64.82	65.18	2.81	2.96
IIIb	7-CH <sub>3</sub>	H	4-NO <sub>2</sub>	60	125	C <sub>23</sub> H <sub>15</sub> NO <sub>5</sub>	0.56 <sup>I</sup>	70.98	71.68	3.82	3.89
IIIc	H	4-OH	4-OCH <sub>3</sub>	56	109–10	C <sub>23</sub> H <sub>16</sub> O <sub>5</sub>	0.71 <sup>II</sup>	73.64	74.19	4.16	4.30
III <sub>d</sub>	H	4-OH	4-NO <sub>2</sub>	54	98	C <sub>22</sub> H <sub>13</sub> NO <sub>6</sub>	0.59 <sup>I</sup>	68.10	68.22	3.10	3.35
IIIe	H	4-OH	4-Cl	50	103	C <sub>22</sub> H <sub>13</sub> O <sub>4</sub> Cl	0.7 <sup>I</sup>	69.58	70.21	3.22	3.46
III <sub>f</sub>	H	4-OH	2-OH	43	110	C <sub>22</sub> H <sub>14</sub> O <sub>5</sub>	0.41 <sup>II</sup>	73.01	73.74	3.75	3.91
III <sub>g</sub>	8-Cl	4-OH	4-OH	40	109	C <sub>22</sub> H <sub>13</sub> O <sub>5</sub> Cl	0.61 <sup>II</sup>	66.85	67.35	3.30	3.31
III <sub>h</sub>	8-Cl	4-OH	2-OH	38	92	C <sub>22</sub> H <sub>13</sub> O <sub>5</sub> Cl	0.45 <sup>II</sup>	66.78	67.35	3.26	3.31
III <sub>i</sub>	8-Cl	4-OH	4-NO <sub>2</sub>	52	74	C <sub>22</sub> H <sub>12</sub> NO <sub>6</sub> Cl	0.6 <sup>I</sup>	62.42	62.71	2.72	2.84

<sup>I</sup> Solvent system: chloroform–benzene (1 : 2)

<sup>II</sup> Solvent system: ethylacetate–chloroform–benzene (1 : 3 : 3)

### 3-Aroylflavones (III)

A mixture of the appropriate chalcone (1 mol) and selenium dioxide (1.1 mol) was refluxed in isoamyl alcohol for 14–20 h. The solvent was removed by steam distillation, the precipitated selenium was filtered off and the residue dissolved in ether. The ethereal layer, after the usual treatment, gave the desired product, which was recrystallized from ethanol. The compounds prepared are recorded in Table III.

#### Fungicidal screening

The flavones listed in Table III were tested for fungicidal activity using two species of fungi at three different concentrations, viz. 1000 ppm (10<sup>3</sup>), 100 ppm (10<sup>4</sup>), and 10 ppm (10<sup>5</sup>). The average percentage inhibition values obtained with these compounds are recorded in Table IV and compared with the effect of Bavistin (Carbendazim) and Dithane M-45 (Maneb).

$$\% \text{ Inhibition} = \frac{(C - T)}{C} \times 100$$

where  $C$  = diameter of fungus colony (in mm) in control plate  
 $T$  = diameter of fungus colony (in mm) in treated plate.  
 The number of repetitions was three in each case.

**Table IV**  
*Fungicidal screening*

Compd. No.	Average percentage inhibition after 96 h					
	<i>Alternaria brassicae</i> , Concentration			<i>H. oryzae</i> , Concentration		
	1000 ppm	100 ppm	10 ppm	1000 ppm	100 ppm	10 ppm
<b>IIIa</b>	60.67	39.5	28.2	44.8	26.3	19.1
<b>IIIb</b>	83.9	65.1	40.2	52.3	30.0	25.1
<b>IIIc</b>	72.5	60.0	36.2	43.3	22.8	17.5
<b>III d</b>	73.3	61.2	39.2	82.5	66.0	41.2
<b>IIIe</b>	78.5	59.6	39.1	49.3	28.2	20.5
<b>III f</b>	64.89	36.3	22.8	75.3	52.2	39.8
<b>III g</b>	76.7	55.2	38.3	46.0	27.4	21.2
<b>III h</b>	90.2	63.3	49.4	63.6	35.2	27.1
<b>III i</b>	78.0	60.1	40.3	90.5	69.3	48.2
Bavistin	95.3	81.4	69.8	93.9	77.4	66.9
Dithane M-45	98.6	89.5	77.2	97.5	88.3	73.9

### Results and Discussion

A critical examination of the fungicidal data reveals that all flavones under investigation were active against *A. brassicae*, while only three compounds (**III d**, **III f**, **III i**) having —OH, —Cl and —NO<sub>2</sub> substituents were active against *H. oryzae*. Compound **III h** having one chloro and two hydroxyl

groups has the highest fungitoxicity of the series. Further tests with this compound is required. Although all compounds investigated have toxophores such as  $-\text{NO}_2$ ,  $-\text{OH}$ ,  $-\text{Cl}$ , none of them are as active as the commercial fungicides Bavistin and Dithane M-45. This indicates that the fungitoxicity of a compound will not be the numerical sum of all toxophoric functions present in the molecule.

\*

The authors express their thanks to Prof. R. P. RASTOGI, Head, Department of Chemistry, University of Gorakhpur, for providing the necessary facilities. One of us (A. K. MISHRA) is thankful to C.S.I.R., New Delhi, for the award of a Junior Research Fellowship.

## REFERENCES

- [1] LINDSTEDT, G.: Acta Chem. Scand., **3**, 755, 759, 1375 (1949)
- [2] MAHESH, V. B., SESHADRI, T. R.: Jour. Sci. Ind. Research, **13B**, 835 (1954)
- [3] NAGRAJAN, G. R., SESHADRI, T. R.: Phytochemistry, **3**, 477 (1964)
- [4] LAUGER, P., MARTIN, H., MULLER, P.: Helv. Chim. Acta, **27**, 892 (1944)
- [5] SESHADRI, T. R., VISHWANATHAN, N.: Proc. Indian Acad. Sci., **25A**, 22 (1947)
- [6] CHARI, N. N., SESHADRI, T. R.: Proc. Indian Acad. Sci., **27A**, 128 (1948)
- [7] SESHADRI, T. R., VARDARAJAN, S.: Proc. Indian Acad. Sci., **35A**, 75 (1952)
- [8] "Organic Synthesis" Coll. Vol. **III**, p. 251.
- [9] JOSHI, K. C., JAUHAR, A. K.: J. Indian Chem. Soc., **39**, 463 (1962)
- [10] MAHAL, H. S., RAI, H. S., VENKETRAMAN, K.: J. Chem. Soc., **1935**, 866
- [11] BUU-HOI, H. P., LAVI, T. D., KUONG, N. D.: J. Org. Chem., **19**, 1617 (1954)
- [12] HEILBRON, I., BUNBURY, H. M.: Dictionary of Organic Compounds, Vol. **I**, pp. 507, Vol. **II**, pp. 712, 783 1953

S. GIRI	}	Chemistry Department, University of Gorakhpur, Gorakhpur (273001), India
NIZAMUDDIN		
A. K. MISHRA		

SYNTHESIS OF 5-METHOXY-2-(3,4-METHYLENE-DIOXYPHENYL)-4H-FURO[2,3-*h*][1]-BENZOPYRAN-4-ONE AND 5-METHOXY-2-PHENYL-4H-FURO[2,3-*h*][1]-BENZOPYRAN-4-ONE

V. P. PATHAK, G. P. GARG and R. N. KHANNA\*

(Department of Chemistry, University of Delhi, Delhi, India)

Received March 31, 1981

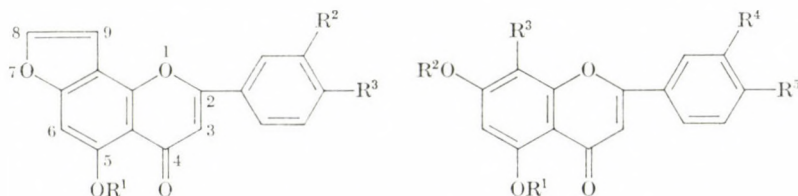
In revised form May 15, 1981

Accepted for publication June 2, 1981

Syntheses of the furanoflavones **1** and **2**, constituents of *Pongamia glabra* were accomplished starting from 5,7-dihydroxy-3',4'-methylenedioxyflavone and 5,7-dihydroxyflavone, respectively.

Furanoflavones such as karanjin are effective against skin diseases like leucoderma [1]. This prompted us to synthesize naturally occurring furanoflavones and we have already published the synthesis of some of them [2–7]. We now report the synthesis of 5-methoxy-2-(3,4-methylene-dioxyphenyl)-4H-furo[2,3-*h*] [1] benzopyran-4-one (**1**) and 5-hydroxy-2-phenyl-4H-furo-[2,3-*h*] [1] benzopyran-4-one (**2**), recently isolated from *Pongamia glabra* [8, 9]. The structures of these furanoflavones have been assigned on the basis of spectral and degradation studies.

The partial synthesis of **1** has also been reported [10] starting from 5-acetyl-4-hydroxy-6-methoxycoumarone and piperonyl chloride. We now report the total synthesis of **1** and **2** starting from 5,7-dihydroxy-3',4'-methylenedioxyflavone (**3**) and chrysin [11], respectively. Compound **3** (prepared



- |   |   |   |   |
|---|---|---|---|
| 1 | $R^1 = \text{CH}_3, R^2 + R^3 = \text{OCH}_2\text{O}$                                     | 3 | $R^1 = R^2 = R^3 = \text{H}, R^4 + R^5 = \text{OCH}_2\text{O}$                            |
| 2 | $R^1 = R^2 = R^3 = \text{H}$  | 4 | $R^1 = R^3 = \text{H}, R^2 = \text{allyl}, R^4 + R^5 = \text{OCH}_2\text{O}$              |
| 5 | $R^1 = \text{CH}_3, R^2 = \text{allyl}, R^3 = \text{H}, R^4 + R^5 = \text{OCH}_2\text{O}$ | 6 | $R^1 = \text{CH}_3, R^2 = \text{H}, R^3 = \text{allyl}, R^4 + R^5 = \text{OCH}_2\text{O}$ |
| 7 | $R^1 = R^3 = R^4 = R^5 = \text{H}, R^2 = \text{allyl}$                                    | 8 | $R^1 = R^2 = R^4 = R^5 = \text{H}, R^3 = \text{allyl}$                                    |

\* To whom correspondence should be addressed

by condensation of phloroacetophenone, piperonyl anhydride and sodium piperonylate by the ROBINSON method [12]) on partial allylation with one mole of allyl bromide, in the presence of potassium carbonate and acetone, afforded 7-allyloxy-5-hydroxy-3',4'-methylenedioxyflavone, which on methylation with dimethyl sulfate, potassium carbonate and acetone, followed by CLAISEN migration under reduced pressure, gave 8-allyl-7-hydroxy-5-methoxy-3',4'-methylenedioxyflavone (6).

The oxidation of 6 with osmium tetroxide/potassium periodate afforded an intermediate aldehyde, which on cyclization with polyphosphoric acid gave 1. The route described above starting from chrysin [11] resulted in 2 *via* 7 [2] and 8. The spectral data of the synthetic samples were in complete agreement with those reported for the natural samples.

## Experimental

All m.p.'s are uncorrected. IR spectra were recorded on a Perkin-Elmer IR spectrophotometer Model-621 ( $\nu$  max in  $\text{cm}^{-1}$ ) in KBr, UV spectra ( $\lambda$  max in nm) on a Beckmann DU-2 spectrophotometer, and NMR spectra on a Perkin-Elmer R-32 (90 MHz) spectrometer using TMS as internal standard. Chemical shifts are given in  $\delta$  ppm.

Anhydrous sodium sulfate was used as drying agent.

### 7-Allyloxy-5-hydroxy-3',4'-methylenedioxyflavone (4)

5,7-Dihydroxy-3',4'-methylenedioxyflavone (1.5 g) was dissolved in acetone (100 mL) and refluxed with allyl bromide (0.5 mL), potassium carbonate (3.5 g) and potassium iodide (0.5 g) for 4 h. The solid was filtrated off and washed with acetone. The acetone was completely evaporated and the residue diluted with water. The separated solid on crystallization from methanol/petroleum ether gave 3 as pale yellow crystals (1.35 g), m.p. 151–153 °C.

$\text{C}_{19}\text{H}_{14}\text{O}_6$ . Calcd. C 67.45; H 4.14. Found C 67.23; H 4.02%. (Acetate, m.p. 143–144 °C.)  
NMR of acetate ( $\text{CDCl}_3$ ): 7.6–7.82 (m, 2H, H-2',6'), 7.2 (d,  $J = 2$  Hz, 1H, H-8), 7.05 (d,  $J = 8.5$  Hz, 1H, H-5'), 6.74 (s, 1H, H-3), 6.42 (d,  $J = 2$  Hz, 1H, H-6), 6.05 (s, 2H,  $-\text{OCH}_2-$ ), 5.5–5.95 (m, 1H,  $-\text{CH}=\text{CH}_2$ ), 5.05–5.43 (m, 2H,  $-\text{CH}=\text{CH}_2$ ), 4.43 (d,  $J = 6$  Hz, 2H,  $-\text{OCH}_2-\text{CH}=\text{CH}_2$ ), 2.1 (s, 3H,  $\text{OCOCH}_3$ ).

‡

### [7-Allyloxy-5-methoxy-3',4'-methylenedioxyflavone (5)

The flavone 4 (1.2 g) was dissolved in acetone (100 mL) and refluxed with dimethyl sulphate (0.55 mL) and potassium carbonate (4.2 g) for 16 h. The solvent was evaporated and water was added to the residue. The separated solid was filtered off and purified by crystallization from ethanol to obtain light yellow crystals (940 mg), m.p. 179 °C.

$\text{C}_{20}\text{H}_{16}\text{O}_6$ . Calcd. C 68.19; H 4.54. Found C 67.82; H 4.43%.  
NMR ( $\text{CDCl}_3$ ): 7.55–7.76 (m, 2H, H-2',6'), 7.15 (m, 2H, H-5',8), 6.66 (s, 1H, H-3), 6.4 (d,  $J = 2$  Hz, 1H, H-6), 6.05 (s, 2H,  $-\text{OCH}_2\text{O}-$ ), 5.45–5.9 (m, 1H,  $-\text{CH}=\text{CH}_2$ ), 5.05–5.4 (m, 2H,  $-\text{CH}=\text{CH}_2$ ), 4.45 (d, 2H,  $J = 5.5$  Hz,  $-\text{OCH}_2-\text{CH}=\text{CH}_2$ ) and 3.98 (s, 3H,  $\text{OCH}_3$ ).

### 8-Allyl-7-hydroxy-5-methoxy-3',4'-methylenedioxyflavone (6)

The flavone 5 (900 mg) was heated in an oil bath at 190–200 °C under reduced pressure (12 mm) for 2 h. The resulting solid was dissolved in ethyl acetate and extracted with 2% aqueous sodium hydroxide (50 mL). The aqueous layer on acidification afforded a solid, which

was filtered off and crystallized from ethanol to give pale yellow needles (550 mg), m. p. 291–292 °C. (Acetate, m.p. 171–173 °C.)

NMR of acetate: 7.65–7.9 (m, 2H, H-2',6'), 7.15 (d,  $J = 9$  Hz, 1H, C-5'), 6.7 (s, 1H, H-3), 6.32 (s, 1H, H-6), 6.15 (s, 2H,  $-\text{OCH}_2\text{O}-$ ), 5.5–6.0 (m, 1H,  $-\text{CH}=\text{CH}_2$ ), 4.95–5.4 (m, 2H,  $-\text{CH}=\text{CH}_2$ ), 3.92 (s, 3H,  $\text{OCH}_3$ ), 3.5 (d,  $J = 6$  Hz, 2H,  $\text{Ar}-\text{CH}_2-\text{CH}=\text{CH}_2$ ) and 2.3 (s, 3H,  $\text{OCOCH}_3$ ).

#### 5-Methoxy-2-(3,4-methylenedioxyphenyl)-4H-furo[2,3-h][1]benzopyran-4-one (1)

The allyl flavone **6** (450 mg) was dissolved in ethyl acetate (80 mL) and an equal amount of water was added. This mixture was treated with osmium tetroxide (50 mg) and stirred for 2 h. During this period potassium periodate (3.5 g) was added to the solution in small portions. The ethyl acetate layer was separated and the aqueous layer extracted with more ethyl acetate (100 mL). The combined extracts were washed with water, dried, and the solvent removed under reduced pressure. The black tarry residue was heated with polyphosphoric acid (15 mL) on a boiling water bath for half an hour. The resulting mixture was added to ice and allowed to stand overnight. The black solid, on purification by column chromatography afforded **1** as a yellow solid (35 mg), m.p. and mixed m.p. 268–269 °C.

$\text{C}_{19}\text{H}_{12}\text{O}_6$  Calcd. C 67.8, H 3.57 Found C 67.76, H 3.52%.

UV(MeOH): 230, 275 and 330 (qualitative).

IR (KBr): 1640 (C=O), 1590 (C=C), 1465, 1400, 1252, 1202, 1140, 1114, 1060, 1030, 960, 911 ( $-\text{OCH}_2\text{O}-$ ), 860, 850, 835, 815, 740, 712 ( $-\text{OCH}_2\text{O}-$ ).

The NMR spectrum could not be recorded owing to the insolubility of the product

#### 8-Allyl-5,7-dihydroxyflavone (8)

The flavone **7** [2] (1.0 g) was heated under reduced pressure (12 mm) at 190–200 °C for 2 h. It was then cooled, dissolved in ethyl acetate and washed with water. The ethyl acetate layer was dried and the solvent evaporated. The purification of the residue by column chromatography afforded **8** as a cream-coloured solid (600 mg), m.p. 233–235 °.

$\text{C}_{18}\text{H}_{14}\text{O}_4$  Calcd. C 73.48; H 4.76. Found C 73.57; H 4.65% (Diacetate, m.p. 160–161 °C).

NMR of diacetate ( $\text{CDCl}_3$ ): 7.75–7.98 (m, 2H, H-2',6'), 7.42–7.6 (m, 3H, H-3', 4', 5'), 6.88 (s, 1H, H-3), 6.68 (s, 1H, H-6), 5.6–6.1 (m, 1H,  $-\text{CH}=\text{CH}_2$ ), 4.9–5.25 (m, 2H,  $-\text{CH}=\text{CH}_2$ ), 3.72 (d, 2H,  $J = 6.5$  Hz,  $-\text{OCH}_2-\text{CH}=\text{CH}_2$ ), 2.44 and 2.37 (2s, 3H, each, 2  $\text{OCOCH}_3$ ).

#### 5-Hydroxy-2-phenyl-4H-furo[2,3-h][1]benzopyran-4-one (2)

The flavone **8** (450 mg) was oxidized with  $\text{OsO}_4/\text{KIO}_4$  and the aldehyde so formed was cyclized with PPA to give **2** (40 mg) as mentioned in the case of **6**, m.p. 195–197 °C (*lit.* [9] m.p. 198 °C).

$\text{C}_{17}\text{H}_{10}\text{O}_2$  Calcd. C 73.38; H 3.5. Found C 73.42; H 3.65%.

IR(KBr): 1650 (C=O) 1608, 1595 (C=C), 1450, 1418, 1345, 1290, 1130, 1060, 1055, 800, 760.

NMR( $\text{CDCl}_3$ ): 12.8 (s, 1H, OH), 7.68–8.0 (m, 2H, H-2',6'), 7.35–7.62 (m, 4H, H-3', 4', 5', 8), 7.05 (m, 1H, H-9), 6.98 (s, 1H, H-6) and 6.65 (s, 1H, H-3).

\*

One of the authors (V.P.P.) is grateful to C.S.I.R. (New Delhi) for the award of Senior Research Fellowship.

#### REFERENCES

- [1] MUSTAFA, A.: *Furopyrans and Furopyrones, in the Chemistry of Heterocyclic Compounds*, p. 183. (A. WEISSBERGER Ed.) John Wiley, New York 1967
- [2] ANEJA, R., KHANNA, R. N., SESHADRI, T. R.: *J. Chem. Soc.*, **1963**, 163
- [3] KHANNA, R. N., SESHADRI, T. R.: *Tetrahedron*, **19**, 219 (1963)

- [4] KHANNA, R. N., SESHADRI, T. R.: Indian J. Chem., **1**, 385 (1963)
- [5] ROY, D., KHANNA, R. N.: Indian J. Chem., **16B**, 525 (1979)
- [6] PATHAK, V. P., KHANNA, R. N.: Gazz. Chim. Ital., **111**, 45 (1981)
- [7] PATHAK, V. P., KHANNA, R. N.: Indian J. Chem., **20B**, 622 (1981)
- [8] GARG, G. P., SHARMA, N. N., KHANNA, R. N.: Indian J. Chem., **16B**, 658 (1978)
- [9] TALAPATRA, S. K., MALIK, A. K., TALAPATRA, B.: Phytochemistry, **19**, 1199 (1980)
- [10] PAVANARAM, S. K., ROW, L. R.: Aust. J. Chem., **9**, 132 (1956)
- [11] ROBINSON, R., VENKATARAMAN, K.: J. Chem. Soc., **1926**, 2344
- [12] KALFF, J., ROBINSON, R.: J. Chem. Soc., **127**, 182 (1925)

Ved Prakash PATHAK }  
Gyan Prakash GARG } Department of Chemistry, University of  
Rajinder Nath KHANNA } Delhi, Delhi-110007, India

## POLAROGRAPHIC DETERMINATION OF POTENTIAL GUEST MOLECULES IN THE PRESENCE OF CYCLODEXTRIN

L. DARUHÁZI<sup>1</sup>, J. SZEJTLI<sup>2</sup> and L. BARCZA<sup>1\*</sup>

(<sup>1</sup> *Institute for Inorganic and Analytical Chemistry, Eötvös Loránd University, Budapest and*  
<sup>2</sup> *Biochemical Research Laboratory of Chinoïn Chem.-Pharm. Works, Budapest)*

Received January 30, 1981

Accepted for publication June 9, 1981

The potential-depending adsorption of  $\beta$ -cyclodextrin on the surface of dropping mercury electrode disturbs the determination of guest molecules if  $E_{1/2}$  is more negative than  $E_{ads}$ . The disturbing effect can be eliminated either by adding competitive guest molecule (which forms a more stable inclusion complex with cyclodextrin) or more conveniently by saturating the mercury surface with  $\beta$ -cyclodextrin. The linearity of wave height *vs.* concentration can be restored by this saturation method, notwithstanding a significant decrease in the slope of calibration curve is observed.

$\beta$ -Cyclodextrin (cycloheptaamylose) forms inclusion complexes with many organic molecules [1] and seems to get interest in pharmacy, too [1]. In aqueous solutions, the dissociation equilibria of the complexes are attained rapidly. Analysing such complexes, unexpected problems often arise [2]. Similar to most of the polyalcohols, cyclodextrins are also adsorbed on the surface of the mercury drop, so it may disturb the polarographic determination of potential guest molecules.

The adsorption of  $\beta$ -cyclodextrin depends on the electrode potential applied, so it can be studied by alternating current polarography. The differential capacity of the double-layer changes on the adsorption potential so a peak can be observed on the alternating current *vs.* potential curve, which consists of only capacitive current [3, 4]. The adsorption potential is about  $-0.1$ – $-0.2$  V (*vs.* S.C.E.); the current *vs.* concentration curve follows the Langmuir isotherm. The first part of the isotherm is linear, so the method is suitable for the determination of small amounts ( $1$ – $20$   $\mu\text{g} \cdot \text{cm}^{-3}$ ) of cyclodextrin [3].

Several authors have investigated the polarographic behaviour of cyclodextrin complexes containing electroactive guest molecules, and attempted to determine stability constants (MATSUI and his co-workers [5];  $\beta$ -cyclodextrin-hydroperoxide complexes; UEHARA and NAKAYA [6]; complexes of azomethin derivatives; YAMAGUCHI *et al.* [7]; hydrogen-peroxide complex). Polarography was used in the study of ferrocene-cyclodextrin complex, too [8].

\* To whom correspondence should be addressed

The reduction of nitrophenols was studied in the presence of cyclodextrin [9, 10]. It was shown that the reduction wave of nitrophenol splits into two waves in the presence of  $\alpha$ -cyclodextrin (cyclodextrin, cyclohexaamylose). This effect cannot be observed with  $\beta$ -cyclodextrin, but the wave height decreases with increasing  $\beta$ -cyclodextrin concentration. It seems to be quite reasonable that a decrease in wave height is a direct consequence of the complexation and only the free nitrophenol gives a polarographic wave. Based on this assumption stability constants were calculated.

Our measurements prove the fact mentioned [3] that decrease in wave height is caused by the inhibiting effect of the adsorbed  $\beta$ -cyclodextrin.

### Experimental

Measurements were carried out on Radelkis OH-105 and Radiometer PO-4 polarographs. Dropping mercury electrode was used with S.C.E. as reference. In alternating current polarography a three-electrode system (with large platinum surface) was used. Supporting electrolytes were Britton-Robinson buffer of pH = 6.8, and 0.1 M formic acid in acidic media. It is proved that there is no complex formation with these electrolytes [12].

The tensammetric curve of the supporting electrolyte and that in the presence of the  $\beta$ -cyclodextrin is shown in Fig. 1. A well-defined capacitive peak can be observed at about  $-0.15$  V. Measurements were carried out both in acidic and in neutral media.

The peak height *vs.* concentration curve follows the Langmuir isotherm; the adsorption constant is  $k = 7.6 \times 10^4 M^{-1}$  in acidic medium, and  $k = 5.8 \times 10^4 M^{-1}$  in neutral medium (in good agreement with [3], where  $k$  is about  $10^5$ ). The maximum surface coverage is reached at  $3 \times 10^{-4} M$   $\beta$ -cyclodextrin concentration.

As the usual concentration range is about this concentration in polarographic measurements, it is obvious that the calibration curve of complex forming depolarizers differs from that obtained in the absence of cyclodextrin.

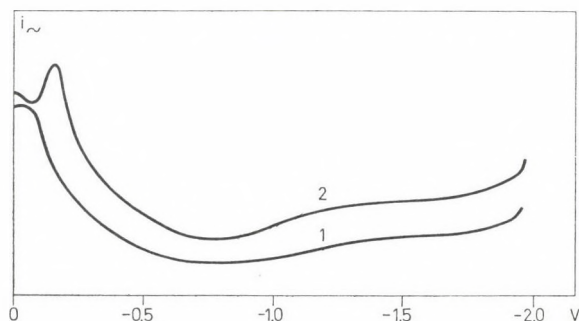


Fig. 1. Tensammetric curve of cyclodextrin; 1: supporting electrolyte without cyclodextrin, 2: with  $10^{-2} M$  cyclodextrin

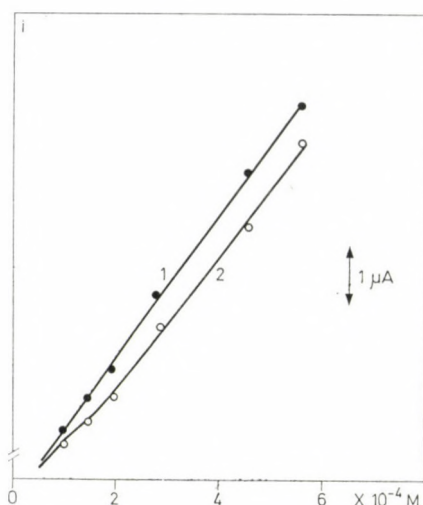


Fig. 2. Calibration curves of the  $K_3$  vitamin (1), and the 1 : 1  $K_3$ - $\beta$ -cyclodextrin complex (2)

When a complex of 1 : 1 stoichiometry is dissolved, the cyclodextrin concentration can be obtained from the following equation:



(where CD is the cyclodextrin and G is the guest molecule). The formation is characterized by the equation:

$$\beta = \frac{[\text{CD} \cdot \text{G}]}{[\text{CD}][\text{G}]} \quad (2)$$

If the stoichiometry is 1 : 1, the correlation between the total concentration of the inclusion complex and the free cyclodextrin is not linear as it is shown in Eq. 3:

$$[\text{CD} \cdot \text{G}]_T = [\text{CD}] + \beta[\text{CD}]^2 \quad (3)$$

In most cases stoichiometry differs from simple ratios (eq. 1 : 1, 1 : 2), therefore the above equations become more complicated — so it is obvious that polarographic determinations in these systems are rather difficult. In Fig. 2, the calibration curves of  $K_3$  vitamin (2-methyl-1,4-naphtoquinone, menadion) are shown, in the absence of cyclodextrin (curve 1); curve 2 is the calibration curve of the 1 : 1 complex.

Cyclodextrin does not disturb the determination of substances with more positive half-wave potential than that of the adsorption, but as it was mentioned, the reduction mechanism may be modified. We observed this phenomenon with Cu(II) ion: the half-wave potential of Cu(II) is more positive than the adsorption potential so inhibition is not likely, however two

steps are observed in the presence of  $\beta$ -cyclodextrin. In the first step, Cu (I)- $\beta$ -cyclodextrin complex is formed at  $-0.05$  V then the complex is reduced at a more negative potential ( $-0.37$  V) to yield  $\text{Cu}(\text{Hg})_X$ .

Theoretically there are three possibilities to eliminate the effect of cyclodextrin:

*i.* to prevent its adsorption with a substance that adsorbs to a greater extent and more strongly than cyclodextrin,

*ii.* to reduce the free cyclodextrin concentration with an electroinactive complex-forming agent added in excess,

*iii.* to increase cyclodextrin concentration adding cyclodextrin to the solution to reach maximum surface coverage.

These possibilities were studied through the reduction of Cu(II) and  $\text{K}_3$  vitamin. (The polarographic behaviour of these substances is rather simple and well known [11].)

The first possibility of the three was examined using gelatine and Triton X-100 (in 0.02 and 0.1% concentration respectively). It was observed that these substances form complexes with cyclodextrin and a very compact layer was formed on the surface. The Cu(II) wave is reduced by this layer to one-third of the original value.

The second possibility for hindering the effect of  $\beta$ -cyclodextrin was examined using aromatic carboxylic acids around pH 7. (They proved to be the most effective among the studied compounds.) The stability constant of their cyclodextrin complexes is about  $10^3 \text{ L} \cdot \text{M}^{-1}$ , so it was supposed that using them in excess, the free cyclodextrin concentration would be decreased in competing reactions, and if the complex is not adsorbed, the surface coverage can be reduced to zero.

Using this method the following problems may arise: *a.* the complex can be adsorbed on the surface, as it was observed with benzoic acid; *b.* if the complex is adsorbed, a more compact layer forms, so further decrease in the wave height can be expected (see Table I); *c.* the solubility of the inactive

Table I

Anti-guest molecule	Decrease in a wave height (%)
none	0.0
$5 \times 10^{-3} \text{ M}$ benzoic acid	-12.5
$5 \times 10^{-3} \text{ M}$ salicylic acid	- 4.3
$5 \times 10^{-3} \text{ M}$ anthranilic acid	- 2.9
$5 \times 10^{-3} \text{ M}$ <i>o</i> -toluic acid	-22.5
$5 \times 10^{-3} \text{ M}$ <i>m</i> -toluic acid	-27.0

$\text{K}_3$  vitamin concentration:  $10^{-4} \text{ M}$ ; cyclodextrin concentration:  $3 \times 10^{-3} \text{ M}$

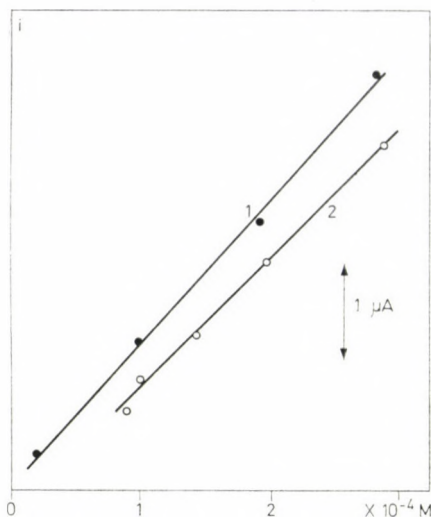


Fig. 3. Calibration curve in the presence of  $\beta$ -cyclodextrin, 1:  $K_3$  calibration curve without  $\beta$ -cyclodextrin, 2: with  $10^{-2}$  M  $\beta$ -cyclodextrin

compounds is usually limited, so it may happen that a great excess in solution cannot be applied.

Table I illustrates all of the mentioned problems. It is noteworthy at every depolarizer to be obtained experimentally, and every depolarizer to be examined would require specific competitive guest molecule. These molecules cannot be selected theoretically, because in the case of complex adsorption, there is a complex equilibrium on the surface of the drop that makes evaluation very difficult.

The third possibility is the simplest, and proved to be utilizable in the majority of the cases examined, so a great excess of cyclodextrin must be added to all solutions. It is obvious that the original calibration curve recorded in the absence of cyclodextrin cannot be used.

Figure 3 shows that the curve is linear in this case as well, only the absolute values of wave height are different, and the slope is less steep.

#### REFERENCES

- [1] BENDER, M. L., KOMILYAMA, M.: *Cyclodextrin Chemistry*. Springer Verlag, Berlin—Heidelberg—New York 1978
- [2] SZEJTLI, J.: *Stärke*, **30**, 427 (1978)
- [3] MATSUI, Y., SAWADA, H., MOCHIDA, K., DATE, Y.: *Bull. Chem. Soc. Japan*, **48**, 3446 (1975)
- [4] MATSUI, Y., SAWADA, H., MOCHIDA, K., DATE, Y.: *Bull. Chem. Soc. Japan*, **48**, 3645 (1975)
- [5] MATSUI, Y., SAWADA, H., MOCHIDA, K., DATE, Y.: *Bull. Chem. Soc. Japan*, **43**, 199 (1970)

- [6] UEHARA, M., NAKAYA, J.: *Nippon Kagaku Zasshi*, **1974**, 2440  
[7] YAMAGUCHI, S., MIYAGI, C., YAMAKAWA, Y., TSUKAMOTO, T.: *Nippon Kagaku Zasshi*, **1975**, 526  
[8] SIEGEL, B., BRESLOW, R.: *J. Am. Chem. Soc.*, **97**, 6869 (1975)  
[9] YAMAGUCHI, S., TSUKAMOTO, T.: *Nippon Kagaku Zasshi*, **1976**, 1856  
[10] OSA, T., MATSUI, T., FUJIHARA, M.: *Heterocycles*, **6**, 1833 (1977)  
[11] BREZINA, A., ZUMAN, P.: *Polarographie in der Medizin Biochemie und Pharmazie* *Academ. Verlagsgesellschaft Leipzig*, 1956  
[12] ROHRBACH, R. P., RODRIGUEZ, L. J., EYRING, L. J., WOJCIK, J. F.: *J. Phys. Chem.*, **81**, 944 (1977)

László DARUHÁZI }  
Lajos BARCZA } H-1443 Budapest, P.O. Box 123

József SZEJTLI H-1026 Budapest, Endrődi Sándor u. 38—40.

## SYNTHESIS OF SOME NEW 2-ARYL-5-ARYL/- ARYLOXYMETHYL-1,3,4-OXADIAZOLO[3,2-*a*]-*s*- -TRIAZINE-7-THIONES AND THEIR PARENT THIOUREAS AS POTENTIAL PESTICIDES<sup>+</sup>

B. K. BHATTACHARYA<sup>1\*</sup>, H. SINGH<sup>2</sup>, L. D. S. YADAV<sup>3</sup> and G. HOORNAERT<sup>1</sup>

(<sup>1</sup> Department of Chemistry, K. U. Leuven, Laboratory for Organic Synthesis, Leuven, Belgium, <sup>2</sup> Department of Chemistry, University of Gorakhpur, Gorakhpur, U.P., India, <sup>3</sup> Tokyo Institute of Technology, Japan)

Received February 13, 1981

In revised form June 1, 1981

Accepted for publication June 25, 1981

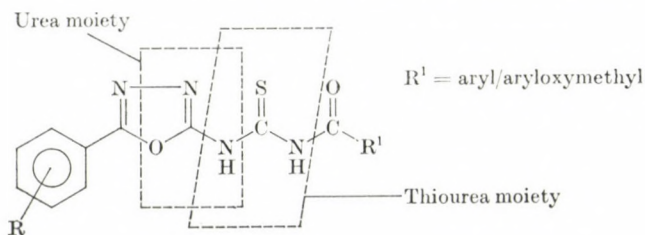
Fifteen 2-aryl-5-aryl/aryloxymethyl-1,3,4-oxadiazolo[3,2-*a*]-*s*-triazine-7-thiones have been synthesized by the cyclization of *N*<sup>1</sup>-aroyl/aryloxy-acetyl-*N*<sup>2</sup>-(5-aryl-1,3,4-oxadiazol-2-yl) thioureas with POCl<sub>3</sub> and PCl<sub>5</sub>. The thioureas were prepared by the reaction of NH<sub>4</sub>SCN and aryl/aryloxyacetyl chlorides.

As examples of an alternative route, six of the oxadiazolo-*s*-triazines were also synthesized by hetero Diels-Alder reaction using 5-aryl-1,3,4-oxadiazol-2-aryl isothiocyanate and aryl/aryloxymethyl cyanide. Nine representative compounds were evaluated for their herbicidal and fungicidal activities against two weeds, *Argemone maxicana* and *Cyperus rotundus*, and two fungal species *viz.* *Aspergillus niger* and *Helminthosporium oryzae*.

Based on the screening data, a possible relationship between structure and pesticidal activity is given.

### Introduction

Thioureas are well known to display a wide range of biocidal activities like bactericidal, fungicidal, herbicidal and insecticidal [1–4] actions. Thus it was presumed that the thioureas (III) synthesized in this investigation might



(III)

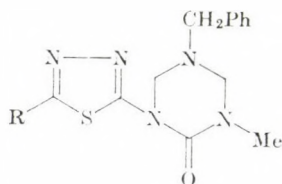
<sup>+</sup> Presented at the Annual Convention of Chemists, Indian Institute of Technology, Bombay, India, 27th December 1980, organized by the Indian Chemical Society.

\* To whom correspondence should be addressed.

\* Post-doctoral research fellow at K.U. Leuven, Belgium (on sabbatical leave from U.N. Post-Graduate College Padrauna, Padrauna, 274304, Deoria, U.P., India).

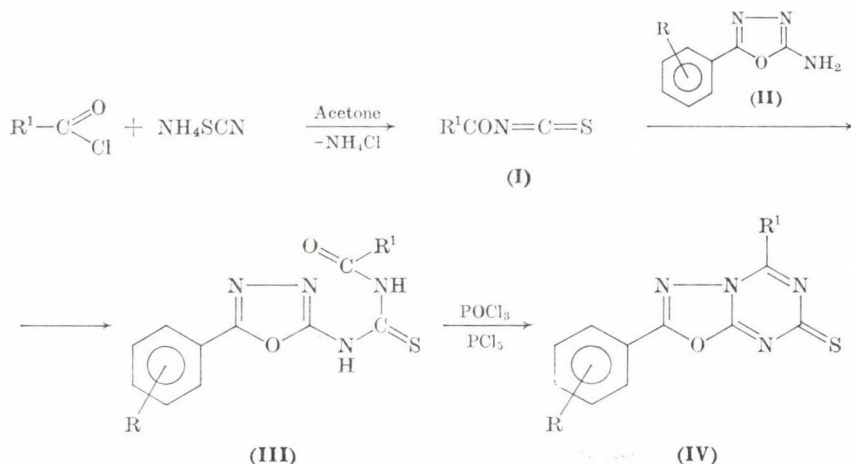
have pesticidal activity of high potency by virtue of incorporating the biologically versatile 1,3,4-oxadiazole moiety [5–8], urea [10], amide [11–13] and thiourea moieties at the same time.

The outstanding selective herbicidal properties of *s*-triazine is well established, and several *s*-triazine herbicides, e.g. Simazine, Atrazine and Prometryn, have gained major recognition in agriculture. Recently, some thiadiazolyl-*s*-triazines (*A*) have been patented as pre- and post-emergence herbicides to control crabgrass and wild oats [14]. Keeping these in view, the title oxadiazolo-*s*-triazines were synthesized in the hope that the fusion of the biolabile *s*-triazine and oxadiazole nuclei might result in pesticides, especially herbicides, of better performance, which have not apparently been recorded in the literature so far.



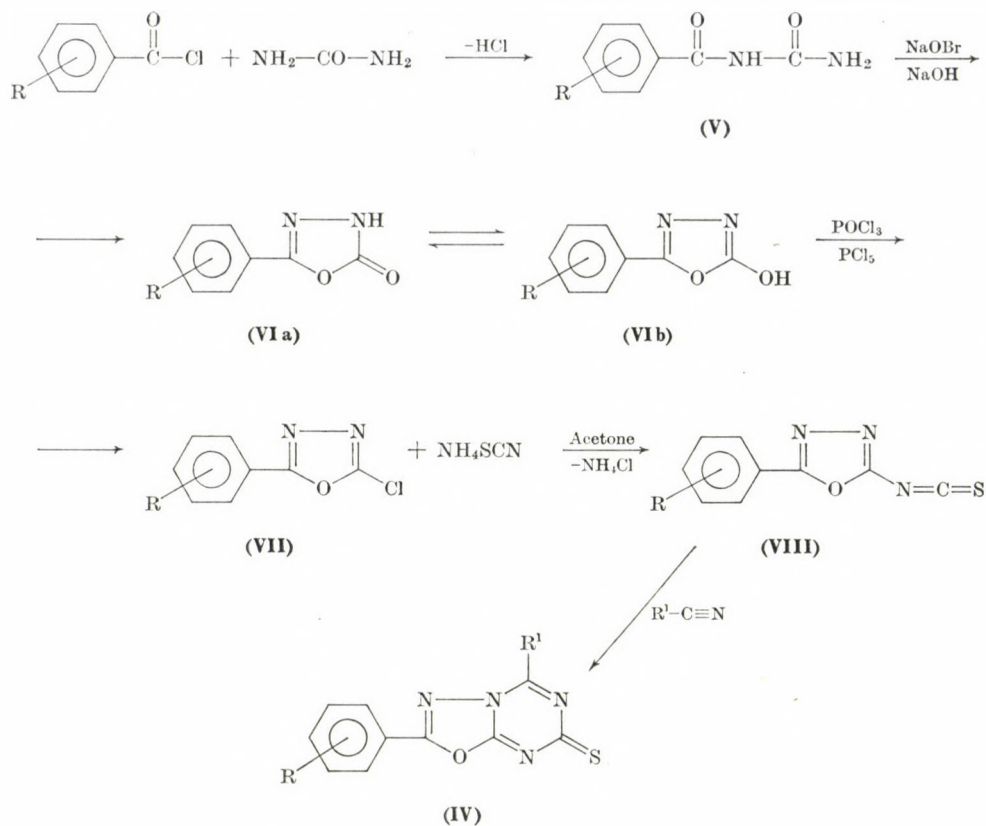
(A)

The synthesis of the title compounds which constitute a novel heterocyclic ring system is depicted in Scheme 1. The novel 1,3,4-oxadiazolo[3,2-*a*]-*s*-triazine-7-thiones (**IV**) were prepared by cyclization of *N*<sup>1</sup>-aroyl//aryloxy-acetyl-*N*<sup>2</sup>-(5-aryl-1,3,4-oxadiazol-2-yl) thioureas **III** using POCl<sub>3</sub> and PCl<sub>5</sub>.



R<sup>1</sup> = aryl/aryloxymethyl

Scheme 1



$R^1 = \text{aryl/aryloxymethyl}$

Scheme 2

The products **IV** were also obtainable by an alternative route outlined in Scheme 2. This route involves the reaction of 5-aryl-1,3,4-oxadiazol-2-yl isothiocyanates and aryl/aryloxymethyl cyanides; as a result of 1,4-cycloaddition, similar to the Diels-Alder reaction, the compounds **IV** were obtained. Employing this method, six representatives of the compounds **IV** were synthesized.

It is evident from the screening data (Table III) that compounds No. 25 and No. 29 (Table II) exhibited a herbicidal activity similar to that of Simazine [2-chloro-4,6-bis (ethylamino)-s-triazine] at 1000 ppm against the test weeds *Argemone mexicana* and *Cyperus rotundus*, and inhibited their germination >50% even at 10 ppm. The compounds Nos 10, 11 and 14 (Table I) had fungicidal action (Table IV) comparable to that of Benomyl [1-(*N-n*-butylcarbamoyl)-2-(methoxycarboxamido)benzimidazole], against the two fungal species, *Aspergillus niger* and *Helminthosporium oryzae* at 1000 ppm.

Table I

*N*<sup>1</sup>-Aroyl/aryloxyacetyl-*N*<sup>2</sup>-(5-aryl-1,3,4-oxadiazol-2-yl)thioureas

No.	R	R <sup>1</sup>	M.p., °C	Yield, %	Mol. formula	Analysis, %	
						Found	Calcd.
1 <sup>a</sup>	H	phenyl	185	85	C <sub>16</sub> H <sub>12</sub> N <sub>4</sub> O <sub>2</sub> S	N 17.31 S 10.00	17.28 9.88
2	H	<i>p</i> -chloro-phenyl	240 <sup>d</sup>	80	C <sub>16</sub> H <sub>11</sub> ClN <sub>4</sub> O <sub>2</sub> S	N 15.87 S 8.85	15.62 8.93
3	<i>p</i> -chloro	phenyl	162–165	90	C <sub>16</sub> H <sub>11</sub> ClN <sub>4</sub> O <sub>2</sub> S	N 15.66 S 9.10	15.62 8.93
4 <sup>b</sup>	<i>p</i> -chloro	<i>p</i> -chloro-phenyl	245 <sup>d</sup>	82	C <sub>16</sub> H <sub>10</sub> Cl <sub>2</sub> N <sub>4</sub> O <sub>2</sub> S	N 14.35 S 8.26	14.25 8.14
5	3,5-di-Br-2-OH	phenyl	132	80	C <sub>16</sub> H <sub>10</sub> Br <sub>2</sub> N <sub>4</sub> O <sub>3</sub> S	N 11.24 S 6.43	11.34 6.43
6	3,5-di-Br-2-OH	<i>p</i> -chloro-phenyl	155–156	75	C <sub>16</sub> H <sub>9</sub> Br <sub>2</sub> ClN <sub>4</sub> O <sub>3</sub> S	N 10.65 S 6.12	10.52 6.0
7	H	phenoxy-methyl	215–218	76	C <sub>17</sub> H <sub>14</sub> N <sub>4</sub> O <sub>3</sub> S	N 15.82 S 9.01	15.82 9.04
8	H	<i>p</i> -chloro-phenoxy-methyl	220	70	C <sub>17</sub> H <sub>13</sub> ClN <sub>4</sub> O <sub>3</sub> S	N 14.03 S 8.31	14.41 8.24
9	H	<i>o</i> -chloro-phenoxy-methyl	176	65	C <sub>17</sub> H <sub>13</sub> ClN <sub>4</sub> O <sub>3</sub> S	N 14.41 S 8.31	14.41 8.24
10	<i>p</i> -chloro	phenoxy-methyl	128–130	80	C <sub>17</sub> H <sub>13</sub> ClN <sub>4</sub> O <sub>3</sub> S	N 14.56 S 8.24	14.41 8.24
11 <sup>c</sup>	<i>p</i> -chloro	<i>p</i> -chloro-phenoxy-methyl	210	75	C <sub>17</sub> H <sub>12</sub> Cl <sub>2</sub> N <sub>4</sub> O <sub>3</sub> S	N 13.33 S 7.55	13.24 7.57
12	<i>p</i> -chloro	<i>o</i> -chloro-phenoxy-methyl	180	68	C <sub>17</sub> H <sub>12</sub> Cl <sub>2</sub> N <sub>4</sub> O <sub>3</sub> S	N 13.24 S 7.61	13.24 7.57

13	3,5-di-Br-2-OH	phenoxyethyl	200	70	$C_{17}H_{12}Br_2N_4O_4S$	N 10.52 S 6.25	10.61 6.06
14	3,5-di-Br-2-OH	<i>p</i> -chloro-phenoxyethyl	175	60	$C_{17}H_{11}Br_2ClN_4O_4S$	N 10.01 S 5.32	9.96 5.69
15	3,5-di-Br-2-OH	<i>o</i> -chloro-phenoxyethyl	140	72	$C_{17}H_{11}Br_2ClN_4O_4S$	N 9.96 S 5.48	9.96 5.69

Significant bands ( $cm^{-1}$ ) in the IR spectrum (in nujol mull)

	C=N	C=O	C—O—C	C=S	—NH—	Substituted benzene nucleus
a	1640	1670	1230 1020	1520	3420	1600, 770, 700
b	1643	1678	1230 1030	1478 1260	3450 3400	1650, 1575, 860
c	1620	1680	1240 1032	1475 1275	3450 3400	1505, 1440, 850
d	Partly melts with decomposition					

**Table II**  
 2-Aryl[5-aryl]aryloxymethyl-1,3,4-oxadiazolo[3,2-a]-s-triazine-7-thiones (IV)

No.	R	R <sup>1</sup>	M.p., °C	Yield, %	Mol. formula	Analysis, %	
						Found	Calcd.
16 <sup>a</sup>	H	phenyl	155	80	C <sub>16</sub> H <sub>10</sub> N <sub>4</sub> OS	C 57.46 H 2.68 N 18.26	57.55 2.88 18.30
17	H	<i>p</i> -chlorophenyl	210	80	C <sub>16</sub> H <sub>9</sub> ClN <sub>4</sub> OS	C 56.46 H 2.58 N 16.72	56.39 2.64 16.45
18	<i>p</i> -Cl	phenyl	110–115	85	C <sub>16</sub> H <sub>9</sub> ClN <sub>4</sub> OS	O 56.53 H 2.64 N 16.55	56.39 2.64 16.45
19 <sup>b</sup>	<i>p</i> -Cl	<i>p</i> -chlorophenyl	205–208	72	C <sub>16</sub> H <sub>8</sub> Cl <sub>2</sub> N <sub>4</sub> OS	C 51.34 H 2.32 N 15.02	51.20 2.13 14.93
20	3,5-di-Br-2-OH	phenyl	190–195	70	C <sub>16</sub> H <sub>8</sub> Br <sub>2</sub> N <sub>4</sub> O <sub>2</sub> S	C 40.14 H 1.69 N 11.67	40.00 1.67 11.67
21	3,5-di-Br-2-OH	<i>p</i> -chlorophenyl	192	85	C <sub>16</sub> H <sub>7</sub> Br <sub>2</sub> ClN <sub>4</sub> O <sub>2</sub> S	C 37.38 H 1.38 N 10.87	27.32 1.36 10.88
22	H	phenoxy-methyl	175	72	C <sub>17</sub> H <sub>12</sub> N <sub>4</sub> O <sub>2</sub> S	C 60.81 H 3.64 N 16.67	60.71 3.57 16.67
23	H	<i>p</i> -chlorophenoxy	165	80	C <sub>17</sub> H <sub>11</sub> N <sub>4</sub> ClO <sub>2</sub> S	C 55.01 H 3.02 N 15.00	55.06 2.97 15.11
24	H	<i>o</i> -chloro-phenoxy-methyl	205 <sup>d</sup>	65	C <sub>17</sub> H <sub>11</sub> ClN <sub>4</sub> O <sub>2</sub> S	C 55.27 H 3.01 N 15.12	55.06 2.97 15.11
25	<i>p</i> -Cl	phenoxy-methyl	170	68	C <sub>17</sub> H <sub>11</sub> ClN <sub>4</sub> O <sub>2</sub> S	C 55.00 H 3.01 N 15.13	55.04 2.97 15.11

26 <sup>c</sup>	<i>p</i> -Cl	<i>p</i> -chloro-phenoxyethyl	152	68	C <sub>17</sub> H <sub>10</sub> Cl <sub>2</sub> N <sub>4</sub> O <sub>2</sub> S	C 50.37 H 2.54 N 13.83	50.37 2.47 13.83
27	<i>p</i> -Cl	<i>o</i> -chloro-phenoxyethyl	150	75	C <sub>17</sub> H <sub>10</sub> Cl <sub>2</sub> N <sub>4</sub> O <sub>2</sub> S	C 50.61 H 2.33 N 10.26	50.37 2.47 10.25
28	3,5-di-Br-2-OH	phenoxyethyl	185	60	C <sub>17</sub> H <sub>10</sub> Br <sub>2</sub> N <sub>4</sub> O <sub>2</sub> S	C 40.23 H 1.75 N 11.01	40.00 1.65 10.98
29	3,5-di-Br-2-OH	<i>p</i> -chloro-phenoxyethyl	150	75	C <sub>17</sub> H <sub>9</sub> Br <sub>2</sub> ClN <sub>4</sub> O <sub>2</sub> S	C 37.47 H 1.75 N 10.26	37.47 1.65 10.28
30	3,5-di-Br-2-OH	<i>o</i> -chloro-phenoxyethyl	180	75	C <sub>17</sub> H <sub>9</sub> Br <sub>2</sub> ClN <sub>4</sub> O <sub>2</sub> S	C 37.82 H 1.55 N 10.15	37.47 1.65 10.28

*Significant bands (cm<sup>-1</sup>) in IR (in nujol mull)*

	C=N	C—O—C	C=S	Substituted benzene nucleus
a	1620	1260 1030	1080	1575, 1470, 760, 710
b	1620	1260 1035	1115	1480, 865
c	1620	1270	1100	1480, 855

d Partly melts with decomposition

## Experimental

M.p.'s were determined in open capillary tubes and are uncorrected. The IR spectra were recorded on a Perkin-Elmer Spectrophotometer (Model 527) in nujol mull.

### 2-Amino-5-aryl-1,3,4-oxadiazoles (II)

These were prepared by oxidative cyclization of the aldehyde semicarbazones with bromine in glacial acetic acid in the presence of anhydrous sodium acetate, according to the method of GIBSON [15]. All the compounds II, (R = H, *p*-Cl and 3,5-di-Br-2-OH) have already been reported in the literature [15, 16, 20].

### *N*<sup>1</sup>-Aroyl/aryloxyacetyl-*N*<sup>2</sup>-(5-aryl-1,3,4-oxadiazol-2-yl) thioureas (III)

These were prepared according to the method of DOUGLASS and DAINS [17]. Thus a mixture of NH<sub>4</sub>SCN (0.06 mol) and aryloxyacetyl chloride/aroyl chloride (0.06 mol) in acetone was heated under reflux for 0.5 h followed by the addition of 2-amino-5-aryl-1,3,4-oxadiazole (0.06 mol), and the mixture was refluxed for further 2 h. The excess of acetone was evaporated and ice-cold water was added to the residue.

The product thus precipitated was filtered off, washed with NH<sub>4</sub>OH, then with water, and recrystallized from acetone-ethanol mixture (50 : 50, *v/v*). The compounds thus obtained are recorded in Table I.

### 2-Aryl-5-aryl/aryloxymethyl-1,3,4-oxadiazolo-[3,2-*a*]-*s*-triazine-7-thiones (IV)

The *N*<sup>1</sup>-aroyl/aryloxyacetyl-*N*<sup>2</sup>-(5-aryl-1,3,4-oxadiazol-2-yl) thioureas III (0.015 mol) were refluxed with a mixture of POCl<sub>3</sub> (15 mL) and PCl<sub>5</sub> (0.015 mol) for 2–3 h. The excess of POCl<sub>3</sub> was removed under reduced pressure, and crushed ice was added to the residue. The products thus obtained were filtered off, washed with water and recrystallized from ethanol-chloroform mixture (60 : 40, *v/v*). These compounds are listed in Table II.

### An alternate procedure for the synthesis of oxadiazolo-*s*-triazines (IV)

*N*-Aroyl ureas (V) were prepared, according to the method of PEAR and OSTROGOVICH [18, 19].

2-Aryl-Δ<sup>2</sup>-1,3,4-oxadiazolin-5-ones (VIa) [21]. Compound V (0.1 mol) was added portionwise, with stirring, to an ice-cold solution of 2 *N* NaOH (168 mL) and bromine (17.6 g). The mixture was poured into water after 15 min to yield the oxadiazolinone VIa in 85–86% yield, which was recrystallized from ethanol; VIa: R = H; *p*-chloro (*lit.* [22]); R = 2-OH-3,5-di-Br, m.p. 165–166 °C.

IR: νC=N 1665 cm<sup>-1</sup>.

C<sub>8</sub>H<sub>4</sub>Br<sub>2</sub>N<sub>2</sub>O<sub>3</sub> Calcd. C 40.66; H 1.05; N 11.91. Found C 40.68; H 1.01; N 11.82%.

5-Aryl-2-chloro-1,3,4-oxadiazoles (VII) [23]. 2-Aryl-Δ<sup>2</sup>-1,3,4-oxadiazolin-5-one (VIa) (0.1 mol) was refluxed in a mixture of PCl<sub>5</sub> (0.009 mol) and POCl<sub>3</sub> (50 mL) for 5 h at 140 °C on an oil bath. The excess of POCl<sub>3</sub> was removed under reduced pressure and the residue was treated with ice water to furnish the desired product. It was filtered off, washed repeatedly with water, and recrystallized from ethanol in 75–85% yield. VII, R=H; *p*-chloro (*lit.* [22]); R = 2-OH-3,5-di-Br, m.p. 145 °C.

IR: νC=N 1660 cm<sup>-1</sup>, νC–O–C 1270–1040 cm<sup>-1</sup>, νC–Cl 750 cm<sup>-1</sup>.

C<sub>8</sub>H<sub>3</sub>ClBr<sub>2</sub>O<sub>2</sub>N<sub>2</sub> Calcd. N 7.99; Cl 9.92. Found N 7.91; Cl 9.88%.

Oxadiazolo-*s*-triazines (VI). 5-Aryl-2-chloro-1,3,4-oxadiazole VII (0.01 mol) and NH<sub>4</sub>SCN (0.01 mol) were refluxed in acetone for 1 h and to this reaction mixture aryl/aryloxymethyl cyanide (0.01 mol) was added. The mixture was refluxed for 6 h. The excess of acetone was evaporated and the residue was mixed with ice-water to precipitate the desired product which was filtered off and washed with dilute NH<sub>4</sub>OH and then with water. Recrystallization from ethanol-DMF (50 : 50; *v/v*) furnished the analytical sample. Employing this procedure, compounds Nos 16, 18, 20, 22 and 28 (Table II) were synthesized in 70–80% yields as examples.

### Herbicidal screening

The test weeds were *Argemone mexicana* and *Cyperus rotundus*. The herbicidal activity was evaluated by pre-emergence tests at three concentrations, viz. 1000 ppm, 100 ppm and 10 ppm, using three replications in each case. Seeds or tubers of the test weeds were soaked for 24 h in the test solutions or suspensions, and then planted for germination. Simazine [2-chloro-4,6-bis(ethylamino)-s-triazine] was also tested under similar conditions with a view to comparing the results. The percentage inhibition produced by the various newly synthesized compounds are recorded in Table III.

$$\% \text{ inhibition} = \frac{G_c - G_t}{G_c} \times 100$$

where  $G_c$  = No. of germinated seeds/tubers in control

$G_t$  = No. of germinated seeds/tubers treated with test solutions/suspension.

### Fungicidal screening

The antifungal activity was evaluated by the agar plate technique [24, 25] at three different concentrations, viz. 1000 ppm, 100 ppm, and 10 ppm. The number of replications in each case was three. The results were compared with the effect of Benomyl [1-(*N*-n-butyl-carbamoyl)-2-(methoxycarboxamido)benzimidazole], a systematic fungicide [26], which was tested under similar conditions. The average inhibition produced by the various compounds are recorded in Table IV.

## Results and Discussion

Out of nine tested substances, the compounds Nos 16, 19, 25 and 29 are by far more active herbicides than the oxadiazolyl thioureas (compounds Nos 1, 4, 10, 14) against both of the test weeds. The higher activity of the oxadiazolo-s-triazines (compounds Nos 16, 19, 25 and 29) is in conformity

**Table III**  
Herbicidal screening

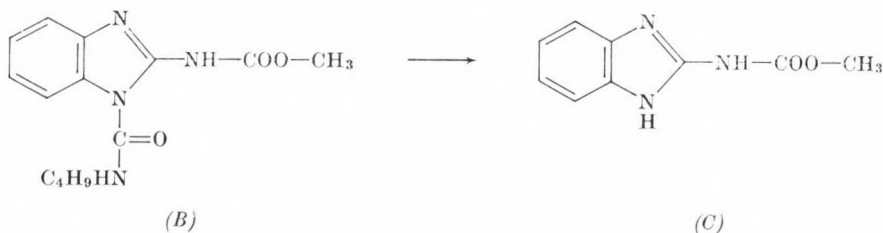
Compound No.	Average percentage inhibition					
	Weed <i>A. mexicana</i>			Weed <i>C. rotundus</i>		
	Concentrations used			Concentrations used		
	1000 ppm	100 ppm	10 ppm	1000 ppm	100 ppm	10 ppm
1	45.4	16.3	07.1	51.0	20.2	09.4
4	50.5	20.7	09.3	53.3	22.5	11.3
10	60.1	35.7	17.2	56.2	23.9	12.1
11	66.2	40.3	22.7	60.1	32.0	16.3
14	70.5	43.5	24.9	65.2	36.7	22.1
16	72.3	50.1	35.2	73.2	51.4	36.0
19	80.5	55.6	41.4	82.4	58.3	44.6
25	100	66.3	52.1	85.7	62.4	50.5
29	100	72.6	55.5	90.3	69.2	52.1
Simazine	100	80.2	60.4	91.3	71.4	56.1

Table IV  
Fungicidal screening

Compound No.	Average percentage inhibition after 96 hours					
	Organism <i>A. niger</i>			Organism <i>H. oryzae</i>		
	Concentrations used			Concentrations used		
	1000 ppm	100 ppm	10 ppm	1000 ppm	100 ppm	10 ppm
1	80.4	48.2	28.6	82.5	45.1	31.9
4	85.5	50.7	38.8	87.6	51.8	39.0
10	98.1	59.4	46.3	94.2	56.1	42.6
11	99.1	63.1	49.2	95.3	60.2	48.4
14	100	68.4	54.6	96.9	65.0	52.1
16	70.3	38.4	20.0	72.4	39.6	22.2
19	76.4	45.3	30.5	74.5	42.0	26.3
25	80.9	50.1	41.3	78.1	45.4	31.8
29	87.6	60.7	44.2	80.7	55.3	39.0
Benomyl	100	80.2	65.2	98.5	70.5	65.8

with the earlier observations that the compact size and planarity of a molecule often augment its herbicidal activity [27–29]. Further, it was observed that triazines cause foliar chlorosis followed by death of the leaf including the loss of membrane integrity and chloroplast destruction [30]. According to the mechanism and mode of action of triazine herbicides, they could inhibit photosynthesis by producing a secondary phytotoxic substance [31–33].

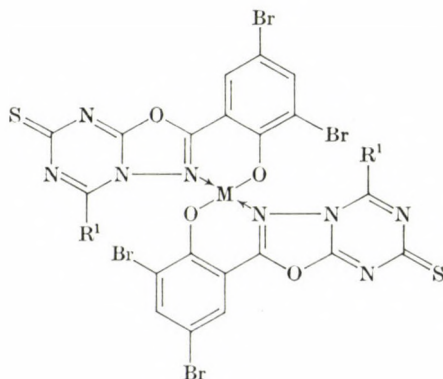
The oxadiazolyl thioureas (compounds Nos 4, 10, 11 and 14) are significantly more toxic to both of the test fungi, *Aspergillus niger* and *Helminthosporium oryzae* at 1000 ppm, than their successor oxadiazolo-s-triazines (compounds Nos 16, 19, 25 and 29). The compounds Nos 10, 11 and 14 incorporating aryl ether moiety have higher fungicidal activity than their aryl analogues (compounds Nos 1 and 4), against both test fungi at 1000 ppm. They exhibit a fungicidal activity comparable with that of Benomyl (B), a systematic fungicide of the benzimidazole group, which decomposes [30] very rapidly to the active form [34], methyl benzimidazol-2-yl carbamate (MBC) (C).



The significant fungitoxicity of the oxadiazolyl thioureas is comparable with the fungitoxicity of phenylthiourea studied by SIJPESTEIJN [35]. Phenylthiourea (PTU) can prevent cucumber diseases due to *Cladosporium cucumerinum* by direct interference with the plant-fungus biochemical relationship and plant metabolism [36]. Three effects of phenylthiourea on cucumber plant have been recognized [35, 37]. It inhibits polyphenol oxidase activity in the plant, increases peroxidase activity and causes the lignification of the plant cell wall in the parenchyma around the penetrating hyphae of fungi [36].

The highest fungitoxicity of compound No. 14 can be explained by its ability to rob essential metals required in the metabolism of fungi. They cause a strong inhibition of polyphenol oxidase activity through chelate formation with the metal containing enzyme system [38-40].

Compounds Nos 25 and 29 were highly active against both test weeds, *Argemone mexicana* and *Cyperus rotundus*, inhibiting their germination >50% even at 10 ppm. The highest toxicity of compound No. 29 might also be attributed to some extent to its ability for bivalent chelate formation [41] with essential metals required in the metabolism of the weeds. A 2 : 1 sym



(D)  $R^1 = p$ -chlorophenoxyethyl

metric metal chelate with compound No. 29, could be formed by two 2-(3,5-dibromo-2-hydroxy)-5-(*p*-chlorophenoxy)methyl-1,3,4-oxadiazolo[3,2-*a*]-s-triazine-7-thione rings and one central metal action, as shown in figure (D).

\*

One of the authors (B.K.B.) is thankful to Professor R. P. RASTOGI, Head of Department of Chemistry, University of Gorakhpur, India, for providing departmental facilities; to U.G.C., New Delhi, India, for financial assistance to complete a part of this work, and also to the authorities of K.U. Leuven, Belgium for providing a fellowship and departmental facilities in the Laboratory for Organic Synthesis.

## REFERENCES

- [1] SCHROEDER, D. C.: Chem. Revs., **55**, 181 (1955)
- [2] LAVY, R., MENORET, Y.: Fr. Pat. 1,193,374 (1959); Chem. Abstr., **55**, 891 (1961)
- [3] JOHNSON, R. S.: U.S. Pat. 3,457,292 (1969); Chem. Abstr., **71**, 101579 (1969)
- [4] GOLDSMITH, E. D., HARNLEY, M. H.: Sciences, **103**, 649 (1946)
- [5] GIRI, S., SINGH, H., YADAV, L. D. S.: J. Agr. Biol. Chem., **40**, 17 (1976)
- [6] OKADA, Y.: Japan Pat. 70 24,982 (1970); Chem. Abstr., **73**, 98953 (1970)
- [7] DEBOURGE, J. C., PILLON, D., TERINH, S.: Ger. Offen. 2,361,613 (1974); Chem. Abstr., **81**, 91537 (1974)
- [8] HAGIMOTO, H., YOSHIKAWA, H., OKADA, Y.: Japan Pat. 74 08258 (1974); Chem. Abstr., **81**, 91537 (1974)
- [9] KUBOTA, H., SHIMIZU, M.: Japan Pat. 7034, 819 (1970); Chem. Abstr., **74**, 87989 (1971)
- [10] KERNEY, P. C., KAUFMAN, D. D.: Herbicides Chemistry, Degradation, and Mode of Action. Vol. I, p. 209. Marcel Dekker, Inc. New York and Basel, 1975
- [11] HAMM, P. C., SPEZIALE, A. J.: J. Agric. Fd. Chem., **4**, 518 (1959)
- [12] YOSHINAGA, E., SUGIYAMA, H., KAWADA, H., ITO, H.: Japan Pat. 74.11,065 (1974); Chem. Abstr., **81**, 131574 (1974)
- [13] CHIYOMARU, I., YOSHINAGA, E., DOHKE, G.: Japan Pat. 73 39 460 (1974)
- [14] KRANZER, J.: U.S. Pat. 3,860,593 (1975); Chem. Abstr., **83**, 101158 (1975)
- [15] GIBSON, M. S.: J. Chem. Soc., **18**, 1377 (1962)
- [16] HOGGARTH, E.: J. Chem. Soc., **1949**, 1918
- [17] DOUGLASS, I. B., DAINS, F. B.: J. Am. Chem. Soc., **56**, 719 (1934)
- [18] PEARL, I. A., DEHM, W. H.: J. Am. Chem. Soc., **61**, 1377 (1939)
- [19] OSTROGOVICH, A.: Bul. Soc. Stinte Cluje, **4**, 538 (1929); Chem. Abstr., **24**, 2119 (1930)
- [20] SINGH, H., YADAV, L. D. S., BHATTACHARYA, B. K.: Indian J. Chem., **17B**, 499 (1979)
- [21] RHONE-POULENC, S. A.: Neth. Appl. 6,500,374 (1965); Chem. Abstr., **64**, 3560 (1966)
- [22] SINGH, H., YADAV, L. D. S., BHATTACHARYA, B. K.: J. Indian Chem. Soc. (1980) (in the press)
- [23] NAKANO, H., SUGIHARA, A., ITO, M., TSUBOUCHI, S.: Japan Pat. 8029 (1967); Chem. Abstr., **67**, 54132 (1967)
- [24] U.S.D.A. Circular No. **198** (1931)
- [25] HORSFALL, J. G.: Bot. Rev., **1945**, 357
- [26] STRINGER, A.: Pestic. Sci., **4**, 165 (1973)
- [27] SUMMER, A.: Tetrahedron, **32**, 615 (1976)
- [28] CHATT, J., DUNCANSON, L. A., VENAZI, L. M.: Nature, **177**, 1042 (1956)
- [29] ROTHWELL, K., WAIN, R. L.: Ann. Appl. Biol., **51**, 161 (1963)
- [30] ASTON, F. M., CRAFTS, A. S.: Mode of action of Herbicides, p. 234, Wiley, New York 1973
- [31] GAST, A.: Experimentia, **13**, 134 (1958)
- [32] RODGERS, E. G.: Weed Sci., **16**, 117 (1968)
- [33] ASHTON, F. M., GIFFORD, E. M., BISALPUTRA, T.: Bot. Gaz., **124**, 329 (1963)
- [34] CLEMONS, G. P., SISLER, H. D.: Phytopathol., **59**, 705 (1969)
- [35] SIJPESTEIJN, A. K., SISLER, H. D.: Neth. Pl. Pathol., **74**, (1968 Suppl. 1) 121 (1968)
- [36] SIJPESTEIJN, A. K.: J. Sci. Food Agric., **20**, 403 (1969)
- [37] SIJPESTEIJN, A. K., VANDER KERK, G. J. M.: Phytopathol., **3**, 127 (1965)
- [38] ZENTHMYER, G. A.: Phytopathol., **33**, 1121 (1943)
- [39] BERNHEIM, F., BERNHEIM, M. L. C.: J. Biol. Chem., **145**, 213 (1942)
- [40] DUBOIS, K. P., ERWAY, W. F.: J. Biol. Chem., **165**, 711 (1946)
- [41] ALBERT, A., GLEDHILL, W. S.: Biochem. J., **41**, 529 (1947)

B. K. BHATTACHARYA      Celestijuenlaan 200F, B-3030 Leuven, Belgium

H. SINGH                      Gorakhpur, 273 001 U.P., India

L. D. S. YADAV              Midori-ku 17-2, Yokohama 227, Japan

G. HOORNAERT              Celestijnenlaan 200F, B-3030 Leuven, Belgium

## ELEKTRONISCHE WECHSELWIRKUNG IN 4-SUBSTITUIERTEN $\omega$ -DIPHENYLPHOSPHINYL- -TRANS-STYRENEEN UND VERWANDTEN VERBINDUNGEN\*

K.-G. BERNDT und D. GLOYNA\*\*

(Humboldt-Universität Berlin, Sektion Chemie, WB Organische Chemie, DDR-1040  
Berlin, DDR)

Eingegangen am 9. Februar 1981  
Zur Veröffentlichung angenommen am 15. Juli 1981

Es werden die UV-Spektren von  $\omega$ -Diphenylphosphinyl-*trans*-styrenen **1** in Ethanol diskutiert. Mit Einführung der Diphenylphosphinyl-Gruppe in  $\omega$ -Position des Styrens ist eine bathochrome Verschiebung der  ${}^1L_b$ - und der  ${}^1L_a$ -Bande des Styrens verbunden. Dabei ist die Verschiebung der  ${}^1L_a$ -Bande bei Anwesenheit eines 4-ständigen Elektronendonator-Substituenten X im Styren-Teil des Moleküls weitaus größer als die der  ${}^1L_b$ -Bande und ausgeprägt abhängig von der Donator-Fähigkeit von X, so daß bei X = N(CH<sub>3</sub>)<sub>2</sub> eine Vertauschung der Reihenfolge beider Banden im Vergleich zu Styren erfolgt. Infolge P(O)-Substitution wird im Benzen-Teil von **1** der  ${}^1L_b$ -Übergang ebenfalls gering bathochrom verschoben. Hinweise für eine mesomere Wechselwirkung zwischen Benzen- und Styren-Teil wurden nicht gefunden. Es besteht jedoch eine Wechselwirkung zwischen den  $\pi$ -Elektronensystemen des Styren-Teils und der P=O-Bindung, so daß sich die P(O)-Gruppe in **1** als selektive Konjugationssperre erweist.

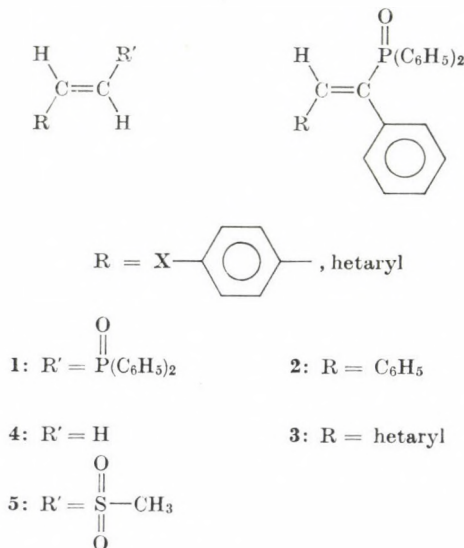
Eine Interpretation photochemischer Messungen [1] an diphenylphosphinyl-substituierten *trans*-Ethylenen **1** erfordert Kenntnisse über den Einfluß des Diphenylphosphinyl-Substituenten auf die Elektronenstruktur des Grundchromophors. Für die relativ große, tetraedrisch konfigurierte (C<sub>6</sub>H<sub>5</sub>)<sub>2</sub>P(O)-Gruppierung muß eine sterische, eine elektronische sowie — bei photochemischen Umsetzungen — möglicherweise auch eine schweratombedingte Wirkung in Betracht gezogen werden. Der sterische Einfluß dieser Gruppierung auf den Grundchromophor zeigt sich deutlich in den Absorptionsspektren von  $\alpha$ -diphenylphosphinyl-substituiertem *cis*-Stilben **2** und verwandten Verbindungen **3** [2]. Die bei **2** und **3** beobachtete hypsochrome Verschiebung der längstwelligeren Absorptionsbande im Vergleich zum unsubstituierten Grundchromophor (z. B. *cis*-Stilben) muß auf ein verstärktes Herausdrehen der  $\alpha$ -ständigen Phenylgruppe aus der Konjugationsebene des Grundchromophors durch die raumfüllende (C<sub>6</sub>H<sub>5</sub>)<sub>2</sub>P(O)-Gruppierung zurückgeführt werden [2, 3].

In dieser Arbeit wird der elektronische Einfluß der relativ stark elektronenziehenden (C<sub>6</sub>H<sub>5</sub>)<sub>2</sub>P(O)-Gruppierung auf das  $\pi$ -System von 4-substituierten

\* 25. Mitteilung über Darstellung und Eigenschaften donator-akzeptor-substituierter Aryl-ethylene

\*\* Korrespondenz bitte an diesen Autor richten

Styrenen sowie vergleichbaren Verbindungen **1** qualitativ diskutiert.<sup>1</sup> Sterische Einflüsse können dabei unberücksichtigt bleiben. Aus der Sicht sterischer Hinderung führen weder R in **1** noch die  $(C_6H_5)_2P(O)$ -Gruppierung zu einer innerhalb der Reihe **1** wechselnden Verdrehung um die  $C-C_{Aryl}$ -Einfachbindung oder die Ethylen-Doppelbindung.<sup>2</sup>



Bei Einführung eines Substituenten tritt im allgemeinen keine prinzipielle Veränderung im Spektrum des Grundchromophors auf [4]. Es können sich Lage, Sequenz, Intensität sowie Schwingungsstruktur der einzelnen Aromatenbanden verändern.<sup>3</sup> Im Styren wirkt jeder Substituent vorwiegend auf ein Grenzorital, wobei in jedem Falle eine bathochrome Verschiebung der  $\pi-\pi^*$ -Absorptionsbande auftritt. Akzeptor-Substituenten senken vorwiegend das tiefste unbesetzte MO ab (LUMO), Donator-Substituenten heben vorwiegend das höchste besetzte MO an (HOMO) [5]. Für die weitere Spektren-diskussion von **1a**—**1g** (siehe Tab. I) kann das Elektronenspektrum des Styrens als Grundlage dienen. Es besteht im nahen UV-Bereich aus vier  $\pi-\pi^*$ -Bandensystemen mit den Schwerpunkten bei 280 nm, 246 nm, 203 nm und 173 nm [6], die in gleicher Reihenfolge wie die  ${}^1L_b$ -,  ${}^1L_a$ - und  ${}^1B_b$ -Banden<sup>4</sup> des Benzens auftreten [7, 8], jedoch bathochrom verschoben sind. Die Einführung des  $(C_6H_5)_2P(O)$ -Substituenten in die  $\omega$ -Position des Styrens bewirkt eine weitere batho-

<sup>1</sup> Die schweratom-bedingte Wirkung dieser Gruppierung soll gesondert besprochen werden [1]

<sup>2</sup> Eine Ausnahme könnte bei **1h** vorliegen, was noch untersucht wird

<sup>3</sup> Siehe auch Abb. 1 in [3]

<sup>4</sup> Notation nach PLATT [10]

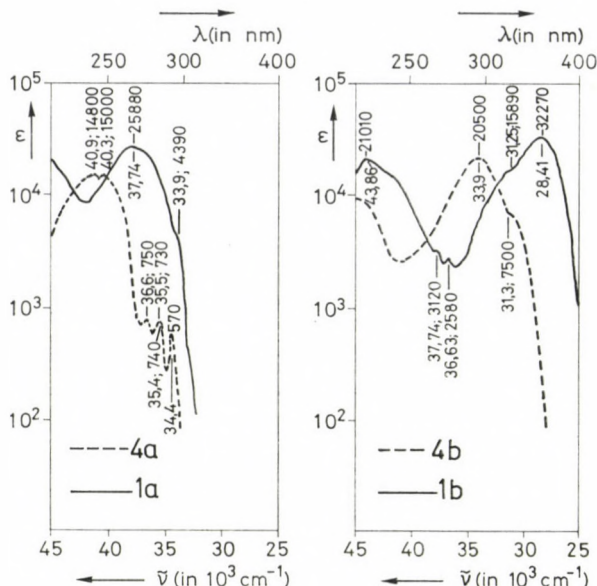


Abb. 1. Absorptionsspektrum von Styren **4a**,  $\omega$ -Diphenylphosphinyl-*trans*-styren **1a**, 4-Dimethylamino-styren **4b** und 4-Dimethylamino- $\omega$ -diphenylphosphinyl-*trans*-styren **1b** in 95-proz. Ethanol bei Raumtemperatur

chrome Verschiebung sowohl der längstwelligen, strukturierten  ${}^1L_b$ -Bande<sup>5</sup> im Bereich von 273–291 nm ( $S_0 \rightarrow S_1$ -Übergang) als auch der intensiveren  ${}^1L_a$ -Bande ( $S_0 \rightarrow S_2$ ) bei 248 nm [8]. Die Verschiebung der  ${}^1L_b$ -Bande beträgt bei **1a** in Ethanol gegenüber Styren **4a**  $470 \pm 200 \text{ cm}^{-1}$ , die der  ${}^1L_a$ -Bande  $2600 \pm 100 \text{ cm}^{-1}$ . Damit resultiert die längstwellige Bande im  $\omega$ -Diphenylphosphinylstyren **1a** aus einer weitgehenden Überlagerung von  ${}^1L_b$ - und  ${}^1L_a$ -Bande (siehe Abb. 1). Das Maximum  $\lambda_{\text{max}}$  der registrierten längstwelligen Bande wird für **1a**–**1g** hauptsächlich durch die Lage der intensiveren  ${}^1L_a$ -Bande bestimmt. Die Schulter bei 295 nm in **1a** deuten wir als bathochrom verschobene längstwellige Schwingungsteilbande (o-o-Übergang) der  ${}^1L_b$ -Bande. Diese Deutung wird durch Lage und Struktur der Fluoreszenzbande bei  $-196^\circ \text{ C}$  in Ethanol gestützt [9].

Erwartungsgemäß ist die mit Einführung des  $(\text{C}_6\text{H}_5)_2\text{P}(\text{O})$ -Substituenten in die  $\omega$ -Position der Styrene **4** verbundene Verschiebung  $\Delta\bar{\nu}_{L_a}$  der  ${}^1L_a$ -Bande stark abhängig von der Natur eines Zweitsubstituenten, wie Tabelle I zeigt. Die größten Verschiebungen werden erreicht, wenn die Substituenten in 4- und  $\omega$ -Position ein Donator-Akzeptor-Paar bilden. Da die Verschiebung der

<sup>5</sup>  ${}^1A_1 \rightarrow {}^1B_2$ -Übergang bei näherungsweise Annahme von  $C_{2v}$ -Symmetrie (siehe auch [5]). Bei Symmetriereduzierung zu  $C_s$  ergibt sich der erlaubte  ${}^1A' \rightarrow {}^1A'$ -Übergang. Siehe dazu Diskussion in [6] und [11]

Tabelle I

Maximum  $\lambda_{\max}$  (in nm) und Intensität  $\epsilon_{\max}$  (in  $L \cdot \text{mol}^{-1} \cdot \text{cm}^{-1}$ ) der längstwelligsten Absorptionsbande für  $\omega$ -Diphenylphosphinyl-transethylen  $\text{R}-\text{CH}=\text{CH}-\text{P}(\text{O})(\text{C}_6\text{H}_5)_2$  **1** und vergleichbare P(O)-freie Ethylene  $\text{R}-\text{CH}=\text{CH}_2$  **4** sowie Verschiebung der  ${}^1\text{L}_a$ -Bande  $\Delta\tilde{\nu}_{\text{L}_a}$  für die Styrene **1a–1g** (in  $\text{cm}^{-1}$  im Vergleich zu **4a**)

R	1		4		$\Delta\tilde{\nu}_{\text{L}_a}$
	$\lambda_{\max}$	$\epsilon_{\max}$	$\lambda_{\max}$	$\epsilon_{\max}$	
<b>a</b> Phenyl	265	25 900	248 [13]	16 000 [13]	2600
<b>b</b> 4-Dimethylaminophenyl	352	32 300	295 [13]	20 500 [13]	5500
<b>c</b> 4-Methoxy-phenyl	287	25 600	259 [13]	19 200 [13]	3800
<b>d</b> 4-Methyl-phenyl	279	27 100 <sup>b)</sup>	252 [14]		3800
			251,5 [15]		
<b>e</b> 4-Chlor-phenyl	272	29 700	253 [13]	19 600 [13]	
			254 [16]	20 000 [16]	2700
<b>f</b> 4-Cyano-phenyl	280	35 700 <sup>b)</sup>			100 <sup>c)</sup>
<b>g</b> 4-Nitro-phenyl	300		301 [13]	13 800 [13]	0
<b>h</b> 3-Indolyl	315	22 600	282 [17]	9 000	

<sup>a)</sup> Jeweils in 95-proz. Ethanol bei Raumtemperatur; für **1** Mittelwerte aus 3 Messungen gleicher Genauigkeit, Fehler für  $\lambda_{\max} \pm 0.5$  nm

<sup>b)</sup> In *n*-Propanol

<sup>c)</sup> Berechnet aus dem Meßwert für  $\omega$ -Cyano-styren [18] in Methanol ( $\lambda_{\max}$  274 nm) unter der Annahme gleicher elektronischer Wirkung der CN-Gruppe in  $\omega$ - und 4-Position; Maximum der  ${}^1\text{L}_a$ -Bande bei **1f** zu 275 nm aus dem Bandenprofil abgeschätzt

${}^1\text{L}_b$ -Bande geringer und weniger substituentenabhängig ist (z. B. bei **1c** und **1e** nur  $230 \pm 100 \text{ cm}^{-1}$ ), fallen infolgedessen bei **1c** bereits  ${}^1\text{L}_b$ - und  ${}^1\text{L}_a$ -Bande zusammen, während bei **1b** die Reihenfolge beider Banden gegenüber **4a** vertauscht ist<sup>6</sup> (siehe Abb. 1). Der gleiche Befund wird experimentell und mittels modifizierter PPP-Rechnung an analogen 4-substituierten  $\omega$ -Methylsulfonyl-styrenen **5** [X = u. a. Cl,  $\text{OCH}_3$ ,  $\text{N}(\text{CH}_3)_2$ ] gewonnen [12], die generell zu **1** sehr ähnliche UV-Spektren aufweisen.

Die durch die  $(\text{C}_6\text{H}_5)_2\text{P}(\text{O})$ -Gruppierung bewirkte Verschiebung  $\Delta\tilde{\nu}_{\text{L}_a}$  korreliert bei Donator-Akzeptor-Substitution in **1** befriedigend mit der elektrophilen Substituentenkonstante  $\sigma_p^+$  [19, 20] des Donators. Die gleiche Beobachtung ergibt sich für **5** bei formaler Einführung der Sulfonyl-Gruppe in 4-donator-substituierte Styrene<sup>7</sup> (siehe Abb. 2). Bei Verwendung der Konstanten  $\sigma_p$  [22] oder  $\sigma_R = 3(\sigma_p - \sigma_m)/2$  [23] ergeben sich für beide Substanzreihen sowie für einige  $\omega$ -nitro-substituierte Styrene [18] schlechtere Korrelationen. Die in **1** durch die Substituenten in  $\omega$ -Position und 4-Position gegenüber Styren **4a** erzielte Gesamtverschiebung  $\Delta\tilde{\nu}_{\text{L}_a}^{\max}$  der  ${}^1\text{L}_a$ -Bande ist bei

<sup>6</sup> Etwa die gleichen Verschiebungswerte für die  ${}^1\text{L}_b$ -Bande findet man bei vergleichbar 4-substituierten  $\omega$ -Methylsulfonyl-styrenen **5** (siehe Tab. III in [12])

<sup>7</sup> Aus Absorptionsspektren von **5** in [21]

Donator-Akzeptor-Substitution um einen bestimmten Energiebetrag  $E_{D-A}$  größer als die Summe der Verschiebungen, die jeder Substituent allein am Styren-Grundchromophor bewirken würde (Gl. 1). Wie bei 1,4-disubstituierten Benzenen [24] ist im Falle einer Akzeptor-Akzeptor-Substitution (bei **If**, **Ig**) die Gesamtverschiebung  $\Delta\tilde{\nu}_{L_a}^{\max}$  auch für 1 etwa so groß, wie sie durch den Substituenten mit dem größeren  $\Delta\tilde{\nu}_{(X)}$ -Wert allein erreicht würde. Die Größe von  $E_{D-A}$  ist selbst abhängig von der Donator-Fähigkeit des 4-ständigen Substituenten.

$$\Delta\tilde{\nu}_{L_a}^{\max} = \Delta\tilde{\nu}_{(D)} + \Delta\tilde{\nu}_{(A)} + E_{D-A} \quad (1)$$

$\Delta\tilde{\nu}_{(D)}$ ,  $\Delta\tilde{\nu}_{(A)}$  Verschiebung der  ${}^1L_a$ -Bande bei Donator-Substitution in 4-Position bzw. Akzeptor-Substitution in  $\omega$ -Position relativ zu Styren

$$\tilde{\nu}_{(X=H)} - \tilde{\nu}_{(X \neq H)} = \Delta\tilde{\nu}_{(X)} \quad (2)$$

$\tilde{\nu}_{(X=H)}$ ,  $\tilde{\nu}_{(X)}$  Wellenzahl für das Maximum der  ${}^1L_a$ -Bande im Styren ( $X = H$ ) bzw. im X-substituierten Styren 4.

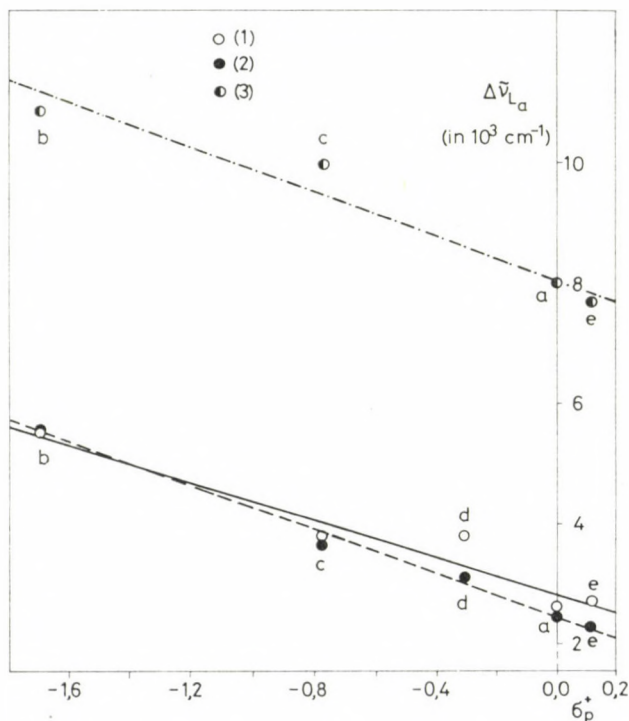


Abb. 2. Verschiebung des Maximums der  ${}^1L_a$ -Bande  $\Delta\tilde{\nu}_{L_a}$  in Ethanol für 4-substituierte *trans*-Styrene 4-X-C<sub>6</sub>H<sub>4</sub>-CH=CH-Z in Abhängigkeit von der Substituentenkonstante  $\sigma_p^+$  des Donators X. X = H (a), N(CH<sub>3</sub>)<sub>2</sub> (b), OCH<sub>3</sub> (c), CH<sub>3</sub> (d), Cl (e); Z = P(O)(C<sub>6</sub>H<sub>5</sub>)<sub>2</sub> (1), Regressionskoeffizienten für  $y = ax + b$ :  $a = -1535 \pm 735$ ,  $b = 2859 \pm 624$ ,  $r = -0,968$ ; Z = SO<sub>2</sub>CH<sub>3</sub> (2),  $a = -1800 \pm 303$ ,  $b = 2457 \pm 258$ ,  $r = -0,996$ ; Z = NO<sub>2</sub> (3),  $a = -1801 \pm 1264$ ,  $b = 8086 \pm 1184$ ,  $r = -0,974$

Diese Befunde zusammen weisen auf eine mesomere Wechselwirkung zwischen  $(C_6H_5)_2P(O)$ -Gruppierung und 4-ständigen Donator-Substituenten im Styren-Teil des Moleküls hin. Für die Methylsulfonyl-Gruppe in **5** ist eine solche mesomere Wechselwirkung bereits sichergestellt [25, 26]. Das vierfach koordinierte P-Atom in **1** erweist sich als Konjugationssperre in Bezug auf die Phenyl-Substituenten. Das Absorptionsspektrum von **1** kann als Summe der beeinflussten («gestörten») Spektren der drei Substituenten am P-Atom betrachtet werden. Die bei **1b** (siehe Abb. 1) und **1h** deutlich sichtbare Strukturierung im Bereich von 265–273 nm wird durch die intensitätsschwache  $^1L_b$ -Bande des Benzen-Chromophors hervorgerufen. Infolge  $p\pi-d\pi$ -Wechselwirkung ist — wie im Styren-Teil — eine geringe bathochrome Verschiebung des  $^1L_b$ -Überganges des Benzens zu verzeichnen. Dieser Übergang wird bei **1b** separiert durch eine maximale Verschiebung der  $^1L_a$ -Bande des Styren-Chromophors auf Grund des 4-ständigen Donator-Substituenten, in den anderen Verbindungen **1** jedoch durch die intensive  $^1L_a$ -Bande des Styren-Chromophors mehr oder weniger überdeckt. Die Zuordnung ergibt sich durch Spektrenvergleich mit Phenyl-butenyl-phosphinsäure-ethylester **6** und Triphenylphosphinoxid **7** (siehe Tab. II). Die Bandenlage ist unabhängig vom Chromophor  $R^2$  (Styryl in **1b–1g**, Phenyl in **7**, Stilbenyl in **8**). Ähnliche Ergebnisse erbrachten UV-Untersuchungen an 4-substituierten Triphenylphosphinoxiden  $4-X-C_6H_4-P(O)(C_6H_5)_2$  [29]. Die Trennung der einzelnen chromophoren Systeme in **1** durch das P-Atom ergibt sich weiterhin aus unserer Beobachtung, daß bei photochemischer Veränderung im Styren- bzw. im Vinyl-indolyl-Teil bei **1b** und **1h** (*trans* → *cis*-Isomerisierung) keine nennenswerten spektroskopischen Veränderungen im Bereich der  $^1L_b$ -Absorptionen des Benzen-Chromophors auftreten [30]. Einen Einfluß übt dagegen bei **1a–1g** der 4-ständige Sub-

Tabelle II

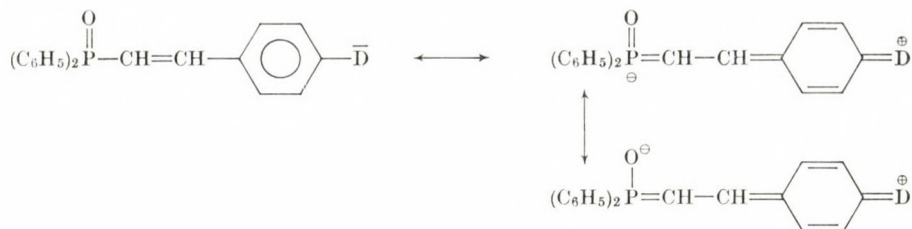
Vibronische Banden  $\tilde{\nu}_{0-i}$  (in  $cm^{-1}$ ) des  $^1L_b$ -Überganges im Benzen-Chromophor von  $C_6H_5-P(O)R^1R^2$  in 95-proz. Ethanol bei 20 °C

	$R^1$	$R^2$	$\tilde{\nu}_{0-i}$	
<b>1b</b>	$C_6H_5$	$CH=CH-C_6H_4-4-N(CH_3)_2$	36 600,	37 700
<b>1c</b>	$C_6H_5$	$CH=CH-C_6H_4-4-OCH_3$	36 600,	37 600
<b>1g</b>	$C_6H_5$	$CH=CH-C_6H_4-4-NO_2$	36 400,	37 300
<b>1h</b>	$C_6H_5$	$CH=CH-3-indolyl$	36 700,	37 600
<b>6</b>	$OC_2H_5$	$CH=CH-C_2H_5$	35 500,	36 700, 37 600, 38 300 <sup>a)</sup>
<b>7</b>	$C_6H_5$	$C_6H_5$	36 900,	37 900, 38 600 [27]
<b>8</b>	$C_6H_5$	$4-C_6H_4-CH=CH-C_6H_5$	36 600,	37 600, 38 500 <sup>b)</sup> [28]

<sup>a)</sup> Im Dampfzustand gemessen

<sup>b)</sup> Werte für *n*-Propanol

stituent im Styren-Teil auf die P=O-Bindung aus. Wir fanden nämlich, daß die Frequenz der P=O-Valenzschwingung mit zunehmender Elektronendonor-Fähigkeit des Substituenten von  $1202\text{ cm}^{-1}$  bei **1g** auf  $1177\text{ cm}^{-1}$  bei **1b**<sup>8</sup> vermindert wird [31]. In Verbindung mit <sup>1</sup>H- und <sup>31</sup>P-NMR-Messungen [32] schlußfolgern wir daraus eine Beteiligung polarer Grenzstrukturen am Grundzustand.



Bei 4-substituierten Triphenyl-phosphinoxiden und -sulfiden,  $4\text{-X-C}_6\text{H}_4\text{-P(Y)(C}_6\text{H}_5)_2$  mit  $\text{Y} = \text{O, S}$ , weisen gemessene und berechnete Dipolmomente ebenfalls auf polare Grenzstrukturen mit im Vergleich zur unsubstituierten Verbindung ( $\text{X} = \text{H}$ ) geschwächter  $\text{P} = \text{Y}$ -Bindung hin, ohne daß jedoch dort eine deutliche Substituentenabhängigkeit sichtbar ist [29]. Unsere Versuche zeigen, daß die P(O)-Gruppe in **1** keine allgemeine, sondern eine selektive Konjugationssperre darstellt.

### Experimenteller Teil

Die Mehrzahl aller Diphenylphosphinyl-*trans*-styrene **1** wurde nach der in [33] angegebenen Methode synthetisiert und ist dort beschrieben. **1d**, **1f** und **1g** wurden via HORNER-Olefinierung aus 4-substituierten Benzaldehyden und Diphenylphosphinylmethyl-diphenylphosphin  $(\text{C}_6\text{H}_5)_2\text{P(O)-CH}_2\text{-P(C}_6\text{H}_5)_2$  mit nachfolgender Oxidation des Olefinierungsproduktes mittels  $\text{H}_2\text{O}_2$  erhalten [34]. Die Darstellung von Phenylbutenyl-phosphinsäure-ethylester **6** erfolgte nach [35]. Die UV-Spektren wurden mit dem Gerät Specord UV/VIS (Fa. VEB Carl Zeiss Jena) in gereinigtem 95-proz. Ethanol bei Raumtemperatur aufgenommen.

\*

Die spektroskopischen Daten der Methylsulfonyl-styrene **5** in Ethanol hat uns Herr Dr. WEGENER, Abteilung Instrumentelle Analytik der Sektion Chemie, vor ihrer Publikation zur Verfügung gestellt, wofür wir ihm herzlich danken. Ebenfalls zu Dank verpflichtet sind wir Herrn Prof. Dr. H.-G. HENNING für sein förderndes Interesse an dieser Arbeit.

### LITERATUR

- [1] GLOYNA, D., BERNDT, K.-G., OTTO, H.: Publikation in Vorbereitung
- [2] LACHMANN, U.: Dissertation A, Humboldt-Universität, Berlin 1973
- [3] HENNING, H.-G.: Z. Chem., **14**, 209 (1974)
- [4] CLAR, E.: Chem. Ber., **82**, 495 (1949)

<sup>8</sup> Jeweils in KBr

- [5] HEILBRONNER, E., BOCK, H.: Das HMO-Modell und seine Anwendung, Weinheim/Bergstraße, Verlag Chemie (1970), S. 109
- [6] ANSARI, B. J., SHARMA, D.: Indian J. pure appl. Physics, **6**, 614 (1968)
- [7] PLATT, J. R.: J. Chem. Physics, **19**, 101 (1951)
- [8] LYONS, A. L. TURRO N. J.: J. Amer. Chem. Soc., **100**, 3177 (1978)
- [9] GLOYNA, D., BERNDT, K.-G., WEGENER, W.: J. Prakt. Chem., **324**, 107 (1982)
- [10] PLATT, J. R.: J. chem. Physics, **17**, 484 (1949)
- [11] HUI, M. H., RICE, S. A.: J. chem. Physics, **61**, 833 (1974)
- [12] SAUER, J., GROHMANN, L., STÖSSER, R., WEGENER, W.: J. prakt. Chem., **321**, 177 (1979)
- [13] UV-Atlas organischer Verbindungen, Weinheim/Bergstraße, Verlag Chemie (1966–1971)
- [14] ELLIOTT, J. H., COOK, E. V.: Ind. Engng. Chem., anal. Edit., **16**, 20 (1944)
- [15] WHEELER, O. H., COVARRUBIAS, C. B.: Canad. J. Chem., **40**, 1224 (1962)
- [16] ADAMSON, D. W., BARRETT, P. A., BILLINGHURST, J. W., JONES, T. S. G.: J. Chem. Soc. (London), **1957**, 2315
- [17] NOLAND, W. E., SUNDBERG, R. J.: J. org. Chemistry, **28**, 884 (1963)
- [18] SKULSKI, L., URBANSKI, T.: Roczniki Chem., **34**, 1307 (1960); siehe dort zitierte Literatur
- [19] BROWN, H. C., OKAMOTO, Y.: J. Amer. chem. Soc., **80**, 4979 (1958)
- [20] EXNER, O. in: Correlation Analysis in Chemistry (ed. N. B. CHAPMAN u. J. SHORTER), Plenum Press, New York, London 1978
- [21] WEGENER, W., MEYER, I.: Publikation in Vorbereitung
- [22] MCDANIEL, D. H., BROWN, H. C.: J. org. Chemistry, **23**, 420 (1958)
- [23] BECKER, H. G. O.: Elektronentheorie organisch-chemischer Reaktionen, 3. Aufl., VEB Deutscher Verlag der Wissenschaften Berlin 1974
- [24] DOUB, L., VANDENBELT, J. M.: J. Amer. chem. Soc., **69**, 2714 (1947)
- [25] ANDRIANOV, V. F., KAMINSKY, A. YA.: Organic Reactivity (Tartu), **14**, 404 (1977)
- [26] SIEGMUND, M., WEGENER, W., SCHLEINITZ, K.-D.: J. prakt. Chem., **322**, 457 (1980)
- [27] LÁNG, L.: Absorption Spectra in the Ultraviolet and Visible Region, Bd. V, S. 190. Akadémiai Kiadó, Budapest 1965
- [28] ALDER, L., GLOYNA, D., HENNING, H.-G., KOZ'MENKO, M. V., KUZ'MIN, M. G.: Vestnik Moskovskogo Univ., Ser. 2 Chim., **20**, 248 (1979)
- [29] GOETZ, H., NERDEL, F., WIECHEL, K.-H.: Liebigs Ann. Chem., **665**, 1 (1963)
- [30] GLOYNA, D., BERNDT, K.-G.: Acta Univ. Szegediensis, Acta physica chem., **26**, 155 (1980), dort Abb. 1 u. 2
- [31] SCHLEINITZ, K.-D., KÖPPEL, H., SIEGMUND, M., GLOYNA, D., ALDER, L.: International Conference on Phosphorus Chemistry, Halle 1979: Abstracts of Papers II, nr. 160, p. 290.
- [32] SCHLEINITZ, K.-D., KÖPPEL, H., GLOYNA, D., BERNDT, K.-G.: International NMR-Symposium in Smolenice, ČSSR, 30.9.1980
- [33] GLOYNA, D., BERNDT, K.-G., KÖPPEL, H., HENNING, H. -G.: J. prakt. Chem., **318**, 327 (1976)
- [34] GLOYNA, D.: Publikation in Vorbereitung
- [35] GLOYNA, D., BERNDT, K.-G., KÖPPEL, H., HENNING, H.-G.: J. prakt. Chem., **319**, 451 (1977)

Kurt-Günter BERNDT  
Dieter GLOYNA

} Sektion Nahrungsgüterwirtschaft und Lebensmitteltechnologie, Bereich Biochemie und Reaktionskinetik, DDR-1040 Berlin, Invalidenstr. 42, DDR

# <sup>1</sup>H-NMR- AND MÖSSBAUER INVESTIGATIONS ON THE ION PAIRS OF TETRACHLOROFERRATE(III) ANION WITH QUATERNARY PHOSPHONIUM CATIONS

L. VINCZE and S. PAPP\*

(*Department of General and Inorganic Chemistry, Veszprém University of Chemical Engineering, Veszprém*)

Received April 7, 1981

Accepted for publication July 29, 1981

Paramagnetic ion pairs were investigated by <sup>1</sup>H-NMR and Mössbauer spectroscopy in chloroform and dimethyl sulphoxide. It has been shown that the chemical shifts of <sup>1</sup>H-NMR peaks arise from a combination of contact and pseudocontact interactions of opposite sign, and the ratio of interactions was definitely influenced by the extent of solvation. On the basis of Mössbauer measurements it was shown that the change of the cation size had an effect on the electron delocalization and symmetry conditions of iron(III) in solid samples, too. In concentrated frozen solutions of ion pairs, different interactions were indicated by Mössbauer spectroscopy in chloroform and dimethyl sulphoxide, in accordance with <sup>1</sup>H-NMR results. However, in dilute solution such an anion-solvent interaction was observed directly, which could be shown by the NMR method only indirectly.

## Introduction

Unpaired electrons of transition metals are known to interact with protons of their environment in complexes *via* two different mechanism, *viz.* contact and dipole interactions [1], both of which may cause signal shifts in the <sup>1</sup>H-NMR spectra. The first interaction permits conclusions to be drawn on the structure of complexes and the delocalization of unpaired electrons, while the geometry of paramagnetic ion pairs and association constants can be deduced from the dipolar effects [2].

The chemical shifts due to the above two effects can be separated by various methods [3–10], but their application gives satisfactory results in relatively few cases. Some investigations are known on the [(C<sub>4</sub>H<sub>9</sub>)<sub>4</sub>N][MX<sub>4</sub>] and [(C<sub>6</sub>H<sub>5</sub>)<sub>3</sub>PC<sub>4</sub>H<sub>9</sub>][MX<sub>4</sub>] systems [3, 11, 12], where X is Cl<sup>-</sup>, Br<sup>-</sup>, or I<sup>-</sup>, and M is Co(II), Ni(II) and Fe(II), containing 2, 3 or 4 unpaired electrons. From <sup>1</sup>H-NMR studies, it was also reported that the spin density removed from the central metal atom of the anion interacts with the protons of the solvent, too [13]. However, the problem of whether or not the total spin density

\* To whom correspondence should be addressed

removed from the paramagnetic center interacts with the associated cation cannot be solved directly by NMR spectroscopy. It seems that Mössbauer spectroscopy gives the possibility to measure the change of spin density departing from the transition metal directly and thus can contribute to the problem in question. In connection with our earlier work on paramagnetic ion pairs [14, 15, 16] the  $[(C_4H_9)_3PR][FeCl_4]$  and  $[(C_6H_5)_3PR][FeCl_4]$  systems were investigated in  $CDCl_3$  and  $DMSO-d_6$  with  $R=Me, Et, Pr, allyl, Bu, Ph$  and benzyl.

## Experimental

### Preparation of $H[FeCl_4]$

The complex is formed in aqueous solution of iron(III) chloride upon adding *conc.* HCl. It cannot be prepared as a solid so its aqueous solution was used.

*Preparation of quaternary phosphonium salts*  $[R_3PR^+]X^-$ , was carried out by quaternization of tributylphosphine and triphenylphosphine.

$[(C_9H_9)_3PCH_3]I$ ,  $[(C_4H_9)_3PC_2H_5]I$ , and  $[(C_4H_9)_3PCH_2CHCH_2]Br$  were prepared by mixing tributylphosphine and the proper alkyl halide. Since the reaction was very vigorous, the components could be mixed in solvent only [17].

$[(C_6H_5)_3PCH_3]I$  was prepared by equimolar mixing of triphenylphosphine and methyl iodide dissolved in benzene.

$[(C_6H_5)_3PH]Cl$  was formed from triphenylphosphine dissolved in *conc.* aqueous HCl. It cannot be prepared as solid so its solutions were used.

$[(C_4H_9)_3PC_3H_7]Br$ ,  $[(C_4H_9)_4P]Br$ ,  $[(C_6H_5)_3PC_2H_5]I$ ,  $[(C_6H_5)_3PC_3H_7]Br$ ,  $[(C_6H_5)_3PC_4H_9]Br$ , and  $[(C_6H_5)_3PCH_2CHCH_2]Br$  were prepared from equimolar mixture of tributyl or triphenylphosphine and the proper alkyl halide. The mixtures were refluxed for 30–60 min, the yields were 30–60%.

$[(C_6H_5)_4P]Br$  was prepared according to the literature [18]. Reaction of tertiary phosphines and benzyl chloride occurred quantitatively upon heating to 200–300 °C of their equimolar mixtures and cooling the  $[(C_4H_9)_3PCH_2C_6H_5]Cl$  and  $[(C_6H_5)_3PCH_2C_6H_5]Cl$  formed.

The products obtained were purified by washing with diethyl ether.

### Preparation of complexes

Since the complexes are soluble in water, aqueous solutions of quaternary phosphonium chlorides and  $H[FeCl_4]$  were mixed, and the solutions were concentrated. The precipitated yellow crystals or powders were filtered and washed with cold *conc.* aqueous HCl. For this procedure  $Br^-$  and  $I^-$  ions of some phosphonium salts had to be substituted for chloride ion. In an aqueous solution of the phosphonium salt, silver chloride was suspended and stirred. Within some hours the substitution had taken place; after filtration the solution is available.

### Analysis of the complexes

Phosphorus and iron contents of the complexes were determined. Digestion was performed in a 1 : 1 (*v/v*) mixture of *conc.*  $HNO_3$  and  $HClO_4$ . Phosphorus was measured by Woy's method and iron was determined iodometrically. Results are collected in Table I.

*NMR spectra* were obtained at 60 MHz on a Varian T 60 spectrometer and at 80 MHz on a Tesla-80 instrument at ambient probe temperature. TMS was used as external reference in all cases. Spectra were recorded in  $DMSO-d_6$  and  $CDCl_3$ . The mole ratio method was used according to the literature [3]. Solutions of the phosphonium halide and the complex were prepared so that to each phosphonium cation concentration belonged four different mole ratios of paramagnetic anion. Plotting the measured shifts against the mole ratio of paramagnetic anion the chemical shift could be obtained at a 1 : 1 mole ratio by extrapolation. Although the mole ratio reached was only 0.30 due to the effect of five unpaired electrons on the high-spin ferric ion, the approximation was reasonable since the chemical shifts were used to evaluate tendencies only.

*Mössbauer spectra* were obtained with a  $^{57}Co/Pt$  source moved at constant acceleration. Activity of the source was  $1.1 \times 10^8$  Bq. Pulses were detected by a Gamma scintillation counter

**Table I**  
*Elemental analysis of complexes*

Formula	Symbol	Fe, calcd. (%)	Fe, found (%)	P, calcd (%)	P, found (%)
$[(C_4H_9)_3PCH_3][FeCl_4]$	A <sub>1</sub>	13.46	13.54	7.46	7.53
$[C_4H_9)_3PC_2H_5][FeCl_4]$	A <sub>2</sub>	13.02	13.19	7.22	7.26
$[C_4H_9)_3PC_3H_7][FeCl_4]$	A <sub>3</sub>	12.60	12.57	6.99	6.85
$[(C_4H_9)_4P][FeCl_4]$	A <sub>4</sub>	12.22	12.31	6.78	6.71
$[(C_4H_9)_3PCH_2CH=CH_2][FeCl_4]$	A <sub>5</sub>	12.66	12.98	7.02	7.12
$[(C_4H_9)_3PCH_2C_6H_5][FeCl_4]$	A <sub>6</sub>	11.37	11.28	6.31	6.68
$[(C_6H_5)_3PH][FeCl_4]$	B <sub>0</sub>	12.12	11.95	6.72	6.71
$[C_6H_5)_3PCH_3][FeCl_4]$	B <sub>1</sub>	11.76	11.67	6.52	6.50
$[(C_6H_5)_3PC_2H_5][FeCl_4]$	B <sub>2</sub>	11.42	11.17	6.33	6.36
$[(C_6H_5)_3PC_3H_7][FeCl_4]$	B <sub>3</sub>	11.10	11.13	6.16	6.00
$[(C_6H_5)_3PC_4H_9][FeCl_4]$	B <sub>4</sub>	10.80	10.86	5.99	6.02
$[(C_6H_5)_3PCH_2CH=CH_2][FeCl_4]$	B <sub>5</sub>	11.15	11.40	6.18	6.17
$[(C_6H_5)_4P][FeCl_4]$	B <sub>6</sub>	10.40	10.38	5.77	5.63
$[(C_6H_5)_3PCH_2C_6H_5][FeCl_4]$	B <sub>7</sub>	10.13	9.89	5.62	5.84

(ND 131/F) equipped with a NaI monocrystal of 0.10 mm thickness and a multichannel analyzer. All measurements were carried out at 77 K, relative to  $^{57}Co$ -Pt source. Rapid freezing was performed dropwise. Next drop was added only when boiling of liquid nitrogen due to the former drop ceased. Spectra were evaluated manually: the errors were estimated.

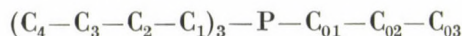
#### Reagents

We used analytical grade  $FeCl_3 \cdot 6 H_2O$  (Reanal), pure  $C_2H_5I$  (Trucizna),  $CH_3I$ ,  $C_3H_7Br$ ,  $CH_2CHCH_2Br$ ,  $C_4H_9Br$ ,  $C_6H_5Br$ ,  $C_6H_5CH_2Cl$  (Reanal), synthesis grade  $(C_6H_5)_3P$  and  $(C_4H_9)_3P$  (Merck-Schuchardt) without further purification.  $CHCl_3$  and DMSO (Reanal) were of analytical grade.  $CDCl_3$  and DMSO- $d_6$  (both were 99% isotopic purity) were obtained from Zentralinstitut für Isotopen- und Strahlungsforschung, Leipzig. Aqueous solutions of  $^{57}FeCl_3$  were prepared from  $^{57}Fe_2O_3$  (95% isotopic purity) by dissolving in hydrochloric acid.

## Results and Discussion

### *NMR spectra*

Designation of the proton groups of the tributyl homologs is:



Peaks of  $C_1$  protons were at the lowest field (2.5–2.9 ppm), those of  $C_2$  and  $C_3$  protons were mixed generally (1.7–2.0 ppm), and the triplets of  $C_4$  protons



**Table II**  
Extrapolated chemical shifts in  $\text{CDCl}_3$

Symbol of compound	$10^2 \times \text{XCR}$	$\Delta\nu$ (Hz)			
		$\text{C}_1$	$\text{C}_2-\text{C}_3$	$\text{C}_4$	$\text{C}_0$
$\text{A}_1$	1.0	—	56	35	—
	10.0	—	372	250	—
	50.0	—	1030	1000	—
$\text{A}_2$	1.0	28	34	-66	—
	10.0	214	251	52	—
	100.0	—	1220	1040	—
$\text{A}_3$	1.0	—	113	107	—
	10.0	—	536	507	—
	100.0	—	$2 \cdot 10^3$	$3 \cdot 10^3$	—
$\text{A}_3$	1.0	—	—	—	—
	1.00	91	61	228	—
	50.0	1099	893	1180	—
$\text{A}_5$	1.0	—	18	16	17
	10.0	—	246	163	168
	100.0	2920	2180	—	2340
		$\text{C}_{\text{Ph}}$	$\text{C}_1$	$\text{C}_2$	$\text{C}_t^a$
$\text{B}_2$	1.0	-47	—	44	—
	10.0	212	101	12	—
	50.0	1390	$6 \cdot 10^3$	2190	—
$\text{B}_3$	1.0	11	15	15	15
	10.0	192	173	227	63
	65.0	1580	—	2900	1280
$\text{B}_4$	1.0	60	11	11 <sup>b</sup>	11
	10.0	180	381	215	80
	55.0	810	944	711	683
$\text{B}_5$	1.0	31	Not evaluated		
	10.0	217			
	60.0	1410			

<sup>a</sup> Terminal protons; <sup>b</sup>  $\text{C}_2-\text{C}_3$  protons

**Table III**  
*Extrapolated chemical shifts in DMSO- $d_6$*

Symbol of compounds	$10^3 X C_R$	$\Delta\nu$ (Hz)				
		$C_1$	$C_2-C_3$	$C_4$	$C_0$	
$A_1$	1.0	116	47	42	—	
	10.0	209	162	167	180	
	50.0	1230	1110	1070	—	
$A_2$	1.0	48	45	47	—	
	10.0	221	232	212	—	
	100.0	970	980	960	—	
$A_3$	1.0	80	55	55	—	
	10.0	160	160	160	—	
	100.0	—	—	—	—	
$A_4$	1.0	33	34	49	—	
	10.0	235	257	206	—	
	50.0	1220	1170	1320	—	
$A_5$	1.0	—	42	53	—	
	10.0	242	155	188	—	
	30.0	620	500	510	—	
		$C_{m-p}$	$C_0$	$C_1$	$C_2$	$C_t^a$
$B_2$	1.0	21	21	—	—	
	10.0	184	193	—	—	
	50.0	817	840	—	—	
$B_3$	0.67	9	11	—	—	—
	5.5	133	142	—	117	138
	33.3	670	630	—	790	740
$B_4$	1.0	15	21	—	60 <sup>b</sup>	60
	10.0	236	225	—	220	234
	20.0	460	420	—	490	460
$B_5$	1.0	13	0	Not evaluated		
	10.0	136	86			
	33.3	800	690			

<sup>a</sup> Terminal protons; <sup>b</sup>  $C_2-C_3$  protons

the anion with the empty 4s or 3d orbitals of phosphorus can be supposed but a hydrogen-bond type interaction between chloride ligands and C<sub>1</sub>-protons is more likely. Shifts of C<sub>1</sub> protons being less than the expected values also point to the latter mechanism as has been pointed out by BROWN and DRAGO [11].

### Mössbauer spectra

#### Solid complexes

Isomer shifts ( $\delta$ ) and quadrupole splittings ( $\Delta E$ ) for the solid compounds are collected in Table IV. It is obvious that in the [(C<sub>6</sub>H<sub>5</sub>)<sub>3</sub>PR][FeCl<sub>4</sub>] series, changes of isomer shifts are closely followed by quadrupole splittings. If  $\delta$  also decreases,  $\Delta E$  increases and conversely, showing that if the 3d-electron density is reduced at the iron(III) nucleus, then the symmetry of the 3d<sup>5</sup> shell will also be lower. In the 3d<sup>5</sup> shell of iron(III) the change of electron density is due to delocalization, which also occurs in solid complexes.

In the [(C<sub>4</sub>H<sub>9</sub>)<sub>3</sub>PR'][FeCl<sub>4</sub>] series the correlation between  $\delta$  and  $\Delta E$  is not too close, which can be caused by too small splittings to be measured by the available instrument. Since  $\Delta E$  of A<sub>4</sub> is about half of  $\Delta E$  of butyl group containing B<sub>4</sub> (Fig. 1), it can be expected that the quadrupole splitting of most

Table IV

Isomer shifts and quadrupole splittings of Mössbauer spectra of solid samples. Error of measurements:  $\pm 0.07$  mm s<sup>-1</sup>

Compounds	Symbol	$\delta$ (mm s <sup>-1</sup> )	$\Delta E_{\text{q}}$ (mm s <sup>-1</sup> )
[(C <sub>4</sub> H <sub>9</sub> ) <sub>3</sub> PCH <sub>3</sub> ][FeCl <sub>4</sub> ]	A <sub>1</sub>	-0.10	0.0
[(C <sub>4</sub> H <sub>9</sub> ) <sub>3</sub> PC <sub>2</sub> H <sub>5</sub> ][FeCl <sub>4</sub> ]	A <sub>2</sub>	0.0	0.0
[(C <sub>4</sub> H <sub>9</sub> ) <sub>3</sub> PC <sub>3</sub> H <sub>7</sub> ][FeCl <sub>4</sub> ]	A <sub>3</sub>	0.0	0.0
[(C <sub>4</sub> H <sub>9</sub> ) <sub>4</sub> P][FeCl <sub>4</sub> ]	A <sub>4</sub>	-0.05	0.30
[(C <sub>4</sub> H <sub>9</sub> ) <sub>3</sub> PCH <sub>2</sub> CH=CH <sub>2</sub> ][FeCl <sub>4</sub> ]	A <sub>5</sub>	+0.06	0.35
[(C <sub>4</sub> H <sub>9</sub> ) <sub>3</sub> P-CH <sub>2</sub> -C <sub>6</sub> H <sub>5</sub> ][FeCl <sub>4</sub> ]	A <sub>6</sub>	-0.05	0.0
[(C <sub>6</sub> H <sub>5</sub> ) <sub>3</sub> PH][FeCl <sub>4</sub> ]	B <sub>0</sub>	0.08	0.20
[(C <sub>6</sub> H <sub>5</sub> ) <sub>3</sub> PCH <sub>3</sub> ][FeCl <sub>4</sub> ]	B <sub>1</sub>	-0.17	0.40
[(C <sub>6</sub> H <sub>5</sub> ) <sub>3</sub> PC <sub>2</sub> H <sub>5</sub> ][FeCl <sub>4</sub> ]	B <sub>2</sub>	-0.05	0.20
[(C <sub>6</sub> H <sub>5</sub> ) <sub>3</sub> PC <sub>3</sub> H <sub>7</sub> ][FeCl <sub>4</sub> ]	B <sub>3</sub>	-0.06	0.30
[(C <sub>6</sub> H <sub>5</sub> ) <sub>3</sub> PC <sub>4</sub> H <sub>9</sub> ][FeCl <sub>4</sub> ]	B <sub>4</sub>	-0.20	0.60
[(C <sub>6</sub> H <sub>5</sub> ) <sub>3</sub> PCH <sub>2</sub> CH=CH <sub>2</sub> ][FeCl <sub>4</sub> ]	B <sub>5</sub>	-0.10	0.20
[(C <sub>6</sub> H <sub>5</sub> ) <sub>4</sub> P][FeCl <sub>4</sub> ]	B <sub>6</sub>	-0.22	0.20
[(C <sub>6</sub> H <sub>5</sub> ) <sub>3</sub> P-CH <sub>2</sub> -C <sub>6</sub> H <sub>5</sub> ][FeCl <sub>4</sub> ]	B <sub>7</sub>	-0.10	0.0

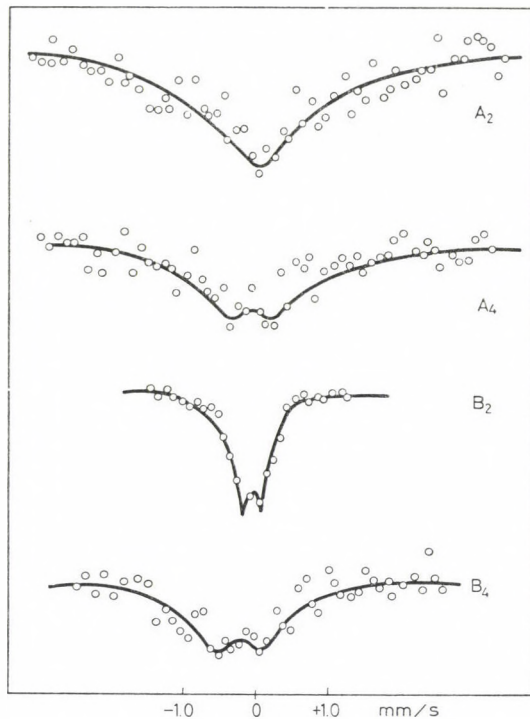


Fig. 1. Mössbauer spectra of some solid samples

$A_1$ — $A_6$  complexes will be less than  $0.20 \text{ mm s}^{-1}$ , which is hardly measurable. As can be seen in Fig. 1, the broadening of the absorption band of  $A_2$  also indicates a hidden  $\Delta E$ .

#### Frozen solutions

Isomer shifts and quadrupole splittings of  $B_2$  in  $\text{CHCl}_3$  and DMSO are shown in Table V and Fig. 2.

The chemical shifts recorded are greater in DMSO than in  $\text{CHCl}_3$  at any concentration. In  $\text{CHCl}_3$  the isomer shifts have a maximum which is hardly lower than that of the solid sample  $-0.10 \text{ mm s}^{-1}$  and  $-0.05 \text{ mm s}^{-1}$  respectively, but in DMSO the increasing curve does not decrease again at higher concentrations. Thus in the case of very dilute solutions the complex has similar properties in both solvents; if the concentration decreases, the 3d-electron density also decreases, and the extent of delocalization increases. This phenomenon cannot be caused by an ion association of great extent, but it can be assumed that unpaired electrons of free anions interact with the protons of solvent molecules [13]. Interestingly, this is directly indicated by Mössbauer data while from  $^1\text{H-NMR}$  studies indirect evidences can be obtained only.

Table V

Mössbauer parameters of  $B_2$  in frozen solutions  
 Error of measurements:  $\pm 0.10 \text{ mm s}^{-1}$

Solution	$C_R$ ( $\text{mol kg}^{-1}$ )	$\delta$ ( $\text{mm s}^{-1}$ )	$\Delta E_Q$ ( $\text{mm s}^{-1}$ )
$\text{CHCl}_3$	0.07	-0.30	<sup>a</sup>
	0.10	-0.25	<sup>a</sup>
	0.175	-0.10	<sup>a</sup>
	0.35	-0.20	0.91
	0.55	-0.30 <sup>b</sup>	0.91 <sup>c</sup>
DMSO	0.07	-0.17	0.98
	0.10	-0.07	0.98
	0.175	+0.04	1.10
	0.36	+0.08	1.14
	0.50	+0.08	1.14

<sup>a</sup> Not evaluated, <sup>b</sup> error  $\pm 0.15 \text{ mm s}^{-1}$ , <sup>c</sup> error  $\pm 0.20 \text{ mm s}^{-1}$

Upon the concentration of dilute solutions the decrease of delocalization of 3d-electrons can be explained by the spherical symmetry conditions of anions being perturbed by cations, which makes the overlapping of 3d-electrons with solvent protons less probable. The further increase of concentration leads again to the spread of electron density *via* increased association and the formation of aggregates in  $\text{CHCl}_3$ , but intensive solvation hinders this procedure in

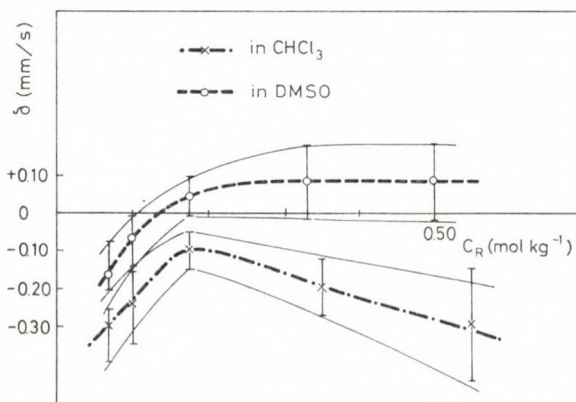


Fig. 2. Isomer shifts of a frozen solution of complex  $B_2$

DMSO. This is supported by the fact that in DMSO the chemical shift tends to a limit.

Quadrupole splitting is increased upon increasing concentration, indicating also a decrease of symmetry due to the formation of ion pairs.

### Conclusions

Information about association conditions of ion pairs can be obtained more directly by Mössbauer than by NMR spectroscopy, which has been used in this area widely and almost exclusively. Furthermore, the interpretation of the NMR spectra requires in many cases extrapolation and lengthy calculations, but the changes of Mössbauer parameters can be directly interpreted. Although, due to the limit of solubility and detection, we could investigate a narrow concentration range only, changes in the association conditions were detected by Mössbauer spectroscopy, which were not indicated at all by NMR studies.

### REFERENCES

- [1] DRAGO, R. S., ZINK, J. I., RICHMAN, R. M., PERRY, W. D.: *J. Chem. Educ.*, **51**, 371 464 (1974)
- [2] EATON, D. R., ZAW, K.: *Coord. Chem. Rev.*, **7**, 197 (1971)
- [3] WALKER, I. M., DRAGO, R. S.: *J. Am. Chem. Soc.*, **90**, 6951 (1968)
- [4] PINKERTON, A. A., EARL, W. L.: *J.C.S. Dalton*, **1973**, 267
- [5] TAN, T. C., LIM, Y. Y.: *Inorg. Chem.*, **12**, 2203 (1973)
- [6] HORROCKS, W. D.: *Inorg. Chem.*, **9**, 690 (1970)
- [7] LA MAR, G. N.: *J. Chem. Phys.*, **41**, 2992 (1964)
- [8] LA MAR, G. N.: *J. Am. Chem. Soc.*, **87**, 3567 (1965)
- [9] WALKER, I. M., ROSENTHAL, L., QUERESHI, M. S.: *Inorg. Chem.*, **10**, 2463 (1971)
- [10] ROSENTHAL, L., WALKER, I. M.: *Inorg. Chem.*, **13**, 2896 (1974)
- [11] BROWN, D. G., DRAGO, R. S.: *J. Am. Chem. Soc.*, **92**, 1871 (1972)
- [12] QUERESHI, M. S., ROSENTHAL, L., WALKER, I. M.: *J. Coord. Chem.*, **5**, 77 (1976)
- [13] LIM, Y. Y., DRAGO, R. S.: *J. Am. Chem. Soc.*, **94**, 84 (1972)
- [14] PAPP, S., KVINTOVICS, P.: *Acta Chim. Acad. Sci. Hung.*, **102**, 247 (1979); **102**, 259 (1979)
- [15] PAPP, S., KVINTOVICS, P.: *Magy. Kém. Folyóirat*, **85**, 202 (1979)
- [16] PAPP, S., VINCZE, L., KERESSZEGI, F.: *Abstracts Internat. Conf. Phosphorus Chem.*, p. 334, Halle (Saale), Sept. 17—21. 1979
- [17] FENTON, G. F., HEY L., INGOLD, C. K.: *J. Chem. Soc. (London)*, **1933**, 989
- [18] CHATT, J., MANN, F. G.: *J. Chem. Soc. (London)*, **1940**, 1192
- [19] LEMIRE, A. E., UL-HASAN, M., WALKER, I. M.: *J. Coord. Chem.*, **3**, 81 (1978)
- [20] BURKERT, P. K., FRITZ, H. P., GRETNER, W., KELLER, H. J., SCHWARZHANS, K. E.: *Inorg. Nucl. Chem. Lett.*, **4**, 237 (1968)
- [21] RETTIG, M. F., DRAGO, R. S.: *J. Am. Chem. Soc.*, **88**, 2966 (1966)
- [22] ALEI, M.: *Inorg. Chem.*, **3**, 44 (1964)

László VINCZE }  
 Sándor PAPP } H-8200 Veszprém, Schönherz Z. u. 12.

## CALCULATION OF ASSOCIATION CONSTANTS AND DISTRIBUTION OF CONTACT AND DIPOLAR INTERACTIONS FOR $[R_3P^+R'] [FeCl_4]^-$ ION PAIRS

L. VINCZE and S. PAPP\*

(Department of General and Inorganic Chemistry, Veszprém University of Chemical Engineering,  
Veszprém)

Received April 7, 1981

Accepted for publication July 29, 1981

On the basis of measured shifts of  $^1H$ -NMR peaks of paramagnetic ion pairs, association constant were calculated according to DRAGO's method. The 1 : 1 association model is valid over a wider range of concentrations in DMSO- $d_6$  than in  $CDCl_3$ . A modified method was developed for estimating the distribution of contact and pseudocontact interactions according to chemical shifts, assuming  $\sigma$  delocalization along the alkyl chains. The effect of changing the concentration and solvent is demonstrated by properly chosen models.

### Introduction

In our previous work [1] detailed NMR studies were carried out by the mole ratio method on ion pairs containing high-spin iron(III) [2]. On the basis of chemical shifts obtained ion pairs were qualitatively found to have both contact and pseudocontact interaction. Two solvents,  $CDCl_3$  and DMSO- $d_6$  were used with different solvation ability, but the expected differences in the extent of chemical shifts were not significant. This could be interpreted by the greater amount of contact ion pairs in the less solvating  $CDCl_3$ . Thus, contact shifts, decreasing the pseudocontact shifts, would be greater in  $CDCl_3$ , and the actual chemical shifts cannot increase to a large extent. In the present paper we wish to support this assumption by mathematical analysis of actual data and to make conclusions more quantitative.

### Procedure and Discussion

#### *Calculation of association constants*

According to LIM and DRAGO [3], the association constant of a 1 : 1 ion pair can be given by the following equation:

$$K_i^{-1} = A_0 \left( \frac{\Delta v_{pi}}{\Delta v_i} - 1 \right) - C_0 \left( \frac{\Delta v_i}{\Delta v_{pi}} - 1 \right) \quad (1)$$

where

$K_i$  — association constant calculated from the chemical shifts of the  $i$ -th proton set ( $kg \cdot mol^{-1}$ ),

\* To whom correspondence should be addressed

Table I

Measured shifts for

Symbols:  $C_0$  concentration of cation ( $\text{mol kg}^{-1}$ );  $n$  mole ratio of paramagnetic anion;  $C_i$  a: overlapped peaks.

[[C <sub>6</sub> H <sub>5</sub> ] <sub>3</sub> PCH <sub>3</sub> ][FeCl <sub>4</sub> ](A <sub>1</sub> )								
C <sub>0</sub>	n	CDCl <sub>3</sub>		C <sub>0</sub>	n	DMSO-d <sub>6</sub>		
		C <sub>2</sub> -C <sub>3</sub>	C <sub>4</sub>			C <sub>1</sub>	C <sub>2</sub> -C <sub>3</sub>	C <sub>4</sub>
0.01	0.02	1	1	0.01	0.02	2	2	2
	0.05	3	2		0.05	5	2	4
	0.10	6	4		0.10	11	6	5
	0.20	11	7		0.20	—	8	10
0.1	0.02	7	9	0.1	0.02	6	5	3
	0.05	20	15		0.05	10	10	7
	0.10	34	27.5		0.10	25	21	20
	0.20	77	48		0.20	41	34	33
0.5	0.02	19	21	0.5	0.02	25	26	24
	0.05	57	50		0.05	69	61	59
	0.10	101	—		0.10	122	—	—

[[C <sub>6</sub> H <sub>5</sub> ] <sub>3</sub> PC <sub>3</sub> H <sub>7</sub> ][FeCl <sub>4</sub> ](A <sub>3</sub> )								
C <sub>0</sub>	n	CDCl <sub>3</sub>		C <sub>0</sub>	n	DMSO-d <sub>6</sub>		
		C <sub>2</sub> -C <sub>3</sub>	C <sub>4</sub>			C <sub>1</sub>	C <sub>2</sub> -C <sub>3</sub>	C <sub>4</sub>
0.01	0.02	1.5	1	0.01	0.02	0	0.5	1
	0.05	5	5		0.05	0	2	2
	0.10	11	9		0.10	0	4	5
	0.20	24	19		0.20	3	8	9
0.1	0.02	4	7	0.1	0.02	2.5	3.5	3
	0.05	15	26		0.05	6	9	8
	0.10	44	48		0.10	21	16	17
	0.20	69	84		0.20	32	33	33
1	0.02	44	64	1	0.02	22	31	34
	0.05	—	—		0.05	77	—	—
	0.10	—	—		—	—	—	—

*paramagnetic ion pairs*

the *i*-th proton set. Ph phenyl protons;  $C_{p-m}$  *para* and *meta* protons;  $C_{or}$  *ortho* protons;  
Shifts are in Hz

[[C <sub>6</sub> H <sub>5</sub> ] <sub>2</sub> PC <sub>2</sub> H <sub>5</sub> ][FeCl <sub>4</sub> ](A <sub>2</sub> )									
C <sub>0</sub>	n	CDCl <sub>3</sub>			C <sub>0</sub>	n	DMSO-d <sub>6</sub>		
		C <sub>1</sub>	C <sub>2</sub> -C <sub>3</sub>	C <sub>4</sub>			C <sub>1</sub>	C <sub>2</sub> -C <sub>3</sub>	C <sub>4</sub>
0.01	0.02	0.5	0.5	- 1.5	0.01	0.02	0.5	1	1
	0.05	1	2	- 3.5		0.05	2	2	2.5
	0.10	2	3	- 6.5		0.10	-	4.5	4.5
	0.20	6	7	-13		0.20	-	10	9
0.1	0.02	6	9	1	0.1	0.02	5	6.5	5
	0.05	12	9	2		0.05	11	12	10
	0.10	18	20	8.5		0.10	22	23	22
	0.20	44	52	11		0.20	44	46	42
1	0.02	22	22.5	21	0.5	0.02	23	22	22
	0.05	-	60.5	52		0.05	50	48	48
						0.10	94	-	-

[[C <sub>6</sub> H <sub>5</sub> ] <sub>2</sub> P][FeCl <sub>4</sub> ](A <sub>1</sub> )									
C <sub>0</sub>	n	CDCl <sub>3</sub>			C <sub>0</sub>	n	DMSO-d <sub>6</sub>		
		C <sub>1</sub>	C <sub>2</sub> -C <sub>3</sub>	C <sub>4</sub>			C <sub>1</sub>	C <sub>2</sub> -C <sub>3</sub>	C <sub>4</sub>
0.01	0.02	-	-	-	0.01	0.02	0.5	0.5	1
	0.05	-	-	-		0.05	2	2	2.5
	0.10	-	-	-		0.10	3	3.5	5
	0.20	-	-	-		0.20	-	7	10
0.1	0.02	6	2	2	0.1	0.02	5	5	6
	0.05	12	3	7		0.05	12	13	12
	0.10	-	4	9		0.10	23	28	22
	0.20	-	8	19		0.20	48	50	40
0.5	0.02	24	21	21	0.5	0.02	24	25	25
	0.05	59	51	54		0.05	65	58	66
	0.10	-	92	-		0.10	120	-	-

Table I

[C <sub>4</sub> H <sub>9</sub> ) <sub>3</sub> PCH <sub>2</sub> CH = CH <sub>2</sub> ] [FeCl <sub>4</sub> ] (A <sub>3</sub> )									
C <sub>0</sub>	n	CDCl <sub>3</sub>			C <sub>0</sub>	n	DMSO-d <sub>6</sub>		
		C <sub>1</sub>	C <sub>2</sub> -C <sub>3</sub>	C <sub>4</sub>			C <sub>1</sub>	C <sub>2</sub> -C <sub>3</sub>	C <sub>4</sub>
0.01	0.02	1	0.5	—	0.01	0.02	—	2	1
	0.05	1	1	—		0.05	—	3	3
	0.10	2	2	—		0.10	—	7	6
	0.20	4	4	—		0.20	—	13	11
0.1	0.02	2	4	3	0.1	0.02	12	5	6
	0.05	6	13	8		0.05	20	12	12
	0.10	16	26	19		0.10	28	19	19
	0.20	32	48	33		0.20	36	27	31
1.0	0.02	48	39	42	0.3	0.02	6	12	11
	0.05	117	109	—		0.05	26	24	24
						0.10	68	50	52

[(C <sub>6</sub> H <sub>5</sub> ) <sub>3</sub> PC <sub>4</sub> H <sub>7</sub> ][FeCl <sub>4</sub> ] (B <sub>3</sub> )										
C <sub>0</sub>	n	CDCl <sub>3</sub>				C <sub>0</sub>	n	DMSO-d <sub>6</sub>		
		Ph	C <sub>1</sub>	C <sub>2</sub>	C <sub>3</sub>			Ph	C <sub>2</sub>	C <sub>3</sub>
0.01	0.02	0.5	—	—	—	0.007	0.02	1	—	—
	0.05	1	—	—	—		0.05	2	—	—
	0.10	2	—	—	—		0.10	1	—	—
	0.30	—	—	—	—		0.20	2	—	—
0.1	0.02	17	2	5	2	0.055	0.02	2	9	3
	0.05	27	13	11	5		0.05	6	12	7
	0.10	36	15	23	10		0.10	12	15	13
	0.30	—	—	—	18		0.20	26	30	27
0.65	0.02	47	34	—	34	0.333	0.02	15	18	16
	0.05	85	—	—	—		0.05	41	41	37
	0.10	165	—	—	—		0.10	68	73	—
	0.20	345	—	—	—		0.20	131	—	—

(contd.)

[(C <sub>6</sub> H <sub>5</sub> ) <sub>2</sub> PC <sub>2</sub> H <sub>5</sub> ][FeCl <sub>2</sub> ](B <sub>2</sub> )								
C <sub>0</sub>	n	CDCl <sub>3</sub>			C <sub>0</sub>	n	DMSO-d <sub>6</sub>	
		Ph	C <sub>1</sub>	C <sub>2</sub>			Ph	alkyl
0.01	0.02	3	3	0	0.01	0.02	1	1.5
	0.05	1.5	1.5	—		0.05	2	3
	0.10	-1.5	3	—		0.10	1	3
	0.30	-13	13	—		0.20	5	6
0.1	0.02	3	8	11	0.1	0.02	3	2
	0.05	8.5	3	8		0.05	9	8
	0.10	17	—	8		0.10	18	15
	0.30	67	—	—		0.20	36	31
0.55	0.02	36	43	48	0.5	0.02	24	8
	0.05	108	—	115		0.05	55	36
	0.10	139	296	—		0.10	102	76
	0.30	262	—	—		0.20	210	—

[(C <sub>6</sub> H <sub>5</sub> ) <sub>2</sub> PC <sub>2</sub> H <sub>5</sub> ][FeCl <sub>2</sub> ](B <sub>2</sub> )									
C <sub>0</sub>	n	CDCl <sub>3</sub>		C <sub>0</sub>	n	DMSO-d <sub>6</sub>			
		Ph	alkyl			C <sub>p-m</sub>	C <sub>or</sub>	C <sub>2-C<sub>3</sub></sub>	C <sub>4</sub>
0.01	0.02	2	0	0.01	0.02	0	0	1	—
	0.05	5	0		0.05	1	1	3	2
	0.10	12	1		0.10	1.5	2	6	6
	0.30	17	4		0.20	3	4	—	—
0.1	0.02	9	4	0.1	0.02	2	3	6	5
	0.05	23	11		0.05	8	7	11	10
	0.10	36	22		0.10	21	19	24	23
	0.30	77	66		0.20	45	43	44	46
0.55	0.02	30	17	0.2	0.02	9	8	12	10
	0.05	57	40		0.05	24	23	25	18
	0.10	101	72		0.10	48	41	46	51
	0.20	178	—		0.20	91	84	—	—

Table I (contd.)

[(C <sub>6</sub> H <sub>5</sub> ) <sub>3</sub> PCH <sub>2</sub> CH = CH <sub>2</sub> ][FeCl <sub>4</sub> ] (B <sub>5</sub> )							
C <sub>0</sub>	n	CDCl <sub>2</sub>	C <sub>0</sub>	n	DMSO-d <sub>6</sub>		
		Ph			C <sub>p-m</sub>	C <sub>or</sub>	alkyl
0.01	0.02	1	0.067	0.02	0	—	—
	0.05	2		0.05	0.5	—	—
	0.10	4		0.10	1	—	—
	0.20	7		0.20	2	—	—
0.1	0.02	7	0.055	0.02	5	5	2
	0.05	13		0.05	8.5	8	6
	0.10	31		0.10	12	9	10
	0.20	52		0.20	28	20	25
0.5	0.02	40	0.333	0.02	24 <sup>a</sup>	—	22
	0.05	68		0.05	41	—	37
	0.10	144		0.10	74	—	74
	0.20	264		—	—	—	—

$A_0$  — concentration of anion (mol · kg<sup>-1</sup>),

$C_0$  — concentration of cation (mol · kg<sup>-1</sup>),

$\Delta\nu_{pi}$  — shift of the  $i$ -th proton set arising in a pure paramagnetic environment (Hz),

$\Delta\nu_i$  — measured shift of the  $i$ -th proton set (Hz).

During the studies chemical shifts have been obtained for each complex at 3 cation concentrations and 3 × 4 anion concentrations (according to the mole ratio method), thus the 1 : 1 association constants and the area of their validity can be established. Data are collected in Table I.

Upon rearrangement Eq. (1) can be written as

$$\frac{C_0}{\Delta\nu_{pi}} (\Delta\nu_i)^2 + (K_i^{-1} + A_0 - C_0) \Delta\nu_i - A_0 \Delta\nu_{pi} = 0 \quad (2)$$

Considering that to each  $C_0$  there belong four different  $A_0$ 's, Eq. (2) can be given as the following vector-vector function:

$$\begin{bmatrix} \Delta\nu_{i1} \\ \Delta\nu_{i2} \\ \Delta\nu_{i3} \\ \Delta\nu_{i4} \end{bmatrix} = F(C_0, [A_{01}, A_{02}, A_{03}, A_{04}], K_i, \Delta\nu_{pi}) \quad (3)$$

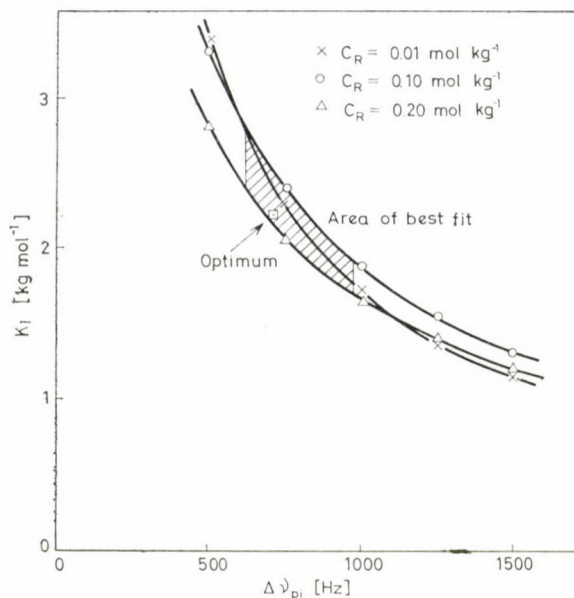


Fig. 1.  $[K_i; \Delta\nu_{pi}]$  vectors of complex  $B_4$  in  $DMSO-d_6$

A set of  $[K_i, \Delta\nu_{pi}]$  vectors can be assigned to each  $[C_0, A_{01}, A_{02}, A_{03}, A_{04}]$  vector which provides  $\Delta\nu_{i\text{calcd}}$  fitting  $\Delta\nu_{i\text{imd}}$  rather well, the  $[K_i, \Delta\nu_{pi}]$  set can be represented by a line in the plane of  $K_i$  and  $\Delta\nu_{pi}$ . Thus, drawing the lines belonging to the different cation concentrations, the area of best fit in the plane of  $K_i$  and  $\Delta\nu_{pi}$  can be visually determined, and the optimum can be easily obtained for each compound by the gradient method. In the case of complex  $B_4$  the procedure is demonstrated in Fig. 1.

Calculations have been carried out using a Hewlett—Packard desk-top computer. The results — summarized in Table II — show that the model is valid over a wider range of concentrations in  $DMSO-d_6$  than in  $CDCl_3$ . The solvation ability of the two solvents proved to be different also in the case of the present systems. It can be supposed that in  $DMSO-d_6$  1 : 1 ion pairs exist also at higher concentrations, while in  $CDCl_3$  aggregates are formed which decrease the chemical shifts due to the increase of contact interaction.

Association constants are always greater in  $CDCl_3$  as is expected, and generally greater for complexes  $B_2$ — $B_5$  than for the respective  $A_2$ — $A_5$  species in agreement with data on the association conditions of other aromatic cations [4].

#### *Distribution of contact and pseudocontact interactions*

On the basis of chemical shifts the rates of contact and pseudocontact interactions also can be estimated, contributing to the picture about the role

of the solvent. Complexes  $A_4$  and  $A_5$  were chosen for investigation, because the shifts of several of their proton groups were readily evaluated.

A rigid model was used, which permitted the internal motion of alkyl chains. Such an orientation was chosen that three butyl chains were in proximity of the anion, the fourth one (butyl or allyl) was on the opposite side along the symmetry axis of the ion pair. Our earlier results supported this orientation [5] especially since "trapping" was not likely for longer chains [6].

The origin of polar coordinates was placed at the phosphorus nucleus and the polar axis coincided with the symmetry axis and pointed toward the anion. Due to the symmetry, it was sufficient to investigate one butyl chain only, and the plane projection of proton groups was considered to simplify calculations. Considering the large freedom of motion of a butyl chain, in

Table II

*Association constants according to the 1 : 1 ion pair model*

Complex	Solvent	Concentration range that can be fitted ( $C_R$ )	$K_i$ (kg/mol)	$\Delta\nu_p$ (Hz)
$A_1$	$CDCl_3$	0.01–0.10	1.25	2000
	$DMSO-d_6$	0.10–0.50	0.74	2100
$A_2$	$CDCl_3$	0.01–0.10	1.3	2000
	$DMSO-d_6$	—	—	—
$A_3$	$CDCl_3$	—	—	—
	$DMSO-d_6$	0.10–1.0	1.5	1000
$A_4$	$CDCl_3$	0.10–0.50	1.4	640
	$DMSO-d_6$	—	—	—
$A_5$	$CDCl_3$	0.01–0.10	2.6	750
	$DMSO-d_6$	0.10–0.30	1.05	1200
$B_2$	$CDCl_3$	0.10–0.55	1.2	1000
	$DMSO-d_6$	0.10–0.50	0.9	1500
$B_3$	$CDCl_3$	0.01–0.10	2.9	850
	$DMSO-d_6$	0.0067–0.05	2.1	1000
$B_4$	$CDCl_3$	—	—	—
	$DMSO-d_6$	0.01–0.20	2.2	700
$B_5$	$CDCl_3$	0.01–0.10	4.5	500
	$DMSO-d_6$	0.007–0.33	1.5	1000

**Table III**  
Residence area of the butyl proton sets

Polar coordinates	C <sub>1</sub>	C <sub>2</sub> -C <sub>3</sub>	C <sub>4</sub>
R(pm)	180-300	200-500	350-600
ϑ (degree)	45-70	70-120	70-110

Table III are summarized the ranges accepted for real residence areas of proton groups according to known C-C and C-H bond distances. Since the C<sub>2</sub>-C<sub>3</sub> protons did not offer essential additional information, only the conditions of shift and position of C<sub>1</sub> and C<sub>4</sub> proton sets were investigated.

Our method can be summarized as follows.

The residence area of C<sub>1</sub> protons was fixed and the arguments were varied to determine the ranges of independent variables over which the calculated and real positions of set C<sub>4</sub> overlap. As is known, the interionic distance in ion pairs generally ranges between 700-1100 pm [2, 7-13] and in the case of  $\sigma$  delocalization the spin density, away from the central atom of the cation, decreases dramatically along the alkyl chain [14-16].

Thus five ionic distances (700, 800, 900, 1000, 1100 pm) and three different decays of contact shift (contact shift of the C<sub>4</sub> set was considered 0, 5, 10% of the contact shift of set C<sub>1</sub>) were assumed.

Pseudocontact shifts of two different proton sets are [10, 15, 17]:

$$\frac{\Delta v_{jpc}}{\nu_0} = F(g_{||}, g_{\perp}) [G.F.]_j \quad (4)$$

$$\frac{\Delta v_{ipc}}{\nu_0} = F(g_{||}, g_{\perp}) [G.F.]_i \quad (5)$$

where  $F(g_{||}, g_{\perp})$  is the same, since the two equations refer to one ion pair. Thus for the ratio of shifts it can be written that

$$\frac{\Delta v_{jpc}}{\Delta v_{ipc}} = \frac{[G.F.]_j}{[G.F.]_i} = \frac{3 \cos^2 \Theta_j - 1}{3 \cos^2 \Theta_i - 1} \cdot \frac{R_i^3}{R_j^3} \quad (6)$$

Since in the present case chemical shifts generally have contact components, too, assuming that

$$\Delta v_{imd} = \Delta v_{ipc} - \Delta v_{ic}, \quad (7)$$

and introducing factors  $\alpha$  and  $\beta$ .

$$\frac{\Delta v_{ic}}{\Delta v_{ipc}} = \alpha_i \quad (8)$$

$$\Delta\nu_{4c} = \beta_4 \Delta\nu_{1c} \quad (9)$$

Equation (6) can be rearranged to

$$\frac{\Delta\nu_{4md} + \Delta\nu_{1md} \beta_4 \frac{\alpha_1}{1 - \alpha_1}}{\Delta\nu_{1md} + \Delta\nu_{1md} \frac{\alpha_1}{1 - \alpha_1}} = \frac{3 \cos^2 \Theta_4 - 1}{3 \cos^2 \Theta_1 - 1} \frac{R_1^3}{R_4^3} \quad (10)$$

Since chemical shifts are known, the term on the left depends on  $\alpha_1$  and  $\beta_4$  only, and the equation can be symbolized as

$$G_4^1(\alpha_1; \beta_2) = F([R_1; \Theta_1], [R_4; \Theta_4]) \quad (11)$$

where  $[R_i; \Theta_i]$  is the position vector of the  $i$ -th proton set. Considering that  $[R_4; \Theta_4]$  is the dependent variable, and assuming that  $R_1$  and  $\Theta_1$  are functions

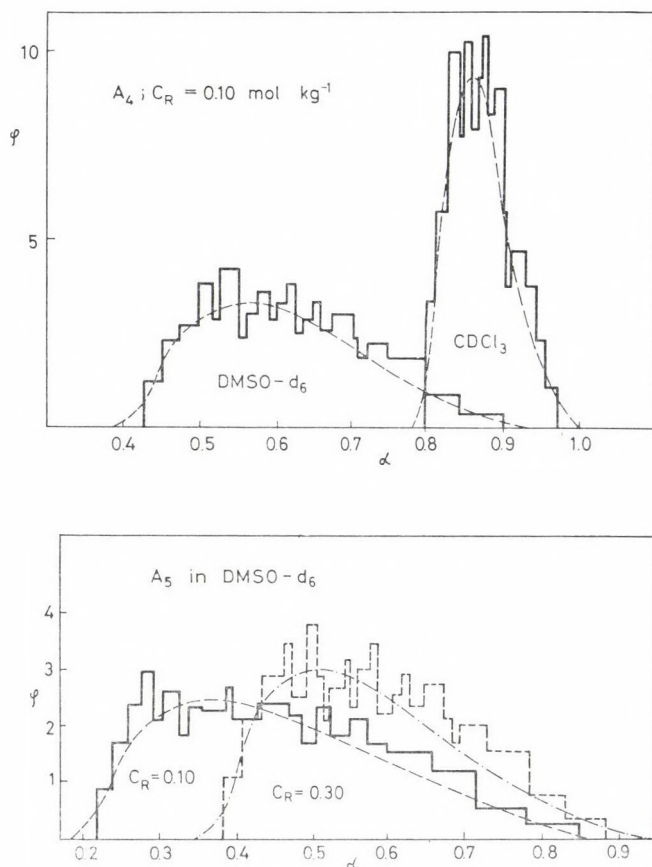


Fig. 2. Empirical distribution functions ( $\varphi$ ) of the ratio of contact and pseudocontact interactions ( $\alpha$ )

of ionic distance  $A$ , one can write that

$$\begin{bmatrix} R_4 \\ \Theta_4 \end{bmatrix} = \Phi(G_4^1(\alpha_1, \beta_4), [R_1(A); \Theta_1(A)]). \quad (12)$$

Replacing the symbols of internal functions, one obtains

$$\begin{bmatrix} R_4 \\ \Theta_4 \end{bmatrix} = \Phi(\alpha_1, \beta_4, A). \quad (13)$$

Equation (13) is nothing else but the transformation of the plane of  $C_1$  protons to the area of  $C_4$  set against  $\alpha_1$ ,  $\beta_4$  and  $A$ . The transformation was investigated for all 15 combinations of  $\beta_4$  and  $A$ , thus  $\alpha_1$  intervals were obtained, over which the transformed  $C_1$  area overlaps with the real  $C_4$  area. Since there is no reason to prefer any combination of  $\beta_4$  and  $A$ , histograms without weighting were plotted according to  $\alpha$  intervals. Empirical distribution functions of  $\alpha_1$  were obtained for different solvents and concentrations. Results are shown in Fig. 2. As can be seen, in line with experiments, the ratio of the contact and the dipolar interactions depends mainly on the solvent and to a minor extent on the concentration, but these results can be elucidated better if they are interpreted in terms of a distribution function rather than of a single number only.

#### REFERENCES

- [1] VINCZE, L., PAPP, S.: *Acta Chim. Acad. Sci. Hung.*, **110**, 153 (1982)
- [2] WALKER, I. M., DRAGO, R. S.: *J. Am. Chem. Soc.*, **90**, 6951 (1968)
- [3] LIM, Y. Y., DRAGO, R. S.: *J. Am. Chem. Soc.*, **94**, 84 (1972)
- [4] HAQUE, R., COSHOW, W. R., JOHNSON, L. F.: *J. Am. Chem. Soc.*, **91**, 3822 (1969)
- [5] PAPP, S., KVINTOVICS, P.: *Acta Chim. Acad. Sci. Hung.*, **102**, 247 (1979)
- [6] TAN, T. C., LIM, Y. Y.: *Inorg. Chem.*, **12**, 2203 (1973)
- [7] HILL, H. A. O., ROBERTS, R. G., WILLIAMS, D.: *J.C.S. Faraday*, **72**, 1267 (1976)
- [8] EATON, D. R.: *Can. J. Chem.*, **49**, 2751 (1971)
- [9] TAKUZO, F., NOBUJI, K., SATOHIRO, Y., KIMIO, T.: *J.C.S. Dalton*, **1977**, 2030
- [10] QUERESHI, M. S., ROSENTHAL, L., WALKER, I. M.: *J. Coord. Chem.*, **5**, 77 (1976)
- [11] LARSEN, D. W.: *Inorg. Chem.*, **5**, 1109 (1966)
- [12] LA MAR, G. N., FISCHER, R. H., HORROCKS, W. D.: *Inorg. Chem.*, **6**, 1798 (1967)
- [13] FISCHER, R. H., HORROCKS, W. D.: *Inorg. Chem.*, **7**, 2659 (1968)
- [14] BROWN, D. G., DRAGO, R. S.: *J. Am. Chem. Soc.*, **92**, 1871 (1970)
- [15] WALKER, I. M., ROSENTHAL, L., QUERESHI, M. S.: *Inorg. Chem.*, **10**, 2463 (1971)
- [16] ROSENTHAL, L., WALKER, I. M.: *Inorg. Chem.*, **11**, 2444 (1972)
- [17] QUERESHI, M. S., WALKER, I. M.: *Inorg., Chem.*, **13**, 2896 (1974)

László VINCZE }  
Sándor PAPP }

H-8200 Veszprém, Schönherz Z. u. 12.



## OXIDATION OF ALKALI METAL IODATES IN MOLTEN ALKALI METAL NITRATES

M. DRÁTOVSKÝ\*, E. DVOŘÁKOVÁ and Z. RYTIŘ

*(Department of Inorganic Chemistry, Charles University, Praha, Czechoslovakia)*

Received April 27, 1981

Accepted for publication July 29, 1981

Alkali metal iodates  $MIO_3$  ( $M = Li, Na, K$ ) were oxidized in the presence of hydroxides  $MOH$  in molten nitrates  $MNO_3$  with oxygen or ozone. The following products were precipitated at variable  $MOH : MIO_3$  ratios and then separated from the melts and identified after purification with liquid ammonia:  $Li_5IO_6$ ,  $Na_4IO_5$ ,  $Na_5IO_6$ ,  $K_2IO_4$ ,  $K_3IO_5$ . Two of these substances,  $Na_4IO_5$  and  $K_2IO_4$  contain formally hexavalent iodine and were studied by X-ray powder method, IR spectroscopy and measurements of the magnetic susceptibility. Their thermodynamic stability was also investigated. Periodates  $Na_5IO_6$  and  $K_3IO_5$  have been prepared for the first time from a homogeneous mixture by precipitation with an oxidizing agent.

### Introduction

The existence of products having an average oxidation number of iodine + VI was observed by DRÁTOVSKÝ at the thermal decomposition of some types of periodates (especially  $M_2^I H_3 IO_6$  and  $M_2^{II} I_2 O_9 \cdot xH_2O$ ) and has been reported in the literature [1–6]. Composition of such products corresponds mostly to the formula  $M_2^I IO_4$  and  $M^{II} IO_4$ . Some of these products were paramagnetic, the paramagnetism was, however, caused by adsorbed molecular oxygen (*i.e.*  $M_2^I IO_4 \cdot xO_2$  and  $M^{II} IO_4 \cdot xO_2$ ) [7]. The products either did not exhibit any X-ray diffraction lines at all, or their diffraction lines corresponded to those of iodates of the same metal, so that their chemical individuality could not be proved by X-ray diffraction method. The materials mentioned were decomposed by water into a mixture of iodates and periodates and therefore could not be prepared in a crystalline form from an aqueous medium.

Also the thermogravimetric study of the thermal decomposition of the corresponding periodates did not give any proof on the thermodynamic stability of products with hexavalent iodine. The record with a plateau corresponding to these products was obtained only at increasing temperature, the products, however were not stable at constant temperature, at which they arose [7].

For this reason experiments were performed with the effort to gain the products containing  $I^{VI}$  from a homogeneous medium of molten salts by

\* To whom correspondence should be addressed

oxidation of iodates, and to reveal their thermodynamic stability, and prepare them in a crystalline form. Our attention was directed especially to the salts of alkali metals because of the relatively low melting points of the alkali metal nitrates.

Beside products of  $I^{VI}$  also anhydrous periodates can be formed by oxidation of iodates in the medium of molten nitrates. Following anhydrous periodates of Li, Na and K are known:  $LiIO_4$ ,  $Li_5IO_6$ ,  $NaIO_4$ ,  $Na_5IO_6$ ,  $KIO_4$ ,  $K_4I_2O_9$  and  $K_3IO_5$  [8].

## Experimental

### *Chemicals and analytical methods*

All chemicals were of A. R. grade. Periodates not available were prepared according to the literature [8–11].

The iodine content of the compounds was determined by argentometric titration after reducing them to iodide. Potentiometric indication was used. The oxidation number of iodine was determined iodometrically.

Alkali metals were determined gravimetrically as chlorides or sulfates. Sodium and potassium were determined also by the AAS method (Varian Techtron).

Nitrates were reduced to ammonia and then determined by the distillation method. Traces of nitrates were also identified by IR spectroscopy.

### *Physical measurements*

X-ray powder diagrams were taken on a Mikrometa equipment with a Chirana chamber ( $\varnothing$  57.3 mm).  $CuK\alpha$  radiation ( $\lambda = 154.18$  pm) was passed through a nickel foil filter.

Infra-red spectra were run on a double beam IR spectrophotometer UR 20 (Carl Zeiss, Jena) within  $40-400$   $mm^{-1}$  in a nujol suspension. Magnetic susceptibility was measured by the FARADAY method on a magnetic balance constructed according to the TERRY principle [12].

## Results and Discussion

The oxidation of alkali metal iodates was carried out in molten nitrates of the corresponding alkali metals. It has been found that the nitrates are sufficiently stable at the temperature of preparation and do not decompose to nitrites. The following results have been obtained by the study of the solubility of iodates and periodates in molten nitrates:

1. Iodates  $LiIO_3$ ,  $NaIO_3$  and  $KIO_3$  are sufficiently soluble in molten nitrates. By the addition of the corresponding hydroxide the solubility of  $NaIO_3$  and  $KIO_3$  decreases, and that of  $LiIO_3$  increases until a limit value (Table I).

2. Periodates  $MIO_4$  are decomposed in molten nitrates into iodates and oxygen. Periodate  $K_4I_2O_9$  is also decomposed under oxygen evolution.

3. Periodates  $Li_5IO_6$ ,  $Na_5IO_6$  and  $K_3IO_5$  are insoluble and do not decompose in the corresponding molten nitrates.

4. From the mixtures of iodates and periodates ( $Li_5IO_6 + LiIO_3$ ;  $Na_5IO_6 + NaIO_3$ ;  $K_3IO_5 + KIO_3$ ) the iodates are dissolved while the periodates remain insoluble in the melt.

Table I

Solubility of iodates  $\text{MIO}_3$ , in molten nitrates,  $\text{MNO}_3$ , in per cent, in dependence of the molar ratio  $\text{MOH} : \text{MIO}_3$  ( $\text{M} = \text{Li, Na, K}$ )

Substance	Ratio $\text{MOH} : \text{MIO}_3$				
	0	1 : 10	1 : 5	1 : 2	1 : 1
$\text{LiIO}_3$	5.5	11.9	13.5	14.0	14.0
$\text{NaIO}_3$	40.5	27.7	24.7	22.7	21.7
$\text{KIO}_3$	22.3	14.0	13.0	12.4	12.0

The oxidations of iodates,  $\text{MIO}_3$ , in molten nitrates,  $\text{MNO}_3$ , were carried out in the presence of hydroxides  $\text{MOH}$  under the following conditions:

	Li	Na	K
Temperature range (K)	545—550	590—603	623—643
Range of molar ratios $\text{MOH} : \text{MIO}_3$	0.3—7.0	1.0—7.0	0.2—7.0

Both oxidizing agents, oxygen and ozone, were used with the same result. During the course of oxidation precipitates appeared at the following molar ratios  $\text{MOH} : \text{MIO}_3 = 1.0$  and higher for  $\text{M} = \text{Li}$ , and at all ratios used for  $\text{M} = \text{Na, K}$ . Dependences of the average oxidation number of iodine in the precipitations on the  $\text{MOH} : \text{MIO}_3$  ratio are illustrated in Fig. 1.

All the precipitates were separated from the melts by sedimentation during heating. Despite this separation, precipitates were considerably contaminated with nitrates. To remove nitrates, some of the precipitates were

Table II

Analyses of substances obtained by the oxidation of iodates,  $\text{MIO}_3$

Substance	% $\text{O}_A^+$		% I		% M	
	found	calc.	found	calc.	found	calc.
$\text{Li}_5\text{IO}_6$	21.60	21.71	49.10	49.22	13.48	13.57
$\text{Na}_4\text{IO}_5$	16.01	16.05	42.61	42.47	29.92	30.77
$\text{Na}_5\text{IO}_6$	16.56	16.57	37.45	37.57	34.15	34.02
$\text{K}_2\text{IO}_4$	17.40	17.84	46.05	47.21	28.77	29.00
$\text{K}_3\text{IO}_5$	17.25	17.28	39.19	39.20	36.16	36.11

<sup>+</sup>  $\text{O}_A$  — the active oxygen determined iodometrically and corresponding to the oxidation number of iodine ( $\text{IV}^{\text{II}} : \text{O}_A = 1 : 3.5$ ,  $\text{IV}^{\text{I}} : \text{O}_A = 1 : 3.0$ ,  $\text{IV} : \text{O}_A = 1 : 2.5$ )

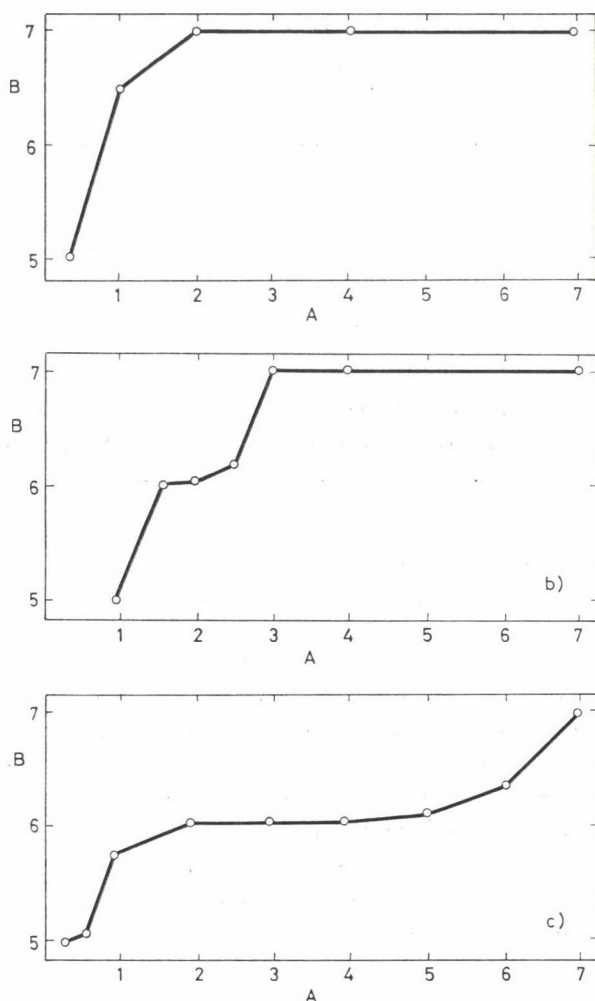


Fig. 1. Dependence of the oxidation number of iodine (B) on the MOH : MIO<sub>3</sub> molar ratio (A).  
a) M = Li, b) M = Na, c) M = K

washed with liquid ammonia (dried over sodium) either at laboratory temperature and high pressure (0.85 MPa) in sealed ampules, or at normal pressure and low temperature (b.p. of ammonia). Some samples containing Li<sub>5</sub>IO<sub>6</sub> were washed with water. The washed substances were then analysed (Table II).

The following conclusions can be made from the data obtained:

1. Li<sub>5</sub>IO<sub>6</sub> periodate is formed by the oxidation of the iodate LiIO<sub>3</sub> at LiOH : LiIO<sub>3</sub> ratios >1.
2. The oxidation of NaIO<sub>3</sub> gives Na<sub>4</sub>IO<sub>5</sub> containing formally hexavalent iodine at NaOH : NaIO<sub>3</sub> ratios between 1.5 and 2.5, while the periodate, Na<sub>5</sub>IO<sub>6</sub>, is formed at NaOH : NaIO<sub>3</sub> ratios >3.

3. By the oxidation of  $\text{KIO}_3$ ,  $\text{K}_2\text{IO}_4$  is formed containing formally hexavalent iodine at  $\text{KOH} : \text{KIO}_3$  ratios between 1.5 and 4.5, while periodate  $\text{K}_3\text{IO}_5$  is formed at  $\text{KOH} : \text{KIO}_3$  ratios  $>6$ .

The mentioned periodates were identified roentgenographically. The X-ray diffraction patterns of the product  $\text{Na}_4\text{IO}_5$  and  $\text{K}_2\text{IO}_4$  were characterized before washing with ammonia (*i.e.* contaminated with about 50% of nitrate) by distinct diffraction lines, which did not belong to nitrate, iodate and periodate. After washing off nitrates with ammonia the diffraction lines became diffuse in case of  $\text{Na}_4\text{IO}_5$  and changed in case of  $\text{K}_2\text{IO}_4$ . The latter product exhibited — after washing — the diffraction lines of  $\text{KIO}_3$ . A similar phenomenon was observed several years ago [1, 3] with  $\text{M}_2\text{IO}_4$  arising by the thermal decomposition of periodates  $\text{M}_2\text{H}_3\text{IO}_6$  ( $\text{M} = \text{Li}$  or  $\text{Na}$ ). X-ray diffraction lines are presented in Tables III and IV.

All the products studied — periodates as well as products with hexavalent iodine — were diamagnetic. Such behaviour does not correspond to the assumption of one unpaired electron of hexavalent iodine, as is (probably incorrectly) claimed by SANYAL and NAG [13]. It is however difficult to explain such a contradiction, because an assumption of polymeric anions containing pentavalent and heptavalent iodine atoms fails too. In such polymeric anions such a high oxygen to iodine ratio cannot be assumed as is required by the formula  $\text{IO}_4^{2-}$  and  $\text{IO}_5^{4-}$ .

An attempt has been made to solve the structure of the products with formally hexavalent iodine by means of their IR spectra. This method has been used also as a tool for the identification of traces of  $\text{NO}_3^-$  in the products studied. Table V presents results of these measurements. Observed bands corresponding to  $\text{O—I—O}$  or  $\text{I—O—I}$  and to  $\text{I—O}$  vibrations cannot be assigned to tetrahedric structure of supposed anion  $\text{IO}_4^{2-}$ . Frequencies of the

Table III

*X-ray diffraction lines of  $\text{K}_2\text{IO}_4$  before washing with liquid ammonia*

<i>I</i>	<i>d</i> (pm)	<i>I</i>	<i>d</i> (pm)	<i>I</i>	<i>d</i> (pm)
7	444	7	218	2	152.3
3	404	4	204.9	1	149.7
10	375	5	193.3	1	140.6
4	316	2	183.4	3	135.9
7	300	1	178.4	1	132.6
4	274	2	168.6	2	125.1
9	264	1	163.4	2	119.4
2	233	1	158.0		

**Table IV**  
*X-ray diffraction lines of Na<sub>4</sub>IO<sub>5</sub>*  
 a) before — b) after washing with liquid ammonia

a)		b)			
<i>I</i>	<i>d</i> (pm)	<i>I</i>	<i>d</i> (pm)	<i>I</i>	<i>d</i> (pm)
6	495	6	140.9	6	498
8	427	5	135.6	10	435
10	305	1	130.1	3	338
8	272	1	122.6	3	318
5	253	3	117.6	9	294
10	243	1	108.2	7	274
5	212	3	105.2	4	248
7	189.2	2	95.9	5	235
2	179.4	1	90.8	1	213
9	166.1	5	79.3	2	189.2
				2	183.4
				3	178.7
				8	166.7
				1	148.0

**Table V**  
*Assignments of absorption bands in the IR spectra*  
*of K<sub>2</sub>IO<sub>4</sub> contaminated with 2.0% KNO<sub>3</sub>*

Frequency (mm <sup>-1</sup> )	Vibration type
42.0 (s)	$\delta(\text{IO}_2)$ , resp. (I—O—I)
61.5 (m)	$\nu(\text{I—O})$
66.5 (w)	$\nu(\text{I—O})$
72.0 (w)	(nujol) + $\delta(\text{NO}_3^-)$
76.5 (vs)	$\nu(\text{I—O})$
81.0 (w)	$\pi(\text{NO}_3^-)$
138.0 (m)	(nujol) + $\nu(\text{NO}_3^-)$
147.0 (m)	(nujol)

absorption bands of K<sub>2</sub>IO<sub>4</sub> correspond to the broad absorption band (42.5—80.0 mm<sup>-1</sup>), observed earlier [14] at Na<sub>2</sub>IO<sub>4</sub> prepared by the thermal decomposition of Na<sub>2</sub>H<sub>3</sub>IO<sub>6</sub>. In the case of our product K<sub>2</sub>IO<sub>4</sub> the broad absorption band is splitted into 4 sharper bands.

## REFERENCES

- [1] DRÁTOVSKÝ, M.: Russ. J. Inorg. Chem., **8**, 1792 (1963)
- [2] DRÁTOVSKÝ, M.: Russ. J. Inorg. Chem., **8**, 2434 (1963)
- [3] DRÁTOVSKÝ, M.: Coll. Czech. Chem. Commun., **29**, 579 (1964)
- [4] DRÁTOVSKÝ, M.: Coll. Czech. Chem. Commun., **29**, 1710 (1964)
- [5] DRÁTOVSKÝ, M.: Z. Anorg. Allg. Chem., **334**, 169 (1964)
- [6] DRÁTOVSKÝ, M., MATĚJČKOVÁ, J.: Chemické zvesti, **19**, 604 (1965)
- [7] JULÁK, J.: Coll. Czech. Chem. Commun., **37**, 1247 (1972)
- [8] SIEBERT, H.: Fortschr. Chem. Forsch., **8**, 470 (1967)
- [9] HESSABY, H., SOUCHAY, P.: Bull. Soc. Chim. France, **20**, 606 (1953)
- [10] ZINTL, E., MORAWIETZ, W.: Z. Anorg. Allg. Chem., **236**, 372 (1938)
- [11] SCHOLDER, R., HUPPERT, K. L.: Z. Anorg. Allg. Chem., **334**, 209 (1964)
- [12] VILÍM, F.: Českoslov. čas. fyz., **5**, 416 (1955)
- [13] SANYAL, G. S., NAG, K.: J. Inorg. Nucl. Chem., **39**, 1127 (1977)
- [14] DRÁTOVSKÝ, M., KOŽÍŠEK, V., STRAUCH, B.: Coll. Czech. Chem. Commun., **32**, 3977 (1967)

Milan DRÁTOVSKÝ      ČSSR, 128 40 Praha 2, Albertov 2030, Dept. of Inorg.  
Chemistry, Charles University

Eliška DVOŘÁKOVÁ      ČSSR, 130 00 Praha 3, Kouřimská Research Institute  
of Pharmacy and Biochemistry

Zdeněk RYTÍŘ      ČSSR, 400 11 Ústí nad Labem, Dzeržinského 26 Spolek  
pro chemickou a hutní výrobu, n.p.



## X-RAY STUDY OF THE LATTICE PARAMETERS OF THE FOUR DICHLORO-*N*-SULFINYLANILINE ISOMERS

Z. CZERWIEC\* and Z. MANDECKI

*(Department of Chemistry and Solid State Physics, Pedagogical University, Czestochowa, Poland)*

Received April 27, 1981

In revised form July 14, 1981

Accepted for publication July 29, 1981

Studies on isomers of dichloro-*N*-sulfinylanilines were made by the use of X-ray powder diffractometry. Interplanar spacings, Miller indices and relative intensities were calculated for 2,3-, 2,4-, 2,5- and 2,6-dichloro-*N*-sulfinylanilines. All of them were hexagonal. The lattice parameters *a* and *c* were calculated.

Recently, the structure of some aromatic *N*-sulfinylamines has been studied [1, 2, 3], however, the crystal structure type was not determined. The aromatic *N*-sulfinylamines Ar-N=S=O, are liquids or low-melting crystalline substances [4], which are very susceptible to moisture, in the presence of which they are subjected to hydrolysis to form the amines and SO<sub>2</sub>. The study of the crystal structure of isomeric dichloro-*N*-sulfinylanilines seemed to be useful as an addition to configurational investigations of these compounds.

### Experimental

#### *Equipment and parameters*

Manganese filter designed to eliminate the K<sub>β</sub> radiation; anode voltage of the X-ray tube  $V_a \approx 35$  kV; plate current  $J_a = 6$  mA; electronic computer measurement range 400 imp/sec; goniometer radius 180 mm; speed of the counter travel 2°/min; recorder tape feed rate 0.5 mm/s; temperature 20° ± 1 °C; silica glass cells.

#### *Sample preparation*

2,3-, 2,4-, 2,5- and 2,6-dichloro-*N*-sulfinylanilines were investigated. The compounds were synthesized according to MICHAELIS [5]. Their purity level was checked by gas chromatography before and after the measurement [6]. The crystalline substances were powdered to obtain a grain size of 100–300 μm and were introduced into the silica glass cell, which was fixed in a goniometric attachment. The thermal stability was also examined.

#### *Measurements*

The study was made by the Debye-Scherrer method using a "DRON-2.0" X-ray diffractometer equipment with a scintillation counter. Since the peaks occurred at small angles 2θ, Mn-filtered Fe K<sub>α</sub> radiation was used. The focussing was done by the Bragg-Brentano method. The slit used was 2, 4, 0.25. The Soller slit divergence was 2.5°. The mean

\* To whom correspondence should be addressed

Table I

*Relative intensity of diffraction lines and interplanar of 2,3-dichloro-N-sulfinylaniline*

Line number	Relative intensity $I/I_{\max}$ (%)	Interplanar spacings $d_{hkl}$ (pm)	Miller indices		
			<i>h</i>	<i>k</i>	<i>l</i>
1	50	908.5	2	0	1
2	50	886.9	1	1	2
3	52	731.4	1	1	3
4	58	707.4	1	2	0
5	80	496.9	0	0	6
6	20	467.8	4	0	0
7	22	454.7	1	1	6
8	17	410.4	3	2	2
9	15	397.8	1	1	7
10	15	390.0	2	0	7
11	16	379.7	4	1	3
12	76	364.7	2	1	7
13	13	357.9	3	3	1
14	100	352.9	3	0	7
15	41	340.8	3	1	7
16	53	324.4	3	3	4
17	21	318.2	5	1	3
18	12	313.4	2	0	9
19	29	302.5	3	2	7
20	33	294.5	4	1	7
21	51	288.7	4	2	6
22	26	282.5	3	2	8
23	45	280.2	6	1	2
24	24	269.3	4	4	3
25	7	263.9	4	4	4
26	6	259.9	5	1	8
27	6	247.9	7	1	10
28	15	243.0	2	2	11
29	12	239.3	6	0	8
30	14	227.0	6	0	9
31	10	223.6	5	1	10
32	18	208.3	7	0	9
33	7	205.1	8	0	7
34	6	202.4	7	3	4
35	8	193.7	7	4	1
36	8	187.3	5	5	8

**Table II**  
*Relative intensity of diffraction lines and interplanar spacings of 2,4-dichloro-N-sulfinylaniline*

Line number	Relative intensity $I/I_{\max}$ (%)	Interplanar spacings $d_{hkl}$ (pm)	Miller indices		
			<i>h</i>	<i>k</i>	<i>l</i>
1	4	1003.3	2	1	0
2	6	744.0	3	1	0
3	5	690.8	3	1	1
4	4	581.4	4	1	0
5	6	542.7	1	1	3
6	40	504.9	2	1	3
7	32	468.5	2	2	3
8	16	454.7	5	0	2
9	13	441.9	3	3	2
10	100	422.6	3	2	3
11	60	393.2	5	0	3
12	7	380.4	2	2	4
13	42	373.7	4	4	1
14	25	346.1	7	1	1
15	10	339.2	6	2	2
16	15	336.8	5	0	4
17	29	332.9	6	3	1
18	22	314.9	—	—	—
19	6	305.9	8	1	1
20	8	292.7	8	1	2
21	7	283.7	7	2	3
22	22	272.6	3	1	6
23	34	270.4	6	4	3
24	5	255.1	6	2	5
25	16	251.1	6	5	3
26	23	244.5	5	4	5
27	4	234.8	4	0	7
28	4	232.7	4	4	6
29	13	186.9	8	4	6
30	3	178.7	5	5	8
31	3	173.2	2	1	10
32	2	152.2	6	4	10
33	2	149.4	8	7	8

wave length was assumed to be  $\lambda = 193.728$  pm. The measurement was carried out with a GUR-5 type goniometer and a GP-4 attachment. The calculations were done using a MERA-217 type computer.

### Results and Discussion

Based on the results obtained from X-ray powder diffractometry the angular position of each diffraction line was measured. Interplanar spacings,  $d_{hkl}$ , which fulfill BRAGG's conditions were calculated [8]. The intensities were taken equal to the height of the diffraction lines (Figs 1, 2). It was found that all four compounds, *i.e.* 2,3-, 2,4-, 2,5- and 2,6-dichloro-*N*-sulfinylaniline, crystallized in the hexagonal system. The result of indexing which was done by the analytical method is a proof for the inherence of hexagonal system.

Table III

Relative intensity of diffraction lines and interplanar spacings of 2,5-dichloro-*N*-sulfinylaniline

Line number	Relative intensity $I/I_{\max}$ (%)	Interplanar spacings $d_{hkl}$ (pm)	Miller indices		
			<i>h</i>	<i>k</i>	<i>l</i>
1	27	663.8	1	0	2
2	1	519.3	1	1	1
3	100	470.9	0	2	0
4	1	417.6	0	2	2
5	1	371.8	0	2	3
6	13	359.7	0	0	5
7	37	331.3	2	1	2
8	19	325.7	0	2	4
9	1	313.4	0	3	0
10	29	297.5	0	3	2
11	18	259.7	3	1	1

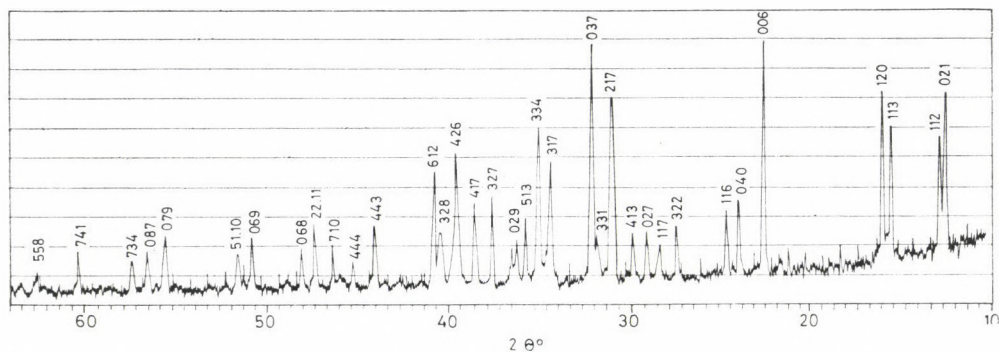


Fig. 1. Diffractogram of 2,3-dichloro-*N*-sulfinylaniline

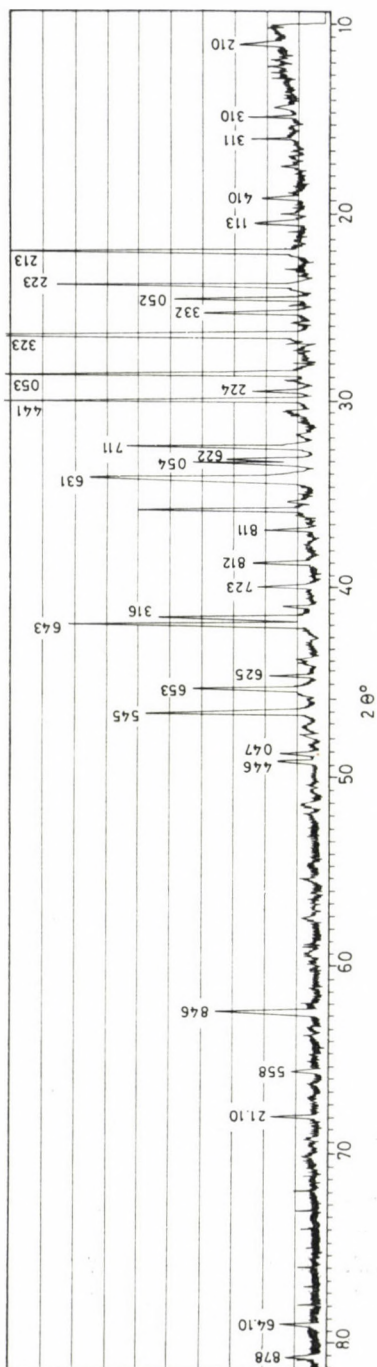


Fig. 2. Diffractogram of 2,4-dichloro-N-sulfinylamine

Table IV

Relative intensity of diffraction lines and interplanar spacings of 2,6-dichloro-*N*-sulfinylaniline

Line number	Relative intensity $I/I_{\max}$ (%)	Interplanar spacings $d_{hkl}$ (pm)	Miller indices		
			<i>h</i>	<i>k</i>	<i>l</i>
1	23	716.4	2	0	0
2	21	681.6	0	0	2
3	33	615.8	1	0	2
4	19	495.6	2	0	2
5	14	402.9	1	1	3
6	18	393.5	3	0	2
7	100	360.4	4	0	0
8	33	343.6	3	1	2
9	80	333.9	1	0	4
10	14	329.9	3	0	3
11	14	309.8	2	0	4
12	63	279.8	5	0	1
13	7	266.8	4	2	1
14	6	249.2	4	0	4
15	12	243.3	2	1	5
16	20	241.1	5	1	2
17	8	226.2	3	1	5
18	8	218.6	6	1	0
19	6	206.9	4	4	0
20	8	180.8	6	3	0
21	8	177.3	5	4	2

Table V

Lattice parameters of 2,3-, 2,4-, 2,5- and 2,6-dichloro-*N*-sulfinylanilines

Dichloro- <i>N</i> -sulfinylaniline	Lattice parameters	
	<i>a</i> (pm)	<i>c</i> (pm)
2,3-dichloro- <i>N</i> -sulfinylaniline	2157.7	2992.1
2,4-dichloro- <i>N</i> -sulfinylaniline	3069.4	1756.4
2,5-dichloro- <i>N</i> -sulfinylaniline	1091.8	1787.6
2,6-dichloro- <i>N</i> -sulfinylaniline	1656.3	1369.0

The said indexing was done for each diffraction line which is characteristic for this lattice type [9]. The results obtained are shown in Tables I, II III and IV. Using the first approximation method [7, 8], parameters  $a$  and  $c$  of the unit cell of the hexagonal lattice of the dichloro-*N*-sulfinylanilines studied have been calculated (Table V).

\*

The authors wish to thank doc. dr. W. LENKOW, Head of the Solid-State Physics Department, Pedagogical University at Czestochowa, for his help in making it possible to do the measurements and for his valuable comments.

#### REFERENCES

- [1] JANNELLI, L., LAMANNA, U., LUMBRISO, H.: *Bull. Soc. Chim. Fr.*, **1966**, 3626
- [2] WOERDEN, H. F., BIJE-VLIEGER, S. H.: *Rec. Trav Chim. Pays-Bas Belg.*, **93**, 85 (197)
- [3] CZERWIEC, Z., MIREK, J.: *Zesz. Nauk. Univ. Jagiellon. Pr. Chem.*, **18**, 183 (1973)
- [4] CZERWIEC, Z.: *J. Thermal Anal.*, **10**, 441 (1976)
- [5] MICHAELIS, A., HERZ, R.: *Ber.*, **23**, 348 (1890)
- [6] CZERWIEC, Z.: *J. Chromatogr.*, **139**, 180 (1977)
- [7] CULLITY, B. D.: *Elements of X-ray Diffraction*. Addison-Wesley Publishing Company Inc. London 1959
- [8] LIPSON, H., STEEPLE, H.: *Interpretation of X-ray Powder Diffraction Patterns*. MacMillan, London—St. Mortins Press, New York 1970
- [9] NEDOMA, J.: *Wskaznikowanie rentgenogramów proszkowych substancji tetragonalnych i heksagonalnych*, 1973, Warszawa, Poland

Z. CZERWIEC } Pedagogical University, Department of Chemistry, Al.  
Z. MANDECKI } Zawadzkiego 13/15, 42—200 Czestochowa, Poland



## VOLTAMETRIC DETERMINATION OF THE DISSOCIATION CONSTANT OF GLYCOLALDEHYDE AND DL-GLYCERALDEHYDE BISULPHITES

S. BALOGH<sup>1\*</sup>, GY. FARSANG<sup>2</sup> and L. MAROS<sup>2</sup>

(<sup>1</sup>REANAL Fine Chemical Works, Budapest, <sup>2</sup>Institute of Inorganic and Analytical Chemistry of Eötvös Loránd University, Budapest)

Received May 18, 1981

Accepted for publication July 29, 1981

A voltametric method (chronoamperometry with linearly changing potential at carbon paste electrode) has been worked out for the determination of the concentration of bisulphite ion in dissociation equilibria with glycolaldehyde and DL-glyceraldehyde bisulphites. The method is based on the distinct oxidation voltametric wave of the  $\text{HSO}_3^-$  ion at pH 4–5 buffered aqueous media. The oxidation results in an irreversible chronoamperometric wave, the oxidation product is sulphate.

The systematic error observed at the titrimetric determination of different monomer as well as dimer hydroxyaldehydes stable in their cyclic half-acetal forms, is mainly due to the stability of their bisulphites, when hydrogensulphite is added for their volumetric determination [1, 2].

According to KERP the aldehyde bisulphites decompose according to the following equation [3]:



Knowing the equilibrium concentration values, the dissociation constant can be written:

$$K_d = \frac{[\text{A}]_e [\text{B}]_e}{[\text{AB}]_e} \quad (1)$$

where

$[\text{AB}]_e$  is the concentration of aldehyde bisulphite

$[\text{A}]_e$  is the concentration of dissociated aldehyde and

$[\text{B}]_e$  is the concentration of dissociated hydrogen bisulphite in equilibrium.

In the knowledge of the total concentration of the aldehyde bisulphite in the solution investigated  $[\text{AB}]_T$ ,  $K_d$  can be calculated according to the following equation:

$$K_d = \frac{[\text{B}]_e^2}{[\text{AB}]_T - [\text{B}]_e} \quad (2)$$

\* To whom correspondence should be addressed

Consequently either the  $[A]_e$  or  $[B]_e$  concentration should be determined in the solutions of different known  $[AB]_T$  concentrations in order to calculate the  $K_d$  value of a given aldehyde bisulphite by using equation 2.

The stability of aldehyde bisulphites is strongly influenced by the pH of the solution [2, 4]. In strongly acidic or basic solutions their decomposition is fast. According to our investigations the decomposition of the glycolaldehyde

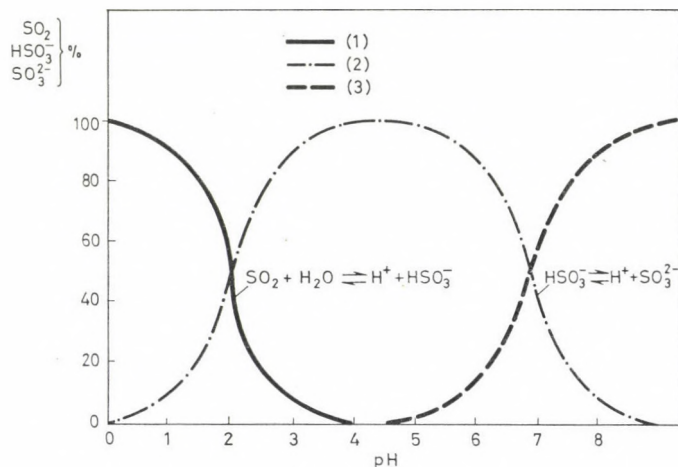


Fig. 1. The percentage distribution of different equilibrium species of  $\text{SO}_2\text{-H}_2\text{O}$  system as a function of pH. (1):  $\text{SO}_2$ , (2):  $\text{HSO}_3^-$ , (3):  $\text{SO}_3^{2-}$

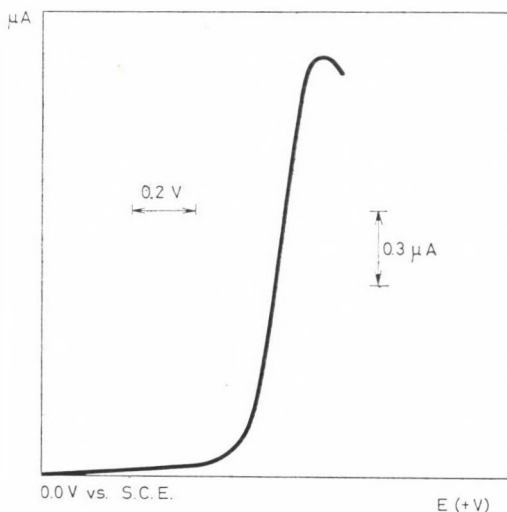


Fig. 2. The oxidation chronoamperometric curve of free bisulphite formed by the dissociation of glycolaldehyde bisulphite. Glycolaldehyde bisulphite concentration:  $1 \times 10^{-4}$  M/dm<sup>3</sup>. Base electrolyte: 0.2 M sodium acetate — acetic acid buffer, pH = 4.6

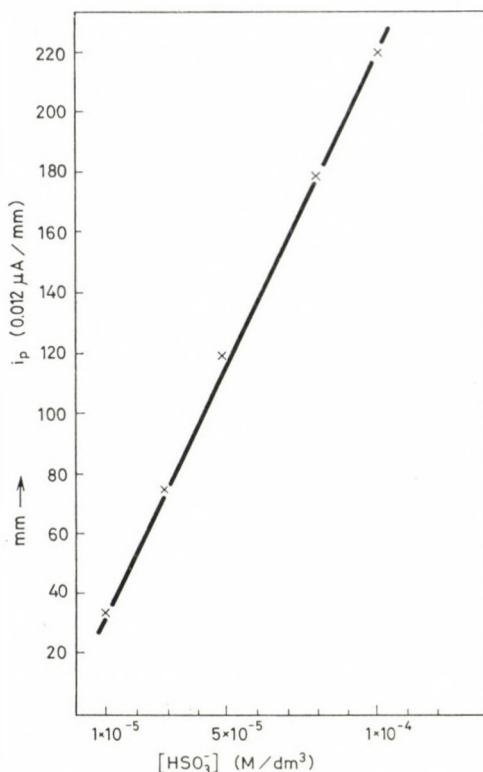


Fig. 3. A plotted calibration curve taken by recording the chronoamperometric oxidation curves of known concentrations of  $\text{HSO}_3^-$ . Base electrolyte: 0.2 M sodium acetate — acetic acid buffer, pH = 4.6

and DL-glyceraldehyde bisulphites is very slow in aqueous solutions of pH 4–5. Under such conditions the only stable species of the pH dependent forms of  $\text{HSO}_3^-$  ion, as it can be seen in Fig. 1, is the  $\text{HSO}_3^-$  ion and its pH dependent equilibria can be neglected.

For the accurate measurement of  $\text{HSO}_3^-$  arising from the dissociation of aldehyde bisulphite, the various titrimetric methods are less applicable because of the danger of shifting of the equilibrium during the titration process [3, 5]. This was the reason that a voltametric method has been worked out for the determination of the concentration of  $\text{HSO}_3^-$ . The basis of the determination is that the bisulphite bonded in the aldehyde bisulphite can be oxidized only at higher positive potential than the free hydrogensulphite species.

The latter ones in pH 4–5 aqueous solutions give a well-developed voltametric wave at the carbon paste electrode, which is well-separated from the oxidation current of aldehyde bisulphite. The study of the voltametric behaviour of  $\text{HSO}_3^-$  at pH 4–5 shows an irreversible two-electron oxidation process at C.P.E. resulting sulphate ion as an oxidation product.

In the experiments a carbon paste electrode prepared with silicone oil has been used [6].

The oxidation current-voltage curve can be recorded either using a rotated carbon paste disc electrode or chronoamperometry with linearly changing potential.

It is interesting to note that after each recording the electrode surface must be removed otherwise a rather serious filming effect is observed in the pH range used.

During the experimental work it was proved that the dissociation rate of both aldehyde bisulphites investigated is very low compared to the rate of polarization used and accordingly the real equilibrium concentrations can be determined. The current is diffusion controlled and is not affected by the dissociation kinetics. This was proved by checking the current peak dependence on the square root of the polarization rate and this function remained linear at as low as 0.4 V/min polarization rate.

A typical linear chronoamperometric curve recorded in a solution containing dissociated free bisulphite is shown in Fig. 2.

The equilibrium free bisulphite concentrations were determined by plotting a calibration curve, and its points in buffered NaHSO<sub>3</sub> solutions; see Fig. 3.

The applied polarization rate for each recorded curves was 0.8 V/min. The measured  $K_d$  resp. pK values at  $25 \pm 0.5$  °C are summarized in Tables I and II.

The systematic error of the volumetric determination based on bisulphite addition of the relatively stable solids of dimer hydroxyaldehydes is determined not solely by the stability of their bisulphite derivates but that of their cyclic

**Table I**  
*Glycolaldehyde bisulphite*

$[AB]_T$ (M/dm <sup>3</sup> )	$K_d$ $t = 25$ °C	pK
$5.0 \times 10^{-5}$	$1.24 \times 10^{-5}$	4.90
$1.0 \times 10^{-4}$	$1.48 \times 10^{-5}$	4.82
$5.0 \times 10^{-4}$	$7.39 \times 10^{-6}$	5.13
$1.0 \times 10^{-3}$	$5.25 \times 10^{-6}$	5.28
$2.0 \times 10^{-3}$	$1.56 \times 10^{-5}$	4.80
$5.0 \times 10^{-3}$	$1.42 \times 10^{-5}$	4.84
$1.0 \times 10^{-2}$	$1.54 \times 10^{-5}$	4.81

$$K_{d\text{mean}} = 1.15 \times 10^{-5} \quad pK_{\text{mean}} = 4.94$$

$$K_s = 3.71 \times 10^4 \quad \text{stdev.} = 0.18$$

**Table II**  
DL-Glyceraldehyde bisulphite

[AB] <sub>T</sub> (M/dm <sup>3</sup> )	K <sub>d</sub> t = 25 °C	pK
5.0 × 10 <sup>-5</sup>	1.82 × 10 <sup>-5</sup>	4.73
1.0 × 10 <sup>-4</sup>	2.87 × 10 <sup>-5</sup>	4.54
2.5 × 10 <sup>-4</sup>	2.16 × 10 <sup>-5</sup>	4.66
5.0 × 10 <sup>-4</sup>	4.57 × 10 <sup>-5</sup>	4.34
1.0 × 10 <sup>-3</sup>	6.20 × 10 <sup>-5</sup>	4.21
2.0 × 10 <sup>-3</sup>	5.07 × 10 <sup>-5</sup>	4.29
5.0 × 10 <sup>-3</sup>	5.62 × 10 <sup>-5</sup>	4.25

$$K_{d\text{mean}} = 4.04 \times 10^{-5} \quad pK_{\text{mean}} = 4.39$$

$$K_s = 2.47 \times 10^4 \quad \text{stdev.} = 0.21$$

half acetals, too [7]. The dimer glycolaldehyde in aqueous solution forms a less stable cyclic half acetal than DL-glyceraldehyde. As a consequence of that for example in the case of glycolaldehyde 99% meanwhile in the case of DL-glyceraldehyde only 96% titration degree can be achieved.

The elaborated voltametric method can be applied in a more thorough study of aldehyde-bisulphite equilibrium in aqueous solutions.

## Experimental

### Chemicals

Glycolaldehyde and DL-glyceraldehyde bisulphites were prepared in solid form and purified.

Their composition was checked by volumetric methods [7, 8]. The base electrolyte was prepared in the usual way from *p.a.* chemicals.

The pH values were checked by using Metrohm combined glass electrode, type EA-120X.

The voltametric purity of base electrolyte was checked by recording *i* - *V* curve at C.P.E. at the sensitivity used for the measurements of bisulphites.

All measurements were carried out at 25 ± 0.1 °C in thermostated cells.

### Measuring devices

Radiometer PO-4g type polarograph was used for recording the chronoamperometric *i* - *V* curves at 0.8 V/min polarization rate and Metrohm E-446 type *iR* compensator. At higher polarization rates a Chemtrix SSP-2 Polarographic Analyser System has been used. Carbon paste working electrode was used as described previously [6].

Reference electrode: S.C.E.

Auxiliary electrode: Pt-foil electrode of 1 cm<sup>2</sup> surface.

## REFERENCES

- [1] KOLTHOFF, I. M., STENGER, V. A.: *Volumetric Analysis I*. 218 p. 2. Edit. Intersci. Publ. New York 1942
- [2] SCHULEK, E., MAROS, L.: *Magyar Kém. Folyóirat*, **64**, 480 (1958)
- [3] KERP, W.: *Arb. kais. Gesundh.*, **21**, 180 (1904); *Chem. Zbl.* **II**, 57 (1904)
- [4] STEWART, T. D., DONNALLY, L. H.: *J. Am. Chem. Soc.*, **54**, 2333, 355, 3559 (1932)
- [5] GUBEREVA, M. A.: *Zhurn. Obsch. Khim.*, **17**, 2259 (1947)
- [6] FARSANG, GY.: *Acta Chim. Acad. Sci. Hung.*, **45**, 165 (1965)
- [7] BALOGH, S., KOLOS, E., GÁLL, G., KOLONITS, P.: *Z. Anal. Chem.*, **276**, 201 (1975)
- [8] MAROS, L., PERL-MOLNÁR, I., SCHULEK, E.: *Magyar Kém. Folyóirat*, **66**, 319 (1960)

Sándor BALOGH            H-1441 Budapest, P.O.Box 54.

György FARSANG    }  
László MAROS        } H-1088 Budapest, Múzeum krt. 4/B

## MÖSSBAUER STUDY OF IRON-SUGAR COMPLEXES

M. TONKOVIĆ<sup>1</sup>, S. MUSIĆ<sup>1</sup>, O. HADŽIJA<sup>1</sup>, I. NAGY-CZAKÓ<sup>2</sup> and A. VÉRTES<sup>2\*</sup>

(<sup>1</sup> "Ruder Bosković" Institute, 41001 Zagreb, Yugoslavia, <sup>2</sup> Eötvös Loránd University, Department of Physical Chemistry and Radiology, Budapest)

Received March 16, 1981

Accepted for publication August 5, 1981

The ferric-fructose complex has been prepared using  $\text{FeCl}_3$  and  $\text{Fe}(\text{NO}_3)_3$  solutions. Molecular weight determination and Mössbauer spectroscopic measurements proved that the ferric-fructose complex is polymeric in solid state and also in aqueous solution. The synthesis of a new iron-sorbose complex has been performed. Its Mössbauer spectra indicate a structure similar to that of the iron-fructose complex.

It is known that reducing sugars and polyols form soluble complexes with ferric iron in alkaline media [1]. These complexes may have an important role in the transport of iron across cell membrane and this fact enables wide investigation possibilities. The basis is LAURELL's [2] postulation which implies that iron leaving transferrin ( $\beta_1$ -globulin, transferrin is the major carrier for serum iron under the physiological conditions [3]) goes into various tissues as iron or as a small soluble complex [4]. The experiments have been performed with citrate, sorbital [5], and several carbohydrates and amino acids [6]. Ferric-fructose has been isolated and well-characterized [1] applying different chemical and physicochemical techniques, such as organic microanalysis, electrophoretic mobility, differences in spectral properties [1], ESR, NMR and susceptibility techniques [7]. It has been suggested that iron-fructose complex precipitated with ethanol from aqueous solution has a molecular weight of 594, and that it contained two molecules of fructose and two atoms of iron linked by oxygen bridges [7].

In the present work the ferric-fructose complex has been prepared using  $\text{FeCl}_3$  and  $\text{Fe}(\text{NO}_3)_3$  solutions as substrates. Chemical characterization and Mössbauer spectroscopic interpretation of the structure proposed are presented. In addition the ferric-sorbose complex was prepared as well, and on the basis of chemical characterization and Mössbauer measurements its structure was discussed.

### Experimental

#### Materials

The carbohydrates used were of AnalaR quality. The iron nitrate and iron chloride were of Pro Analyti grade. The other chemicals used were of analytical grade too.

\* To whom correspondence should be addressed

*Methods of preparation*

## a) Reaction of fructose with ferric iron.

The following experimental conditions were used:

1. 0.2 M FeCl<sub>3</sub> (10 mL) was mixed with 2.0 M fructose (10 mL). The pH of the solution was 2.3 and by the addition of NaOH it was adjusted to 9.3. Deep brown solution of the complex was obtained. Ferric-fructose complex was precipitated by the addition of ethanol and isolated by centrifugation. Deep brown precipitate was redissolved in a small volume of water, the pH was again adjusted to 9.3 and the solution made 80% in ethanol, the precipitate was isolated by centrifugation, washed with ethanol, acetone and ether, and dried over P<sub>2</sub>O<sub>5</sub>.

Table I

*Experimental conditions for the preparation of the complexes*

Complex	pH	Molar ratio sugar/iron	Reaction time
Ferric-fructose (FeCl <sub>3</sub> )	9.3	10 : 1	24 h
Ferric-fructose [Fe(NO <sub>3</sub> ) <sub>3</sub> ]	9.3	10 : 1	24 h
Ferric-sorbose (FeCl <sub>3</sub> )	10.5	10 : 1	24 h

2. 0.2 M Fe(NO<sub>3</sub>)<sub>3</sub> (10 mL) was mixed with 2.0 M fructose (10 mL). By the addition of NaOH the pH of the solution was adjusted to 9.3. Deep brown solution was obtained. Complex ferric-fructose was isolated and recrystallized as described above. Yellowish-brown precipitate of ferric-fructose was obtained.

## b) Reaction of sorbose with ferric iron.

0.2 M FeCl<sub>3</sub> (10 mL) was mixed with 2.0 M sorbose (10 mL). The reaction mixture was kept at room temperature for 24 h. By the addition of NaOH the pH of the solution was adjusted to 10.5. Brown complex was precipitated. The isolation and recrystallization of the ferric-sorbose obtained was performed as described above (a. 1).

The experimental conditions used are summarized in Table I.

*Methods of analysis*

## a) Iron.

Iron was analysed by two methods:

- the complex was decomposed by mixed acids and the resulted iron(III) was determined by atomic absorption spectrophotometry
- the complex was burned in oxygen stream and iron was determined in Fe<sub>2</sub>O<sub>3</sub> obtained.

b) Carbon and hydrogen were determined by the standard microanalytical procedure.

c) Sodium was determined from the acid solution (obtained by the acidic decomposition of the complex) using flame spectrophotometry.

d) Nitrogen was determined by the standard Dumas microanalytical procedure.

e) Thin-layer chromatography was performed on silica gel plates (5×10 cm) with *n*-BuOH : acetone : HCl : acetylacetone : H<sub>2</sub>O (60 : 40 : 1 : 0.5 : 20) for about 80 min. Sulphuric acid (10%) and K<sub>4</sub>[Fe(CN)<sub>6</sub>] (2%) sprays were used for the identification of carbohydrates and iron, respectively.

f) Conductivity measurements were performed using a CD-7A conductivity bridge (Tacussel Electronique, France) with a cell constant of 1.304 cm<sup>-1</sup>.

g) Molecular weight determination was performed by comparing elution volumes of the Fe-sugar complexes against elution volumes of the sugar standard molecules of known molecular weights. Molecular sieve of Sephadex type was used in the experiments.

h) Mössbauer spectra were recorded in absorption geometry using a "RANGER ELECTRONICS" Mössbauer spectrometer in conjunction with a multichannel analyser. <sup>57</sup>Co-Pd source of 3.7×10<sup>8</sup> Bq activity was used but the reference material for the isomer shift was α-iron. The Mössbauer spectra of the solid complexes and those of the frozen solutions were recorded at room and liquid nitrogen temperature, respectively. The computer evaluation of the spectra was performed by the least square fitting of the linear combination of Lorentzian curves.

## Results and Discussion

### Chemical part

Evidence for the existence of Fe-sugar complexes has been based on the measurements: its solubility, direct isolation of the water soluble complex, conductometric measurements, chemical elemental microanalysis, thin-layer

**Table II**  
*Elemental analysis of the ferric sugar complexes*

Sample	Complex	% (w/w)				
		C	H	Fe	Na	N
A	Ferric-fructose (FeCl <sub>3</sub> )	27.28	4.96	21.17	3.91	—
B	Ferric-fructose [Fe(NO <sub>3</sub> ) <sub>3</sub> ]	27.18	4.90	21.04	3.51	0.84
C	Ferric-sorbose (FeCl <sub>3</sub> )	27.91	4.65	20.84	4.68	—

chromatographic analysis, molecular weight determinations and Mössbauer studies (separately discussed).

Thin-layer chromatography showed the existence of the compounds containing iron and sugar.  $R_f$  values of the compounds differed from those of the original sugars or iron salts.

The elemental analysis data are presented in Table II.

The conductivity measurements indicate the presence of 1 : 1 electrolytes.

Molecular weight determination was performed by the use of molecular sieves of Sephadex type, suggesting polymer structure of Fe-sugar complexes.

Fe-sugar complexes were eluted on Sephadex G-15 with void volume, what indicates molecular weight greater than 1500.

With Sephadex G-150 and G-200 elution volumes corresponds to molecular weights <10 000. The elution volumes of compounds of known molecular weights were used to determine the molecular weight of Fe-sugar complexes and a value of about 5000 was obtained.

### Mössbauer part

The Mössbauer spectrum of iron-sorbose complex is shown in Fig. 1. The parameters of the solid sugar complexes obtained by the computer evaluation of the Mössbauer spectra are summarized in Table III. They indicate that iron(III) is in the high-spin state [8]. Moreover, these parameters support a dimeric or polymeric structure [9, 10, 11, 12] proposed in the literature [1, 7].

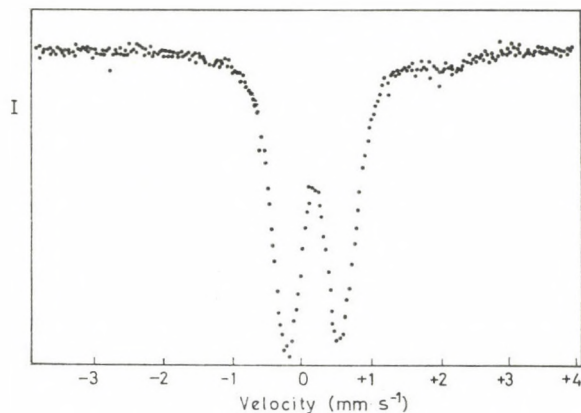


Fig. 1. Mössbauer spectrum of the solid ferric-sorbose complex at room temperature

To get a conclusive proof, we have recorded the Mössbauer spectra of the dilute aqueous solutions (0.02–0.05 *M*) of the iron-sugar complexes. It is known that in high-spin iron(III) salt solutions the Mössbauer study of the paramagnetic spin relaxation can give information about the structure of the dissolved compound [13, 14, 15]. Briefly, the appearance of magnetic hyperfine structure (MHS) on the Mössbauer spectrum depends only on the distance between Fe(III) spins. When Fe(III) ions are far apart, a MHS spectrum will be observed, while on the other hand, when the Fe(III) ions are close together, such as in dimeric iron complexes, the MHS is diminished and a single line or a doublet appears. Thus the Mössbauer spectroscopy can give unambiguous information concerning the mono- or binuclear (or polynuclear) structure of the iron-sugar complex in the solution.

The Mössbauer spectra of the frozen iron-sugar complex solutions measured by us did not show any MHS at liquid nitrogen temperature and this experimental result in accordance with the molecular weight determination proves

Table III

*Mössbauer parameters of the solid iron-sugar complexes at room temperature*

Sample	Complex	$^*\delta_{\text{Fe(III)}}$ $\text{mms}^{-1}$	$\Delta E_{\text{Fe(II)}}$ $\text{mms}^{-1}$	$I_{\text{Fe(III)}}$ $\text{mms}^{-1}$	$\delta_{\text{Fe(II)}}$ $\text{mms}^{-1}$	$\Delta E_{\text{Fe(II)}}$ $\text{mms}^{-1}$	** <i>A</i> %Fe(II)
A	Iron-fructose	0.363	0.770	0.465	1.177	2.387	7.0
B	Iron-fructose	0.367	0.804	0.500	1.161	2.352	4.0
C	Iron-sorbose	0.362	0.789	0.490	1.131	2.294	3.4

\* Values are referred to metallic iron

\*\* *A* is the area of the line as percentage of the whole area  
The uncertainty of the given results is  $\pm 0.005 \text{ mms}^{-1}$

**Table IV**  
*Mössbauer parameters of the frozen iron-sugar complex solutions at liquid nitrogen temperature*

Sample	Complex	$\delta_{\text{Fe(III)}}$ mms <sup>-1</sup>	$\Delta E_{\text{Fe(III)}}$ mms <sup>-1</sup>	$\Gamma_{\text{Fe(III)}}$ mms <sup>-1</sup>
A	Iron-fructose	0.435	0.689	0.472
B	Iron-fructose	0.472	0.788	0.436
C	Iron-sorbose	0.507	0.788	0.450

that in dissolved state the iron-sugar complexes are in polymeric form and hence they are polymeric in solid state, too. The Mössbauer parameters of the frozen solutions are tabulated in Table IV. The changes in the Mössbauer parameters can be attributed to the hydration of the iron(III)-sugar complexes.

In this work the synthesis of a new iron-sorbose complex has been performed. The complex has been characterized by classical chemical methods and Mössbauer spectroscopy. The Mössbauer results indicate a structure similar to that of the iron-fructose complex. The small quantity of iron(II) present is owing to the reducing action of the sugars investigated.

In the paper of AASA *et al.* [7] a suggestion is given that the complex is formed by the replacement of two molecules of water for one molecule of fructose on each side of the iron dimer; the latter being proposed by HEDSTRÖM [16]. The compounds of high molecular weight are probably aggregates of several dimers.

#### REFERENCES

- [1] CHARLEY, P. J., SARKAR, B., STITT, C. F., SALTMAN, P.: *Biochim. Biophys. Acta*, **69**, 313 (1963)
- [2] LAURELL, C. B.: *Blood*, **6**, 183 (1951)
- [3] WALLENIUS, C.: *Scand. J. Clin. & Lab. Invest.*, **4**, 24 (1952)
- [4] CHARLEY, P., ROSENSTEIN, M., SHORE E., SALTMAN, P.: *Arch. Biochem. Biophys.*, **88**, 222 (1960)
- [5] HERNDON, J. F., RICE, E. G., TUCKER, H. G., VAN LOON, E. J., GREENBERG, S. M.: *J. Nutrition*, **64**, 615 (1958)
- [6] FURNIER, P., DUPUIS, Y., SUSBIELLE, H., ALLE, M., TARDY, N.: *J. Physiol.*, **47**, 339 (1955)
- [7] AASA, R., MALSTRÖM, B., SALTMAN, P., VANNGARD, T.: *Biochim. Biophys. Acta*, **88**, 430 (1964)
- [8] VÉRTES, A., KORECZ, L., BURGER, K.: *Mössbauer Spectroscopy*, Elsevier, Amsterdam 1979
- [9] WROBLENSKI, J. T., BROWN, D. B.: *Inorg. Chim. Acta*, **35**, 109 (1979)
- [10] STEIN, G. E., MARINSKY, J. A.: *J. Inorg. Nucl. Chem.*, **37**, 2421 (1975)
- [11] REIF, W. M., BAKER, W. A. JR., ERICKSON, N. E.: *J. Am. Chem. Soc.*, **90**, 4794 (1968)
- [12] REIF, W. M., LONG, G. J., BAKER, W. A. JR.: *J. Am. Chem. Soc.*, **90**, 6347 (1968)
- [13] VÉRTES, A., PARAK, F.: *J. Chem. Soc.*, **1972**, 2062; *MTA Kémiai Közlemények*, **36**, 429 (1971)

- [14] PLATCHINDA, A. S., KOMOR, M., VÉRTES, A.: J. Radioanal. Chem., **10**, 89 (1972)  
[15] VÉRTES, A., NAGY-CZAKÓ, I., BURGER, K.: J. Phys. Chem., **82**, 1469 (1978)  
[16] HEDSTRÖM, B. O. A.: Arkiv Kemi, **6**, 1 (1953)

Maja TONKOVIĆ }  
Svetozar MUSIĆ } 41001 Zagreb, P.O. Box 1016, Yugoslavia  
Olga HADŽIJA }  
  
Ilona NAGY-CZAKÓ }  
Attila VÉRTES } H-1088 Budapest, Puskin u. 11—13.

## ELECTROCHEMISTRY OF STAINLESS STEELS, I

### POTENTIODYNAMIC POLARIZATION CURVES

G. VÉRTES

*(General Design Institute for the Engineering Industry, Budapest)*

Received March 16, 1981

Accepted for publication August 5, 1981

It was established that the cyclic voltammogram of steel KO 36, cleaned by polishing and kept for 30 minutes under open circuit conditions in a solutions containing  $0.1 \text{ mol/dm}^3 \text{ Na}_2\text{SO}_4$  and  $0.5 \text{ mol/dm}^3 \text{ H}_3\text{BO}_3$ , can be well reproduced between  $E_{\text{SCE}} = -800$  and  $+1400 \text{ mV}$  after the first anodic sweep. The curve reveals between the regions of hydrogen and oxygen evolution three anodic and two cathodic maxima.

The first anodic peak indicates surely the ionization of hydrogen absorbed in the metal, but the dissolution of the basic metal cannot be completely excluded. The second peak will be discussed in the study of pretreatments. The third peak represents the formation of the passive film, the reduction of which is jointly indicated by the two cathodic peaks, and presumably reduction continues also during hydrogen evolution.

The name stainless steel indicates that in practical application a layer or a film is formed on the surface, which considerably diminishes, virtually prevents their further corrosion. Though passive films of this type can be formed on several metals, thus on iron, our knowledge of these layers is rather limited from both theoretical and practical aspects.

HORVÁTH and RAUSCHER [1] have recently published a review on the passivity formed on iron, containing also a detailed evaluation of the relevant literature. It can be established also from this paper that in certain instances even the most elementary cases are under discussion between various research schools. The situation is still more complicated in the case of stainless steels containing chromium and mostly also nickel. In spite of the fact that detailed data have been known more than 20 years (*e.g.* Ref. [2]) on the chemical composition of the passive layer, and even certain structural investigations yielded information, several theoretical and practical problems still have to be elucidated.

Most of the investigations were aimed at single characteristic current and potential data, such as corrosion current, passive current, corrosion potential, passivation potential, activation potential, Flade potential *etc.* Experiments were carried out to detect relationships between the above values and the single chemical or possibly physical processes. However, in addition to these problems, and sometimes even independently of these, the practical user needs informations whether this protective layer is developed under the given conditions, and if so, at what rate, under which conditions can the

layer formed be maintained, and what properties and durability does the layer possess.

The object of the present series is to investigate how far these questions can be answered by electrochemical measurements. It is sought necessary to investigate in certain concrete cases the conditions of layer formation and the properties of the layers, but we also consider it as our task to develop simple methods, which help the user to obtain with relative ease data most important for him.

## Experimental

Austenitic steel rods, type KO 36, of 20 mm in diameter and 20 cm<sup>2</sup> surface were used for the investigations.

Composition of steel: Cr = 17.4%, Ni = 10.4%, C = 0.08%, S = 0.030%, P = 0.035%, Si = 0.33%, Mn = 1.4%, Ti = 0.8%.

Most of the steels used as materials of construction are first mechanically worked by turning, grinding, polishing, *etc.*, so that it seemed suitable to carry out also the investigations on surfaces purified mechanically and not chemically. Accordingly, the steel was polished blank with water resistant abrasive paper No. 400 before each measuring series, then washed first with a strong water jet, then with distilled water. Differences between surfaces obtained with various cleaning and pretreatment processes will be discussed in a later communication.

A solution containing 0.1 mol/dm<sup>3</sup> Na<sub>2</sub>SO<sub>4</sub> and 0.5 mol/dm<sup>3</sup> H<sub>3</sub>BO<sub>3</sub> of pH 4.3 was used as electrolyte. Investigations were carried out at 25 °C, the auxiliary electrode was a platinum plate, the reference electrode a saturated calomel electrode, so that electrode potentials are referred to this electrode in the paper. The reference electrode was communicating through a Luggin-capillary with the part of the cell, deoxygenized with nitrogen, containing the test sample.

A potentiostat AFKEL Model 412/1 was used for the measurements, which is able to compensate resistance polarization (in our case 0.1 to 0.2 Ω). Current density values above 1 μA/cm<sup>2</sup> were well reproducible both in potentiostatic and potentiodynamic measurements.

Results given in this paper were obtained in the following way: after the preparation described above the steel rod was placed into the electrolyte and was allowed to stand in open circuit for 30 minutes. The electrode potential was then shifted at a velocity of 1.7 mV/s in the negative direction, and after reaching the lower limit of  $E_k = -800$  mV, at the same velocity in the positive direction, up to a value of  $E_a = +1400$  mV, from where we started again in the negative direction. The extent of polarization was continuously changed in alternating directions between the two extreme values. Experiments showed that voltammograms determined after the first potentiodynamic curve coincide within the limits of measuring errors and can be well reproduced. In the following only these curves will be shown, while the analysis of the first curves will be discussed in a later publication. Measurements at various polarization rates were carried out by starting after a polarization rate of 1.7 mV/s in each case from  $E_a = +1400$  mV, and going over from this rate to other sweep rates.

In potentiostatic measurements, in the predominant part of the cases current is rapidly stabilized within an accuracy of 0.1 μA at the single potentials. If this did not happen within half an hour, current values read-off in the 30th minute are given.

## Results

Figure 1 shows the potentiostatic, and at a rate of 1.7 mV/s the potentiodynamic polarization curves of steel KO 36. The potential of the reversible hydrogen electrode, immersed in the same solution, was also determined in the electrolyte investigated, by bubbling gaseous hydrogen to the platinized

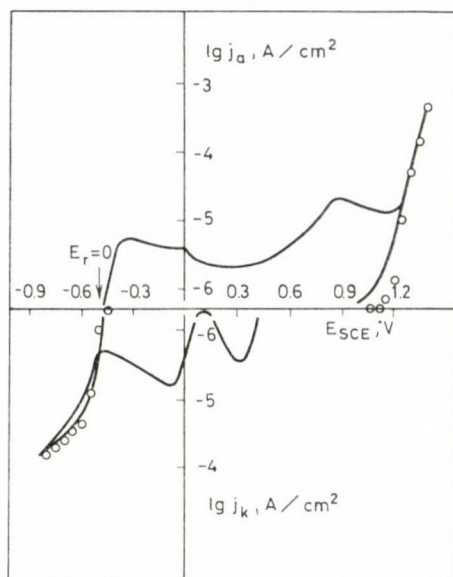


Fig. 1. Potentiostatic (marked with circlets) and potentiodynamic (1.7 mV/s) curves of steel K0 36 in 0.1 mol/dm<sup>3</sup> Na<sub>2</sub>SO<sub>4</sub>, 0.5 mol/dm<sup>3</sup> H<sub>3</sub>BO<sub>3</sub> solution of pH = 4.3, in N<sub>2</sub> atmosphere

platinum electrode and measuring the potential difference against a saturated calomel electrode. In Fig. 1 this value is marked with the arrow  $E_r = 0$ .

In accordance with the chemical resistance, *i.e.* the good polarizability of stainless steel, no current appears on the potentiostatic curve in a wide potential range. At  $E_{SCE} < -500$  mV and  $E_{SCE} > +1000$  mV, resp., an abrupt increase of current can be observed. This is doubtless attributable to hydrogen and oxygen evolution, since already before reaching a current density of  $10^{-4}$  A/cm<sup>2</sup> gas evolution can be observed. Naturally, this does not exclude the proceeding of other reactions, *e.g.* the possibility of transpassive dissolution, but this has to be proved by other methods. The potentiostatic curve alone does not permit further interpretation.

It should be mentioned that the anodic branch of the curve can be well reproduced independently of the fact whether switching to a given value was approached from a more positive or a more negative potential and generally current was stabilized in 30 minutes. As contrary to this, the value of the current on the cathodic side considerably depends in certain cases on the measure in which the surface has been previously reduced. In the experiment presented the single points were determined in the direction of decreasing negative potentials.

The potentiodynamic curve may furnish further information at the polarization rate shown in Fig. 1. In the two extreme potential ranges the course of the two curves is similar but in the middle section, where potentiostatically

no current was observed, *i.e.* no steady state process takes place, the potentiodynamic curve is divided into anodic and cathodic branches, the anodic revealing three, the cathodic two maxima. The first anodic peak appears after a steep raise as a flat slightly inclining plateau with a maximum near  $-300$  mV. Along the descending branch a slight shoulder can be observed at  $-20$  mV, which is already terminated at about  $0$  mV, where the descending branch of the first maximum continues. Next a long extended minimum appears on the polarization curves. The third anodic maximum is to be found between  $800$  and  $900$  mV, and the curve reached then after a slight decrease the oxygen evolution branch of the potentiostatic curve.

In potential shift in the cathodic direction, in the beginning, while anodic current is flowing, we move in the vicinity of the potentiostatic curve. At  $E_{SCE} = 1000$  mV current practically drops to zero and the cathodic current appears only at a value more negative than  $+500$  mV. The first cathodic peak appears now with a maximum of  $+300$  mV. After a brief current-free section a steep raise can be again observed. After the second cathodic maximum near  $-100$  mV a mild extended descending branch follows. It reaches the potentiostatic curve at about  $-500$  mV, where the steep ascent certainly indicates the neutralization of hydrogen ions.

For a better interpretation of the single maxima the change of the shape of the potentiodynamic curve at different potential sweep rates has been investigated (Fig. 2). A changing of the sweep rate within two orders of magnitude did virtually not change the character of the polarization curves.

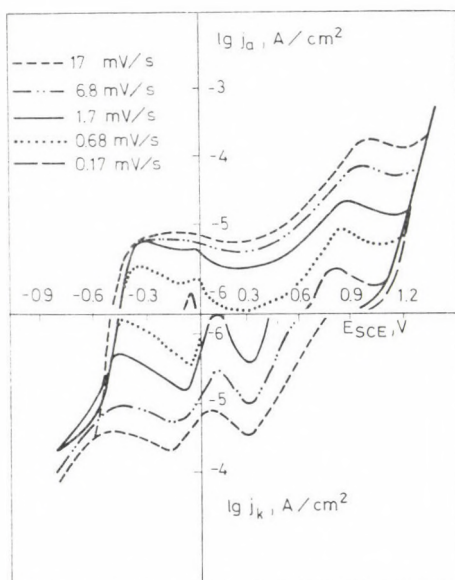


Fig. 2. Potentiodynamic curves of steel KO 36 determined at different sweep rates

At lower rates there is a certain similarity to the potentiostatic curves, thus *e.g.* at 0.17 mV/s the cathodic branch completely disappears, to reappear only at the value of hydrogen evolution. However, it can be seen that in the given system even this decidedly slow potential sweep does not provide for steady state conditions at the anodic side. As can be noted from Fig. 2, the logarithms of the current density values of the single peaks are directly proportional to the logarithms of the sweep rate. This statement is not valid for peak  $A_1$ , which attains at higher sweep rates a limit value.

### Discussion

In the electrochemical investigation of stainless steels steady state methods were not widely used. The reason for this is to be sought in three factors. First of all, in certain regions the reaching of the steady state conditions may occasionally require days [3], and this time factor introduces high uncertainty in the measuring results. It should be mentioned as second aspect that in the 1500 mV region of the polarization curve, particularly at the very potentials most often met in practice, steady state current is very low, and the slightest interfering factor or impurity may cause important changes at the well polarizable surface. The third factor, formulated by W. LORENZ *et al.* [4] for the case of pure iron, is the following: due to the high number of parallel and series reactions complicated by the specific adsorption of intermediate products, and to the transport-inhibiting effect of the oxide membrane formed at the surface, kinetic informations obtained under steady state conditions are unsatisfactory. On the basis of all this, they recommend so-called non-steady state methods, but call the attention to the fact that thermodynamical and even kinetic results obtained in this way are rather of qualitative than of quantitative character.

The findings of GREEN and LEONARD [3] are apparently in contrast with this statement. They studied in detail the potentiostatic and potentiodynamic curves of stainless steel. However, in their experiments they did not compare the true steady state conditions with the potentiodynamic data, but changed the potential at given time intervals and compared the currents measured at the end of the intervals with the current measured at continuously changed potential. They hold non-steady state measurements unsuitable on the basis of the experience that the pretreatment of the metal may considerably influence the individual characteristic current or potential values. This finding calls the attention to the very fact that the method can be advantageously used in the investigation of the effect of various pretreatments, as will be shown in detail in our next communication.

During the application of non-steady state methods one of the crucial problems is the reproducibility of the measurements. This problem occasion-

ally arises within a single measuring series, but more frequently measurements carried out at another laboratory cannot be reproduced. The main difficulty is caused by the circumstance that one part of the variables cannot be controlled [5]. The solution most often recommended is the application of a generally rather energetic pretreatment [4, 5, 6, 7], after which potentiodynamic polarization curves can be easily reproduced. This pretreatment is primarily aimed at the removal of the passive layer spontaneously formed at the surface of steel and means thus adequate cathodic polarization. To a certain extent the same effect can be achieved by allowing to stand the stainless steel under open circuit conditions in a sufficiently acid medium. More generally, cathodic polarization from an external source is used for the promotion of reduction [4, 5, 8, 13], to provide thereby for a clean metal surface and for the reproducibility of the measurements. It follows probably from the exaggerated demand on the purity of the surface that the polarization curves of stainless steels have been determined in most of the cases proceeding from the more negative to the more positive electrode potentials, *i.e.* in the anodic direction.

In this question too, GREENE and LEONARD [3] hold an opposite view, recommending as far as possible the avoidance of cathodic treatment and even of the potential range of possible active dissolution, because these result in unwanted changes.

In the present work the following train of thoughts was followed. First, conditions of good reproducibility must be provided. It is possible that results obtained in this way do not reflect processes proceeding at the "original" surface, but after the comprehension of these processes a comparison with results obtained for surfaces, which can be considered as original, offers a possibility for their better understanding. Thus, our investigations were first concentrated on the interpretation of the polarization curves of good reproducibility, obtained in the way as described in the "Experimental".

The five maxima appearing on the potentiodynamic curve must correspond to five well-defined processes. It would seem obvious to assign two anodic peaks to the two cathodic maxima, and to treat the four peaks pairwise as the redox reaction of a surface or of an adsorbed layer. In first approximation this is conceivable in the case of the first cathodic ( $K_1$ ) and the third anodic ( $A_{III}$ ) peaks, but then nothing can be assigned to the second cathodic peak  $K_{II}$  on the anodic side. Evidently, the shoulder  $A_{II}$ , representing a very small charge quantity, does not come into consideration in this respect. On the other hand, the maximum  $A_I$  cannot be linked with  $K_{II}$  because of theoretical considerations.

In the case of a reversible process the anodic and the cathodic peaks appear at an identical electrode potential, while in the case of irreversible surface reactions the anodic peak is located at a more positive, the cathodic a more negative potential, than values measurable under reversible conditions.

Since the location of maximum  $A_I$  is more negative than that of any of the cathodic peaks,  $A_I$  cannot be linked with the latter in a redox reaction.

Accordingly, the maximum  $A_I$  may mean an oxidation process, the reduction step of which proceeds only at potential values more negative than that of the beginning of hydrogen evolution. The absorption or adsorption of hydrogen may be such a process. In the literature several authors dealt with the interpretation of the first maximum appearing on the anodic polarization curve of pure iron. Some of the authors [4] attribute it to the oxidation of hydrogen, while others [5] deny this possibility. In the case of austenitic steels investigations were mostly carried out in acid solutions. However, also in this case opinions vary whether the oxidation of adsorbed hydrogen appears on the polarization curve [8, 10] or not [14, 15].

In our case, the maximum  $A_I$  cannot be merely explained by the oxidation of adsorbed hydrogen, because it can be seen from Fig. 2 that the maximum approaches with increasing potential sweep rate a limit value, *i.e.* the process reaches some limit rate, and at the given slow rate this makes some transport process very similar. KIM and WILDE [8] clearly proved the hydrogen absorption of austenitic steel by diffusion through a 0.1 mm thick steel foil of type AISI 304. The limit rate in Fig. 2 can also be readily interpreted as a diffusion limit value.

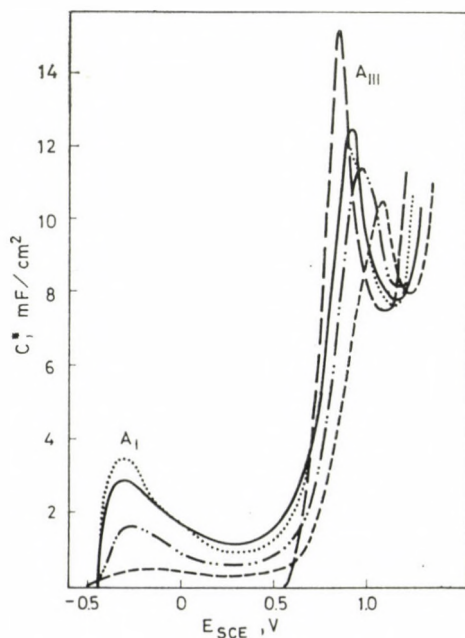


Fig. 3. Pseudocapacities calculated from the anodic polarization curves of Fig. 2

However, it should be mentioned that experimental data presented so far do not exclude the possibility that peak  $A_I$  is connected with the dissolution of the base metal. Though steel is passivated under steady state conditions in this region, the covering of the whole surface takes a longer time, and applying polarization of a higher rate than 0.6 mV/s, there is no time for complete passivation.

For the better interpretation of the single peaks, the charge quantity represented by these peaks was investigated. With a view to this, first the pseudocapacity of the electrode was determined from the ratio of current density and polarization rate, as shown in Figs 3 and 4. It should be mentioned here that according to data in the literature [5, 16] the capacity of the double layer is lower than 0.1 mF/cm<sup>2</sup>, so that it can be neglected in the present case. The peak  $A_{II}$ , involving a very narrow potential range was not taken into consideration in the investigation of the curve.

By the integration of the area enclosed by the curve, the charge quantities belonging to the single peaks are given in Table I.

It can be seen from the Table that only the charge quantities belonging to peaks  $A_{III}$  and  $K_{II}$  remain unchanged, when sweep rate is changed by two orders of magnitude.  $A_I$  was discussed already earlier. The charge quantity belonging to peak  $K_I$  decreases with decreasing sweep rate. This fact, but particularly a comparison of the charge quantities belonging to the maxima

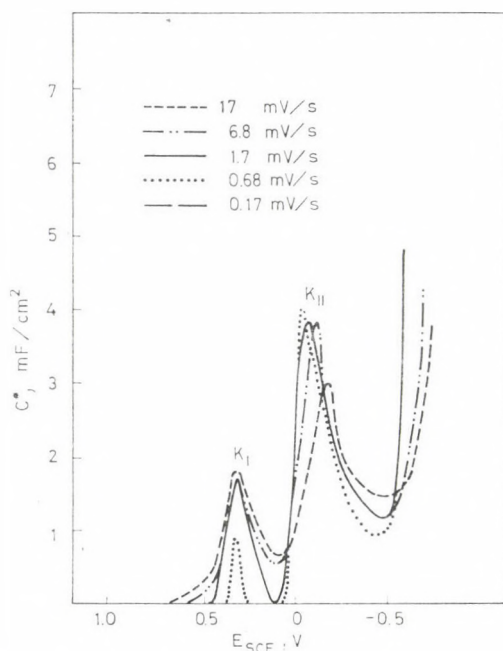


Fig. 4. Pseudocapacities calculated from the cathodic polarization curves of Fig. 2

Table I

Charge quantities belonging to the single peaks  
of the voltammogram, mC/cm<sup>2</sup>

Sweep rate	A <sub>I</sub> -300 mV	A <sub>III</sub> 8-900 mV	K <sub>I</sub> 300 mV	K <sub>II</sub> -100 mV
17.0 mV/s	0.4	3.9	0.5	1.0
6.8 mV/s	1.0	4.3	0.4	1.1
1.7 mV/s	1.7	4.6	0.25	1.1
0.68 mV/s	1.7	4.1	0.05	1.1
0.17 mV/s	0.6	4.2	—	—

K<sub>I</sub> and A<sub>III</sub>, exclude the possibility of linking the processes corresponding to the two peaks into a single redox reaction.

The considerable difference between the anodic and cathodic charge quantities must be discussed separately. It was found in investigation of pure iron [4] that in alkaline medium charges measured during anodic and cathodic polarizations are near identical, and between 12 and 120 mV/s independent of polarization rate. Under similar conditions as above, SCHREBLER-GUZMAN *et al.* [5] link the peaks A<sub>I</sub> and A<sub>II</sub> with K<sub>II</sub>, and peak A<sub>III</sub> with K<sub>I</sub>. They establish, however, that the structure of the layer changes during repeated cyclic polarization and certain rearrangements take place. They mention as one explanation of this phenomenon that the density of the more highly oxidized FeOOH is higher than that of Fe(OH)<sub>2</sub>, so that parts of the surface become free during reduction, which behave differently in the next oxidation.

In our case the quantity of charge introduced along peak A<sub>III</sub> considerably surpasses even the sum of charges introduced during complete cathodic polarization. This can be explained in two ways. The difference can arise from the facts that a reaction proceeds in the potential range of peak A<sub>III</sub>, the product of which leaves the surface, and thus, can not appear during reduction. The other possible explanation is that reduction proceeds at the surface in a potential range where it cannot be any more observed because of the current of hydrogen evolution.

The probability of the first possibility, of active or transpassive dissolution is rather small, because at potentials more negative than +1000 mV no reaction can be observed under steady state conditions at the location of maximum A<sub>III</sub>. Theoretically it is conceivable that the reaction appears only in non-steady state measurements, because the surface is passivated in time, and thus, no potentiostatic current can be obtained. However, the charge quantity belonging to peak A<sub>III</sub> is independent of sweep rate, and thus it is unlikely that the dissolution of a surface gradually passivated with time were to take place.

It can be assumed on the basis of the aforesaid that even at potentials more negative than  $-500$  mV there remains some kind of oxygen or oxide at the surface, which can be then reduced up to  $-800$  mV. Here primarily the oxides have to be taken into consideration, the reduction of which either to  $\text{Cr}^{2+}$  or to metallic Cr always proceed at a potential more negative than that of the reversible hydrogen electrode [17, 18]. This is indicated also in communication [19] reporting on the polarization curve of chromium, where it has been established that at  $\text{pH} > 3$  hydrogen evolution takes place at the oxide. FRANKENTHAL [6] assumed in the case of stainless steels that the surface cannot be completely oxide-free at the corrosion potential (by 250 mV more negative, than the potential of the reversible hydrogen potential).

Let us return here in detail to the measuring uncertainties along the cathodic branch of the potentiostatic curve in Fig. 1, mentioned earlier. Evidently, hydrogen overvoltage will not be the same at a pure metal surface and at a surface covered with oxide. The attention has been called already in the case of iron to hydrogen evolution at the oxide in certain cases [20]. This possibility can by no means be left out of consideration in the case of stainless steels because of the chromium content. In principle, the phenomenon observed on stainless steels in  $0.5$  M  $\text{H}_2\text{SO}_4$  [3] may be identical: in a range more negative than the passivation potential, *i.e.* in active dissolution, the potentiostatically measurable current decreases with time, indicating that the surface is also passivated at potentials more negative than that of the reversible hydrogen electrode.

However, as a cause of the uncertainty in conjunction with hydrogen overvoltage other possible differences between the reduced and the oxidized surfaces cannot be disregarded. It has been observed also in the case of iron that hydrogen overvoltage changes during the voltammogram cycles and this is attributed to the chemical and structural changes of the surface [5]. In the case of stainless steels this means further complications, since by the dissolution of certain elements others may get enriched at the surface, which can affect hydrogen evolution.

#### REFERENCES

- [1] HORVÁTH, J., RAUSCHER, Á.: *Korróziós Figyelő*, **18**, 88, 115, 145 (1978)
- [2] NIELSEN, N. A., RHODIN, T. N.: *Z. Elektrochem.*, **62**, 707 (1958)
- [3] GREENE, N. D., LEONARD, R. B.: *Electrochim. Acta*, **9**, 45 (1964)
- [4] GEANA, D., EL MILIGY, A. A., LORENZ, W. J.: *J. Appl. Electrochem.*, **4**, 337 (1974)
- [5] SCHREBLER-GUZMÁN, R. S., VILCHE, J. R., ARVIA, A. J.: *Electrochim. Acta*, **24**, 395 (1979)
- [6] FRANKENTHAL, R. P.: *J. Electrochem. Soc.*, **116**, 1646 (1969)
- [7] ASTM G5-72 Standard Reference Method
- [8] KIM, C. D., WILDE, B. E.: *Corr. Sci.*, **10**, 735 (1970)
- [9] EL-BASIOUNY, M. S.: *Br. Corros. J.*, **12**, 89 (1977)
- [10] CIGADA, A., RE, G., SINIGAGLIA, D., BORILE, F.: *Corrosion*, **34**, 407 (1978)

- [11] AZZERI, N. A., BOMBARA, G.: J. Appl. Electrochem., **3**, 285 (1973)
- [12] BULMAN, G. M., TSEUNG, A. C. C.: Corr. Sci., **12**, 451 (1972)
- [13] OKAMOTO, G., SHIBATA, T.: Corr. Sci., **10**, 371 (1970)
- [14] ROCKEL, M. B.: Corrosion, **27**, 95 (1971)
- [15] RIGGS, O. L.: Corrosion, **31**, 413 (1975)
- [16] KIM, C. D., WILDE, B. E.: Corrosion, **28**, 26 (1972)
- [17] EVANS, U. R.: The Corrosion and Oxidation of Metals. Arnold Ltd. London 1961. p. 226.
- [18] DE BETHUNE, A. J., SWENDEMAN LOUD, N. A.: Standard Aqueous Electrode Potentials. C. A. Hampel Ltd. Skokie, Ill., 1964
- [19] EL-BASIOUNY, M. S., HARUYAMA, S.: Corr. Sci., **17**, 405 (1977)
- [20] NAGAYAMA, M., COHEN, M.: J. Electrochem Soc., **109**, 781 (1962)

György VÉRTES      H-1012 Budapest, Kuny Domokos u. 2.



# POLYETHYLENE GLYCOL DERIVATIVES AS COMPLEXING AGENTS AND PHASE-TRANSFER CATALYSTS, IV

BEHAVIOUR OF PHASE-TRANSFER CATALYSTS IN SOLID-LIQUID  
PHASE EQUILIBRIA

G. T. SZABÓ, K. ARANYOSI and L. TÓKE\*

(Department of Organic Chemical Technology, Technical University, Budapest)

Received December 15, 1980

In revised form June 17, 1981

Accepted for publication August 28, 1981

Linear polyethers and other phase-transfer catalysts have been studied in equilibria simulating solid-liquid phase-transfer conditions. Salt concentrations of the organic phases have been determined. Polyethylene glycols, crown ether and tricaprylmethylammonium chloride exhibited high salt extracting power in benzene, chlorobenzene, dichloromethane and acetonitrile. Tetramethylethylenediamine does not influence the equilibrium salt concentration of the organic phase. The ratio  $K_{sol} = \text{dissolved complex}/\text{total ligand}$  is used to characterize the equilibria of solid-liquid systems.

## Introduction

It is known that polyethylene glycols have a moderate solid-liquid phase-transfer catalytic effect [1, 4, 5, 6]. Nevertheless, neither the physicochemical approach of this phenomenon nor a comparison of different phase-transfer catalysts in solid-liquid systems has been made.

This is why we have studied solid-liquid phase equilibria influenced by polyoxyethylenes [1, 2, 3].

Solid 2,4-dinitro-phenolate salts were stirred with aprotic solvents in the presence of phase-transfer catalysts and the ion concentrations of the saturated solutions were measured. The concentrations are given in this paper, and the equilibria are discussed.

The present considerations are related to system (a) catalyzed by *complexing agents* (b) in which *no reaction occurs*. A 1:1 complexing stoichiometry is considered.

Figure 1 shows the theoretically possible equilibria existing between the cation and the ligand.\*\*

\* To whom correspondence should be addressed

\*\* In Fig. 1 anions are not shown. In a one-anion system  $c_{\text{anion, sol}} = c_{\text{Me}^{\oplus}, \text{sol}} + c_{[\text{Lig Me}]^{\oplus}, \text{sol}}$   
 $c_{\text{anion, dis}} = c_{\text{Me}^{\oplus}, \text{dis}} + c_{[\text{Lig Me}]^{\oplus}, \text{dis}}$

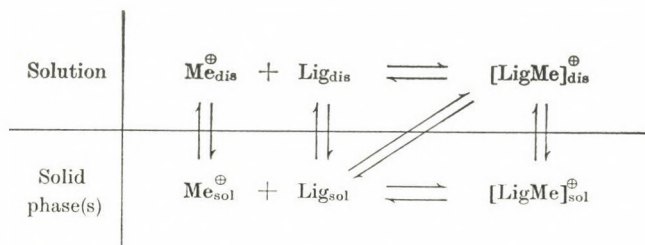


Fig. 1. Equilibrium of a solid-liquid phase-transfer system catalyzed by complexing agent

We attempt to find a possibility for quantitative characterization of catalyst efficiency. Theoretically, the best way is to give the stability constant of the complex in solution\*

$$K_{\text{stab}} = \frac{c_{[\text{LigMe}]^{\oplus}, \text{dis}}}{c_{\text{Me}^{\oplus}, \text{dis}} c_{\text{Lig}, \text{dis}}} \quad (1)$$

To determine  $K_{\text{stab}}$ ,  $c_{\text{Me}^{\oplus}, \text{dis}}$  should be measured, and in solid-liquid systems it is a difficult task. An approximation can be taken. If the ligand concentration is low enough (so the polarity of the medium is unchanged), the concentration of the dissolved but uncomplexed cation is not changed by the addition of ligand:

$$c_{\text{Me}^{\oplus}, \text{dis}} \approx c_{\text{Me}^{\oplus}, \text{dis}}^0 \quad (2)$$

Where  $c_{\text{Me}^{\oplus}, \text{dis}}^0 = \text{Me}^{\oplus}$ -ion concentration of the solution in the absence of any ligand.

The values of  $K_{\text{stab}}$  can be calculated using approximations (2) and (8) but (a) it is uncertain how correct approach (2) is, (b)  $c_{\text{Me}^{\oplus}, \text{dis}}^0$  values carry a high experimental error; and (c)  $K_{\text{stab}}$  gives information only for the liquid phase.

We suppose that it is more informative to define how many mol of complex are solubilized by one mol of ligand [ $K_{\text{sol}}$ , Eq. (3)].

$$K_{\text{sol}} = \frac{c_{[\text{LigMe}]^{\oplus}, \text{dis}}}{c_{\text{Lig}}^0} \quad (3)$$

where  $c_{\text{Lig}}^0 =$  the total ligand concentration

$$c_{\text{Lig}}^0 = \frac{m_{\text{Lig}}}{M_{\text{Lig}} V_{\text{Liq}}} \quad (4)$$

$m_{\text{Lig}}$  = weight of the ligand added,

$M_{\text{Lig}}$  = molecular weight of the ligand

$V_{\text{Liq}}$  = volume of the liquid phase.

\* Symbols used: Lig = complexing compound,  $\text{Me}^{\oplus}$  = cation,  $[\text{Lig Me}]^{\oplus}$  = complex cation,  $\text{DNP}^{\ominus}$  = 2,4-dinitrophenolate ion. Index "sol" refers to the solid, "dis" refers to the solution phase.  $K_{\text{stab}}$  = complex stability constant [Eq. (1)];  $K_{\text{sol}}$  = solubility constant [Eq. (3)].

To clarify the behaviour of  $K_{\text{sol}}$  we investigated the solubilization equilibrium and sought for the connection between  $K_{\text{sol}}$  and  $K_{\text{stab}}$ .

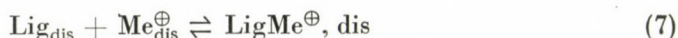
If the quantity of ligand in the solid phase is negligible

$$V_{\text{sol}} c_{\text{Lig, sol}} \ll V_{\text{Liq}} c_{\text{Lig, dis}} \quad (5)$$

and the quantity of complex in the solid phase is negligible

$$V_{\text{sol}} c_{[\text{Lig Me}]^{\oplus}} \ll V_{\text{Liq}} c_{[\text{Lig Me}]^{\oplus}, \text{dis}} \quad (6)$$

where  $V_{\text{sol}}$  = volume of the solid phase; all the concentrations in process (7) are known,



because

$$c_{\text{Lig}}^0 = c_{\text{Lig, dis}} + c_{[\text{Lig Me}]^{\oplus}, \text{dis}} \quad (8)$$

Combining Eqs (1), (2), (3) and (8), we get

$$K_{\text{sol}} = \frac{K_{\text{stab}} c_{\text{Me}^{\oplus}, \text{dis}}}{1 + K_{\text{stab}} c_{\text{Me}^{\oplus}, \text{dis}}} \quad (9)$$

This expression of  $K_{\text{sol}}$  contains only constants and  $c_{\text{Me}^{\oplus}, \text{dis}}$ ; the concentration of uncomplexed cation, *i.e.* the cation solvated by the aprotic solvent. This concentration may be supposed to remain low and hardly changing (at least by low ligand concentrations). Thus Eq. (8) shows the ratio  $K_{\text{sol}}$  to be characteristic for a solvent (ligand) salt system at a given temperature and at low ligand concentration (if the complexing stoichiometry is stable 1 : 1).

In practice  $K_{\text{sol}}$  was observed to be remarkably constant in a given system.

## Experimental

### Materials

Polyethylene glycols: commercial product supplied by Fluka and dried by benzene azeotropic distillation. Other polyethers were prepared in this Laboratory [2]. Tricaprylmethylammonium chloride (Aliquat 336<sup>®</sup>) was supplied by Fluka.

### Measurements of solid-liquid phase-transfer equilibria

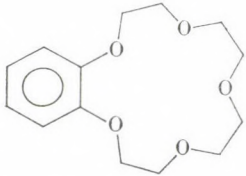
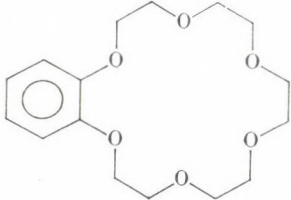
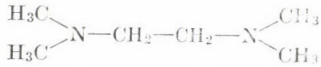
Catalyst (0.1 g), dry solvent (10 cm<sup>3</sup>) and solid 2,4-dinitrophenol alkali salt (in excess) were stirred in a thermostated flask until an equilibrium was achieved. The salt concentration was determined by measuring the absorbance of the solution at  $\lambda = 370$  nm.

## Results and Discussion

The behaviour of  $K_{\text{sol}}$  was checked by varying the concentration of polyethylene glycols in benzene solutions at 25 °C, and monitoring the value of  $K_{\text{sol}}$ . Between 0.005 and 0.015  $\frac{\text{g}}{\text{cm}^3}$  ( $1.7 \times 10^{-2}$  and  $5 \times 10^{-2}$  M) PEG concentrations,  $K_{\text{sol}}$  was constant and independent of the (moderate) excess of solid.

Table I

Equilibrium  $\text{DNP}^{\ominus}\text{Me}^{\oplus}$  concentration of benzene solutions at different temperatures in the presence of different catalysts\*

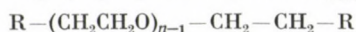
Catalyst $C = 10 \frac{\text{g}}{\text{dm}^3}$	Me	Salt concentration $\frac{\text{mg}}{\text{dm}^3}$				
		$t = 25 \text{ }^{\circ}\text{C}$	$t = 30 \text{ }^{\circ}\text{C}$	$t = 35 \text{ }^{\circ}\text{C}$	$t = 40 \text{ }^{\circ}\text{C}$	$t = 50 \text{ }^{\circ}\text{C}$
PEG 300	Li	600	800		1400	1200
	Na	1400	1300	1700		1700
	K	2700	2400	2500	2300	2300
PEG 600	Li	700	600		900	1200
	Na	600	800		1100	800
	K	1000	1000		1700	1500
PEG 2000	Li	30	200		1000	1200
	Na	100	100		100	100
	K	200	200		600	600
Tricaprylmethyl-ammonium-chlorid	Li	830	440		390	590
	Na	3000	2800	2900	3100	3100
	K	3500	3700	4100	3900	3600
	Li	80	200		1200	1100
	Na	2600	3000	3600	3300	3800
	K	160	270		570	1000
	Li	220	420		530	870
	Na	1700	1900		2800	4200
	K	5200	4600		5400	4600
	Na	13				
	Li	0.08				
	Na	0.45				
No catalyst	K	0.54				

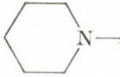
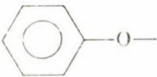
\* Concentrations are given as  $\text{DNP}^{\ominus}$  content though mainly  $\text{DNP}^{\ominus} [\text{LigMe}]^{\oplus}$  is present

Table II

DNP<sup>⊖</sup>Me<sup>⊕</sup> concentration of benzene solutions at 25 °C in the presence of symmetrically

$\alpha,\omega$ -disubstituted polyoxyethylene compounds.  $c_{\text{catalyst}} = 10 \frac{\text{g}}{\text{dm}^3}$



R	$C \frac{\text{mg}}{\text{dm}^3}$	
	$\bar{n} = 64.0 \bar{M} = 300^*$	$\bar{n} = 48 \bar{M} = 2000^*$
HO—	1400	100
	74	57
	44	57

\* Average molecular weight of the polyethylene glycols used as starting material

These results lead to the conclusion that conditions (5) and (6) are valid and  $K_{\text{sol}}$  can be used to characterize the solubilizing effect.

The concentrations of dissolved salt in Tables I—III are given as weight concentrations. In Table IV  $K_{\text{sol}}$  and  $K_{\text{stab}}$  values are collected.

Tables I, III and IV show some systems catalyzed by agents other than polyethers. Though the mechanism of dissolution is different here, the solubility data can be compared with the other ones.

Table I shows the salt-extracting power of polyethylene glycols with different chain lengths and that of some ether catalysts.

In benzene-aqueous phase equilibria [3] salt extraction can be increased by modifying the end groups of polyethylene glycols to form more lipophilic polyethers. Recently we examined the effect of such substitutions on solid-liquid phase-transfer (see Table II).

Equilibrium data for different solvents are collected in Table III.

These results allow to draw the following conclusions.

1) The polyethylene glycols have a significant solubilizing power in solid-liquid systems. The ion concentration under the influence of PEG's may be  $10^2$ — $10^3$  times higher in solid-liquid phase equilibria than in the liquid-liquid case.

2) Concentration produced in the organic phase is not independent of the average molecular weight of the polyethylene glycol. The dependence is shown in Fig. 2.

Table III

DNP<sup>⊖</sup>Me<sup>⊕</sup> concentrations of aprotic solvents in the presence of different catalysts  
(*t* = 25 °C)

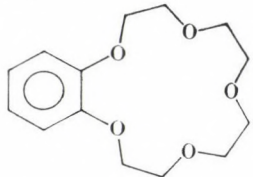
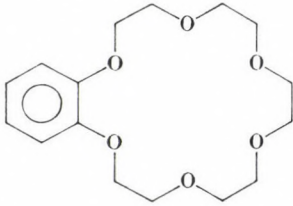
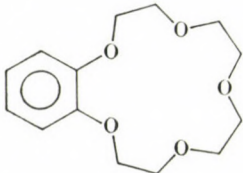
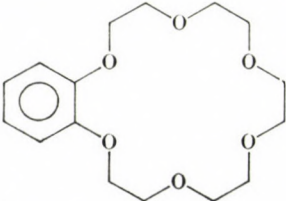
Catalyst $c = 10 \frac{\text{g}}{\text{dm}^3}$	Me	Salt concentration $\frac{\text{mg}}{\text{dm}^3}$		
		Chlorobenze	Dichloromethane	Acetonitrile
PEG 300	Li	5000	12,000	
	Na	2600	4300	12,000
	K	3800	3900	6000
PEG 600	Li	4500	7900	
	Na	1800	1700	9600
	K	3100	2900	4300
PEG 2000	Li	1700	7300	
	Na	800	2500	8100
	K	2300	1700	4000
Tricaprylmethyl-ammonium chloride	Li	3900	4600	7000
	Na	4800	3400	7800
	K	4300	3500	4200
	Li	6900	6300	
	Na	5300	5300	12,500
	K	2500	3400	7400
	Li	2000	4800	
	Na	2900	1700	10,300
	K	4900	2900	9600
No catalyst	Li	30	13	$>2.5 \cdot 10^5$
	Na	13	3	7800
	K	8	4	2000

Table IV

 $K_{sol}$  and  $K_{stab}$  for solid-liquid phase-transfer equilibria in different solvents

Catalysr	Me	Benzene		Cholorobenzene		Dichloromethane		Acetonitrile	
		$K_{sol}$	$\log K_{stab}$	$K_{sol}$	$\log K_{stab}$	$K_{sol}$	$\log K_{stab}$	$K_{sol}$	$\log K_{stab}$
PEG 300 $c_{Lig}^0 = 3.33 \times 10^{-3} M$	Li	0.095	5.4	0.79	4.3	1.9*			
	Na	0.20	5.1	0.38	4.0	0.63	5.0	0.61	1.6
	K	0.37	5.4	0.51	4.5	0.53	4.8	0.54	2.1
PEG 600 $c_{Lig}^0 = 1.67 \times 10^{-3} M$	Li	0.22	5.8	1.4*		2.5*			
	Na	0.17	5.0	0.52	4.2	0.49	4.8	0.52	1.4
	K	0.27	5.2	0.83	5.2	0.78	5.3	0.62	2.3
PEG 2000 $c_{Lig}^0 = 5.0 \times 10^{-3} M$	Li	0.031	5.0	1.8*		7.7*			
	Na	0.097	4.7	0.77	4.7	2.4*		0.26	1.0
	K	0.18	5.0	2.1*		1.5*		1.8*	
 $c_{Lig}^0 = 2.73 \times 10^{-2} M$	Li	0.011	4.4	0.97	5.3	0.89	5.1		
	Na	0.34	5.4	0.69	4.5	0.69	5.2	0.61	1.6
	K	0.019	3.9	0.30	4.1	0.41	4.6	0.65	2.3
 $c_{Lig}^0 = 3.21 \times 10^{-2} M$	Li	0.036	4.9	0.32	3.5	0.78	4.7		
	Na	0.26	5.2	0.44	4.1	0.26	4.4	0.37	1.2
	K	0.73	6.1	0.69	4.8	0.41	4.6	1	
$c_{DNP}^0 \ominus Me^{\oplus}$	Li	$4.2 \cdot 10^{-7}$		$1.6 \cdot 10^{-4}$		$6.8 \times 10^{-5}$		$>1.3$	
	Na	$2.2 \cdot 10^{-6}$		$6.3 \cdot 10^{-5}$		$1.5 \cdot 10^{-5}$		$3.8 \cdot 10^{-2}$	
	K	$2.4 \cdot 10^{-6}$		$3.6 \cdot 10^{-5}$		$1.8 \cdot 10^{-5}$		$9.0 \cdot 10^{-3}$	

\* This high  $K_{sol}$  value may point to other than 1 : 1 complexation

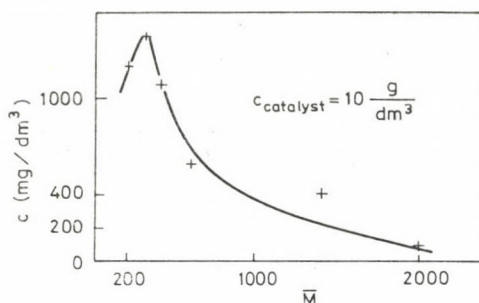


Fig. 2. Equilibrium  $\text{DNP}^{\ominus}\text{Me}^{\oplus}$  concentration of benzene solutions at  $t = 25^{\circ}\text{C}$  as a function of the average molecular weight of polyethylene glycol

We have observed the highest salt concentration for  $\bar{M} = 300$  polyethylene glycol. A similar decrease was found above  $\bar{M} = 300$  also at other temperatures and in other solvents.

3) Modifications of the end-groups (to increase lipophilicity) resulted in no improvement of solid-liquid phase-transfer. Polyethers containing OH end-groups (polyethylene glycols) gave the best results.

4) Different types of phase-transfer catalysts have been compared with each other. A quaternary ammonium salt (tricaprylmethylammonium chloride) gives the highest concentration. The following best ones are the crown ethers with optimum hole-size (benzo-15-crown-5 for  $\text{Na}^{\oplus}$  and benzo-18-crown-6 for  $\text{K}^{\oplus}$ ). PEG 300 is the next in the order of activity. Crown ethers with non-optimal holes exhibit lower activities than PEG 300 does. The concentration with PEG 300, tricaprylmethylammonium chloride and crown ethers are in the same order of magnitude (even in nonpolar solvents). In more polar solvents the differences become smaller. From 25 to  $50^{\circ}\text{C}$  in benzene the concentrations do not show any remarkable temperature dependence when using PEG's or tricaprylmethylammonium chloride. If the size of the crown ether and the cation do not fit well some temperature dependence can be observed.

The solvents in our experiments are the ones generally used in phase-transfer catalysis. These are in order of increasing polarity: benzene ( $\epsilon = 2.3$ ), chlorobenzene ( $\epsilon = 5.7$ ), dichloromethane ( $\epsilon = 9.1$ ), and acetonitrile ( $\epsilon = 37.5$ )

The cation concentration increases in this order. In this general tendency the quality of the cation also plays a role. For polyethylene glycols in benzene, the order of solubility is  $\text{Li}^{\oplus} < \text{Na}^{\oplus} < \text{K}^{\oplus}$ . When increasing the solvent polarity, it turns step by step to its opposite, so that in acetonitrile lithium 2,4-dinitrophenolate is soluble without any catalyst. In this case phase-transfer catalysis has no significance (at least with such a soft anion).

In Table IV,  $K_{\text{sol}}$  and  $K_{\text{stab}}$  values are listed. Values of  $K_{\text{sol}}$  were calculated using Eq. (10)

$$K_{\text{sol}} = \frac{c_{\text{DNP}^{\ominus}, \text{dis}} - c_{\text{DNP}^{\ominus}, \text{dis}}^0}{c_{\text{Lig}}^0} \quad (10)$$

where

$c_{\text{DNP}^\ominus, \text{dis}}$  = 2,4-dinitrophenolate concentration of the solution,

$c_{\text{DNP}^\ominus, \text{dis}}^0$  = 2,4-dinitrophenolate concentration of the solution in the absence of catalyst.

Equation (10) is derived from Eqs (3) and (2) by substituting the cation concentrations by the equivalent anion concentrations.

In benzene, chlorobenzene and dichloromethane, the concentrations  $c_{\text{DNP}^\ominus}^0$  are low, while in acetonitrile higher, so the  $K_{\text{sol}}$  values referring to acetonitrile systems are uncertain (being small differences between large numbers).

Constants  $K_{\text{stab}}$  are also tabulated. They are computed from Eq. (11)

$$K_{\text{stab}} = \frac{c_{\text{DNP}^\ominus, \text{dis}} - c_{\text{DNP}^\ominus, \text{dis}}^0}{(c_{\text{Lig}}^0 - c_{\text{DNP}^\ominus, \text{dis}} + c_{\text{DNP}^\ominus, \text{dis}}^0) c_{\text{DNP}^\ominus}^0} \quad (11)$$

Because of the large experimental error of  $c_{\text{DNP}^\ominus, \text{dis}}^0$ ,  $K_{\text{stab}}$  is only an estimation. Nevertheless, the data show that upon increasing the solvent polarity,  $K_{\text{sol}}$  becomes higher while  $K_{\text{stab}}$  lower that is more of the complex appears in the solutions, though the complex stability decreases.

This phenomenon can be explained in the following way. An increase of the medium polarity 1) is favourable for the formation of a more polar species



In equilibrium (12),  $c_{[\text{LigMe}]^\oplus_{\text{dis}}}$  increases. 2) For higher solvating power of the solvent there is an enhancement in  $c_{\text{Me}^\oplus, \text{dis}}^0 = c_{\text{DNP}^\ominus, \text{dis}}^0$ .

As a consequence,

$$c_{[\text{LigMe}]^\oplus, \text{dis}} - c_{\text{Me}^\oplus, \text{dis}} = c_{\text{DNP}^\ominus, \text{dis}} - c_{\text{DNP}^\ominus, \text{dis}}^0$$

increases, but  $K_{\text{stab}}$  decreases because of the stronger improvement of

$$c_{\text{Me}^\oplus, \text{dis}} = c_{\text{DNP}^\ominus, \text{dis}}^0$$

The relation between  $K_{\text{stab}}$  and  $K_{\text{sol}}$  is shown by Eq. (9) and by its inverse form (13)

$$K_{\text{stab}} = \frac{1}{c_{\text{Me}^\oplus, \text{dis}}} \frac{K_{\text{sol}}}{1 - K_{\text{sol}}} \quad (13)$$

We will try to extrapolate these results to the real phase-transfer catalytic processes.

1) If a polyethylene glycol is used as solid-liquid phase-transfer agent, PEG 300 should be chosen.

2) Lithium salts are supposed to have a solid-liquid phase-transferring power in acetonitrile.

3) As the salt concentration was found to have no significant temperature dependence, and the chemical reactions are faster with increasing temperature, solid-liquid phase-transfer reactions have to be carried out at the highest temperature permitted by the solvent and other materials. To check forecasts 1-2, experiments are in progress.

\*

We are indebted to Prof. I. RUSZNÁK for his helping in every respect, for Mr. S. Bozsó for technical assistance and the National Committee for Technical Development, for financial support.

#### REFERENCES

- [1] TÓKE, L., SZABÓ, G. T.: *Acta Chim. (Budapest)*, **93**, 421 (1977)
- [2] TÓKE, L., SZABÓ, G. T., ARANYOSI, K.: *Acta Chim. Acad. Sci. Hung.*, **100**, 257 (1979)
- [3] TÓKE, L., SZABÓ, G. T. SOMOGYI-WERNER, K.: *Acta Chim. Acad. Sci. Hung.*, **101**, 47 (1979)
- [4] LEHMKUHL, H., RABET, F., HAUSCHILD, K.: *Synthesis*, **1977**, 1984
- [5] LEE, D. G., CHANG, V. S.: *J. Org. Chem.*, **43**, 1532 (1975)
- [6] SANTANIELLO, E., MANZOCCHI, A., SOZZANI, P.: *Tetrahedron Lett.*, **1979**, 4581

Gábor Tamás SZABÓ	}	H-1502 Budapest, Műegyetem rkp. 3.
Katalin ARANYOSI		
László TÓKE		

# POLYETHYLENE GLYCOLS AS COMPLEXING AGENTS AND PHASE-TRANSFER CATALYSTS, V

## REACTION RATES IN THE ORGANIC PHASE

G. T. SZABÓ, K. ARANYOSI and L. TÓKE\*

(Department of Organic Chemical Technology, Technical University, Budapest)

Received December 16, 1980

In revised form June 17, 1981

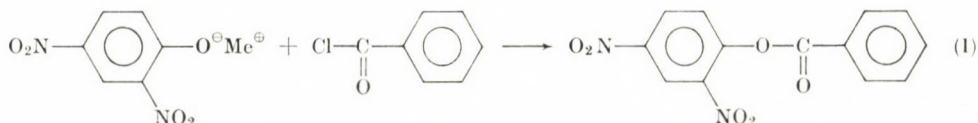
Accepted for publication August 28, 1981

Rates of the reaction between benzoyl chloride and 2,4-dinitrophenolates have been studied in benzene solution containing polyethers. Tertiary amines have been found to accelerate these reactions. A model was proposed for tertiary amine catalyzed phase-transfer acylation processes.

### Introduction

Complexation and interphase behaviour of polyoxyethylenes have been reported in previous papers [1–4]. Polyethylene glycols have been found to produce a significant increase of salt concentration in aprotic solvents [4] under circumstances simulating phase-transfer catalysis. It is the reactivity of ions transferred into the organic phase that will be discussed in the present paper.

The rate of reaction (1)



was studied in benzene solution.

### Experimental

Abbreviations used: DNP = 2,4-dinitrophenol,  $\text{DNP}^\ominus$  = 2,4-dinitrophenolate ion, TEMEDA = *N,N,N',N'*-tetramethylethylenediamine, DAP = 4-dimethylaminopyridine, BzCl = benzoyl chloride, PEG = polyethylene glycol  $\bar{M}$  = 300, DBN = 1,5-diaza-bicyclo-4,3,0-non-5-ene, TEA = triethylamine.

#### Materials

Polyethylene glycol: industrial product (FLUKA) dried by azeotropic distillation with benzene. Benzoyl chloride was freshly distilled after purification from hydrochloric acid.  $\text{DNP}^\ominus$  alkali salts were prepared from DNP and the corresponding alkali hydroxides in alcohol solution. DAP was prepared by the method of VORBRÜGGEN *et al.* [5, 6]. The other amines were industrial products distilled from solid NaOH.

\* To whom correspondence should be addressed

*Benzene solution of 1,4-dinitrophenol alkali salt*

Lithium, sodium or potassium salt of 2,4-dinitrophenol ( $5 \times 10^{-5}$  mol) and 0.1 g ( $3.33 \times 10^{-4}$  mol) of PEG were dissolved in dry benzene and the solution was filled up to 10.0 cm<sup>3</sup> total volume with dry benzene.

*Kinetic measurements*

Dry benzene solutions of the catalyst, 2,4-dinitrophenol alkali salt ( $2 \times 10^{-3}$  M) and of benzoyl chloride ( $2 \times 10^{-3}$  M) were measured into a thermostated flask and kept at 25 °C in N<sub>2</sub> atmosphere. Total volume: 5–7 cm<sup>3</sup>. The mixture was sampled 5–10 times. Quenching: 1–50 μL of the sample was immediately diluted to 20–100 fold volume.

The 2,4-dinitrophenolate concentration was determined from the absorbance at  $\lambda = 370$  nm. No interference by other components has been found.

**Results and Discussion**

The kinetics of the reaction at different mole ratios are first order with respect both reactants.

$$-\frac{dc_{\text{DNP}^{\ominus}}}{d\tau} = w = k_2 c_{\text{DNP}^{\ominus}} c_{\text{BzCl}} \cdot * \quad (2)$$

In the reaction mixture DNP<sup>⊖</sup> is not the only nucleophile, PEG is also capable of being esterified. In such a case the DNP<sup>⊖</sup> consumption could be similar.

In the concentration range examined we could rule out PEG acylation because: 1) the rate constant is independent of the PEG concentration, and 2) the same rate constant has been found when benzo-15-crown-5 was used instead of PEG (see Table I).

The rate constants collected in Table I show that

1) The reaction rate (the nucleophilicity of DNP<sup>⊖</sup>) is the same when complexing the cation either by PEG or benzo-15-crown-5.

2) The rate constant depends upon the nature of the cation. The order is

$$\text{K}^{\oplus} \geq \text{Na}^{\oplus} \gg \text{Li}^{\oplus} \quad (3)$$

3) The dryness of the reaction mixture is one of the unclarified factors [9] in phase-transfer reactions. This is why we have studied the effect of water.

In non-catalyzed reactions the addition of water does not change the rate constant. In the presence of amines, the DNP<sup>⊖</sup> consumption becomes faster when water is present. (It is not known what the role of hydrolysis processes is.)

We have also studied how tertiary amines act in the homogeneous reactions.

This group of catalysts was introduced by NORMANT, CUVIGNY and SAVIGNAC [7]. The catalytic effect was attributed to complexation. One of

\*  $k_2$  is second order rate constant,  $c_{\text{DNP}^{\ominus}}$  and  $c_{\text{BzCl}}$  are concentrations of DNP<sup>⊖</sup> and BzCl, respectively

**Table I**  
Rate constants of the reaction  $\text{DNP}^{\ominus} + \text{BzCl}$  in benzene solution  $t = 25^{\circ}\text{C}$

$C^{\circ}$ $\frac{\text{BzCl}}{\text{mol}} \cdot \frac{\text{L}}{\text{L}}$	$C^{\circ}$ $\frac{\text{DN}^{\ominus}}{\text{mol}} \cdot \frac{\text{L}}{\text{L}}$	$C^{\circ}$ $\frac{\text{PEG}}{\text{mol}} \cdot \frac{\text{L}}{\text{L}}$	Cation	$\frac{k_2^a}{\text{mol} \times \text{s}}$
$3.25 \times 10^{-3}$	$1.77 \times 10^{-3}$	b	$\text{Na}^{\oplus}$	0.13
$1.03 \times 10^{-3}$	$7.62 \times 10^{-4}$	$5.69 \times 10^{-3}$	$\text{Na}^{\oplus}$	0.13
$1.55 \times 10^{-3}$	$1.99 \times 10^{-3}$	c	$\text{Na}^{\oplus}$	0.13
$1.02 \times 10^{-3}$	$8.31 \times 10^{-4}$	$2.24 \times 10^{-2}$	$\text{Na}^{\oplus}$	0.13
$1.49 \times 10^{-3}$	$8.80 \times 10^{-4}$	$7.56 \times 10^{-3}$	$\text{Na}^{\oplus}$	0.13
$1.85 \times 10^{-3}$	$1.09 \times 10^{-3}$	$7.66 \times 10^{-3}$	$\text{Na}^{\oplus}$	2.66
				0.11 M $\text{H}_2\text{O}$
				0.11 M $\text{H}_2\text{O} + 1.77 \cdot 10^{-5} \frac{\text{mol}}{\text{L}}$
				TEMEDA
$2.15 \times 10^{-3}$	$1.08 \times 10^{-3}$	$7.66 \times 10^{-3}$	$\text{Na}^{\oplus}$	0.27
$2.15 \times 10^{-3}$	$1.08 \times 10^{-3}$	$7.66 \times 10^{-3}$	$\text{Na}^{\oplus}$	0.70
$1.15 \times 10^{-3}$	$1.06 \times 10^{-3}$	$7.82 \times 10^{-3}$	$\text{Na}^{\oplus}$	1.04
$2.11 \times 10^{-3}$	$1.08 \times 10^{-3}$	$7.62 \times 10^{-3}$	$\text{Na}^{\oplus}$	0.25
$1.85 \times 10^{-3}$	$9.68 \times 10^{-4}$	$8.80 \times 10^{-3}$	$\text{K}^{\oplus}$	0.16
$2.98 \times 10^{-3}$	$2.03 \times 10^{-3}$	$1.28 \times 10^{-2}$	$\text{Li}^{\oplus}$	0.01

a) Average of more than one runs; when catalyzed:  $k_2'$

b)  $c = 9.93 \times 10^{-3}$  M benzo-15-crown-5 as solubilizing agent

c)  $c = 1.85 \times 10^{-2}$  M benzo-15-crown-5 as solubilizing agent

these compounds, TEMEDA has become a frequently utilized phase-transfer catalyst.

In solid-liquid equilibrium experiments, TEMEDA was found to produce no significant anion concentration in the organic phase [4], so it can not be a complexing catalyst.

Earlier GOKEL and GARCIA [8] proved that in alkylation reactions it is the monoquaternary derivative of TEMEDA which acts as a catalyst. But the mechanism of acylation processes catalyzed by TEMEDA has not been clarified.

To obtain new information about phase-transfer acylations catalyzed by TEMEDA, we have measured homogeneous reaction rates in the presence of TEMEDA.

When TEMEDA was added, the reaction  $\text{BzCl} + \text{DNP}^{\ominus}$  kept following a second-order kinetics, but with a higher rate constant than otherwise. When varying the TEMEDA concentrations, the following dependence was found (Figs 1, 2, 3).

$$k_2 = k_2 + k_{2, \text{TEM}} c_{\text{TEM}} \quad (4)$$

\*  $k_2$  = second order rate constant of catalyzed reaction,  $k_{2, \text{TEM}}$  = slope of line in Figs 1-3,  $c_{\text{TEM}}$  = TEMEDA concentration

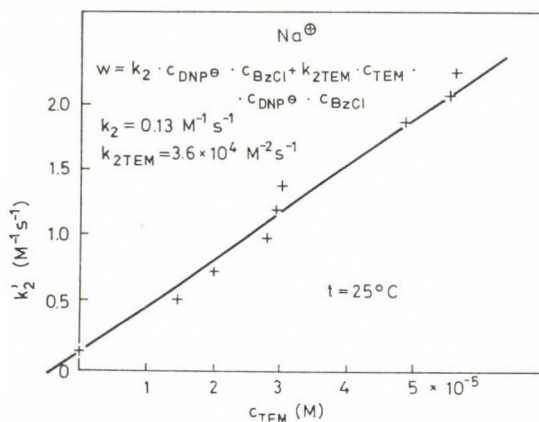


Fig. 1. Second order rate constant of the reaction  $\text{DNP}^{\ominus}\text{Na}^{\oplus} + \text{BzCl}$  as a function of TEMEDA concentration

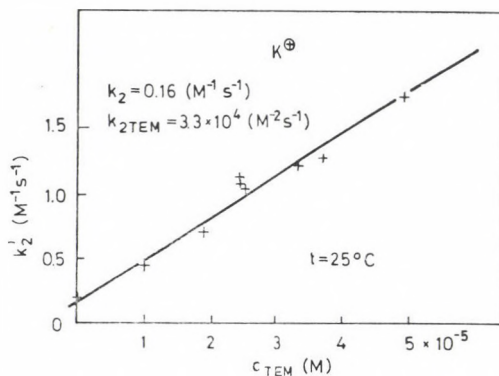


Fig. 2. Second order rate constant of the reaction  $\text{DNP}^{\ominus}\text{K}^{\oplus} + \text{BzCl}$  as a function of TEMEDA concentration

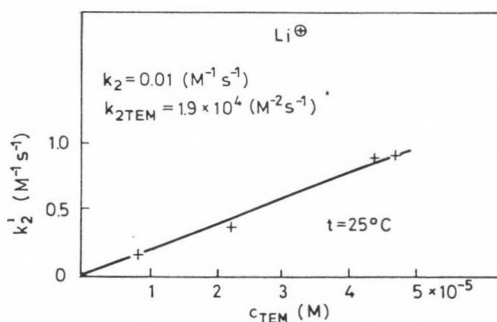
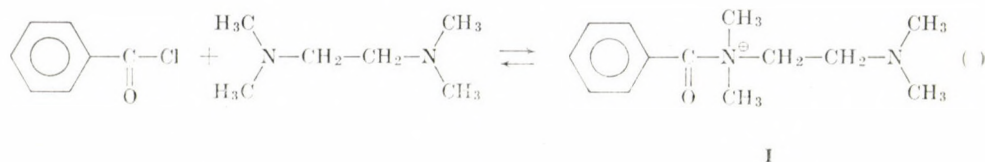


Fig. 3. Second order rate constant of the reaction  $\text{DNP}^{\ominus}\text{Li}^{\oplus} + \text{BzCl}$  as a function of TEMEDA concentration

Kinetics equation (4) can be explained by supposing the formation of and catalysis by the acylammonium ion **I** if its concentration is either small or stationary  $\left(\frac{dc\mathbf{I}}{d\tau} \approx 0\right)$ .



In non-phase-transfer acylations, this is a generally accepted way of catalysis. In tertiary amine catalyzed phase-transfer acylation processes, the acylammonium ion must also play a role.

Based on Eq. (4), the homogeneous catalytic effect can be evaluated.

As Table I and Figs 1–3 show,  $k_{2,\text{TEM}}$  is almost the same ( $3.6 \times 10^{-4}$  and  $3.3 \times 10^{-4} \text{ M}^{-2} \text{ s}^{-1}$  respectively) in presence of sodium and potassium ions. With lithium, it is remarkably lower ( $1.9 \times 10^{-4} \text{ M}^{-2} \text{ s}^{-1}$ ). The difference in the behaviour of the lithium salt can be explained by supposing a weaker dissociation of the ion pair.

In addition to its electrophilicity-increasing effect, acylammonium ion **I** can have a phase-transferring power. On the basis of this statement, we constructed a model for solid–liquid phase-transfer acylation processes catalyzed by tertiary amines (Fig. 4). Without any catalysis, nucleophilic species can enter into the organic phase at a low concentration. When an amine is present, the reaction is faster (homogeneous catalysis).

The acylammonium ion (if its concentration is high enough) acts also as a phase-transfer catalyst (phase-transfer catalysis in Fig. 4).

Both effect can contribute to determine the overall rate of the process.

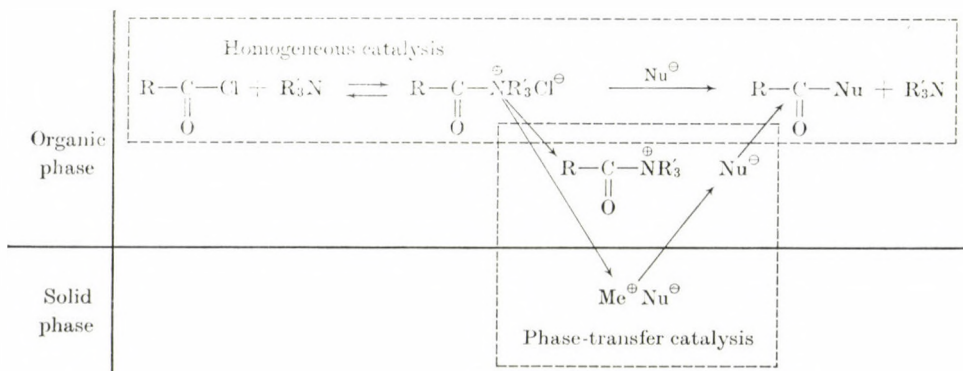


Fig. 4. Catalytic effect of a tertiary amine on phase transfer acylation

Experiments checking the validity of this model are in progress.\*

We also examined the catalytic activity of some other tertiary amines (see Table I). Pyridine, DBN and TEA were less active than TEMEDA. In a homogeneous reaction, DAP was found to have a very strong catalytic effect, so we wish to try it as phase-transfer catalyst.

#### REFERENCES

- [1] TÓKE, L., SZABÓ, G. T.: *Acta Chim. (Budapest)* **93**, 421 (1977)
- [2] TÓKE, L., SZABÓ, G. T., ARANYOSI, K.: *Acta Chim. Acad. Sci. Hung.*, **100**, 257 (1979)
- [3] TÓKE, L., SZABÓ, G. T., SOMOGYI-WERNER, K.: *Acta Chim. Acad. Sci. Hung.*, **101**, 47 (1979)
- [4] SZABÓ, G. T., ARANYOSI, K., TÓKE, L.: *Acta Chim. Acad. Sci. Hung.* (in press)
- [5] VORBRÜGGEN, H., KOTTWITZ, I., KROLIKIEWICZ, J.: *Chem. Ber.* (in press)
- [6] HÖFLE, G., STEGLICH, W., VORBRÜGGEN, H.: *Angew. Chem.*, **90**, 602 (1978)
- [7] NORMANT, H., CUVIGNY, T., SAVIGNAC, P.: *Synthesis*, **1975**, 805
- [8] GOKEL, W., GARCIA, B. I.: *Tetrahedron Lett.*, **1978**, 1743
- [9] WEBER, W. P., GOKEL, G. W.: *Phase Transfer Catalysis in Organic Synthesis*, p. 14. Springer Verlag, Berlin, Heidelberg, New York 1977

Gábor Tamás SZABÓ  
Katalin ARANYOSI  
László TÓKE

H-1502 Budapest, Műegyetem rkp. 3.

\* One of the results of our preliminary experiments: i) When stirring 0.4 g ( $1.9 \times 10^{-3}$  mol) of solid DNP Na salt with 10 mL benzene solution of 0.12 g ( $8.5 \times 10^{-4}$  mol) of benzoyl chloride, no reaction occurs ( $t = 25^\circ\text{C}$ , stirring rate = 500 rpm, 4 h). ii) After addition of 0.3 mg ( $2.6 \times 10^{-6}$  mol) of TEMEDA to this system and stirring for 4 h, 50% conversion can be observed. Analysis of the kinetics shows a probably diffusion controlled process. The initial reaction rate is  $w = 3.3 \times 10^{-8} \frac{\text{mol}}{\text{s}}$ . Had no phase-transfer catalysis occurred, the starting reaction rate would have been  $w = 1.0 \times 10^{-8} \frac{\text{mol}}{\text{s}}$ .

## REACTIONS OF MONO- AND DIARYLIDENECYCLOALKANONES WITH THIOUREA AND AMMONIUM THIOCYANATE, VI\*

Z-E-ISOMERIZATION OF 2-ALKYLMERCAPTO-4-PHENYL-8-  
-BENZYLIDENE-5,6,7,8-TETRAHYDROQUINAZOLINES

T. LÓRÁND<sup>1</sup>, D. SZABÓ<sup>1\*\*</sup>, A. FÖLDESI<sup>2</sup> and A. NESZMÉLYI<sup>3</sup>

<sup>1</sup> *Chemical Department, Medical University, Pécs,*

<sup>2</sup> *Theoretical Central Laboratory, Medical University, Pécs and*

<sup>3</sup> *Central Chemical Research Institute, Hungarian Academy of Sciences, Budapest*

Received January 27, 1981

In revised form May 29, 1981

Accepted for publication August 28, 1981

Compounds **IIIa–g** having the known *E*-configuration were converted into the *Z* isomers (**IVa–g**) by photoisomerization, and these isomers were isolated in the pure state in the case of compounds **IVa–c** and **IVe**; the <sup>1</sup>H-NMR technique has been employed to develop a method suitable for the determination of these isomers in the presence of each other. The structures of **IVa–g** were confirmed partly by thermal isomerization catalyzed by I<sub>2</sub>, partly by spectroscopic methods (UV, <sup>1</sup>H-NMR, <sup>13</sup>C-NMR). The equilibrium of photoisomerization was also investigated from both directions and the characteristic constants of the equilibrium were calculated.

*Z-E* isomerization processes have been known for a long time. In certain cases this is the only method for the preparation of a given isomer. Most researchers studied the isomerization of olefins on stilbene and its derivatives [2–4]; attention has been paid to the isomerization of unsaturated dicarboxylic acids [3–5] and carotenoids belonging to the natural polyenes [8]. There are only few papers dealing with isomerizations taking place in the side-chain of heterocyclic compounds [9–10].

In the previous papers the synthesis of some 2-alkylmercaptohexahydroquinazoline derivatives (**Ia–g** salts and **IIa–g**, bases) [11] was described these yielded 2-alkylmercaptotetrahydroquinazoline derivatives (**IIIa–g**) on oxidation [12].

Compounds **IIIa–g** were prepared by two methods: singlet O<sub>2</sub> or potassium hexacyanoferrate were used in the oxidation reaction. In the first method two products were obtained in some cases. This was indicated by the <sup>1</sup>H-NMR spectrum: in the reaction of **Ie**, the following signals appeared in the spectrum, beside those belonging to **IIIe** [12]: δ 0.8 ppm (t) (CH<sub>3</sub>), δ 2.3 ppm (t) (SCH<sub>2</sub>), δ 6.7 ppm (t) (=CH); this latter signal very probably corresponds to the ole-

\* Part V: Ref. [1]

\*\* To whom correspondence should be addressed

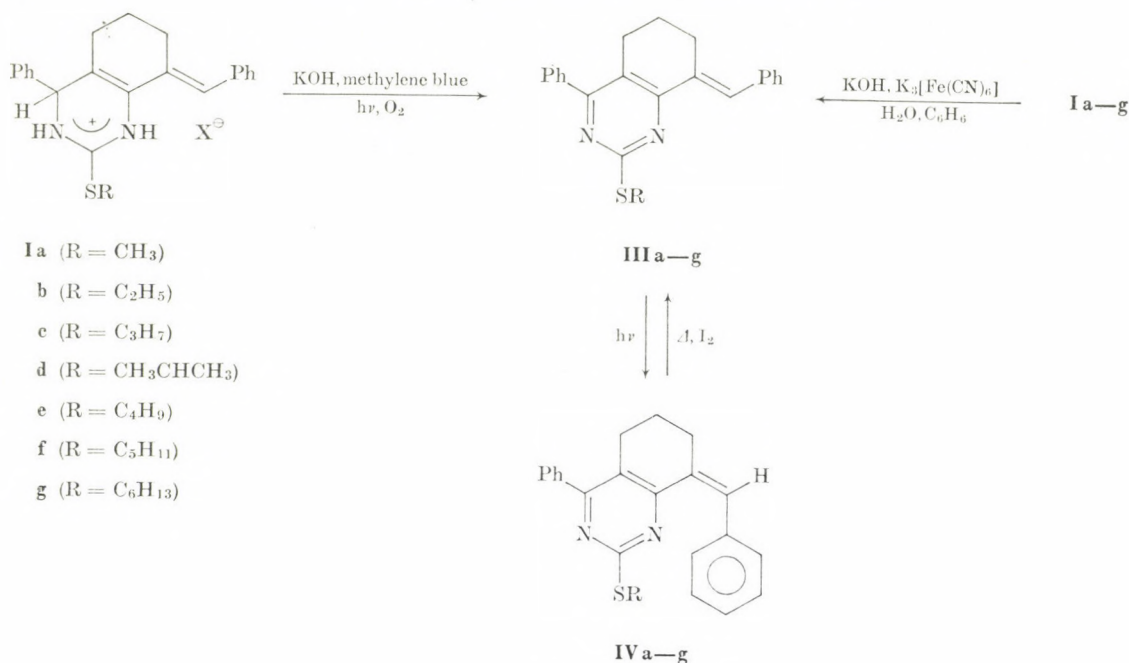


Fig. 1

finic proton at  $\delta$  8.2 ppm in **IIIe**. This fact pointed to the possibility of *Z-E* isomerization. (It must be noted that oxidation with  $\text{K}_3[\text{Fe}(\text{CN})_6]$  never yielded an isomeric mixture, **IIIa-g** were always obtained.)

In the present work we aimed at: (a) an investigation and confirmation of *Z-E* isomerization in the above case; (b) preparation of *Z* isomers (**IVa-g**) corresponding to **IIIa-g** and verification of their structures; (c) studying the isomerization equilibrium.

First, the mixture of *Z-E* isomers (**IIIe** + **IVe**) obtained in the above aromatization reactions was refluxed with iodine in toluene to effect the thermal isomerization catalyzed by a halogen [13]. After refluxing for 3 hours, only **IIIe** could be detected in the reaction mixture by the  $^1\text{H-NMR}$  technique. (The composition of the isomeric mixture was examined in all cases without recording the whole spectrum, only by measuring the integral of the olefin protons.)

Preparation of the *Z* isomers **IVa-g** was achieved by photoisomerization. Traces of methylene blue were present in the solution. (In the absence of this reagent, the products were more contaminated, having a deeper yellow colour). The duration of illumination was determined from the equilibrium experiments, and it was usually 15 h. Under these conditions the equilibrium concentration of the *Z* isomer was obtained. (Photoisomerization effected in the absence of methylene blue yielded the same equilibrium ratio of the *Z*

isomer also after 15 h.) Separation of the **IIIa–g** and **IVa–g** isomer pairs by the TLC technique failed with the solvents employed by us; however, good results were obtained by the HPLC technique (see Experimental).

The structures **IVa–g** were confirmed by the elemental analysis data and spectral results (UV,  $^1\text{H-NMR}$ ,  $^{13}\text{C-NMR}$ ) (Table I). (Raman spectra and IR spectra of **IVa–c** and **e** in comparison with the corresponding *E* isomers will be discussed in a later paper.)

In the  $^1\text{H-NMR}$  spectrum of **IVa**, the signal of the methyl group was shifted diamagnetically, due to the effect of the phenyl ring in the arylidene group (**IIIa**:  $\delta$  2.6 ppm, **IVa**:  $\delta$  1.7 ppm), the signal of the  $\text{CH}_2$  protons in the cyclohexene ring remained practically unchanged. The change in the shift of the only olefinic proton is the most significant in the whole spectrum (**IIIa**:  $\delta$  8.2 ppm, **IVa**:  $\delta$  6.8 ppm), and this change also points to the *Z* isomer [12, 14]. The structure of the aromatic multiplet is also significantly altered.

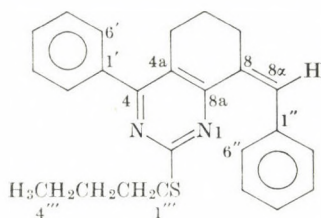
Table I

Compound	M.p., °C	Molecular formula M.w. Yield, %	UV (ethanol)		$^1\text{H-NMR}$ $\delta$ ppm, CDCl
			$\lambda_{\text{max}}$ (nm)	log $\epsilon$	
<b>IVa</b>	103–108	$\text{C}_{22}\text{H}_{20}\text{N}_2\text{S}$ 344.48 57 <sup>a</sup>	260	4.41	1.7 s 3H $\text{SCH}_3$
			345	4.08	1.6–2.2} m 6H $\text{CH}_2$ 2.5–2.9} t 1H =CH 6.8 m 10H Ar 7.1–7.5
<b>IVb</b>	85–90	$\text{C}_{23}\text{H}_{22}\text{N}_2\text{S}$ 358.51 19 <sup>a</sup>	260	4.42	1.0 t 3H $\text{CH}_3$
			345	4.04	1.5–2.1} m 6H $\text{CH}_2$ 2.4–2.9} q 2H $\text{SCH}_3$ $J=6$ Hz 2.3 t 1H =CH 6.7 m 10H Ar 7.0–7.6
<b>IVc</b>	134–137	$\text{C}_{24}\text{H}_{24}\text{N}_2\text{S}$ 372.53 62 <sup>a</sup>	261	4.42	0.8 t 3H $\text{CH}_3$
			346	4.06	1.1–2.1} m 8H $\text{CH}_2$ 2.5–3.0} t <sup>b</sup> 2H $\text{SCH}_3$ 2.3 s 1H =CH 6.7 m 10H Ar 7.2–7.7
<b>IVe</b>	110–114	$\text{C}_{25}\text{H}_{26}\text{N}_2\text{S}$ 386.57 60 <sup>a</sup>	261	4.43	0.8 t <sup>b</sup> 3H $\text{CH}_3$
			346	4.08	1.0–2.1} m 10H $\text{CH}_2$ 2.5–2.9} t <sup>b</sup> 2H $\text{SCH}_3$ 2.3 t 1H =CH 6.7 m 10H Ar <sup>c</sup> 7.1–7.7

<sup>a</sup> Yields are expressed in percentage of the 100% "ideal" conversion by isomerization; the substance obtained in pure, crystalline state is considered

<sup>b</sup> First order approximation

<sup>c</sup> Compounds **IVd**, **IVf** and **IVg** could not be isolated in the pure state. The clearly assigned signals characteristic of them in the  $^1\text{H-NMR}$  spectra are the following: **IVd**  $\delta$  1.05 ppm (d) 3H  $\text{CH}_3$  (**IIIc**:  $\delta$  1.5 ppm),  $\delta$  6.8 ppm (t) 1H =CH (**IIIc**:  $\delta$  8.2 ppm); **IVf**  $\delta$  0.8 (t<sup>b</sup>) 3H  $\text{CH}_3$ ,  $\delta$  2.3 (t<sup>b</sup>) 2H  $\text{SCH}_3$ ,  $\delta$  6.8 ppm (t) 1H =CH; **IVg**  $\delta$  0.8 pp. (t<sup>b</sup>) 3H  $\text{CH}_3$ ,  $\delta$  2.3 ppm (t<sup>b</sup>) 2H  $\text{SCH}_3$ ,  $\delta$  6.8 ppm (t) 1H =CH



IVe

Fig. 2

In the  $^1\text{H-NMR}$  spectra of **IVb–g**, the shift changes for group R decrease with increasing R, as compared with the corresponding **IIIb–e**, compounds, except the signal assigned to  $\text{SCH}_2$  (cf. Table I) [12].

In the  $^{13}\text{C-NMR}$  spectrum, the *Z-E* isomerism results in altered shifts for each aromatic C in the benzal group and at C-7, since the benzalphenyl

Table II

Assignment	IIIe	IVe
	Chemical shift	Chemical shift
	$\delta$ ppm	$\delta$ ppm
4'''	13.8	13.7
6	22.3	21.9
3'''	22.8	23.5
2'''	27.2	26.8
1'''	27.8	29.7
5	30.8	31.1
7	31.8	33.9
8a	122.2	123.1
4*	127.6	126.7
2'', 6''	129.9 <sup>b</sup>	128.8 <sup>b</sup>
3'', 5''	128.3 <sup>b</sup>	127.8 <sup>b</sup>
3', 5'	129.1 <sup>a,c</sup>	128.9 <sup>a,c</sup>
2', 6'	128.2 <sup>c</sup>	128.2 <sup>c</sup>
4''	131.0	133.3
8	134.0	134.6
1''	137.3	138.6
1'	138.3	138.3
4a	160.6	160.9
4	166.3	166.4
2	168.3	168.2

<sup>a</sup> The signal assigned to C-8 $\alpha$  can be found at the same site

<sup>b,c</sup> Shifts with the same alphabetical notation are interchangeable

group is not coplanar with the molecule. It is noteworthy, that the signal of the  $\text{SCH}_2$  group in the alkyl chain is paramagnetically shifted, owing to the steric vicinity which is also demonstrated by the Dreiding model (see Fig. 2 and Table II).

In the UV spectra (*cf.* Table I) two maxima appear; both of them suffered some hypsochromic shift as compared with the corresponding maxima in **IIIa–g** (**IVa**:  $\lambda_1$  260 nm,  $\lambda_2$  345 nm; **IIIa**:  $\lambda_1$  265 nm,  $\lambda_2$  350 nm). This phenomenon often occurs with *Z-E* isomers [15].

The equilibria of the photoisomerization reactions were also studied and the results are summarized in Table III and Fig. 3.

The isomerization mixture attained equilibrium after 15 h at 38 °C, where the *Z* isomer is present, on the average, in 70%, practically irrespective of the nature of R, when considering the error of measurement. The preponderance of the *Z* isomer can be understood when taking into account that at the wave length of irradiation ( $\lambda$  366 nm) the extinction coefficients the *E* isomers **IIIa–g** are higher than those of the corresponding *Z* isomers **IVa–g** (**IIIa**:  $\epsilon_{366 \text{ nm}}$ : 10 700; **IVa**:  $\epsilon_{366 \text{ nm}}$ : 6940) [16].

The equilibrium of photoisomerization was also investigated starting from the *Z* isomer: compound **IVa** was irradiated at 38 °C. After 15 h, the equilibrium concentration of isomer *Z* was obtained ( $72.3 \pm 5.3\%$ ).

Table III

Compound	<i>Z</i> isomer at equilibrium, % ( <i>t</i> = 38 °C)	<i>K</i> <i>Z/E</i>	$G_{Z-E}^0$	
			Kcal/mol	Joule/mole · 10 <sup>3</sup>
<b>IVa</b>	67.7 ± 2.8	2.09 ± 0.27	-0.456 ± 0.079	-1.91 ± 0.331
<b>IVb</b>	71.8 ± 1.3	2.54 ± 0.16	-0.577 ± 0.040	-2.42 ± 0.167
<b>IVe</b>	73.0 ± 1.8	2.70 ± 0.25	-0.614 ± 0.056	-2.57 ± 0.234
<b>IVg</b>	68.2 ± 1.5	2.15 ± 0.15	-0.472 ± 0.042	-1.98 ± 0.176

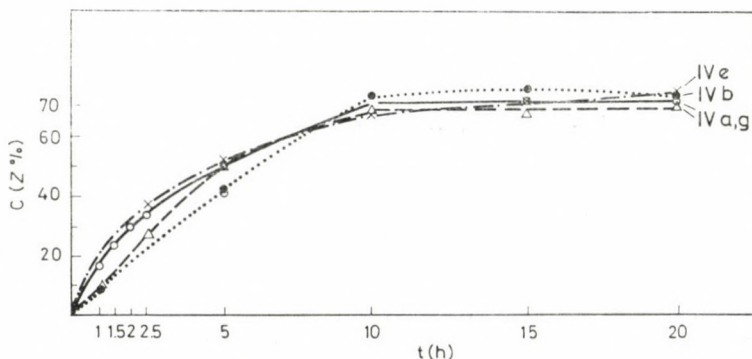


Fig. 3

## Experimental

The  $^1\text{H-NMR}$  spectra were recorded with a Perkin-Elmer R-12 (60 MHz) spectrometer. The  $^{13}\text{C-NMR}$  spectrum of **IVe** was obtained with a VARIAN XL-100-15 FT (25.16 MHz) instrument in  $\text{CDCl}_3$  at  $50^\circ\text{C}$ , internal standard TMS. The UV spectra were recorded with a HITACHI 124 spectrometer. In the irradiation reactions the UV lamp used was Analysenlampe, Hanau,  $\lambda$  366 nm, power: 125 W. In the reactions, external illumination was employed. The elemental analysis data were within the limits of experimental error.

Preparation of the starting materials **IIIa-g** has already been published [12].

### Photoisomerization of 2-alkylmercapto-4-phenyl-8-*E*-benzylidene-5,6,7,8-tetrahydroquinazolines

#### 2-Methylmercapto-4-phenyl-8-*Z*-benzylidene-5,6,7,8-tetrahydroquinazoline (IVa)

Compound **IIIa** (1 g; 0.0029 mole) and methylene blue (5 mg) were dissolved in methanol (300 mL), and the solution was externally illuminated with a UV lamp in an Erlenmeyer flask (Ergon) at  $38^\circ\text{C}$  for 15 h. At the end of the reaction, the precipitate was filtered off, washed until colourless with cold methanol; according to the  $^1\text{H-NMR}$  spectrum, this was the *Z* isomer. The mother liquor was evaporated to dryness, and the evaporation residue was dissolved in benzene. This solution was washed with 10% HCl and water until colourless, then dried over  $\text{MgSO}_4$ . After evaporation of the solution, the oily residue was subjected to fractional crystallization from methanol. The purity of the fractions was checked by the  $^1\text{H-NMR}$  technique as stated above.

Preparation of **IVb, c, e** was effected similarly, by the irradiation of the corresponding compounds, **IIIb, c, e**. The amounts of compounds **IVd, f** and **g**, not isolated in the pure state, were estimated on the basis of the  $^1\text{H-NMR}$  spectra again; the *Z* isomers were present in about 70% (see Table III, compound **IVg**).

#### Thermal isomerization of 2-butylmercapto-4-phenyl-8-*Z*-benzylidene-5,6,7,8-tetrahydroquinazoline (IVe) catalyzed by iodine

A mixture of **IIIe** and **IVe** (46% and 54%) (0.16 g; 0.00043 mole) was dissolved in toluene (100 mL) and  $\text{I}_2$  (50 mg) was added to the solution. After refluxing for 3 h, the  $^1\text{H-NMR}$  spectrum showed no *Z* isomer in the mixture. The brown solution was washed with a solution of  $\text{Na}_2\text{S}_2\text{O}_3$ , then with water and dried over anhydrous  $\text{MgSO}_4$ . The toluene solution was evaporated to dryness and the oily residue crystallized from methanol to obtain **IIIe** (0.11 g; 69%).

#### Investigations on the photoisomerization equilibria of **IIIa, b, c, g**

Compound **IIIa, b, e** or **g** (1 g) was dissolved in methanol (300 mL) and methylene blue (5 mg) was added to the solution, which was then irradiated externally with a UV lamp, in an Erlenmeyer flask (Ergon). Samples were withdrawn periodically from the reaction mixture and, after evaporation to dryness, the  $^1\text{H-NMR}$  spectrum of the oil obtained was recorded to determine the isomeric composition of the mixture (see Fig. 3).

#### Experimental conditions for the separation of **IIIa** and **IVa** by the HPLC technique

A Liquochrom 307 instrument was used with a column of 20 cm  $\times$  4.2 mm dimensions packed with Partisil 10  $\mu$ ; the eluent was benzene. Flow rate (*F*): 1.34 cm<sup>3</sup>/min, the column pressure drop was 37 bar. Detection: UV spectrophotometric detector, the volume of the cell: 8  $\mu\text{L}$ ,  $\lambda$  276 nm, *A* = 0.1. Results: **IIIa**: *k'* 0.94; **IVa**: *k'* 1.79; **IIIa**: *t<sub>R</sub>* 2.35 min; **IVa**: *t<sub>R</sub>* 3.40 min; peak resolution (*R<sub>s</sub>*): 4.2.

\*

The authors' thanks are due to Dr. R. OHMACHT for the IR spectra, to Dr. P. MOLNÁR and Dr. Mrs. L. KISIMRE for the UV spectra, to Miss É. TÓTH for the  $^1\text{H-NMR}$  spectra to Mrs. M. OTT and Dr. R. OHMACHT for the analyses, to Mr. Z. MATUS for the HPLC separations and to Miss E. MÁTRAI, Miss H. TENCZ and Mrs. E. BLESZITY for technical assistance.

## REFERENCES

- [1] LÓRÁND, T., SZABÓ, D., FÖLDESI, A., NESZMÉLYI, A.: Acta Chim. Acad. Sci. Hung. **108**, 197 (1981)
- [2] FISCHER, G., MUSCHAT, A., FISCHER, E.: J. Chem. Soc., (B), **1968**, 1156
- [3] MUSCHAT, K. A., GEGIOU, D., FISCHER, E.: J. Am. Chem. Soc., **89**, 4814 (1967)
- [4] BALLASTEV, M., ROSA, J.: Tetrahedron, **9**, 156 (1960)
- [5] OLSON, A. R., HUNDSON, F. L.: J. Am. Chem. Soc., **65**, 1410 (1930)
- [6] WISLICENUS, J.: Ber., **29**, 1080 (1897)
- [7] STÖRNER, R.: Ber., **42**, 4864; **44**, 637 (1911)
- [8] ZECHMEISTER, L.: *Cis-trans* Isomeric Carotenoids, Vitamins A and Arylpolyenes. Springer Verlag, Vienna 1962
- [9] ULLMANN, E. F.: J. Am. Chem. Soc., **90**, 4157 (1968)
- [10] BRODY, B. A., KENNEDY, J. A., O'SULLIVAN, W. I.: Tetrahedron, **29**, 359 (1973)
- [11] LÓRÁND, T., SZABÓ, D., FÖLDESI, A.: Acta Chim. Acad. Sci. Hung., **104**, 147 (1980)
- [12] LÓRÁND, T., SZABÓ, D., FÖLDESI, A., NESZMÉLYI, A.: Acta Chim. Acad. Sci. Hung. **108**, 91 (1981)
- [13] STEINMETZ, H., NOYES, R. M.: J. Am. Chem. Soc., **74**, 4141 (1952)
- [14] KEVILL, D. N., WEILER, E. D.; CROMWELL, N. H.: J. Org. Chem., **29**, 1276 (1964)
- [15] HOUBEN-WEYL: Methoden der organischen Chemie, Photochemie, Teilband I, p. 191. Vierte Auflage. Georg Thieme Verlag, Stuttgart 1975
- [16] CHAPMAN, O. L.: Organic Photochemistry. Vol. I. p. 205. Marcel Dekker, New York 1969

Tamás LÓRÁND

Dezso SZABÓ

András FÖLDESI

H-7643 Pécs, Szigeti út 12.

András NESZMÉLYI

H-1525 Budapest, Pusztaszeri út 57—59.

## INDEX

### PHYSICAL AND INORGANIC CHEMISTRY

<sup>1</sup> H-NMR- and Mössbauer Investigations on the Ion Pairs of Tetrachloroferrate(III) Anion with Quaternary Phosphonium Cations, L. VINCZE, S. PAPP .....	153
Calculation of Association Constants and Distribution of Contact and Dipolar Interactions for [R <sub>3</sub> P <sup>+</sup> R'] [FeCl <sub>4</sub> ] <sup>-</sup> Ion Pairs, L. VINCZE, S. PAPP .....	163
Oxidation of Alkali Metal Iodates in Molten Alkali Metal Nitrates, M. DRÁTOVSKÝ, E. DVOŘÁKOVÁ, Z. RYTIŘ .....	175
X-Ray Study of the Lattice Parameters of the Four Dichloro- <i>N</i> -sulfinylaniline Isomers, Z. CZERWIEC, Z. MANDECKI .....	183
Voltametric Determination of the Dissociation Constant of Glycolaldehyde and DL-Glyceraldehyde Bisulphites, S. BALOGH, GY. FARSANG, L. MAROS .....	191
Electrochemistry of Stainless Steels, I. Potentiodynamic Polarization Curves, GY. VÉRTES	203

### ORGANIC CHEMISTRY<sub>1</sub>

Synthesis of Some 3-Aroylflavones as Potential Fungicides, S. GIRI, NIZAMUDDIN, A. K. MISHRA .....	117
Synthesis of 5-Methoxy-2-(3,4-methylenedioxyphenyl)-4 <i>H</i> -furo[2,3- <i>h</i> ][1]-benzopyran-4-one and 5-Methoxy-2-phenyl-4 <i>H</i> -furo[2,3- <i>h</i> ][1]-benzopyran-4-one, V. P. PATHAK, G. P. GARG, R. N. KHANNA .....	123
Synthesis of Some New 2-Aryl-5-aryl/aryloxymethyl-1,3,4-oxadiazolo-[3,2- <i>a</i> ]- <i>s</i> -triazine-7-thiones and their Parent Thioureas as Potential Pesticides, B. K. BHATTACHARYA, H. SINGH, L. D. S. YADAV, G. HOORNAERT .....	133
Electronic Interactions in $\omega$ -Diphenylphosphinyl- <i>trans</i> -styrenes Substituted in Position 4 and in their Derivatives, K. -G. BERNDT, D. GLOYNA (in German) .....	145
Mössbauer Study of Iron-Sugar Complexes, M. TONKOVIĆ, S. MUSIĆ, O. HADŽIJA, I. NAGY-CZAKÓ, A. VÉRTES .....	197
Polyethylene Glycol Derivatives as Complexing Agents and Phase-Transfer Catalysts, IV. Behaviour of Phase-Transfer Catalysts in Solid-Liquid Phase Equilibria, G. T. SZABÓ, K. ARANYOSI, L. TŐKE .....	215
Polyethylene Glycols as Complexing Agents and Phase-Transfer Catalysts, V. Reaction Rates in the Organic Phase, G. T. SZABÓ, K. ARANYOSI, L. TŐKE .....	225
Reactions of Mono- and Diarylidencycloalkanones with Thiourea and Ammonium Thiocyanate, VI. <i>Z-E</i> -Isomerization of 2-Alkylmercapto-4-phenyl-8-benzylidene-5,6,7,8-tetrahydroquinazolines, T. LÓRÁND, D. SZABÓ, A. FÖLDESI, A. NESZMÉLYI	231

### ANALYTICAL CHEMISTRY

Polarographic Determination of Potential Guest Molecules in the Presence of Cyclodextrin, L. DARUHÁZI, J. SZEJTLI, L. BARCZA .....	127
--	-----

PRINTED IN HUNGARY

82.10267 Akadémiai Nyomda, Budapest

Les Acta Chimica paraissent en français, allemand, anglais et russe et publient des mémoires du domaine des sciences chimiques.

Les Acta Chimica sont publiés sous forme de fascicules. Quatre fascicules seront réunis en un volume (3 volumes par an).

On est prié d'envoyer les manuscrits destinés à la rédaction à l'adresse suivante:

*Acta Chimica*  
Budapest, P.O.B. 67, H-1450, Hongrie

Toute correspondance doit être envoyée à cette même adresse.

La rédaction ne rend pas de manuscrit.

Abonnement en Hongrie à l'Akadémiái Kiadó (1363 Budapest, P.O.B. 24, C. C. B. 215 11488), à l'étranger à l'Entreprise du Commerce Extérieur «Kultura» (H-1389 Budapest 62, P.O.B. 149. Compte-courant No. 218 10990) ou chez représentants à l'étranger.

---

Die Acta Chimica veröffentlichen Abhandlungen aus dem Bereich der chemischen Wissenschaften in deutscher, englischer, französischer und russischer Sprache.

Die Acta Chimica erscheinen in Heften wechselnden Umfangs. Vier Hefte bilden einen Band. Jährlich erscheinen 3 Bände.

Die zur Veröffentlichung bestimmten Manuskripte sind an folgende Adresse zu senden:

*Acta Chimica*  
Budapest, Postfach 67, H-1450, Ungarn

An die gleiche Anschrift ist jede für die Redaktion bestimmte Korrespondenz zu richten: Manuskripte werden nicht zurückerstattet.

Bestellbar für das Inland bei Akadémiái Kiadó (1363 Budapest, Postfach 24, Bankkonto Nr. 215 11488), für das Ausland bei »Kultura« Aussenhandelsunternehmen (H-1389 Budapest 62, P.O.B. 149. Bankkonto Nr. 218 10990) oder seinen Auslandsvertretungen.

---

«Acta Chimica» издают статки по химии на русском, английском, французском и немецком языках.

«Acta Chimica» выходит отдельными выпусками разного объёма, 4 выпуска составляют один том и за год выходят 3 тома.

Предназначенные для публикации рукописи следует направлять по адресу:

*Acta Chimica*  
Budapest, P.O.B. 67, H-1450, ВНР

Всякую корреспонденцию в редакцию направляйте по этому же адресу.

Редакция рукописей не возвращает.

Отечественные подписчики направляйте свои заявки по адресу Издательства Академии Наук (1363 Budapest, P.O.B. 24, Текущей счет 215 11488), а иностранные подписчики через организацию по внешней торговле «Kultura» (H-1389 Budapest 62, P.O.B. 149. Текущий счет 218 10990) или через ее заграничные представительства и уполномоченных.

Reviews of the Hungarian Academy of Sciences are obtainable  
at the following addresses:

**AUSTRALIA**

C B.D. LIBRARY AND SUBSCRIPTION SERVICE.  
Box 4886, G.P.O., Sydney N.S.W. 2001  
COSMOS BOOKSHOP, 145 Ackland Street, St.  
Kilda (Melbourne), Victoria 3182

**AUSTRIA**

GLOBUS, Höchstädtplatz 3, 1200 Wien XX

**BELGIUM**

OFFICE INTERNATIONAL DE LIBRAIRIE, 30  
Avenue Marnix, 1050 Bruxelles  
LIBRAIRIE DU MONDE ENTIER, 162 Rue du  
Midi, 1000 Bruxelles

**BULGARIA**

HEMUS, Bulvar Ruski 6, Sofia

**CANADA**

PANNONIA BOOKS, P.O. Box 1017, Postal Sta-  
tion "B", Toronto, Ontario M5T 2T8

**CHINA**

CNPICOR, Periodical Department, P.O. Box 50,  
Peking

**CZECHOSLOVAKIA**

MAD'ARSKÁ KULTURA, Národní tr'ada 22,  
115 33 Praha

PNS DOVOZ TISKU, Vinohradská 46, Praha 2

PNS DOVOZ TLACE, Bratislava 2

**DENMARK**

EJNAR MUNKSGAARD, Norregade 6, 1165  
Copenhagen

**FINLAND**

AKATEMINEN KIRJAKAUPPA, P.O. Box 128,  
SF-00101 Helsinki 10

**FRANCE**

EUROPÉRIODIQUES S.A., 31 Avenue de Ver-  
sailles, 78170 La Celle St. Cloud

LIBRAIRIE LAVOISIER, 11 rue Lavoisier 75008  
Paris

OFFICE INTERNATIONAL DE DOCUMENTA-  
TION ET LIBRAIRIE, 48 rue Gay-Lussac, 75240  
Paris Cedex 05

**GERMAN DEMOCRATIC REPUBLIC**

HAUS DER UNGARISCHEN KULTUR, Karl-  
Liebknecht-Strasse 9, DDR-102 Berlin

DEUTSCHE POST ZEITUNGSVERTRIEBSAMT,  
Strasse der Pariser Kommüne 3-4, DDR-104 Berlin

**GERMAN FEDERAL REPUBLIC**

KUNST UND WISSEN ERICH BIEBER, Postfach  
46, 7000 Stuttgart 1

**GREAT BRITAIN**

BLACKWELL'S PERIODICALS DIVISION, Hythe  
Bridge Street, Oxford OX1 2ET

BUMPUS, HALDANE AND MAXWELL LTD.,  
Cover Works, Olney Bucks MK46 4BN

COLLET'S HOLDINGS LTD., Denington Estate,  
Wellingborough, Northants NN8 2QT

WM. DAWSON AND SONS LTD., Cannon House,  
Folkestone, Kent CT19 5EE

H. K. LEWIS AND CO., 136 Gower Street, London  
WC1E 3BS

**GREECE**

KOSTARAKIS BROTHERS, International Book-  
sellers, 2 Hippokratous Street, Athens-143

**HOLLAND**

MEULENHOFF-BRUNA B.V., Beulingstraat 2,  
Amsterdam  
9-11, Den Haag

SWETS SUBSCRIPTION SERVICE 347b Heere-  
weg, Lisse

**INDIA**

ALLIED PUBLISHING PRIVATE LTD., 13/14  
Asaf Ali Road, New Delhi 110001

150 B-6 Mount Road, Madras 600002

INTERNATIONAL BOOK HOUSE PVT. LTD.,  
Madame Cama Road, Bombay 400069

THE STATE TRADING CORPORATION OF  
INDIA LTD., Books Import Division, Chandralok,  
36 Janpath, New Delhi 110001

**ITALY**

EUGENIO CARLUCCI, P.O. Box 252, 70100 Bari

INTERSCIENTIA, Via Mazzè 28, 10149 Torino

LIBERIA COMMISSIONARIA SANSONI, Via  
Lamarmora 45, 50121 Firenze

SANTO VANASIA, Via M. Macchi 58, 20124  
Milano

D. E. A., Via Lima 28, 00198 Roma

**JAPAN**

KINOKUNIYA BOOK-STORE CO. LTD., 17-7  
Shinjuku-ku 3 chome. Shinjuku-ku, Tokyo 160-91

MARUZEN COMPANY LTD., Book Department,  
P.O. Box 5050 Tokyo International, Tokyo 100-61

NAUKA LTD. IMPORT DEPARTMENT, 2-40-19  
Minami Ikebukuro, Toshima-ku, Tokyo 171

**KOREA**

CHULPANMUL, Phenjan

**NORWAY**

TANUM-CAMMERMEYER, Karl Johansgatan  
41-43, 1000 Oslo

**POLAND**

WEGIERSKI INSTYTUT KULTURY, Marszal-  
kowska 80, Warszawa

CKP I W ul. Towarowa 28 00-958 Warszawa

**ROUMANIA**

D. E. P., Bucureşti

ROMLIBRI, Str. Biserica Amzei 7, Bucureşti

**SOVIET UNION**

SOJUZPETCHATJ — IMPORT, Moscow

and the post offices in each town

MEZHDUNARODNAYA KNIGA, Moscow G-200

**SPAIN**

DIAZ DE SANTOS, Lagasca 95, Madrid 6

**SWEDEN**

ALMQVIST AND WIÖSELL, Gamla Brogatan 26,  
101 20 Stockholm

GUMPERS UNIVERSITETSBOKHANDEL AB.  
Box 346, 401 25 Göteborg 1

**SWITZERLAND**

KARGER LIBRI AG, Petersgraben 31, 4011 Basel

**USA**

EBSCO SUBSCRIPTION SERVICES, P.O. Box  
1943, Birmingham, Alabama 35201

F. W. FAXON COMPANY, INC., 15 Southwest  
Park, Westwood, Mass. 02090

THE MOORE-COTTRELL SUBSCRIPTION  
AGENCIES, North Cohocton, N. Y. 14868

READ-MORE PUBLICATIONS, INC., 140 Cedar  
Street, New York, N. Y. 10006

STECHELT-MACMILLAN, INC., 7250 Westfield  
Avenue, Pennsauken N. J. 08110

**VIETNAM**

XUNHASABA, 42, Hai Ba Trung, Hanoi

**YUGOSLAVIA**

JUGOSLAVENSKA KNJIGA, Terazije 27, Beograd  
FORUM, Vojvode Mišića 1, 21000 Novi Sad

# ACTA CHIMICA

ACADEMIAE SCIENTIARUM  
HUNGARICAE

ADIUVANTIBUS

M. T. BECK, R. BOGNÁR, GY. HARDY,  
K. LEMPert, B. LENGYEL, K. POLINSZKY,  
E. PUNGOR, G. SCHAY,  
Z. G. SZABÓ, P. TÉTÉNYI

REDIGUNT

F. MÁRTA et GY. DEÁK

TOMUS 110

FASCICULUS 3



AKADÉMIAI KIADÓ, BUDAPEST

1982

ACTA CHIM. ACAD. SCI. HUNG.

ACASA2 110 (3) 239-355 (1982)

# ACTA CHIMICA

A MAGYAR TUDOMÁNYOS AKADÉMIA  
KÉMIAI TUDOMÁNYOK OSZTÁLYÁNAK  
IDEGEN NYELVŰ KÖZLEMÉNYEI

FŐSZERKESZTŐ  
MÁRTA FERENC

SZERKESZTŐ  
DEÁK GYULA

TECHNIKAI SZERKESZTŐ  
HAZAI LÁSZLÓ

SZERKESZTŐ BIZOTTSÁG  
BECK T. MIHÁLY, BOGNÁR REZSŐ, HARDY GYULA,  
LEMPERT KÁROLY, LENGYEL BÉLA, POLINSZKY KÁROLY,  
PUNGOR ERNŐ, SCHAY GÉZA, SZABÓ ZOLTÁN,  
TÉTÉNYI PÁL

Acta Chimica is a journal for the publication of papers on all aspects of chemistry in English, German, French and Russian.

Acta Chimica is published in 3 volumes per year. Each volume consists of 4 issues of varying size.

Manuscripts should be sent to

*Acta Chimica*  
Budapest, P.O. Box 67, H-1450, Hungary

Correspondence with the editors should be sent to the same address. Manuscripts are not returned to the authors.

Hungarian subscribers should order from Akadémiai Kiadó, 1363 Budapest, P.O. Box 24. Account No. 215 11488.

Orders from other countries are to be sent to "Kultura" Foreign Trading Company (H-1389 Budapest 62, P.O. Box 149. Account No. 218 10990) or its representatives abroad.



# MULTIPLE STEADY STATES AND HYSTERESIS DURING STIRRED FLOW OXIDATION OF CEROUS ION BY BROMATE

EXPERIMENTS AND MODELS\*

K. BAR-ELI<sup>1</sup> and W. GEISELER<sup>2\*\*</sup>

<sup>1</sup> *Department of Chemistry, Tel-Aviv University, Tel-Aviv, Israel,*

<sup>2</sup> *Institute of Technical Chemistry, Technical University, Berlin, Germany)*

Received March 6, 1981

Accepted for publication April 20, 1981

Multiple steady states (bistability), threshold properties, and hysteresis behavior are observed when cerous ions are oxidized by acidic bromate in a continuously stirred tank reactor (CSTR). The theoretical behavior of the system is investigated under various experimental conditions by use of both a detailed and a simple model. The predictive abilities of the models are compared—with experimental findings. The agreement is remarkably good and thus gives further confidence to the mechanism used and to estimates of various rate constants applied.

## Introduction

The oxidation of cerous ions by acidic bromate which is one of the most important steps of the oscillating BELOUSOV—ZHABOTINSKII reaction [1] is a very complex reaction and exhibits peculiar kinetic features [2]. The kinetics have been studied by several investigators [2, 3]. All of the studies were conducted in batch reactors. A detailed mechanism has been proposed by NOYES, FIELD and THOMPSON [3] (NFT mechanism). Recently GEISELER and FÖLLNER [4] conducted the reaction in a continuously stirred tank reactor (CSTR). They observed that two different stable steady states may exist for identical input conditions. After a perturbation the system can either return to its previous steady state or move to the other one. BAR-ELI and NOYES [5] pointed out that all these phenomena are accounted for by the NFT mechanism. In a recent paper [6] they investigated the theoretical behavior of the system under various experimental conditions and predicted results of further feasible experiments. Their detailed calculations showed that the system being bistable can convert from one steady state to the other *via* a hysteresis loop. The hysteresis limits, *i.e.* the limits of the domain of bistability, depend sensitively on the rate constants of the mechanism and on the constraints of the system. Valuable

\* Presented on the joint session of the Working Committees on Reaction Kinetics and Catalysis, and Coordination Chemistry, Budapest, October 29, 1980.

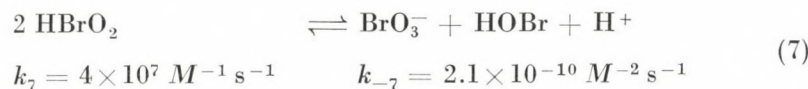
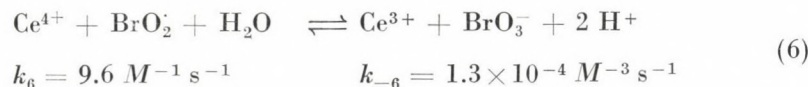
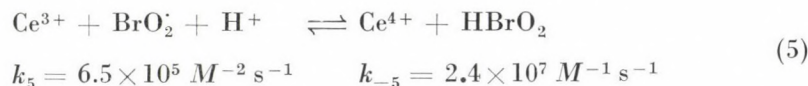
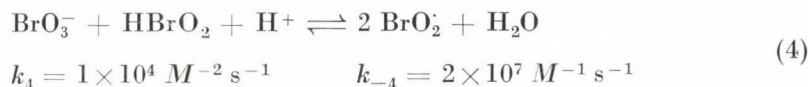
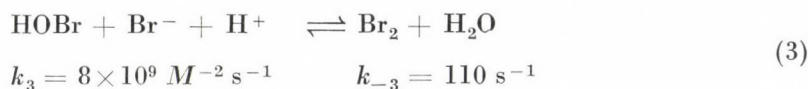
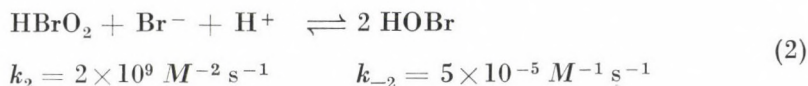
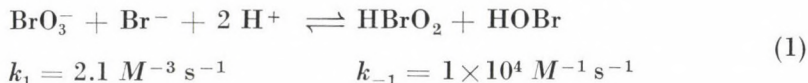
\*\* To whom correspondence should be addressed

information is therefore expected from studies of the hysteresis limits as function of the constraints. Comparison of calculated and measured limits could contribute independent tests that would serve either to refine the rate constant estimates or to refute the mechanism.

In the present paper we extend the investigations of BAR-ELI and NOYES [5, 6] for various experimental conditions. We compare previous and new calculated data with experimental results, check hysteresis limits and provide further support to the NFT mechanism. Moreover, we give accuracy limits for some of the rate constants used. We also investigate the predictive abilities of a reduced model of two variables which has been derived from the Oregonator model by GEISELER and FÖLLNER [4]. Recently TYSON [7] studied this model analytically and subsequently NOYES [8] made use of it when examining relative dynamic stabilities. Although the predictive power of the reduced model is restricted a priori due to several assumptions, it is shown to describe fairly well the characteristic features of the system.

### Mechanism and computations

The NFT mechanism consists of seven potentially reversible reactions, to which the indicated rate constants at 25 °C are assigned:



The rate constants are defined so that solvent water does not enter the rate expressions, but is treated as at unit activity. For each of the other nine chemical species in these equations the chemical mechanism generates a differential equation. To each such equation a term describing the outflow of chemicals from the CSTR was added. The four species  $\text{BrO}_3^-$ ,  $\text{Br}^-$ ,  $\text{Ce}^{3+}$  and  $\text{H}^+$  were assumed added to the reactor at a constant rate and instantaneously mixed as is done experimentally. For these species inflow terms were added to their differential equation. The rate of the inflow and outflow is described by  $k_0$ . This quantity is equal to  $T_R^{-1}$ , where  $T_R$  is the residence time of the CSTR. The stiff differential equation system thus formed was solved numerically by the method of GEAR [9] to obtain an estimate of  $dc_i/dt = 0$  and then Newton's method was used to pinpoint the concentrations at which  $\dot{c}_i = 0$ .

When only the hysteresis limits were necessary any steady state (SS) was calculated. Then one of the constraints was changed as slow as to remain on the same SS. When the limit was arrived at the solution suddenly jumped to a quite new SS. Slow enough changes in the constraints give the same results as the point by point calculation.

## Experimental

The experimental details and the device have been described elsewhere [4, 10]. The external parameters or constraints for the system are  $[\text{BrO}_3^-]_0$ ,  $[\text{Br}^-]_0$ ,  $[\text{Ce}^{3+}]_0$ , and  $[\text{H}^+]_0$  standing for the inflow concentrations,  $k_0$  and temperature. Temperature was held constant at 25 °C during all experiments. The concentration of bromide has been followed by an electrode specific to bromide ions (ORION Research Inc.). As a reference electrode we used the system  $\text{Hg}/\text{Hg}_2\text{SO}_4/\text{sat. K}_2\text{SO}_4$ .

## Computational and experimental results

### 1. Detailed model

Figure 1 shows calculated and measured hysteresis curves of the steady state bromide concentration as a function of the bromide inflow concentration. The values of the other constraints were constant and imitate the experimental conditions used by GEISELER and FÖLLNER [4]. The actual measured bromide concentrations at the steady states differ from the calculated ones due to the method of measurement, but they are unimportant in obtaining the hysteresis limits. These limits were reliably indicated by the bromide electrode. The same limits were obtained within experimental error, when a Pt electrode was used, thus giving confidence to the experimental procedure. Both the calculated and measured results show clearly the existence of two stable steady states (SSI and SSII). In between there exists an unstable steady state (SSIII) which is calculated only. Being an unstable SS it cannot appear experimentally.

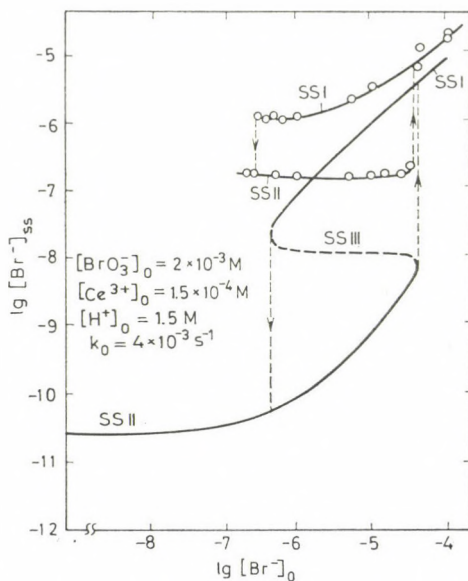


**Fig. 1.** Calculated and measured hysteresis loops: plot of  $\lg [\text{Br}^-]_{\text{ss}}$  vs.  $\lg [\text{Br}^-]_0$ . Solid line — calculated stable steady states SSI and SSII. Dashed line — calculated unstable steady states SSIII. Line with dots — measured steady states SSI and SSII. Other constraints:  $k_0 = 4 \times 10^{-3} \text{ s}^{-1}$ ,  $[\text{BrO}_3^-]_0 = 2 \times 10^{-3} \text{ M}$ ,  $[\text{Ce}^{3+}]_0 = 1.5 \times 10^{-4} \text{ M}$ ,  $[\text{H}^+]_0 = 1.5 \text{ M}$ . The arrows indicate the limits of the hysteresis loops and the direction of transitions

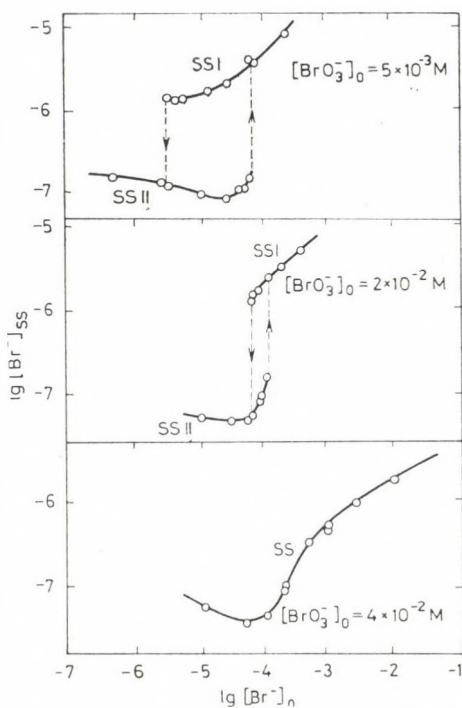


**Fig. 2.** Measured hysteresis loops for different values of  $[\text{BrO}_3^-]_0$ . Other constraints:  $k_a = 4 \times 10^{-3} \text{ s}^{-1}$ ,  $[\text{Ce}^{3+}]_0 = 1.5 \times 10^{-4} \text{ M}$ ,  $[\text{H}^+]_0 = 1.5 \text{ M}$

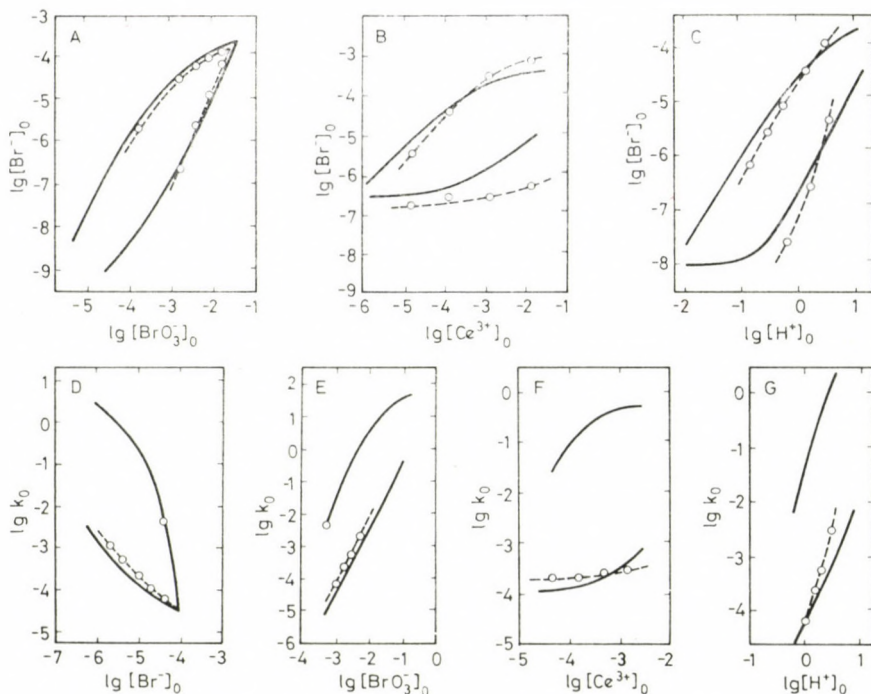


Fig. 3. Domains of bistability in various planes of the constraints: (A)  $\lg [\text{Br}^-]_0$  vs.  $\lg [\text{BrO}_3^-]_0$ , (B)  $\lg [\text{Br}^-]_0$  vs.  $\lg [\text{Ce}^{3+}]_0$ , (C)  $\lg [\text{Br}^-]_0$  vs.  $\lg [\text{H}^+]_0$ , (D)  $\lg k_0$  vs.  $\lg [\text{Br}^-]_0$ , (E)  $\lg k_0$  vs.  $\lg [\text{BrO}_3^-]_0$ , (F)  $\lg k_0$  vs.  $\lg [\text{Ce}^{3+}]_0$ , (G)  $\lg k_0$  vs.  $\lg [\text{H}^+]_0$ . The fixed constraints were:  $[\text{BrO}_3^-]_0 = 2 \times 10^{-3} M$ ,  $[\text{Br}^-]_0 = 1 \times 10^{-5} M$ ,  $[\text{Ce}^{3+}]_0 = 1.5 \times 10^{-4} M$ ,  $[\text{H}^+]_0 = 1.5 M$ , and  $k_0 = 4 \times 10^{-3} \text{ s}^{-1}$ . Solid lines — calculated limits, dashed line with dots — measured limits

In Fig. 2 are shown measured hysteresis curves for different bromate inflow concentration. As has been predicted in [6] the curves and its limits depend sensitively on the set of constraints used. In the present example the hysteresis curves shift to larger  $[\text{Br}^-]_0$  with increasing  $[\text{BrO}_3^-]_0$ . Thereby the limits approach each other and coincide at a sufficiently large  $[\text{BrO}_3^-]_0$ . For  $[\text{BrO}_3^-]_0 > 4 \times 10^{-2} M$  changing of  $[\text{Br}^-]_0$  causes only a smooth change in  $[\text{Br}^-]_{SS}$  without any hysteresis. Similar coalescence will occur of course also at very low values of  $[\text{BrO}_3^-]_0$ . These values of the constraints, however, are much below the experimental feasible ones.

The hysteresis limits which define the domain of bistability were calculated and measured for various sets of the constraints. The results are depicted in Fig. 3. Since we have five constraints,  $k_0$ ,  $[\text{Br}^-]_0$ ,  $[\text{BrO}_3^-]_0$ ,  $[\text{Ce}^{3+}]_0$ , and  $[\text{H}^+]_0$ , we can calculate and measure ten such domains of bistability in the 2-dimensional planes of the constraints, seven of which are shown in the Figure. No new information is expected from the other three domains of bistability.

Generally there is a good agreement between the calculated and measured data. Some deviations, however, occur in the limits of  $[\text{H}^+]_0$  vs.  $[\text{Br}^-]_0$  (C) and  $[\text{H}^+]_0$  vs.  $k_0$  (G) subspaces of the constraints. In these cases, changes in the activity coefficients can cause rather drastic changes in the rate constants, which are not accounted for in the model. At the moment we are unable to explain the rather strong deviation in the lower hysteresis limit of the subspace  $[\text{Ce}^{3+}]_0$  vs.  $[\text{Br}^-]_0$  (B), however, similar deviation is observed, when  $\text{Mn}^{2+}$  is used instead of  $\text{Ce}^{3+}$  [11]. Other deviations occur near the limits of the bistability. In these cases there is a tendency for the measured limits to approach each other faster than the calculated ones. This is most clearly seen in (A).

The computed results obtained above depend only on the rate constants of the reactions (1)–(7) and the applied constraints. Some of the rate constants were obtained earlier [3] on the basis of kinetic and thermodynamic arguments, while others were measured directly. The agreement between measured and computed data proves that the NFT mechanism used is basically correct and only slight variations in the rate constants may be needed to improve it. Of course, only those rate constants which influence the hysteresis limits most drastically can be reestimated. Taking into consideration the thermodynamic constraints we find that the sensitive rate constants are probably correct within a factor of two or even less.

## 2. Simple model

As has been shown by GEISELER and FÖLLNER [4] the full NFT mechanism can be reduced so that the kinetics of the bistable system can be described by four essential reaction steps:



with the rate constants at 25 °C:

$$k_{R3} = 2.1 \text{ M}^{-1} \text{ s}^{-1}$$

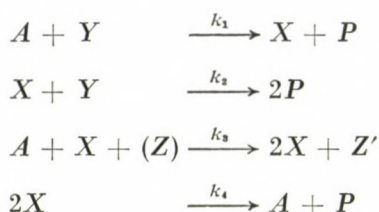
$$k_{R2} = 2 \times 10^9 \text{ M}^{-2} \text{ s}^{-1}$$

$$k_{R5} = 1 \times 10^4 \text{ M}^{-2} \text{ s}^{-1}$$

$$k_{R4} = 4 \times 10^7 \text{ M}^{-1} \text{ s}^{-1}.$$

The reaction (10) is an autocatalytic and consecutive one with the first step being rate limiting.

By introducing appropriate abbreviations we obtain a simple reaction scheme:



with  $A \equiv \text{BrO}_3^-$ ,  $P \equiv \text{HOBr}$ ,  $X \equiv \text{HBrO}_2$ ,  $Y \equiv \text{Br}^-$ ,  $Z \equiv 2 \text{Ce}^{3+}$ , and  $Z' \equiv 2 \text{Ce}^{4+}$ . The new rate constants are given by:

$$k_1 = k_{R3} [\text{H}^+]^2$$

$$k_2 = k_{R2} [\text{H}^+]$$

$$k_3 = k_{R5} [\text{H}^+]$$

$$k_4 = k_{R4}$$

Since the reactions are treated as irreversible and acidity effects are included in the rate constants, we can derive from this scheme a differential equation system, which contains only four chemical species, namely  $A$ ,  $X$ ,  $Y$ , and  $Z$  standing for the concentrations of bromate, bromous acid, bromide, and cerous ion:

$$\frac{dX}{dT} = k_1 AY - k_2 XY + k_3 AX - 2k_4 X^2 - k_0 X \quad (12)$$

$$\frac{dY}{dT} = -k_1 AY - k_2 XY + k_0(Y_0 - Y) \quad (13)$$

$$\frac{dZ}{dT} = -2k_3 AXZ + k_0(Z_0 - Z). \quad (14)$$

The differential equation system includes again additional terms describing material flux due to the-flow reactor,  $k_0(c_{i0} - c_i)$ .

A further simplification was made by assuming that the bromate concentration, being in large excess, is equal to that of the inflow concentration. In other words  $A = A_0 = \text{constant}$  and the appropriate differential equation is therefore omitted.

On closer inspection of the equation system we realize that the differential equation of  $Z$  (cerous ion) can be integrated once the solution of  $X(T)$  is

known. Thus the differential equation system reduces to two variables:

$$\frac{dX}{dT} = k_1AY - k_2XY + k_3AX - 2k_4X^2 - k_0X = F(X, Y) \quad (15)$$

$$\frac{dY}{dT} = -k_1AY - k_2XY + k_0(Y_0 - Y) = G(X, Y). \quad (16)$$

Such systems can be investigated by means of some well established mathematical methods. Since we are interested in the steady states, we first determine the equations of the isocline by division of  $G(X, Y)$  by  $F(X, Y)$ :

$$\frac{dY}{dX} = \frac{-k_1AY - k_2XY + k_0(Y_0 - Y)}{k_1AY - k_2XY + k_3AX - 2k_4X^2 - k_0X}. \quad (17)$$

Since  $G(X, Y)$  and  $F(X, Y)$  do not depend explicitly on time, time  $T$  is eliminated by this procedure. The solution of this equation defines trajectories of the system in the  $X, Y$  phase plane. The intersections of the isoclines represent the steady states of the system. They can be calculated easily by means of the nullclines, which can be derived from the general equation of the isocline:

$$\text{Nullcline } I_0(dY/dT = 0): \quad Y = \frac{k_0Y_0}{k_1A + k_0 + k_2X} \quad (18)$$

$$\text{Nullcline } I_\infty(dX/dT = 0): \quad Y = \frac{2k_4X^2 - (k_3A - k_0)X}{k_1A - k_2X}. \quad (19)$$

Both of them represent hyperbolas. When calculating the SS we obtain a cubic equation:

$$X^3 - \frac{k_2(k_3A - k_0) - 2k_4(k_1A + k_0)}{2k_2k_4} X^2 + \frac{k_0k_2Y_0 - (k_3A - k_0)(k_1A + k_0)}{2k_2k_4} X - \frac{k_0k_1AY_0}{2k_2k_4} = 0. \quad (20)$$

From the sequence of the signs of the coefficients (+ - + -) we conclude that three SS may exist in the physically relevant positive quadrant provided that the parameters  $k_0$  and  $Y_0$  are suitable chosen.

Indeed, with the actual parameters and constraints of the system we calculate three stationary solutions of  $X$  ( $\text{HBrO}_2$ ) for certain values of the constraint  $Y_0$  (bromide inflow concentration  $[\text{Br}^-]_0$ ). The computed results are shown in Fig. 4. The stationary concentrations of the variable  $Y$  ( $\text{Br}^-$ ) are calculated *via* the nulleline equation. The general shape of the curves resembles very well to the corresponding curves obtained from the detailed model [6]. The curve of  $X$  is z-shaped and the stationary concentrations of

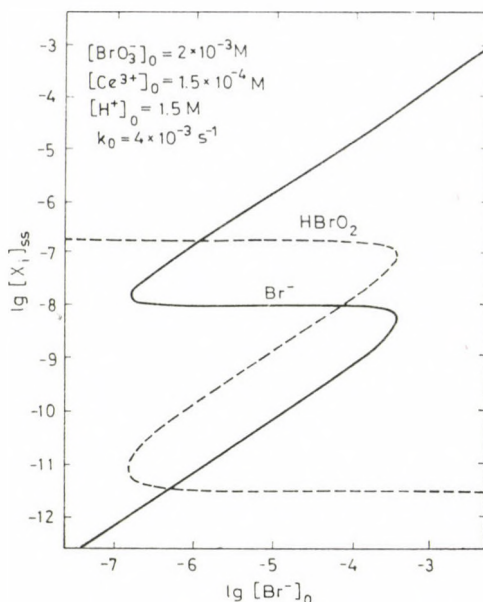


Fig. 4. Changes of steady state concentrations of bromous acid,  $[\text{HBrO}_2]_{\text{ss}}$ , and bromide,  $[\text{Br}^-]_{\text{ss}}$ , with  $[\text{Br}^-]_0$  ( $\lg$ - $\lg$  plot). Other constraints:  $[\text{BrO}_3^-]_0 = 2 \times 10^{-3} \text{ M}$ ,  $[\text{Ce}^{3+}]_0 = 1.5 \times 10^{-4} \text{ M}$ ,  $[\text{H}^+]_0 = 1.5 \text{ M}$ ,  $k_0 = 4 \times 10^{-3} \text{ s}^{-1}$ .

SSI and SSII are independent of the bromide inflow. On the other hand the curve of  $Y$  is s-shaped and the stationary concentrations of SSI and SSII depend linearly on the constraint  $[\text{Br}^-]_0$ . Thus the simple model also predicts hysteresis behavior and the hysteresis limits agree tolerably to measured results.

From the discriminant of equation (20), which is cubic with respect to  $Y_0$ , we can calculate the limits of the hysteresis curves for various values of  $A$  ( $\text{BrO}_3^-$ ). By plotting these limits in the plane  $[\text{Br}^-]_0$  vs.  $[\text{BrO}_3^-]_0$  we obtain the domain of bistability of Fig. 5. The computed and calculated data agree reasonably well for low bromate concentrations, however, for large concentrations of bromate the model fails and an upper limit of the domain of bistability is not predicted [12]. This is a contradiction to the experimental findings and a consequence of oversimplification. For any constant value of  $A$  we are able to calculate from equation (20) the domain of bistability in the plane of constraints  $k_0$  vs.  $[\text{Br}^-]_0$ . This domain is very similar to that obtained from the detailed model [see (D) in Figure 3], however, it is somewhat wider. The dynamic behaviour of the model has been calculated by numerical integration of the equations system (15)–(16). The kinetics are described reasonably well, but peculiar features are not simulated.

Figure 6 shows the calculated trajectories of the model in the plane of  $[\text{HBrO}_2]$  vs.  $[\text{Br}^-]$ . The trajectories represent the non-steady states along

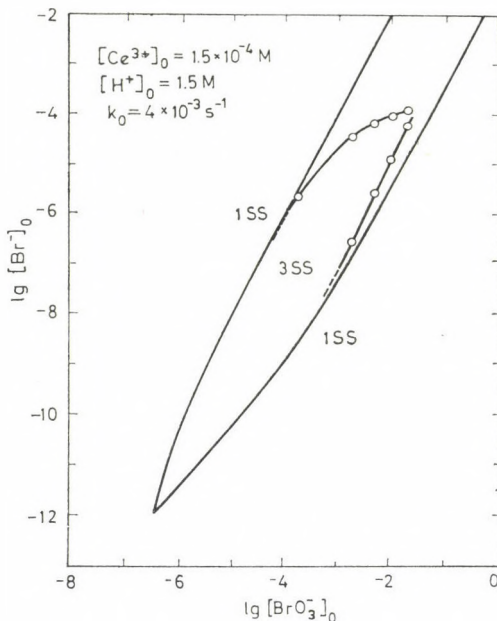


Fig. 5. Domain of bistability in the plane  $\lg [Br^-]_0$  vs.  $\lg [BrO_3^-]_0$ . Other constraints:  $k_0 = 4 \times 10^{-3} s^{-1}$ ,  $[Ce^{3+}]_0 = 1.5 \times 10^{-4} M$ ,  $[H^+]_0 = 1.5 M$ . Solid lines — calculated limits, dashed lines with dots — measured limits

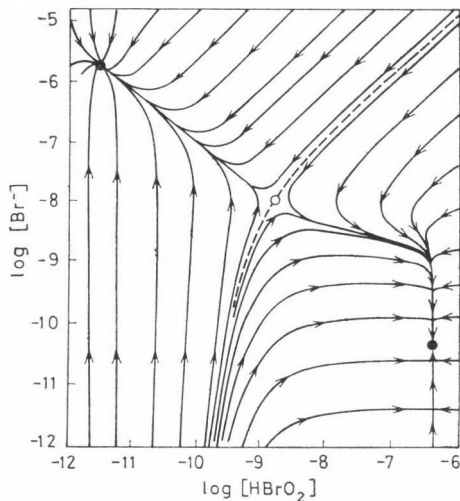


Fig. 6. Trajectories in the plane  $\lg [Br^-]$  vs.  $\lg [HBrO_2]$ . Other constraints:  $[BrO_3^-]_0 = 2 \times 10^{-3} M$ ,  $[Br^-]_0 = 1 \times 10^{-5} M$ ,  $[Ce^{3+}]_0 = 1.5 \times 10^{-4} M$ ,  $[H^+]_0 = 1.5 M$ ,  $k_0 = 4 \times 10^{-3} s^{-1}$

which the system moves to the stable steady states. Both of them are nodes and are separated by a separatrix which is part of the third SS. This SS is unstable and referred to as a saddlepoint. Any transition from one stable SS to the other one requires perturbations [4], which overcome the separatrix (super-threshold perturbations). Otherwise the system returns to its previous SS (sub-threshold perturbations).

## REFERENCES

- [1] BELOUSOV, B. P.: Sb. Referat. Radiats. Med., 1958, Medgiz, Moscow, 145 (1959); ZHABOTINSKII, A. M.: Biofizika, **9**, 306 (1964); FIELD, R. J., KÖRÖS, E., NOYES, R. M.: J. Am. Chem. Soc., **94**, 8649 (1972)
- [2] VAVILIN, V. A., ZHABOTINSKII, A. M.: Kinet. Katal., **10**, 83 (1969); KASPEREK, G. J., BRUCE, T. C.: Inorg. Chem., **10**, 382 (1971); THOMPSON, R. C.: J. Am. Chem. Soc., **93**, 7315 (1971); HERBO, C., SCHMITZ, G., VAN GLABBEKE, M.: Can. J. Chem., **54**, 2628 (1976); BARKIN, S., BIXON, M., NOYES, R. M., BAR-ELI, K.: Int. J. Chem. Kinet., **9**, 841 (1977)
- [3] NOYES, R. M., FIELD, R. J., THOMPSON, R. C.: J. Am. Chem. Soc., **93**, 7315 (1971)
- [4] GEISELER, W., FÖLLNER, H. H.: Biophys. Chem., **6**, 107 (1977)
- [5] BAR-ELI, K., NOYES, R. M.: J. Phys. Chem., **81**, 1988 (1977)
- [6] BAR-ELI, K., NOYES, R. M.: J. Phys. Chem., **82**, 1352 (1978)
- [7] TYSON, J. J.: Ann. New York Acad. Sci., **316**, 279 (1979)
- [8] NOYES, R. M.: J. Chem. Phys., **72**, 3454 (1980)
- [9] GEAR, C. W.: Numerical Initial Value Problems in Ordinary Differential Equations, Prentice-Hall, Englewood Cliffs, N. J., 1971, pp. 209—29; HINDMARSH, A. C.: Gear: Ordinary Differential Equation System Solver, VCID-2001 rev. 3, University of California, Livermore, CA, Dec. 1974
- [10] GEISELER, W., BAR-ELI, K.: J. Phys. Chem., **85**, 908 (1981)
- [11] GEISELER, W.: unpublished results
- [12] The same result was obtained analytically by TYSON (private communication)

Kedma BAR-ELI } Department of Chemistry, Tel-Aviv University IL-  
69978 Ramat-Aviv, Israel

Wolfgang GEISELER } Institute of Technical Chemistry Technical University  
of Berlin D-1000 Berlin 12, Germany



## BrO<sub>2</sub> AS AN INTERMEDIATE IN THE BELOUSOV—ZHABOTINSKY REACTION\*

H. D. FÖRSTERLING,\*\* H. J. LAMBERZ, H. SCHREIBER and W. ZITTLAU

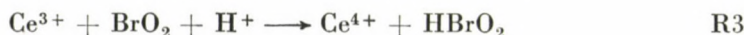
(*Fachbereich Physikalische Chemie der Philipps-Universität  
Hans-Meerwein-Straße, D-3550 Marburg, W. Germany*)

Received March 6, 1981

Accepted for publication April 20, 1981

BrO<sub>2</sub> is found to be an intermediate in the oscillating system as well as in the set of inorganic reactions (reaction between HBrO<sub>2</sub> and bromate, reaction between Ce<sup>3+</sup> and bromate). The kinetics of these reactions is modeled by including the BrO<sub>2</sub>/Br<sub>2</sub>O<sub>4</sub>-equilibrium; the theoretical results are in good agreement with our experiments. Moreover, an attempt was made to detect Br<sub>2</sub> as an intermediate in the oscillating system; it is concluded that Br<sub>2</sub>-oscillations cannot be detected spectroscopically in the cerium-catalysed system.

Within the reaction scheme proposed by FIELD, KÖRÖS and NOYES (FKN theory) [1] BrO<sub>2</sub> is assumed to be an important intermediate in the BELOUSOV—ZHABOTINSKY reaction [2]. We have been able to detect BrO<sub>2</sub> spectroscopically in the oscillating system [3] as well as in the set of inorganic reactions [4, 5, 6]:



### Experimental results

#### Oscillating system

A closed oscillating system (composition  $1 \cdot 10^{-4} \text{ m Ce}^{4+}$ ,  $0.1 \text{ m}$  bromate and  $0.1 \text{ m}$  malonic acid in  $1 \text{ m}$  sulfuric acid) in a 200 mL reaction cell was thermostated at 20 °C and stirred with a magnetic stirrer. N<sub>2</sub> was bubbled through the solution for half an hour before injecting the cerium solution; after starting the reaction, a stream of N<sub>2</sub> was passed above the surface of the solution in order to keep away oxygen from the reaction mixture. Under these conditions, stable oscillations were obtained for about 100 hours (Fig. 1).

The oscillations were monitored spectroscopically. In the region from 345 to 400 nm the absorbance changes were measured by using a double beam spectrometer (Beckman ACTA III); in the region from 400 to 600 nm, however, the signal to noise ratio had to be improved by using the dual wave length technique [3].

\* Presented on the joint session of the Working Committees on Reaction Kinetics and Catalysis, and Coordination Chemistry, Budapest, October 29, 1980.

\*\* To whom correspondence should be addressed

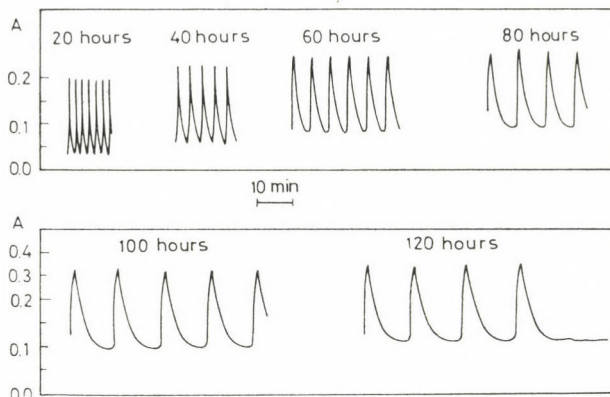


Fig. 1. Absorbance  $A$  at  $\lambda = 400$  nm of an oscillating system (composition  $1 \cdot 10^{-4}$   $m$   $\text{Ce}^{4+}$   $0.1$   $m$  bromate and  $0.1$   $m$  malonic acid in  $1$   $m$  sulfuric acid) as a function of time at 20, 40, 60, 80, 100 and 120 h after starting the reaction. Temperature  $20^\circ\text{C}$ , optical path length  $10$  cm, elimination of  $\text{O}_2$  by applying a stream of  $\text{N}_2$

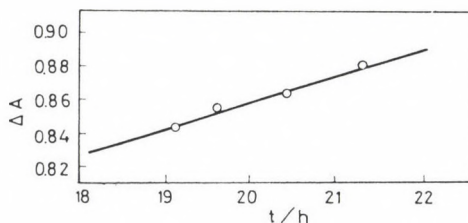


Fig. 2. Oscillation amplitudes  $\Delta A$  at  $\lambda = 345$  nm of an oscillating system ( $1 \cdot 10^{-4}$   $m$   $\text{Ce}(\text{SO}_4)_2$ ,  $0.1$   $m$   $\text{NaBrO}_3$  and  $0.1$   $m$  malonic acid in  $1$   $m$  sulfuric acid) as a function of time. Temperature  $20^\circ\text{C}$ , optical path length  $10$  cm. Zero point of the time scale is the time when the reaction was started

### Region 345 to 400 nm

The amplitudes  $\Delta A$  of the absorbance changes in the oscillating system were measured at fixed wavelengths. In the course of the experiment, the oscillation amplitudes were not constant, but increased slightly with time (Fig. 2). From this reason interpolated values  $\Delta A_0$  at time  $t_0$  ( $t_0 = 20$  h after starting the reaction) were taken from the time dependence curves and relative values

$$\Delta A_{\text{rel}}^{\lambda} = \Delta A_{0,\lambda} / \Delta A_{0,400} \quad (1)$$

( $\Delta A_{0,\lambda} = \Delta A_0$  at wavelength  $\lambda$ ;  $\Delta A_{0,400} = \Delta A_0$  at wavelength  $400$  nm) were calculated (Table I, column 2). Additionally, the  $\text{Ce}^{4+}$  spectrum was taken by measuring the absorbance  $A$  of a solution of  $\text{Ce}(\text{SO}_4)_2$  in  $1$   $m$  sulfuric acid at the same wavelengths as in the case of the oscillating system. By an appropriate choice of the  $\text{Ce}^{4+}$  concentration ( $2.4 \cdot 10^{-5}$   $\text{mol} \cdot \text{L}^{-1}$ ) the absorbance  $A$  at  $400$  nm was chosen equal to  $\Delta A_{0,400}$ . The relative values

$$A_{\text{rel}} = A_{\lambda} / A_{400} \quad (2)$$

(Table I, column 3) are compared to  $\Delta A_{\text{rel}}$  by calculating the ratio  $\Delta A_{\text{rel}}/A_{\text{rel}}$ . From Table I (column 4) it is clearly to be seen that this ratio is equal to 1.00 within the experimental error of about 1%.

Table I

Relative absorbance changes  $\Delta A_{\text{rel}}$  (eq. 1) of the oscillating system and relative absorbance  $A_{\text{rel}}$  (eq. 2) of an acid solution of  $\text{Ce}(\text{SO}_4)_2$ . Temperature 20 °C, optical path length 10 cm. Composition of the oscillating system:  $1 \cdot 10^{-4}$  m  $\text{Ce}(\text{SO}_4)_2$ , 0.1 m  $\text{NaBrO}_3$  and 0.1 m malonic acid in 1 m sulfuric acid.  $\text{Ce}(\text{SO}_4)_2$  spectrum taken in 1 m sulfuric acid

$\frac{\lambda}{\text{nm}}$	$\Delta A_{\text{rel}}$	$A_{\text{rel}}$	$\frac{\Delta A_{\text{rel}}}{A_{\text{rel}}}$
400	1	1	1
385	1.75	1.74	1.01
370	2.71	2.69	1.01
357	3.73	3.75	1.00
345	4.83	4.83	1.00

This result seems to contradict the experimental finding of VIDAL, ROUX and ROSSI [7] that in their oscillating system the absorbance changes at 400 nm were about 10% larger than calculated from the  $\text{Ce}^{4+}$  spectrum. The authors conclude that this difference is due to oscillations of  $\text{Br}_2$ ; from this difference they calculate maximum  $\text{Br}_2$  concentrations which are in the same order of magnitude as the maximum  $\text{Ce}^{4+}$  concentrations.

Since in their system the experimental conditions ( $2.5 \cdot 10^{-4}$  m  $\text{Ce}(\text{SO}_4)_2$ , 0.036 m  $\text{KBrO}_3$  and 0.08 m malonic acid in 1.5 m sulfuric acid; temperature 40 °C) were slightly different from ours we have repeated their experiments. In Table II the relative oscillation amplitudes  $\Delta A_{\text{rel}}$  are compared again to  $A_{\text{rel}}$  [ $\text{Ce}(\text{SO}_4)_2$  spectrum taken at 20 °C as in Table I]. Indeed, from column

Table II

Relative absorbance changes  $\Delta A_{\text{rel}}$  (eq. 1) of the oscillating system and relative absorbance  $A_{\text{rel}}$  (eq. 2) of an acid solution of  $\text{Ce}(\text{SO}_4)_2$ . Temperatures as given in the headline, optical path length 10 cm. Composition of the oscillating system:  $1 \cdot 10^{-4}$  m  $\text{Ce}(\text{SO}_4)_2$ , 0.036 m  $\text{NaBrO}_3$  and 0.08 m malonic acid in 1.5 m sulfuric acid.  $\text{Ce}(\text{SO}_4)_2$ -spectrum taken in 1.5 m sulfuric acid

$\frac{\lambda}{\text{nm}}$	$\frac{\Delta A_{\text{rel}}}{A_{\text{rel}}}$ (40 °C)	$\frac{A_{\text{rel}}}{A_{\text{rel}}}$ (20 °C)	$\frac{\Delta A_{\text{rel}}}{A_{\text{rel}}}$	$\frac{\Delta A_{\text{rel}}}{A_{\text{rel}}}$ (40 °C)	$\frac{A_{\text{rel}}}{A_{\text{rel}}}$ (40 °C)	$\frac{\Delta A_{\text{rel}}}{A_{\text{rel}}}$
400	1	1	1	1	1	1
385	1.71	1.76	0.97	1.71	1.70	1.00
370	2.55	2.75	0.93	2.55	2.57	0.99
357	3.50	3.86	0.91	3.50	3.53	0.99
345	4.41	4.95	0.89	4.41	4.44	0.99

4 it is evident that the ratio  $\Delta A_{\text{rel}}/A_{\text{rel}}$  at 400 nm is about 10% larger than at 345 nm as claimed by VIDAL, ROUX and ROSSI. From the chemistry of acid  $\text{Ce}(\text{SO}_4)_2$  solutions it is clear, however, that  $\text{Ce}^{4+}$  ions are forming sulfato complexes in sulfuric acid [8]; hence the  $\text{Ce}^{4+}$  spectrum may change with temperature, and it may be problematic to use the 20 °C values for  $A_{\text{rel}}$ . Indeed, taking the  $\text{Ce}^{4+}$  spectrum at 40 °C, the ratio  $\Delta A_{\text{rel}}/A_{\text{rel}}$  is found to be 1.0 within the experimental error of 1% again (Table II, column 7).

From these experimental results we conclude that the absorbance changes in the range from 345 to 400 nm are due to concentration changes of  $\text{Ce}^{4+}$  only, and that oscillations of  $\text{Br}_2$  cannot be detected spectroscopically.

### Region 400 to 600 nm

With increasing wavelength, the oscillation amplitudes  $\Delta A$  are rapidly decreasing; hence a very poor signal to noise ratio is obtained if a normal double beam spectrometer is used. This fact is mainly due to the evolution of  $\text{CO}_2$  bubbles disturbing the optical light path. By using a dual wavelength spectrometer [3] the signal to noise ratio is drastically improved (Fig. 3). In Fig. 4 the oscillation amplitudes at different wavelengths are given as a function of time. The slopes of the curves at 400 and 450 nm are positive as in Fig. 2; these slopes become negative with increasing wavelength indicating that there is another species oscillating than  $\text{Ce}^{4+}$ . In the same way as pointed out in the previous section, the relative absorbance changes  $\Delta A_{\text{rel}}$  were calculated and compared to the relative absorbance  $A_{\text{rel}}$  of  $\text{Ce}^{4+}$  (Table III).

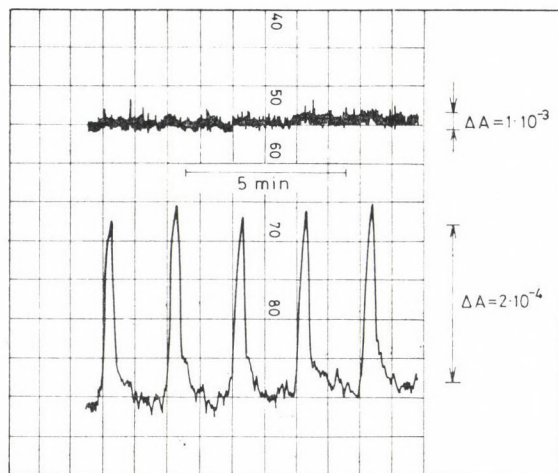


Fig. 3. Improvement of the signal to noise ratio, when an oscillating system (composition as given in Fig. 1) is monitored using a dual wavelength spectrometer (lower curve) instead of a double beam spectrometer (upper curve). Optical path length 10 cm, monitoring wavelength 600 nm

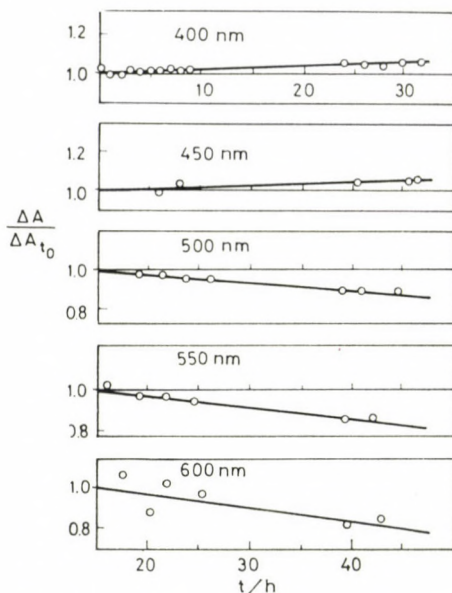


Fig. 4. Time dependence of the oscillation amplitudes  $\Delta A$  of an oscillating system (composition as given in Fig. 1) as a function of time after starting the reaction.  $\Delta A_{t_0}$  is the change of absorbance at time  $t_0 = 16$  h. Optical path length 10 cm, temperature 20 °C

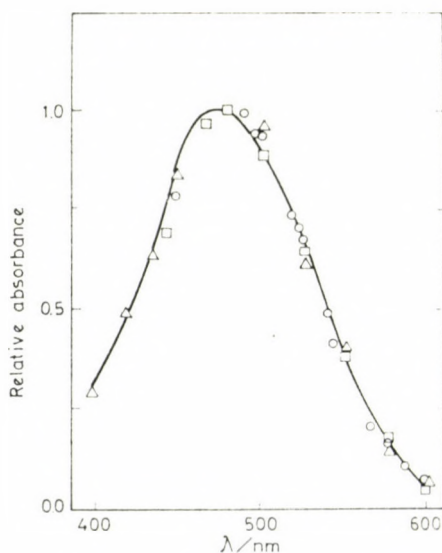


Fig. 5. Relative absorbance of  $\text{BrO}_2$  as a function of wavelength (maximum value set to 1.0). Full line: Values from BUXTON and DAINTON [9]. Circles: Values  $A_{\text{rel}}$  from the oscillating reaction according to (3). Triangles: Values  $\Delta A_{\text{max}}$  (Fig. 6a) from the reaction of  $\text{HBrO}_2$  with bromate. Squares: Values  $\Delta A_{\text{max}}$  (Fig. 6b, corrected for the  $\text{Ce}^{4+}$  absorbance) from the reaction of  $\text{Ce}^{3+}$  with bromate. In the case of the oscillating reaction, the experimental conditions are the same as given in Table I

Contrary to the wavelength region from 400 to 345 nm (Table I), the ratio  $\Delta A_{\text{rel}}/A_{\text{rel}}$  is drastically increasing towards larger wavelengths. If the difference

$$A'_{\text{rel}} = \Delta A_{\text{rel}} - A_{\text{rel}} \quad (3)$$

is calculated (Table III) and plotted as a function of wavelength (Fig. 5) the experimental values are found to be in good agreement with the absorption spectrum of  $\text{BrO}_2$  reported by BUXTON and DAINTON [9].

Table III

Relative absorbance changes  $\Delta A_{\text{rel}}$  of the oscillating system and relative absorbance  $A_{\text{rel}}$  of an acid solution of  $\text{Ce}(\text{SO}_4)_2$ . The experimental conditions are the same as given in Table I

$\frac{\lambda}{\text{nm}}$	$\Delta A_{\text{rel}}$	$A_{\text{rel}}$	$\frac{\Delta A_{\text{rel}}}{A_{\text{rel}}}$	$\Delta A_{\text{rel}} - A_{\text{rel}}$
400	1	1	1	—
450	0.174	0.146	1.19	0.028
480	0.0913	0.0557	1.64	0.0356
490	0.0570	0.0219	2.60	0.0351
496	0.0483	0.0148	3.26	0.0335
500	0.0458	0.0126	3.63	0.0332
518	0.0310	0.0051	6.07	0.0259
521	0.0294	0.0043	6.84	0.0251
525	0.0277	0.0038	7.29	0.0239
539	0.0185	0.0015	12.3	0.0170
542	0.0162	0.0014	11.6	0.0148
550	0.0145	0.0009	16.1	0.0136
566	0.0078	0.0005	15	0.0073
576	0.0064	0.0004	16	0.0060
586	0.0042	0.0002	21	0.0040
600	0.0026	0.0001	26	0.0025

From these experimental results we conclude that the absorbance changes in the range from 400 to 600 nm are due to concentration changes of  $\text{Ce}^{4+}$  and  $\text{BrO}_2$ . At  $\lambda = 500$  nm the contribution of  $\text{BrO}_2$  to the total absorbance change is about 70%; it is about 95% at  $\lambda = 600$  nm.

#### Reaction of $\text{HBrO}_2$ with bromate (R1, R2)

This reaction was started by injecting an alkaline solution of  $\text{NaBrO}_2$  into a 1 m solution of  $\text{NaBrO}_3$  in 1 m  $\text{H}_2\text{SO}_4$  (assuming that the reaction  $\text{BrO}_2^- + \text{H}^+ \rightarrow \text{HBrO}_2$  is much faster than all other reactions under consideration). Using a monitoring wavelength of 488 nm, a fast rise of the absorbance

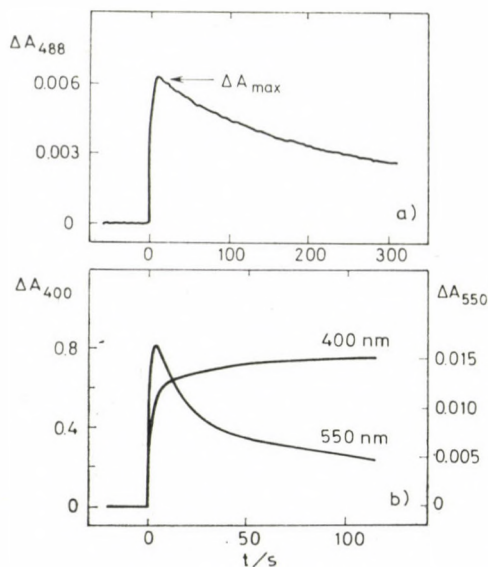


Fig. 6. Kinetics of the reaction of  $\text{HBrO}_2$  (a) and of the reaction of  $\text{Ce}^{3+}$  (b) with bromate. The reactions were carried out in 1 *m* bromate solutions in 1 *m* sulfuric acid at 20 °C. The initial concentrations of  $\text{NaBrO}_2$  and of  $\text{Ce}^{3+}$  were  $1.2 \cdot 10^{-6}$  *m* and  $1.0 \cdot 10^{-4}$  *m*, respectively. The kinetics were monitored by measuring the absorbance change  $\Delta A$  ( $\text{BrO}_2$  at 488 and 550 nm,  $\text{Ce}^{4+}$  at 400 nm)

A and a slow decay were observed (Fig. 6a). Changing the monitoring wave length in the range from 400 to 600 nm, the maximum absorbance change  $\Delta A_{\text{max}}$  was measured and plotted in Fig. 5 as a function of wavelength (triangles). The experimental values are well fitted by the  $\text{BrO}_2$  absorption spectrum [9].

Using the  $\varepsilon$ -values of BUXTON and DAINTON [9] the maximum concentration of  $\text{BrO}_2$  in Fig. 6a is calculated to be  $0.63 \cdot 10^{-6}$  mol  $\cdot$  L $^{-1}$ . On the other hand, from the stoichiometry of the reactions R1, R2 and the initial concentration of  $\text{NaBrO}_2$  of  $1.2 \cdot 10^{-6}$  mol  $\cdot$  L $^{-1}$  the  $\text{BrO}_2$  concentration is expected to be  $2.4 \cdot 10^{-6}$  mol  $\cdot$  L $^{-1}$ , if  $\text{Br}_2\text{O}_4$  is treated as a transient of negligible concentration. The reason for this discrepancy is that a considerable amount of the dimer  $\text{Br}_2\text{O}_4$  is formed according to the equilibrium R2 and that the competitive reaction



must be taken into account.

On the basis of the reaction scheme R1, R2, R4 we were able to calculate the equilibrium constant of R2

$$K = \frac{c_{\text{BrO}_2}^2}{c_{\text{Br}_2\text{O}_4}} = 1.5 \cdot 10^{-6} \text{ mol} \cdot \text{L}^{-1}$$

and the ratio  $k_1/k_4 = 5.0 \cdot 10^{-6} \text{ mol} \cdot \text{L}^{-1}$  of the rate constants of the reactions R1 and R4 [6].

### Reaction of $\text{Ce}^{3+}$ with bromate (R1, R2, R3, R4)

This reaction was started by injecting a solution of  $\text{Ce}_2(\text{SO}_4)_3$  into a 1 *m* solution of  $\text{NaBrO}_3$  in 1 *m*  $\text{H}_2\text{SO}_4$ . The absorbance change was monitored at 400 nm and 550 nm simultaneously (Fig. 6b). The 400 nm curve was found to be identical with the well-known kinetics of  $\text{Ce}^{4+}$  formation. From the shape of the 550 nm curve it must be concluded that an intermediate is formed in the course of the reaction. In order to identify this intermediate by its absorption spectrum, the experiment was repeated by changing the monitoring wavelength (550 nm) in the range from 450 to 600 nm. In each case the maximum absorbance change was measured and corrected for the  $\text{Ce}^{4+}$  contribution; the corrected values  $\Delta A_{\text{max}}$  plotted in Fig. 5 (squares) are found to be in excellent agreement with the  $\text{BrO}_2$  absorption spectrum.

### Discussion

From our experiments it is concluded that  $\text{BrO}_2$  is an intermediate as well in the oscillating system as in the set of inorganic reactions R1 to R4. Within the error of our experiments, no  $\text{Br}_2$  was to be detected.

In one of our preceding papers [4] it was pointed out that the kinetics of the  $\text{Ce}^{3+}$ /bromate reaction experimentally observed was not in quantitative agreement with the kinetics calculated from the rate constants assumed by FIELD, KÖRÖS and NOYES [1]; the maximum  $\text{BrO}_2$  concentration was larger by a factor of ten compared to the experimental value; the calculated rise time of  $\text{BrO}_2$  was one tenth of the experimental value only. On the basis of the values  $k_1/k_4 = 5.0 \cdot 10^{-6} \text{ mol} \cdot \text{L}^{-1}$  and  $K = 1.5 \cdot 10^{-6} \text{ mol} \cdot \text{L}^{-1}$  for the equilibrium R2 given in this paper modified calculations were performed.

Since absolute values of  $k_1$  or  $k_4$  were not available,  $k_4$  was chosen as in [1] ( $k_4 = 4 \cdot 10^7 \text{ L} \cdot \text{mol}^{-1} \text{ s}^{-1}$ ) and  $k_1$  was calculated from our value for  $k_1/k_4$  ( $k_1 = 200 \text{ L} \cdot \text{mol}^{-1} \text{ s}^{-1}$ ). For the same experimental conditions as in Fig. 6a the reaction of  $\text{HBrO}_2$  with bromate was simulated by numerical integration of the rate equations for R1, R2, R4. A good agreement with experiment was obtained if the value  $k_{-1} = 5.0 \text{ s}^{-1}$  was used for the reverse of reaction R1 (Fig. 7). According to the maximum concentration of  $\text{BrO}_2$  the calculated value is about 30% larger than observed; possible explanations for this discrepancy are discussed in detail in a preceding paper [6].

Using the same set of rate constants the reaction of  $\text{Ce}^{3+}$  with bromate was simulated by numerical integration of the rate equations for R1, R2,

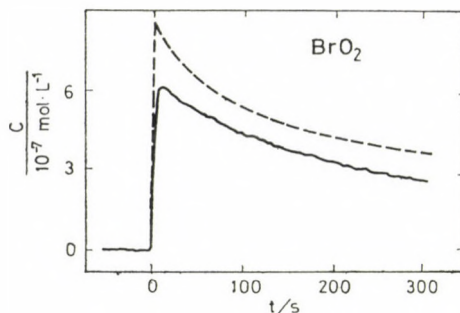


Fig. 7. Reaction of  $\text{HBrO}_2$  with bromate; concentrations of  $\text{BrO}_2$  as a function of time. Full line: Experimental curve, calculated from Fig. 6a using the value  $\varepsilon_{488} = 975 \text{ L} \cdot \text{mol}^{-1} \cdot \text{cm}^{-1}$ . Dashed line: Theoretical curve, obtained by numerical integration of the rate equations for R1, R2, R4 by GEAR's method [11]. The rate constants used are  $k_1 = 200 \text{ L} \cdot \text{mol}^{-1} \text{ s}^{-1}$ ,  $k_{-1} = 5 \text{ s}^{-1}$ ,  $k_4 = 4 \cdot 10^7 \text{ L} \cdot \text{mol}^{-1} \text{ s}^{-1}$ ,  $k_{-4} = 0$ ; R2 was assumed to be a fast equilibrium ( $K = 1.5 \cdot 10^{-6} \text{ mol} \cdot \text{L}^{-1}$ .) Initial values as given in Fig. 6a

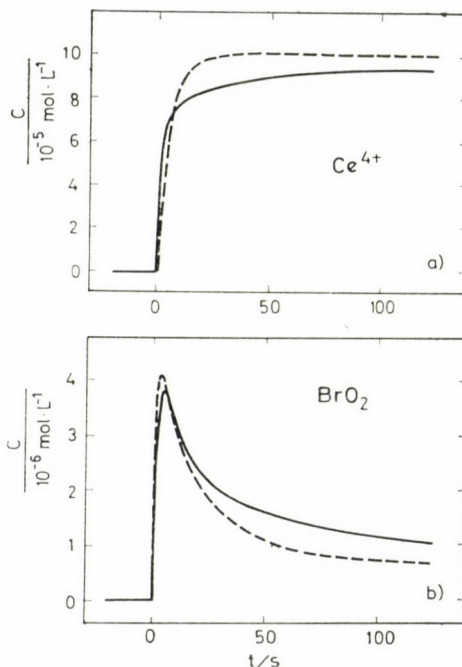


Fig. 8. Reaction of  $\text{Ce}^{3+}$  with bromate; concentration of  $\text{Ce}^{4+}$  (a) and  $\text{BrO}_2$  (b) as a function of time. Full line: Experimental curves, calculated from Fig. 6b using the values  $\varepsilon_{400} = 800 \text{ L} \cdot \text{mol}^{-1} \cdot \text{s}^{-1}$  and  $\varepsilon_{550} = 0.0009 \text{ L} \cdot \text{mol}^{-1} \text{ cm}^{-1}$  for  $\text{Ce}^{4+}$  and  $\varepsilon_{550} = 387 \text{ L} \cdot \text{mol}^{-1} \text{ cm}^{-1}$  for  $\text{BrO}_2$  and subtracting the  $\text{Ce}^{4+}$  contribution to the absorbance at 550 nm. Dashed line: Theoretical curves, obtained by numerical integration of the rate equations for R1–R4 by GEAR's method [11]. The rate constants for R1, R2, R4 are the same as in Fig. 7; for R3 the rate constants  $k_3 = 6.5 \cdot 10^4 \text{ L}^2 \cdot \text{mol}^{-2} \text{ s}^{-1}$ ;  $k_{-3} = 0$  were used. Initial values as given in Fig. 6b; the initial value for  $\text{HBrO}_2$  was arbitrarily chosen  $c = 10^{-9} \text{ mol} \cdot \text{L}^{-1}$  as in [4]

R3, R4 for the same experimental conditions as in Fig. 6b. A good agreement with experiment (Fig. 8) was obtained if the value  $k_3 = 6.5 \cdot 10^4 \text{ L}^2 \text{ mol}^{-2} \text{ s}^{-1}$  was used; this is 1/10 of the value assumed in [1]. The rise time of Ce<sup>4+</sup> is nearly the same in theory and experiment; the only difference is that the final value of the Ce<sup>4+</sup> concentration is reached within 30 s in the calculated curve, whereas the experimental curve is converging very slowly to this value. The reason for this discrepancy is that our reaction scheme has been simplified; the reaction between BrO<sub>2</sub> and Ce<sup>4+</sup> must be added to overcome this difficulty. On the other hand, the reverse of reaction R3 (reaction of Ce<sup>4+</sup> with HBrO<sub>2</sub>) plays a negligible role as pointed out by SULLIVAN and THOMPSON [10]. The small differences between the curves for BrO<sub>2</sub> may be due to the neglect of all reactions including Br<sub>2</sub> and Br<sup>-</sup>.

From our calculations we conclude that the chemistry of the inorganic set of reactions proposed by FIELD, KÖRÖS and NOYES [1] is essentially valid in the BELOUSOV-ZHABOTINSKY system; the only difficulty seems to be the choice of the right set of rate constants. The aim of our work was to calculate these constants by a stepwise approach. It must be pointed out, however, that the values given in this paper are preliminary values only. They must be improved by extending the set of reactions under consideration and by further experiments.

\*

The authors wish to thank the Fonds der Chemischen Industrie and the Deutsche Forschungsgemeinschaft for financial support.

#### REFERENCES

- [1] FIELD, R. J., KÖRÖS, E., NOYES, R. M.: *J. Am. Chem. Soc.*, **94**, 8649 (1972)
- [2] BELOUSOV, B. P.: Collection of Reports on Radiation Medicine During 1958, Moscow 1959, p. 145; ZHABOTINSKY, A. M.: *Biofizika*, **9**, 306 (1964)
- [3] FÖRSTERLING, H. D., SCHREIBER, H., ZITTLAU, W.: *Z. Naturforsch.*, **33a**, 1552 (1978)
- [4] FÖRSTERLING, H. D., LAMBERZ, H., SCHREIBER, H.: *Z. Naturforsch.*, **35a**, 329 (1980)
- [5] FÖRSTERLING, H. D., LAMBERZ, H., SCHREIBER, H.: *Ber. Bunsenges. Phys. Chem.*, **84**, 407 (1980)
- [6] FÖRSTERLING, H. D., LAMBERZ, H. J., SCHREIBER, H.: *Z. Naturforsch.*, **35a**, 1354 (1980)
- [7] VIDAL, C., ROUX, J. C., ROSSI, A.: *J. Am. Chem. Soc.*, **102**, 1241 (1980)
- [8] HARDWICK, T. J., ROBERTSON, E.: *Can. J. Chem.*, **29**, 828 (1951)
- [9] BUXTON, G. V., DAINTON, F. S.: *Proc. Roy. Soc.*, **A304**, 427 (1968)
- [10] SULLIVAN, J. C., THOMPSON, R. C.: *Inorganic Chemistry*, **13**, 2375 (1979)
- [11] GEAR, C. W.: *Numerical Initial Value Problems in Ordinary Differential Equations*, Prentice Hall, Englewood Cliffs, New Jersey 1971

Horst-Dieter FÖRSTERLING Hubert-Josef LAMBERZ Helmut SCHREIBER Werner ZITTLAU	}	Hans-Meerwein-Straße, D-3550 Marburg, W.-Germany
--	---	---

## ON THE APPLICABILITY OF THE LOTKA—VOLTERRA SCHEME FOR DIFFERENT TYPES OF THE BELOUSOV—ZHABOTINSKII REACTION\*

Z. NOSZTICZIUS\*\* and A. FELLER

(*Institute of Physics, Department for Chemical Engineering, Technical University,  
Budapest*)

Received March 6, 1981

Accepted for publication May 26, 1981

It is shown that in theory the well-known Lotka—Volterra scheme can be applied as a general mechanistic “core” for different types of the BZ reaction. The problem of the limit cycle behaviour and the role of the catalyst are also discussed briefly. Looking for a “basic” BZ oscillator as a reference system for the others it was found experimentally that the classical BZ oscillator (substrate: malonic acid) is not the best choice because of the presence of some unidentified intermediates.

### Introduction

Recently a new mechanism was proposed for the BZ reaction [1–3] based on the well known LOTKA—VOLTERRA (LV) scheme [4, 5]. That novel mechanism was introduced because new experimental facts had been discovered [6–9] which were difficult to explain by the previous theories [10, 11] regarding the bromide ion as a control intermediate. The LV model was developed originally for the acetone-oxalic acid mixed substrate system. In this paper we want to examine the applicability of that model for other BZ systems and to discuss other problems of the proposed mechanism. Some new experimental results are also presented.

#### **The LV mechanism of the acetone-oxalic acid mixed substrate system. Basic ideas leading to the LV scheme**

The LV scheme of the BZ reaction with a substrate mixture is depicted in Fig. 1 in its original form [1]. Our aim was to construct a *simple* and *bromide-free* mechanism which is *easy to generalize* for all the known BZ systems. In the followings we should like to show how these main ideas are leading to our model.

\* Presented on the joint session, of the Working Committees on Reaction Kinetics and Catalysis, and Coordination Chemistry, Budapest, October 29, 1980

\*\* To whom correspondence should be addressed

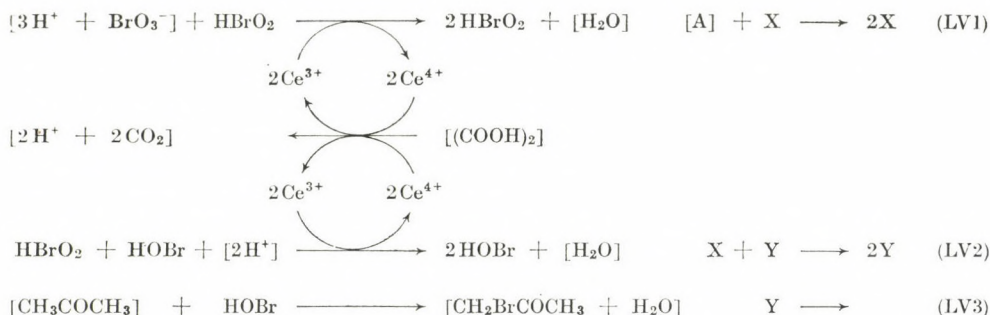


Fig. 1. The LV model of the BZ oscillator with a mixed substrate. Components with  $q$  as steady concentrations or components of no further interest are in brackets. The analogy with LOTKA's original scheme [4] can be recognized by denoting  $\text{HBrO}_2 \equiv \text{X}$ ,  $\text{HOBr} \equiv \text{Y}$ , Acidic bromate  $\equiv \text{A}$

### Simplicity

First of all we think that a *simple explanation* for the oscillations in the BZ reaction should exist. As the LV scheme is the simplest chemical oscillator, we suspect that it might be the "core" of a real mechanism.

### General validity

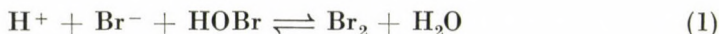
Regarding all the variants of the BZ reaction it is the presence of the bromate which is crucial, all the other components can be substituted. *E.g.* there are other organic substrates (citric, malic, oxalacetic acids [12]) and other catalysts as well ( $\text{Mn}^{2+}$ , ferroin), and even so called non-catalysed BZ systems were discovered [13] in the case of which a metal ion catalyst was not added to the system. Now if we assume that all BZ systems have basically the same mechanism (a general "core") we have to construct a scheme which includes only the characteristic inorganic bromo compounds but not the substrate or the catalyst. These supplementary components play an important role in special cases but not in the invariant core.

Naturally if we want to understand the different behaviour of the different types of the BZ reaction then all of these supplementary compounds and auxiliary reactions have to be included into some more complex reaction schemes.

### Bromide- and bromine-free core

An important feature of the previous theories is a delayed negative feedback loop where the bromide ions play a crucial role. However, recently non-bromide controlled BZ oscillations were found [8] and the presence of bromide in the classical BZ reaction was questioned [9]. Naturally the non-bromide controlled oscillations can be explained as exceptional cases where

some general rules are not valid any more. Nevertheless it is better to look for a general scheme which can be applied without such limitations. In other words the core of a general mechanism must be free of bromide ions. Regarding that idea we can exclude the elementary bromine as well from the core of our scheme because bromide can generate bromine and *vice versa* according to the following reaction:



Thus a control role for bromine would mean an indirect control role for bromide too. More convincingly there are BZ systems where the bromine concentration is below the level of spectroscopic detection [14].

These bromine-free systems would be exceptions again from the viewpoint of a mechanism containing bromine as an important intermediate. Consequently we can *exclude bromide and bromine* from the characteristic inorganic bromo compounds of the core.

Summarizing the above requirements the core of our proposed mechanism is depicted in Fig. 2.

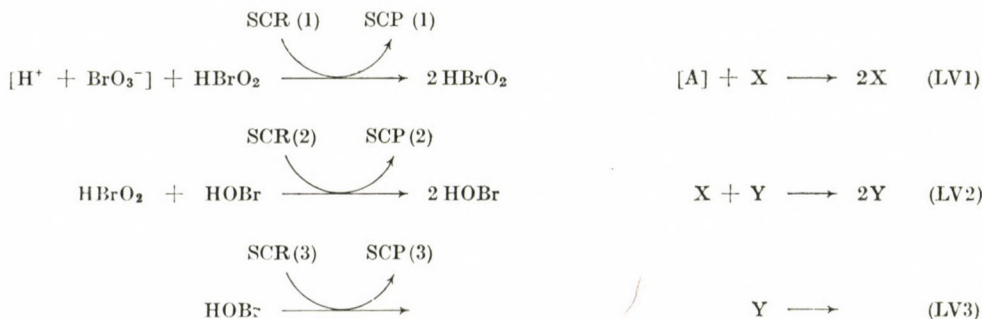


Fig. 2. The LV core of the BZ oscillations SCR(i): supplementary components of the "i"-th reaction step (reagents). SCP(i): supplementary components of the "i"-th reaction step (products)

### Application of the LV scheme for different BZ systems

#### The heterogeneous BZ oscillator

It was observed that oxalic acid alone can be a substrate of cerous catalysed BZ oscillations [6] provided elementary bromine is scrubbed from the reaction mixture by a stream of inert gas. If we want to apply the LV scheme for this special system the reaction LV3 causes some problems. (The other steps remain the same as in Fig. 1.) The removal of hypobromous acid is a duty of oxalic acid now. That is possible according to KNOLLER and PERLMUT-





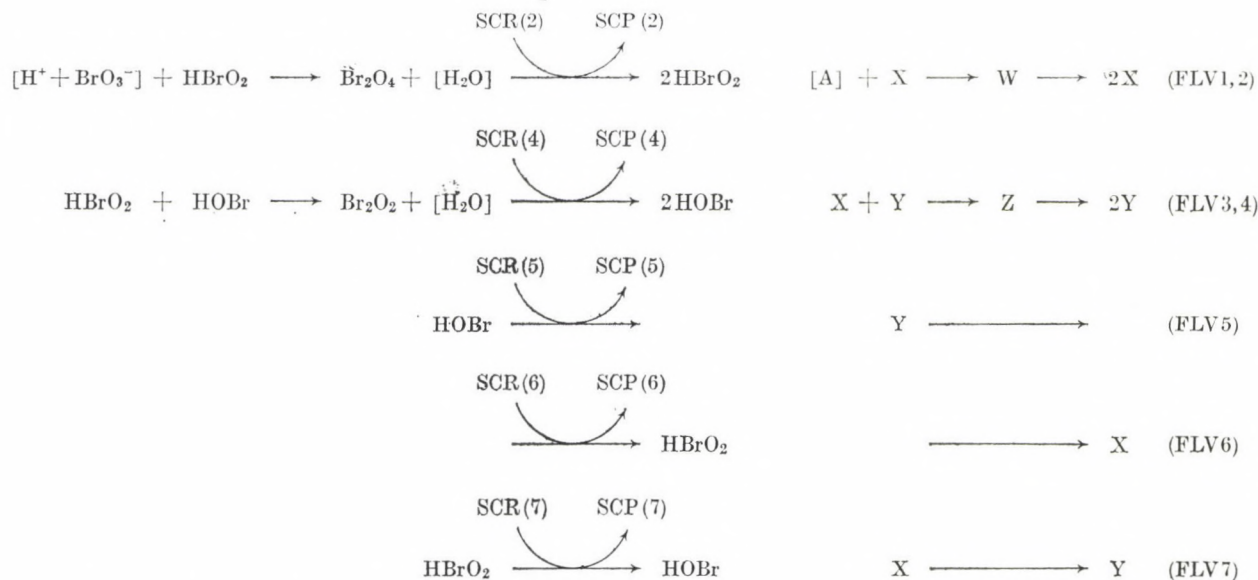


Fig. 6. The general core of the FLV model of the BZ oscillations. The new intermediates  $\text{Br}_2\text{O}_4 \equiv \text{W}$  and  $\text{Br}_2\text{O}_2 \equiv \text{Z}$  were introduced into our scheme to show some details of the autocatalytic processes. The new reactions (FLV6) and (FLV7) provide independent sources for  $\text{HBrO}_2 \equiv \text{X}$  and for  $\text{HOBr} \equiv \text{Y}$ . SCR(i) and SCP(i) are supplementary components of the "i"-th reaction step (reagents and products, respectively)

model is oversimplified: it can be regarded only as a "first" and rough approximation of a real BZ system. This simplest model exhibits the most important feature of the BZ reaction (the oscillating behaviour) but it cannot account for a limit cycle. To explain such a behaviour we have to develop an extended LV scheme showing some more details of the mechanism.

In our opinion the simple LV model contains two essential assumptions from a chemical point of view: it describes the autocatalytic processes as elementary steps and it neglects the reactions producing the first  $X$  and  $Y$  species ( $\text{HBrO}_2$  and  $\text{HOBr}$ , respectively). To overcome these difficulties we have constructed a four-variable LV (FLV) scheme [2] the core of which is depicted in Fig. 6.

A mathematical analysis of that scheme and of some derived three and two variable systems [3] proves that the above mentioned modification results in the appearance of the desired limit cycle even a bifurcation occurs in the parameter space. Finally it is interesting to remark that reaction schemes closely related to the FLV mechanism were proposed by other authors as well [19–21].

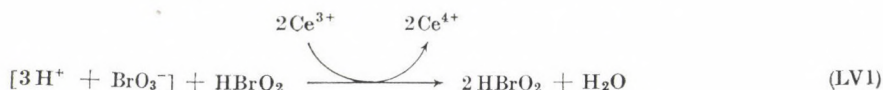
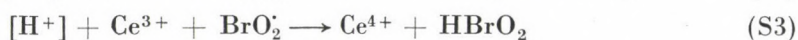
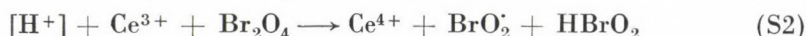
#### *On the role of the catalyst in the LV schemes*

Another problem of the LV mechanism proposed by us that it does not contain the catalyst in its core and our mathematical treatment [3] regards its concentration as a quasi constant. Nevertheless the colour changes observable during the BZ oscillations are due to usually just the changes in the concentration of the oxidized and reduced form of the catalyst.

That objection is well founded because there are numerous systems where our assumption [according to which the reduced form of the catalyst (*e.g.*  $\text{Ce}^{3+}$  see Fig. 1) has a quasi constant concentration] is not valid any more. At the same time in many cases most of the catalyst is in its reduced form during the oscillatory regime. See *e.g.* [22]. In other words regarding the special example of Fig. 1 the relative change of the  $\text{Ce}^{3+}$  concentration ( $\Delta[\text{Ce}^{3+}]/[\text{Ce}^{3+}]_0$  where  $\Delta[\text{Ce}^{3+}]$  is the absolute change and  $[\text{Ce}^{3+}]_0$  some reference level of the  $\text{Ce}^{3+}$  concentration) is small. This is not the case for  $\text{Ce}^{4+}$  because its relative changes can be quite large. However  $\text{Ce}^{4+}$  does not play an important role in our scheme: it is removed by oxalic acid and that reaction is not included in our mathematical scheme. Thus the colour changes due to the temporal accumulation of  $\text{Ce}^{4+}$  by the speeding up of the reaction producing it does not mean necessarily that the  $\text{Ce}^{3+}$  concentration is depleted seriously. Summarizing our considerations: there are systems where our assumption is valid and other cases where it is not. The main point is that it is not essential to suppose changes in the  $\text{Ce}^{3+}$  concentration to get an oscillating scheme and there are real systems where these changes are really minimal.

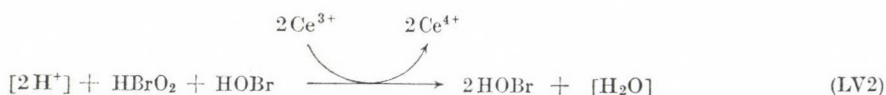
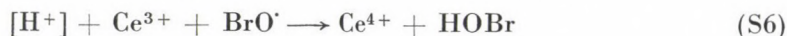
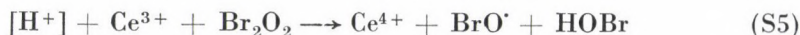
Naturally the simple four variable mathematical model can be applied in the latter cases only. To describe the effects due to the concentration variations of the oxidized and reduced form of the catalyst we need new variables e.g. "Ox" and "Red", respectively. (In a closed system  $[Ox] + [Red] = \text{const}$  as the total concentration of the catalyst does not change.) Such a new six variable ("SLV") model showing limit cycle oscillations [23] is a natural extension of the FLV mechanism.

At this point a new problem emerges, however: what is the detailed mechanistic role of the catalyst? This problem is inevitable if we want to use kinetic equations containing  $[Ox]$  and  $[Red]$ . For the sake of simplicity let us regard the mixed substrate system depicted in Fig. 1. For the oxidation of  $Ce^{3+}$  the following steps were proposed [1, 2]:



the sum of which steps is the equation (LV1) of Fig. 1.

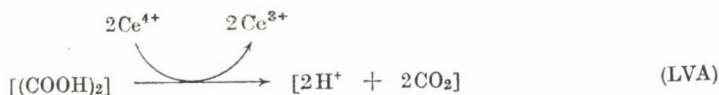
It is a convenient hypothesis to regard step (S2) as a rate determining one. Similar considerations can be repeated for the net process (LV2)



Here the step (S5) can be regarded to be rate determining. The reduction of the catalyst consists of two steps



The sum of steps (S7) and (S8) gives an auxiliary reaction of our scheme in Fig. 1:



If we regard (S7) as a rate determining step then both the oxidation and the reduction rate of the catalyst is a first order reaction in [Ox] and [Red]. We propose to use these assumptions as a first approximation. Nevertheless it is important to remark that some systems may behave differently: e.g. KOCH [24] studying some BZ system found a second order kinetics in respect of the catalyst.

Thus we can see that even in our simplest model the catalyst plays an implicit role: as a first approximation the rate of reaction is proportional to its concentration. Some experimental facts seem to support that picture: the amount of  $\text{CO}_2$  produced in one period of several oscillatory systems is roughly proportional to the concentration of the catalyst [25].

### Search for a "basic" BZ oscillator

#### *Formulation of the problem*

In the previous parts of this work the LV model and its problems were discussed from a theoretical point of view. That new mechanism provides some remarkable theoretical advantages (simplicity, general core) but naturally it needs an experimental verification at first for a special case. Thus the next logical step would be now to select one of the special BZ oscillators and perform a quantitative comprehensive study of experimental facts and theoretical calculations. Such a study exceeds by far the possibilities of the present work and here we want to concentrate only to the selection of the "basic" BZ system which should be the most suitable one to check a theoretical model. In this respect the classical BZ system has some advantages over the others: it is the most studied oscillator providing a considerable amount of important experimental data, it was already the basis of another theoretical model and it requires only one organic substrate. At the same time it has a serious disadvantage: the induction period caused by some partly unidentified intermediate. As it would be desirable to know all the important "supplementary" components in the following we shall examine that problem experimentally.

#### *Attempts to shrink the induction period of the classical BZ system*

Our plan to find the unknown intermediate consisted of two steps

1. At first we wanted to produce a mixture of malonic acid and the molecular intermediates showing no induction period if it is applied as a substrate mixture in the BZ reaction. It was also a requirement to get similar oscillations (period and shape) as can be observed in the unmodified classical system (with malonic acid as the sole substrate) after the induction period.

2. Having found such a mixture we wanted to check whether those intermediates were really present in a classical BZ system at the beginning of the oscillatory regime.

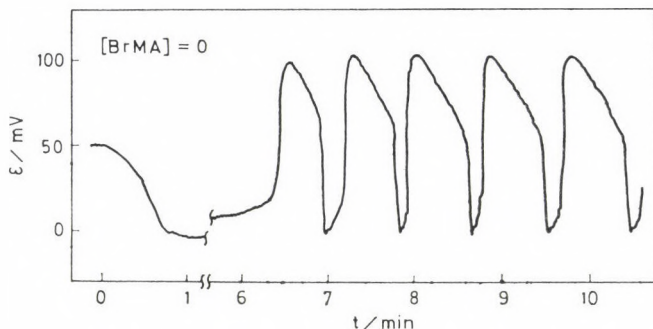
It has been well-known [26–28] that the bromomalonic acid is an important induction period reducing intermediate thus at first we studied its effect on the induction period alone. The results are depicted in Figs 7a–d. In our experiments bromomalonic acid was produced on the spot according to the following reaction:



that is a known amount of a KBr solution was added to the reaction mixture before starting the reaction by the introduction of the catalyst. (A “waiting period” of some minutes was inserted between the addition of the KBr solution and the catalyst to mix the reactants and to make the reaction (3) complete. Our results were independent of the length of that waiting period if it was between 3 and 30 minutes.)

This way a part of the bromate and of the malonic acid is also consumed and the product is not a pure monobromo derivative. This method was chosen because of its simplicity and because there are similar changes during the induction period: a part of the bromate and of the malonic acid is used up and the formation of some other bromoderivatives also may occur.

A similar method was applied by TREINDL and DROJAKOVA [29]. Our results agree with theirs: at first the induction period shrinks with the increasing bromomalonic acid concentration but after reaching a minimum it grows again and at these higher concentrations the frequency of the oscillation decreases considerably (see Fig. 7d). (Applying different initial conditions the minimum value of the induction period can be reduced even to zero. *E.g.* FKN [11] report that in their case “The induction period can be suppressed entirely if bromomalonic acid is deliberately added to the solution initially”. However in this case the potentiometric behaviour of the first oscillation was



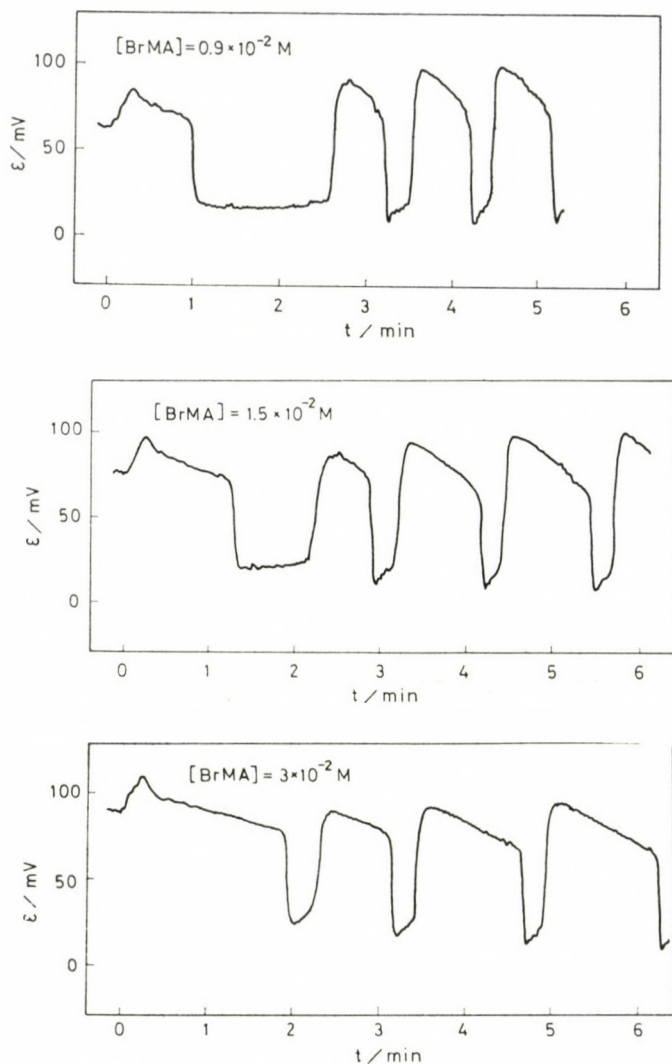


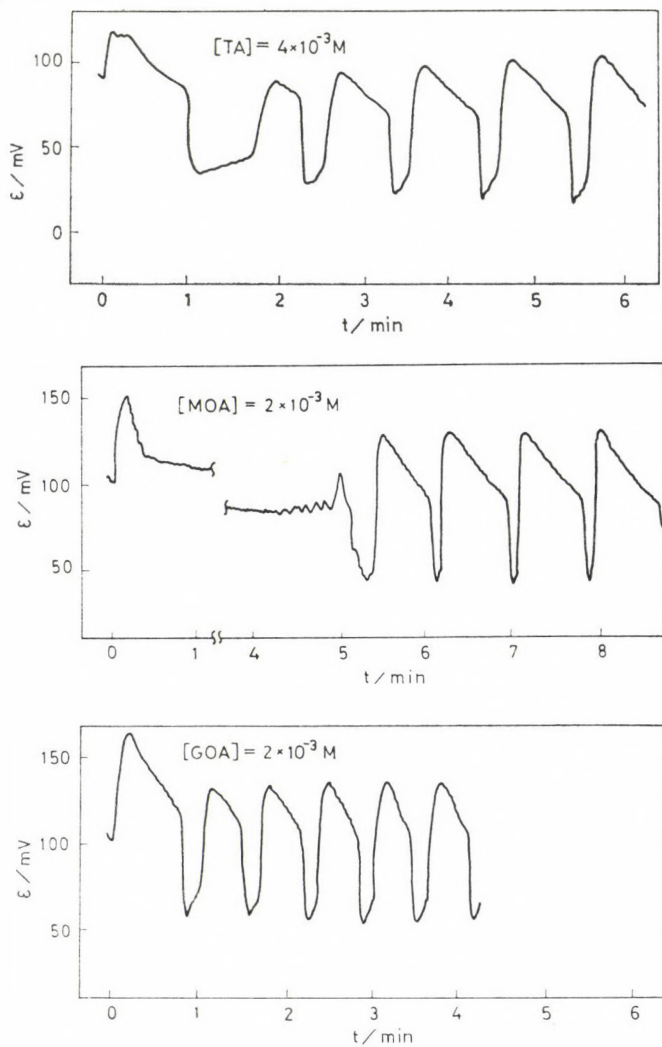
Fig. 7. Effect of bromomalonic acid concentration ( $[\text{BrMA}]$ ) on the induction period of the classical BZ oscillator. Bromomalonic acid was produced on the spot and its concentration is given in the figures. Other initial concentrations (valid after mixing at  $t = 0$ ):  $[\text{H}_2\text{SO}_3] = 1.5 \text{ M}$ ,  $[\text{Ce}(\text{SO}_4)_2] = 10^{-3} \text{ M}$ ,  $[\text{MA}] = 10^{-1} \text{ M} - [\text{BrMA}]$ ,  $[\text{KBrO}_3] = 4 \times 10^{-2} - [\text{BrMA}]/3$ . The reaction was started by the addition of the cerium catalyst at  $t = 0$ . The figures show potentiometric traces of a bromide sensitive electrode without absolute calibration

atypical and they concluded: "Apparently the behaviour is significantly affected by small amounts of some unidentified reaction product or intermediate."

In other words the bromomalonic acid alone does not meet our requirements. It was straightforward to assume — like FKN [11] — that some other

intermediates were also needed to get the complete oscillating system. Jwo and NOYES [30] studied the reactions of some possible molecular intermediates, namely the tartronic (TA) mesoxalic (MOA) glyoxalic (GOA) oxalic (OA) and formic (FA) acids. According to our experiments these acids alone do not provide the desired effect either, thus we applied a mixture of bromomalonic acid and one of the above mentioned intermediates. Some of our results are displayed in Fig. 8a—d. The presence of formic acid did not change the kinetic behaviour of the system as it was expected [31].

It can be seen that only the substrate mixture of oxalic, bromomalonic and malonic acids gives rise of immediate oscillations resembling to the classical ones.



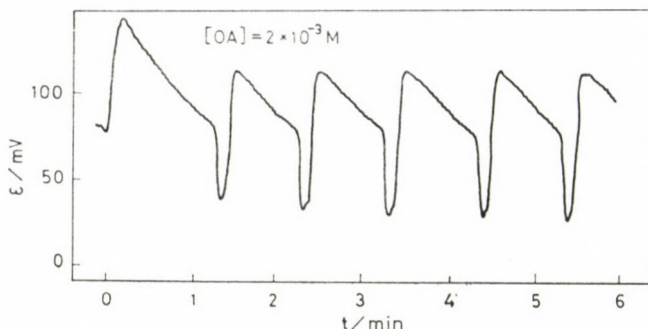


Fig. 8. Effect of different intermediates on the classical BZ oscillator. The concentration of different intermediates is given in the figures (See text for abbreviations). The tartronic acid (TA) was applied in a higher concentration because its effect was not so pronounced. Other initial concentrations:  $[H_2SO_4] = 1.5 M$ ,  $[Ce(SO_4)_2] = 10^{-3} M$ ,  $[MA] = 8.5 \times 10^{-2} M$ ,  $[BrMA] = 1.5 \times 10^{-2} M$ ,  $[KBrO_3] = 3.5 \times 10^{-2} M$ . The figures show " $\epsilon$ " the potential of a bromide sensitive electrode as a function of time " $t$ " without absolute calibration

### Determination of oxalic acid in an oscillating medium

At this stage of our investigations we thought that oxalic acid is an important molecular intermediate in the classical BZ system. To prove that hypothesis we analysed the oscillating solutions by the following method.

#### Analytical procedure

An excess of  $Ca(OH)_2$  powder (Merck) was added to the solution to be analysed. In the alkaline media formed this way all reactions stop practically and a great quantity of  $CaSO_4$  precipitate appears which serves as a carrier for the  $Ca(COO)_2$  precipitate. The precipitate mixture was filtered and washed with distilled water to remove other organic compounds, the cerium catalyst and the bromate.

Then the precipitate was treated with 1.5 molar sulfuric acid for 15 minutes to get the oxalic acid into solution. The mixture was filtered again washed with 1.5 molar sulfuric acid and the collected filtrate was titrated with a 0.05 molar  $KMnO_4$  solution.

The separation and regeneration of oxalic acid were not quantitative: the yield was only 80 percent due to some unidentified losses. This was determined by a calibration procedure measuring a known amount of oxalic acid added to a 1.5 molar sulfuric acid solution. It is probable that a part of  $Ca(COO)_2$  remains occluded in the precipitate mixture.

### Results

In the artificial mixture of Figure 8d we could measure an oxalic acid content equivalent to the  $80 \pm 10$  percent of the originally introduced one if the addition of  $Ca(OH)_2$  followed the start of the reaction within one minute. That is during such a short time losses in oxalic acid due to its reactive decomposition were within the error of our analytical procedure.

In the classical BZ system, however, we were not able to find any measurable quantity of oxalic acid at the beginning of the oscillatory regime. More exactly speaking the concentration of oxalic acid was less than 10 per cent of

the concentration applied in the artificial mixture of Fig. 8d. Experiments show that such a low concentration of oxalic acid has no effect on the induction period.

Summarizing our results we were not able to assign the missing intermediate among the above mentioned compounds. It is possible that the formation of bromomalonic acid and of a complicated mixture of more than one molecular intermediate are responsible for the induction period. Nevertheless in our opinion it is more probable that some organic radical plays an important role in this respect. The radical can be *e.g.* a product of a reaction between bromomalonic acid and some inorganic radicals of  $Ce^{4+}$ .

### Conclusion

We have shown that the LV model originally developed for the oxalic acid — acetone mixed substrate system, can be generalized for other BZ systems as well. Naturally this is a theoretical possibility only and the validity of the generalization and of the LV mechanism itself must be proved experimentally.

Searching for a simple "basic" BZ oscillator we examined the classical one. According to our experiments the classical BZ system contains some unidentified intermediates consequently is not the best choice as a reference system in spite of the great amount of available data. Therefore from a theoretical point of view the heterogeneous BZ oscillator seems to be the simplest one, and the mixed substrate system is probable the simplest homogeneous one.

\*

The authors thank Dr. Gy. BAZSA and Prof. A. M. ZHABOTINSKII for valuable discussions, Prof. B. L. CLARKE and Dr. C. ESCHER for helpful correspondence.

### REFERENCES

- [1] NOSZTICZIUS, Z.: *Kémiai Közlemények*, **54**, 79 (1980)
- [2] NOSZTICZIUS, Z., BÓDISS, J.: *Ber. Bunsen Gesell. Phys. Chem.*, **84**, 366 (1980)
- [3] NOSZTICZIUS, Z., FARKAS, H.: "An Old Model as a New Idea in the Modelling of the Oscillating BZ Reaction" in: "Workshop on Modelling Chemical Reaction Systems" Heidelberg 1980 Sept. (in press)
- [4] LOTKA, A. J.: *J. Am. Chem. Soc.*, **42**, 1595 (1920)
- [5] VOLTERRA, V.: *Animal Ecology*, ed. R. N. CHAPMAN Mc Graw Hill, New York, 1931 409—448 p.
- [6] NOSZTICZIUS, Z., BÓDISS, J.: *J. Am. Chem. Soc.*, **101**, 3177 (1979)
- [7] NOSZTICZIUS, Z.: *Magyar Kémiai Folyóirat*, **85**, 330 (1979)
- [8] NOSZTICZIUS, Z.: *J. Am. Chem. Soc.*, **101**, 3660 (1979)
- [9] NOSZTICZIUS, Z.: *Acta Chim. Acad. Sci. Hung.*, **106**, 347 (1981)
- [10] ZHABOTINSKII, A. M.: *Concentration Self-oscillations* (in Russian), Nauka, Moscow, 1974
- [11] FIELD, R. J., KÖRÖS, E., NOYES, R. M.: *J. Am. Chem. Soc.*, **94**, 8649 (1972)

- [12] ZHABOTINSKII, A. M.: Dokl. Akad. Nauk SSR, **157**, 392 (1964)  
[13] ORBÁN, M., KÓRÖS, E., NOYES, R. M.: J. Phys. Chem., **83**, 3056 (1979)  
[14] FÖRSTERLING, H. D., SCHREIBER, Z. W.: Naturforsch., **33a**, 1552 (1978)  
[15] KNOLLER, Y., PERLMUTTER-HAYMAN, B.: J. Am. Chem. Soc., **77**, 3212 (1955)  
[16] NOYES, R. M.: J. Am. Chem. Soc., **102**, 4644 (1980)  
[17] KÓRÖS, E., ORBÁN M.: Nature (London), **273**, 371 (1978)  
[18] ORBÁN, M., KÓRÖS, E.: J. Phys. Chem., **82**, 1672 (1978)  
[19] KORZUKHIN, M. D., ZHABOTINSKII, A. M.: Molekularnaya Biofizika Moscow, **1965**, 5 (Equation 6) (1965)  
[20] TOCKSTEIN, A., HANDLIŘOVA, M.: Kinetics of Physicochemical Oscillations, Preprints of Submitted Papers, p. 143. Aachen 1979  
[21] CLARKE, B. L.: "Stability of Complex Reaction Networks" (Figures 46 and 47), Advances in Physical Chemistry, Vol. **16**, 1980  
[22] VIDAL, C., ROUX, J. C., ROSSI, A.: J. Am. Chem. Soc., **102**, 1241 (1980)  
[23] CLARKE, B. L.: Personal communication  
[24] KOCH, E., STILKERIEG, B.: Thermochim. Acta, **29**, 205 (1979)  
[25] BÓDISS, J., NOSZTICZIUS, Z.: Work in progress  
[26] DEGN, H.: Nature (London), **213**, 589 (1967)  
[27] BURGER, M., KÓRÖS, E.: J. Phys. Chem., **84**, 496 (1980)  
[28] BURGER, M., KÓRÖS, E.: Ber. Bunsen Gesell Phys. Chem., **84**, 363 (1980)  
[29] TREINDL, L., DROJAKOVA, S.: Coll. Czech. Chem. Comm., **43**, 1561 (1978)  
[30] JWO, J. J., NOYES, R. M.: J. Am. Chem. Soc., **97**, 5431 (1975)  
[31] NOSZTICZIUS, Z., BÓDISS, J.: Magyar Kém. Folyóirat, **86**, 2 (1980)

Zoltán NOSZTICZIUS }  
Antal FELLER } H-1521 Budapest, Budafoki út 8.



## STUDY OF PSEUDO-WAVES IN PERIODIC REACTIONS\*

G.Y. PÓTA, G.Y. BAZSA\*\* and M. T. BECK

(*Institute of Physical Chemistry, Kossuth Lajos University, Debrecen*)

Received April 27, 1981

Accepted for publication June 1, 1981

The effect of diffusion on the propagation of one-dimensional chemical waves initiated by the concentration gradient of the acid in the system malonic acid-bromate-ferroin-cerium(III)-sulphuric acid was studied photographically. It was found, that the waves penetrate the impermeable wall, which means that the diffusion practically has no role in the propagation of the waves.

### Introduction

The formation of periodic structures or chemical waves in the so-called one-dimensional space was first observed by BUSSE [1]. Upon dropping ferroin to the homogeneous system malonic acid—bromate—Ce(III)—sulphuric acid a red-blue stripe system is formed parallel to the surface of the solution. He interpreted his experience as a diffusion effect governed by the autocatalytic reaction proceeding in the system and the concentration gradient together.

An acceptable explanation was first provided by BECK and VÁRADI [2]. The essential points in this explanation are the following. In the system studied a homogeneous periodic reaction takes place under constant stirring. If this reaction is arranged in such a way that along one of the space coordinates a gradient is created for one of the reactants significantly influencing the rate of the reaction, the reaction rate will change along this space coordinate. Thus — unlike in the homogeneous case — the red-blue colour variations corresponding to the periodic ferroin-ferrin transformation occur shifted in time along the space coordinate, *i.e.* red and blue stripes are apparently migrating in the solution. Diffusion plays a negligible role in the formation of this stripe system.

KOPELL and HOWARD [3] arrived at the same conclusion in their paper.

BECK, VÁRADI and HAUCK [4] tried to describe quantitatively the one-dimensional waves on the basis of the above concept. Their model calculations

\* Presented on the joint session of the Working Committees on Reaction Kinetics and Catalysis, and Coordination Chemistry, Budapest, October 29, 1980.

\*\* To whom correspondence should be addressed

reflect correctly the main characteristics of the phenomena studied. In the course of the investigation of two-dimensional waves formed in the system malonic acid—bromate—ferroin—sulfuric acid—bromomalonic acid, WINFREE [7] concluded that the chemical waves are of two types: the so-called pseudo-waves without mass transfer, and the trigger waves which involve mass transfer. He believes that pseudo-waves can penetrate impermeable walls placed in the way of their migration, while the passage of trigger waves is prevented by such a wall. FIELD and NOYES [5] clarified the essential features of trigger waves. SMOES says in a paper published recently [6] that in the Zhabotinskii system catalyzed by ferroin an impenetrable wall can prevent the migration of every type of waves, consequently, the differentiation between the two types of waves is artificial, and the phenomenon can be treated on the basis of a uniform theory. However, this theory has not been discussed in detail in the paper.

According to the above mentioned papers [2, 3, 4], the one-dimensional chemical waves are pseudo-waves in terms of the classification of WINFREE, consequently, they should be able to penetrate an obstacle placed in their way.

Such a simple experiment for clarifying the role of diffusion in the case of one-dimensional chemical waves has been carried out — to our knowledge — only by KOPELL and HOWARD [3]. Their results, however, concern only the case of temperature gradients, and can be interpreted only indirectly.

The paper of SMOES [6] mentioned earlier makes the experimental settlement of the question especially justified.

In order to check experimentally the description of pseudo-waves mentioned earlier, we studied the penetration of one-dimensional waves coming about as a result of concentration gradients through hindrances.

## Experimental

Experiments were performed according to the concentration conditions described in the paper of BECK and VÁRADI [4] as follows:

malonic acid:  $3 \times 10^{-1}$  mol dm<sup>-3</sup>

potassium bromate:  $7 \times 10^{-2}$  mol dm<sup>-3</sup>

ferroin:  $6.7 \times 10^{-4}$  mol dm<sup>-3</sup>

cerium(III) nitrate:  $1.3 \times 10^{-3}$  mol dm<sup>-3</sup>.

The wave propagation was studied in a cell etched vertically into a transparent lucite block with the size of  $1 \times 1 \times 7$  cm. The block was split into two pieces at the half height of the cell, and a slight groove was etched into the fitting plane which served as a guide rail, so that we could fit a plastic foil of 0.1 mm thickness between the two planes. A hole identical in size to that of the cell was cut into the foil. These three parts were fastened together with springs in such a way that the liquid could not leak at the fittings, but the foil could be moved in the guide rail to and fro between the two half blocks. When the opening in the foil gets into the axis of the cell, the cell volume is united, when the foil is pulled off from this position, the cell is separated into two volumes with this impermeable wall. The moving of the foil, i.e. the joining or separating of the cell volumes lasted for 1 s in the cell filled with liquid.

According to our preliminary experiments, the material of the cell and the foil had no observable effect on the reaction. The operation of the cell is seen in Fig. 1. Experiments were

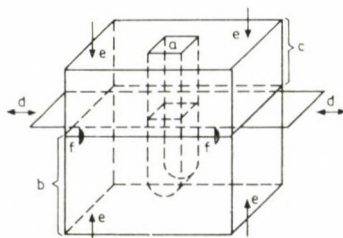


Fig. 1. Design and operation principle of the cell used in the experiments; a — cell volume, b — bottom of the lucite block, c — top of the lucite block, d — thin plastic foil separating the cell volume with the  $1 \text{ cm}^2$  opening, e — compression points of springs with the pressure direction (springs are not represented for the sake of clarity), f — wedges ensuring the two half blocks against moving from each other

carried out as follows:  $6 \text{ cm}^3$  of the mixture of the above composition was filled into the unseparated cell after careful homogenization, then  $0.2 \text{ cm}^3$  conc. sulfuric acid was added. After the damping of convection flow (i.e. after about 8 s) the cell was separated with the slide-in wall. The phenomenon was photographed from the moment of dropping the sulfuric acid with a Pentacon automatic camera provided with a quick exposure equipment, which was placed at the same level as the cell, in every 9 (sometimes 12) s.

The migration of chosen stripes was also studied, in this case pictures were taken in every 3 s. Black and white negative material was used. The blue and red stripes were best visible when applying a blue filter.

The experiment was carried out also in such a way that the cell was not separated after the damping of the flow, only later, after the beginning of the migration of stripes. Pictures were here also taken from the moment of  $\text{H}_2\text{SO}_4$  addition.

Waves were also generated and studied by injecting distilled water into the mixture. In this case, to the  $6 \text{ cm}^3$  mixture described earlier,  $0.2 \text{ cm}^3$  conc.  $\text{H}_2\text{SO}_4$  was added, homogenized and filled into the cell. After awaiting one change of colour (the solution changed colour at the same time in the whole cell), about  $0.5 \text{ cm}^3$  of distilled water was injected into the mixture. The cell was separated after the damping of the convective flow, or in other experiments after the starting of stripe migration. Pictures were taken in the same way as with acid addition. Experiments were also made with ferroin only as catalyst.

## Results and Discussion

After dropping concentrated sulfuric acid into the mixture the following events happened. The high density sulfuric acid quickly sank, causing thereby a convective flow in the cell. Its damping needed 8 s. The initially red solution suddenly turned blue — except for a surface layer of several mm — upon addition of the acid, then became slowly red again. About 30 s after the dropping of the acid, blue stripes appeared on the bottom of the cell moving upwards with a speed of about  $1 \text{ mm s}^{-1}$ . The migration of the stripes lasted for about 15 min, then the stripe system was slowly destroyed by the gas bubbles formed. One deviation from the observations of BECK and VÁRADI was noticed: according to our experience, though the speed of the migration of stripes decreased by more than one order of magnitude, it did not become zero.

For the stripes starting from the bottom of the cell after dropping in the acid, the wall slid in did not represent any obstacle.

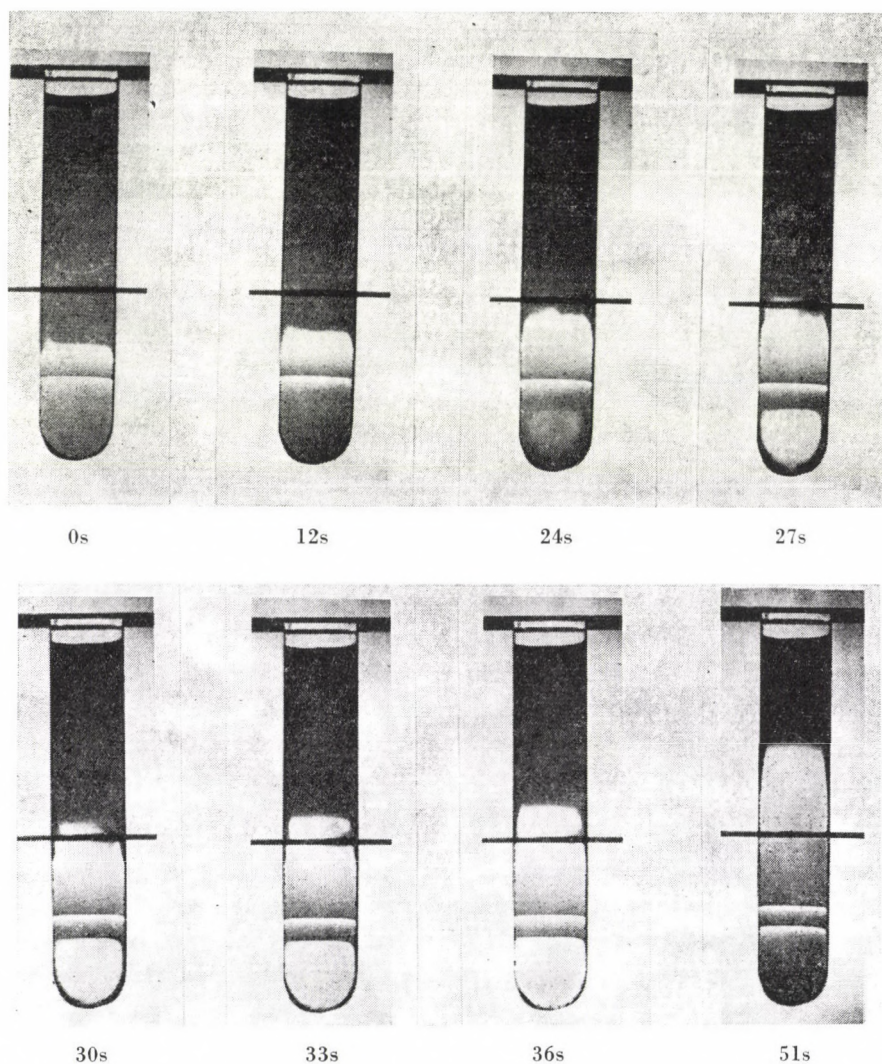


*Fig. 2.* Note: On the photographs in Fig. 2 only the front view of the cell is shown. Penetration of waves generated by injecting of distilled water through the separating wall in the system bromate-malonic acid-sulfuric acid, containing cerium-ferroin mixed catalyst. Times are given on a relative time scale beginning with the first picture

Within the limits of experimental error, every stripe penetrated reproducibly the separating wall without any breaking or weakening.

The same was found in the case of waves created by injection of distilled water. The phenomenon is independent of whether the catalyst is cerium and ferroin together or only pure ferroin.

Figure 2 shows the penetration of waves created by injection of distilled water through the separating wall. The stripe formed on the bottom of the cell

proceeds first slowly, then with increasing speed upwards and reaches the separating wall marked with a black line in the pictures, and apparently passes through it.

For comparison, the corresponding phenomenon was also photographed in the unseparated cell. The pictures prove that the wave propagation is practically the same in both the separated and unseparated cells.

Our results confirm that the concept of BECK and VÁRADI [2, 4] and that of KOPELL and HOWARD [3] is right: wave propagation in the system studied is the result of a periodic reaction proceeding with a changing rate along the space coordinate. Mass transfer caused by diffusion does not play a basic role in the propagation of waves. It is obvious, however, that the consideration of the effect of diffusion cannot be neglected in the *full* description of the stripe structure.

The extent of this effect was studied by developing further the concept of BECK and VÁRADI [4], which was proved to be right by our experiments, and the propagation of the one-dimensional waves was modelled by taking diffusion into account. In the knowledge of initial acid gradient and the diffusion constant of sulfuric acid we reckoned with the diffusional levelling of the acid gradient, but we neglected the diffusion of the other components between the stripes. Our calculations provided the stripe system originating from the model not considering diffusion for the existence of the phenomenon of about 15 minutes. That means that in the modification of the stripe system only the diffusion between the stripes can play a role. Considering, however, that as a consequence of the periodic reaction, the gradients between the stripes steadily change their direction — in relatively short intervals — the role of diffusion between the stripes seems also to be negligible.

That means that in the formation of one-dimensional stripe systems generated by a concentration gradient, diffusion does not play a role, these one-dimensional waves can be considered unambiguously as pseudo-waves.

#### REFERENCES

- [1] BUSSE, H. G.: J. Phys. Chem., **73**, 750 (1969)
- [2] BECK, M., VÁRADI, Z.: Magy. Kém. Folyóirat, **77**, 167 (1971)
- [3] KOPELL, N., HOWARD, L. N.: Science, **180**, 1171 (1973)
- [4] BECK, M., VÁRADI, Z., HAUCK, K.: Magy. Kém. Folyóirat, **81**, 86 (1975); VÁRADI, Z. B., BECK, M. T.: BioSystems, **7**, 77 (1975)
- [5] FIELD, R. J., NOYES, R. M.: J. Amer. Chem. Soc., **96**, 2001 (1974)
- [6] SMOES, M. L.: Bull. Amer. Phys. Soc., **24**, 477 (1979)
- [7] WINFREE, A. T.: Faraday Symp. Chem. Soc., **9**, 43 (1974)

György PÓTA }  
György BAZSA } H-4010 Debrecen, P.O.Box 7  
Mihály BECK }



## SELF-OSCILLATING CHEMICAL REACTIONS

### MECHANISM OF OSCILLATING OXIDATIONS WITH BROMATE\*

A. M. ZHABOTINSKII

*(Institute of Biological Tests of Chemical Compounds Kupavna Moscow Region, USSR)*

Received April 28, 1981

Accepted for publication June 13, 1981

Approaches to the analysis of the mechanism of oscillatory oxidation with bromate and the use of models of various depths of detail are discussed. The detailed scheme of oxidation of transition metal ions with bromate is analyzed together with semiempirical dynamic models for the complete oscillating system and a controlled experiment based on a "black box" model. New data are reported, which further specify the generally accepted basis scheme.

Since the discovery of the first example of this group of reaction by BELOUSOV [1] and the proposal of a crude flow-chart for its description [2], *cf.* Fig. 1, studies have been conducted in three main directions:

#### 1. Search for new oscillating systems

The most important recent findings in this direction were the discovery of uncatalyzed oscillating reactions [3, 4] and reductants that cannot be brominated [5], observation of oscillations during intramolecular ligand oxidation in complexes [6, 7], and the application of mixed substrates [8]. One of the most interesting results is the discovery of oscillations in systems with very low, and apparently constant bromide ion concentrations [9].

#### 2. Search for new dynamic regimes in ideally mixed, closed and flow reactors

A wide variety of simple, complex and stochastic oscillations has been discovered [2, 10–17], including switchover between regimes [12, 14]. For checking the mathematical models, the most valuable tool is the study of boundaries between various dynamic regimes in the space of controllable parameters, *viz.* the initial reactant concentrations [10–12, 18].

\* Presented on the joint session of the Working Committees on Reaction Kinetics and Catalysis, and Coordination Chemistry, Budapest, October 29, 1980

### 3. Study of behaviour in space

This field has led to most important results involving the discovery of new types of wave structures [19–24] and steady-state periodic concentration distributions [25–28].

#### What does it mean to know the mechanism of the phenomenon? Problems and models

The mechanism of the phenomenon can be regarded as known when it is capable of describing adequately all the most important characteristics of the concept of process and of predicting new experimental facts. As concerns predictive value, the knowledge of a mechanism depends on the type of problem posed. Several alternatives are possible, for instance the mechanism of a given system can be considered as known if it is capable of predicting:

1. Possibility of oscillations upon replacing one or another chemical reactant by others;
2. The qualitative behaviour of the system, *i.e.* the occurrence of certain dynamic regimes and the structural (parametric) diagram of the system;
3. The quantitative behaviour of the system, *i.e.* the exact description of dynamically important variables at various values of the controllable parameters; and
4. Most important, qualitatively new dynamic regimes.

The mechanistic descriptions of a given system required for solving the above problems may bear no resemblance whatsoever to one another.

The following descriptions of mechanism have been already used:

1. Flow-charts with the basic substrates and products, key intermediates, and their transformations as well as their effects on the rate of the basic process [2, 29].
2. Schemes including non-elementary reactions together with their kinetics [30].
3. Detailed schemes in terms of elementary steps [31, 32].
4. Dynamic models, consisting of systems of differential equations in terms of the key intermediates, their coefficients depending on the controllable parameters [30, 33–37].
5. Active media, every point of which is finite automaton [27].

In numerous cases mixed models are used, where various parts of the mechanism are described in different depths of detail [38].

Naturally, the ideal model is a detailed scheme including all the essential elementary steps and the values of rate constants or at least their order of

magnitude. Such a complete model would in principle permit to describe and predict all the details of behaviour and also to obtain simple asymptotic models by correct methods [29, 39]. Unfortunately, the emergence of such models cannot be realistically expected in the near future.

Similarly, insufficient information is available at present for predicting the possibility of oscillations upon significant changes in the nature of starting reactants. In such cases intuition is based on a "zoo" of theoretical models, involving, in one way or another, autocatalysis, retardation/inhibition or other types of negative feedback, permitting instability and oscillations [29]. From the complete scheme of such a simplex system, *e.g.* BELOUSOV's reaction, it is possible to select, ignoring the values of constants, a variety of sub-schemes that can generate oscillations separately. However, the existence of self-oscillating sub-schemes is a necessary but not sufficient condition for self-oscillations in the complete system.

Despite the lack of a fully consistent model for the Belousov reaction, the various partial models permit to draw a number of important conclusions. In what follows, we shall demonstrate examples of the efficient utilization of models at various levels of sophistication.

**Detailed scheme. Mechanism of the  $\text{Me}^{n+} \xrightarrow{\text{HBrO}_3} \text{Me}^{(n+1)+}$  reaction**

Let us denote the total  $\text{BrO}_3^-$  concentration by  $A$  and the sum  $[\text{Me}^{n+}] + [\text{Me}^{(n+1)+}]$  by  $C$ . Of the various characteristics of the reaction



the following are the most important with respect to oscillations.

1. Reaction (1) is autocatalytic, the autocatalyst being an intermediate of bromate reduction.

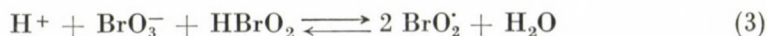
2. At  $C/A \ll 1$ , the maximum reaction rate is [40]

$$v_{\max} = d[\text{Me}^{(n+1)+}]/dt = q_1 h_0 AC \quad (2)$$

This expression is valid in a wide interval of parameters.

3. The reaction is strongly inhibited by bromide ions.

The nucleus of the scheme is the autocatalytic reaction. Of the multitude of possible versions, the simplest is the scheme proposed by FIELD, KŐRÖS and NOYES (FKN) [41]:



Since  $pK_{\text{HBrO}_3} \approx 0.7$  [42], reaction (3) should be replaced by



Within the simplest scheme (4, 5] autocatalysis can be obtained in a wide interval of rate constants. These constants have been estimated from various indirect data [31, 41]. However, it is more correct to study the quantitative behaviour of the system at various values of the constants. The corresponding system of equations has the form:

$$\begin{aligned} \dot{x} &= k_4 y(C - x) - k_{-4} ux \\ \dot{y} &= -k_4 y(C - x) + k_{-4} ux + 2k_{-5} Au - 2k_{-5} y^2 \\ \dot{u} &= k_4 y(C - x) - k_4 ux - k_5 Au + k_{-5} y^2 \end{aligned} \quad (6)$$

where

$$x = [\text{Ce}^{4+}], \quad y = [\text{BrO}_2^\cdot], \quad u = [\text{HBrO}_2]$$

It is easy to see that

$$x = y + 2u$$

According to analysis, expressions of type (1) can only be obtained if the rate of radical disproportionation (-4) is small compared to that of reaction (+5). In this case, the model gives a  $\text{BrO}_2^\cdot$  concentration that is comparable with  $x$ . Disagreement with the data of BUXTON and DAINTON [43] and the observed linear dependence of  $v_{\text{max}}$  on  $h_0$  [40] clearly indicates protonation of the radicals. Thus, scheme (4)–(5) should be replaced by



Estimates made in Ref. [32] yielded

$$pK_{\text{HBrO}_2^+} \geq 4.5 \quad (11)$$

FÖRSTERLING's data [44, 45] indicate that at  $[\text{H}_2\text{SO}_4] = 1.5 \text{ M}$ , there is a sharp increase in the lifetime of  $\text{BrO}_2^\cdot$  radicals as compared to neutral solution [43]. Thus a direct qualitative confirmation of this model is now available.

A comparison of the results in Refs [31, 32, 46, 47] clearly shows that the occurrence of autocatalysis and bistability does not depend on the details of the chemical scheme. It is easy to achieve a quantitative fit of the results at one point having with a large number of uncertain kinetic constants. However, the quality of fit in a wide range of chemical parameters depends strongly on the correctness of the scheme in a strictly chemical sense. In the example given, it is the acidity that permits to make a suitable selection.

On the other hand, the analysis of asymptotic subsystems, obtained by approaching some of the constants (or their ratios) to zero or infinity:

$$k_i(k_i/k_j) \longrightarrow 0 \quad \text{or} \quad k_i(k_i/k_j) \longrightarrow \infty$$

provides a qualitative picture of how the system behaves. In the above example, it was the analysis of such subsystems that revealed the importance of reaction (-10) for the correct description of the kinetic behaviour [48].

### Qualitative and quantitative description of oscillatory regimes by semiempirical models

In numerous cases the quantitative, and sometimes the qualitative description of oscillatory regimes in selected points of the parameter space is performed in terms of rather detailed models. This approach is justified only if the reaction scheme and the constants involved are accurately known. If the coincidence with experiments is achieved by arbitrary variation of the constants of the large scheme, then the procedure involves extensive uncertainty. It is easy to show that the majority of dynamic regimes observed in the system under consideration can be described by a second-order dynamic model in which the slow variable is the concentration of one of the catalyst species ( $x$ ), and the fast variable is the concentration of the  $\text{Br}^-$  inhibitor ( $z$ ) or the autocatalyst —  $\text{HBrO}_2$  ( $\text{HBrO}_2^+$ ) ( $y$ ). The phase planes of such models are shown in Fig. 2a and b. On the other hand, the flow-chart in Fig. 1 indicates the existence of at least three essential dynamic variables ( $x, y, z$ ), therefore the starting model is naturally constructed with respect to these 3 variables. Such a model can be immediately written down from the kinetics of the individual blocks [30] or may be obtained more or less accurate-

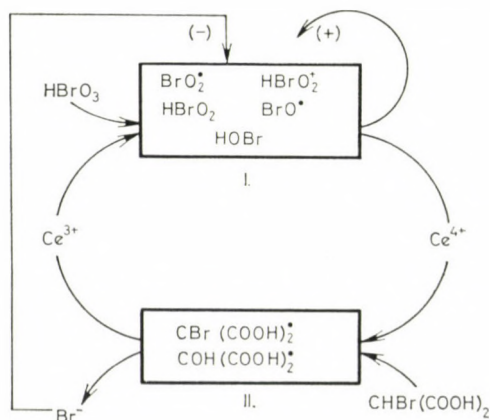


Fig. 1. Basic flow-chart of the oscillating reaction bromate, cerium, bromomalonic acid (BCB)

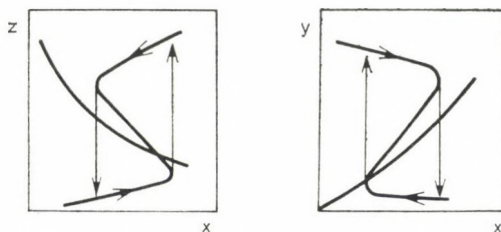


Fig. 2. Phase planes of the simplest self-oscillating models for bromate oxidation;  $x = [\text{Ce}^{4+}]$ ;  $y = [\text{HBrO}_2^+]$ ;  $z = [\text{Br}^-]$

ly from the detailed reaction scheme [33–37]. Consequently, a third-order model with respect to  $(x, y, z)$ , which reduces asymptotically to the second order relaxation model relative to  $(x, z)$  or  $(x, y)$  (Fig. 2), describes quantitatively practically all of the observed regimes. The starting third-order model is capable of describing also stochastic oscillations or oscillations with complicated periodicity [36, 49]. It has been shown that good quantitative description is possible if the coefficients of the dynamic model are chosen as simple functions of the parameters of the system [30]. On the basis of the FKN mechanism, TYSON has obtained a very simple asymptotic model, which, for two empirical sets of parameters, gives good quantitative agreement in a sufficiently wide interval of the experimental parameters [36, 37].

It seems to be that the structural diagram of the dynamic system has the greatest informative value as it shows the distribution of regions for the various dynamic regimes in the space of experimentally controllable parameters [10–12, 18, 50]. The experimental construction of the structural diagram requires no quantitative measurements but good agreement between theory and experiment is only possible if both the dynamic and chemical features of the system are taken into account. There have already been limited attempts at comparing the theoretical and experimental structural diagrams [30, 34, 35, 50]. However, it remains the task of future research to develop a complete diagram including the regions of simple self-oscillations, oscillations of complicated periodicity, stochastic oscillations and several steady states.

### Possibility of new chemical mechanisms providing oscillations

The basic mechanism responsible for oscillations in the majority of new chemical compositions is apparently close to the original flow-chart (Fig. 1). However, the results of NOSZTICZIUSZ [8, 9] induce thoughts about the possibility of new chemical and dynamic mechanisms. For example, he observed oscillations when  $\text{Br}_2$  was continuously removed from systems involving oxalic and glyoxylic acid as reducing agents [8]. Also, oscillations occurred in

the bromate, Ce, malonic acid system when the bromide ion concentration was strongly reduced by the addition of  $\text{Ag}^+$  ions [9]. Even if the first of these findings can be reconciled with the basic flow-chart and the available data, the second observation clearly contradicts this scheme.

NOSZTRICZIUSZ has suggested new basic schemes for the mechanism of oscillations [51]. The validity of these schemes can at present be discussed only on the basis of indirect data. From the full set of steps possible in this complex scheme, it is also possible to select other theoretical mechanisms leading to oscillations.

The desirability of finding a simple, unified scheme describing self-oscillations in the majority of bromate-containing systems has been emphasized [51]. However, it is quite conceivable that in one and the same chemical system, oscillations are due to different sub-schemes at various parameter values. This may be the reason for the very wide oscillatory region for the bromate, Ce, malonic acid system [10].

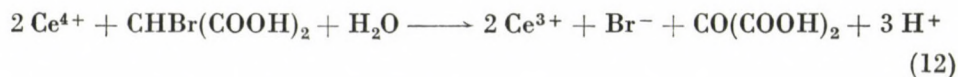
A final answer can only be obtained from direct experiments on the role of the suspected compounds, HOBr and  $\text{Br}_2$ . As the accurate determination of HOBr and  $\text{Br}_2$  in this system is rather difficult, it would be more convenient to apply the controlled introduction of these compounds into the reacting solution.

### The controlled experiment. Refinement of the flow-chart

The controlled experiment is a convenient means of checking the details of a complex reaction. Here we report some preliminary data on checking the simplest mechanistic hypothesis (SMH) for the BELOUSOV reaction, based on the flow-chart in Fig. 1 [38, 52]. This hypothesis implies the following simplifying assumptions.

1. The free radicals involved in reaction (I) play no role in reaction (II) and, conversely, the radicals generated in (II) do not affect reaction (I).

2.  $\text{Br}^-$  is produced proportionally to the reduction of  $\text{Ce}^{4+}$ , in the simplest case via the reaction



There are sufficient data indicating that reaction (12) is not the only source of bromide ions. In this case the SMH implies that



The oscillatory model based on the SMH is of the form:

$$\begin{aligned}\dot{x} &= f_x - bx \\ \dot{y}_i &= f_i \\ \dot{z} &= f_z + qbx\end{aligned}\quad (14)$$

where  $x = [\text{Ce}^{4+}]$ ,  $z = [\text{Br}^-]$ ,  $y_i$  — the concentrations of other intermediates, and  $q = m/n$ . According to Ref. [53],

$$b = \frac{KB}{K + B} \quad (15)$$

where  $B$  is the concentration of bromomalonic acid.

The model of reaction (1) in an ideally stirred flow reactor is

$$\begin{aligned}\dot{x} &= f_x - \delta x \\ \dot{y}_i &= f_i - \delta y_i \\ \dot{z} &= f_z - \delta z + \delta_z z_0\end{aligned}\quad (16)$$

where  $\delta = v/V$ ,  $\delta_z = v_z/V$ ,  $v$  is the volume flow rate,  $v_z$  is the rate of introduction of  $\text{Br}^-$  and  $V$  is the volume of the reactor.

Models (14) and (16) coincide under the conditions:

$$\delta = b \quad (17)$$

$$\delta_z z_0 = qbx \quad (18)$$

$$\delta z \ll \alpha z \quad (19a)$$

$$\delta y_i \ll \beta_i y_i \quad (19b)$$

where  $\alpha z$  and  $\beta_i y_i$  are the corresponding terms of  $f_z$  and  $f_i$ .

Thus, if the SMH is valid, then the Ce, BMA, bromate system can be precisely modelled, conducting reaction (1) in a flow reactor with additional feeding of  $\text{Br}^-$ . The  $\text{Br}^-$  feed rate should be proportional to the  $\text{Ce}^{4+}$  concentration of the solution.

The experiment has been carried out in the cells of a Specord UV-Vis double-beam spectrophotometer under intense stirring. The solution volume was 2.5 cm<sup>3</sup>, the temperature 40 °C. The solutions of  $\text{Ce}_2(\text{SO}_4)_3$  and  $\text{KBrO}_3$  in 1.5 M  $\text{H}_2\text{SO}_4$  were fed into the cell at a constant rate. The  $\text{KBr}$  solution in 1.5 M  $\text{H}_2\text{SO}_4$  was added at a rate proportional to the optical density at 320 nm, *i.e.* to the  $\text{Ce}^{4+}$  concentration.

The experimental setup is shown schematically in Fig. 3.

The results shown in the Table I indicate that a relatively good agreement is observed if  $q$  is in the range of 1.1–2.6. The experiments have been carried

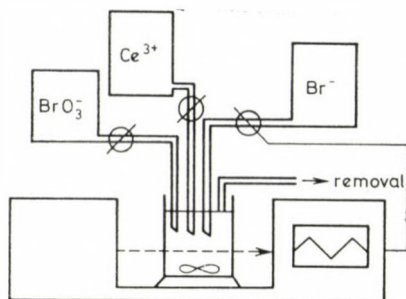


Fig. 3. Scheme of setup for modelling the self-oscillating BCB system; oxidation of  $Ce^{3+}$  by bromate with controlled feed of  $Br^-$ . Feed rate of  $Br^-$  is proportional to the optical density at 320 nm

out at small  $A$ ,  $B$  and  $C$ . More complete information is obtained upon comparison in the whole  $ABC$  space of oscillations. Unfortunately, higher initial  $Br^-$  ( $z_0$ ) concentrations could not be used in our setup. In the latter case the results obtained depended on the intensity of stirring. Consequently, these experiments require accurate control of the conditions of ideal mixing.

Table I

$q$ \ $A(M)$	0.001	0.0025	0.005
0.55		1: St.; 6.4	2: St.; 6.6
0.65	3: St.; 5.6		
1.1		4: 26; 1.9; 5; 15	5: 29; 7.4; 6; 10
1.3	6: 20; 2.1; 13.5; 12		
2.2		7: 24; 1.6; 3.3; 21	8: 29; 4.5; 3; 16.5
2.6	9: 20; 2.4; 4; 13.5		
4.4			10: 26; 2.1; 2; 18
8.8	11: 16; 1; 1.5; 15		
$B$	12: 16; 2.7; 3.3; 17	13: 27; 6.6; 3; 9	14: 29; 16; 2.5; 7.5

*Explanation of codes:*

Sets of 5 numbers are given as: No;  $M$ ;  $N$ ;  $T_1$ ;  $T_2$ , where

No is the number of run;

$M$  is the maximum  $Ce^{4+}$  concentration (in  $10^{-6} M$ );

$N$  is the minimum  $Ce^{4+}$  concentration (in  $10^{-6} M$ );

$T_1$  and  $T_2$  are in minutes.

St. denotes a steady state; it is followed by  $[Ce^{4+}]$  in  $10^{-6} M$  units.

$C = 5 \times 10^{-5} M$ ;  $B = 4.5 \times 10^{-3} M$ ;  $t = 40^\circ C$ .

Average values for 2–3 runs are given

It is apparent from the Table I that at  $A/B \approx 0.2$  (No. 12 in the Table) good agreement can be obtained at  $q = 2.6$  (No. 9). However, at  $A/B \approx 1$  (No. 14) no coincidence of the oscillation pattern can be achieved at any values of  $q$ . Nos 14, 5 and 8 are compared in Fig. 4.

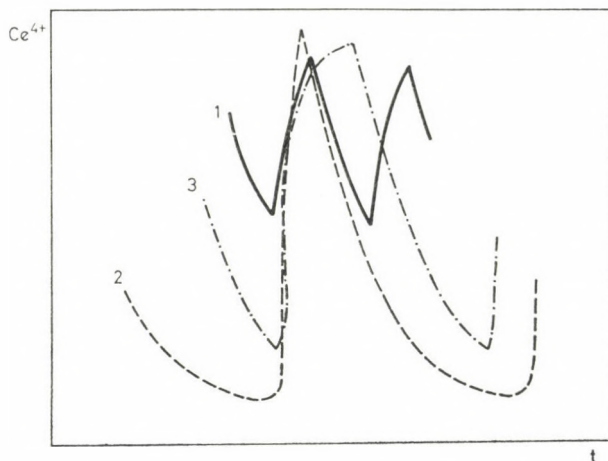


Fig. 4. Comparison of self-oscillations in the BCB system and in the controlled experiment; (1): BCB (No. 14); (2):  $q = 1.1$  (No. 5); (3):  $q = 2.2$  (No. 8). Numbers correspond to the Table I; initial concentrations are given in the Table I. The results of single experiments are listed

On comparing the characteristics of oscillations obtained via mathematical models in controlled experiments with the bromate/cerium/BMA system, the following can be established:

1. The mathematical models based on the SMH can be brought to good agreement with the results of the controlled experiment.

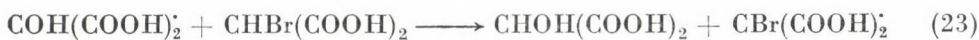
2. At small  $A/B$  values, agreement is obtained at  $q \approx 3$ .

3. At  $A/B \geq 1$ , the value of  $N$  in the controlled experiment is much smaller than in the initial oscillating system. It appears that in the vicinity of the maximum  $Ce^{4+}$  concentration, inhibition is significantly stronger and around the minimum it is significantly weaker than predicted by the SMH.

The question arises how one should obtain the required value of  $q$ . One of the possibilities is to assume a chain reaction. To the steps



giving together the overall reaction (12), one can add the chain propagation step

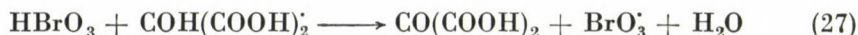


In order to obtain a better agreement at  $A/B \geq 1$ , one should apparently include additional interaction between blocks I and II in Fig. 1. In fact, it

has been shown that the intermediates of bromate reduction may participate in  $\text{Br}^-$  production [54]. The following reactions can be assumed



On the other hand, the products of block II may activate reaction (1), e.g.:



Consequently, there are sufficient grounds to state that the free-radical intermediates of blocks I and II may produce additional interactions between these blocks.

\*

The author is indebted to all of his Hungarian colleagues for the interesting discussions which have lead to the writing of this paper and especially to Prof. M. T. BECK, Prof. E. KÖRÖS and Dr. Z. NOSZTICZIUSZ for their warm hospitality.

#### REFERENCES

- [1] BELOUSOV, B. P.: Collection of Abstracts in Radiation Medicine 1958 (In Russian), p. 145. Medgiz, Moskva 1959
- [2] ZHBOTINSKII, A. M.: Dokl. Akad. Nauk SSSR, **157**, 392 (1964)
- [3] ORBÁN, M., KÖRÖS, E.: J. Phys. Chem., **82**, 1672 (1978)
- [4] ORBÁN, M., KÖRÖS, E.: React. Kinet. Catal. Lett., **8**, 273 (1978)
- [5] BECK, M. T., VÁRADY, Z. B.: React. Kinet. Catal. Lett., **6**, 275 (1977)
- [6] BECK, M. T., BAZSA, Gy. HAUCK, J.: Kinetics of Physicochemical Oscillations, Preprints **1**, 123 (1979)
- [7] YATSIMIRSKII, K. B., ZAKREVSAYA, L. N., KOLCHINSKII, A. G., TIKHONOVA, L. P.: Dokl. Akad. Nauk SSSR, **251**, 132 (1980)
- [8] NOSZTICZIUSZ, Z.: Magy Kém. Folyóirat, **85**, 330 (1979)
- [9] NOSZTICZIUSZ, Z.: J. Am. Chem. Soc., **101**, 3660 (1979)
- [10] VAVILIN, V. A., ZHBOTINSKII, A. M., YAGUZHINSKII, L. S.: Oscillatory processes in biological and chemical systems (In Russian), p. 181. Nauka, Moskva 1967
- [11] VAVALIN, V. A., ZHBOTINSKII, A. M., KRUPYANKO, V. I.: Oscillatory processes in biological and chemical systems (In Russian), p. 199. Nauka, Moskva 1967
- [12] DE KEPPER, P., ROSSI, A., PACAULT, A.: C. R. Acad. Sci. Paris, **C283**, 371 (1976)
- [13] VAVILIN, V. A., ZHBOTINSKII, A. M., ZAIKIN, A. N.: Zh. Fiz. Khim., **42**, 3091 (1968)
- [14] MAREK, M., SVOBODOVA, E.: Biophys. Chem., **3**, 263 (1975)
- [15] GRAZIANI, K. R., HUDSON, J. L., SCHMITZ, R. A.: Chem. Eng. J., **12**, 9 (1976)
- [16] SCHMITZ, R. A., GRAZIANI, K. R., HUDSON, J. L.: J. Chem. Phys., **67**, 3040 (1977)
- [17] ROSSLER, O., WEGMANN, K.: Nature, **271**, 89 (1978)
- [18] KOVALENKO, A. S., TIKHONOVA, L. P., ROIZMAN, O. M., PROTOPOPOV, E. B.: Teor. Eksp. Khim., **16**, 46 (1980)
- [19] ZAIKIN, A. N., ZHBOTINSKII, A. M.: Nature, **225**, 535 (1970)
- [20] WINFREE, A. T.: Science, **175**, 634 (1972)
- [21] BUSSE, H.-J., HESS, B.: Nature, **244**, 203 (1973)
- [22] JESSEN, W., BUSSE, H.-J., HAVSTEEN, B. H.: Angew. Chem., **15**, 689 (1976)
- [23] ZHBOTINSKII, A. M., ZAIKIN, A. N.: Oscillatory processes in biological and chemical systems, V. 2, ed. Selkov E. E. (In Russian), p. 279. Pushchino 1971

- [24] WINFREE, A. T.: *Science*, **181**, 937 (1973)
- [25] BUSSE, H.-J.: *J. Phys. Chem.*, **73**, 750 (1969)
- [26] ZAIKIN, A. N., ZHABOTINSKII, A. M.: *Zh. Fiz. Khim.*, **45**, 265 (1971)
- [27] ZHABOTINSKII, A. M., ZAIKIN, A. N.: *J. Theor. Biol.*, **40**, 45 (1975)
- [28] VÁRADI, Z. B., BECK, M. T.: *Bio Systems*, **7**, 77 (1975)
- [29] ZHABOTINSKII, A. M.: *Concentration Self-oscillations*. Nauka, Moskva 1974
- [30] ZHABOTINSKII, A. M., ZAIKIN, A. N., KORZUKHIN, M. D., KREITSER, G. P.: (a) *Oscillatory processes in biological and chemical systems*, V. 2. Ed. Selkov, E. E., p. 269. Pushchino 1971.; (b) *Kinet. Katal.*, **12**, 584 (1971)
- [31] BARKIN, S., BIXON, M., NOYES, R. M., BAR-ELI, K.: *Intern. J. Chem. Kinet.*, **11**, 841 (1977)
- [32] ROVINSKII, A. B., ZHABOTINSKII, A. M.: *Teor. Eksp. Khim.* **14**, 183 (1978)
- [33] FIELD, R. J., NOYES, R. M.: *J. Chem. Phys.*, **60**, 1877 (1974)
- [34] WEISBUCH, G., SALOMON, J., ATLAN, H.: *J. Chim. Phys.*, **72**, 71 (1975)
- [35] TOMITA, K., ITO, A., OHTA, T.: *J. Theor. Biol.*, **68**, 459 (1977)
- [36] TYSON, J. J.: *J. Math. Biol.*, **5**, 351 (1978)
- [37] TYSON, J. J.: *Ann. N. Y. Acad. Sci.*, **316**, 279 (1979)
- [38] SHOWALTER, K., NOYES, R. M., BAR-ELI, K.: *J. Chem. Phys.*, **69**, 2514 (1978)
- [39] ZHABOTINSKY, A. M.: *Ber. Bunsenges. Phys. Chem.*, **84**, 303 (1980)
- [40] VAVILIN, V. A., ZHABOTINSKII, A. M.: *Kinet. Katal.*, **10**, 83 (1969)
- [41] FIELD, R. J., KÖRÖS, E., NOYES, R. M.: *J. Am. Chem. Soc.*, **94**, 8649 (1972)
- [42] *Chemical Handbook*, Vol. 3, p. 1005. Khimiya, Leningrad—Moskva 1964
- [43] BUXTON, G. V., DANTON, F. S.: *Proc. Roy. Soc.*, **A304**, 427 (1968)
- [44] FÖRSTERLING, H.-D., LAMBERZ, H., SCHREIBER, H.: *Z. Naturforsch.*, **35a**, 329 (1980)
- [45] FÖRSTERLING, H.-D.: *Acta Chim. Acad. Sci. Hung.* (this issue)
- [46] GEISELER, W., FOLLNER, H. H.: *Biophys. Chem.*, **6**, 107 (1977)
- [47] BAR-ELI, K., NOYES, R. M.: *J. Phys. Chem.*, **82**, 1352 (1978)
- [48] ROVINSKII, A. B., ZHABOTINSKII, A. M.: *Teor. Eksp. Khim.*, **15**, 25 (1979)
- [49] TOMITA, K., TSUDA, I.: *Phys. Lett.*, **71A**, 489 (1979)
- [50] DE KEPPER, P., BOISSONADE, J.: *Kinetics of Physicochemical Oscillations*, Preprints **1**, 21 (1979)
- [51] NOSZTICZIUSZ, Z., BÓDISS, J.: *Ber. Bunsenges. Phys. Chem.*, **84**, 366 (1980)
- [52] ZHABOTINSKII, A. M., ROVINSKII, A. B.: *Teor. Eksp. Khim.*, **16**, 386 (1980)
- [53] KASPEREK, G. I., BRUCE, T. C.: *Inorg. Chem.*, **10**, 382 (1971)
- [54] ROVINSKII, A. B., ZHABOTINSKII, A. M.: *Teor. Eksp. Khim.*, **15**, 457 (1979)

A. M. ZHABOTINSKII } Institute of Biological Test of Chemical Compound,  
 } Kupavna, Moscow Region, USSR

## PERTURBATION OF BROMATE OSCILLATORS, I

### PERTUBATION BY $\gamma$ IRRADIATION\*

E. KŐRÖS<sup>1\*\*</sup>, G. PUTIRSKAYA<sup>2</sup> and M. VARGA<sup>1</sup>

<sup>(1)</sup> Institute of Inorganic and Analytical Chemistry, Eötvös Loránd University, Budapest,

<sup>(2)</sup> Central Research Institute for Chemistry, Budapest)

Received May 25, 1981

Accepted for publication July 27, 1981

Reacting BZ systems of different catalyst [ $\text{Ce}^{3+}$ ,  $\text{Mn}^{2+}$ ,  $\text{Fe}(\text{phen})_3^{2+}$ ,  $\text{Ru}(\text{dipy})_3^{2+}$ ] have been perturbed by  $^{60}\text{Co}$   $\gamma$  irradiation. At high bromate concentrations (between 0.15 and 0.1 mol · dm<sup>-3</sup>)  $\gamma$  irradiation has no effect on the chemical oscillation irrespectively of the catalyst used. At lower bromate concentrations the oscillation is either quenched or considerably decreased in frequency in the case of cerium(III) or manganese(II). BZ systems with  $\text{Fe}(\text{phen})_3^{2+}$  or  $\text{Ru}(\text{dipy})_3^{2+}$  as a catalyst are not effected by  $\gamma$  irradiation. The major role of H atoms — produced in the radiolysis of water — is discussed, and the claim of earlier authors that the inhibitory effect can be attributed to bromide ions formed in the  $\text{BrMA} + \text{H}$  reaction is criticized.

### Introduction

The BELOUSOV—ZHABOTINSKY (BZ) oscillatory chemical system has been investigated from a large variety of aspects. A part of the investigations has been performed with the aim in mind to try to reveal what chemical conditions a reacting BZ system should meet for an oscillatory behaviour to occur.

Also in our Laboratories we have been dealing with this problem and for various BZ systems we could calculate the crucial bromomalonic acid concentration which is actually a threshold concentration at which the preoscillation period terminates and the system starts to exhibit concentration oscillation [1]. It is also well known that the reacting BZ systems can be perturbed in many ways, *e.g.* by the addition of ions of inhibitory property (halides) [2, 3], by the supply of  $\text{O}_2$  [4, 5], by keeping low of the bromide concentration (additions of  $\text{Ag}^+$ ) [6], and by changing of the temperature [7, 8]. From the effect the perturbation exerts important information can be gained as regards to the overall or to the part mechanism of the oscillatory reaction.

One of the recently applied perturbations is the  $\text{Co}^{60}$   $\gamma$  irradiation of the BZ system, which has been studied by RAMA RAO and PRASAD [9]. These

\* Presented on the joint session of the Working Committees on Reaction Kinetics and Catalysis, and Coordination Chemistry, Budapest, October 29, 1980.

\*\* To whom correspondence should be addressed

authors have reported on some rather interesting observations and on the basis of their experimental results they attempted to explain the occurring phenomena. The most important finding of the authors was that the oscillation ceased a certain period of time after the start of the irradiation or immediately at the start of the irradiation. This depended on the composition of the reaction mixture, especially on the bromate concentration. They claimed that a certain amount of the bromate should be converted to bromomalonic acid (BrMA) before the irradiation could quench the oscillation. They introduced the concept of effective bromate concentration  $[\text{BrO}_3^-]_{\text{eff}}$ . When the reacting system reached  $[\text{BrO}_3^-]_{\text{eff}}$  the effect of irradiation became evident. They found a linear correlation between  $[\text{BrO}_3^-]_{\text{eff}}$  and  $[\text{H}^+]$ : the higher was  $[\text{H}^+]$  the lower was  $[\text{BrO}_3^-]_{\text{eff}}$ .

The oscillation quenching by  $\gamma$  irradiation has been explained by the authors considering a reaction between H atoms and BrMA



The rate constant of the reaction is  $k = 2.0 \times 10^8 \text{ dm}^3 \cdot \text{mol}^{-1} \cdot \text{s}^{-1}$ . Bromide is generated in this reaction, and thus radiolysis contributes to the formation of the control intermediate. They claim that the irradiation sustains a higher than critical bromide concentration, which hampers chemical oscillation.

For the quantitative explanation of their results the authors slightly modified the OREGONATOR model [10] and included the radiolytic route of bromide formation (see Eq. 1). They have demonstrated that if the radiolysis parameter,  $r$ , is above a given value ( $r > r_{\text{min}} \sim 4$ ) the system reaches a stable steady state thus chemical oscillation is no more observable.

We have not been convinced by the authors explanation and doubted the important contribution of reaction (1) to the overall process. This fact and our intention to compare the behaviour of BZ systems of different catalysts prompted us to look again at the effect of  $\gamma$  irradiation. We also hoped to get additional information as to the prerequisites of chemical oscillation.

## Experimental

### Chemicals

Chemicals used in the experiments ( $\text{KBrO}_3$ ,  $\text{H}_2\text{SO}_4$ ,  $\text{Ce}(\text{NH}_4)_2(\text{SO}_4)_3$ ,  $\text{MnSO}_4 \cdot 7 \text{H}_2\text{O}$ ,  $\text{KNO}_3$ ) were of analytical purity. Malonic acid was of purissimum grade. Tris(2,2'-dipyridine)-ruthenium(II) hexahydrate was purchased from G. F. Smith Chemical Co. A  $0.025 \text{ mol} \cdot \text{dm}^{-3}$  solution of tris(phenanthroline)iron(II) was prepared from 1,10-phenanthroline and  $\text{Fe}(\text{NH}_4)_2(\text{SO}_4)_2 \cdot 6 \text{H}_2\text{O}$  (both of analytical grade).

Bromomalonic acid was prepared as described by CONRAD and REINBACH [11]. The potassium salt of bromomalonic acid was recrystallized from 90% ethanol. The bromomalonate content of the obtained white, crystalline material was determined iodometrically.

#### *Oscillatory reactions*

Potassium bromate, malonic acid, sulphuric acid and a catalyst [ $\text{Ce}^{3+}$ ,  $\text{Mn}^{2+}$ ,  $\text{Fe}(\text{phen})_3^{2+}$  or  $\text{Ru}(\text{dipy})_3^{2+}$ ] were mixed in various proportions. The reaction was started by the addition of the catalyst solution. The total volume was 50 cm<sup>3</sup>. Purified nitrogen was bubbled through the reaction mixture before the addition of the catalyst and also during the course of the reaction. The potential change in the reacting system was continuously monitored with a smooth platinum electrode and a  $\text{Hg}(\text{Hg}_2\text{SO}_4)\text{K}_2\text{SO}_4$  reference electrode which were connected to a Yokogawa Technicorder F Type 3052 recorder.

The reacting oscillatory systems were irradiated from a Co-60 radiation source of  $6 \times 10^{13}$  Bq output at two dose rates:  $2.74 \times 10^{18} \text{ eV} \cdot \text{dm}^{-3} \cdot \text{s}^{-1}$  and  $1.37 \times 10^{18} \text{ eV} \cdot \text{dm}^{-3} \cdot \text{s}^{-1}$ , respectively. The dose rate was measured by the use of the FRICKE solution.

#### *The course of the reaction*

In certain experiments 2.00 cm<sup>3</sup> aliquots were withdrawn from the reacting solution at different reaction times interrupting the irradiation for 1 minute and the total oxidation power of the solution was determined iodometrically.

In a few runs the amount of carbon dioxide evolved during the reaction was also measured. In these experiments the total volume of the reaction mixture was 200 cm<sup>3</sup>. Carbon dioxide was removed from the solution with high purity nitrogen and introduced into a gas chromatograph of Perkin-Elmer Type 451. The carbon dioxide content of the gas mixture was measured on a thermal conductivity detector periodically. The column length was 1 m, with an inner diameter of 2 mm, and was filled with PORAPACK-T of 0.16 mm particle diameter. The instrument was calibrated before the experiments.

#### *Auxiliary measurements*

In separate runs the spontaneous hydrolytic and radiation-induced decomposition, respectively, of bromomalonic acid was followed iodometrically by withdrawing samples in every 30 minute from a 1 mol · dm<sup>-3</sup> sulphuric acid solution of a 0.02 mol · dm<sup>-3</sup> bromomalonic acid solution and their bromomalonate content determined.

In order to reveal the effect of H atoms the behaviour of the reacting oscillatory system under  $\gamma$  irradiation containing potassium nitrate of different concentrations (0.5–1.5 mol · dm<sup>-3</sup>), was investigated.

### **Results and Discussion**

RAMA RAO and PRASAD determined the  $G(\text{Br}^-)$  during the irradiation of bromomalonic acid solutions ( $1 \times 10^{-2}$  —  $5 \times 10^{-2}$  mol · dm<sup>-3</sup>) and obtained a value of about 3 ion per 100 eV [9]. The rate of bromide ion formation was  $4.16 \times 10^{-7}$  mol · dm<sup>-3</sup> · s<sup>-1</sup> at the dose rate ( $8.357 \times 10^{18}$  eV · dm<sup>-3</sup> · s<sup>-1</sup>) applied by the authors.

We also measured the radiation-induced decomposition of bromomalonic acid irradiating  $2 \times 10^{-2}$  mol · dm<sup>-3</sup> bromomalonic acid solution at a dose rate of  $2.74 \times 10^{18}$  eV · dm<sup>-3</sup> · s<sup>-1</sup>, and in separate experiments we followed the spontaneous hydrolytic decomposition of bromomalonic acid under identical conditions at 20 °C. The following values were obtained (averages of three

runs) for the initial rate:

	$-\frac{d[\text{BrMA}]}{dt}$
	$\text{mol} \cdot \text{dm}^{-3} \cdot \text{s}^{-1}$
Hydrolytic	$0.9 \times 10^{-7}$
Radiolytic	$2.0 \times 10^{-7}$

The rate of bromomalonic acid decomposition is equal with the rate of bromide formation. Unfortunately the latter can not be followed directly in acidic solution because of its very low value. The two values given above are very close to each other and this fact indicates that  $\gamma$  irradiation has very slight effect on the decomposition of bromomalonic acid. This involves that reaction (1) can be neglected at the interpretation of the radiation-induced phenomena. In a separate run we have found that the chemical oscillation did not terminate earlier if the starting reaction mixture contained some bromomalonic acid.

Having considered that the supposition on the radiolysis-effected decomposition of bromomalonic acid to be questionable a detailed investigation has been launched in order to try to clarify the effect of  $\gamma$  irradiation on the reacting BZ systems.

First a BZ system of the following composition was  $\gamma$ -irradiated at the two dose rates:  $0.05 \text{ mol} \cdot \text{dm}^{-3} \text{ KBrO}_3$ ,  $0.20 \text{ mol} \cdot \text{dm}^{-3}$  malonic acid,  $1.0 \text{ mol} \cdot \text{dm}^{-3} \text{ H}_2\text{SO}_4$  and  $0.002 \text{ mol} \cdot \text{dm}^{-3} \text{ Ce}(\text{NH}_4)_2(\text{SO}_4)_3$ .

The overall reaction was followed iodometrically and by means of gas chromatography, respectively. The course of the reaction is shown in Figs 1 and 2. For comparison the unirradiated system is also shown in the Figures.

The curves in Figs 1 and 2 show that as a result of irradiation the overall rate of the reaction decreases and chemical oscillation is no more observable. The decrease in rate is more pronounced at the higher dose rate. Interrupting the irradiation the rate of reaction increases abruptly and chemical oscillation starts immediately.

The chemical reaction, however, is not completely quenched even during irradiation (in the non-oscillatory phase), only its rate became much lower. We assumed that probably the catalyst is hampered in its function. We shall come back to this point later in this paper.

Earlier we have reported that the reaction between acid bromate and malonic acid (*i.e.* the oxidative bromination of malonic acid) proceeds — though rather slowly — even in the absence of a catalyst [1, 12]. It is also known that there is a close-to-linear correlation between the initial rate and the catalyst concentration.

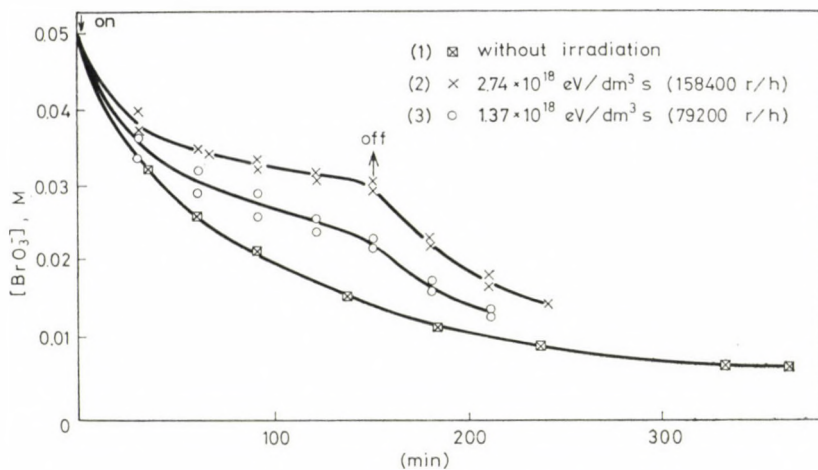


Fig. 1. The decrease of bromate concentration in time in a reacting system with the composition:  $0.05 \text{ mol} \cdot \text{dm}^{-3} \text{ KBrO}_3$ ,  $0.20 \text{ mol} \cdot \text{dm}^{-3}$  malonic acid,  $1.0 \text{ mol} \cdot \text{dm}^{-3} \text{ H}_2\text{SO}_4$  and  $0.002 \text{ mol} \cdot \text{dm}^{-3} \text{ Ce(IV)}$ . (1) without irradiation, (2) irradiation at a dose rate of  $2.74 \times 10^{18} \text{ eV} \cdot \text{dm}^{-3} \cdot \text{s}^{-1}$ , (3) irradiation at a dose rate of  $1.37 \times 10^{18} \text{ eV} \cdot \text{dm}^{-3} \cdot \text{s}^{-1}$ .

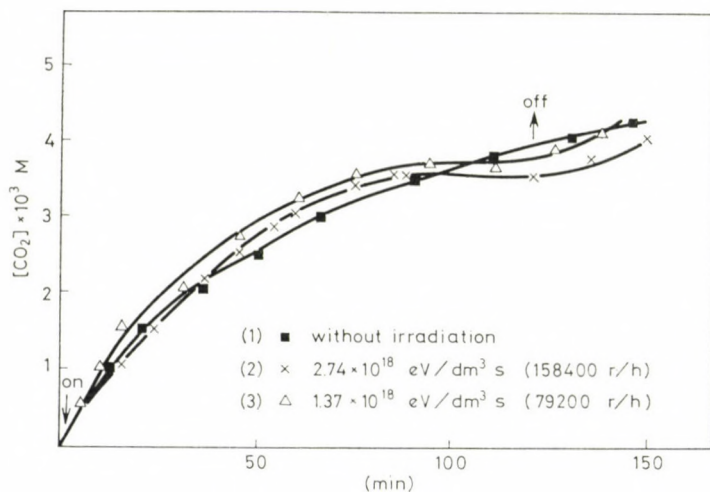


Fig. 2. The evolution of carbon dioxide in time in a reacting system with the composition:  $0.05 \text{ mol} \cdot \text{dm}^{-3} \text{ KBrO}_3$ ,  $0.20 \text{ mol} \cdot \text{dm}^{-3}$  malonic acid,  $1.0 \text{ mol} \cdot \text{dm}^{-3} \text{ H}_2\text{SO}_4$  and  $0.002 \text{ mol} \cdot \text{dm}^{-3} \text{ Ce(IV)}$ , (1) without irradiation, (2) irradiation at a dose rate of  $2.74 \times 10^{18} \text{ eV} \cdot \text{dm}^{-3} \cdot \text{s}^{-1}$ , (3) irradiation at a dose rate of  $1.37 \times 10^{18} \text{ eV} \cdot \text{dm}^{-3} \cdot \text{s}^{-1}$ .

We also looked at the effect of irradiation on BZ systems of different bromate concentrations. The results are given in Table I.

The  $\gamma$  irradiation of the reacting systems was started practically at the start of the chemical reaction. The once-and-ever termination of the oscillation could not be experienced; very rare and aperiodical "stray"

Table I

The composition of the BZ system:  $0.20 \text{ mol} \cdot \text{dm}^{-3}$  malonic acid,  $1.0 \text{ mol} \cdot \text{dm}^{-3} \text{H}_2\text{SO}_4$  and  $0.002 \text{ mol} \cdot \text{dm}^{-3} \text{Ce}(\text{NH}_4)_2(\text{SO}_4)_3$ ; temperature:  $20^\circ \text{C}$

$[\text{BrO}_3^-]$ $\text{mol} \cdot \text{dm}^{-3}$	Observation
0.15	$\gamma$ irradiation does not quench the oscillation
0.10	the same
0.07	after 16 oscillations the frequency of oscillation decreases, the oscillation, however, does not terminate even after 60 minutes
0.06	$\sim 10$ oscillations
0.055	$\sim 5$ oscillations
0.050	$\sim 0-4$ oscillations

oscillations always occurred. This involves that the reacting system is at the margin of its excitability. The numbers given in Table I are oscillations of unchanged period time.

Replacing cerium with manganese in the BZ system similar results have been obtained. Further experiments were performed with  $\text{Fe}(\text{phen})_3^{2+}$ , respectively,  $\text{Ru}(\text{dipy})_3^{2+}$ -catalyzed BZ systems containing  $0.05 \text{ mol} \cdot \text{dm}^{-3} \text{KBrO}_3$ ,  $0.2 \text{ mol} \cdot \text{dm}^{-3}$  malonic acid,  $0.5 \text{ mol} \cdot \text{dm}^{-3} \text{H}_2\text{SO}_4$  and  $4 \times 10^{-4} \text{ mol} \cdot \text{dm}^{-3} \text{Fe}(\text{phen})_3^{2+}$ , respectively,  $0.05 \text{ mol} \cdot \text{dm}^{-3} \text{KBrO}_3$ ,  $0.2 \text{ mol} \cdot \text{dm}^{-3}$  malonic acid,  $1.0 \text{ mol} \cdot \text{dm}^{-3} \text{H}_2\text{SO}_4$  and  $4 \times 10^{-4} \text{ mol} \cdot \text{dm}^{-3} \text{Ru}(\text{dipy})_3^{2+}$ .

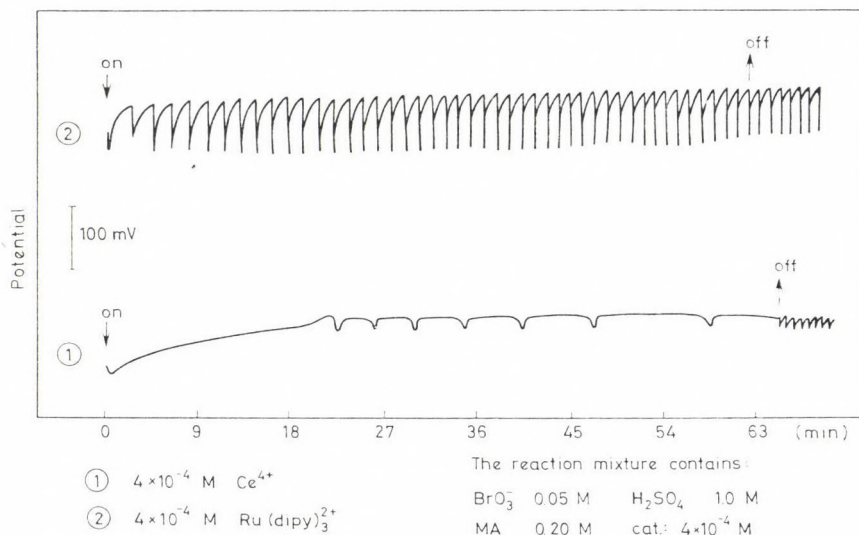


Fig. 3. The behaviour of BZ oscillating systems during irradiation and without irradiation. The reacting BZ systems contain:  $0.05 \text{ mol} \cdot \text{dm}^{-3} \text{KBrO}_3$ ,  $0.20 \text{ mol} \cdot \text{dm}^{-3}$  malonic acid,  $1.0 \text{ mol} \cdot \text{dm}^{-3} \text{H}_2\text{SO}_4$ , and (1)  $4 \times 10^{-4} \text{ mol} \cdot \text{dm}^{-3} \text{Ce}(\text{IV})$ , (2)  $4 \times 10^{-4} \text{ mol} \cdot \text{dm}^{-3} \text{Ru}(\text{dipy})_3^{2+}$

It has been found that even in the case of prolonged (60 min) irradiation the chemical oscillation sustained and the parameters of oscillation did not change as compared with unirradiated systems.

We also compared a cerium-catalyzed system with a  $\text{Ru}(\text{dipy})_3^{2+}$ -catalyzed one using the same catalyst concentration ( $4 \cdot 10^{-4} \text{ mol} \cdot \text{dm}^{-3}$ ) in both systems and irradiating them at the higher dose rate.

The recordings on Fig. 3 show that the irradiation does not influence the chemical oscillation in the  $\text{Ru}(\text{dipy})_3^{2+}$ -catalyzed system, however, in the cerium-catalyzed one the frequency of oscillation decreased dramatically and after a rather long reaction time the period of oscillation was more than 8 minutes. The termination of irradiation resulted in an abrupt increase in the frequency of oscillation.

Our experiments revealed that the behaviour of the simple ion- ( $\text{Ce}^{3+}$ ,  $\text{Mn}^{2+}$ ) catalyzed systems and that of the complex ion [ $\text{Fe}(\text{phen})_3^{2+}$ ,  $\text{Ru}(\text{dipy})_3^{2+}$ ] ones differs considerably and it is likely that reaction of H atoms with the catalyst is of great importance.

We also studied the effect of  $\gamma$  irradiation on the sulphuric acid solution of  $\text{Ce}^{3+}$ , respectively,  $\text{Ce}^{4+}$ . The irradiation of a  $10^{-3} \text{ mol} \cdot \text{dm}^{-3}$  cerium(III)-solution at a dose rate of  $2.74 \times 10^{18} \text{ eV} \cdot \text{dm}^{-3} \cdot \text{s}^{-1}$  for 1 hour did not result cerium(IV) of detectable amount. Cerium(IV), however, was reduced to cerium(III) due to the  $\gamma$  irradiation of its  $10^{-3} \text{ mol} \cdot \text{dm}^{-3}$  solution. (See Fig. 4.) These results can be explained by assuming that the irradiation-generated H atoms reduce  $\text{Ce}^{4+}$  with a higher rate than do OH radicals oxidize  $\text{Ce}^{3+}$ . The rate constant of this latter reaction ( $\text{Ce}^{3+} + \text{OH} + \text{H}^+ \rightarrow \text{Ce}^{4+} + \text{H}_2\text{O}$ ) is  $7.2 \times 10^7 \text{ dm}^3 \cdot \text{mol}^{-1} \cdot \text{s}^{-1}$ . It is important to note that

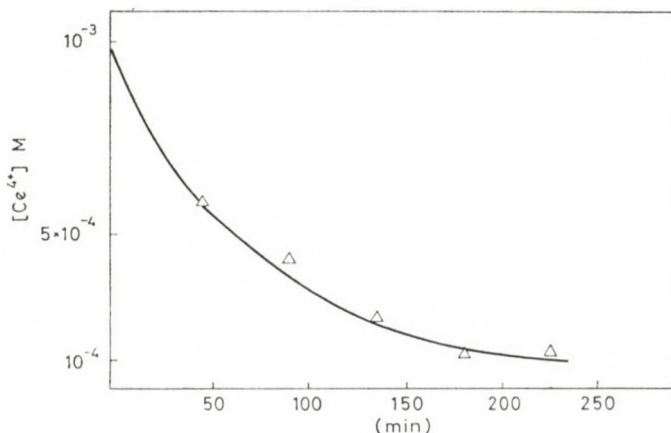


Fig. 4. The decrease of cerium(IV) concentration in time during the irradiation of a  $10^{-3} \text{ mol} \cdot \text{dm}^{-3}$  cerium(IV) solution in  $1.0 \text{ mol} \cdot \text{dm}^{-3} \text{ H}_2\text{SO}_4$  at a dose rate of  $2.74 \times 10^{18} \text{ eV} \cdot \text{dm}^{-3} \cdot \text{s}^{-1}$

also  $\text{H}_2\text{O}_2$  (one of the products of water radiolysis) can reduce  $\text{Ce}^{4+}$  to  $\text{Ce}^{3+}$ . The rate constant of the  $\text{Ce}^{4+} + 1/2 \text{H}_2\text{O}_2 \rightarrow \text{Ce}^{3+} + 1/2 \text{O}_2 + \text{H}^+$  reaction is  $1.0 \times 10^6 \text{ dm}^3 \cdot \text{mol}^{-1} \cdot \text{s}^{-1}$ . This reaction, however, is an inferior one since the rate of formation of  $\text{H}_2\text{O}_2$  is  $3.3 \times 10^{-8} \text{ mol} \cdot \text{dm}^{-3} \cdot \text{s}^{-1}$ , and that of H atoms  $1.67 \times 10^{-7} \text{ mol} \cdot \text{dm}^{-3} \cdot \text{s}^{-1}$  [13].

The decisive role of H atoms in quenching chemical oscillations was supported by further series of experiments. In one series of runs nitrate was added to cerium-catalyzed BZ systems in various amounts. Namely, nitrate reacts with H atoms with a rate constant of  $1.4 \times 10^6 \text{ dm}^3 \cdot \text{mol}^{-1} \cdot \text{s}^{-1}$  it, however, is ineffective towards the OH radicals. Irradiating a cerium-catalyzed BZ system containing 0.5 sodium nitrate no change in the parameters of chemical oscillation was observable.

From our experimental results obtained so far the following considerations can be made:

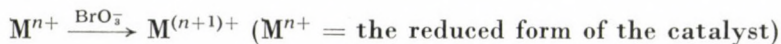
a) the termination of chemical oscillation in some BZ systems can not be attributed to the inhibitory effect of bromide ions supposed to be generated from BrMA by its reaction with H atom, since the rate of bromide formation is a very low value (see above).

b) the continuous formation of H atoms during irradiation, however, is important to account for the phenomena observed. If a H atom scavenger (e.g.  $\text{NO}_3^-$ ) is present in a considerable concentration the oscillation does not terminate. The same happens in reacting BZ systems of higher bromate concentrations, being bromate also a trap for the H atom. At lower bromate concentrations a decrease in the frequency of oscillation is observable, which can be attributed to competitive reactions involving H atoms,

c) the termination of chemical oscillation by  $\gamma$  irradiation can not be explained by the reactions between the radiolysis products and the transient reduction products of bromate ( $\text{BrO}_2$ ,  $\text{HBrO}_2$ ,  $\text{HOBr}$  etc.). These latter are present in very low steady state concentrations ( $< 10^{-6} \text{ mol} \cdot \text{dm}^{-3}$ ) and thus the probability of their reaction with H or OH is extremely low. In addition these transients occur in every BZ systems and as it has been described above  $\gamma$  irradiation has effect only if cerium or manganese is the catalyst.

d) the absence of any effect of the  $\gamma$  irradiation on reacting BZ systems containing complex catalysts [ $\text{Fe}(\text{phen})_3^{2+}$  or  $\text{Ru}(\text{dipy})_3^{2+}$ ] should not be attributed to the organic component of the complex (phenanthroline or dipyridine). Namely, we performed experiments in which the BZ system contained cerium(III) as a catalyst and also  $1.2 \times 10^{-3} \text{ mol} \cdot \text{dm}^{-3}$  of phenanthroline or dipyridine. (This concentration is equal to that one which is present in the  $\text{Fe}(\text{phen})_3^{2+}$  or  $\text{Ru}(\text{dipy})_3^{2+}$ -catalyzed systems.) The  $\gamma$  irradiation of the above system behaved as a BZ system containing cerium(III), but not the heteroaromatics, i.e. the oscillation terminated due to irradiation.

The results suggest us to assume that H atoms inhibit the



autocatalytic reaction if the catalyst is present as a labile complex (cerium- or manganese-sulphato complex), but exert no effect on inert complex catalysts [ $Fe(phen)_3^{2+}$ ,  $Ru(dipy)_3^{2+}$ ]. This probably can be attributed among others to the difference in mechanisms by which the H atoms reach the metal ion center across a labile inorganic and an inert organic coordination sphere, respectively.

Further experiments are in progress to reveal the fine details of these rather involved phenomena.

#### REFERENCES

- [1] BURGER, M., KÖRÖS, E.: *J. Phys. Chem.* **84**, 496 (1980)
- [2] JACOBS, S. S., EPSTEIN, J. R.: *J. Am. Chem. Soc.*, **98**, 1721 (1976)
- [3] KANER, R. J., EPSTEIN, J. R.: *J. Am. Chem. Soc.*, **100**, 4073 (1978)
- [4] BAR-ELI, K., HADDAD, S.: *J. Phys. Chem.*, **83**, 2952 (1979)
- [5] VÁRADI, Z., BECK, M. T.: *J. Chem. Soc. Chem. Comm.* **1970**, 30; TREINDL, L., FABIAN, P.: *Coll. Czech. Chem. Comm.*, **45**, 1168 (1980)
- [6] NOSZTICZIUS, Z.: *J. Am. Chem. Soc.*, **57**, 3660 (1979)
- [7] KÖRÖS, E.: *Nature*, **251**, 703 (1974)
- [8] BLANDAMER, M. J., MORRIS, S. H.: *J. Chem. Soc. Faraday Trans. I.*, **71**, 2319 (1975)
- [9] RAMA RAO, K. V. S., PRASAD, D.: "Kinetics of Physicochemical oscillations", Vol. III. Aachen 1979 p. 724,
- [10] FIELD, R. J., NOYES, R. M.: *J. Chem. Phys.* **60**, 1877 (1974)
- [11] CONRAD, M., REINBACH, M.: *Ber.*, **35**, 1816 (1907)
- [12] KÖRÖS, E.: *Faraday Symp. Chem. Soc. No. 9*, p. 92 (1974)
- [13] PIKAEV, A. K., KABAKCHI, S. A., MAKAROV, I. E., ERLOV, B. G.: "Impulznyi radioliz i evo primenenie" (Impulse radiolysis and its application), Moskva, Atomizdat, 1980

Endre KÖRÖS }  
Margit VARGA } H-1088 Budapest, Múzeum krt. 4/b

Galina PUTIRSKAYA H-1025 Budapest, Pusztaszeri u. 59-67.



## OSCILLATORY REACTIONS: MODEL CONSTRUCTION AND POSSIBILITIES OF REALIZATION\*

B. TURCSÁNYI

*(Central Research Institute for Chemistry of the Hungarian Academy of Sciences,  
Budapest)*

Received July 22, 1981

Accepted for publication September 18, 1981

The construction of a relatively simple oscillatory model is described. It is shown, that reactions of an organic redox couple (in the given example the hydroxylamine/nitroso system) may fulfil the criteria raised by this model, thus, an experimental realization seems to be possible.

### Introduction

In the last ten years, homogeneous reaction systems with oscillatory kinetics have been the object of intensive study. The goal of these studies was the understanding of the nature of oscillatory reactions on the ground of an acceptable kinetic-mechanistic description. It has been claimed [1, 2] that this was achieved for both classical oscillatory systems, the BRAY reaction and the BELOUSOV—ZHABOTINSKY reaction.

It is remarkable, that during the above time no fundamentally new liquid-phase homogeneous oscillatory reaction was found, although many variants of the BELOUSOV—ZHABOTINSKY reaction were discovered (for a review see [3]). By the BRIGGS—RAUSCHER reaction the possible connection of the two classical systems was demonstrated only. The great number of known oscillatory gas reactions and periodic processes in continuous reactors are clearly incomparable with the above systems.

Thus, the theoretically founded construction of a truly new homogeneous oscillatory reaction is a very ambitious goal. A possibility to reach this mark, given by the specific chemistry of some organic redox systems, will be discussed here.

### Model construction

The mathematical analysis of a differential equations system, corresponding to some chemical reaction mechanism, gives explicitly whether the reaction is oscillatory or not. On the other hand, from the mathematical criteria it is

\* Presented on the joint session of the Working Committees on Reaction Kinetics and Catalysis, and Coordination Chemistry, Budapest, October 29, 1980

generally impossible to construct straightforwardly a kinetic scheme, possessing the desired oscillatory characteristics.

Earlier we have shown [4] that oscillatory model schemes may be constructed by the following way: At first, a kinetic equilibrium system possessing multiple equilibrium states must be formulated for the intermediates of the reaction. Then the total intermediate concentration must be modulated by suitable input and output reactions. As the actual state of the kinetic equilibrium depends on the total intermediate concentration and, on the other hand, the input and output rates (*i.e.* the variation of the total intermediate concentration) are depending on the actual equilibrium state, an oscillatory kinetics may be established.

It must be emphasized that the kinetic equilibrium system is only a construction tool here. In the oscillatory system there is no equilibrium any more, although this may be approximated during the intervals of slow concentration changes, if the input and output rates are low enough in relation to the rates of the kinetic equilibrium system.

To have a relatively simple oscillatory system, we must choose also the simplest possible kinetic equilibrium system with multiple stable states. A two-component system may be formulated with the following realistic rate laws:

$$\text{rate } (x \rightarrow y) = c_1 xy \quad (\text{autocatalytic}) \quad (1)$$

$$\text{rate } (y \rightarrow x) = c_2 y / (1 + \gamma y) \quad (\text{limited rate}) \quad (2)$$

The equilibrium states are given by equation (3):

$$y\{c_1 x(1 + \gamma y) - c_2\} = 0 \quad (3)$$

It is immediately seen, that  $y = 0$  corresponds always to an equilibrium state. In the other factor of Eq. (3)  $x$  may be substituted by  $x \equiv s - y$  (when  $s \equiv x + y$  is the total intermediate concentration) giving a quadratic equation for  $y$  in function of  $s$ :

$$y^2 + \left(\frac{1}{\gamma} - s\right)y + \frac{1}{\gamma} \left(\frac{c_2}{c_1} - s\right) = 0. \quad (4)$$

The equilibrium system has two stable states (one of these is the  $y = 0$  state), if (4) has two positive roots in some domain of  $s$ . The condition of this behaviour is:

$$\gamma > \frac{c_1}{c_2}. \quad (5)$$

and the domain of multiple stable states is given by

$$2 \sqrt{\frac{c_2}{c_1} \frac{1}{\gamma}} - \frac{1}{\gamma} < s < \frac{c_2}{c_1} \quad (6)$$

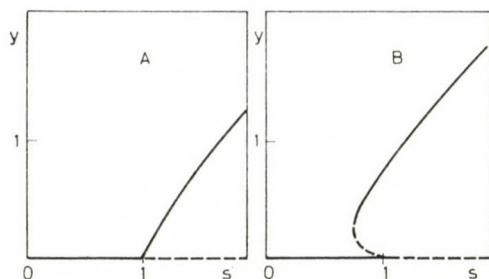


Fig. 1. Stable (solid lines) and unstable (broken lines) equilibrium concentrations of  $y$  in function of  $s$ . A:  $\gamma = 0.5 < c_1/c_2 = 1$ ; B:  $\gamma = 4 > c_1/c_2 = 1$

Figure 1 shows the equilibrium curves of  $y$  in function of  $s$  for the cases  $\gamma < \frac{c_1}{c_2}$  and  $\gamma > \frac{c_1}{c_2}$ .

For the input and output reactions it is advisable to choose the simplest processes too. By these is provided, that at low values of  $y$  an increase, at high  $y$  values a decrease of the total intermediate concentration takes place. With constant input rate and with an output rate proportional to  $y$  the differential equation for  $s$  is as follows:

$$ds/dt = w_1 - c_3 y \quad (7)$$

The stationary point of the system (where  $ds/dt = dy/dt = 0$ ) is — on this level of approximation — unstable, if condition (5) and the following one

$$\frac{w_1}{c_3} < \frac{1}{\sqrt{\gamma}} \sqrt{\frac{c_2}{c_1}} - \frac{1}{\gamma} \quad (8)$$

is fulfilled. Figure 2 gives a hint about these relations.

On the ground of Eq. (7) input of  $x$  or  $y$  seems to be equivalent for this oscillatory system. This is, however, not true. Detailed analysis shows, that only in case of  $x$  input are the conditions of instability (*i.e.* of the oscillatory kinetics) as given by (5) and (8). In case of  $y$  input the domain of the limit-cycle behaviour is more restricted and damped oscillations are observed between this and the non-oscillatory region.

The time variation of  $s$  may be formulated alternatively by the following equation (9):

$$ds/dt = w_1 - c_3 xy \quad (9)$$

*i.e.* the output corresponds to a bimolecular reaction of  $x$  and  $y$ . The criteria of oscillatory kinetics are more complex in this case and are not discussed here. This output process is, however, more easily realizable chemically than the unimolecular one (see below).

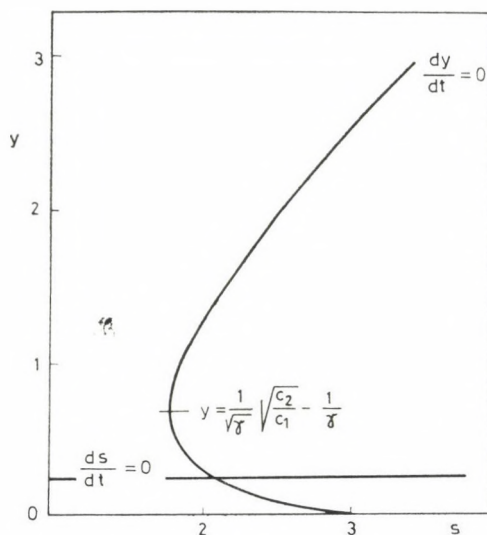
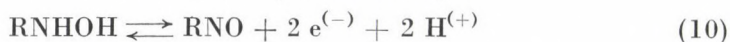


Fig. 2. Phase portrait of the oscillatory model system for  $w_1/c_3 = 0.25 < \frac{1}{\sqrt{\gamma}} \sqrt{\frac{c_2}{c_1}} - \frac{1}{\gamma} = 0.695$ .  
The stationary point is an unstable focus, producing counterclockwise rotations

### Chemical considerations

In this Section a plausible chemical realization of the above system will be described. It must be emphasized, that no experimental work has been done yet on this field and the presented chemistry is purely illustrative. We feel, however, that the reaction system chosen gives good chances for the experimental realization too.

The phenylhydroxylamine/nitrosobenzene system is a redox couple corresponding to a two electron + two proton change:

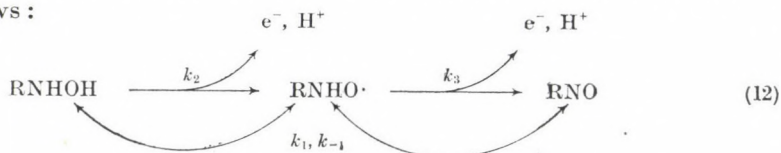


The system has, however, a one-electron intermediate too:



The existence of the phenyl nitroxide radical was demonstrated by EPR spectroscopy [5].

Reactions between this system and one-electron oxidants are formulated as follows:



The kinetics of the phenylhydroxylamine  $\rightarrow$  nitrosobenzene (denoted thereafter by X and Y) conversion by a one-electron oxidant is correspondingly complex. For the radical intermediate Z we can apply — under suitable circumstances — the steady-state condition:

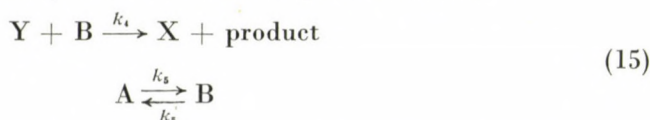
$$dz/dt = 2k_1xy - 2k_{-1}z^2 + k_2x - k_3z = 0 \quad (13)$$

(where the constant oxidant concentration is combined into the rate constants  $k_2$  and  $k_3$ ). A fairly simple rate expression can be obtained, if the  $z^2$  term drops out in case of high oxidant concentration ( $k_3 \gg k_{-1}z$ ):

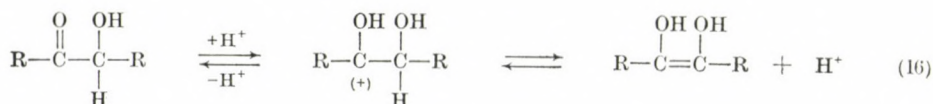
$$\text{rate (X} \rightarrow \text{Y)} = k_1xy + k_2x \quad (14)$$

The above rate law differs from expression (1) only in the  $x$  term. This term must be small enough, but not strictly zero, to provide the desired oscillatory kinetics. It is hoped, that by proper choice of the hydroxylamine/nitroso compound and of the oxidant respectively, this condition can be fulfilled.

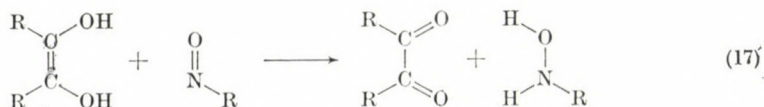
The reverse reaction, the reduction of nitrosobenzene must be a limited-rate process. The corresponding rate law (2) can be approximated, if the reductant is formed reversibly from an inactive pool reactant:



In this scheme the pool reactant A is an  $\alpha$ -oxyketone or reductone and the active form B is produced by enolisation:



The reduction of nitrosobenzene may then proceed in a concerted reaction:



To obtain an approximate rate law, we assume again the steady state for the active form:

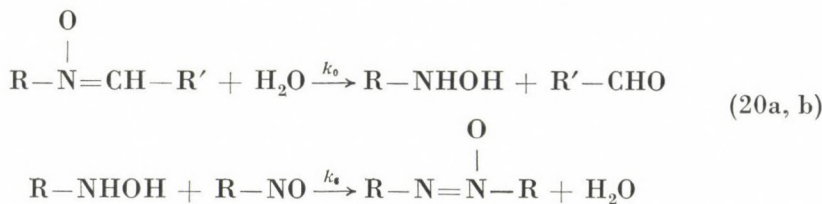
$$db/dt = -k_4by + k_5a - k_{-5}b = 0 \quad (18)$$

giving

$$\text{rate (Y} \rightarrow \text{X)} = k_4k_5ay/(k_4y + k_{-5}) = k_4 \frac{k_5}{k_{-5}} ay \left( 1 + \frac{k_4}{k_{-5}} y \right) \quad (19)$$

of the same form, as (2). Note that the complex rate constant  $c_2$  may be varied by the pool reactant concentration and the  $\gamma$  factor by the modification of the tautomerization rates depending on the acidity of the solution.

The input and output reactions can be formulated as follows:



where (20a) corresponds to the hydrolytic decomposition of a nitron, giving hydroxylamine and aldehyde as inactive product. The nitron is a further pool reactant of the system and the input rate of hydroxylamine,  $w_1 \equiv k_0$  [nitron] may be taken as constant. The output reaction (20b) is the well-known condensation process of phenylhydroxylamine and nitrosobenzene.

### System dynamics: a numerical example

The differential equations describing the dynamics of the above system are as follows:

$$\begin{aligned} dx/dt &= w_1 - (k_1 + k_6)xy - k_2x + k_4by \\ dy/dt &= (k_1 - k_6)xy + k_2x - k_4by \\ db/dt &= k_5a - k_{-5}b - k_4by \end{aligned} \quad (21a-c)$$

By direct calculation and, in part, by trial and error, the following set of constants resulting in an oscillatory behaviour was determined (Table I).

Table I

$w_1$	0.1	(conc. unit) (time unit) <sup>-1</sup>
$k_{5a}$	1.2	
$k_2$	0.01	(time unit) <sup>-1</sup>
$k_3$	100	
$k_{-5}$	4	
$k_1$	1	(conc. unit) <sup>-1</sup> (time unit) <sup>-1</sup>
$k_{-1}$	100	
$k_4$	10	
$k_6$	0.1	

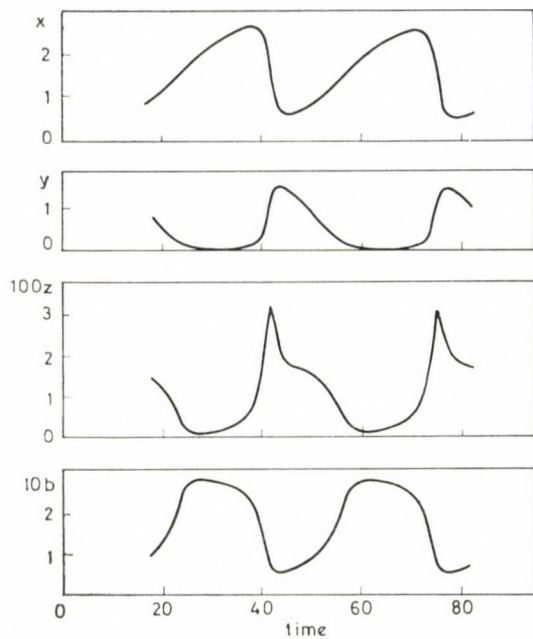


Fig. 3. Kinetic curves of the oscillatory system corresponding to the differential equations system (21). Rate constant values in Table I

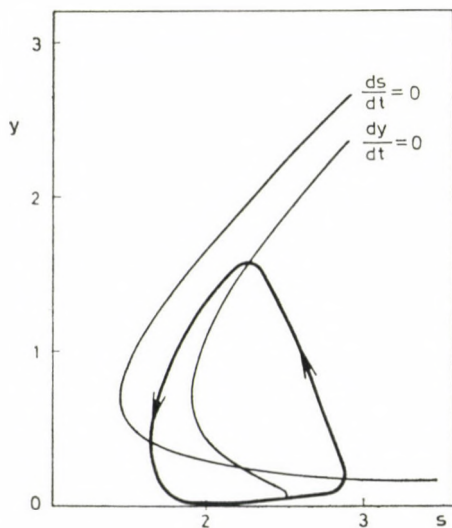


Fig. 4. Stable limit cycle (thick line) of the system (21) in the  $s - y$  plane

The given values of  $k_1$ ,  $k_{-1}$ ,  $k_2$  and  $k_3$  permitted the approximation (14) and thus the reduction of the originally four-variable system. This resulted in the substantial reduction of calculation time. The calculation was done on a HP 9830 A Calculator by a self-developed integration routine based on the DIMSDALE iteration [6]. The time-concentration curves are shown in Fig. 3, where the concentrations of the intermediate Z were calculated by Eq. (13).

The system exhibits limit-cycle oscillations with a cycle time of about 33 units. In Fig. 4 this limit cycle is shown, together with the  $ds/dt = 0$  and the  $dy/dt = 0$  curves (compare this with Fig. 2).

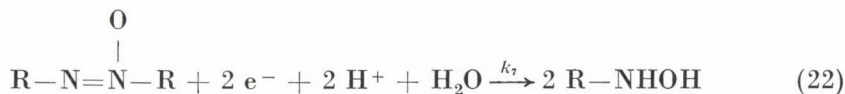
The stoichiometry of this reaction system is interesting too. During one cycle 3.3 units of hydroxylamine, 33.9 units of one-electron oxidant and 15.3 units of bivalent reductant are consumed, producing 1.65 units of the azoxy compound. The significance of this stoichiometry will be discussed below.

### Conclusions

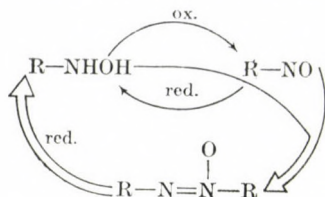
In the foregoing sections it was shown, that plausible reactions of the organic hydroxylamine/nitroso system give theoretical possibility to establish — under suitable conditions — an oscillatory reaction regime. It seems that many other organic redox systems (*e.g.* quinones, various dye molecules, *etc.*) may have a similar capacity. Experimental research on this field has promising perspective.

The theoretical system discussed above allows some mechanistic generalizations too. To see this, we must remind that in the construction of the model we concentrated on the reactions of the hydroxylamine/nitroso system and, consequently, the essential net process seems to be the hydroxylamine  $\rightarrow$  azoxy conversion. However, the stoichiometry of the reaction shows clearly, that the main reaction proceeds between the one-electron oxidant and the bivalent reductant (*i.e.* between the outer components) and the other components only mediate this "forbidden" reaction. The approximately tenfold difference between the oxidant/reductant consumption rate and the azoxybenzene formation rate correspond clearly to the ratio  $k_1/k_6$ . Lowering of this ratio, however, results in the cessation of the oscillatory regime, showing that this type of stoichiometry is essential for an oscillatory reaction.

If we assume a further reaction, the reduction of the azoxy compound to the hydroxylamine:



the constant rate input of hydroxylamine may be replaced by this process giving a closed system for the catalyst, as seen on the following scheme:



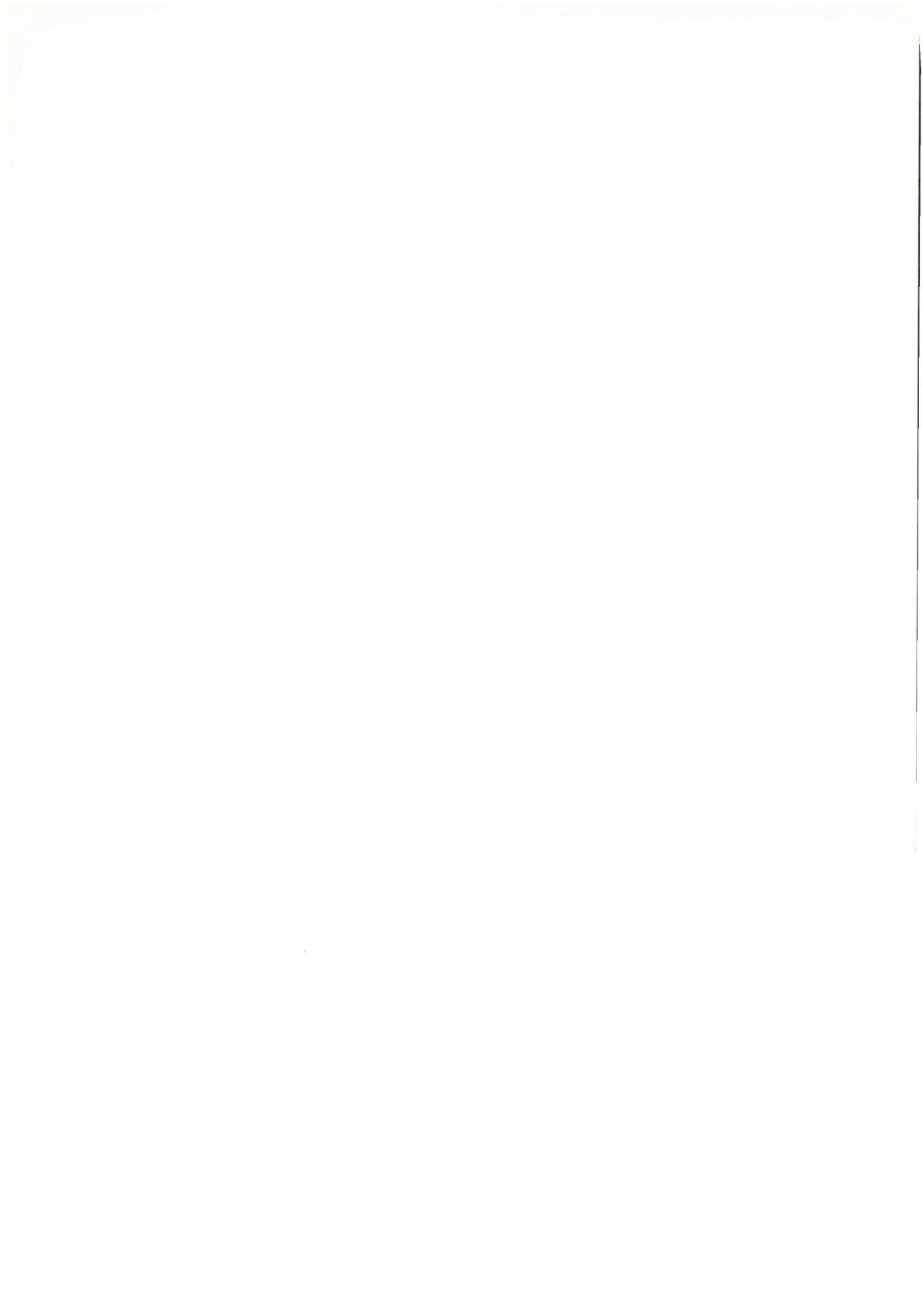
In oscillatory regime the mean rate in the smaller circle (single lines) is substantially greater than in the greater circle (double lines). The azoxy compound is a "switching component" here in the sense, that the total concentration of the other intermediates varies inversely with the variation of this compound, resulting in "switches" at high and low concentrations.

The classical BRAY reaction shows remarkable similarities with the system discussed above. Here the hydrogen peroxide is both oxidant and reductant, but the direct disproportionation process is forbidden and must be mediated by the oxyiodine system. As early as in 1921 BRAY [7] pointed out, that the amount of hydrogen peroxide consumed during one cycle is substantially greater, as would correspond to the observed variation of the amount of iodine during the same time. Thus, iodine has very probably a similar status in this mechanism as the azoxybenzene in our hypothetical system, and the other oxyiodine species are forming a kinetic quasi-equilibrium system with multiple stable states, driven by the oxidation and reduction processes of hydrogen peroxide.

#### REFERENCES

- [1] SHARMA, K. R., NOYES, R. M.: *J. Am. Chem. Soc.*, **98**, 4345 (1976); EDELSON, D., NOYES, R. M.: *J. Phys. Chem.*, **83**, 212 (1979)
- [2] EDELSON, D., FIELD, R. J., NOYES, R. M.: *Int. J. Chem. Kinet.*, **7**, 417 (1975); EDELSON, D., NOYES, R. M., FIELD, R. J.: *Int. J. Chem. Kinet.*, **11**, 155 (1979)
- [3] NOYES, R. M.: *J. Am. Chem. Soc.*, **102**, 4644 (1980)
- [4] TURCSÁNYI, B., KELEN, T.: *Z. Phys. Chem. Neue Folge*, **109**, 17 (1978)
- [5] AYSCOUGH, P. B., SARGENT, F. P., WILSON, R.: *J. Chem. Soc. B.*, **1966**, 903
- [6] KUNZ, K. S.: *Numerical Analysis*. Wiley, New York 1957
- [7] BRAY, W. C.: *J. Am. Chem. Soc.*, **43**, 1262 (1921)

Béla TURCSÁNYI     H-1025 Budapest, Pusztaszeri út 59—67.



## ON THE PREOSCILLATORY PERIOD OF THE BELOUSOV—ZHABOTINSKY REACTION

A SEARCH FOR INTERMEDIATES\*

M. BURGER\*\* and K. RÁCZ

(*Institute of Inorganic and Analytical Chemistry, Eötvös Loránd University, Budapest*)

Received June 12, 1981

Accepted for publication September 29, 1981

Having determined the  $[\text{BrMA}]_{\text{crit}}$  values in the  $\text{MA}-\text{BrO}_3^--\text{Mn}^{2+}-\text{HNO}_3$  ( $5.0 \text{ mol/dm}^3$ ) Belousov—Zhabotinsky system, in order to clarify whether BrMA alone was responsible for the start of oscillation or other organic intermediates played also an important role, the effect of added BrMA on the preoscillatory period was studied. The addition of BrMA to the reaction mixture shortens the preoscillatory period, but oscillation does not start when  $[\text{BrMA}]_{\text{added}}$  is equal to  $[\text{BrMA}]_{\text{crit}}$ . However, the preoscillatory period always disappears when the reaction mixture contains about  $10^{-3} \text{ mol/dm}^3$  glyoxylic acid or oxalic acid beside the crucial BrMA concentration. By elaborating an analytical method, glyoxylic acid was determined during the preoscillatory period of the  $\text{MA}-\text{BrO}_3^--\text{Mn}^{2+}-\text{HNO}_3$  ( $5.0 \text{ mol/dm}^3$ ) reacting system.

### Introduction

Most of the chemical investigations on oscillatory reactions are devoted to the study of the Belousov—Zhabotinsky systems, namely the catalytic oxidative bromination of malonic acid (MA) with bromate. Probably the most difficult feature of this reaction to characterize experimentally is the preoscillatory period. During this part of the reaction some intermediates form and adjust the system to a quasi-steady state. Their presence in definite concentrations is necessary to switch the reaction from the non-oscillatory to the oscillatory state.

The first qualitative statement that the length of the induction period depends on the initial reagent concentration was given by FIELD, KÓRÖS and NOYES [1]. ADAMČIKOVA and TREINDL [2] as well as RASTOGI *et al.* [3–5] gave a quantitative correlation between the duration of the preoscillatory period and the initial reagent concentrations.

BAR-ELI and HADDAD [6] investigated the induction time of the Belousov—Zhabotinsky reaction in detail as a function of the catalyst,  $\text{BrO}_3^-$  and MA concentrations in a closed system. The experimental data were compared to computations performed on the basis of an improved Oregonator.

\* Presented on the joint session of the Working Committees on Reaction Kinetics and Catalysis, and Coordination Chemistry, Budapest, October 29, 1980

\*\* To whom correspondence should be addressed

TREINDL and DROJAKOVA [7] studied the effect of  $\text{Br}^-$ ,  $\text{Cl}^-$ ,  $\text{ClO}_4^-$  and the different cations on the length of the induction period. Their data concerning the influence of  $\text{Br}^-$ , were used by EDELSON [8] as a basis for comparison with the behaviour of a revised theoretical mechanism of the Belousov—Zhabotinsky system [9]. Here EDELSON, NOYES and FIELD [9] took into account the detailed structure of the organic reaction subset beside the inorganic reactions.

In our previous papers [10, 11] we have pointed out that in the  $\text{MA}-\text{BrO}_3^-$ -catalyst (cerium or manganese) systems the accumulation of bromomalonic acid (BrMA) plays an important role. The amount of BrMA formed during the preoscillatory period was denoted as crucial BrMA concentration ( $[\text{BrMA}]_{\text{cru}}$ ) and these values in different conditions were determined experimentally and calculated from the rate equations describing the BrMA formation in this part of the reaction. We thought that at the end of the preoscillatory period the catalyst is reduced by the accumulated BrMA.

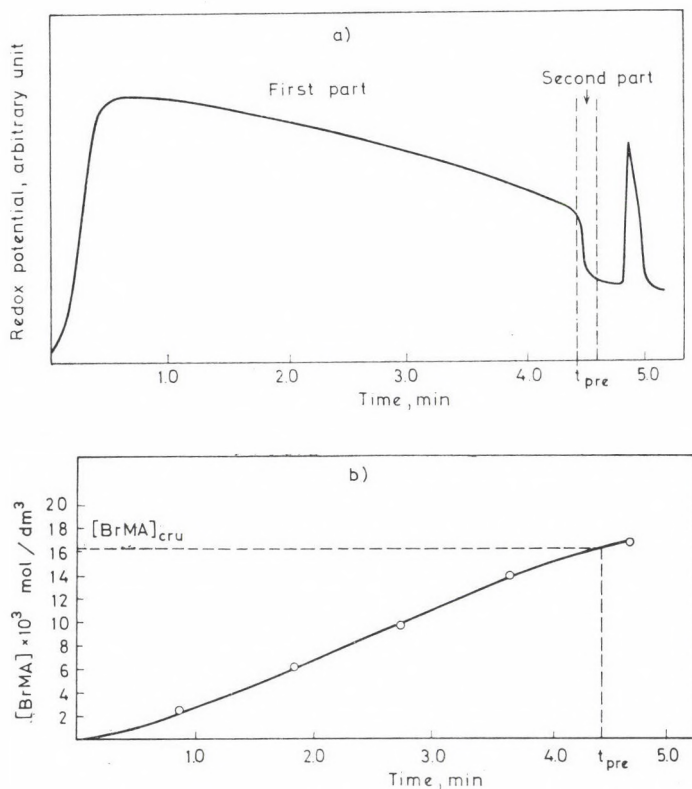


Fig. 1. Change of the redox potential (a) and BrMA concentration (b) in time. Initial conditions:  $[\text{MA}] = 0.2 \text{ mol/dm}^3$ ,  $[\text{BrO}_3^-] = 5 \times 10^{-2} \text{ mol/dm}^3$ ,  $[\text{Mn}^{2+}] = 2 \times 10^{-3} \text{ mol/dm}^3$ ,  $[\text{HNO}_3] = 5.0 \text{ mol/dm}^3$ . Temperature:  $15^\circ\text{C}$

During this period the catalyst is present always in the higher oxidation state. The first oscillation is preceded by a fast decrease in the redox potential and by the disappearance of the colour of the oxidized form of the catalyst. An example is shown in Fig. 1 for the manganese-catalyzed MA—BrO<sub>3</sub><sup>-</sup>—HNO<sub>3</sub> (5.0 mol/dm<sup>3</sup>) system. The oxidation of the catalyst with BrO<sub>3</sub><sup>-</sup> and the reduction with the organic compound(s) occur simultaneously during the first part of the preoscillatory period. The sudden decrease in the redox potential in the second part (*i.e.* the fast reduction of the catalyst) was attributed to BrMA on the basis of our previous results [10, 11] measuring the values of [BrMA]<sub>crit</sub> at various acid concentrations. The actual redox potential of the BrO<sub>3</sub><sup>-</sup>/HOBr system increases with the increase of [H<sup>+</sup>], while that of the Mn<sup>3+</sup>/Mn<sup>2+</sup> system is practically independent of [H<sup>+</sup>]. Thus the following reaction



is thermodynamically favourable at higher acid concentrations. Therefore the higher the acid concentration is, the higher amount of the organic reducing agent is required to reduce the catalyst during the second part of the preoscillatory period (see Fig. 1). In accordance with this statement the values of [BrMA]<sub>crit</sub> is about five times higher in the 5.0 mol/dm<sup>3</sup> HNO<sub>3</sub>, manganese-catalyzed system, than in the 1.5 mol/dm<sup>3</sup> HNO<sub>3</sub> solution, as it can be seen in Table I.

**Table I**  
[BrMA]<sub>crit</sub> values at different HNO<sub>3</sub> concentrations  
Temperature: 15 °C

[MA], mol/dm <sup>3</sup>	[BrO <sub>3</sub> <sup>-</sup> ] × 10 <sup>2</sup> , mol/dm <sup>3</sup>	[Mn <sup>2+</sup> ] × 10 <sup>3</sup> , mol/dm <sup>3</sup>	[HNO <sub>3</sub> ] mol/dm <sup>3</sup>	[BrMA] <sub>crit</sub> × 10 <sup>3</sup> , mol/dm <sup>3</sup>
0.2	5.0	2.0	1.5	3.1
			5.0	16.3
0.2	10.0	2.0	1.5	6.1
			5.0	29.1
0.4	5.0	2.0	1.5	3.0
			5.0	21.1

On the basis of these considerations in the present paper we try to answer the following questions:

(1) Is the BrMA formation the only important reaction during the preoscillatory period, or should we consider further reactions of BrMA too?

(2) Is BrMA alone responsible for the start of oscillation, or do other organic intermediates play also an important role?

## Experimental

### Reagents

All but two reagent were of analytical grade, malonic acid and glyoxylic acid were of purissimum grade. BrMA was prepared from malonic acid according to CONRAD and REINBACH [12].

### Methods

#### Determination of manganese

The concentration of the manganese stock solution (0.1 mol/dm<sup>3</sup>) was measured by complexometric titration: 5.0 cm<sup>3</sup> Mn<sup>2+</sup> solution was pipetted to a mixture containing 0.2 g hydroxylamin hydrochlorid, 2 drops of distilled HCl, 10 cm<sup>3</sup> conc. NH<sub>4</sub>OH and 25 cm<sup>3</sup> distilled water. This solution was titrated with 0.05 mol/dm<sup>3</sup> EDTA solution in the presence of methylthymol blue as an indicator.

#### Determination of BrMA

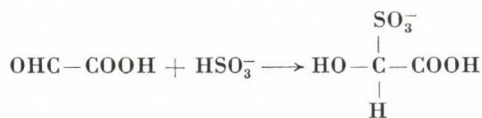
The purity of BrMA was checked by iodometric titration, and it was always higher than 95%.

The concentration of BrMA in the reaction mixture was determined polarographically as described in Ref. [10].

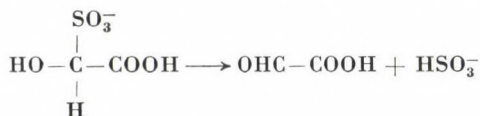
#### Determination of glyoxylic acid

The measurement of the glyoxylic acid concentration was based on the specific reaction of the aldehyde group of this compound with Na<sub>2</sub>SO<sub>3</sub>. The analytical procedure was the following:

20.0 cm<sup>3</sup> of the reaction mixture was pipetted into a glass-stoppered Erlenmeyer flask containing KI in excess to reduce BrO<sub>3</sub><sup>-</sup> and BrMA. Iodine formed was reacted with a 1.5 mol/dm<sup>3</sup> Na<sub>2</sub>SO<sub>3</sub> solution. After the disappearance of the colour of I<sub>2</sub>, further 1 cm<sup>3</sup> of Na<sub>2</sub>SO<sub>3</sub> solution was added to the reaction mixture. Then the pH was adjusted to 2–3 with 10 mol/dm<sup>3</sup> NaOH (which neutralizes the 5.0 mol/dm<sup>3</sup> HNO<sub>3</sub> sample solution) and 20% CH<sub>3</sub>COOH solutions. At this pH value the following reaction takes place:



The excess of Na<sub>2</sub>SO<sub>3</sub> was titrated with a 10% KI-I<sub>2</sub> solution in the presence of starch indicator. NaHCO<sub>3</sub> was then added to the solution to adjust the pH to 7, and aldehyde bisulphite hydrolysed according to the reaction:



HSO<sub>3</sub><sup>-</sup>, which is equivalent with the aldehyde, was titrated with a 0.05 mol/dm<sup>3</sup> KI-I<sub>2</sub> solution in the presence of starch. Blank solutions containing 5.0 mol/dm<sup>3</sup> HNO<sub>3</sub>-BrO<sub>3</sub><sup>-</sup>-Mn<sup>2+</sup>, 5.0 mol/dm<sup>3</sup> HNO<sub>3</sub>-MA-Mn<sup>2+</sup> and 5.0 mol/dm<sup>3</sup> HNO<sub>3</sub>-MA-BrMA, were also titrated parallel with the samples. The method was checked with the titration of glyoxylic acid in different concentrations and the results were 100 ± 4%.

*Procedure*

The concentration range investigated was the following:

[MA]: 0.1–0.4 mol/dm<sup>3</sup>,

[KBrO<sub>3</sub>]: 2.5 × 10<sup>-2</sup> – 10 × 10<sup>-2</sup> mol/dm<sup>3</sup>,

[MnSO<sub>4</sub>]: 1.0 × 10<sup>-3</sup> – 5.0 × 10<sup>-3</sup> mol/dm<sup>3</sup>,

[HNO<sub>3</sub>]: 5.0 mol/dm<sup>3</sup>, was constant in every experiment.

The reaction vessel was thermostated to 15 °C ± 0.1 °C.

The redox potential was recorded using a Pt-electrode and a Hg/Hg<sub>2</sub>SO<sub>4</sub> reference electrode.

In the investigation of the effect of BrMA, in order to get comparable results, the initial MA and BrO<sub>3</sub><sup>-</sup> concentrations were corrected on the basis of the following stoichiometric equation:



and so  $[\text{MA}]_{0,\text{corr.}} = [\text{MA}]_0 - 1.5 \times [\text{BrMA}]_{\text{added}}$ ,

$[\text{BrO}_3^-]_{0,\text{corr.}} = [\text{BrO}_3^-]_0 - [\text{BrMA}]_{\text{added}}$ .

When glyoxylic acid (GOA) and oxalic acid (OA) were added to the reaction mixture further reactions were also considered:



and so  $[\text{MA}]_{0,\text{corr.}} = [\text{MA}]_0 - 1.5 \times ([\text{BrMA}]_{\text{added}} + [\text{GOA}]_{\text{added}} + [\text{OA}]_{\text{added}})$ ,

$[\text{BrO}_3^-]_{0,\text{corr.}} = [\text{BrO}_3^-]_0 - ([\text{BrMA}]_{\text{added}} + [\text{GOA}]_{\text{added}} + [\text{OA}]_{\text{added}})$

supposing that the stoichiometry of these reactions is the same even when manganese is used as a catalyst.

**Results and Discussion***Effect of BrMA on the preoscillatory period*

The addition of BrMA to the reaction mixture shortens the length of the preoscillatory period. The rate of BrMA formation during the remaining non-oscillatory phase of the reaction is constant. But oscillation does not start at  $[\text{BrMA}]_{\text{cru}}$ : the higher is the amount of BrMA added initially to the reacting system, the higher is the BrMA concentration at which oscillations start. It is valid, even if  $[\text{BrMA}]_{\text{added}}$  is equal to  $[\text{BrMA}]_{\text{cru}}$ . These results are shown in Fig. 2. Extrapolating the values of BrMA determined at the end of the preoscillatory periods (dotted line in Fig. 2),  $t_{\text{pre}}$  becomes zero, when  $[\text{BrMA}]_{\text{added}}$  is equal to  $1.5 \times [\text{BrMA}]_{\text{cru}}$ . The correctness of this extrapolation was proved experimentally: adding this amount of BrMA to the reaction mixture, preoscillatory period could not be observed.

In order to clarify that this phenomenon is a general one or it is characteristic only to the initial reagent concentrations shown in Fig. 2, the MA, BrO<sub>3</sub><sup>-</sup> and Mn<sup>2+</sup> concentrations were varied. The results, summarized in Table II and Fig. 3, show that the  $[\text{BrMA}]_{\text{added}}/[\text{BrMA}]_{\text{cru}}$  ratio approximates to 1, when [MA] is relatively high, and [BrO<sub>3</sub><sup>-</sup>] is low; it is independent of the manganese ion concentration.

From these data it is clear that in general the accumulation of BrMA alone is not enough to start oscillation, but other organic compounds should accumulate too. Adding BrMA to the reaction mixture, the BrMA producing reaction proceeds without oscillation after reaching the  $[\text{BrMA}]_{\text{cru}}$ . Generally the  $[\text{BrMA}]_{\text{added}}$  values have to exceed the values of the  $[\text{BrMA}]_{\text{cru}}$  to start prompt oscillations.

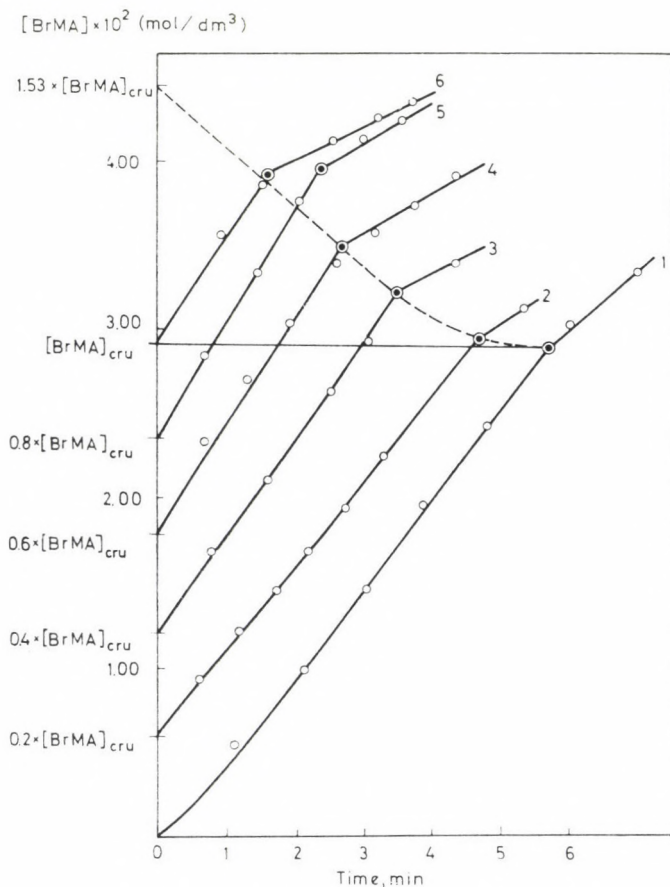
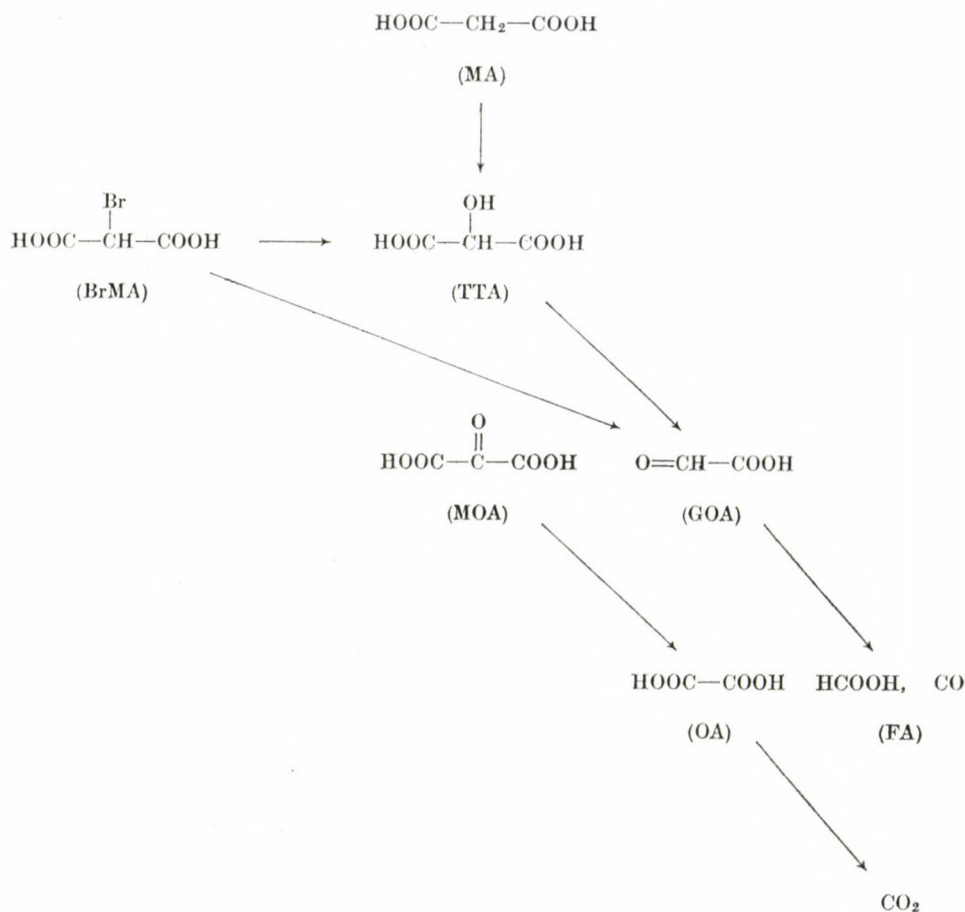


Fig. 2. BrMA accumulation during the preoscillatory period without (curve 1) and with the various amount of BrMA added initially to the reaction mixture (curves 2–6). The amounts of BrMA added are equal to the intercepts of these curves. ⊙ — at this point the oscillation starts. Initial conditions:  $[\text{MA}] = 0.2 \text{ mol/dm}^3 - 1.5 \times [\text{BrMA}]_{\text{added}}$ ,  $[\text{BrO}_3^-] = 0.1 \text{ mol/dm}^3 - [\text{BrMA}]_{\text{added}}$ ,  $[\text{Mn}^{2+}] = 2 \times 10^{-3} \text{ mol/dm}^3$ ,  $[\text{HNO}_3] = 5.0 \text{ mol/dm}^3$ , temperature:  $15^\circ \text{C}$

We supposed that the organic intermediates were formed from BrMA in the course of the reaction with the catalyst, and this reaction took place simultaneously with the BrMA formation. This assumption was based on the

results of JWO and NOYES [13] who studied the reduction of  $Ce^{4+}$  with BrMA, and investigated the conceivable intermediates of this reaction:



Of these possible intermediates formic acid (FA) and  $\text{CO}_2$  do not react with  $Ce^{4+}$  [14] and therefore they are disregarded. However, tartronic acid (TTA), mesoxalic acid (MOA), glyoxylic acid (GOA) and oxalic acid (OA) show an accelerating effect on the  $Ce^{4+}$  reduction with BrMA of the following order [13]:



In the cases of TTA and MA the contributions are almost what would be predicted from independent behaviour, so TTA can not be responsible for the fast reduction of the catalyst in the second part of the preoscillatory period (see Fig. 1a). Further, there is no evidence that MOA is produced from MA

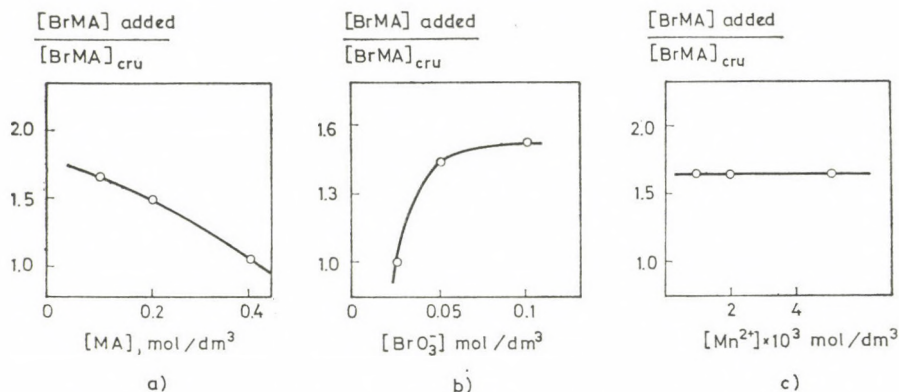


Fig. 3. Dependence of the  $[\text{BrMA}]_{\text{added}}/[\text{BrMA}]_{\text{cru}}$  ratios (a) on the initial MA concentrations,  $[\text{BrO}_3^-] = 5 \times 10^{-2} \text{ mol}/\text{dm}^3$ ,  $[\text{Mn}^{2+}] = 2 \times 10^{-3} \text{ mol}/\text{dm}^3$ , (b) on the initial  $\text{BrO}_3^-$  concentration,  $[\text{MA}] = 0.2 \text{ mol}/\text{dm}^3$ ,  $[\text{Mn}^{2+}] = 2 \times 10^{-3} \text{ mol}/\text{dm}^3$ , (c) on the initial  $\text{Mn}^{2+}$  concentration,  $[\text{MA}] = 0.1 \text{ mol}/\text{dm}^3$ ,  $[\text{BrO}_3^-] = 5 \times 10^{-2} \text{ mol}/\text{dm}^3$

Table II

Dependence of the  $[\text{BrMA}]_{\text{added}}/[\text{BrMA}]_{\text{cru}}$  ratios on the initial reagent concentrations, at  $15^\circ\text{C}$

$[\text{MA}]^*$ , $\text{mol}/\text{dm}^3$	$[\text{BrO}_3^-]^* \times 10^2$ , $\text{mol}/\text{dm}^3$	$[\text{Mn}^{2+}] \times 10^3$ , $\text{mol}/\text{dm}^3$	$[\text{BrMA}]_{\text{cru}}^{**} \times 10^2$ , $\text{mol}/\text{dm}^3$	$[\text{BrMA}]_{\text{added}}^{***} \times 10^2$ , $\text{mol}/\text{dm}^3$	$\frac{[\text{BrMA}]_{\text{added}}}{[\text{BrMA}]_{\text{cru}}}$
0.1	5.0	2.0	1.35	2.24	1.6
0.2	2.5	2.0	0.89	0.89	1.0
0.2	5.0	2.0	1.62	2.41	1.5
0.2	10.0	2.0	2.91	4.45	1.5
0.4	5.0	2.0	2.11	2.22	1.1
0.1	5.0	5.0	1.35	2.17	1.6
0.1	5.0	1.0	1.35	2.30	1.7

\* These values were corrected as described in the Experimental section;

\*\*  $[\text{BrMA}]_{\text{cru}}$ : the BrMA concentration at which the oscillation starts without any additives;

\*\*\*  $[\text{BrMA}]_{\text{added}}$ : the amount of BrMA which has to be added initially, to diminish the preoscillatory period

or BrMA, according to JWO and NOYES [13]. But on the contrary of Ref. [13], on the basis of the results of NOSZTICZIUS [14], we supposed that OA might be formed from GOA according to the following reaction:



This assumption is plausible, because  $\text{HCOOH}$  is very likely not an intermediate in the oscillating system [14], and GOA is not a final product. It is probably that the  $\text{CO}_2$  production from GOA goes through OA.

The above-mentioned facts prompted us to examine the effect of GOA and OA on the preoscillatory period of the  $\text{MA}-\text{BrO}_3^- - \text{Mn}^{2+} - \text{HNO}_3$  ( $5.0 \text{ mol/dm}^3$ ) system.

### *The effect of GOA and OA on the preoscillatory period*

GOA and OA were applied as additives beside BrMA, which were added in crucial concentration to the reaction mixture. The results were the following:

#### *Experiment (1)*

In the reaction mixture with the initial concentrations of  $0.1 \text{ mol/dm}^3$  MA,  $5 \times 10^{-2} \text{ mol/dm}^3$   $\text{BrO}_3^-$ ,  $2 \times 10^{-3} \text{ mol/dm}^3$   $\text{Mn}^{2+}$  and  $5.0 \text{ mol/dm}^3$   $\text{HNO}_3$  the length of the preoscillatory period is 6.0 min, and  $[\text{BrMA}]_{\text{cru}} = 1.35 \times 10^{-2} \text{ mol/dm}^3$  at  $15^\circ\text{C}$ . The preoscillatory period is no more observable when

- a)  $1.35 \times 10^{-2} \text{ mol/dm}^3$  BrMA and  $3.4 \times 10^{-3} \text{ mol/dm}^3$  GOA, or
- b)  $1.35 \times 10^{-2} \text{ mol/dm}^3$  BrMA and  $1.1 \times 10^{-3} \text{ mol/dm}^3$  OA are added to the reaction mixture.

#### *Experiment (2)*

The initial reagent concentrations were:  $0.2 \text{ mol/dm}^3$  MA,  $5 \times 10^{-2} \text{ mol/dm}^3$   $\text{BrO}_3^-$ ,  $2 \times 10^{-3} \text{ mol/dm}^3$   $\text{Mn}^{2+}$ ,  $5.0 \text{ mol/dm}^3$   $\text{HNO}_3$  and temperature  $15^\circ\text{C}$ . During the 4.4 min preoscillatory period  $[\text{BrMA}]_{\text{cru}} = 1.63 \times 10^{-2} \text{ mol/dm}^3$  accumulates.

The  $t_{\text{pre}}$  disappears, when

- a)  $1.63 \times 10^{-2} \text{ mol/dm}^3$  BrMA and  $2.4 \times 10^{-3} \text{ mol/dm}^3$  GOA, or
- b)  $1.63 \times 10^{-2} \text{ mol/dm}^3$  BrMA and  $8.1 \times 10^{-4} \text{ mol/dm}^3$  OA are the additives. These can be seen in Fig. 4.

At this low concentration neither GOA nor OA alone react in an oscillatory manner with bromate in the presence of manganese(II) ion.

On the basis of these experiments we attempted to determine GOA in the oscillatory system. OA, in the presence of BrMA, reacts with the catalyst very fast [13], thus very likely it can not accumulate in detectable concentration.

### *Determination of GOA*

With the analytical method described in the Experimental section, GOA was determined during the preoscillatory period in the concentration range of  $10^{-4} \text{ mol/dm}^3$ . Its concentration reaches a maximum value during the preos-

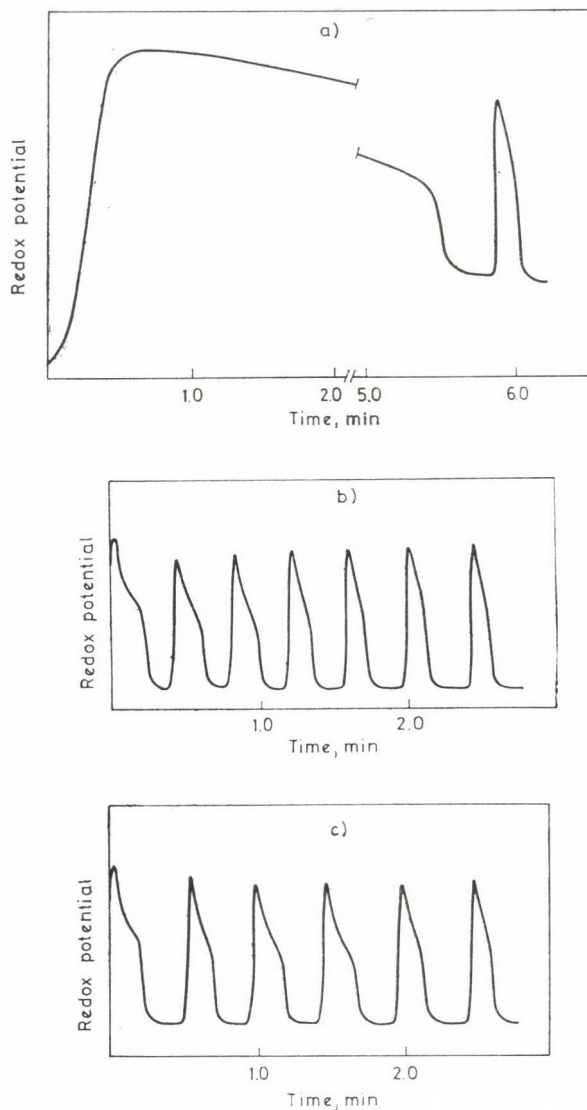


Fig. 4. The effect of GOA and OA on the preoscillatory period. The redox potential curves (a) without any additives, (b)  $[\text{BrMA}]_{\text{cru}} + \text{GOA}$ , (c)  $[\text{BrMA}]_{\text{cru}} + \text{OA}$ . In detail see the text

cillatory period, but this maximum is not at the end of the non-oscillatory phase of the reaction (Fig. 5).

In the case of the initial reagent concentrations, shown in Fig. 5, the GOA concentration required to start prompt oscillation, is  $2.4 \times 10^{-3} \text{ mol/dm}^3$  (see *Experiment (2)* in the above section). At the end of the preoscillatory period GOA determined is  $3.3 \times 10^{-4} \text{ mol/dm}^3$ . The difference between these

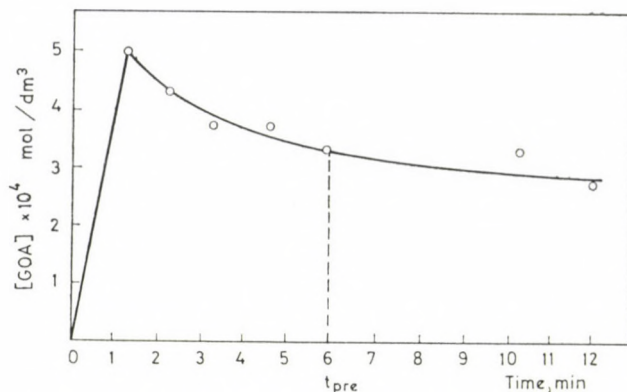


Fig. 5. Change of GOA concentration in time in the  $[MA] = 0.1 \text{ mol/dm}^3$ ,  $[BrO_3^-] = 5 \times 10^{-2} \text{ mol/dm}^3$ ,  $[Mn^{2+}] = 2 \times 10^{-3} \text{ mol/dm}^3$  and  $[HNO_3] = 5.0 \text{ mol/dm}^3$  reacting system at  $15^\circ C$

two values and the decrease of the GOA concentration during the preoscillatory period show, that GOA is only a precursor of another compound, which react faster with the catalyst, than BrMA and GOA together. This compound might be OA, according to our experiments.

### Conclusions

Our experiments show that

(1) BrMA forms during the preoscillatory period in the reaction [10, 11]:



(2) Simultaneously with this reaction BrMA reduces  $Mn^{3+}$ . In this reaction intermediates are formed which react with the catalyst faster than BrMA, and these compounds are important in the initiation of the oscillation. If we add BrMA to the reacting system, then a certain time has to elapse to produce these intermediates. Probably this is the reason, that oscillation does not start reaching the  $[BrMA]_{\text{crit}}$  or adding the  $[BrMA]_{\text{crit}}$  to the reaction mixture. When we use higher  $[BrMA]$  than  $[BrMA]_{\text{crit}}$  as an additive, then we can establish conditions under which these intermediates are produced instantaneously in the  $BrMA + Mn^{3+}$  reaction, and the preoscillatory period disappears.

(3) When the MA concentration is high, its reaction with the catalyst becomes emphasized, therefore the addition of the crucial amount of BrMA initiates the oscillation.

(4) The presence of GOA in the reacting system brings into connection the oscillating systems containing MA or GOA as organic substrates: the main

feature of these two oscillators must be similar. And if our assumption, that in the MA-containing system OA is formed at the end of the preoscillatory period, will be proved, then we can consider these three types of oscillating systems belonging to one group: in the cases of MA and GOA preoscillatory period is necessary to form the active component, OA; while OA can produce oscillations without preoscillatory period.

\*

Thanks are due to Dr. L. MAROS for his suggestions in the analysis of glyoxylic acid, and to Prof. E. KŐRÖS for his interest in this work.

## REFERENCES

- [1] FIELD, R. J., KŐRÖS, E., NOYES, R. M.: *J. Am. Chem. Soc.*, **94**, 8649 (1972)
- [2] ADAMČIKOVÁ, L., TREINDL, L.: *Coll. Czech. Chem. Commun.*, **41**, 3521 (1976)
- [3] RASTOGI, R. P., YADAVA, K. D. S., PRASAD, K.: *Ind. J. Chem.*, **12**, 974 (1974)
- [4] RASTOGI, R. P., YADAVA, K. D. S.: *Ind. J. Chem.*, **12**, 687 (1974)
- [5] RASTOGI, R. P., RASTOGI, P., KUMAR, A.: *Ind. J. Chem.*, **15A**, 163 (1977)
- [6] BAR-ELI, K., HADDAD, S.: *J. Phys. Chem.*, **83**, 2944 (1979)
- [7] TREINDL, L., DROJÁKOVÁ, S.: *Coll. Czech. Chem. Commun.*, **43**, 1561 (1978)
- [8] EDELSON, D.: *Int. J. Chem. Kin.*, **11**, 1231 (1979)
- [9] EDELSON, D., NOYES, R. M., FIELD, R. J.: *Int. J. Chem. Kin.*, **11**, 155 (1979)
- [10] BURGER, M., KŐRÖS, E.: *J. Phys. Chem.*, **84**, 496 (1980)
- [11] BURGER, M., KŐRÖS, E.: *Ber. Bunsenges. Phys. Chem.*, **84**, 363 (1980)
- [12] CONRAD, M., REINBACH, M.: *Ber.*, **35**, 1816 (1907)
- [13] JWO, J. J., NOYES, R. M.: *J. Am. Chem. Soc.*, **97**, 5422 (1975)
- [14] NOSZTICZIUS, Z., BÓDISS, J.: *Magy. Kém. Foly.*, **86**, 2 (1980)
- [15] NOSZTICZIUS, Z.: *Magy. Kém. Foly.*, **85**, 330 (1979)

Mária BURGER }  
Krisztina RÁCZ } H-1088 Budapest, Múzeum krt. 4/b.

## A SIMPLE RULE FOR PREDICTING CIRCULAR DICHROISM INDUCED IN AROMATIC GUESTS BY CYCLODEXTRIN HOSTS IN INCLUSION COMPLEXES

M. KAJTÁR<sup>1\*</sup>, Cs. HORVÁTH-TORÓ<sup>1</sup>, É. KUTHI<sup>1</sup> and J. SZEJTLI<sup>2</sup>

(<sup>1</sup> *Institute of Organic Chemistry, Eötvös Loránd University, Budapest and*  
<sup>2</sup> *CHINOIN Biochemical Research Laboratory, Budapest*)

Received June 19, 1981

Accepted for publication September 23, 1981

Circular dichroism (CD) spectra of inclusion complexes of a number of aromatic hydrocarbons, mono- and disubstituted benzene and naphthalene derivatives, and of vitamin K<sub>3</sub> with water-soluble  $\beta$ -cyclodextrin polymer, 2,6-dimethyl- $\beta$ -cyclodextrin and  $\beta$ -cyclodextrin, respectively, have been recorded. To interpret the phenomenon of induced optical activity in these complexes, a descriptive model, based on the theory of coupled oscillators, is presented. The correlation between structure and chiroptical properties of cyclodextrin complexes of aromatic molecules is expressed in the form of a simple rule by which the relative arrangement of guest and host in a cyclodextrin complex can be estimated from the CD spectrum.

The appearance of circular dichroism in the absorption bands of achiral molecules of various structures as a result of their complexing with cyclodextrins has been observed by a number of authors during the last decade [1–9]. A deeper analysis of the experimental material shows the sign and intensity of the induced CD bands to be dependent on the polarization and dipole strength of the electronic transitions in the guest molecule, from which it may be concluded that (a) the appearance of induced CD is indicative of the formation of an inclusion complex with well-defined structure, and (b) the origin of induced optical activity has to be attributed to an analogous mechanism in the case of complexes with guest molecules of different structures. By revealing, either theoretically or, at least, phenomenologically, the correlation between the induced CD spectrum and the structure of the complex, as well as the nature of the electronic transitions of the guest molecule, the recording of CD spectra can serve as a simple tool to estimate either the structures of cyclodextrin complexes or the polarization of the transitions in the guest molecule.

Because of the large size of cyclodextrin complexes, an exact theoretical calculation of the rotational strengths connected with the electronic transitions seems at present to be out of the scope of quantum chemical methods even at the semiempirical level. For calculating the induced Cotton effects

\* To whom correspondence should be addressed

of the cyclodextrin complexes of some naphthalene derivatives, HARATA and UEDAIRA [7] used the TINOCO [10] formulation of the coupled oscillator model of KIRKWOOD [11]. The same method was applied by SHIMIZU *et al.* [8] in their calculations on the complexes of substituted benzene derivatives. From a comparison of the signs of experimental CD bands with those of the rotational strengths calculated for complexes of different structures, conclusions have been made on the orientation of the guest molecules in the cyclodextrin cavity [7, 8]. In spite of the "qualitative" success of these calculations, no quantitative agreement with the experimental data can be expected from them, because of the crude simplifications involved in the coupled oscillator model. On the other hand, in our opinion, a simple qualitative model, based also on the classical electrodynamical principles of the coupled oscillators and completed with quantitative features taken from experiments, might be of the same predicting capability as the rather complicated and still unexact calculations and, at the same time, might be more easily applicable in studies aimed at correlating structure and chiroptical properties of cyclodextrin complexes.

Based on the analysis of experimental results obtained from the CD spectra of inclusion complexes of simple aromatic compounds with  $\beta$ -cyclodextrin and its derivatives, and on a simple descriptive model of induced optical activity, in the present publication we propose a rule for expressing the correspondence between the structure and the CD spectra of cyclodextrin complexes of aromatic molecules.

### Materials and Methods

For the preparation of the complexes  $\beta$ -cyclodextrin, 2,6-dimethyl- $\beta$ -cyclodextrin [12] and a water-soluble polymer built up of  $\beta$ -cyclodextrin residues connected by glycerol epichlorohydrin [13] were used. The  $\beta$ -cyclodextrin content of the polymer was of about 50%. The advantage of using the above  $\beta$ -cyclodextrin derivatives instead of  $\beta$ -cyclodextrin lies in the higher water solubility of the former compounds. With solutions of relatively high concentration of the host, it is easier to create the conditions needed for practically complete complexation even of guests with low complexing ability. Simple aromatic hydrocarbons like benzene and its homologues, which cannot be dissolved at any suitable concentration in the saturated solution of  $\beta$ -cyclodextrin, can easily be brought to complexation with a 10% solution of the  $\beta$ -cyclodextrin polymer. The latter solutions were prepared by adding, with a pipette of 0.1  $\mu$ L scale, 2–3  $\mu$ L ( $2-3 \cdot 10^{-5}$  mole) of the aromatic hydrocarbon to 10 mL of a 11.3% aqueous solution of the polymer (about  $5 \cdot 10^{-2}$  mole/L for  $\beta$ -cyclodextrin). After shaking for a few seconds, the solutions became homogeneous. Because of the inaccurate addition of the solute, the concentrations of the aromatic hydrocarbons in these solutions ( $2-3 \cdot 10^{-3}$  mole/L;  $[\beta\text{-CD}]/[\text{arom}] \sim 20$ ) were only known within an experimental error of about 10%. The UV and the CD spectra were measured by using the same solutions, therefore the values of the anisotropy numbers ( $g = \Delta\varepsilon/\varepsilon$ ) are more correct than those of  $\Delta\varepsilon$  and  $\varepsilon$  themselves. The complex of naphthalene was prepared by adding 38  $\mu$ L of a 10% solution of naphthalene in trimethyl phosphate to 10 mL of a 11.3% solution of  $\beta$ -cyclodextrin polymer ( $[\text{naphthalene}] = 3 \cdot 10^{-3}$  mole/L). In the experiments with 2,6-dimethyl- $\beta$ -cyclodextrin,  $10^{-3}$  molar solutions of the guest substances (substituted benzene derivatives) in a  $5 \cdot 10^{-2}$  molar solution of 2,6-dimethyl- $\beta$ -cyclodextrin in water were used. The complexes of 1- and 2-naphthol were prepared by mixing equal volumes of a  $2 \cdot 10^{-2}$  molar solution of  $\beta$ -cyclodextrin (over-

saturated) and a  $10^{-3}$  molar solution of the naphthol in water ( $[\text{naphthol}] = 5 \cdot 10^{-4}$ ,  $[\beta\text{-CD}] = 10^{-2}$  mole/L;  $[\beta\text{-CD}]/[\text{naphthol}] = 20$ ). In the case of the preparation of the complex of vitamin  $\text{K}_3$ , to 1.72 mg (0.01 mmole) of the substance dissolved in a few drops of ethanol was added 20 mL of a  $10^{-2}$  molar  $\beta$ -cyclodextrin solution ( $[\text{vitamin K}_3] = 5 \cdot 10^{-4}$  mole/L;  $[\beta\text{-CD}]/[\text{vit}] = 20$ ). The solutions of the complexes were prepared at least two hours before the measurement.

The UV and CD spectra were measured at ambient temperature in quartz cells using a SPECORD spectrophotometer and a Roussel—Jouan Dichrograph N<sup>o</sup> III (Jobin—Yvon), respectively.

## Results

### (1) Inclusion complexes of aromatic hydrocarbons and $\beta$ -cyclodextrin polymer

The UV and CD data of the inclusion complexes of benzene, toluene, *t*-butylbenzene, *p*-xylene, 1,2,3,5- and 1,2,4,5-tetramethylbenzene, and naphthalene with  $\beta$ -cyclodextrin polymer are summarized in Table I. The spectra of benzene and its homologues were recorded only in the wavelength range of 280–230 nm. At lower wavelengths the spectra are too noisy and could not be evaluated correctly. Under experimental conditions used for the other measurements, *o*- and *m*-xylene failed to form complexes of measurable CD effect.

The CD spectra of the complexes show the vibrational fine structures characteristic of the  ${}^1L_b$  band of aromatic hydrocarbons. As an example, the UV and CD spectra of the complex of *p*-xylene are shown in Fig. 1. Also the

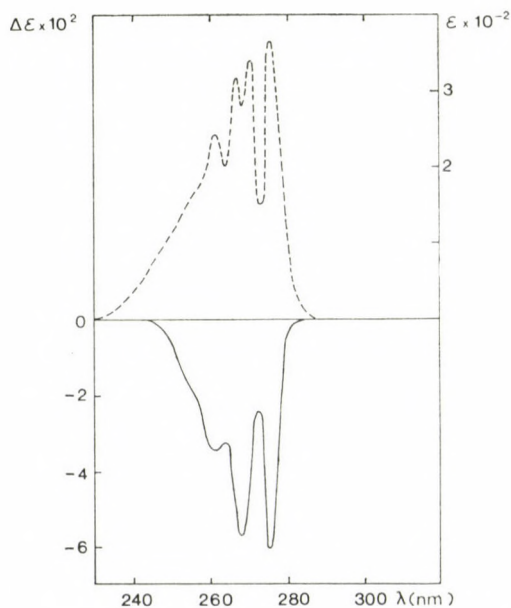


Fig. 1. CD (—) and UV (---) spectra of the inclusion complex of *p*-xylene and  $\beta$ -cyclodextrin polymer in water

Table I

CD and UV data of inclusion complexes of aromatic hydrocarbons with  $\beta$ -cyclodextrin polymer in water

Guest molecule	$\lambda$ , nm ( $\Delta\epsilon$ )	$\lambda$ , nm( $\epsilon$ )	$g = \frac{\Delta\epsilon}{\epsilon} \times 10^4$
Benzene	261 (-0.0054)	261 (160)	-0.34
	255 (-0.0076)	255 (230)	-0.33
	249 (-0.0064)	249 (200)	-0.32
	244 (-0.0045)	244 (140)	-0.32
	239 (-0.0034)	239 (100)	-0.34
Toluene	269 (-0.023)	269 (240)	-0.96
	263 (-0.023)	262 (250)	-0.92
	256 (-0.013)	256 (160)	-0.81
<i>t</i> -Butylbenzene	268 (-0.022)	268 (150)	-1.47
	261 (-0.022)	261 (190)	-1.16
	255 (-0.013)	255 (150)	-0.87
<i>p</i> -Xylene	275 (-0.061)	275 (620)	-0.98
	268 (-0.057)	268 (500)	-1.14
	261 (-0.034)	260 (330)	-1.03
1,2,3,5-Tetramethylbenzene	278 (-0.023)	278 (210)	-1.10
	269 (-0.021)	269 (250)	-0.84
1,2,4,5-Tetramethylbenzene	279 (+0.031)	279 (580)	+0.53
	271 (+0.021)	273 (540)	+0.39
Naphthalene	312 (-0.019)	312 (170)	-1.12
	305 (-0.019)	304 (230)	-0.83
	298s (-0.034)	297s (320)	-1.06
	286 (-0.40)	286 (3900)	-1.03
	278 (-0.47)	276 (5700)	-0.82
	267s (-0.23)	266 (5100)	-0.45

UV data given in Table I are our own measurements. The values agree, in most cases, quite well with those found in the literature [14, 15] for ethanolic solutions. Some differences in the  $\epsilon$  values may be attributed either to the special solvational state of the guest molecules in the cyclodextrin cavity, or to experimental inaccuracies occurring in the preparation of the solutions (see above).

The CD spectrum of the  $\beta$ -cyclodextrin complex of naphthalene was measured down to 250 nm (Table I). In this spectral range two band systems appear. The positions of the vibronic components of both bands correspond to those found in the UV spectrum measured in ethanol [15]. Below 258 nm the CD of the naphthalene complex is positive. This accounts for the smaller  $g$  value of the 267 nm shoulder. In the UV spectrum the overlapping of the very intensive  ${}^1B$  band [16] with the lower wavelength part of the  ${}^1L_a$  band causes the  $\epsilon$  values of the latter to increase. In the CD spectrum, however, the situation is just the opposite with the strong positive CD band of low wavelength shifting the neighbouring part of the  ${}^1L_a$  band towards the positive direction and resulting in a smaller negative value of  $\Delta\epsilon$  at 267 nm.

(2) *Inclusion complexes of mono- and disubstituted benzene derivatives with 2,6-dimethyl- $\beta$ -cyclodextrin*

The UV and CD data of the title substances investigated by us can be found in Table II. The UV data relating to ethanolic solutions have been taken from the literature [14]. As it was determined by systematic experiments using solutions of different concentrations and different [host]/[guest] ratios, the induced optical activity ( $\Delta\epsilon$ ) shown by the solutions used for the measurements was of maximal intensity, indicating that practically the total amount of the aromatic component was bound in the complex.

In several cases, instead of water, a dilute solution of hydrochloric acid (pH 2) or of sodium hydroxide (pH 12) was used for preparing the complexes, but no systematic experiments were performed to investigate the pH dependence of the chiroptical properties. As a result of these qualitative experiments it was found that neither phenol in basic solution, nor aniline in acidic solution form complexes with dimethyl- $\beta$ -cyclodextrin in any detectable measure. In the case of the aminobenzoic acids, however, the shape of the CD spectrum does not change on protonation of the amino group, only the intensity of the bands is somewhat reduced.

The CD spectra of the 2,6-dimethyl- $\beta$ -cyclodextrin complexes of phenol, aniline and, in particular, of benzoic acid are, in the positions of their bands as well as in their intensity, very similar to those described by SHIMIZU *et al.* [8] for the complexes of unsubstituted  $\beta$ -cyclodextrin with the same compounds.

It is remarkable that the CD spectrum of the complex of anthranilic acid is completely different from those of the other aromatic compounds studied by us. The two maxima appearing in the CD spectrum at the wavelengths of the first two UV bands assigned to the  ${}^1L_b$  and  ${}^1L_a$  type transitions are both of positive sign and of low intensity. Also the  $g$  values of these CD bands are small as compared with those of the other complexes of this type.

Table II

*CD and UV data of inclusion complexes of mono- and disubstituted benzene derivatives with 2,6-dimethyl- $\beta$ -cyclodextrin in water*

Guest molecule	$\lambda$ , nm ( $\Delta\epsilon$ )	$\lambda$ , nm ( $\epsilon$ )	$g = \frac{\Delta\epsilon}{\epsilon} \times 10^4$
Phenol	272 (-0.14)	273 (1 900)	-0.74
Aniline	287 (-0.10)	285 (1 740)	-0.57
Benzoic acid	280 (-0.08)	280 (815)	-0.98
	233 (+2.32)	228 (11 400)	+2.04
2-Hydroxybenzoic acid	304 (-0.21)	302 (4 170)	-0.50
	240 (+1.22)	234 (7 420)	+1.64
3-Hydroxybenzoic acid	297 (-0.26)	296 (2 760)	-0.94
	242 (+1.54)	234 (6 900)	+2.23
4-Hydroxybenzoic acid	256 (+3.38)	254 (14 100)	+2.40
	208 (-7.30)	212 (10 700)	-6.82
2-Aminobenzoic acid	340 (+0.09) <sup>a</sup>	332 (4 500)	+0.20
	247 (+0.29)	247 (6 700)	+0.43
4-Aminobenzoic acid	287 (+2.66) <sup>b</sup>	288 (19 000)	+1.40

<sup>a</sup> at pH 2: 340 (+0.05)

<sup>b</sup> at pH 2: 287 (+1.28)

### 3) Inclusion complexes of 1-naphthol and 2-naphthol with $\beta$ -cyclodextrin

The characteristically different CD spectra of the inclusion complexes of the two naphthol isomers with  $\beta$ -cyclodextrin, together with the corresponding UV spectra, are shown in Fig. 2. The spectral data are summarized in Table III. The  $\beta$ -cyclodextrin complex of 2-naphthol has also been studied by HARATA [9] with similar results.

In accordance with the three bands in the UV spectrum, the CD spectrum of 2-naphthol exhibits three induced Cotton effects with maxima at 329, 287 and 225 nm. The first two bands belonging to the  $^1L_b$  and  $^1L_a$  transitions are of negative sign, while the third one of  $B_b$  origin is positive. The anisotropy numbers of the negative bands are of about the same value ( $-1.16$  and  $-1.26 \cdot 10^{-4}$ ), but that of the positive band is somewhat higher ( $+1.64 \cdot 10^{-4}$ ).

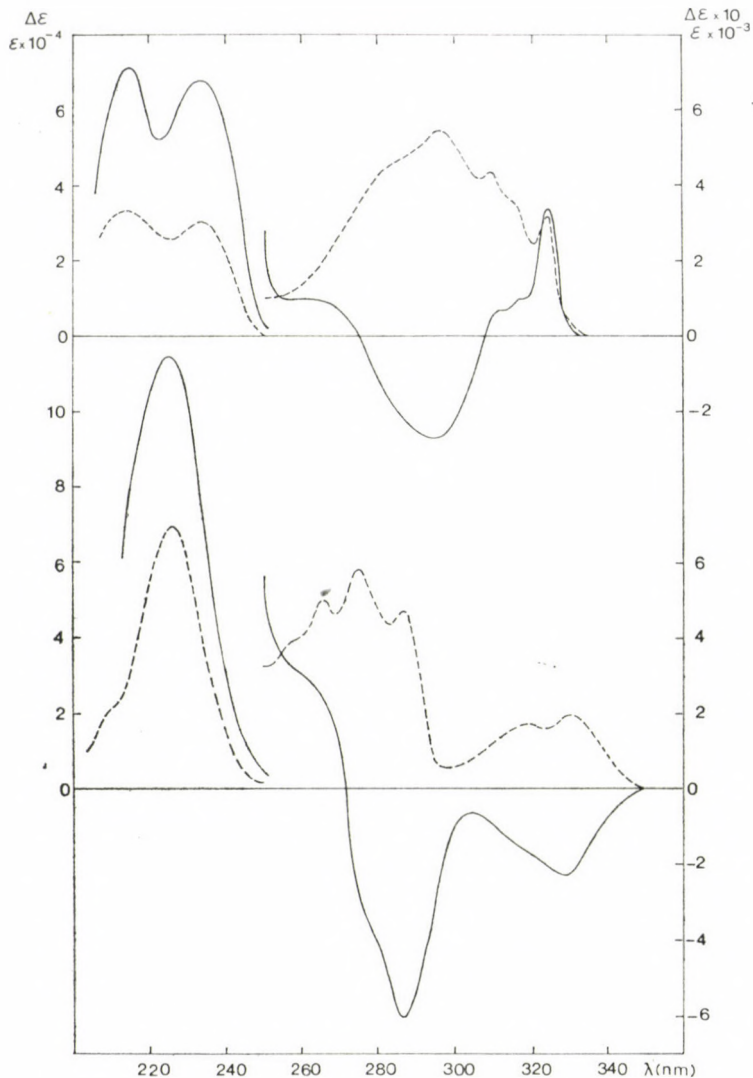


Fig. 2. CD (—) and UV (---) spectra of the inclusion complexes of 1-naphthol (top) and 2-naphthol (bottom) with  $\beta$ -cyclodextrin in water. (The scale at the left refers to the left side part of the spectra, that at the right to the right side part)

In the UV spectrum of 1-naphthol, the first two bands are overlapping each other, nevertheless, the vibronic components of the  ${}^1L_b$  band can be well distinguished on the long wavelength side of the more intensive  ${}^1L_a$  band. In the short wavelength region of the UV spectrum two distinct maxima can be found assigned to mixtures of several transitions [17]. In contrast to their strong overlapping found in the UV spectrum, the  ${}^1L_b$  and  ${}^1L_a$  transitions

Table III

CD and UV data of inclusion complexes of 1-naphthol and 2-naphthol with  $\beta$ -cyclodextrin in water

Guest molecule	$\lambda$ , nm ( $\Delta\epsilon$ )	$\lambda$ , nm ( $\epsilon$ )	$g = \frac{\Delta\epsilon}{\epsilon} \times 10^4$
1-Naphthol	324 (+0.34)	324 (3 180)	+1.07
	317 (+0.10)	315 (3 600)	+0.28
	311 (+0.07)	309 (4 400)	+0.16
	295 (-0.27)	296 (5 480)	-0.49
	285s (-0.15)	284s (4 580)	-0.33
	260 (+0.10)		
	234 (+6.88)	234 (30 900)	+2.23
	215 (+7.20)	214 (33 200)	+2.17
2-Naphthol	329 (-0.23)	330 (1 980)	-1.16
	319s (-0.17)	319 (1 720)	-0.99
	287 (-0.60)	287 (4 740)	-1.26
	276s (-0.31)	275 (5 840)	-0.53
	265s (+0.25)	266 (5 000)	+0.50
		257 (3 860)	
	225 (-11.50)	226 (70 000)	+1.64

appear in the form of two well separated maxima of opposite sign in the CD spectrum of the  $\beta$ -cyclodextrin complex of 1-naphthol. The longest wavelength CD band (at 324 nm) is of positive sign whereas the next one (at 295 nm) is negative. The fine structures of the CD bands are in good correlation with those of the UV bands. The two short wavelength UV maxima also have their equivalents in the CD spectrum, both of them of positive sign. The anisotropy values belonging to the individual vibronic components of the first band apparently decrease with decreasing wavelengths. This anomaly can be attributed to the strong overlapping of the intensive  ${}^1L_a$  band with the short wavelength components of the  ${}^1L_b$  band in the UV spectrum. Therefore the  $\epsilon$  values read directly from the spectrum are much higher than the real intensity of these band components. It is only the  $g$  value of the well separated first vibronic component ( $+1.07 \cdot 10^{-4}$ ) which can be considered as the anisotropy of the first, positive band. The negative band assigned to the  ${}^1L_a$  transition is rather weak as compared with the intensity of the corresponding UV maximum. Its  $g$  value amounts to only  $-0.49 \cdot 10^{-4}$ . The two intensive positive bands at short wavelengths, however, are of high  $g$  values ( $+2.2 \cdot 10^{-4}$ ).

(4) *Inclusion complex of vitamin K<sub>3</sub> (2-methyl-1,4-naphthoquinone) with  $\beta$ -cyclodextrin*

This complex first prepared by FRÖMMING and SANDMANN [18], and investigated by SZEJTLI *et al.* [19] in connection with efforts to provide pharmacologically active substances with a protecting capsule of molecular size, can also be chosen as a substance for the study of the correlation between structure and chiroptical properties of cyclodextrin complexes with aromatic molecules. The CD and UV spectra of the aqueous solution of the complex are shown in Fig. 3. The spectral data are summarized in Table IV. In addition

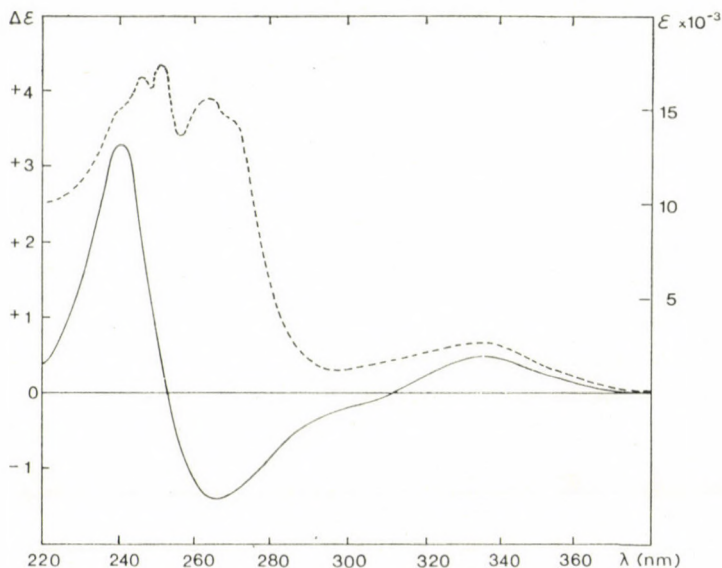


Fig. 3. CD (—) and UV (---) spectra of the inclusion complex of vitamin K<sub>3</sub> (2-methyl-1,4-naphthoquinone) with  $\beta$ -cyclodextrin in water

to the values of  $\epsilon$ ,  $\Delta\epsilon$  and  $g$ , the directions of polarization of the electronic transitions responsible for the individual bands are also given in the Table ( $\parallel$  and  $\perp$  indicating the direction of polarization to be parallel with or perpendicular to the long axis of the naphthoquinone molecule).

The maxima appearing in the CD spectrum correlate well with the corresponding UV bands. The band belonging to the electrically forbidden  $n \rightarrow \pi^*$  transition of the carbonyl groups appears around 420 nm in the form of a hardly detectable shoulder in the UV spectrum and of a very weak and broad negative maximum in the CD. (Because of its low intensity, this band is not indicated in Fig. 3.) However, the  $g$  value of this band is fairly high in comparison with those of the others. It is very probable that this value is

Table IV

CD and UV data of the inclusion complex of vitamin K<sub>3</sub> (2-methyl-1,4-naphthoquinone) with  $\beta$ -cyclodextrin in water

Band	$\lambda$ , nm	$\Delta\epsilon$	$\epsilon$	$g = \frac{\Delta\epsilon}{\epsilon} \times 10^4$	Polarization
$n \rightarrow \pi^*$	430	-0.03	50	-6.00	$\perp$
${}^1L_b$	334	+0.51	2 500	+2.04	$\parallel$
${}^1L_a$	266	-1.42	15 000	-0.95	$\perp$
$B_b$	241	+3.35	17 000	+1.97	$\parallel$

unrealistic, resulting only from the fact that the  $\epsilon$  value of the shoulder cannot be determined correctly without performing a curve resolving procedure. It is worthy of note that the magnitudes of the  $g$  values belonging to the two positive CD bands at 334 and 241 nm are two times greater than that of the negative band at 266 nm.

The positive maximum appearing at 334 nm in the CD and UV spectrum can be assigned to a transition localized mainly on the benzene ring and polarized parallel to the long axis of the molecule [20]. This can be regarded as the  ${}^1L_b$  transition of an *ortho* disubstituted benzene derivative. The maximum of negative sign found around 260 nm in the CD spectrum is composed of several transitions [21–23]. The most intensive of them can be attributed to the quinone chromophore with a polarization along the axis of the two carbonyl groups, *i.e.* perpendicular to the long axis of the naphthalene ring. Because of its intensity and polarization, this “quinonoid” band is often referred to as the  ${}^1L_a$  band of the naphthalene chromophore [20]. The highest energy band system has been assigned to transitions analogous to the degenerated  ${}^1B$  transition pair of benzene [20]. The main component of this band system is considered again as originating mainly from a “benzenoid” transition polarized parallel to the long axis of the molecule [21–23]. The CD within this last band is rather intensive and of positive sign.

### Discussion

In inclusion complexes, the electronic system of the achiral guest molecule and that of the chiral cyclodextrin are in interaction, therefore, the total system being chiral, all the transitions attributed to the complex as a whole must in principle be connected with rotational strength [24].

In the simplified picture of the excited states used for rationalizing the experimental facts in chemical spectroscopy, however, the change caused by excitation on the state of the electronic system is usually considered as localized to the chromophore, *i.e.* to a smaller or larger part of the whole molecule [25]. In the inclusion complexes of cyclodextrins with aromatic guests, the latter can be regarded as the chromophores responsible for the transitions assigned to the absorption bands above 200 nm. This simplification seems to be justified by the close similarity in the positions and intensities of the bands found in the anisotropic absorption spectra of solutions of the complexes as well as in those of the guest molecules themselves. In this respect the effect of the environment represented by the host cannot be regarded as being significantly different from that of a common solvent (*e.g.* alcohol or ether). Nevertheless, the appearance of circular dichroism within the absorption bands assigned to the transitions of the inherently achiral aromatic guest indicates that the electronic system of the chiral host, too, must take some part in these transitions.

Since no exact description of the ground and excited states of such a big electronic system as a whole complex, can, at present, be achieved by the more sophisticated methods of quantum chemistry, for solving problems like this, the simplified approximations of the perturbation theory are usually employed [10, 26]. According to this theory, the electronic transitions of an inherently achiral chromophore can acquire the missing transition moment (in this case the magnetic one) necessary to render the rotational strength nonzero, by interacting with the transitions of other chromophores arranged chirally with respect to it within or around the molecule.

For interpreting the induced optical activity of the inclusion complexes of aromatic guests and cyclodextrin hosts, HARATA and UEDAIRA [7], and using their method, also SHIMIZU *et al.* [8], have applied the simple model of coupled oscillators described first by KUHN [27] and by KIRKWOOD [11], and incorporated later in perturbation theory by TINOCO [10]. This model is based on the dipole-dipole interaction between the electric transition dipole moment of the aromatic guest molecule and the weak electric moment induced by the oscillating electric field of light in the  $\sigma$ -bonds of the chirally arranged  $\alpha$ -D-glucosyl residues of the cyclodextrin host. The results of calculations performed by applying this method to the complexes of a number of substituted naphthalene [7] and benzene derivatives [8] are in qualitative, but not in reliably good quantitative, agreement with the experimental data. As a matter of fact, no reliable numerical results on such an intricate physical quantity as the rotational strength, can be expected from a calculation involving crude simplifications. Nevertheless, the investigations of the Japanese authors [7, 8] have shown that the coupled oscillator model can well be used to explain the main features of the optical activity induced in the cyclodextrin complexes

of aromatic molecules. But, since the application of their method to other compounds requires rather laborious and still inaccurate computations for each individual case, we are going to give here a qualitative description of the coupled oscillator model as applied to the inclusion complexes of aromatic molecules and, on the basis of this model and of experimental data, to formulate a simple rule for correlating the chiroptical properties of the complexes with their structure and with the nature of their electronic transitions. In our opinion, this simple rule can be more easily and generally applied in practice than the calculations and, at the same time, with almost the same reliability.

### *The descriptive model and the sector rule*

According to the model of coupled oscillators [11, 28], an optically active system is composed of (at least) two oscillating electric dipoles which must not be either coplanar or perpendicular simultaneously to each other and to the line connecting their centers. The system formed by the coupling of these oscillating dipoles will possess not only a resultant oscillating electric moment but also an oscillating magnetic moment, which, being either parallel or antiparallel to the electric moment, will give rise in the system to a positive or negative rotational strength, respectively. The relative directions of the resultant electric and magnetic moments, *i.e.* the sign of the rotational strength, depend on the spatial arrangement of the two oscillators.

The interaction of the two oscillating dipoles can be described in the following way, too. An oscillator possessing an electric dipole moment can acquire also a magnetic moment if perturbed by another oscillating dipole. The phenomenon is reciprocal, *i.e.* the second oscillator also gets hold of a magnetic moment from the interaction, being perturbed by the first one [28].

Without entering into any details of mathematical deductions, their results can be summarized in the following descriptive form. If two oscillators of different energy are in such a disposition to each other that, when in phase,\* they determine a right handed helix, the electric and magnetic moments resulting from their coupling will be parallel, and the rotational strength belonging to the oscillator of lower energy will be of positive sign (Fig. 4a). In the inverse case, *i.e.*, if the relative position of the pair of oscillators can be characterized by a left handed helix, the resulting electric and magnetic moments are antiparallel, and the rotational strength belonging to the lower energy oscillator will be negative (Fig. 4b).\*\* (It is always the direction of the resultant

\* That mode of coupling of the two oscillating dipoles is to be chosen in which the dihedral angle of the two dipole moment vectors is smaller than  $90^\circ$ .

\*\* The rotational strength belonging to the higher energy oscillator is always of inverse sign (*cf.* [28]), but this is not relevant for the present discussion.

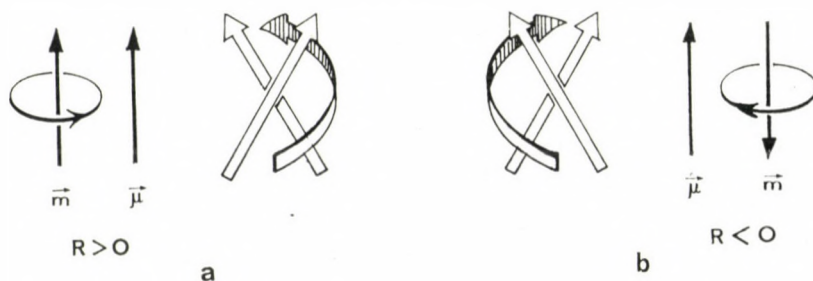


Fig. 4. Coupling of two oscillators determining a right handed (a) and a left handed (b) helix. The two pairs of empty arrows represent the pair of oscillators in two different relative positions, the curved arrows showing how the helicity of the given pair has to be interpreted. The black arrows indicate the direction of the electric ( $\mu$ ) and magnetic ( $m$ ) transition moment vectors resulting from the coupling. ( $R$  means rotational strength)

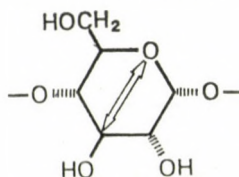


Fig. 5. Direction of the oscillating induced dipole attributed to a single glucose unit of the cyclodextrin molecule

electric vector which is to be regarded as that of the propagation of the helix. The direction of the magnetic moment can be determined by the "right hand rule".)

This qualitative model of the coupled oscillators can be applied to the cyclodextrin complexes of aromatic molecules. The electric transition moment which belongs to a selected electronic transition of the aromatic molecule occupying the cavity of the cyclodextrin host can be regarded as the oscillator of lower energy. In the calculations of HARATA and UEDAIRA [7], the perturbing dipoles, *i.e.* the oscillators of higher energy, are represented by the individual  $\sigma$ -bonds of the cyclodextrin molecule brought into oscillation by the oscillating electric field of light. The electric moment belonging to these oscillators are proportional to the polarizability of the individual bonds. The moments induced in the  $\sigma$ -bonds of an individual  $\alpha$ -glucopyranose unit, however, can be summed up to a resultant induced electric moment attributable to a glucose unit. It can easily be seen that, in consequence of the structural symmetry of the glucose unit, this "resultant" induced oscillator is lying nearly along the line connecting the C<sup>3</sup> and O<sup>5</sup> atoms (Fig. 5). The induced dipoles belonging to the individual glucose units of the cyclodextrin host are regarded in our model as "perturbers" which, by coupling with the electric transition dipole of the aromatic guest, give rise to the rotational strength of the latter.\*

\* The rotational strength arising in the "perturbers" in consequence of the reciprocal nature of the coupling will not be dealt with here.

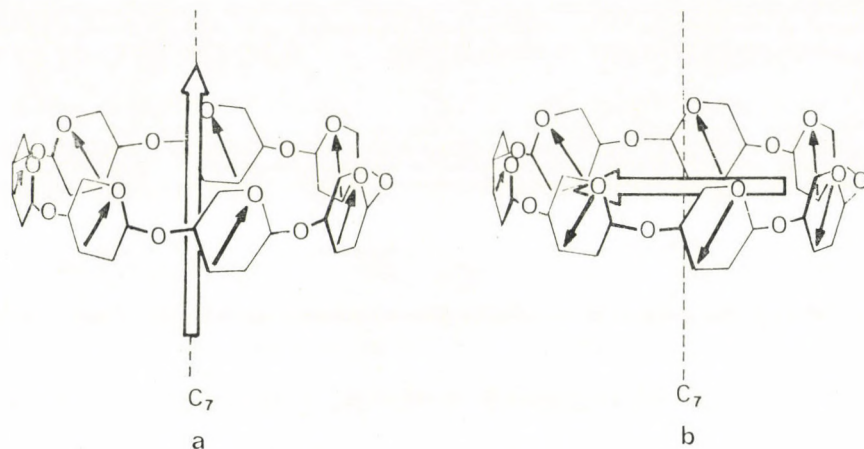


Fig. 6. Coupled oscillator systems composed, on the one hand, of the induced dipoles of the individual glucose units of a  $\beta$ -cyclodextrin molecule (represented by black arrows) and, on the other, of the electric transition moment of the guest polarized parallel (a) with and perpendicular (b) to the  $C_7$  symmetry axis of the host (represented by empty arrows). For details, see text

If the direction of the transition dipole moment due to the investigated electronic transition of the aromatic guest occupying the cavity of the  $\beta$ -cyclodextrin molecule coincides with the  $C_7$  symmetry axis of the latter, the relative positions of the coupled oscillator pairs composed, on the one hand, of the central dipole of the aromatic transition and, on the other, of the induced dipole of any of the individual glucose units determine, when in phase, a right handed helix (Fig. 6a). Therefore, this geometric arrangement of the transition moments of the guest and of the "perturbers" in the host induces a rotational strength of positive sign in the discussed transition of the aromatic molecule.

It is to be expected that the induced rotational strength will be of a relatively large magnitude in this case, because, in consequence of symmetry, the contributions of the individual oscillator pairs add up favourably.

The chirality of the geometric arrangement remains unchanged even in cases when the direction of the transition moment of the guest somewhat deviates from that of the symmetry axis of the cyclodextrin. At an angle of about  $30^\circ$ , however the transition moment becomes parallel with one of the glucose dipoles, and, by further increase of the deviation, the relative arrangement of some of the coupled oscillator pairs will change from the right handed to a left handed helix. It can easily be seen that, at an angle of about  $30-40^\circ$  between the directions of the transition moment and the symmetry axis, the contributions of the different oscillator pairs compensate each other and the rotational strength vanishes. By further increasing the angle between the transition moment and the symmetry axis, we arrive at a geometry at which most of the local oscillator pairs become of left handed type and the resulting

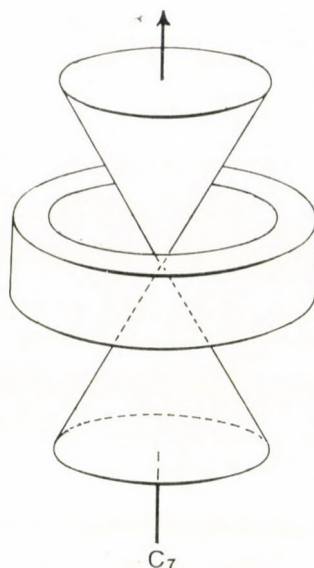


Fig. 7. The imaginary double cone distributing the environment of a cyclodextrin molecule (represented by a ring) into sectors of different signs

rotational strength of the system changes to negative sign. The optimal situation for a negative rotational strength is the one with the transition moment of the aromatic guest perpendicular to the symmetry axis of the host (Fig. 6b). However, even at this arrangement the geometry of the central transition moment and of the seven perturbing dipoles is only of  $C_2$  and not of  $C_7$  symmetry, and thus the contributions of the individual oscillator pairs cannot be all simultaneously optimal. Therefore, the magnitude of the maximal negative rotational strength (at the "perpendicular" position of the transition moment) does not reach that of the positive one (at the "parallel" position).

The conclusions from this simple model can be summarized in the following rule. If the electric moment belonging to the investigated transition of the aromatic guest molecule falls within an imaginary double cone whose center coincides with that of the cyclodextrin and whose constructor forms an angle of about  $30^\circ$  with the  $C_7$  symmetry axis (Fig. 7), then the induced rotational strength and the sign of the CD maximum will be positive, while the sign of the rotational strength (and the CD maximum) induced in a transition with its electric moment outside of this double cone will be negative. The positive or negative induced circular dichroism is of maximal magnitude if the transition dipole moment is parallel or perpendicular, respectively, to the symmetry axis of the cyclodextrin. By an angle of about  $30^\circ$  between the directions of the transition moment and the symmetry axis, no induced Cotton effect can be expected within the absorption band in question.

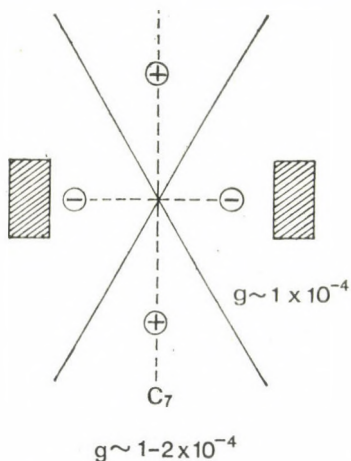


Fig. 8. Sector diagram for predicting the sign and approximate anisotropy ( $g$ ) of CD bands induced in inclusion complexes of aromatic molecules with cyclodextrins. For details, see text

The above considerations are in good agreement with the calculations of SHIMIZU *et al.* [8], according to which the magnitude of the positive rotational strength belonging to a transition parallel with the symmetry axis is two times larger than that of the negative rotational strength connected with a "perpendicular" transition.

The rule deduced from the simple model is demonstrated in the diagram of Fig 8. It shows a plane section of the cyclodextrin molecule containing the symmetry axis. The hatched rectangles represent the two parts of the cross section of the cyclodextrin ring, and the full lines indicate the cross section of the double cone. The plus and minus signs in the sector pairs give the sign of the induced CD band belonging to the transition of the aromatic guest the electric moment of which falls into the respective sector pair. The dashed lines show the directions of the transition moments connected with the positive or negative induced Cotton effects of maximal anisotropy (see below). This cross sectional representation of the inclusion complexes is sufficient for the formulation of the rule, because, in most complexes, the guest molecule can freely rotate around the symmetry axis in the cyclodextrin cavity and can occupy many equivalent positions with respect to the host.

For the characterization of the intensity of induced CD bands, the value of the anisotropy number ( $g = \Delta\epsilon/\epsilon$  [24, 25]) is more appropriate than that of the experimentally measured  $\Delta\epsilon$ . It may be supposed that the dipole moments induced by the light in the glucose units of the cyclodextrin molecule are of about the same magnitude within the spectral range of the aromatic bands investigated in our measurements. The magnitude of the perturbing dipoles being constant, the value of the induced rotational strength due to the coupled oscillator mechanism must be proportional to the electric moment

of the investigated aromatic transition and, therefore, the value of the anisotropy ( $\Delta\epsilon/\epsilon$ ) must always be the same, irrespective of the intensity ( $\epsilon$ ) of the band in question. Though this reasoning is not completely correct, since the magnitude of the induced dipole moments somewhat increases with the decreasing wavelength of the light (*cf.* p. 348) [7, 8], our conclusion drawn from it seems to be justified, in a good approximation, by experiment. As can be seen from the data in Tables I–IV, the anisotropy values ( $g$ ) belonging to the induced Cotton effects of different cyclodextrin complexes are of the same order of magnitude ( $10^{-4}$ ). This value is of about one order of magnitude smaller than in the more usual cases, when the electrically allowed transition acquires the missing magnetic transition moment from an intramolecular perturbational interaction [24]. Therefore, a  $g$  value of the magnitude of  $10^{-4}$  of an induced CD band originating from an electrically allowed transition of the guest molecule may be considered as an indication of the formation of a true inclusion complex. The assumption that the optical activity of the inclusion complexes of cyclodextrins with different types of guest molecules is due to a common mechanism, is also supported by the relatively constant value of the anisotropy of the induced CD bands.

According to our model, the variations falling within one order of magnitude of the values of anisotropy of the induced CD bands reflect the geometric arrangement of guest and host in the inclusion complexes (see below).

Based on the experimental data, approximate values relating to the anisotropy number ( $g$ ) of the induced CD maxima can also be assigned to the sector pairs in the diagram.

Now we will try to discuss our experimental results in the light of the simple sector rule.

#### *Inclusion complexes of aromatic hydrocarbons*

The 260 nm band of benzene originates from the  ${}^1L_b$  transition (in PLATT's notation [16]) of the  $\pi$ -system [25]. Because of the high symmetry of the benzene molecule ( $D_{6h}$ ), this transition is electrically forbidden (*i.e.* the value of its electric transition moment is zero), however, by coupling with a vibrationally excited state of  $e_{2g}$  symmetry, it acquires a small electric transition moment polarized along one of the lines connecting the midpoints of the opposite C–C bonds [16, 30]. Being relatively small and highly symmetric, the benzene molecule can be accommodated by the  $\beta$ -cyclodextrin host (inner diameter 0.75 nm) in any of the possible orientations. In the most symmetric of the imaginable arrangements, the  $D_6$  axis of the benzene molecule is coincident with the  $C_7$  axis of the  $\beta$ -cyclodextrin. The plane of the benzene molecule being perpendicular to the axis of the cyclodextrin in this position, all the possible directions of the electric moment belonging to the  ${}^1L_b$  transition

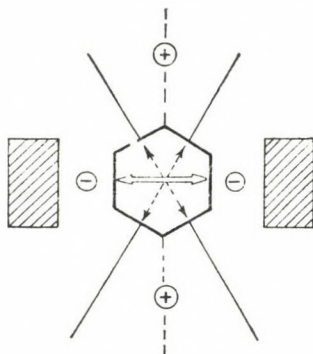


Fig. 9. The sector diagram as applied for the explanation of the negative sign of the  ${}^1L_b$  Cotton effect induced in benzene by  $\beta$ -cyclodextrin. (The empty arrow indicates the direction of polarization of the  ${}^1L_b$  transition leading to the negative Cotton effect. The broken arrows show two other possible directions of the transition moment coinciding with nodal lines)

(polarized in the plane of the ring) must be concomitant with an induced rotational strength of negative sign. Of the other possible positions of the benzene ring, those having the longer axis of the molecule (crossing the opposite C atoms) along the symmetry axis of the cyclodextrin allow more favourable van der Waals interactions with the host than those in which the same axis of benzene ring is perpendicular to the cyclodextrin axis. In arrangements of the former type, one of the possible directions of the electric moment of the  ${}^1L_b$  transition is lying along the line of the maximal negative rotational strength as shown in the sector diagram, while the other directions coincide with the section lines of the double cone, *i.e.* with the directions of zero rotational strength (Fig. 9). Thus, the negative sign of the Cotton effect induced in the  ${}^1L_b$  band of benzene, the most symmetric one of aromatic molecules, can well be explained by applying the sector rule.

In the case of the benzene complex, the  $g$  value is constant for all the vibronic components of the  ${}^1L_b$  band. The relatively low value of anisotropy ( $g = -0.3 \cdot 10^{-4}$ ) can be explained by the fact that neither the benzene molecules inside the cavity of the cyclodextrin, nor the direction of the transition moment in the benzene molecule are fixed. Some of the possible orientations may be optically inactive, others may induce Cotton effects of opposite signs partly compensating each other.

At the most probable arrangement of a toluene molecule in the complex, its  $C_2$  axis is coincident with the symmetry axis of the cyclodextrin. The  ${}^1L_b$  transition being polarized perpendicularly to the  $C_2$  axis [25, 31], the induced Cotton effect of the toluene complex must, according to the sector rule, be of negative sign in agreement with experience. Because of the fixed direction of the transition moment within the molecule and because of the fixed position of the toluene molecule relative to the cyclodextrin, the  $g$  value belong-

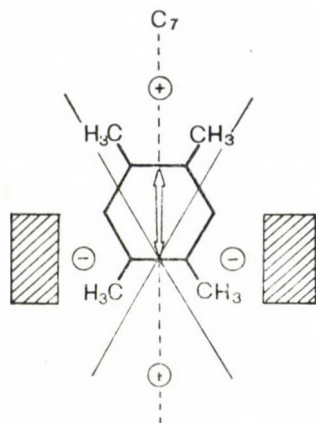


Fig. 10. The sector diagram as applied to the cyclodextrin complex of durene (1,2,4,5-tetramethylbenzene). The guest molecule cannot accommodate symmetrically in the cyclodextrin cavity

ing to the  ${}^1L_b$  transition is more than three times higher than in the case of the benzene complex.

The same agreement between the sector rule and the experimental data can be found with the complexes of *t*-butylbenzene, *p*-xylene and 1,2,3,5-tetramethylbenzene, too. The direction of polarization of the  ${}^1L_b$  band in these molecules with either one or more identical substituents can easily be established, by using PLATT's spectroscopic moments, to be perpendicular to the  $C_2$  symmetry axis (in the case of *p*-xylene, to the one running through the two methyl groups) [25, 31]. The relative orientation of guest and host in these complexes can be taken as unambiguous from simple geometric considerations, for the above mentioned molecules may best accommodate the cavity with their symmetry axis lying parallel to that of the cyclodextrin. The *g* values of the negative bands found in the CD spectra of all the three complexes are of about the same magnitude ( $-1 \cdot 10^{-4}$ ).

In contrast to the negative maxima found in the CD spectra of the complexes discussed above, the  $\beta$ -cyclodextrin complex of durene (1,2,4,5-tetramethylbenzene) exhibits a weak positive induced band in the CD spectrum. This fact provides an opportunity to prove the reliability of our sector rule. As can be determined by PLATT's method [16, 25, 31], the direction of the electric moment of the  ${}^1L_b$  transition in durene coincides with the  $C_2$  axis crossing the molecule between the methyl groups in *orto* position. The most favourable position for the durene molecule in the cyclodextrin cavity is the one with the above mentioned axis lying in the symmetry axis of the cyclodextrin. At such an arrangement of guest and host, the transition moment falls in a positive sector pair, enabling us to predict an induced Cotton effect of positive sign, as it can indeed be found in the spectrum (Fig. 10). Although

according to the rule this positive CD band should be of a higher  $g$  value than the negative ones in the former complexes, the actual value of  $g$  is even lower. The relatively small value of anisotropy may be ascribed to the asymmetrical position of the benzene ring inside the cyclodextrin. The pair of *ortho* methyl groups entering the cavity first do not let the benzene ring itself reach the center of the cyclodextrin. In a complex with such an asymmetrical structure, the interaction of the coupled dipoles must decrease in intensity [7, 8].

As can be seen from the above examples, the proposed rule can be applied with success for rationalizing the chiroptical properties of the cyclodextrin complexes of simple benzene homologues.

The explanation of the induced CD spectrum of the complex of naphthalene with  $\beta$ -cyclodextrin polymer causes some difficulties. The first two transitions of naphthalene referred to as the  ${}^1L_b$  and the  ${}^1L_a$  transitions according to PLATT [16, 25, 31], are polarized parallel and perpendicular, respectively, to the long axis of the naphthalene molecule. These transitions with mutually perpendicular electric moments should give rise, according to our rule, to induced Cotton effects of opposite signs, but the two bands found in the experimental CD spectrum are both of negative sign. This finding cannot be brought into accordance with the rule by supposing any of the conceivable structures for the complex. In the light of other data relating to the structure of the cyclodextrin complexes of naphthalene derivatives [7, 9], it may be supposed that the naphthalene molecule penetrates the cavity with its longer axis parallel to the symmetry axis of the cyclodextrin. A complex with this structure must indeed give a negative Cotton effect in the  ${}^1L_a$  band as found experimentally. The  ${}^1L_b$  Cotton effect induced in this complex should, however, be of positive sign, in contrast to our experimental results. One could try to explain this anomaly by supposing that the overlapping of the weak  ${}^1L_b$  and of the much stronger  ${}^1L_a$  bands makes the former one shift in the direction of the latter. However, the first vibronic component of the  ${}^1L_b$  band is clearly separated in the CD spectrum and is, nevertheless, negative. The induced CD spectra of the naphthols, on the other hand, are in good accordance with the proposed rule (see below).

#### *Inclusion complexes of substituted benzene derivatives*

The chiroptical properties of  $\beta$ -cyclodextrin complexes of a number of simple benzene derivatives substituted with one hydroxyl, amino, carboxyl or nitro group, or with a pair of these groups in *para* position, have been studied earlier by SHIMIZU *et al.* [8]. Our results with the 2,6-dimethyl- $\beta$ -cyclodextrin complexes of some of these compounds are in good agreement with those of the Japanese authors, indicating that the perturbing effect of the 2,6-dimethyl- $\beta$ -glucopyranose units does not markedly differ from that of the

glucose units of unsubstituted  $\beta$ -cyclodextrin. The data collected in Table II can, at least in most of the instances, be easily explained on the basis of our simple rule.

The crystal structures of  $\alpha$ -cyclodextrin complexes of several benzene derivatives have been determined by X-ray diffraction [32–36]. As indicated by the results of these studies, the hydroxyl or the amino group is usually emerging from the cavity near the secondary hydroxyl side of the cyclodextrin molecule, whereas the carboxyl or the nitro group, forming hydrogen bonds with the primary hydroxyl groups of the host, is located in the inside of the hole. These structural features of the complexes found in the crystalline phase may be supposed to be valid also in solution.

As far as the signs of the induced Cotton effects are concerned, however, it is irrelevant whether the substituent of the guest is located at one or the other side of the cyclodextrin molecule. In this respect, the only important feature of the structure is that the monosubstituted derivatives of benzene are oriented with their  $C_2$  axes lying in the symmetry axis of the cyclodextrin ring. In these complexes the electric moments of the  ${}^1L_b$  and  ${}^1L_a$  transitions being polarized perpendicular and parallel, respectively, to the  $C_2$  axes of the aromatic molecules, fall into the negative and the positive sector pairs, respectively, of the sector diagram, in agreement with the longer wavelength negative and shorter wavelength positive induced Cotton effects found in the experimental CD spectra. The  $g$  values of the negative  ${}^1L_b$  Cotton effects are smaller than  $1 \cdot 10^{-4}$ , whereas those of the positive  ${}^1L_a$  bands are between 1 and  $2 \cdot 10^{-4}$  indicating also the quantitative predictions of the rule to be valid.

Of the complexes of disubstituted benzene derivatives, those of *p*-hydroxybenzoic acid and of *p*-aminobenzoic acid behave regularly. As it can be regarded as unambiguous on simple geometric grounds, and as it has been established on the example of the  $\alpha$ -cyclodextrin complex of *p*-hydroxybenzoic acid [34], these molecules are situated with their long axes parallel to the cyclodextrin axis. The carboxyl group is immersed into the cavity, whereas the hydroxyl or the amino group is emerging from it. In these complexes the  ${}^1L_b$  and the  ${}^1L_a$  bands are polarized perpendicular and parallel, respectively, to the common symmetry axis of the aromatic guest and the cyclodextrin host.

The first intensive band in the CD spectra of the complexes of *p*-hydroxybenzoic and *p*-aminobenzoic acids has to be assigned, according to its spectral position and to the high  $\epsilon$  value of the corresponding band in the UV spectra, to the  ${}^1L_a$  transition. Thus the positive sign of this band is in agreement with the rule. Neither the CD nor the UV spectrum of *p*-hydroxybenzoic acid show any trace of the band belonging to the  ${}^1L_b$  type transition. It is presumably hidden by the much stronger  ${}^1L_a$  band.

In the CD spectrum of *p*-hydroxybenzoic acid a second, negative band of very high intensity can also be found at 208 nm. This originates from a

$^1B$  type transition polarized nearly perpendicular to the  $C_2$  axis of the molecule with an angle of polarization\* of  $76^\circ$  according to PPP calculations [37]. The electric moment belonging to this transition gets into a negative sector pair, thus its negative sign is in accordance with the sector rule. As to the anisotropy of the two induced CD bands of *p*-hydroxybenzoic acid, it is of interest to note that while the first one is also of a rather high  $g$  value, the second transition is of exceptional intensity, its  $g$  value amounting to  $-6.8 \cdot 10^{-4}$ . As it has already been mentioned above, the magnitude of the induced dipoles in the glucose units somewhat increases with the decreasing of the wavelength of light [7, 8]. This means that the intensity of the rotational strength resulting from the interaction of the coupled oscillators must also increase as the wavelength of the aromatic transition decreases. This is why, with the other parameters equal, an induced Cotton effect of lower wavelength is connected with a greater absolute value of anisotropy. (The analogous  $^1B$  bands were not measured for the other benzene derivatives.)

As far as the signs and the  $g$  values of the individual bands are concerned, the CD spectrum of the cyclodextrin complex of *m*-hydroxybenzoic acid is very similar to that of benzoic acid. To our knowledge, no X-ray data are at present available on the structure of this complex. However, based on the similarity between the structures of the complexes containing *p*-hydroxybenzoic acid and *p*-nitrophenol as guest molecules [34], the structure of the cyclodextrin complex of *m*-hydroxybenzoic acid can be regarded as analogous to the known structure of the *m*-nitrophenol complex [35]. It is therefore very probable that the carboxyl group is situated at the "bottom" of the cyclodextrin cavity, forming hydrogen bonds with the primary hydroxyl groups, while the

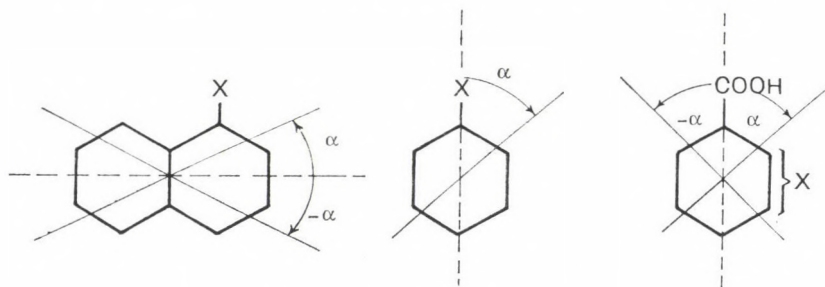


Fig. 11. Definition of the sign of the angle of polarization for transition moments of substituted naphthalene and benzene derivatives

\* Here and on the following pages, the angle of polarization ( $\alpha$ ) of a transition is taken as measured from the long axis of the benzene or naphthalene molecule. In case of the substituted benzoic acids, this axis is running through the C atom of the carboxyl group. The sign of the angle is positive if the smaller angle falls toward the second substituent being in *ortho* or *meta* position relative to the carboxyl group as shown in Fig. 11. According to this definition, the angle of polarization can be positive or negative, but its magnitude cannot be higher than  $90^\circ$ .

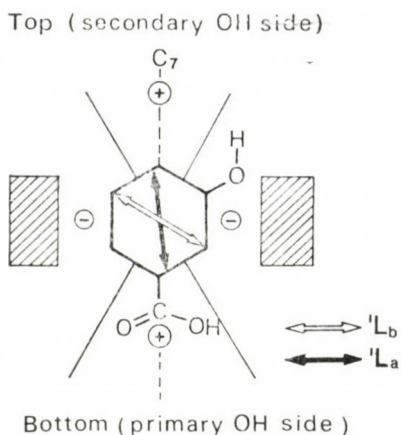


Fig. 12. The sector diagram as applied to the cyclodextrin complex of *m*-hydroxybenzoic acid

phenolic hydroxyl group is bound to the secondary hydroxyls of the cyclodextrin molecule at the wider border of the cavity. The angles of polarization of the  ${}^1L_b$  and  ${}^1L_a$  transitions have been calculated by KISS and SZŐKE [38] to be of about  $+60^\circ$  and  $+6^\circ$ , respectively. Supposing the orientation of the molecule in the cyclodextrin cavity to be as shown in Fig. 12, the sector rule predicts a weaker negative and a stronger positive induced CD band for the  ${}^1L_b$  and the  ${}^1L_a$  transitions, respectively, in full agreement with the experimental data. Thus the proposed structure of the complex is supported by the analysis of its chiroptical properties.

The complex of salicylic acid with 2,6-dimethyl- $\beta$ -cyclodextrin exhibits a CD spectrum similar to that of *m*-hydroxybenzoic acid. There is, however, a characteristic difference in the anisotropy values of the CD bands belonging to the two complexes, with those of the salicylic acid complex being remarkably smaller than those of its *meta* isomer. This difference can probably be attributed either to the less fixed accommodation of the former guest in the complex or to the different orientations of the transition moments relative to the perturbing system of the cyclodextrin in the two complexes. At present, no data relating to the structure of the cyclodextrin complex of an *ortho* disubstituted benzene derivative can be found in the literature. Calculations on the excited states of salicylic acid have given  $-40^\circ$  and  $-19^\circ$  for the values of the polarization angles of the  ${}^1L_b$  and the  ${}^1L_a$  transitions, respectively [38]. Having these data and supposing the predictions of our sector rule to be correct, we may try to make some proposals for the structure of the complex. Two structures can be brought into accordance with the chiroptical properties: the one with both functional groups outside the cyclodextrin cavity and the other with both groups penetrating into it. The line connecting the C<sup>1</sup> and C<sup>4</sup> atoms of the benzene ring must either run parallel with the symmetry axis of

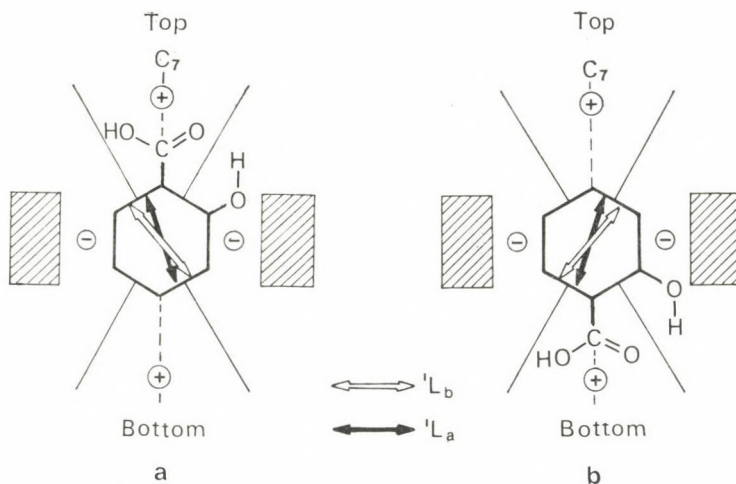


Fig. 13. Sector diagrams as applied for two possible structures of the cyclodextrin complex of salicylic acid

the cyclodextrin or form an angle not wider than  $10^\circ$  with it. The directions of the electric transition moments of the  ${}^1L_b$  and  ${}^1L_a$  bands get, in both structures, in negative and positive sector pairs, respectively (Fig. 13). Anyway, both the transition moments fall, in any of the two structures, near the nodal lines separating the positive and negative sectors, thus no intensive induced optical activity can be expected. This might account for the relatively small values of anisotropy found experimentally.

We encounter some difficulties when trying to deduce a structure for the cyclodextrin complex of anthranilic acid from its induced CD spectrum. The electric moments of the first two transitions in anthranilic acid are of almost the same direction, with the calculated angles of polarization for the  ${}^1L_b$  and  ${}^1L_a$  bands being of  $-49^\circ$  and  $-56^\circ$ , respectively [37]. This seems to be in accordance with the two induced CD bands also of the same sign. As a plausible structure for the complex, the apolar benzene ring may be assumed to be absorbed by the apolar cavity of the cyclodextrin with the two polar functional groups sticking out of it and forming hydrogen bonds with the neighbouring water molecules. In a complex like this, however, the electric moments of the two transitions would get in negative sector pairs (Fig. 14a), therefore, according to the sector rule, two negative CD bands would be expected in contrast to the experimental ones which are both positive. Approaching the problem from the side of the experimental CD spectrum, another structure can also be proposed for the complex which is compatible with the two positive CD maxima, as well as with the sector rule. In this structure both functional groups of anthranilic acid should be located in the cavity of the cyclodextrin (Fig. 14b). Although at first sight this structure seems to be fairly improbable, there are several experimental facts likely to support it.

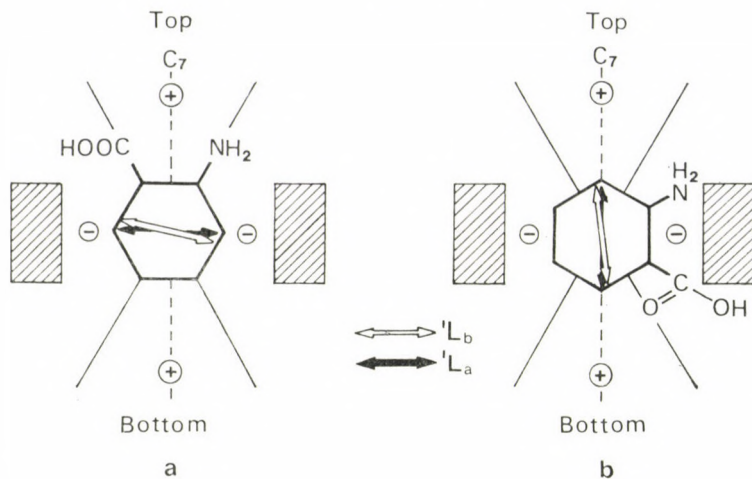


Fig. 14. The sector diagram as applied to the inclusion complex of anthranilic acid with both its functional groups being either outside (a) or inside (b) the cyclodextrin cavity

(a) While aniline does not form a complex with  $\beta$ -cyclodextrin at pH 2, anthranilic acid does. From this fact it can be concluded that it is the undissociated carboxyl group which is mainly responsible for anchoring the latter molecule in the cyclodextrin, therefore, it must be in the inside of the cavity. Under such circumstances, the amino group, being in *ortho* position to the carboxyl, can easily get into the inside of the complex, too.

(b) The thermodynamic parameters of the complex equilibrium between  $\beta$ -cyclodextrin and the *ortho* and *para* isomers of hydroxy- and aminobenzoic acids show a remarkable trend. The values of  $\Delta G$ ,  $\Delta H$  and  $\Delta S$  determined by us [39] can be found in Table V.

It can be seen that, whereas the  $\Delta G$  values belonging to the different benzoic acid derivatives do not differ too much, there is a significant difference

Table V

Thermodynamic parameters of the complex formation of 2- and 4-substituted benzoic acids with  $\beta$ -cyclodextrin in water

Guest molecule	$\Delta G$ (20 °C) kJ mol <sup>-1</sup>	$\Delta H$ kJ mol <sup>-1</sup>	$\Delta S$ J mol <sup>-1</sup> deg <sup>-1</sup>
2-Hydroxybenzoic acid	-12.6	-33.5	-72.0
2-Aminobenzoic acid	-15.6	-35.6	-68.3
4-Hydroxybenzoic acid	-14.7	-20.0	-21.1
4-Aminobenzoic acid	-16.9	-19.9	-10.1

in the enthalpy and entropy changes connected with the complex formation of the two *ortho* isomers on the one hand, and the two *para* isomers, on the other. Both  $\Delta H$  and  $\Delta S$  related to the formation of a cyclodextrin complex in water solution have been attributed, in the first place, to changes in the hydrogen bonds of the system [9, 40]. The greater negative values of  $\Delta H$  and  $\Delta S$  connected with the complex forming equilibrium of the *ortho* substituted benzoic acid derivatives as compared to those of their *para* isomers, seem to indicate that the formation of the cyclodextrin complex from the former compounds is followed by a greater change in the solvational state of the guest and results in a more rigid structure of the complex than in the case of the *para* isomers. This reasoning is compatible with the assumption that in the complexes of *ortho* substituted benzoic acids the guest molecule is accommodated with both its functional groups embedded in the cyclodextrin cavity, while in those of the *para* isomers the carboxyl and the hydroxyl or amino groups protrude out of the host molecule with partial retention of their original hydrational state.

Another possible solution of the discrepancy between the signs of the CD bands and the more plausible structure of the anthranilic acid complex can be achieved by supposing that the guest molecule is in dissociated state in which the polarizations of the transitions responsible for the signs of the induced CD bands are different from those calculated for the undissociated molecules. As a matter of fact, without X-ray data on the structure or, at least, a detailed study on the pH dependence of the formation and the stability of the anthranilic acid complex, the problem of the validity of the sector rule for this special case cannot be settled.

### *Complexes of 1-naphthol and 2-naphthol*

The CD study on the cyclodextrin complexes of the two naphthol isomers has been included in this article to show that the sector rule can also be applied for estimating the polarizations of the transitions in aromatic molecules. In the case of the naphthols, the directions of the electric moments belonging to the different electronic transitions have been determined experimentally [41] as well as calculated theoretically [17]. Figure 15 shows the results of the calculations by SUZUKI *et al.* [17] which are in good agreement with those of experimental studies. (For the sake of clarity the numerical values of the polarization angles are also indicated; with respect to them, *cf.* p. 40.)

By comparing the CD spectra shown in Fig. 2 with the data on the polarizations of the individual bands, a full agreement between the experimental data and the predictions of the sector rule can be established if we assume that the naphthol molecules accommodate in the cavity of the host with their long axes parallel to the symmetry axis of the  $\beta$ -cyclodextrin. The same arrange-

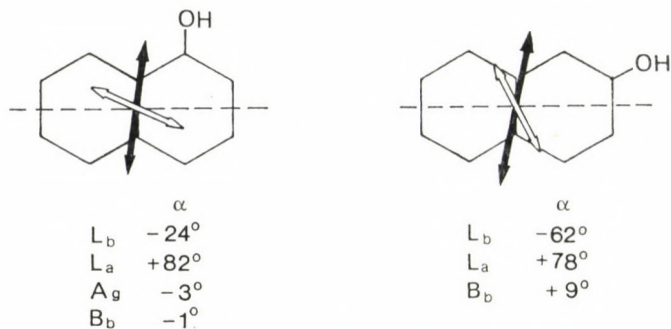


Fig. 15. Directions of polarization of the  $^1L_b$  and  $^1L_a$  bands in 1-naphthol (a) and 2-naphthol (b) as calculated by SUZUKI *et al.* [17]. (Below the figures the values of polarization angles of all the transitions are also indicated)

ment of the naphthalene ring has been deduced from the calculations of HARATA and UEDAIRA [7], as well as from the negative sign of the band assigned to the  $^1L_a$  transition found by us in the CD spectrum of the cyclodextrin complex of naphthalene (see above).

The most remarkable feature of the CD spectra of the naphthol complexes is the nice separation of the  $^1L_b$  and  $^1L_a$  bands of 1-naphthol, though the corresponding bands in the UV spectrum are strongly overlapping. The separation of overlapping bands of different signs is often mentioned as an important advantage of the CD spectra over the UV spectra in the assignment of the electronic transitions [42]. The possibility of recording the CD spectra of *achiral* aromatic compounds in the form of their cyclodextrin complexes offers a good opportunity for extending this method of spectral analysis.

In many cases, especially when dealing with molecules of larger size, the most probable arrangement of guest and host can be predicted on the basis of simple geometric considerations. In those cases when the structure of the complex is known, the approximate directions of polarization of the different transitions in the guest molecule can be estimated by applying the sector rule.

It is worth mentioning that, in addition to the sign pattern of the CD spectra, the magnitudes of the  $g$  values belonging to the different induced bands are in good agreement with the predictions of the sector rule.

#### $\beta$ -Cyclodextrin complex of 2-methyl-1,4-naphthoquinone

The last substrate we investigated for correlating the chiroptical properties with the relative geometry of guest and host in inclusion complexes was the  $\beta$ -cyclodextrin complex of vitamin  $K_3$  (2-methyl-1,4-naphthoquinone). The assignment of the bands in the UV spectrum to transitions of different polarization was achieved by both theoretical calculations [21–23] and

experimental analysis of the spectra of substituted naphthoquinone derivatives [20]. Though there are some inconsistencies between the results of the different theoretical works [21–23], it can be accepted with good reason that the polarizations of the subsequent bands in the spectrum are mutually perpendicular to each other [20], as shown in Table IV. This feature of the transitions is reflected in the alternating signs of the induced bands in the CD spectrum of the cyclodextrin complex of vitamin K<sub>3</sub>. Leaving now the very weak band assigned to the  $n \rightarrow \pi^*$  transitions of the carbonyl groups out of consideration, it can be stated that the positive signs of the first and the third CD bands assigned to the  $^1L_b$  and  $^1B$  transitions, respectively, of the naphthalene chromophore and both of them polarized parallel to the long axis of the molecule, as well as the negative sign of the second band assigned to the perpendicularly polarized  $^1L_a$  transitions, are in agreement with the predictions of the sector rule. The bands assigned to the  $^1L_a$  and  $^1B$  transitions are strongly overlapping in the UV spectrum, whereas the two corresponding CD maxima, being of opposite sign, are well separated indicating the individuality of these bands. The values of the anisotropy of the different bands fit well to those given by the sector rule. It is only the lowest wavelength band the  $g$  value of which is too small in comparison to the formerly discussed examples. This can probably be attributed to the complex nature of this band composed of several components with different polarizations [21–23].

The structure of the vitamin K<sub>3</sub> complex with the long axis of the guest molecule lying parallel to the cyclodextrin symmetry axis can be regarded as the most plausible one on the basis of simple geometric considerations. The same structure can be deduced from the sector rule in the knowledge of the polarizations of the different bands of the guest molecule. Had the latter not been known already, they could have been established by the present CD study of the cyclodextrin complex. These results can, therefore, be regarded as an example for the applicability of the sector rule in the spectroscopic analysis of aromatic compounds.

#### REFERENCES

- [1] SENSSE, K., CRAMER, F.: Chem. Ber., **102**, 509 (1968)
- [2] TAKEO, K., KUGE, T.: Stärke, **24**, 281 (1972)
- [3] TAKENAKA, S., MATSUURA, N., TOKURA, N.: Tetrahedron Lett., **1974**, 2325
- [4] IKEDA, K., UEKAMA, K., OTAGIRI, M., HATANO, M.: J. Pharm. Sci., **63**, 1168 (1974)
- [5] IKEDA, K., UEKAMA, K., OTAGIRI, M.: Chem. Pharm. Bull., **23**, 201 (1975)
- [6] BERGERON, R. J., MCPHIE, P.: Bioorg. Chem., **6**, 465 (1977)
- [7] HARATA, K., UEDAIRA, H.: Bull. Chem. Soc. Japan, **48**, 375 (1975)
- [8] SHIMIZU, H., KAITO, A., HATANO, M.: Bull. Chem. Soc. Japan, **52**, 2678 (1979)
- [9] HARATA, K.: Bull. Chem. Soc. Japan, **52**, 1807 (1979)
- [10] TINOCO, I. Jr.: Adv. Chem. Phys., **4**, 113 (1962)
- [11] KIRKWOOD, J. P.: J. Chem. Phys., **5**, 479 (1937)
- [12] SZEJTLI, J., DÓSA, É., LIPTÁK, A., NÁNÁSI, P., JODÁL, I., JÁNOSY, L.: Hung. Patent Appl. 1140/80
- [13] SZEJTLI, J., ZSADON, B., FENYVESI, É., SZILAS, M., TÜDŐS, F.: Hung. Patent Appl.

- [14] KAMLET, M. J. (Ed.): *Organic Electronic Spectral Data*, Vol. I, 1946—1952. Interscience, New York, 1960
- [15] ROE, E. M. F. (Ed.): *DMS UV Atlas of Organic Compounds*, Vol. III. Verlag Chemie, Weinheim, 1966
- [16] PLATT, J. R.: *J. Chem. Phys.*, **17**, 484 (1949); **19**, 263 (1951)
- [17] SUZUKI, S., FUJII, T., BABA, H.: *J. Mol. Spectrosc.*, **47**, 243 (1973)
- [18] FRÖMMING, K. H., SANDMANN, R.: *Archiv. Pharmazie*, **303**, 371 (1970)
- [19] SZEJTLI, J., BOLLA, É., KAJTÁR, M., SZABÓ, P., FERENCZY, T.: To be published
- [20] HILL, R. R., MITCHELL, G. H.: *J. Chem. Soc. (B)*, **1969**, 61
- [21] LEIBOVICI, C., DESCHAMP, J.: *Theor. Chim. Acta*, **4**, 321 (1966)
- [22] EDWARDS, T. G.: *Theor. Chim. Acta*, **30**, 267 (1973)
- [23] NOVÁK, A., TITZ, M., NEPRAŠ, M.: *Collection Czechoslov. Chem. Commun.*, **39**, 1532 (1974)
- [24] SNATZKE, G.: *Angew. Chem. Int. Ed.*, **18**, 363 (1979)
- [25] JAFFE, H. H., ORCHIN, M.: *Theory and Applications of Ultraviolet Spectroscopy*. Wiley, New York, 1962
- [26] SCHELLMAN, J. A.: *Acc. Chem. Res.*, **1**, 144 (1968)
- [27] KUHN, W. in FREUDENBERG, K. (Ed.): *Stereochemie*. p. 317. Deuticke, Leipzig, 1933
- [28] URRY, D. W. (Ed.): *Spectroscopic Approaches to Biomolecular Conformation*. p. 65. American Medical Association, Chicago, 1970
- [29] KUHN, W.: *Trans. Faraday Soc.*, **46**, 293 (1930)
- [30] PETRUSKA, J.: *J. Chem. Phys.*, **34**, 1120 (1961)
- [31] STEVENSON, P. E.: *J. Chem. Educ.*, **41**, 234 (1964)
- [32] HARATA, K.: *Bull. Chem. Soc. Japan*, **48**, 2409 (1975)
- [33] HARATA, K.: *Carbohydr. Res.*, **48**, 265 (1976)
- [34] HARATA, K.: *Bull. Chem. Soc. Japan*, **50**, 1416 (1977)
- [35] HARATA, K., UEDAIRA, H., TANAKA, J.: *Bull. Chem. Soc. Japan*, **51**, 1627 (1978)
- [36] HARATA, K.: *Bull. Chem. Soc. Japan*, **53**, 2782 (1980)
- [37] KISS, Á. I., SZŐKE, J.: Unpublished results
- [38] KISS, Á. I., SZŐKE, J.: *Acta Chim. (Budapest)*, **90**, 133 (1976)
- [39] To be published later
- [40] PIEROTTI, R. A.: *J. Phys. Chem.*, **69**, 281 (1965)
- [41] GANGAKHEDKAR, N. S., NAMJOSHI, A. V., TAMHANE, P. S., CHAUDHURI, N. K.: *J. Chem. Phys.*, **60**, 2584 (1974)
- [42] ROSENFELD, J. S., MOSCOWITZ, A. in CIARDELLI, F., SALVADORI, P. (Eds.): *Fundamental Aspects and Recent Developments in Optical Rotatory Dispersion and Circular Dichroism*. p. 41. Heyden, London, 1973

Márton KAJTÁR

Csilla HORVÁTH-TORÓ

Éva KUTHI

} H-1088 Budapest, Múzeum krt. 4/B

József SZEJTLI

H-1026 Budapest, Endrődi S. u. 38—40.

## INDEX

### PHYSICAL AND INORGANIC CHEMISTRY

Multiple Steady States and Hysteresis During Stirred Flow Oxidation of Cerous Ion by Bromate. Experiments and Models, K. BAR-ELI, E. GEISELER.....	239
BrO <sub>2</sub> as an Intermediate in the Belousov-Zhabotinsky Reaction H. D. FÖRSTERLING, H. J. LAMBERZ, H. SCHREIBER, W. ZITTLAU.....	251
On the Applicability of the Lotka-Volterra Scheme for Different Types of the Belousov-Zhabotinskii Reaction, Z. NOSZTICZIUS, A. FELLER .....	261
Study of Pseudo-Waves in Periodic Reactions, Gy. PÓTA, Gy. BAZSA, M. T. BECK.....	277
Self-Oscillating Chemical Reactions. Mechanism of Oscillating Oxidations with Bromate, A. M. ZHABOTINSKII .....	183
Perturbation of Bromate Oscillators, I. Perturbation by $\gamma$ Irradiation, E. KÖRÖS, G. PUTIRSKAYA, M. VARGA .....	295
Oscillatory Reactions: Model Construction and Possibilities of Realization, B. TURCSÁNYI	305
On the Preoscillatory Period of the Belousov-Zhabotinsky Reaction. A Search for Intermediates, M. BURGER, K. RÁCZ.....	315

### ORGANIC CHEMISTRY

A Simple Rule for Predicting Circular Dichroism Induced in Aromatic Guests by Cyclodextrin Hosts in Inclusion Complexes, M. KAJTÁR, Cs. HORVÁTH-TORÓ, É. KUTHI, J. SZEJTLI.....	327
---	-----

PRINTED IN HUNGARY  
Akadémiai Nyomda, Budapest

Les Acta Chimica paraissent en français, allemand, anglais et russe et publient de mémoires du domaine des sciences chimiques.

Les Acta Chimica sont publiés sous forme de fascicules. Quatre fascicules seront réunis en un volume (3 volumes par an).

On est prié d'envoyer les manuscrits destinés à la rédaction à l'adresse suivante:

*Acta Chimica*  
Budapest, P.O. Box 67, H-1450, Hongrie

Toute correspondance doit être envoyée à cette même adresse.

La rédaction ne rend pas de manuscrit.

Abonnement en Hongrie à l'Akadémiái Kiadó (1363 Budapest, P.O.B. 24, C. C. B. 215 11488), à l'étranger à l'Entreprise du Commerce Extérieur «Kultura» (H-1389 Budapest 62, P.O.B. 149 Compte-courant No. 218 10990) ou chez représentants à l'étranger.

---

Die Acta Chimica veröffentlichen Abhandlungen aus dem Bereich der chemischen Wissenschaften in deutscher, englischer, französischer und russischer Sprache.

Die Acta Chimica erscheinen in Heften wechselnden Umfanges. Vier Hefte bilden einen Band. Jährlich erscheinen 3 Bände.

Die zur Veröffentlichung bestimmten Manuskripte sind an folgende Adresse zu senden

*Acta Chimica*  
Budapest, Postfach 67, H-1450, Ungarn

An die gleiche Anschrift ist jede für die Redaktion bestimmte Korrespondenz zu richten. Manuskripte werden nicht zurückerstattet.

Bestellbar für das Inland bei Akadémiái Kiadó (1363 Budapest, Postfach 24, Bankkonto Nr. 215 11488), für das Ausland bei »Kultura« Außenhandelsunternehmen (H-1389 Budapest 62, P.O.B. 149. Bankkonto Nr. 218 10990) oder seinen Auslandsvertretungen.

---

«Acta Chimica» издают стили по химии на русском, английском, французском и немецком языках.

«Acta Chimica» выходит отдельными выпусками разного объема, 4 выпуска составляют один том и за год выходят 3 тома.

Предназначенные для публикации рукописи следует направлять по адресу:

*Acta Chimica*  
Budapest, P.O. Box 67, H-1450, ВНР

Всякую корреспонденцию в редакцию направляйте по этому же адресу.

Редакция рукописе не возвращает.

Отечественные подписчики направляйте свои заявки по адресу Издательств Академии Наук (1363 Budapest, P.O.B. 24. Текущий счет 215 11 488), а иностранные одписчики через организацию по внешней торговле «Kultura» (H-1389 Budapest 62, P.O.B. 149. Текущий счет 218 10990) или через ее заграничные представительства и уполномоченных.

Periodicals of the Hungarian Academy of Sciences are obtainable  
at the following addresses:

**AUSTRALIA**

C.B.D. LIBRARY AND SUBSCRIPTION SERVICE  
Box 4886, G.P.O., Sydney N.S.W. 2001  
COSMOS BOOKSHOP, 145 Ackland Street  
St. Kilda (Melbourne), Victoria 3182

**AUSTRIA**

GLOBUS, Höchstädtplatz 3, 1206 Wien XX

**BELGIUM**

OFFICE INTERNATIONAL DE LIBRAIRIE  
30 Avenue Marnix, 1050 Bruxelles  
LIBRAIRIE DU MONDE ENTIER  
162 rue du Midi, 1000 Bruxelles

**BULGARIA**

HEMUS, Bulvar Ruszki 6, Sofia

**CANADA**

PANNONIA BOOKS, P.O. Box 1017  
Postal Station "B", Toronto, Ontario M5T 2T8

**CHINA**

CNPICOR, Periodical Department, P.O. Box 50  
Peking

**CZECHOSLOVAKIA**

MAD'ARSKÁ KULTURA, Národní třída 22  
115 66 Praha

PNS DOVOZ TISKU, Vinohradská 46, Praha 2

PNS DOVOZ TLAČE, Bratislava 2

**DENMARK**

EJNAR MUNKSGAARD, Norregade 6  
1165 Copenhagen K

FEDERAL REPUBLIC OF GERMANY  
KUNST UND WISSEN ERICH BIEBER  
Postfach 46, 7000 Stuttgart 1

**FINLAND**

AKATEEMINEN KIRJAKAUPPA, P.O. Box 128  
SF-00101 Helsinki 10

**FRANCE**

DAWSON-FRANCE S. A., B. P. 40, 91121 Palaiseau  
EUROPÉRIODIQUES S. A., 31 Avenue de Ver-  
sailles, 78170 La Celle St. Cloud  
OFFICE INTERNATIONAL DE DOCUMENTA-  
TION ET LIBRAIRIE, 48 rue Gay-Lussac  
75240 Paris Cedex 05

GERMAN DEMOCRATIC REPUBLIC  
HAUS DER UNGARISCHEN KULTUR

Karl Liebknecht-Straße 9, DDR-102 Berlin  
DEUTSCHE POST ZEITUNGSVERTRIEBSAMT  
Straße der Pariser Kommüne 3-4, DDR-104 Berlin

**GREAT BRITAIN**

BLACKWELL'S PERIODICALS DIVISION

Hythe Bridge Street, Oxford OX1 2ET  
BUMPUS, HALDANE AND MAXWELL LTD.  
Cowper Works, Olney, Bucks MK46 4BN

COLLET'S HOLDINGS LTD., Denington Estate  
Wellingborough, Northants NN8 2QT

WM. DAWSON AND SONS LTD., Cannon House  
Folkstone, Kent CT19 5EE

H. K. LEWIS AND CO., 136 Gower Street  
London WC1E 6BS

**GREECE**

KOSTARAKIS BROTHERS INTERNATIONAL  
BOOKSELLERS, 2 Hippokratous Street, Athens-143

**HOLLAND**

MEULENHOF-BRUNA B.V., Beulingstraat 2,  
Amsterdam

MARTINUS NIJHOFF B.V.  
Lange Voorhout 9-11, Den Haag

**SWETS SUBSCRIPTION SERVICE**

347b Heereweg, Lisse

**INDIA**

ALLIED PUBLISHING PRIVATE LTD., 13/14  
Asaf Ali Road, New Delhi 110001

150 B-6 Mount Road, Madras 600002

INTERNATIONAL BOOK HOUSE PVT. LTD.  
Madame Cama Road, Bombay 400039

THE STATE TRADING CORPORATION OF  
INDIA LTD., Books Import Division, Chandralok  
36 Janpath, New Delhi 110001

**ITALY**

INTERSCIENTIA, Via Mazzè 28, 10149 Torino

LIBRERIA COMMISSIONARIA SANSONI, Via  
Lamarmora 45, 50121 Firenze

SANTO VANASIA, Via M. Macchi 58  
20124 Milano

D. E. A., Via Lima 28, 00198 Roma

**JAPAN**

KINOKUNIYA BOOK-STORE CO. LTD.

17-7 Shinjuku 3 chome, Shinjuku-ku, Tokyo 160-91

MARUZEN COMPANY LTD., Book Department,

P.O. Box 5050 Tokyo International, Tokyo 100-31

NAUKA LTD. IMPORT DEPARTMENT

2-30-19 Minami Ikebukuro, Toshima-ku, Tokyo 171

**KOREA**

CHULPANMUL, Phenjan

**NORWAY**

TANUM-TIDSKRIFT-SENTRALEN A.S., Karl  
Johansgatan 41-43, 1000 Oslo

**POLAND**

WEGIERSKI INSTYTUT KULTURY, Marszał-  
kowska 80, 00-517 Warszawa

CKP I W, ul. Towarowa 28, 00-958 Warszawa

**ROUMANIA**

D. E. P., București

ILEXIM, Calea Grivitei 64-66, București

**SOVIET UNION**

SOJUZPECHAT - IMPORT, Moscow

and the post offices in each town

MEZHDUNARODNAYA KNIGA, Moscow G-200

**SPAIN**

DIAZ DE SANTOS, Lagasca 95, Madrid 6

**SWEDEN**

ALMQVIST AND WIKSELL, Gamla Brogatan 26  
101 20 Stockholm

GUMPERS UNIVERSITETSBOKHANDEL AB  
Box 346, 401 25 Göteborg 1

**SWITZERLAND**

KARGER LIBRI AG, Petersgraben 31, 4011 Basel

**USA**

EBSCO SUBSCRIPTION SERVICES

P.O. Box 1943, Birmingham, Alabama 35201

F. W. FAXON COMPANY, INC.

15 Southwest Park, Westwood Mass. 02090

THE MOORE-COTTRELL SUBSCRIPTION

AGENCIES, North Cohocton, N. Y. 14868

READ-MORE PUBLICATIONS, INC.

140 Cedar Street, New York, N. Y. 10006

STECHELT-MACMILLAN, INC.

7250 Westfield Avenue, Pennsauken N. J. 08110

**YUGOSLAVIA**

JUGOSLOVENSKA KNJIGA, Terazije 27, Beograd

FORUM, Vojvode Mišića 1, 21000 Novi Sad

# ACTA CHIMICA

ACADEMIAE SCIENTIARUM  
HUNGARICAE

ADIUVANTIBUS

M. T. BECK, R. BOGNÁR, GY. HARDY,  
K. LEMPÉRT, B. LÉNGYEL, K. POLINSZKY,  
E. PUNGOR, G. SCHAY,  
Z. G. SZABÓ, P. TÉTÉNYI

REDIGUNT

F. MÁRTA et GY. DEÁK

TOMUS 110

FASCICULUS 4



AKADÉMIAI KIADÓ, BUDAPEST

1982

ACTA CHIM. ACAD SCI. HUNG.

ACASA2 110 (4) 357-484 (1982)

# ACTA CHIMICA

A MAGYAR TUDOMÁNYOS AKADÉMIA  
KÉMIAI TUDOMÁNYOK OSZTÁLYÁNAK  
IDEGEN NYELVŰ KÖZLEMÉNYEI

FŐSZERKESZTŐ

MÁRTA FERENC

SZERKESZTŐ

DEÁK GYULA

TECHNIKAI SZERKESZTŐ

HAZAI LÁSZLÓ

SZERKESZTŐ BIZOTTSÁG

BECK T. MIHÁLY, BOGNÁR REZSŐ, HARDY GYULA,  
LEMPERT KÁROLY, LENGYEL BÉLA, POLINSZKY KÁROLY,  
PUNGOR ERNŐ, SCHAY GÉZA, SZABÓ ZOLTÁN,  
TÉTÉNYI PÁL

Acta Chimica is a journal for the publication of papers on all aspects of chemistry in English, German, French and Russian.

Acta Chimica is published in 3 volumes per year. Each volume consists of 4 issues of varying size.

Manuscripts should be sent to

*Acta Chimica*  
Budapest, P.O. Box 67, H-1450, Hungary

Correspondence with the editors should be sent to the same address. Manuscripts are not returned to the authors.

Hungarian subscribers should order from Akadémiai Kiadó, 1363 Budapest, P.O.B. 24. Account No. 215 11488.

Orders from other countries are to be sent to "Kultura" Foreign Trading Company (H-1389 Budapest 62, P.O.B. 149. Account No. 218 10990) or its representatives abroad.



## LIQUID CRYSTALS, IV\*

### CORRELATION BETWEEN THE THERMAL STABILITY AND MOLECULAR STRUCTURE IN CHOLESTERYL 2-ETHOXYETHYL-CARBONATE AND ITS SULFUR CONTAINING ANALOGUES

P. M. AGÓCS<sup>1\*\*</sup>, G. MOTIKA<sup>1</sup> and P. ZSÉDENYI<sup>2</sup>

(<sup>1</sup> *Institute of Organic Chemistry, József Attila University, Szeged,*  
and <sup>2</sup> *Jókai Mór Economical High-School, Pápa*)

Received March 9, 1981

In revised form July 1, 1981

Accepted for publication August 28, 1981

The change in thermal stability was investigated when the oxygen in cholesteryl 2-ethoxyethyl-carbonate was replaced by sulfur. Four compounds were prepared and their phase transitions were measured with the aid of differential scanning calorimetry and a polarizing microscope equipped with a hot stage.

One of the most important properties of liquid crystals is their thermal stability\*\*\* [1]; its knowledge is important, because the upper limit of applications may be governed by it. Many authors have investigated in detail the occurrence of mesomorphic properties and the thermal stability of compounds as functions of the position, number and length of the side chains in the case of numerous different homologous series [2].

From the investigations of LEDER [3] and ELSER *et al.* [4] it appeared that 3 $\beta$ -mercapto-cholest-5-ene and cholesteryl chlorothiocarbonate, in contrast with cholesterol and cholesteryl chloroformate, are mesomorphic materials. 3 $\beta$ -Mercapto-cholest-5-ene benzoate, synthesized by BERNSTEIN and SAX [5], also formed a cholesteric mesophase, and both the crystalline-cholesteric and cholesteric-isotropic transitions ensued at higher temperatures, than in the case of cholesteryl benzoate [6]. The syntheses and investigations of homologous series of cholesteryl-*n*-alkanoates [7] and thiocholesteryl-*n*-alkanoates [7] and thiocholesteryl-*n*-alkanoates [8]; cholesteryl- $\omega$ -phenylalkanoates [9] and thiocholesteryl- $\omega$ -phenylalkanoates [10]; cholesteryl-*n*-alkylcarbonates [11], cholesteryl-*S-n*-alkylthiocarbonates [12] and *S*-cholesteryl-*n*-alkylthiocarbonates [13], as well as 5 $\alpha$ -cholestan-3 $\beta$ -yl-*n*-alkylcarbonates and 5 $\alpha$ -cholestan-3 $\beta$ -yl-*S-n*-alkylcarbonates [14] presented the possibility of assessing the influence of changing the oxygen atoms next to the cholesterol skeleton for sulfur atoms.

\* Part III: *Acta Phys. et Chem. Szeged*, XXVI, 71 (1980)

\*\* To whom correspondence should be addressed

\*\*\* The thermal stability is the thermal value (temperature) at which the liquid crystalline properties are lost and the substance is transformed into the isotropic liquid state

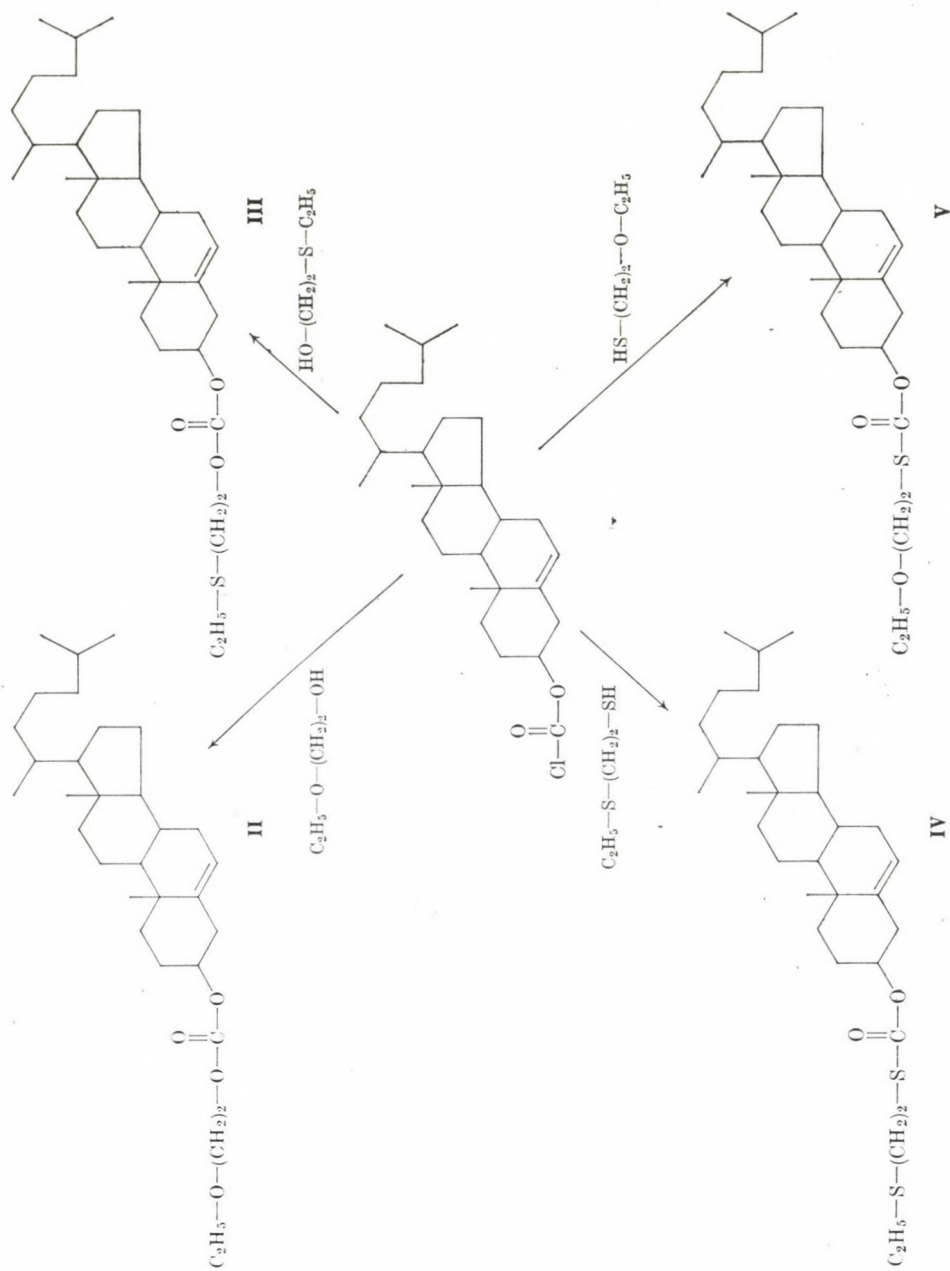


Fig. 1. The synthesis route

According to the reviews by ELSER [14] and ENNULAT [15, 16], the substitution of oxygen by sulfur next to the carbonyl group increases both the cholesteric-isotropic and the smectic-cholesteric transition temperatures of the thioesters and thiocarbonates. This finding is in accordance with the data measured by BERNSTEIN and SAX [5]: replacement by sulfur atom increases the thermal stability. In addition to this, the presence of the sulfur atom accentuates the odd-even effect.

Our purpose was to synthesize cholesterol derivatives containing ether and carbonate structural units and to substitute the oxygen atoms by sulfur atoms. By the changing of the atoms, we wished to observe what influence is exerted on the liquid crystalline properties by the incorporation of sulfur atoms in place of the oxygen atoms at different distances from the steran skeleton.

The starting material of the synthesis was cholesteryl chloroformate (I), which was prepared from cholesterol and phosgene in dry benzene [17]. This compound (I) was allowed to react with the corresponding hydroxy-[18] or thiol derivatives [19, 20] to give the required compounds (II, III, IV, V). The synthesis route is shown in Fig. 1.

The processes were effected in dry benzene, and pyridine was used as acid acceptor. The reactions were followed by thin-layer chromatography and the products obtained in the usual manner were purified by column chromatography and thereafter crystallized. The analytical data of the compounds prepared are shown in Table I.

Table I

Analytical data for the compounds II, III, IV and V

No.	Compound	Mol. formula	Mol. weight	M, p., K	Analysis, %	
					Found	Calculated
II	Cholesteryl 2-ethoxy-ethyl-carbonate	C <sub>32</sub> H <sub>54</sub> O <sub>4</sub>	502.75	343.5	C = 76.16 H = 10.68	C = 76.44 H = 10.82
III	Cholesteryl 2-ethyl-thioethyl-carbonate	C <sub>32</sub> H <sub>54</sub> O <sub>3</sub> S	518.81	381.5	C = 73.92 H = 10.51	C = 74.07 H = 10.49
IV	Cholesteryl 2-ethylthio-ethyl-S-thiocarbonate	C <sub>32</sub> H <sub>54</sub> O <sub>2</sub> S <sub>2</sub>	534.88	365.5	C = 71.60 H = 10.12	C = 71.85 H = 10.17
V	Cholesteryl 2-ethoxy-ethyl-S-thiocarbonate	C <sub>32</sub> H <sub>54</sub> O <sub>3</sub> S	518.81	338.5	C = 74.22 H = 10.34	C = 74.07 H = 10.49

## Results and Discussion

On the basis of the thermograms and the optical observations, the phase transition schemes can be given as shown in Fig. 2.

The abbreviations are as follows:

*I* = isotropic liquid

Ch = cholesteric mesophase

C, C<sub>I</sub>, C<sub>II</sub> = crystalline modifications.

The heating direction is indicated by a continuous line, the cooling direction by a dashed line, and the transitions during thermostating by a dotted line.

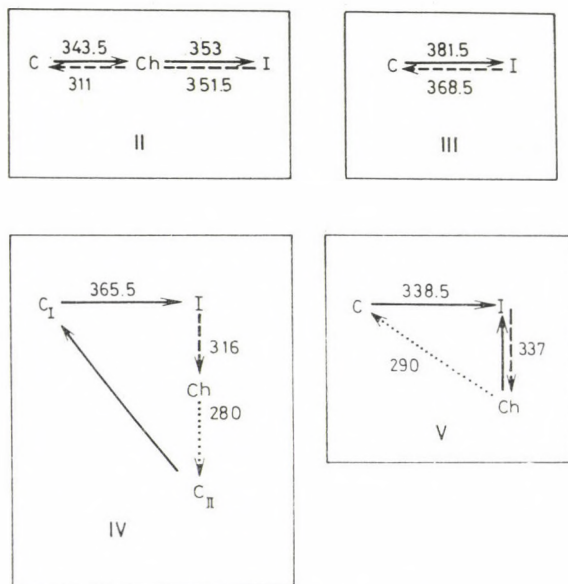


Fig. 2. The phase transition schemes

### Cholesteryl 2-ethoxyethyl-carbonate (II)

The compound displays an enantiotropic cholesteric mesophase.

### Cholesteryl 2-ethylthioethyl-carbonate (III)

On the basis of the thermograms, the compound does not form a liquid crystalline phase. During rapid cooling (quenching) to below 368.5 K, however, an unstable cholesteric mesophase is observable optically, which did not appear in the calorimeter.

### Cholesteryl 2-ethylthioethyl-S-thiocarbonate (IV)

The compound exhibited a monotropic cholesteric mesophase, which began to crystallize only during a longer thermostating period. Depending on the duration of the thermostating period and the temperature, several polymorphic transitions were observable between  $C_{II}$  and  $C_I$ .

### Cholesteryl 2-ethoxyethyl-S-thiocarbonate (V)

This compound shows a monotropic cholesteric mesophase. The crystalline state was reformed on cooling only after a 24 h thermostating period at 290 K.

From the results, we may conclude that the properties of the compounds are significantly altered when the ether oxygen atom is exchanged for sulfur (*cf.* the difference between compounds **II** and **III**). The melting point rises and only an unstable liquid crystalline phase is formed.

The exchange of the carbonate oxygen for sulfur resulted in a more moderate change (*cf.* the difference between compounds **II** and **V**). The melting point changes only insignificantly, and the mesophase formed is cholesteric in both cases.

The compounds containing sulfur atoms in the carbonate group (**IV** and **V**) are similar in that both form monotropic cholesteric mesophase. The exchange of the ether oxygen atom for sulfur results in a considerable rise of the melting point.

In summary, we may conclude that in the case of the compounds we have synthesized (with the exception of compound **V**) substitution by a sulfur atom increases the thermal stability. This is in accordance with previous observations [5, 14, 15, 16]. As regards the change in the properties of the compounds, replacement of oxygen by sulfur further from the steran skeleton has a greater influence.

## Experimental

The calorimetric measurements were made with a PERKIN-ELMER DSC-2 calorimeter in a highly purified nitrogen atmosphere. The temperature axis was calibrated with the melting point of indium standard and the melting point of bidistilled water. The weights of the samples lay in the range 3–5 mg. The temperatures of the phase transitions could be reproduced with an accuracy of  $\pm 1$  K.

For the determination of the textures of the mesophases, a PHMK (VEB Analytik, Dresden) apparatus and an AMPLIVAL POL-U (Carl Zeiss, Jena) polarizing microscope (equipped with a hot stage) were used.

All melting points were measured on a Boetius hot-stage apparatus.

TLC was carried out on silica gel plates (MERCK, DC-Fertigplatten, Kieselgel 60); development was performed with an acetone-benzene (1 : 30) mixture. Visualization was achieved by sparying with 50% phosphoric acid and heating.

Column chromatography was performed using silica gel (REANAL, Kieselgel 60, 0.063—0.2 mm) and a 1 : 2 mixture of benzene—petroleum ether.

The IR spectra were recorded in KBr pellets on a UNICAM SP 200 spectrometer, while the PMR spectra were obtained on a JEOL 60-HL spectrometer in  $\text{CDCl}_3$ , with TMS as internal standard.

### Cholesteryl 2-ethoxyethyl-carbonate (II) and its sulfur-containing derivatives (III, IV, V)

The hydroxy or thiol compound (0.01 mole) and 2 mL of pyridine were dissolved in 10 mL of dry benzene, and 0.01 mole cholesteryl chloroformate (I) in 15 mL dry benzene was added dropwise during 10—15 min, with stirring. Stirring was continued, and the reaction was followed by thin-layer chromatography. When the reaction was complete, the benzene solution was washed with cold dilute hydrochloric acid and water, and dried over anhydrous sodium sulfate. The benzene was evaporated and the crude product purified by column chromatography and finally crystallized from a mixture of benzene and ethyl alcohol.

\*

The authors are grateful to the Hungarian Technical Committee for considerable technical assistance of this research. Thanks are expressed to Mrs. Dr. BARTÓK-BOZÓKI and É. GÁCS-GERCELY for the combustion analyses, to Mr. A. GAJDACSI for technical assistance, to Dr. Gy. DOMBI for the PMR spectra, and to Dr. J. KISS for the IR spectra and helpful discussions.

### REFERENCES

- [1] GRAY, G. W., WINSOR, P. A.: *Liquid Crystals and Plastic Crystals*. Vol. I. pp. 103—152. Ellis Horwood Limited, Chichester 1974
- [2] KELKER, H., HATZ, R.: *Handbook of Liquid Crystals*. pp. 34—113. Verlag Chemie, Weinheim—Deerfield Beach, Florida—Basel 1980
- [3] LEDER, L. B.: *J. Chem. Phys.*, **55**, 2649 (1971)
- [4] ELSER, W., ENNULAT, R. D., POHLMANN, J. L. W.: *Mol. Cryst. Liq. Cryst.*, **27**, 375 (1974)
- [5] BERNSTEIN, S., SAX, K. J.: *J. Org. Chem.*, **16**, 679 (1961)
- [6] DEMUS, D., DEMUS, H., ZASCHKE, H.: "Flüssige Kristalle in Tabellen." p. 285. VEB Deutsche Verlag für Grundstoffindustrie, Leipzig 1974
- [7] GRAY, G. W.: *J. Chem., Soc.*, **1956**, 3733
- [8] ELSER, W., POHLMANN, J. L. W., BOYD, P. R.: *Mol. Cryst. Liq. Cryst.*, **11**, 279 (1970)
- [9] POHLMANN, J. L. W., ELSER, W., BOYD, P. R.: *Mol. Cryst. Liq. Cryst.*, **20**, 87 (1973)
- [10] ELSER, W., POHLMANN, J. L. W.: *Mol. Cryst. Liq. Cryst.*, **27**, 325 (1974)
- [11] ELSER, W., POHLMANN, J. L. W., BOYD, P. R.: *Mol. Cryst. Liq. Cryst.*, **20**, 77 (1973)
- [12] ELSER, W., ENNULAT, R. D.: *J. Phys. Chem.*, **74**, 1545 (1970)
- [13] ELSER, W., ENNULAT, R. D., POHLMANN, J. L. W.: *Mol. Cryst. Liq. Cryst.*, **27**, 375 (1974)
- [14] ELSER, W.: *Mol. Cryst. Liq. Cryst.*, **3**, 219 (1969)
- [15] ENNULAT, R. D.: *Mol. Cryst. Liq. Cryst.*, **3**, 274 (1969)
- [16] ENNULAT, R. D., BROWN, A. J.: *Mol. Cryst. Liq. Cryst.*, **12**, 367 (1971)
- [17] MCKAY, A. F., VAVASOUR, G. R.: *Can. J. Chem.*, **31**, 688 (1953)
- [18] MERCK Reagents for Organic Synthesis
- [19] SWALLEN, L. C., BOORD, C. E.: *J. Am. Chem. Soc.*, **52**, 651 (1930)
- [20] KABACHNIK, M. I., GODOVKOV, N. N., PAIKIN, D. M., SHABANOVA, M. P., EFIMOVA, L. F., GAMPER, N. M.: *Zh. Obshch. Khim.*, **29**, 2182 (1959)

Pál Mihály AGÓCS }  
Gábor MOTIKA } H-6720 Szeged, Dóm tér 8.

Piroska ZSÉDENYI H-8501 Pápa, Felszabadulás u 45.

## A NEW ROUTE FOR THE PREPARATION OF *N*-SUBSTITUTED *N*-DEMETHYLAPOCODEINE DERIVATIVES

S. BERÉNYI, S. HOSZTAFI, S. MAKLEIT\* and I. SZEIFERT  
(*Institute of Organic Chemistry, Kossuth Lajos University, Debrecen*)

Received May 13, 1981

Accepted for publication August 28, 1981

Transformation of 6-*O*-mesylneopine into 6-demethoxythebaine in a good yield is the first experimental proof for the assumed mechanism of the codein → apocodeine rearrangement. 6-Demethoxythebaine proved to be an important starting material for the preparation of *N*-alkyl-*N*-demethylapocodeine derivatives affording better yields than procedures used so far.

In the recent past our studies on neopine unequivocally proved that this morphine alkaloid can conveniently be transformed into important derivatives which are otherwise difficult of access.

Our investigations made possible to develop the first procedure for the industrial isolation of natural neopine from ripe poppy head [1] and, on the other hand, to work out a new route for its preparation starting from thebaine [2] which provides the highest yield in comparison with the known procedures.

In the course of our studies numerous new derivatives have been prepared by the nucleophilic substitution reactions of 6-*O*-mesylneopine (II) [3]. In the present paper, the synthesis in a good yield of 6-demethoxythebaine (3-methoxy-4,5 $\alpha$ -epoxy-6,7,8,14-tetrahydro-17-methylmorphinan) (III) is reported. Starting from this compound, *e.g.*, 14-hydroxyallopseudocodeine (1,2-addition) can be prepared in a very convenient way. Neopine is also an important starting material in the synthesis of B/C-*trans* morphine derivatives, since it has proved to be suitable for transformation into isoneopine by using a simple procedure providing a good yield and large-scale applicability [4].

The preparation of 6-demethoxythebaine in a high yield is noteworthy in two respects:

(a) 6-Demethoxythebaine is an intermediate in the assumed mechanism of the codeine → apocodeine rearrangement (on the analogy of the assumed mechanism [5] of the morphine → apomorphine transformation);

(b) if the mechanism is true, the rearrangement 6-demethoxythebaine → apocodeine (VIb) can also be realized. Besides the first experimental corroboration of the assumed mechanism, this provides a new possibility for the

\* To whom correspondence should be addressed



preparation of apocodeine and *N*-substituted *N*-demethylapocodeine derivatives (VI), detailed studies of which appear desirable.

On the basis of the literature data, the following combinations can be taken into account for the preparation of these compounds:

(1) codeine  $\xrightarrow{a}$  apocodeine  $\xrightarrow{b}$  *N*-demethylapocodeine  $\xrightarrow{c}$  *N*-alkyl-*N*-demethylapocodeine

(2) codeine  $\xrightarrow{a}$  *N*-demethylcodeine  $\xrightarrow{b}$  *N*-alkyl-*N*-demethylcodeine  $\xrightarrow{c}$  *N*-alkyl-*N*-demethylapocodeine

(3) codeine  $\xrightarrow{a}$  *N*-demethylcodeine  $\xrightarrow{b}$  *N*-demethylapocodeine  $\xrightarrow{c}$  *N*-alkyl-*N*-demethylapocodeine.

The following facts should be taken into consideration for the realization of the above combinations:

(1a) The yield of the codeine  $\rightarrow$  apocodeine transformation is very low: 12.8% with oxalic acid [6], 30% or 20% with phosphoric acid [7, 8], and 32% with methanesulfonic acid [9].

(1b) The apocodeine  $\rightarrow$  *N*-demethylapocodeine transformation is unknown, and the *N*-demethylation of aporphine alkaloids has not yet been satisfactorily solved. The use of cyanogen bromide [10, 11, 12], alkyl chloroformates [13, 14], azodicarboxylic acid diesters [15] and nitrous acid [12, 16] did not give the desired result. Though the *N*-demethylation of some aporphine alkaloids has been achieved *via* *N*-oxide, the yields are generally low [17]; the best yield was 34% in the case of the nuciferine  $\rightarrow$  *N*-demethylnuciferine conversion. According to KIM, J. C. [Org. Prep. Proc. Int., 9, 1 (1977)], apomorphine can be *N*-demethylated with methyl chloroformate in 87% yield. This result, however, has not been corroborated by our own studies. We also investigated the case of apocodeine using 2,2,2-trichloroethyl chloroformate, but the product obtained was not identical with *N*-demethylapocodeine (VIa).

(1c) No data are available in the literature concerning the *N*-alkylation of *N*-demethylaporphines, only the *N*-methylation has hitherto been published [18].

(2a) The codeine  $\rightarrow$  *N*-demethylcodeine transformation has been thoroughly studied and solved: the yields were 38% with cyanogen bromide [19], 16% with azodicarboxylic acid diester [19], 30% with nitrous acid [20], and in the case of chloroformates they were 71% ( $-\text{CH}_3$ ) [21], 43% [ $-\text{C}_2\text{H}_5$ ] [22], 65% ( $\text{Cl}_3\text{CCH}_2-$ ) [23], and 89% ( $\text{C}_6\text{H}_5-$ ) [24].

(2b) According to our own experiences, the *N*-alkylation of *N*-demethylmorphinan derivatives can generally be performed in 50% yield by means of the usual procedures. In this field our studies are in progress.

(2c) For the transformation of the *N*-alkyl-*N*-demethylcodeine derivatives into *N*-alkyl-*N*-demethylapocodeine derivatives only one example has hitherto been published in the literature: the conversion of the *N*-hydroxyethyl

derivative (**VIc**) in 42% yield [9]. We performed this reaction of the *N*-allyl derivative (**VIId**) in 30% yield.

(3a) see (2a).

(3b) The yields are very low: 6% with phosphoric acid [12], 13% with oxalic acid [12] and 23% with methanesulfonic acid [9].

(3c) see (1c).

According to our recent studies, 6-*O*-mesylneopine (**II**) obtained from neopine (**I**) in 90% yield can be transformed into 6-demethoxythebaine (**III**) in 93% yield by means of tetrabutylammonium fluoride (TBAF); **III** gave apocodeine (**VIb**) quantitatively on treatment with methanesulfonic acid, or in 84% yield calculated for neopine.

On the basis of our results concerning the *N*-demethylation of morphine alkaloids by using azodicarboxylic acid diethyl ester (ADDE) [25], we managed to transform 6-demethoxythebaine into *N*-demethyl-6-demethoxythebaine (**IV**) in 70% yield. Compound **IV** quantitatively gave *N*-demethylapocodeine (**VIa**) on treatment with methanesulfonic acid. *N*-Demethyl-6-demethoxythebaine (**IV**) afforded **Vd** (in 45%) on allylation and **Ve** (in 43%) on 2-hydroxyethylation, which compounds could be quantitatively rearranged into *N*-(2-hydroxyethyl)-*N*-demethylapocodeine (**VIId**) and *N*-allyl-*N*-demethylapocodeine (**VIc**), respectively. The yields calculated for neopine were 25.2% and 26.4%.

Of the possibilities (1, 2, 3) outlined earlier, the best one (codeine  $\xrightarrow{89\%}$  *N*-demethylcodeine  $\xrightarrow{34\%}$  *N*-(2-hydroxyethyl)-*N*-demethylcodeine  $\xrightarrow{42\%}$  *N*-(2-hydroxyethyl)-*N*-demethylapocodeine) provided 12.8% overall yield [9, 24].

## Experimental

M.p.'s were measured with a Koffler apparatus and are uncorrected. Thin-layer chromatography was performed on Merck 5554 silica gel 60 F<sub>254</sub> foils using benzene : methanol (8 : 2) or chloroform : acetone : diethylamine (5 : 4 : 1) developing mixtures. The detecting agent was Dragendorff reagent. Preparative thin-layer chromatography was performed on Merck 5717 silica gel 60 F<sub>254</sub> (20 × 20 cm, layer thickness 2 mm) and the detection was done in UV light. The <sup>1</sup>H-NMR spectra were obtained with a JEOL 100 MHz spectrometer.

### 6-*O*-Mesylneopine (**II**)

From neopine (**I**) according to [3].

### 6-Demethoxythebaine (**III**)

According to [3], but with the following modification.

Compound **II** (5.0 g; 13.25 mmoles) was dissolved in anhydrous acetonitrile (300 mL) and TBAF (15.0 g; 59 mmoles) was added; the mixture was then refluxed for 2.5 h. The solvent was evaporated and the oily residue extracted with ether (3 × 50 mL). The materials obtained after evaporation of the ether crystallized on standing to yield 3.45 g (93%) of the crystalline product.

<sup>1</sup>H-NMR (CCl<sub>3</sub>): δ (ppm) 2.42s (3H, N-CH<sub>3</sub>), 3.9s (3H, O-CH<sub>3</sub>), 5.4–6m (4H, 5 βH, 6H, 7H, 8H), 6.62dd (2H, Ar-H).

**N-Demethyl-6-demethoxythebaine (IV)**

A mixture of compound **III** (1.12 g; 4.0 mmoles) and ADDE (0.89 g; 5.1 mmoles) was refluxed in anhydrous benzene (15 mL) for 8 h. The solvent was evaporated, the residue dissolved in anhydrous ethanol (20 mL) and an aqueous solution 10 mL of ammonium chloride (3.5 g) was added. The mixture was allowed to stand at room temperature for 24 h, then the ethanol was evaporated to leave 0.8 g (70%) of the hydrochloride, m.p. 253–255 °C, after washing with anhydrous ethanol.

$[\alpha]_D^{20}$  –176° (0.5, water). The free base was an oil.

$C_{17}H_{17}NO_2 \cdot HCl$ . Calcd. N 4.6, C 67.2, H 5.97,  $Cl^-$  11.6. Found N 4.8, C 67.7, H 6.0,  $Cl^-$  11.4.

$^1H$ -NMR ( $CDCl_3$ ):  $\delta$  (ppm) 3.8s (3H, O–CH<sub>3</sub>), 5.4–6m (4H, 5  $\beta$ H, 6H, 7H, 8H) 6.6dd (2H, Ar–H).

**N-(2-Hydroxyethyl)-N-demethyl-6-demethoxythebaine (Vc)**

A mixture of compound **IV** (1.0 g; 3.74 mmoles) and 2-bromoethanol (0.53; 4.24 mmoles) was refluxed for 6 h in anhydrous ethanol (17 mL) in the presence of sodium hydrogen carbonate (0.53 g; 6.3 mmoles). The solid material was filtered off, the solvent evaporated and the residue dissolved in acetone. The inorganic salt was filtered off and the acetone evaporated to yield 1.0 g of an oily product; 500 mg of this material was purified by preparative TLC (developing mixture: benzene–methanol 1 : 1) to obtain a substance (250 mg; 43%) on elution with methanol, which then crystallized from *n*-hexane. M.p. 122–122.5 °C.

$[\alpha]_D^{20}$  –136° (0.5, chloroform).

$^1H$ -NMR ( $CDCl_3$ ):  $\delta$  (ppm) 2.8m (2H, CH<sub>2</sub>), 3.6m (2H, CH<sub>2</sub>), 3.8s (3H, O–CH<sub>3</sub>), 5.4–5.9m (4H, 5  $\beta$ H, 6H, 7H, 8H), 6.6dd (2H, Ar–H).

$C_{19}H_{21}NO_3$ . Calcd. N 4.5, C 73.26, H 6.79, Found C 4.2, C 72.8, H 6.65.

**N-allyl-N-demethyl-6-demethoxythebaine (Vd)**

A mixture of compound **IV** (0.9 g; 3.38 mmoles) and allyl bromide (0.49 g; 4.06 mmoles) was refluxed for 20 h in anhydrous ethanol (15 mL) in the presence of sodium hydrogencarbonate (0.43 g; 5.0 mmoles). The solid residue was filtered off, washed with ethanol, the solvent evaporated and the residue dissolved in ether. The insoluble material was filtered off and the solvent evaporated to obtain an oil, homogeneous in TLC, which gave the hydrochloride of **Vd** (520 mg; 43%) on treatment with hydrogenchloride in anhydrous ethanol. M.p. 207–211 °C (decomp.).

$[\alpha]_D^{20}$  –108° (0.25, water).

$^1H$ -NMR ( $CDCl_3$ ):  $\delta$  (ppm) 3.1–3.4m (2H, N–CH<sub>2</sub>–), 3.8s (3H, O–CH<sub>3</sub>), 5.0–5.9m (7H, olefinic protons), 6.6dd (2H, Ar–H).

$C_{20}H_{21}NO_2 \cdot HCl$ . Calcd. N 4.07, C 69.85, H 6.45,  $Cl^-$  10.3. Found N 3.75, C 69.1, H 6.5,  $Cl^-$  10.8.

**N-Demethylapocodeine (VIa)**

Compound **IV** (600 mg; 2.24 mmoles) was dissolved in methanesulfonic acid (3 mL) and heated at 95 °C for 45 min. After cooling, the mixture was poured into a stirred aqueous (50 mL) solution of potassium hydrogen carbonate (8.0 g), and stirred for further 1 h. The precipitated material was filtered off and dried under reduced pressure to afford 600 mg (100%) of a crystalline substance, which was homogeneous in TLC. Its hydrochloride formed with hydrogenchloride in anhydrous ethanol, decomposed between 270 and 280 °C (*lit.* [9] m.p. 277–280 °C).

$[\alpha]_D^{20}$  –48° (0.5, water).

$^1H$ -NMR (base,  $CDCl_3$ ):  $\delta$  (ppm) 3.8s (3H, O–CH<sub>3</sub>), 7.0–7.2m (4H, Ar–H), 8.2dd (1H, Ar–H).

**Apocodeine (VIb)**

Compound **III** (1.0 g; 3.35 mmoles) was dissolved in methanesulfonic acid (5 mL) and heated at 95 °C for 45 min. After cooling, the mixture was poured into an aqueous (75 mL) solution of potassium hydrogencarbonate (14.0 g) and worked up as described for compound

**Vla** to yield 1.0 g (100%) of the product. The m.p. of its hydrochloride, formed with hydrogen-chloride in anhydrous ethanol, was 246 °C (decomp.) (*lit.* [9] m.p. 257–260 °C).

The free base was crystallized from methanol, m.p. 121–124 °C (methanolic solvate) (*lit.* [9] m.p. 125–127 °C).

The <sup>1</sup>H-NMR data were identical with those published in Ref. [25] and with those of authentic apocodeine obtained from codeine with 85% phosphoric acid [8] or methanesulfonic acid [9].

#### N-allyl-N-demethylapocodeine (VI<sub>d</sub>)

Compound **Vd** (1.0 g; 3.25 mmoles) was allowed to react with methanesulfonic acid (5 mL) and worked up as described above to yield 1.0 g (100%) of **VI<sub>d</sub>**, m.p. 59–63 °C.

$[\alpha]_D^{20} -90.8^\circ$  (0.5, chloroform).

The m.p. of the hydrochloride was 216–220 °C.

$[\alpha]_D^{20} -157^\circ$  (0.27, water).

<sup>1</sup>H-NMR (base, CDCl<sub>3</sub>): δ (ppm) 3.1m (2H, –CH<sub>2</sub>–), 3.85s (3H, O–CH<sub>3</sub>), 5.1–5.3m (3H, olefinic protons), 6.9–7.2m (4H, Ar–H), 8.1dd (1H, Ar–H).

C<sub>20</sub>H<sub>21</sub>NO<sub>2</sub>HCl. Calcd. N 4.07, C 69.86, H 6.45, Cl<sup>–</sup> 10.3. Found N 3.75, C 69.6, H 6.38, Cl<sup>–</sup> 10.6.

\*

The authors' thanks are due to the First Department of Sciences of the Hungarian Academy of Sciences and to the Alkaloida Chemical Works, Tiszavasvári, Hungary for financial support, and to Mr. Attila LÖKI for the <sup>1</sup>H-NMR spectra.

#### REFERENCES

- [1] BERÉNYI, S., DOBÁNY, Zs., MAKLEIT, S.: To be published
- [2] MAKLEIT, S., BERÉNYI, S., BOGNÁR, R.: *Acta Chim. (Budapest)*, **94**, 165 (1977)
- [3] BERÉNYI, S., MAKLEIT, S., BOGNÁR, R., TEGDES, A.: *Acta Chim. Acad. Sci. Hung.,* **103**, 365 (1980); (some identical results were also published by L. MAAT *et al.*: *Synth. Commun.*, **9**, 713 (1979). Their paper was received for publication on April 27, 1979, whereas our communication [3] on March 2, 1979)
- [4] BERÉNYI, S., MAKLEIT, S.: *Acta Chim. Acad., Sci. Hung.*, **104**, 97 (1980)
- [5] BENTLEY, K. W.: *The Chemistry of Morphine Alkaloids*. p. 309. Clarendon Press, Oxford 1975
- [6] FOLKERS, K.: *J. Am. Chem. Soc.*, **58**, 1814 (1936)
- [7] SMALL, L., FARIS, B. E., MALLONEE, J. L.: *J. Org. Chem.*, **5**, 334 (1940)
- [8] KOCH, M. V., CANNON, J. G., BURKMAN, A. M.: *J. Med. Chem.*, **11**, 977 (1968)
- [9] GRANCHELLI, F. E., FILER, C. N., SOLOWAY, A. H., NEUMEYER, J. L.: *Org. Chem.*, **45**, 2275 (1980)
- [10] von BRAUN, J., AUST, E.: *Ber.*, **50**, 43 (1917)
- [11] SMISSMAN, E. E., MAKRIYANNIS, A. C., WALASZEK, E. J.: *J. Med. Chem.* **13**, 640 (1970)
- [12] CORRODI, H., HARDEGGER, E.: *Helv. Chim. Acta*, **38**, 2038 (1955)
- [13] GADAMER, J., KNOCH, F.: *Arch. Pharm.*, **259**, 135 (1921)
- [14] ATKINSON, E. R., BATTISTA, S. P., ARY, I. E., RICHARDSON, D. G., HARRIS, L. S., DEWEY, W. L.: *J. Pharm. Sci.*, **65**, 1682 (1976)
- [15] SMISSMAN, E. E., MAKRIYANNIS, A.: *J. Org. Chem.*, **38**, 1652 (1973)
- [16] HENSIKAK, J. F., CANNON, J. G., BURKMAN, A. M.: *J. Med. Chem.*, **8**, 577 (1965)
- [17] CAVA, M. P., SRINIVASAN, M.: *J. Org. Chem.*, **37**, 330 (1972)
- [18] JOHNS, S. R., LAMBERTON, J. A., LI, C. S., SIOUMIS, A. A.: *Austr. J. Chem.*, **23**, 363 (1970)
- [19] von BRAUN, J.: *Ber.*, **47**, 2312 (1914)
- [20] SPEYER, E., WALTER, L.: *Ber.*, **63**, 852 (1930)
- [21] BRINE, G. A., BOLDT, K. G., HART, C. K., CAROLL, F. I.: *OPPI*, **8**, 103 (1976)
- [22] ABDEL-MONEM, M. M., PORTHOGESE, P. S.: *J. Med. Chem.*, **15**, 208 (1972)

- [23] DEGRAW, J. I.,—LAWSON, J. A., CRASE, J. L., JOHNSON, H. L., ELLIS, M., UYENO, E. T., LOEW, G. H., BERKOWITZ, D. S.: *J. Med. Chem.*, **21**, 415 (1978)
- [24] RICE, K. C.: *J. Org. Chem.*, **40**, 1850 (1975); RICE, K. C., MAY, E. L.: *J. Heterocyclic Chem.*, **14**, 665 (1977)
- [25] HOSZTAFI, S., MAKLEIT, S., BOGNÁR, R.: *Acta Chim. Acad. Sci. Hung.*, **103**, 371 (1980)
- [26] CANNON, J. G., SMITH, R. V., MODIRI, A., SOOD, S. P., BORGMAN, R. J., ALEEM, M. A., LONGE, J. P.: *J. Med. Chem.*, **15**, 273 (1972)

Sándor BERÉNYI  
Sándor HOSZTAFI  
Sándor MAKLEIT  
Ilona SZEIFERT

H-4010 Debrecen, P.O.Box 20.



## THERMAL DECOMPOSITION OF OXETANE AND OXETANE- $d_2$ IN THE PRESSURE INDEPENDENT RANGE

ZS. HUNYADI-ZOLTÁN, L. ZALOTAI, T. BÉRCES\* and F. MÁRTA

(Central Research Institute for Chemistry, Hungarian Academy of Sciences, Budapest)

Received May 22, 1981

Accepted for publication August 28, 1981

The thermal decomposition of oxetane and oxetane-2,2- $d_2$  has been studied at high pressures. Over the temperature range of 668–757 K, oxetane decomposes into ethylene and formaldehyde *via* a clean unimolecular process with a rate constant

$$\log(k_{\infty}/s^{-1}) = 15.42 \pm 0.31 - (259.5 \pm 3.8) \text{ kJmol}^{-1}/RT \ln 10$$

Oxetane-2,2- $d_2$  was found to decompose by a similar unimolecular reaction, and in the temperature range of 673–758 K the rate constants fitted the equation

$$\log(k_{\infty}/s^{-1}) = 15.54 \pm 0.16 - (262.8 \pm 1.9) \text{ kJmol}^{-1}/RT \ln 10$$

A preliminary study of the pressure dependence of the first order rate constant of oxetane and oxetane- $d_2$  decomposition has been carried out at 732.2 K. The fall-off curves were analyzed using the RRK treatment. The best fits were obtained with the  $s_K$  parameters 18 and 19 for oxetane and oxetane- $d_2$ , respectively. The relation of these  $s_K$  parameters to theoretical estimates are discussed.

### Introduction

Apart from the early studies by WALTERS and co-workers on oxetane [1] and 3,3-dimethyl-oxetane [2], the kinetics of the thermal decomposition of oxetanes have been investigated only recently. Although kinetic data for various substituted oxetanes are available today, the reported Arrhenius parameters seem to involve a certain inconsistency "Low" Arrhenius parameters ( $A$  factors around  $10^{14.5} \text{ s}^{-1}$  and activation energies less than  $250 \text{ kJ mol}^{-1}$ ) were obtained for the 2-alkyl derivatives [3, 4] and "high" Arrhenius parameters ( $A$  factors of about  $10^{15.5} \text{ s}^{-1}$  and activation energies around or above  $250 \text{ kJ mol}^{-1}$ ) were reported for the 3-alkyl oxetanes [2, 5]. The order of magnitude difference in the  $A$  factors is difficult to elucidate, provided that all compounds decompose by the same mechanism.

Arrhenius parameters determined for the pyrolysis of *cis*- and *trans*-2,3-dimethyloxetane [6] clearly belong to the data designated here as "high" values. On the other hand, the results obtained for *cis*-2,4-dimethyl-*trans*-3-

\* To whom correspondence should be addressed

-vinyloxetane decomposition [7] fit in with low values of the 2-alkyl derivatives but cannot be reconciled with the "high" values of the dimethyloxetanes [7].

Regarding the decomposition of oxetane itself, the early study of BITTKER and WALTERS [1] gave

$$\log(k_{\infty}/s^{-1}) = 14.79 - 251.2 \text{ kJ mol}^{-1}/RT \ln 10 \quad (1)$$

while more recently HOLBROOK and SCOTT [8] found

$$\log(k_{\infty}/s^{-1}) = 15.71 - 263.7 \text{ kJ mol}^{-1}/RT \ln 10 \quad (2)$$

The "high" Arrhenius parameters obtained in the latter study fit in more with the kinetic parameters of cyclobutane decomposition [9].

Transition state estimates for the Arrhenius parameters of oxetane decomposition made by BENSON and O'NEAL [15] ( $\log A_{\infty} = 14.7$  and  $E_{\infty} = 247 \text{ kJ mol}^{-1}$ ) seem to support the "low" values, while those reported by HOLBROOK and SCOTT [8] appear to confirm the "high" ones. Further studies are obviously required.

In this paper we report our results on the decomposition of oxetane and oxetane-2,2- $d_2$  in the pressure independent range, and present some preliminary data on the pressure dependence of the unimolecular rate constants as well as the analysis based on the KASSEL (RRK) theory.

## Experimental

Oxetane and oxetane-2,2- $d_2$  were prepared from acrylic acetate through 3-chloropropyl acetate, trimethylene chlorohydrin and 3-chloropropyl acetate. Reduction of chloropropyl acetate to trimethylene chlorohydrin was carried out by  $\text{LiAlH}_4$  and  $\text{LiAlD}_4$ , respectively. Ring closure was brought about in the presence of potassium hydroxide, as described in [10]. The trimethylene oxide raw products were distilled from KOH. Final purification was carried out by bulb to bulb distillation in vacuum. The chemical purity of the samples was shown to be better than 99.5% by g.l.c. Mass spectrometric analysis of the oxetane- $d_2$  sample showed an isotopic purity better than 98%.

Kinetic experiments were carried out in a conventional static vacuum apparatus equipped with greaseless stopcocks. A cylindrical pyrex vessel of 450  $\text{cm}^3$  volume was used with a surface/volume ratio of 0.80  $\text{cm}^{-1}$ . The reaction vessel temperature was kept constant by means of a regulated air thermostat; long term stability and temperature gradient along the vessel was  $\pm 0.2 \text{ K}$ . Temperature measurements were carried out with a calibrated iron-constantan thermocouple.

Reactant pressure measurements were made with a quartz spiral manometer (TEXAS Model 145). After a pressure increase of 15–25%, the reaction was quenched by expansion into a glass bulb. Gas samples were transferred into a gas sampling valve. The reaction was followed by g.l.c. analysis which was carried out on an HP 5840A type gas chromatograph. Reaction products were separated on a 3 m Chromosorb 101 column using a temperature program from 333 to 423 K.

## Results

Oxetane and oxetane- $d_2$  decomposed with a reproducible rate in the seasoned reaction vessel. (Seasoning was achieved by carrying out a few runs in the new vessel.) Ethylene was the only reaction product which could be

detected under the conditions of g.l.c. analysis. Non-condensable products were not formed. Conversion calculated from the analysis of ethylene and oxetane agreed within the limits of experimental error with that obtained from pressure measurements. In agreement with previous investigations [8], we found that oxetane decomposed under our experimental conditions in a clean unimolecular reaction according to a simple stoichiometry:



Reaction was carried out up to 15–25% conversion and first order rate coefficients were obtained from the analytical results:

$$k = \frac{1}{t} \ln \left( 1 + \frac{[\text{ethylene}]}{[\text{oxetane}]} \right) \quad (4)$$

“High pressure” rate coefficients for oxetane decomposition were determined at pressures of  $p_0 \geq 7$  kPa over the temperature range of 668–757 K. The results are given in Table I and Fig. 1. A least-squares treatment of the data yields

$$\log(k_\infty/\text{s}^{-1}) = 15.42 \pm 0.31 - (259.5 \pm 3.8) \text{ kJ mol}^{-1}/RT \ln 10 \quad (5)$$

where the error limits are the standard deviations.

“High pressure” rate coefficients obtained for oxetane- $d_2$  decomposition at pressures of  $p_0 \geq 7$  kPa, in the temperature range 673 to 758 K, are given

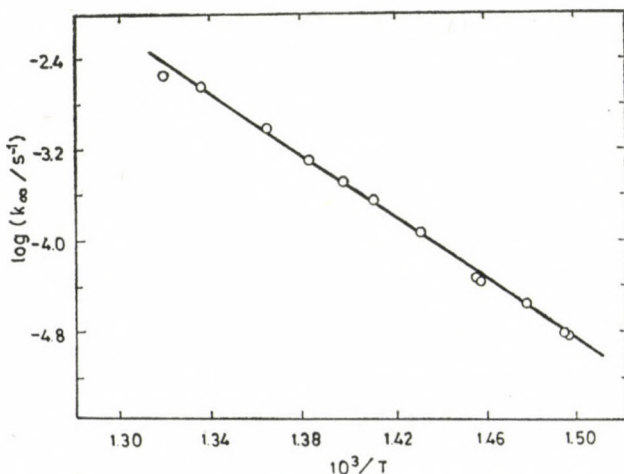


Fig. 1. Arrhenius plot for oxetane decomposition

**Table I**  
First order rate coefficients for oxetane decomposition

T (K)	$p_0$ (kPa)	$10^4 \times k_{\infty}$ (s <sup>-1</sup> )	T (K)	$p_0$ (kPa)	$10^4 \times k_{\infty}$ (s <sup>-1</sup> )
668.1	7.24	0.145	708.7	7.83	2.24
669.2	6.98	0.148	715.1	6.99	3.26
677.0	6.97	0.277	722.5	8.69	5.06
686.3	7.64	0.423	732.0	15.21	8.86
686.7	8.99	0.454	748.2	7.37	22.8
699.0	6.40	1.16	757.3	7.24	28.6

in Table II and Fig. 2. A least-squares treatment of the data yields

$$\log(k_{\infty}/\text{s}^{-1}) = 15.54 \pm 0.16 - (262.8 \pm 1.9) \text{ kJ mol}^{-1}/RT \ln 10 \quad (6)$$

where the error limits are again the standard deviations.

One may obtain a kinetic isotope effect from the rate coefficients determined for oxetane and oxetane- $d_2$ . Thus, one calculates  $k_{\text{H}}/k_{\text{D}} = 1.4$  at 732 K. Using Eqs (5) and (6),  $A_{\text{H}}/A_{\text{D}} = 0.76$  and  $E_{\text{H}} - E_{\text{D}} \cong -3.3 \text{ kJ mol}^{-1}$  are estimated.

The pressure dependence of the first order rate coefficients of oxetane and oxetane- $d_2$  decomposition was studied at 732.2 K at pressures down to about 10 Pa. The fall-off plots of the data, together with theoretical curves (see Discussion), are presented in Figs 3 and 4.

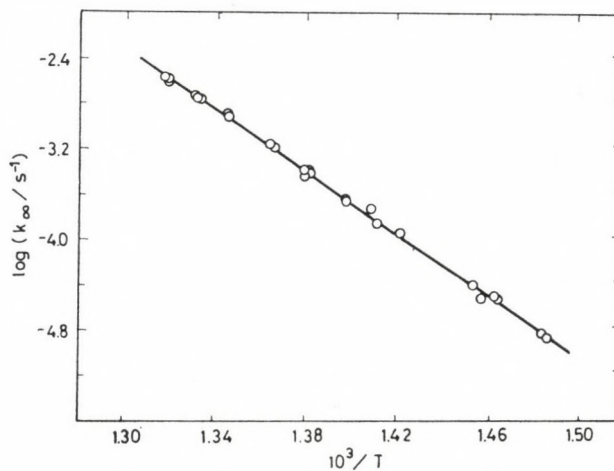


Fig. 2. Arrhenius plot for oxetane-2,2- $d_2$  decomposition

Table II

First order rate coefficients for oxetane-d<sub>2</sub> decomposition

<i>T</i> (K)	<i>p</i> <sub>0</sub> (kPa)	10 <sup>4</sup> × <i>k</i> <sub>∞</sub> (s <sup>-1</sup> )	<i>T</i> (K)	<i>p</i> <sub>0</sub> (kPa)	10 <sup>4</sup> × <i>k</i> <sub>∞</sub> (s <sup>-1</sup> )
673.1	7.09	0.131	724.4	9.56	3.90
674.1	8.29	0.150	724.8	9.35	3.66
683.1	7.83	0.297	732.2	12.00	6.30
683.1	7.75	0.301	734.0	8.43	6.40
686.8	8.21	0.288	743.1	7.76	12.20
688.1	6.61	0.394	743.1	7.73	11.70
702.9	8.06	1.06	749.4	11.28	17.40
708.2	8.80	1.29	749.9	9.40	16.50
709.3	7.05	1.78	750.2	9.05	17.70
715.1	10.13	2.16	750.2	9.01	16.70
715.1	6.97	2.18	757.2	11.01	25.80
723.0	7.77	3.61	757.5	10.87	24.60
732.0	7.75	3.62	758.2	8.72	25.90

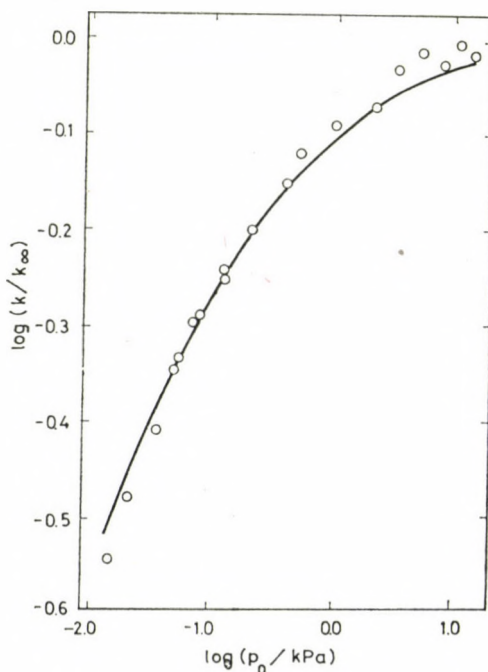


Fig. 3. Calculated and experimental fall-off curves for oxetane decomposition at 732.2 K; ○ experimental points; — RRK curve with  $s_K = 18$ ,  $\log A_\infty(\text{s}^{-1}) = 15.42$ ,  $E_\infty(\text{kJ mol}^{-1}) = 259.5$

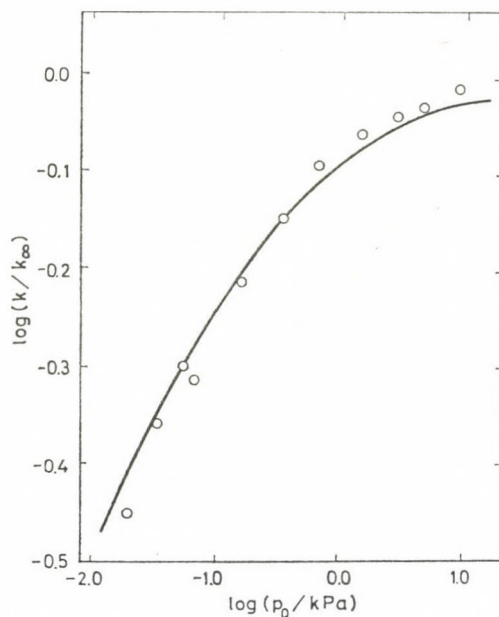


Fig. 4. Calculated and experimental fall-off curves for oxetane-2,2- $d_2$  decomposition at 732.2 K;  $\circ$  experimental points; — RRK curve with  $s_K = 19$ ,  $\log A_\infty(\text{s}^{-1}) = 15.54$ ,  $E_\infty(\text{kJ mol}^{-1}) = 262.8$

### Discussion

The “high pressure” kinetic data obtained for oxetane decomposition in this study are compared in Table III with the early results of BITTKER and WALTERS [1] and the more recent data of HOLBROOK and SCOTT [8]. It can be seen from the Table that the rate coefficients originating from the three sources show remarkably good agreement; they all agree within 4 per cent at 713 K (which is the mean temperature of our investigations). However, the comparison of the Arrhenius parameters is not satisfying at all, indicating the known difficulties involved in the precise determination of  $A$  and  $E_A$

Table III

Comparison of kinetic data for oxetane decomposition

$\log(A_\infty/\text{s}^{-1})$	$E_A^\infty(\text{kJ mol}^{-1})$	$10^4 \times k_\infty(\text{s}^{-1})$ at 713 K	Ref.
$15.42 \pm 0.31$	$259.5 \pm 3.8$	2.56	This work
$15.71 \pm 0.31$	$263.7 \pm 3.5$	2.46	HOLBROOK and SCOTT [8]
14.79	251.0	2.52	BITTKER and WALTERS [1]

from  $k$  measurements. Our parameters are in between the "high values" of HOLBROOK and SCOTT and the "low values" of BITTKER and WALTERS, but definitely closer to the former ones.

The rate coefficients and Arrhenius parameters obtained for oxetane- $-2,2-d_2$  are in line with those determined in this work for oxetane itself. Thus the kinetic results on deuterated oxetane decomposition seem to substantiate the kinetic parameters determined for the decomposition of oxetane in this study.

It is clear from the above discussion as well as from an inspection of the Arrhenius parameters reported for the decomposition of substituted oxetanes (see the Introduction) that all sorts of available theoretical and experimental information other than  $k$  measurements as a function of  $T$  have also to be consulted in order to come to a reliable conclusion regarding the precise value of the Arrhenius parameters of oxetane decomposition. Such information can be expected from the interpretation of the pressure dependence of the first order rate coefficient and of the kinetic isotope effect.

In this paper we examine the experimental data on the pressure dependence of the first order rate coefficient at 732.2 K using the RICE—RAMSPERGER—KASSEL (RRK) theory [11] of unimolecular reactions. According to the RRK theory, the first order rate coefficient at any pressure is given by

$$\frac{k}{k_\infty} = \frac{1}{(s-1)!} \int_0^\infty \frac{x^{s-1} \exp(-x) dx}{1 + \frac{A}{\omega} \left(\frac{x}{b+x}\right)^{s-1}} \quad (7)$$

where  $x = (E - E_0)/RT$ ,  $b = E_0/RT$ ,  $A$  and  $E_0$  are to be identified as the high pressure pre-exponential factor and activation energy, respectively, and  $\omega$  is the collision frequency at pressure  $p$ . (In the calculation of  $\omega$ , the collision diameter was taken as  $5 \times 10^{-8}$  cm.) In Eq. (7)  $s$  is the fall-off parameter; regarding its value used in the calculations see the discussion that follows.

RRK calculations were carried out for oxetane and oxetane- $-d_2$  decomposition at 732.2 K using the Arrhenius parameters obtained in this study. The fall-off curves were computed with a series of  $s$  values in order to find the fall-off parameters giving the best fit to the experimental data. In this way  $s_K = 18$  and  $s_K = 19$  were obtained in case of oxetane and oxetane- $-d_2$ , respectively. The solid curves of Figs 3 and 4 were computed with  $s_K$  parameters assigned in this manner.

Similar good fits to the experimental fall-off data could be obtained if the Arrhenius parameters determined by HOLBROOK and SCOTT or those reported by BITTKER and WALTERS were used. Naturally, different  $s_K$  values were required in each case. The  $s_K$  parameters that gave the best fits to our fall-off data at 732.2 K are presented in the second column of Table IV.

**Table IV**  
Comparison of KASSEL fit parameter  $s_K$  with calculated  $s$  values (732.2 K)

	$s_K$ best fit	$s = C_{vib}/R$ Eq. (8)	$s = (\langle E_{th}^\infty \rangle_f - E_0)/RT$ Eq. (9)	$s = \langle E_{all} \rangle_K / RT$ Eq. (10)
Oxetane	18 <sup>a</sup> 19 <sup>b</sup> 17 <sup>c</sup>	12.50	7.18	5.34
Oxetane- $d_2$	19 <sup>a</sup>	13.52	7.79	5.60

<sup>a</sup> With Arrhenius parameters from this work

<sup>b</sup> with Arrhenius parameters determined by HOLBROOK and SCOTT [8]

<sup>c</sup> with Arrhenius parameters reported by BITTKER and WALTERS [1]

Analysis of the fall-off curves, on the basis of the RRK theory, could support one or the other of the Arrhenius parameters reported for oxetane decomposition provided that the  $s$  parameter were available from independent sources. GOLDEN *et al.* [12] suggested that the  $s$  parameter is uniquely defined by the vibrational heat capacity of the decomposing molecule as

$$s = C_{vib}/R = \sum_i \frac{u_i^2 \exp(u_i)}{[\exp(u_i) - 1]^2} \quad (8)$$

where  $u_i = hv_i/kT$ , and  $\bar{\nu}_i$  being the molecular frequencies.

PLACZEK *et al.* [13] as well as TSCHUIKOW-ROUX [14] examined the estimation of the "effective" number of oscillators in terms of the average energy of the reacting species (which is also the non-fixed energy of the activated complex):

$$s(\langle E_{th}^\infty \rangle_f - E_0)/RT = \frac{1}{2}(r^+ + 2) + \sum_{i=1}^{s^+} (H^\circ - H_0^\circ)_i^+ / RT \quad (9)$$

where  $s^+$  and  $r^+$  designate the number of vibrational degrees of freedom and the number of active internal rotations of the activated complex and  $\sum_i (H^\circ - H_0^\circ)_i^+$  are the Planck-Einstein harmonic oscillator functions for the complex. Still another method of finding the  $s$  parameter is by fitting the average internal energy of all the molecules at the temperature in question [13, 14]:

$$s = \langle E_{all} \rangle_K / RT = \frac{r}{2} + \sum_{i=1}^t (H^\circ - H_0^\circ)_i / RT \quad (10)$$

where  $t$  and  $r$  are the total number of vibrational degrees of freedom and the number of internal rotations of the molecule and  $\sum_i (H^\circ - H_0^\circ)_i / RT$  are the Planck-Einstein harmonic oscillator functions for the molecule.

Determinations of the fall-off parameter from Eqs (8)–(10) were carried out using the molecular and activated complex models summarized in the Appendix. The results are given in Table IV. All the theoretical estimates of the  $s$  parameter are considerable less than the  $s_K$  parameters giving the best fit. Theoretical prediction of the fall-off parameter is clearly not good enough either to support or to reject any of the reported Arrhenius parameters of oxetane decomposition. A more sophisticated treatment, the RRKM theory is required to analyze the fall-off data. This work is in progress.

### Appendix

The following vibrational frequency assignment ( $\text{cm}^{-1}$ ) was adopted in the theoretical estimation of the  $s$  parameters.

*Oxetane*: Molecular frequencies were taken 2959, 2930, 3000, 2966, 3007, 2940, 1473, 1447, 1498, 1342, 1410, 1363, 1283, 1185, 1225, 986, 1142, 836, 1134, 1018, 908, 1228, 931, 90. Activated complex assignment was 2967(6), 1422(6), 1209(4), 911(2), 390(4), 50(1).

*Oxetane- $d_2$* : Molecular frequencies 2966(4), 2179(2), 1430(4), 1167(5), 988(4), 871(3), 724(1), 87(1). Activated complex assignment 2966(4), 2179(2), 1430(4), 1167(3), 988(3), 871(1), 724(1), 430(4), 50(1).

\*

The authors are indebted to Prof. M. BARTÓK for assistance in the preparation of oxetane- $d_2$ .

### REFERENCES

- [1] BITTKER, D. A., WALTERS, W. D.: J. Amer. Chem. Soc., **77**, 2326 (1955)
- [2] COHOE, G. F., WALTERS, W. D.: J. Phys. Chem., **71**, 2326 (1967)
- [3] CLARKE, M. J., HOLBROOK, K. A.: J.C.S. Faraday I, **73**, 890 (1976)
- [4] COHOE, C. F.: Ph. D. Thesis (University of Rochester, 1965), cited in ref. [3]
- [5] CLEMENTS, A. D., FREY, H. M., FREY, J. G.: J.C.S. Faraday I, **71**, 2485 (1975)
- [6] HOLBROOK, K. A., SCOTT, R. A.: J.C.S. Faraday I, **70**, 43 (1974)
- [7] CARLESS, H. A., MAITRA, A. K., POTTINGER, R., FREY, H. M.: J.C.S. Faraday I, **76**, 1849 (1980)
- [8] HOLBROOK, K. A., SCOTT, R. A.: J.C.S. Faraday I, **71**, 1849 (1975)
- [9] GENAUX, C. T., WALTERS, W. D.: J. Amer. Chem. Soc., **73**, 4497 (1951)
- [10] BARTÓK, M., APJOK, J.: Acta Phys. Chem. Univ. Szeged, **8**, 133 (1962)
- [11] KASSEL, L. S.: "Kinetics of Homogeneous Gas Reactions". Reinhold, New York 1932
- [12] GOLDEN, D. M., SOLLY, R. K., BENSON, S. W.: J. Phys. Chem., **75**, 1333 (1971)
- [13] PLACZEK, D. W., RABINOVITCH, B. S., WHITTEN, G. Z., TSCHUIKOW-ROUX, E.: J. Chem. Phys., **43**, 4071 (1965)
- [14] TSCHUIKOW-ROUX, E.: J. Phys. Chem., **73**, 3891 (1969)
- [15] BENSON, S. W., O'NEAL, H. E.: "Kinetic Data on Gas Phase Unimolecular Reactions", NSRDS-NBS 21, Washington, 1970

Zsuzsa HUNYADI-ZOLTÁN  
Lajos ZALOTAI  
Tibor BÉRCES  
Ferenc MÁRTA

H-1025 Budapest, Pusztaszeri út 59–67.



## ZUM EINFLUSS VON DISPERSIONSWECHSELWIRKUNGEN AUF DIE ABSCHIRMKONSTANTE DER KERNMAGNETISCHEN RESONANZ

U. POHLE and G. GROSSMANN\*

(Sektion Chemie der Technischen Universität Dresden, Dresden, DDR)

Eingegangen am 25. Mai 1981

Zur Veröffentlichung angenommen am 28. August 1981

Es wird der Einfluß der Dispersionswechselwirkungen auf die Abschirmung mittels Störungsrechnung theoretisch beschrieben. Zunächst wird der Einfluß der Dispersionswechselwirkungen zwischen zwei Teilchen auf die Abschirmung untersucht und dann eine Verallgemeinerung auf viele Umgebungsteilchen durchgeführt. Die theoretischen Ergebnisse werden zur Auswertung experimenteller Befunde aus  $^{31}\text{P}$ - und  $^{129}\text{Xe}$ -NMR-Spektren genutzt.

### Einleitung

Seit 1951 [1] ist die Abhängigkeit der chemischen Verschiebung vom Lösungsmittel bekannt. Zunächst versuchte man sie allein durch das entmagnetisierende Feld zu erklären. Bald fanden BOTHNER-BY und GLICK [2], daß diese Erklärung nicht ausreichend ist. Es wurde der Einfluß von Dispersionswechselwirkungen diskutiert. MARSHALL und POPE [3] und STEPHEN [4] veröffentlichten 1958 theoretische Arbeiten über den Einfluß eines äußeren elektrischen Feldes auf die Abschirmung. Stephen erhielt den einfachen Ausdruck

$$\delta = -BF^2, \quad (1)$$

wonach die Verschiebung proportional dem mittleren Quadrat des elektrischen Feldes am Ort des untersuchten Kernes ist. Bei Versuchen zur Berechnung dieses Feldes wurde deutlich, daß sich die direkten elektrischen Felder, die von den Nachbarpartikeln erzeugt werden, in hohem Maße ausmitteln, so daß das mittlere Quadrat des elektrischen Feldes am Ort des untersuchten Kernes klein bleibt und in guter Näherung durch die Wirkung eines Nachbarpartikels beschreibbar sein sollte [5]. In Gasen wurde mit diesem Modell gute Übereinstimmung zwischen Experiment und Theorie gefunden.

Untersucht man aber die theoretischen Ergebnisse hinsichtlich ihres Verhaltens beim Übergang zum Kontinuum [6], so findet man, daß die Dichteabhängigkeit der Abschirmung nicht verschwindet. Das mittlere Quadrat des

\* Korrespondenz bitte an diesen Autor richten

direkten elektrischen Feldes muß aber in einem Kontinuum verschwinden. Man kann daraus ersehen, daß dieses Modell auch die Wirkung des Reaktionsfeldes der induzierten Momente des untersuchten Moleküls auf die Abschirmung für den Fall zweier Teilchen mit enthält. Dieses Reaktionsfeld ist aber additiv, und man muß bei höherer Dichte — insbesondere in Flüssigkeiten — alle Umgebungsmoleküle berücksichtigen. Die einfache Multiplikation mit einer mittleren Koordinationszahl [7], ausgehend vom mittleren Quadrat des elektrischen Feldes, das von einem Molekül am Ort des untersuchten Kerns erzeugt wird, enthält die prinzipiell fehlerhafte Voraussetzung, daß sich das mittlere Quadrat des elektrischen Feldes an diesem Ort additiv aus den mittleren Quadraten der von den einzelnen Umgebungsmolekülen erzeugten Felder zusammensetzt. Es lag nahe, daß das Reaktionsfeld wegen seiner Additivität allein für die Abhängigkeit der Abschirmung von Dispersionswechselwirkungen verantwortlich ist.

Für die Einführung des Reaktionsfeldes  $R$  anstelle des mittleren Quadrats des elektrischen Feldes in die Beziehung (1) wurden zwei unterschiedliche Ansätze verwendet. Einmal setzte DE MONTGOLFIER [8] einfach  $F^2 \sim R^2$ , und daraus leitete RUMMENS [9] letztlich ab:  $\delta \sim [(n^2 - 1)/(2n^2 + 1)]^2$ . Andererseits führt LINDER [10] das Reaktionsfeld so ein, daß die Änderung des Potentials des untersuchten Moleküls im Reaktionsfeld gleich der im gedachten fluktuierenden Feld  $F$  ist:  $W = -mR/2 = \alpha F^2$ , und so erhält er  $\delta \sim (n^2 - 1)/(2n^2 + 1)$ ;

$n$  Brechungsindex,

$m$  fluktuierendes Dipolmoment des untersuchten Moleküls,

$\alpha$  dessen Polarisierbarkeit,

$W$  Potentielle Energie

In beiden Modellen ist die gleiche fragwürdige Grundlage enthalten. Man muß davon ausgehen, daß die Änderung der Abschirmung eine Folge der Veränderung der Wellenfunktion des untersuchten Moleküls bei Wechsel der Umgebung ist. Betrachtet man Dipolwechselwirkungen, so erzeugt jede Veränderung mit nicht verschwindenden Matrixelementen des Dipoloperators ein stabilisierend wirkendes Reaktionsfeld, dessen Richtung von der Veränderung der Wellenfunktion des untersuchten Moleküls abhängig ist. STEPHEN hat aber die Beziehung (1) für ein von außen angelegtes, vom betrachteten Molekül völlig unabhängiges elektrisches Feld abgeleitet, und nur deshalb verschwindet das linear vom elektrischen Feld abhängige Glied in seiner Ableitung bei Mittelung über alle Orientierungen. Die Beziehung (1) ist also streng genommen für ein Reaktionsfeld nicht anwendbar. Deshalb ist es notwendig, mit Hilfe der Störungsrechnung quantenmechanisch die Abhängigkeit der Abschirmkonstanten von der molekularen Dipol-Dipol-Wechselwirkung zu untersuchen. Dabei muß eine Zerlegung des erhaltenen Ergebnisses für

Molekülpaare in Reaktionsfeldanteil und Anteil des direkten Feldes durchgeführt werden. Danach soll eine Verallgemeinerung auf viele Umgebungsteilchen bei isotroper Umgebung für den Reaktionsfeldanteil mit Hilfe eines Kontinuummodells betrachtet werden. Einflüsse der Anisotropie der Umgebung durch Bildung von Komplexen aus wenigen Teilchen in Gasen können durch einen statistischen Ansatz berücksichtigt werden.

### Theorie

RAMSAY [11, 12] zeigte, daß die Berechnung des Abschirmtensors mit der Störungsrechnung zweiter Ordnung möglich ist. Für die Untersuchung des Abschirmtensors unter dem Einfluß eines äußeren Mediums bei Verwendung der Dipol-Dipol-Wechselwirkung ist diese Ableitung ungünstig, da Glieder die beide Einflüsse — das magnetische Feld und die Dipol-Dipol-Wechselwirkung — enthalten, erst in 3. und 4. Ordnung auftreten. Eine beträchtliche Vereinfachung läßt sich erzielen, wenn man einen Operator findet, der es erlaubt, die Elemente des Abschirmtensors mit der Grundzustandswellenfunktion des betrachteten Moleküls zu berechnen. Dieser Operator existiert nach dem Theorem der doppelten Störungsrechnung [13]. Seine Struktur ist für das hier zu behandelnde Problem ohne Belang.

Es gilt:

$$\sigma_{\alpha\beta} = \langle 0 | \hat{\sigma}_{\alpha\beta} | 0 \rangle \quad (2)$$

$$= [\partial^2 \langle 0 | \hat{h}_{\mu_\alpha B_\beta} | 0 \rangle / \partial \mu_\alpha \partial B_\beta] \mu = 0, B = 0 \quad (3)$$

$$= [\partial^2 (E - \mu_\gamma B_\gamma) / \partial \mu_\alpha \partial B_\beta] \mu = 0, B = 0 \quad (4)$$

$\hat{\sigma}_{\alpha\beta} = \partial^2 \hat{h}_{\mu_\alpha B_\beta} / \partial \mu_\alpha \partial B_\beta$  sei der Operator der Abschirmung,

$B_\beta$  — die Komponenten der magnetischen Induktion am Ort des untersuchten Kerns,

$\mu_\alpha$  — die Komponenten des magnetischen Moments des untersuchten Kerns.

Die Verschiebung durch Paarwechselwirkung  $\delta_{\alpha\beta}$  erhält man zu:

$$\delta_{\alpha\beta} = \delta_{\alpha\beta, \text{Paar}} - \delta_{\alpha\beta}^{(0)} \quad (5)$$

$$= [\partial^2 (E_{\text{Paar}} - E_0) / \partial \mu_\alpha \partial B_\beta] \mu = 0, B = 0 \quad (6)$$

$$= [\partial^2 (w^{(2)} + w^{(3)}) / \partial \mu_\alpha \partial B_\beta] \mu = 0, B = 0 \quad (7)$$

Dabei bedeuten :

$E^0$  — die Energie des Molekülpaares ohne Wechselwirkungen bei angelegtem Magnetfeld<sup>1</sup>

$E_{\text{Paar}}$  — die Energie des Molekülpaares mit Wechselwirkungen im Magnetfeld.

Es treten erst in zweiter und dritter Ordnung nicht trivial verschwindende Beiträge zur Verschiebung auf. Diese sind in den sowohl vom Operator  $\hat{h}_{\mu\alpha B\beta}$  als auch vom Dipol-Dipol-Wechselwirkungsoperator  $\hat{h}_{\alpha\beta}$  abhängenden Anteilen der Störungsenergien in zweiter ( $w^{(2)}$ ) und dritter Ordnung ( $w^{(3)}$ ) enthalten. Die Paarwechselwirkung soll durch den Operator  $\hat{h}_{ab}$  in Punktdipolnäherung hinreichend beschrieben sein :

$$\hat{h}_{ab} = -M^a M^b R_{ab}^{-3} = -M^a \vec{E}^{ba} = -M^b \vec{E}^{ab} \quad (8)$$

Hierin bedeuten :

$M^a$  — das Dipolmoment des Moleküls  $a$

$M^b$  — das Dipolmoment des Moleküls  $b$

$R_{ab}$  — der Abstand der Ladungsschwerpunkte der Moleküle  $a$  und  $b$

$\vec{E}^{ba}$  — das vom Dipol  $M^b$  am Ort des Moleküls  $a$  erzeugte elektrische Feld

$\vec{E}^{ab}$  — das vom Dipol  $M^a$  am Ort des Moleküls  $b$  erzeugte elektrische Feld.

Im Zustand ohne Wechselwirkungen erhalte man die Wellenfunktionen  $|n_{ab}^{(0)}\rangle$  der Molekülpaare als Produkt der Wellenfunktionen der einzelnen Moleküle :

$$|n_{ab}^{(0)}\rangle = |r_a^{(0)}\rangle |u_b^{(0)}\rangle \equiv |ru\rangle \quad (9)$$

Bei der Durchführung der Störungsrechnung ergibt sich :

$$\delta_{\alpha\beta}^{(2)} = [\partial^2 w^{(2)} / \partial \mu_\alpha \partial B_\beta]_{\mu=0, B=0} = 0, \quad (10)$$

wenn die Orientierung der einzelnen Moleküle zueinander nicht festgelegt ist.

$$\begin{aligned} \delta_{\alpha\beta}^{(3)} &= [\partial^2 w^{(3)} / \partial \mu_\alpha \partial B_\beta]_{\mu=0, B=0} \\ &= \sum_{\substack{r \\ r+u}} \sum_{\substack{u \\ u \neq 0}} \frac{(\sigma_{\alpha\beta rr} - \sigma_{\alpha\beta 00}) \langle 00 | h_{ab} | ru \rangle \langle ru | h_{ab} | 00 \rangle}{(W_{0,\alpha}^{(0)} + W_{0,b}^{(0)} - W_r^{(0)} - W_u^{(0)})^2}. \end{aligned} \quad (11)^*$$

Diesen Beitrag kann man in drei Anteile zerlegen, die sich hinsichtlich ihrer physikalischen Bedeutung unterscheiden:

1.  $r = 0, u \neq 0$ ; Wechselwirkung des statischen Dipolmoments des Moleküls  $a(m_{0,a})$  mit dem induzierten Moment des Moleküls  $b(m_{i,b})$

2.  $r \neq 0, u = 0$ : Wechselwirkung von  $m_{i,a}$  und  $m_{0,b}$

3.  $r \neq 0, u \neq 0$ : Wechselwirkung von  $m_{i,a}$  und  $m_{i,b}$ .

Der zum 1. Fall gehörende Beitrag  $\delta_{\alpha\beta 1}^{(3)}$  verschwindet, weil der erste Klammerausdruck in Gl. (11) Null wird.

Für  $\delta_{\alpha\beta 2}^{(3)}$  erhält man (2. Fall):

$$\delta_{\alpha\beta 2}^{(3)} = \sum_{r \neq 0} \vec{E}_{00}^{ba} \frac{(\sigma_{\alpha\beta rr} - \sigma_{\alpha\beta 00}) \langle 0 | M^a | r \rangle \langle r | M^a | 0 \rangle}{(W_{0,a}^{(0)} - W_r^{(0)})^2} \vec{E}_{00}^{ba} \quad (12)$$

$\delta_{\alpha\beta 2}^{(3)}$  gibt die Abhängigkeit der Abschirmung vom direkten elektrischen Feld an, das der statische Dipol des Nachbarmoleküls am Ort des untersuchten Moleküls erzeugt.

Für den 3. Fall erhält man:

$$\delta_{\alpha\beta 3}^{(3)} = \sum_{r \neq 0} \sum_{u \neq 0} \frac{(\sigma_{\alpha\beta rr} - \sigma_{\alpha\beta 00}) \langle 00 | h_{ab} | ru \rangle \langle ru | h_{ab} | 00 \rangle}{(W_{0,a}^{(0)} + W_{0,b}^{(0)} - W_r^{(0)} - W_u^{(0)})^2}. \quad (13)$$

Dieser Term läßt sich in zwei Teile zerlegen:

$$\delta_{\alpha\beta 3}^{(3)} = \delta_{\alpha\beta 31}^{(3)} + \delta_{\alpha\beta 32}^{(3)} \quad (14)$$

Der erste Teil ergibt sich bei Berücksichtigung von  $W_{0,a}^{(0)} - W_r^{(0)} = h\nu_{0r}^a$  und  $W_{0,b}^{(0)} - W_u^{(0)} = h\nu_{0u}^b$  zu:

$$\delta_{\alpha\beta 31}^{(3)} = \sum_{r \neq 0} \sum_{u \neq 0} \frac{\sigma_{\alpha\beta rr} - \sigma_{\alpha\beta 00}}{h^2 (\nu_{0r}^a + \nu_{0u}^b)} \vec{E}_{0u}^{ba} \frac{\nu_{0r}^a \langle 0 | M^a | r \rangle \langle r | M^a | 0 \rangle}{(\nu_{0r}^a)^2 - (\nu_{0u}^b)^2} \vec{E}_{0u}^{ba}. \quad (15)$$

Gl. (15) gibt den Einfluß des direkten elektrischen Feldes, das von den induzierten Dipolen des Moleküls  $b$  am Ort des untersuchten Moleküls  $a$  erzeugt wird, an.

$$\delta_{\alpha\beta 32}^{(3)} = \sum_{r \neq 0} \sum_{u \neq 0} \frac{(\sigma_{\alpha\beta rr} - \sigma_{\alpha\beta 00})}{h^2 (\nu_{0r}^a + \nu_{0u}^b)} \vec{E}_{0r}^{ab} \frac{\nu_{0u}^b \langle 0 | M^b | u \rangle \langle u | M^b | 0 \rangle}{(\nu_{0u}^b)^2 - (\nu_{0r}^a)^2} \vec{E}_{0r}^{ab}. \quad (16)$$

Gl. (16) enthält den stabilisierenden Einfluß des Nachbarmoleküls auf Veränderungen der Wellenfunktion des untersuchten Moleküls und läßt sich nach

\* Die detaillierte Ableitung ist in [6] dargelegt

Näherungen zur Beseitigung der Doppelsumme als Reaktionsfeldterm schreiben:

$$\delta_{\alpha\beta 32}^{(3)} = \frac{I_a}{I_a + I_b} \sum_{r \neq 0} \frac{(\sigma_{\alpha\beta rr} - \sigma_{\alpha\beta 00})}{h^2 \nu_{0r}^a} \sum_{u \neq 0} \vec{E}_{0r}^{ab} \frac{\nu_{0u}^b \langle 0 | M^b | u \rangle \langle u | M^b | 0 \rangle}{(\nu_{0u}^b)^2 - (\nu_{0r}^a)^2} \vec{E}_{0r}^{ab} \quad (17)$$

$$= \frac{I_a}{I_a + I_b} \sum_{r \neq 0} \frac{(\sigma_{\alpha\beta rr} - \sigma_{\alpha\beta 00})}{h \nu_{0r}^a} \vec{E}_{0r}^{ab} \alpha^b(\nu_{0r}^a) \vec{E}_{0r}^{ab} \quad (18)$$

$$= \frac{I_a}{I_a + I_b} \sum_{r \neq 0} \frac{(\sigma_{\alpha\beta rr} - \sigma_{\alpha\beta 00})}{h \nu_{0r}^{ab}} \vec{E}_{0r}^{ab} m_i^b(\nu_{0r}^a) \quad (19)$$

$$= \frac{I_a}{I_a + I_b} \sum_{r \neq 0} \frac{(\sigma_{\alpha\beta rr} - \sigma_{\alpha\beta 00})}{h \nu_{0r}^a} \langle 0 | M^a | r \rangle e_{0r}^b. \quad (20)$$

Dabei bedeuten :

- $I_{a,b}$  — mittlere Anregungsenergien der Moleküle  $a$  bzw.  $b$   
 $m_i^b(\nu_{0r}^a)$  — induziertes Dipolmoment des Moleküls  $b$  auf der Frequenz  $\nu_{0r}^a$   
 $\vec{e}_{0r}^b$  — Reaktionsfeld auf der Frequenz  $\nu_{0r}^a$ .

Ausgehend davon, daß das direkte Feld bei näherungsweise isotroper Umgebung im Vergleich zum Reaktionsfeld einen vernachlässigbaren Einfluß auf die Abschirmung ausübt, braucht man in guter Näherung nur den Einfluß des Terms  $\delta_{\alpha\beta 32}^{(3)}$  bei der Verallgemeinerung auf viele Umgebungsteilchen zu berücksichtigen. Das Reaktionsfeld stimmt bekanntlich in der Richtung mit dem erzeugenden Moment überein und ist additiv, weshalb die Anwendung eines Kontinuummodells sinnvoll ist. Es wird das Modell nach ONSAGER [14] in der Version nach BÖTTCHER [15] verwendet. Danach befindet sich der erzeugende Dipol im Zentrum einer Hohlkugel mit dem dichteunabhängigen Radius  $a$ . Außerhalb dieser Kugel befindet sich ein Kontinuum, das gekennzeichnet ist durch die frequenz- und dichteabhängige Dielektrizitätskonstante  $\epsilon\nu$ . Bei Summation über alle Moleküle  $b$  erhält man mit

$$\sum_b \vec{e}_{0r}^b = R_{0r} \quad (21)$$

$$\delta_{\alpha\beta 32}^{(3)} = \frac{I_a}{I_a - I_b} \sum_{r \neq 0} \frac{(\sigma_{\alpha\beta rr} - \sigma_{\alpha\beta 00})}{h \nu_{0r}^a} \langle 0 | M^a | r \rangle R_{0r} \quad (22)$$

Das Kontinuummodell liefert :

$$R_{0r} = \frac{2(\epsilon\nu - 1)}{2\epsilon\nu + 1} \frac{\langle r | M^a | 0 \rangle}{a^3} \quad (23)$$

und somit ergibt sich:

$$\delta_{\alpha\beta 32}^{(3)} = \frac{I_a}{I_a + I_b} \frac{2}{a^3} \sum_{r \neq 0} (\sigma_{\alpha\beta rr} + \sigma_{\alpha\beta 00}) \frac{\langle 0 | M^a | r \rangle \langle r | M^a | 0 \rangle}{h\nu_{0r}^a} \frac{\varepsilon_\nu - 1}{2\varepsilon_\nu + 1} \quad (24)$$

Auch dieser Ausdruck ist für die experimentelle Auswertung noch zu kompliziert, da die Kenntnis aller Molekülzustände, aller Übergangsmomente und der Abschirmtensoren in allen Molekülzuständen des untersuchten Moleküls sowie die vollständige Frequenzabhängigkeit der Dielektrizitätskonstanten des Mediums benötigt wird. Zweckmäßig ist die Einführung einer gemittelten Dielektrizitätskonstanten  $\bar{\varepsilon}$ , so daß gilt:

$$\delta_{\alpha\beta 32}^{(3)} = \frac{I_a}{I_a + I_b} \frac{t_{\alpha\beta}}{a^3} \frac{\bar{\varepsilon} - 1}{2\bar{\varepsilon} + 1} \quad (25)$$

mit

$$t_{\alpha\beta} = 2 \sum_{r \neq 0} (\sigma_{\alpha\beta rr} - \sigma_{\alpha\beta 00}) \frac{\langle 0 | M^a | r \rangle \langle r | M^a | 0 \rangle}{h\nu_{0r}^a} \quad (26)$$

Für die Änderung der Abschirmkonstanten folgt:

$$\delta_{32}^{(3)} = \frac{I_a}{I_a + I_b} \frac{t}{a^3} \frac{\bar{\varepsilon} - 1}{2\bar{\varepsilon} + 1} \quad (27)$$

Schließlich kann man noch eine Frequenz  $\bar{\nu}$  einführen, so daß gilt:

$$\bar{\varepsilon} = \varepsilon(\bar{\nu}) \quad (28)$$

Dann gilt unter Verwendung der üblichen Näherung für die Frequenzabhängigkeit der Dielektrizitätskonstanten:

$$\frac{\bar{\varepsilon} - 1}{\bar{\varepsilon} + 2} = \frac{\nu_b^2}{\nu_b^2 - \bar{\nu}^2} \frac{\varepsilon_\sigma - 1}{\varepsilon_0 + 2} = \frac{\nu_b^2}{\nu_b^2 - \bar{\nu}^2} \frac{4\pi N_L \alpha_{0b}}{3M_b} d_b \quad (29)$$

$$\frac{\bar{\varepsilon} - 1}{2\bar{\varepsilon} + 1} = \left( 1 + \frac{\bar{\varepsilon} + 2}{\bar{\varepsilon} - 1} \right)^{-1} = \left( 1 - \frac{\nu_b^2 - \bar{\nu}^2}{\bar{\nu}_b^2} \frac{3M_b}{4\pi N_L \alpha_{0b}} d_b^{-1} \right)^{-1} \quad (30)$$

Für die Dichteabhängigkeit der Abschirmung ergibt sich:

$$(\delta_{32}^{(3)})^{-1} = \frac{I_a + I_b}{I_a} \frac{a^3}{t} \left( 1 + \frac{\nu_b^2 - \bar{\nu}^2}{\nu_b^2} \frac{3M_b}{4\pi N_L \alpha_{0b}} d_b^{-1} \right) \quad (31)$$

In Gasen ist die Dichte im allgemeinen klein genug, um in Gl. (31) die 1 in der Klammer zu vernachlässigen. Dann ist  $\delta_{32}^{(3)}$  in guter Näherung linear von

der Dichte abhängig und man erhält:

$$\delta_{32}^{(3)} = \frac{I_a}{I_a + I_b} \frac{t}{a^3} \left( \frac{v_b^2}{v_b^2 - \bar{v}^2} \frac{4\pi N_L \alpha_{0b}}{3M_b} d_b \right). \quad (32)$$

Dafür treten aber in der Nähe und unterhalb der kritischen Temperatur Anteile auf, die durch Bildung von Komplexen aus wenigen Teilchen hervorgerufen werden. Bezeichnet man die Verschiebung der freien Teilchen durch Umgebungseffekte mit  $(\delta)_1$ , die im Komplex aus zwei Teilchen mit  $(\delta)_2$  und die im Komplex aus drei Teilchen mit  $(\delta)_3$  sowie die Anteile der Teilchen mit  $x_1$  (freie Teilchen),  $x_2$  (Teilchen im Zweierkomplex) und  $x_3$  (Teilchen im Dreierkomplex), so erhält man für die Verschiebung:

$$\delta = x_1(\delta)_1 + x_2(\delta)_2 + x_3(\delta)_3 + \dots \quad (33)$$

Es wird ein reines einatomiges Gas untersucht und angenommen, daß die Anteile der Teilchen in den Komplexen klein gegenüber denen der freien Teilchen sind.

$$x_{2,3} \ll x_1 \quad x_1 \cong 1 \quad (34)$$

$$x_2/2 = x'_2 = K_2 \quad (35)$$

$$x_3/3 = x'_3 = K_3 \quad (36)$$

Dabei bedeuten  $x'_i$  die Molenbrüche der Komplexe und  $K_i$  die Komplexbildungskonstanten. Für einatomige Gase lassen sich für die Komplexbildungskonstanten unter Verwendung der aus der statistischen Thermodynamik bekannten Formeln für die absolute Entropie idealer Gase folgende Ausdrücke ableiten:

$$K_2 = \frac{2\sqrt{2} r^2 N_L}{e^{5/2} V_{M_2}} \left( \frac{h^2}{2\pi m k T} \right)^{1/2} \exp \left( - \frac{\Delta U_2}{RT} \right) \quad (37)$$

$$K_3 = \frac{36\sqrt{3} \pi^2 N_L^2}{e^5 V_{M_3}^2} \left( \frac{I_x I_y I_z}{m^3} \right)^{1/2} \left( \frac{h^2}{2\pi m k T} \right)^{3/2} \exp \left( - \frac{\Delta U_3}{RT} \right). \quad (38)$$

Mit  $V_M = M/d$  und  $(\delta)_1 = \delta_{32}^{(3)}$  sowie

$$K_2 = K'_2 \frac{d}{T^{1/2}} \exp \left( - \frac{\Delta U_2}{RT} \right) \quad (39)$$

$$K_3 = K'_3 \frac{d^2}{T^{3/2}} \exp \left( - \frac{\Delta U_3}{RT} \right) \quad (40)$$

gilt schließlich :

$$\delta = \delta_{32}^{(3)} + 2K'_2 \frac{d}{T^{1/2}} \exp\left(-\frac{\Delta U_2}{RT}\right) (\delta)_2 + 3K'_3 \frac{d^2}{T^{3/2}} \exp\left(-\frac{\Delta U_3}{RT}\right) (\delta)_3. \quad (41)$$

Bedeutung der Symbole :

- $\Delta U_{2,3}$  — molare Komplexbildungsenergien
- $V_M$  — Molvolumen
- $N_L$  — Loschmidtsche Konstante
- $M$  — Molmasse
- $d$  — Dichte
- $m$  — Teilchenmasse
- $r$  — Abstand der Teilchen im Zweierkomplex
- $I_{x,y,z}$  — Komponenten des Trägheitsmoments
- $k$  — Boltzmannkonstante
- $h$  — Planksches Wirkungsquantum

### Resultate und Diskussion

#### *Dichte- und Temperaturabhängigkeit der Abschirmkonstanten von Xenon in der Gasphase*

Mit den Untersuchungen von JAMESON, JAMESON und COHEN [16] zur Dichte- und Temperaturabhängigkeit der  $^{129}\text{Xe}$ -Abschirmung in der Gasphase liegt eine experimentelle Arbeit vor, die hervorragend geeignet ist zur Überprüfung theoretischer Modelle.

Die Autoren geben folgende Abhängigkeit der chemischen Verschiebung von Dichte und Temperatur an :

$$\delta = c_1(t)d + c_2(t)d_2 \quad (42)$$

$$c_1(t) = (0,536 - 0,135 \cdot 10^{-2} t + 0,132 \cdot 10^{-4} t^2 - 0,598 \cdot 10^{-7} t^3 + 0,663 \cdot 10^{-10} t^4) \text{ppm/amagat} \quad (43)$$

mit  $t = (T - 300) \text{ K}$  und  $1 \text{ amagat} = 5,85 \text{ g/L}$ .

$c_2(t)$  wird in Form einer Tabelle angegeben.

Nach Gl. (41) sollte für  $c_2$  gelten :

$$c_2 = 3 K'_3 T^{-3/2} (\delta)_3 \exp\left(-\frac{\Delta U_3}{RT}\right) \quad (44)$$

$$\ln(c_2 T^{3/2}) = \ln(3K'_3(\delta)_3) - \frac{\Delta U_3}{RT} \quad (45)$$

Der Zusammenhang (45) ist in Abb. 1 dargestellt. Die erhaltene Gerade hat einen Korrelationsfaktor von 0,99. Aus dem Anstieg ermittelt man eine Komplexbildungsenergie von  $-29,75$  kJ/mol. Da  $\delta_{32}^{(3)}$  in Gasen in guter Näherung linear von der Dichte abhängt, setzt sich  $c_1$  aus einem nicht von der Temperatur abhängigen Anteil  $c'_1$  und einem temperaturabhängigen Anteil  $c''_1$  additiv zusammen, wie man aus den Gleichungen (32) und (41) ersehen kann.

$$c_1(T) = c'_1 + c''_1(T) \quad (46)$$

$$\ln [(c_1 - c'_1) T^{1/2}] = \ln [2 \cdot 0,264 \cdot 5,85 K'_2(\delta)_2] - \frac{\Delta U_2}{RT}. \quad (47)$$

Die beste Gerade mit einem Korrelationsfaktor von 0,99 erhält man für  $c'_1 = 0,375$  ppm/amagat. (s. Abb. 2). Aus dem Anstieg der Geraden berech-

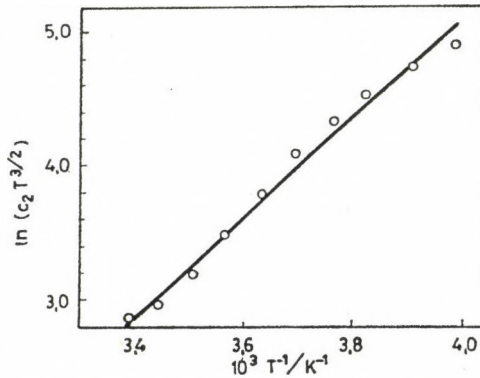


Abb. 1. Temperaturabhängigkeit des Koeffizienten  $c_2(T)$  in der Potenzreihenentwicklung der Mediumverschiebung nach der Dichte für Xenongas im Temperaturbereich zwischen 250 und 295 K

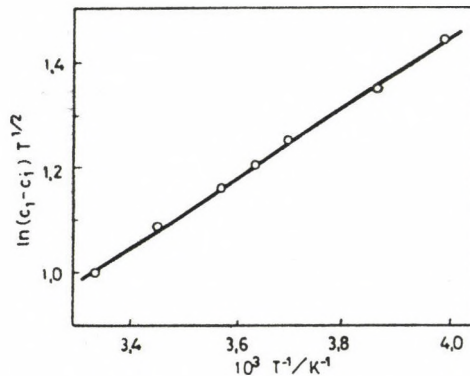


Abb. 2. Temperaturabhängigkeit des Koeffizienten  $c_1$  in der Potenzreihenentwicklung der Mediumverschiebung nach der Dichte für Xenongas im Temperaturbereich zwischen 250 und 300 K

net man eine Komplexbildungsenergie von  $-6,12$  kJ/mol. Ermittelt man  $K'_2$  unter der Annahme eines Xe-Xe-Abstandes von  $450$  pm (Minimum des LENNARD-JONES-Potentials [17]), so erhält man:

$$K'_2 = 3,286 \cdot 10^{-5} \text{ g}^{-1} \text{LK}^{-1/2} \quad (48)$$

Somit kann man aus dem Ordinatenabschnitt der Geraden (47) die chemische Verschiebung des Komplexes aus zwei Atomen bezogen auf freie Xe-Atome zu  $(\delta)_2 = 2237$  ppm berechnen (Faktoren in Gl. (47):  $0,264$  — natürliche Häufigkeit von  $^{129}\text{Xe}$ ;  $5,85$  — Umrechnung der Dichtemaßeinheit).

#### Dichteabhängigkeit der Gas-Flüssigkeitsverschiebung von $\text{P}_4\text{O}_6$

Die  $^{31}\text{P}$ -chemische Verschiebung von  $\text{P}_4\text{O}_6$  in der Gasphase wurde zu  $115,57$  ppm gegen externen Standard ermittelt (85%ige  $\text{H}_3\text{PO}_4$ ,  $T = 300$  K, Eichung über externen Lock. Die Temperaturabhängigkeit des Locks wurde eliminiert. Der angegebene Wert ist nicht susceptibilitätskorrigiert.). Eine Temperaturabhängigkeit konnte im Bereich zwischen  $450$  K (Linienbreite  $79$  Hz) und  $400$  K (Linienbreite  $140$  Hz) im Rahmen der durch die hohe Linienbreite eingeschränkten Meßgenauigkeit nicht festgestellt werden. Alle Messungen wurden bei  $36,44$  MHz durchgeführt. Für die Dichteabhängigkeit der

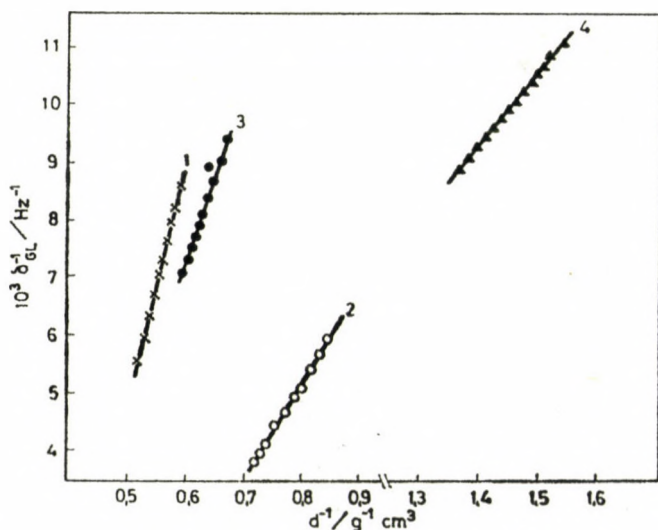


Abb. 3. Abhängigkeit der  $^{31}\text{P}$ -Gas-Flüssigkeitsverschiebung von der Dichte der Lösung. Die Werte sind susceptibilitätskorrigiert. (1)  $\text{P}_4\text{O}_6$  in Substanz, (2)  $\text{P}_4\text{O}_6$  in  $\text{CCl}_4$  ( $0,1$  M), (3)  $\text{P}_4\text{O}_6$  in  $\text{CS}_2$  ( $0,1$  M), (4)  $\text{P}_4\text{O}_6$  in *n*-Dodecan ( $0,1$  M)

Gas-Flüssigkeitsverschiebung ergeben sich die in Abb. 3 dargestellten Geraden:

$$-(\delta_{32}^{(3)})^{-1} 10^3 = \delta_{GL}^{-1} 10^3 = -15,91 (\text{Hz})^{-1} + 41,399 \text{ d}^{-1} \text{ g cm}^{-3} (\text{Hz})^{-1}$$

Korrelationsfaktor:  $r_{xy} = 0,997$  für  $\text{P}_4\text{O}_6$  in Substanz

$$-(\delta_{32}^{(3)})^{-1} 10^3 = \delta_{GL}^{-1} 10^3 = -11,49 (\text{Hz})^{-1} + 31,107 \text{ d}^{-1} \text{ g cm}^{-3} (\text{Hz})^{-1}$$

mit  $r_{xy} = 0,998$  für  $\text{P}_4\text{O}_6$  in  $\text{CCl}_4$

$$-(\delta_{32}^{(3)})^{-1} 10^3 = \delta_{GL}^{-1} 10^3 = -8,03 (\text{Hz})^{-1} + 16,438 \text{ d}^{-1} \text{ g cm}^{-3} (\text{Hz})^{-1}$$

mit  $r_{xy} = 0,998$  für  $\text{P}_4\text{O}_6$  in  $\text{CS}_2$

$$-(\delta_{32}^{(3)})^{-1} 10^3 = \delta_{GL}^{-1} 10^3 = -7,68 (\text{Hz})^{-1} + 12,074 \text{ d}^{-1} \text{ g cm}^{-3} (\text{Hz})^{-1}$$

mit  $r_{xy} = 0,999$  für  $\text{P}_4\text{O}_6$  in *n*-Dodecan.

Somit wird in unpolaren Medien, in denen das untersuchte  $\text{P}_4\text{O}_6$ -Molekül eine näherungsweise isotrope Umgebung besitzt, die Dichteabhängigkeit der Gas-Flüssigkeitsverschiebung durch Gl. (31) prinzipiell richtig beschrieben. Wie man aus dieser Gleichung ersieht, gilt für den Ordinatenabschnitt der Geraden:

$$c_0 = \frac{I_a + I_b}{I_a} \frac{a^2}{t} \quad (48)$$

$t$  ist eine Konstante des untersuchten Moleküls.

$(I_a + I_b)/I_a$  ist näherungsweise konstant gleich 2.

$$c_0 = 2a^3/t \quad (49)$$

Also muß der Hohlkugelradius  $a$  veränderlich sein. Für reines  $\text{P}_4\text{O}_6$  gilt die Beziehung (49) exakt.  $a^3$  kann man nach BÖTTCHER [15] in reinen unpolaren Substanzen aus der Abhängigkeit der Dielektrizitätskonstanten von der Dichte ermitteln. Das wurde für reines  $\text{P}_4\text{O}_6$  durchgeführt, wobei sich  $a^3 = 55,9 \cdot 10^{-24} \text{ cm}^3$  ergab. Damit erhält man  $t = 7,027 \cdot 10^{-21} \text{ cm}^3 \text{ Hz}$  bei 36,44 MHz. Somit ist es möglich,  $a^3$  für  $\text{P}_4\text{O}_6$  in den anderen Lösungsmitteln zu berechnen. Andererseits kann man  $a^{-3}$  als Erwartungswert der reziproken sechsten Potenz des Teilchenabstandes über die radiale Abstandsverteilungsfunktion betrachten:

$$a^{-3} \sim \int \frac{W(r)}{r^6} r^2 dr \quad (50)$$

In Flüssigkeiten ist das bei gegebener Dichte keine Funktion der Temperatur. Wenn man als untere Integrationsgrenze den Radius  $r_{00}$  setzt, der für das untersuchte Molekül charakteristisch ist, so erhält man:

$$a^{-3} \sim Z_{\text{eff}} r_{00}^{-3} \quad (51)$$

$Z_{\text{eff}}$  ist eine effektive Koordinationszahl. Für die Berechnung einer solchen Koordinationszahl schlagen BERNSTEIN und RAYNES [7] vor:

$$Z = \frac{\pi(r_a + r_b)^2}{r_b^2} \quad (52)$$

Dabei berechnen sie die Molekülradien von untersuchtem Molekül  $r_a$  und Lösungsmittelmolekül  $r_b$  aus dem Molvolumen nach der ONSAGER-Näherung. Das führt zu einer Dichteabhängigkeit von  $Z$ . Im hier beschriebenen Modell wird die Dichteabhängigkeit der Abschirmung durch die Dichteabhängigkeit der Dielektrizitätskonstanten beschrieben. Deshalb darf  $Z$  keine Funktion der Dichte sein. Das erreicht man dadurch, daß man für  $r$  die Molekularradien nach BÖTTCHER [15] einsetzt. Dabei erhält man die in Tabelle I zusammengestellten Ergebnisse.

Trägt man nun die aus den NMR-Experimenten erhaltenen Werte von  $a^{-3}$  gegen die Koordinationszahl  $Z$  auf (Abb. 4), so erhält man die Gerade  $a^{-3} = (-5,293 + 1,967 Z)\text{nm}^{-3}$  mit einem Korrelationsfaktor  $r_{xy} = 0,9999$ . Damit ist es möglich, die Koordinationszahl von  $\text{P}_4\text{O}_6$  in  $n$ -Dodecan zu bestimmen. Man ermittelt  $Z = 21,6$ . Eine solch hohe Koordinationszahl ist nur möglich, wenn die  $n$ -Dodecanmoleküle das  $\text{P}_4\text{O}_6$ -Molekül mit den Kettenenden umgeben. Dieses Verhalten sollten dann alle genügend langkettigen  $n$ -Alkane zeigen. Deshalb kann man annehmen, daß  $a^{-3}$  in  $n$ -Alkanen eine Konstante ist.

Wenn man die charakteristischen Frequenzen  $\nu_b$  der Lösungsmittel durch die langwelligen UV-Absorptionsgrenzen ausdrückt, verbleibt in Gl. (31) als

Tabelle I

Molekülradien  $r$ , Koordinationszahlen  $Z$  und Böttcherradien  $a$  für  $\text{P}_4\text{O}_6$  in verschiedenen Lösungsmitteln

Lösungsmittel	$r$ in pm	$Z$	$a$ in pm
$\text{P}_4\text{O}_6$	382	12,56	382
$\text{CCl}_4$	305 [15]	15,94	343*
$\text{CS}_2$	236 [15]	31,54	304*
$n$ -Dodecan	—	—	300*

\* Aus den Ordinatenabschnitten in Abb. 3 berechnet

einzig unbekannt Größe die mittlere Frequenz  $\bar{\nu}$ . Für  $P_4O_6$  in *n*-Dodecan läßt sich  $\bar{\nu}$  aus der Dichteabhängigkeit der chemischen Verschiebung berechnen. Es ist aber infolge der enthaltenen Mittelung nicht anzunehmen, daß  $\bar{\nu}$  vom Lösungsmittel unabhängig ist. Für ähnliche Lösungsmittel kann man erwarten, daß  $\bar{\nu}^2$  sich in eine Potenzreihe nach  $\nu_b$  entwickeln läßt und das erste

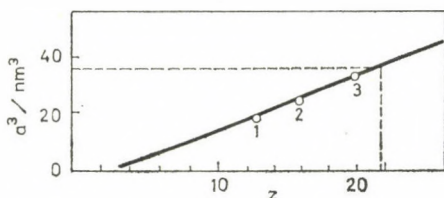


Abb. 4. Abhängigkeit der reziproken dritten Potenz des Böttcherradius von der Koordinationszahl für  $P_4O_6$  in verschiedenen Lösungsmitteln. 1:  $P_4O_6$  in Substanz, 2:  $P_4O_6$  in  $CCl_4$ , 3:  $P_4O_6$  in  $CS_2$

Tabelle II

Experimentelle und berechnete  $^{31}P$ -chemische Verschiebungen  $\delta_{GL}$  von  $P_4O_6$  in *n*-Alkanen

Lösungsmittel	UV-Limits in nm	$\delta_{GL, exp}^*$ in Hz		$\delta_{GL, ber}^*$ in Hz	
			$\bar{\nu}^2 \sim \nu_b^2$	$\bar{\nu}^2 \sim \nu_b$	$\bar{\nu} = konst$
<i>n</i> -Hexan	170	107	97,8	107	118,1
<i>n</i> -Oktan	171	113,9	107,8	114,9	121,2
<i>n</i> -Decan	172,5	117,6	114,4	116,1	118,2
<i>n</i> -Dodecan	173	118,8	118,8	118,8	118,8

\*  $\delta_{GL} = \delta_{L\ddot{o}s} - \delta_{Gas}$ . Die chemischen Verschiebungen gelten für eine Meßfrequenz von 36,44 MHz. Die experimentellen Werte sind susceptibilitätskorrigiert

Glied der Entwicklung ausreichend ist. Es ergeben sich die Möglichkeiten:  $\bar{\nu}^2 = konst$ ,  $\bar{\nu}^2 \sim \nu_b$  und  $\bar{\nu}^2 \sim \nu_b^2$ . Für diese Fälle wurden die Gas-Flüssigkeitsverschiebungen für  $P_4O_6$ -Lösungen in *n*-Alkanen bei 24 °C vorausberechnet und den experimentellen Ergebnissen in Tabelle II gegenübergestellt. Für den Fall  $\bar{\nu}^2 \sim \nu_b$  ergibt sich eine sehr gute Übereinstimmung.

Somit ist die prinzipielle Anwendbarkeit der vorgelegten Theorie an experimentellen Ergebnissen nachgewiesen. Es wurden aber auch die Grenzen deutlich, die die Vorausberechnung der Dichteabhängigkeit der chemischen Verschiebung bei Wechsel des Lösungsmittels erschweren.

#### LITERATUR

- [1] DICKINSON, W. C.: Phys. Rev., **81**, 717 (1951)
- [2] BOTHNER-BY, A. A., GLICK, R. E.: J. Am. Chem. Soc., **78**, 1071 (1956)
- [3] MARSHALL, T. W., POPLER, J. A.: Mol. Phys., **1**, 199 (1958)

- [4] STEPHEN, M. J.: *Mol. Phys.*, **1**, 223 (1958)
- [5] RAYNES, W. T., BUCKINGHAM, A. D., BERNSTEIN, H. J.: *J. Chem. Phys.*, **36**, 3481 (1962)
- [6] POHLE, U.: Dissertation, Technische Universität Dresden 1979
- [7] BERNSTEIN, H. J., RAYNES, W. T.: Presented at the NMR Symposium Boulder (Colorado) 1962; Ref.: *NMR Basic Principles and Progress*, **10**, Springer-Verlag Berlin 1975, p. 27
- [8] DE MONTGOLFIER, PH.: *J. Chim. Phys.*, **64**, 639 (1967)
- [9] RUMMENS, F. H. A.: *J. Chim. Phys.*, **72**, 448 (1975)
- [10] LINDER, B.: *J. Chem. Phys.*, **33**, 668 (1960)
- [11] RAMSAY, N. F.: *Phys. Rev.*, **73**, 339 (1950)
- [12] RAMSAY, N. F.: *Phys. Rev.*, **86**, 243 (1952)
- [13] DALGARNO, A., STEWART, A. L.: *Proc. Roy. Soc.*, **A247**, 245 (1958)
- [14] ONSAGER, L.: *J. Am. Chem. Soc.*, **58**, 1486 (1936)
- [15] BÖTTCHER, C. J. W.: *Theorie of Electric Polarization*, Vol. **1**, Elsevier Scientific Publishing Company, Amsterdam 1973
- [16] JAMESON, C. J., JAMESON, A. K., COHEN, S. M.: *J. Chem. Phys.*, **59**, 4540 (1973)
- [17] MASON, E. A.: *J. Chem. Phys.*, **23**, 49 (1954)

Ulrich POHLE            }   Sektion Chemie der Technischen Universität  
Gisbert GROSSMANN    }   Dresden, DDR-8027 Dresden, Mommsenstr. 13.



## SIMULATION OF THE INSTABILITIES OBSERVED IN POTENTIOSTATIC STUDIES OF ACTIVE–PASSIVE TRANSITION

B. LENGYEL\* and L. MÉSZÁROS

*(Research Laboratory for Inorganic Chemistry, Research Group of Electrochemistry  
and Corrosion, Hungarian Academy of Sciences, Budapest)*

Received July 7, 1981

Accepted for publication September 4, 1981

The instability occurring in the potential range of active–passive transition in the anodic polarization of metals was studied by means of a dummy cell simulating the polarization curve. The oscillatory behaviour was found to depend on the transfer properties of the potentiostat and on the impedance of the measuring cell.

Current oscillations were often observed in potentiostatic studies of passivable metals in the potential range corresponding to active–passive transition [1–8]. This phenomenon, however, was not reported by several other authors engaged in studies of metal passivity [9–17].

WOJTOWICZ [18] recently published an excellent review of the works on the chemical and electrochemical causes of oscillations. It is believed that oscillation phenomena are caused by the combined effect of consecutive interfacial and diffusion processes.

Oscillatory behaviour of electrochemical systems have been studied by several authors recently. HORÁNYI *et al.* [19] noted that under suitable conditions electrochemical oscillations could occur even without polarizing current. JEHRING *et al.* studied oscillation phenomena caused by the inhomogeneity of surface tension [20], and by the negative resistance encountered during the potential dependent adsorption of an inhibitor on a mercury electrode [21].

The control characteristics of potentiostats were widely studied during the development of modern potentiostatic techniques as the cell impedance constituting the negative feed-back circuit considerably affects the stability of the measuring system [22–24]. The study of the stability of such systems is especially important in the case of potentiostats with  $iR$  compensation, as the transfer characteristics and the stability can considerably deteriorate when positive feed-back is combined with negative feed-back [25–28]. It was generally assumed in the above studies that the real part of the cell impedance is positive, while the imaginary part is negative *i.e.* capacitive. However, the polarization curves of various electrode processes exhibit negative  $AC$  differential resistance in certain potential range, *i.e.* the current density decreases

\* To whom correspondence should be addressed

as the potential is increased. This phenomenon can be observed in the active—passive transition region of the anodic polarization curves of passivating metals [29].

According to SALIE [30] an impedance having a negative real part is encountered in the cases of anomalous potential and coverage dependence of the rate of reactions, *e.g.* in processes with short-lived intermediates at least one symmetry factor must be negative.

WOJTOWICZ [18] also reported on spontaneous oscillations due to a negative impedance.

Negative differential resistance can also cause the instability of the potentiostatic measuring system in addition to spontaneous oscillations. Thus it was deemed interesting to study whether or not the instability of the measuring system consisting of the potentiostat and cell contributed to the generation of oscillations when electrochemical effects were excluded.

The potentiostat is essentially an amplifier with a large negative feedback, the latter being constituted by the measuring cell. Consequently an integral system is formed by the potentiostat and the cell, the former having a relatively wide-band frequency response and the latter corresponding to an equivalent circuit composed of frequency dependent elements. The transfer properties of the system are determined mainly by the impedance of the measuring cell, assuming that the potentiostat does not cause linear distortion in the case of pure ohmic load *i.e.* the gain and phase characteristics of the potentiostat are frequency independent in a wide frequency range. These are essential conditions of the potentiostatic technique where the input voltage controlling the potentiostat (polarizing voltage) and the output current generated by it (the current flowing through the cell) are measured and recorded. In other words, the polarizing curve is the relationship between the input voltage and output current of the system consisting of the potentiostat and the measuring cell, where the latter constitutes the feed-back circuit.

The basic potentiostatic circuit is shown in Fig. 1a. Differential amplifier *A* is controlled by voltage  $E_1$  at the non-inverting input. Output voltage  $E_3$  is connected to the measuring cell. The cell current is denoted by *J*. Voltage  $E_2$  developed between the reference and the working electrode is applied to the inverting input of the differential amplifier. This constitutes the negative feed-back. The following relationship exists [22] between voltages  $E_2$ , and  $E_1$ :

$$E_2 = \frac{A\beta}{1 + A\beta} E_1 \quad (1)$$

where  $\beta$  is the feed-back factor

$$\beta = \frac{E_2}{E_3} = \frac{Z}{R_k + Z} \quad (2)$$

The equivalent circuit of the cell is shown in Fig. 1b. The impedance of an auxiliary electrode with a sufficiently large surface area can be neglected. Thus the resistance compensated by the potentiostat consists of the resistance

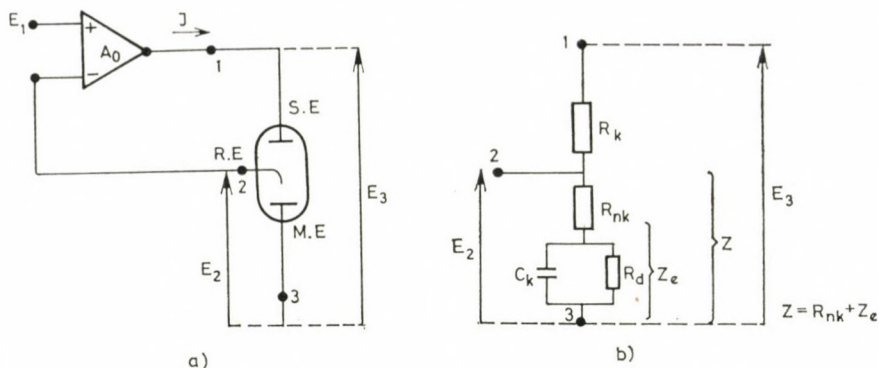


Fig. 1a. Block diagram of the potentiostatic circuit; b. equivalent circuit of the measuring cell

of the solution between the auxiliary and the reference electrodes ( $R_k$ ). Impedance  $Z$  between the reference and working electrodes is the sum of electrode impedance  $Z_e$  and uncompensated solution resistance  $R_{nk}$ . The cell impedance constitutes a voltage divider between the output voltage  $E_3$  and  $E_2$ .

The condition for the correct functioning of the potentiostat is that 1 is negligible as compared to  $A\beta$ , i.e.,

$$|A\beta| \gg 1 \quad (3)$$

thus

$$E_2 = \frac{A\beta}{1 + A\beta} E_1 \approx E_1 \quad (4)$$

i.e. the potential difference between the reference and working electrodes is very nearly equal to the control voltage of the potentiostat ( $E_1$ ).

However, both  $A$  and  $\beta$  depend on frequency. The absolute value of both quantities decreases as the frequency is increased. It can also occur that the negative feed-back voltage becomes positive, because of the frequency dependence of the phase shift and the system becomes unstable i.e. undesirable oscillation may be set up. The problems concerning the stability of feed-back amplifiers are well known in literature (cf. BODE [31]).

In the present communication the low-frequency oscillatory behaviour of electrochemical systems is studied in the potential range of the active—passive transition. In this potential range the current—voltage curve exhibits

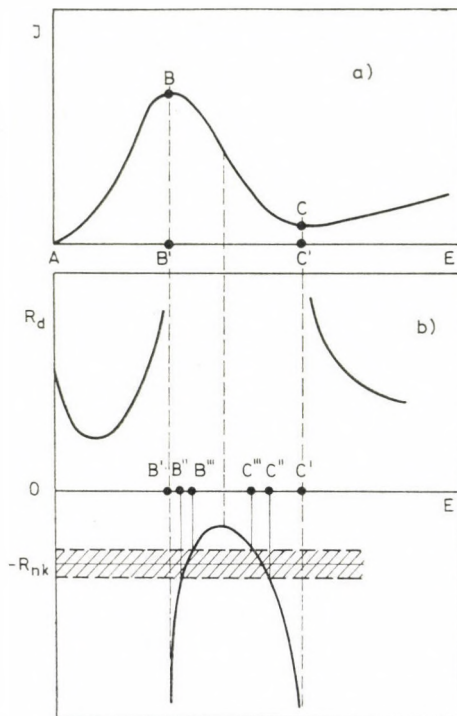


Fig. 2a. Current—voltage characteristics of the dummy cell; b. variation of the differential resistance  $R_d$  with the potential

negative AC resistance. If the differential (AC) resistance is negative (Fig. 2)

$$R_d = \frac{dE}{dJ} < 0, \quad (5)$$

the feed-back factor

$$\beta = \frac{Z}{R_k + Z} = \frac{R_d + R_{nk}}{R_k + R_{nk} + R_d} \quad (6)$$

may become positive. (As this type of oscillation occurs mainly at very low frequencies, the double layer capacity is neglected in Eq. (6) as a first approximation.) The transfer coefficient of the potentiostat ( $E_2/E_1$ ) can be obtained by combining Eqs (6) and (1)

$$\frac{E_2}{E_1} = \frac{A_0 (R_d + R_{nk})}{R_k + R_d + R_{nk} + A_0 (R_d + R_{nk})} \quad (7)$$

where  $A_0$  is the low-frequency (frequency independent) gain of the differential amplifier. It is apparent from Eq. (7) that the potentiostat operates normally

when

$$|A_0(R_d + R_{nk})| \gg |R_k + R_d + R_{nk}| \quad (8)$$

as in this case  $E_2/E_1 \approx 1$  regardless of the sign of  $R_d + R_{nk}$ . If the above condition is not satisfied electrode potential  $E_2$  does not follow control voltage  $E_1$  i.e. either

$$E_2/E_1 < 1 \quad (9) \quad \text{or} \quad E_2/E_1 > 1 \quad (10)$$

depending on the values of  $R_d, R_{nk}, R_k$  and  $A_0$ . In both cases, so-called relaxation oscillation can occur i.e. the electrode potential set in the range of negative differential resistance (cf. Fig. 2) is shifted either to a larger potential or a smaller one depending on the condition expressed by either Eq. (9) or Eq. (10) in order to satisfy the stability conditions. However, in this instance potential  $E_2$  is set again to an unstable value and the above process is repeated.\*

In addition to relaxation oscillations a high-frequency instability (oscillation) can also occur in many cases due to the frequency dependence of both the absolute value and the phase of  $\beta A$ . The high-frequency current is rectified because of the non-linear current—voltage characteristics of the cell and the electrode current is increased by this DC component and consequently the polarization curve is distorted.

The instability conditions are shown in Fig. 2. Figure 2a represents the polarization curve modelling the active—passive transition, while the differential resistance  $R_d = dE/dJ$  as a function of the polarizing voltage is shown in Fig. 2b. It is apparent that the differential resistance is negative in region B—C. Uncompensated resistance  $R_{nk}$  is shown in the Figure with a negative sign. At given  $R_k$  and  $R_{nk}$  values the stability condition given by Eq. (8) is satisfied outside the hatched area, and relaxation oscillation does not occur ( $B'B''$ ,  $B'''C'''$ ,  $C''C'$ ). Whereas in regions  $B''B'''$  and  $C'''C''$  the above stability condition is not satisfied and relaxation oscillation is generated. It is also clear from the Figure that the position and width of the above potential ranges can be changed by varying  $R_{nk}$ , and if  $R_{nk}$  is sufficiently decreased the instability can even be eliminated. The width of the stability and instability regions respectively depends on the value of compensated resistance  $R_k$  according to Eq. (8). The instability regions  $B''B'''$  and  $C'''C''$  are broadened as  $R_k$  is increased whereas relaxation oscillations are considerably diminished by a decrease in  $R_k$ . Figure 3 represents a polarization curve illustrating the above considerations.

In order to verify the above considerations a dummy cell was constructed having a current—voltage characteristics similar to the stationary polarization curves observed in passivation studies (Fig. 4).

\* It should be noted that the stability conditions are also affected by the double layer capacity [32] which has been neglected in these considerations, however, the above discussion remains qualitatively valid in the present case.

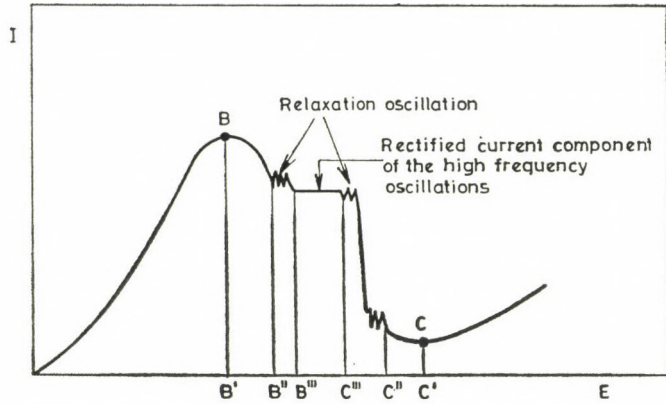


Fig. 3. The current—voltage characteristics expected on the basis of theoretical considerations

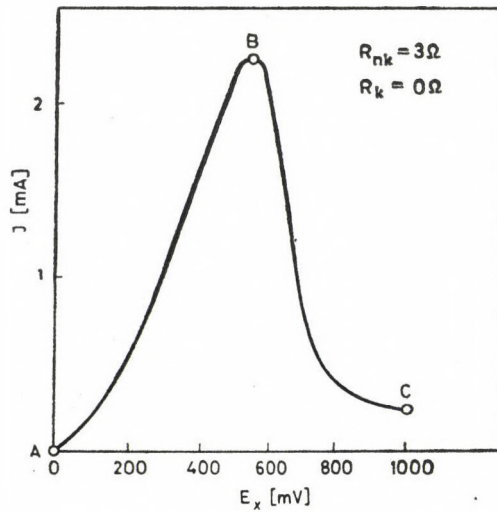


Fig. 4. The current—voltage characteristics of the circuit in Fig. 5

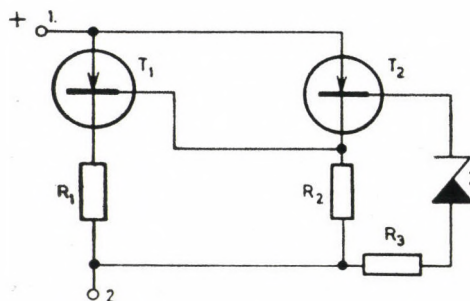


Fig. 5. Circuit of the dummy cell modelling the active—passive transition

The differential resistance is positive ( $R_d = dE/dJ > 0$ ) in region  $A - B$  of the curve, whereas it is negative ( $R_d = dE/dJ < 0$ ) in region  $B - C$ . The latter corresponds to the active—passive transition.

The circuit diagram of the above set-up is shown in Fig. 5. If the input voltage impressed between points 1 and 2 is increased the current initially increases also. However, when the current of transistor  $T_2$  is increased above a certain limit the voltage on resistance  $R_2$  gradually cuts off transistor  $T_1$ , which in turn causes a decrease of the current flowing through the circuit, *i.e.* the circuit exhibits a negative differential resistance in this range. The above circuit modelling the polarization curve of a working electrode of differential resistance  $R_d$ , connected in series with resistance  $R_{nk}$  and  $R_k$  simulated the electrochemical cell in the usual potentiostatic experiment as shown in Fig. 6, where  $C$  is the capacity of the double layer, variable resistance,  $R_{nk}$  is the uncompensated cell resistance while  $R_k$  is the cell resistance compensated by the potentiostat.

Experiments were carried out in order to study the effect of resistances  $R_{nk}$  and  $R_k$  and capacity  $C$  on the current—voltage characteristics of the above circuit.

Type Tacussel PIT 20 — 2X and Jaisse 1000 T potentiostats respectively were employed in the measurements. The voltage across the impedance between points 2 and 3 ( $E_y$ ), which corresponds to the electrode potential and the potential across resistance  $R_{nk}$  proportional to current ( $J$ ) were recorded with an  $X - Y_1 - Y_2$  recorder as a function of the control voltage of the potentiostat ( $E_x$ ) impressed by means of function generator  $G$ . The uncompensated resistance  $R_{nk}$  was used as a measuring resistance. The results obtained with the Tacussel potentiostat are represented in Figs 7—9 while Figs 11—14 show the plots obtained with the Jaisse potentiostat.

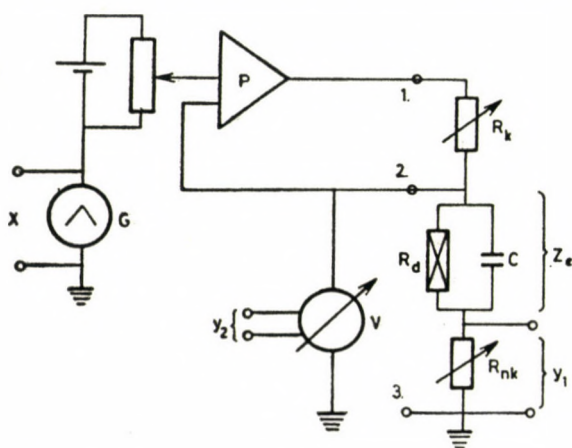


Fig. 6. Block diagram of the measuring system

The effect on the current—voltage curve of the variation of resistance  $R_k$  between 0 and 3 k $\Omega$  is shown in Fig. 7 in the case of  $R_{nk} = 3\Omega$  and  $C = 0$ . It is apparent that the distortion of the curve became more marked in the negative resistance range when  $R_k$  was increased in accordance with Eq. (8),

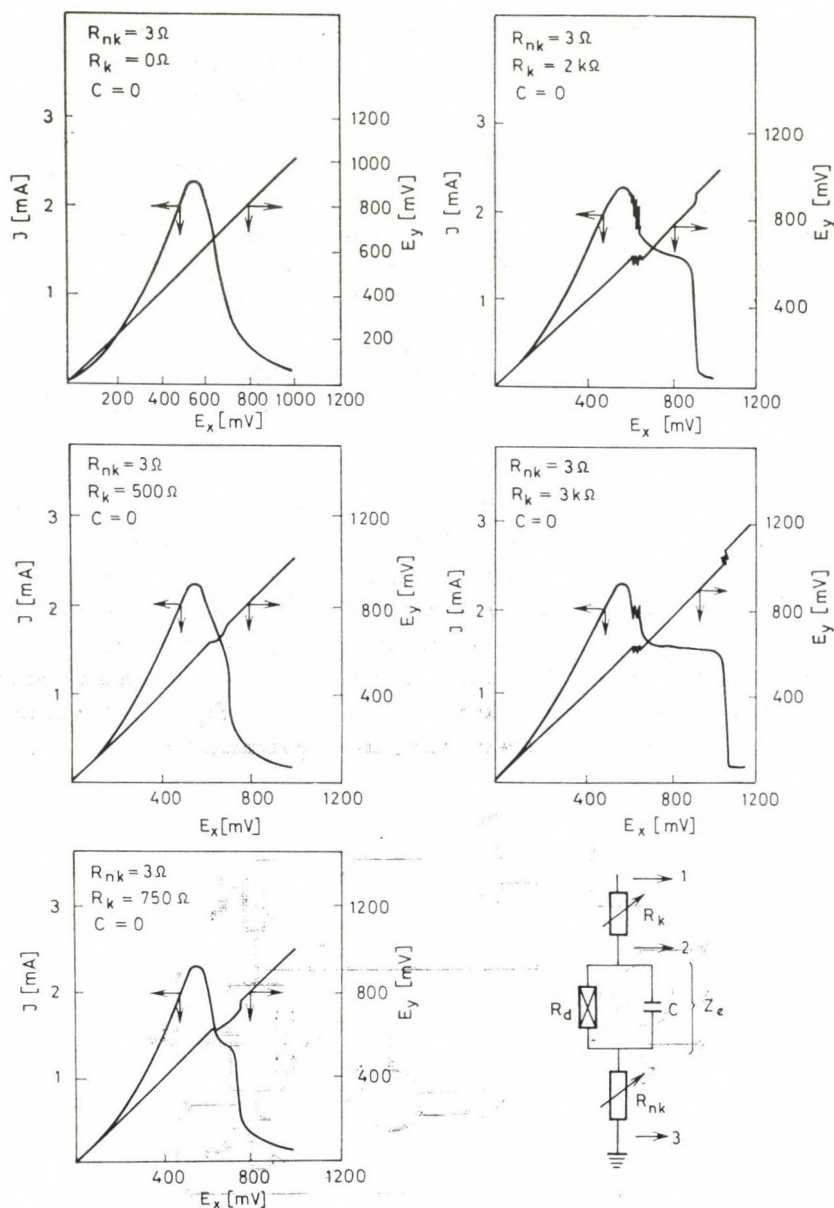


Fig. 7. Current—voltage characteristics at different  $R_k$  values measured with type PIT 20 — 2X Tacussel potentiostat

e.g. at  $R_k = 2 \text{ k}\Omega$  current and potential oscillations could be observed. It is also apparent that in this case the voltage across resistance  $R_k + R_{nk}$  ( $E_y$ ) and the control voltage of the potentiostat ( $E_x$ ) differed in the negative resistance range i.e., the potentiostat could not stabilize the potential in this region.

The effect of the variation of  $R_{nk}$  between  $3 \Omega$  and  $100 \Omega$  on the potential and current oscillations is shown in Fig. 8 for the case of  $R_k = 3 \text{ k}\Omega$ .

It is apparent that the potential range of relaxation oscillations decreased as  $R_{nk}$  was increased. The oscillations totally disappeared at sufficiently large values of  $R_{nk}$ , however, the current—voltage curve was distorted in the region of negative differential resistance by the rectified current component of high-frequency oscillations. The decrease in the susceptibility to relaxation oscillations of the system can be explained by the following consideration. The increase of  $R_{nk}$  reduced regions  $B''B'''$  and  $C'''C''$  where relaxation oscillations occurred according to Fig. 2b.

The effect on the oscillatory behaviour of capacitor  $C$  simulating the electrochemical double layer is shown in Fig. 9.

It can be observed that both the relaxation and high-frequency oscillations decreased as the capacity was increased. The difference between the potential across impedance  $Z_e + R_{nk}(E_y)$  and the control voltage of the potentiostat ( $E_x$ ) decreased as the capacity  $C$  was increased. A distortion-free current—voltage curve was obtained with a capacitor of  $10 \mu\text{F}$  as shown in (Fig. 4). The decrease in the tendency of oscillations can be explained in terms of the shunting and phase-shifting effects of the capacitor connected in parallel to the negative  $AC$  resistance.

As it has already been mentioned, the development of undesirable oscillations is considerably influenced also by the gain ( $A$ ) of the potentiostat.

In order to study the latter effect the above-mentioned measurements were also carried out with type Jaissle 1000 T potentiostat. A built-in phase correcting circuit permitted the variation of the frequency response characteristics of this potentiostat. The switch of phase corrector had 8 positions.

The frequency response characteristics of the system are shown in Fig. 10 at various positions of the phase corrector.

The gain of the potentiostat with an ohmic load at  $\beta = 1$  was plotted as the function of the frequency in the Figure. It is apparent that the frequency response of the potentiostat was practically constant in the frequency range from 1 to 10 kHz, independently of the position of the phase corrector. In the range from 10 to 100 kHz the gain was found to vary as the position of the phase corrector was changed.

Results obtained with the dummy cell are shown in Figs 11 to 14. The effect of the variation of resistance  $R_k$  is represented in Fig. 11, for the case of  $R_{nk} = 3 \Omega$  and  $C = 0$ , in position 1 of the phase corrector. It is apparent that the increase of  $R_k$  above  $1 \text{ k}\Omega$  caused a distortion in the current—voltage

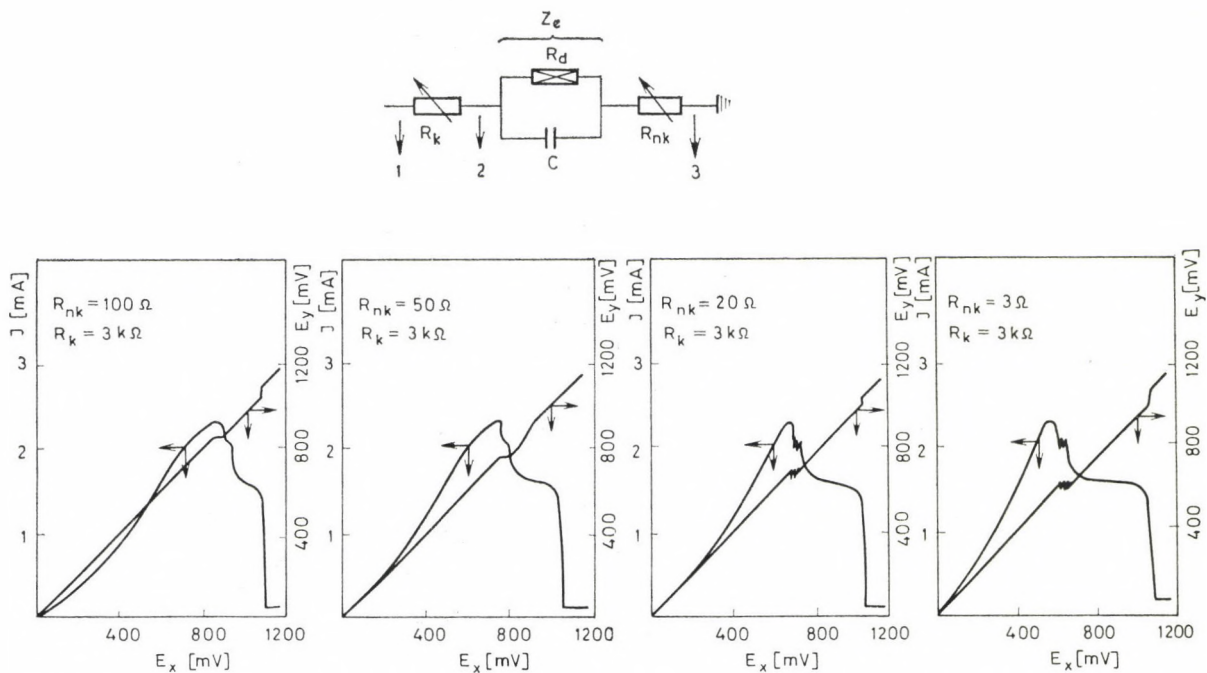


Fig. 8. Current—voltage characteristics at different  $R_{nk}$  values measured with type PIT 20 — 2X Tacussel potentiostat

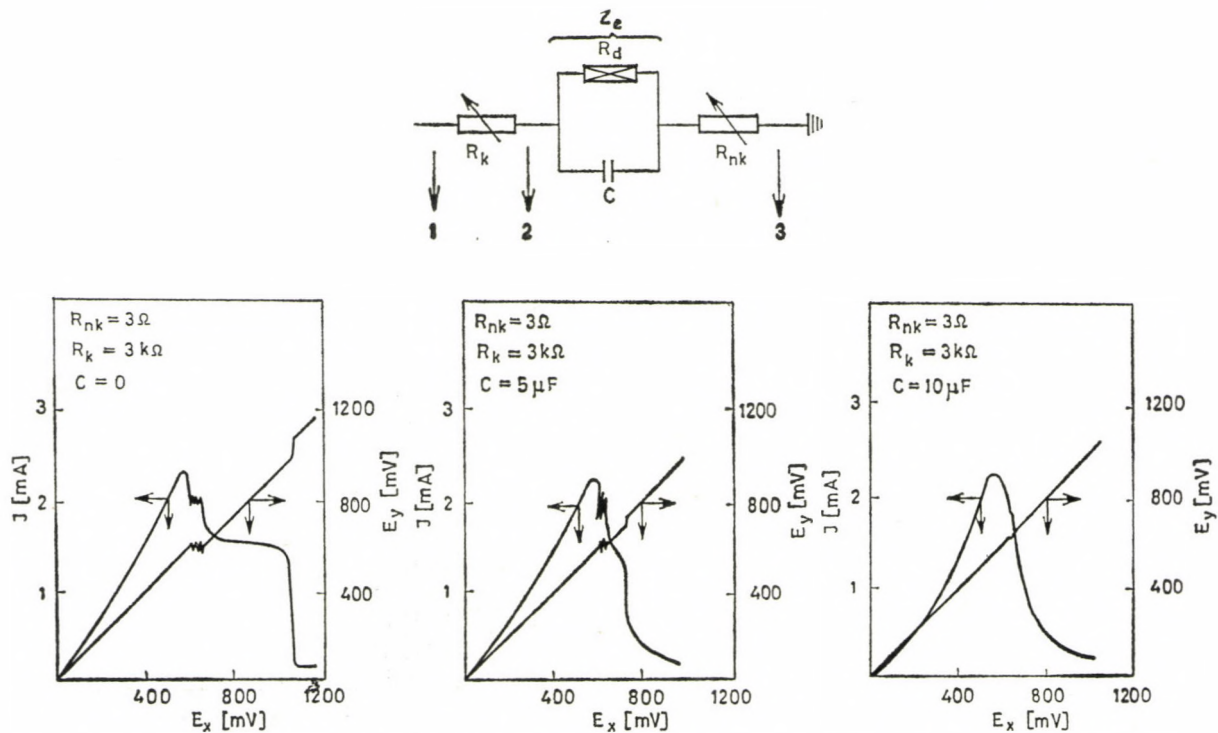


Fig. 9. Current-voltage characteristics at different  $C$  values measured with type PIT 20 - 2X Tacussel potentiostat

curve in the range of negative differential resistance, due to the rectified current component of high-frequency oscillations occurring in this region. Relaxation oscillations were also observed if resistance  $R_k$  was larger than 3 k $\Omega$ . The potential across impedance  $Z_e + R_{nk}(E_y)$  and the control voltage ( $E_x$ ) significantly differ in this case. Comparing the latter results with the curves in Fig. 7, it can be concluded that high-frequency oscillations are generated at higher values of resistance  $R_k$  when type Jaisle potentiostat was employed. As expected, both potentiostats were unsuitable for the stabilization of the potential in the range of negative differential resistance.

Results obtained with various phase corrector positions are shown in Fig. 12. It is apparent that the variation of the frequency response characteristics affected both relaxation oscillations and high-frequency oscillations as well as the difference between the control voltage and the potential across impedance  $Z_e + R_{nk}$ .

The effect of the capacity on the oscillatory behaviour is shown in Fig. 13. It is clear from the Figure that the tendency of both relaxation oscillations and high-frequency oscillations at identical phase corrector positions decreased as the capacity was increased. This effect is due to the shunting effect of the latter.

The effect of the variation of the frequency response characteristics under the same conditions as in the above experiment is shown in Fig. 14. The

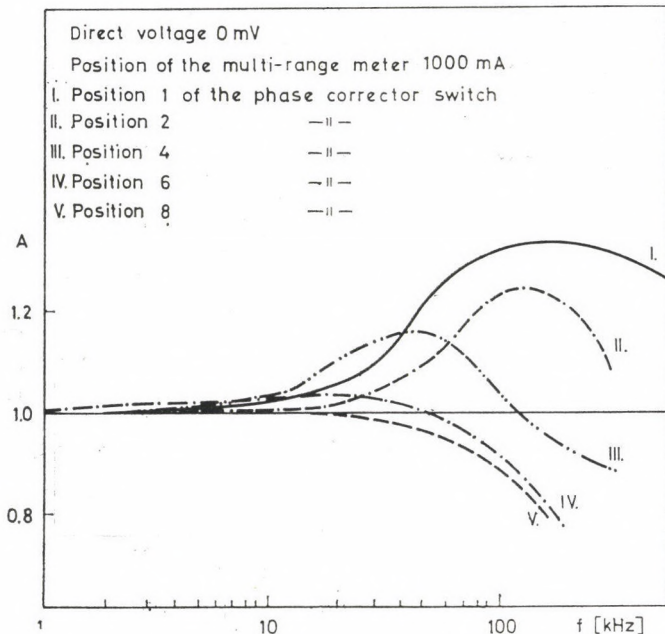


Fig. 10. The frequency response of type 1000 T Jaisle potentiostat measured across an ohmic resistance at  $\beta = 1$

improper choice of the frequency response can considerably counteract the effect of the capacity namely the decrease of the oscillations. The above results are in accordance with theoretical considerations predicting that relaxation oscillations and high-frequency oscillations can also occur in the absence of

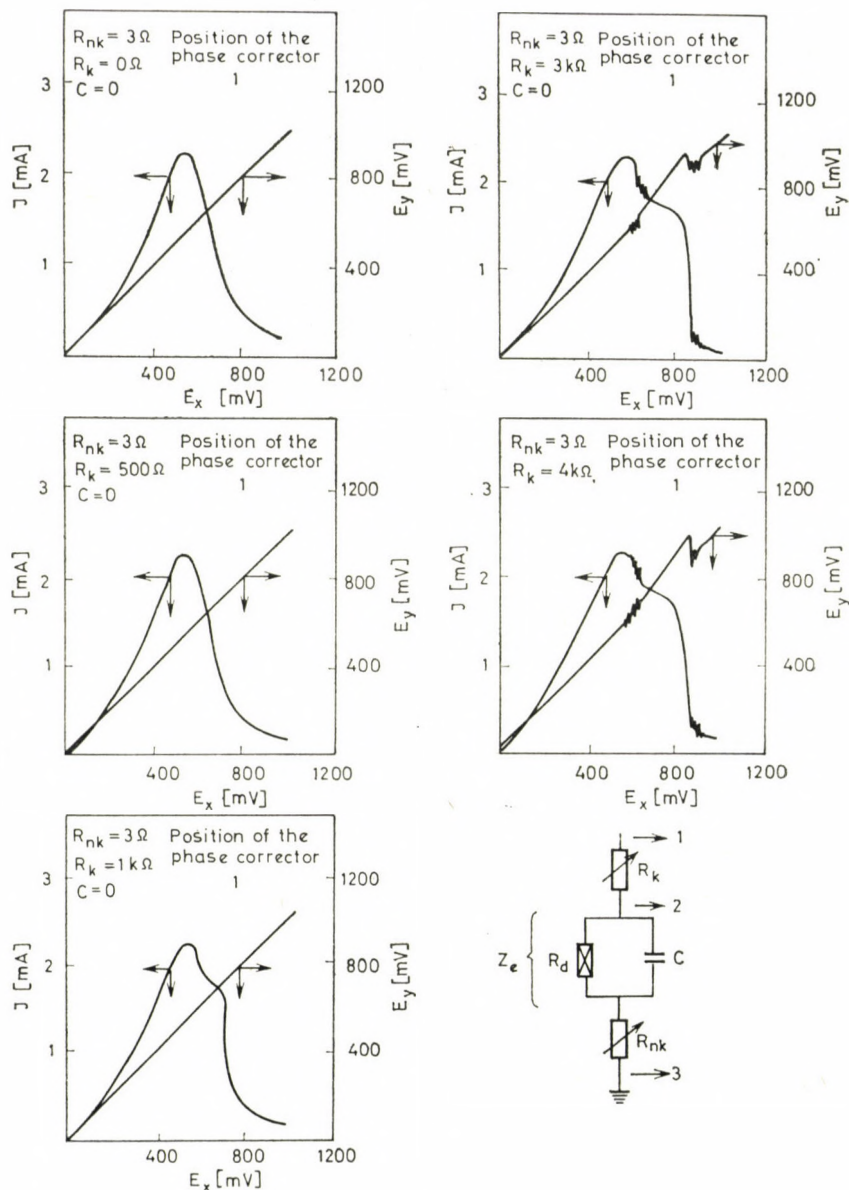
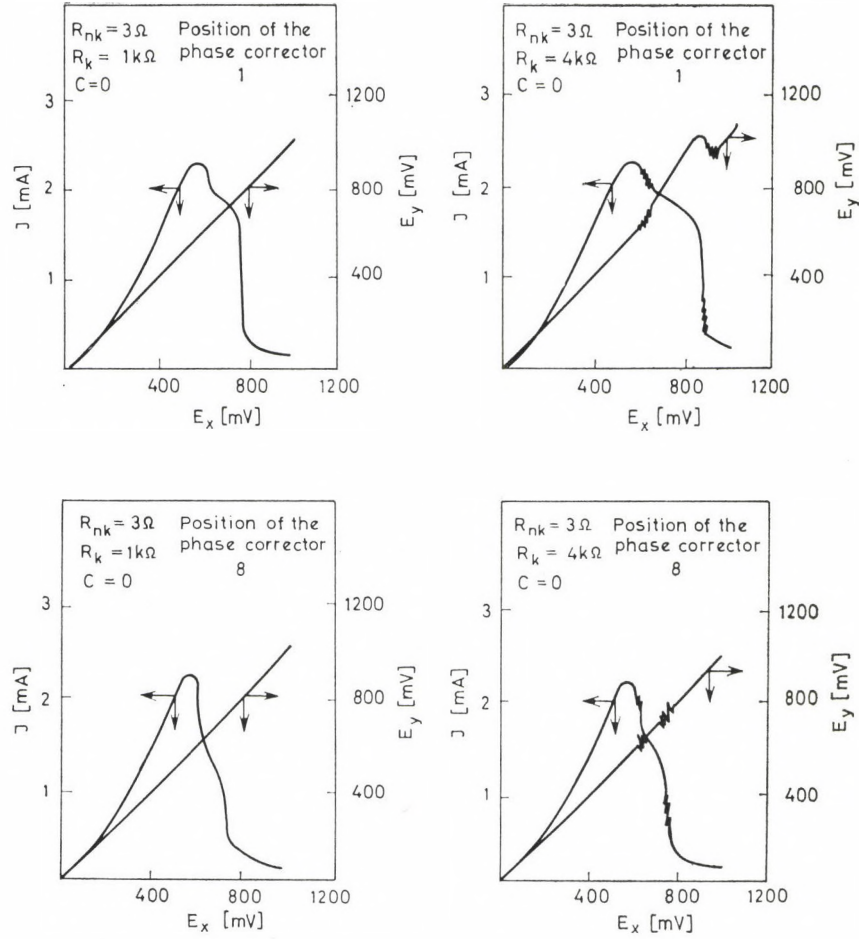
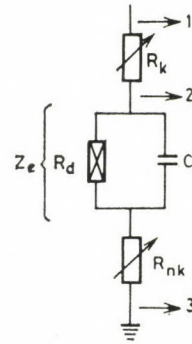


Fig. 11. Current-voltage characteristics at various  $R_k$  values measured in the first position of the phase corrector with type 1000 T Jaislle potentiostat



**Fig. 12.** Current—voltage characteristics at various  $R_k$  values in positions 1 and 8 respectively of the phase corrector measured with type 1000 T Jaisle potentiostat



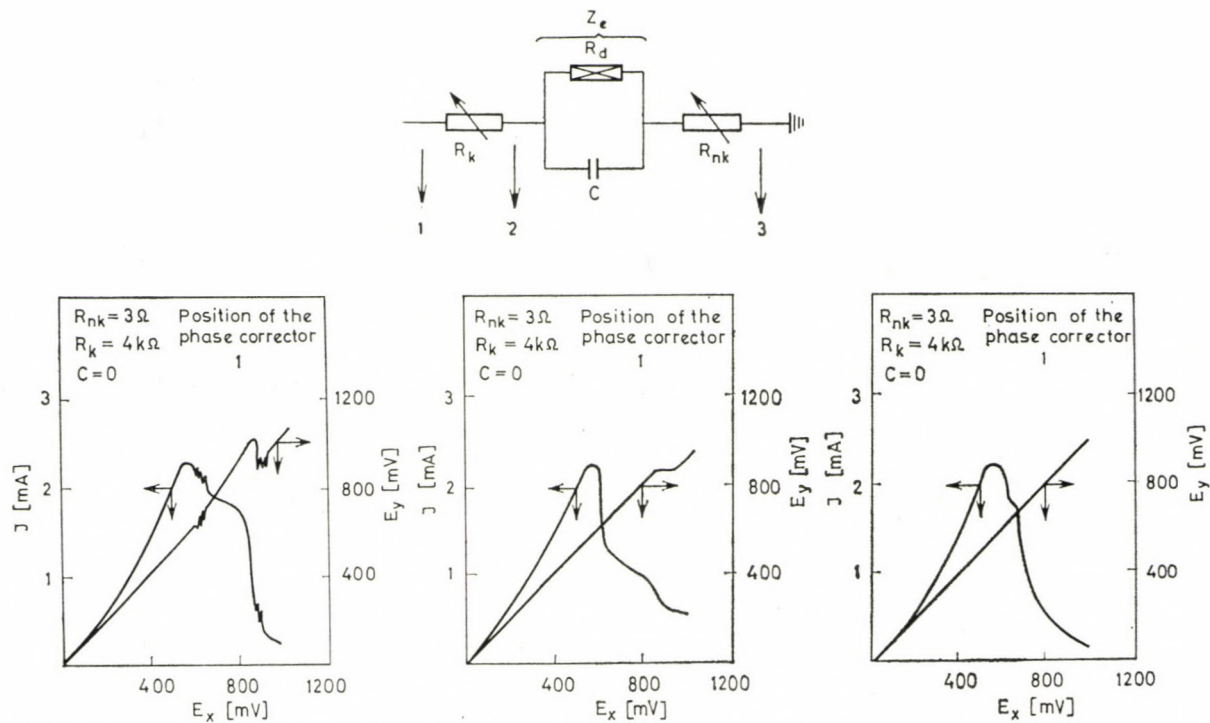


Fig. 13. Current—voltage characteristics at various  $C$  values in position 1 of the phase corrector measured with type 1000 T Jaisse potentiostat

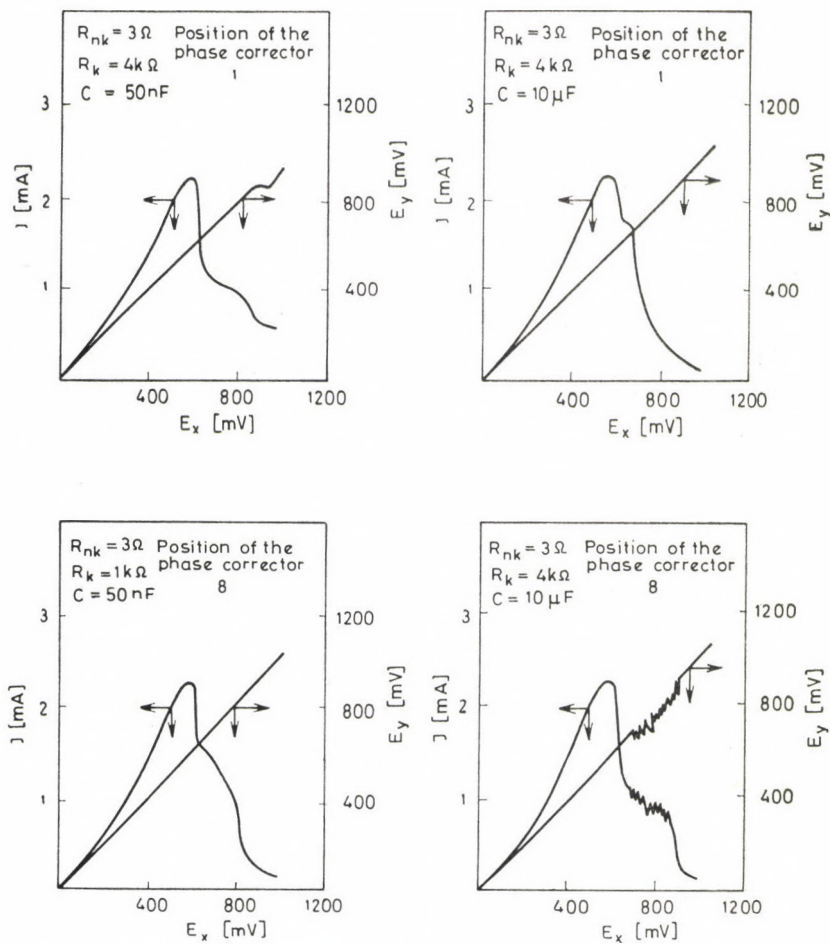


Fig. 14. Current-voltage characteristics at various  $C$  values in positions 1 and 8 respectively of the phase corrector measured with type 1000 T Jaisse potentiostat

electrochemical reactions, as a consequence of the instability of the feed-back system in the range of negative differential resistance. Accordingly, the results obtained in the cases of circuits having critical stability are considerably affected by the response characteristics of the potentiostat and the impedance of the measuring cell. The cell can be considered as a critical circuit in passivity studies where, in addition to chemical effects, the electric parameters of the potentiostat and the measuring cell may also influence the instabilities occurring in the active—passive transition. Therefore, when oscillations phenomena are observed in potentiostatic conditions, it should carefully be studied whether the phenomenon is caused by the instability of the measuring system or by the electrochemical process.

## REFERENCES

- [1] DOSS, K. S. G., DESHMUKH, D.: *J. Electroanal. Chem.*, **70**, 141 (1976)
- [2] FRANCK, U. F.: *Werkstoffe u. Korrosion*, **9**, 504 (1958)
- [3] FRANCK, U. F.: *Z. Elektrochem.*, **62**, 649 (1958)
- [4] FRANCK, U. F., HUGH, R. F.: *Z. Elektrochem.*, **65**, 156 (1961)
- [5] OSTERWALD, J.: *Z. Elektrochem.*, **66**, 401 (1962)
- [6] REINOEHL, J. E., BECK, F. H., FONTANA, M. G.: *Corrosion*, **26**, 141 (1976)
- [7] EPELBOIN, I., GABRIEL, C., KEDDAM, M.: *Corros. Sci.*, **15**, 135 (1975)
- [8] GERISCHER, H.: *Angew. Chemie*, **70**, 285 (1958)
- [9] HEUMANN, T., DIEKÖTTER, F. W.: *Z. Elektrochem.*, **62**, 745 (1958)
- [10] HEUSLER, K. E., WEIL, K. G., BONHOFFER, K. F.: *Z. Phys. Chem., N. F.*, **15**, 149 (1958)
- [11] OSTERWALD, J., UHLIG, H. H.: *J. Electrochem. Soc.*, **108**, 515 (1961)
- [12] NAGAYAMA, M., COHEN, M.: *J. Electrochem. Soc.*, **109**, 781 (1962)
- [13] FRANKENTHAL, R. P.: *J. Electrochem. Soc.*, **114**, 542 (1967)
- [14] FRANKENTHAL, R. P.: *J. Electrochem. Soc.*, **116**, 580 (1969)
- [15] HERBSLEB, G., SCHWENK, W.: *Werkstoffe u. Korrosion*, **20**, 995 (1969)
- [16] OSE, E. K., ROSENFELD, N. L., DOROSENKO, V. G.: *Zashchita Metallov*, **7**, 38 (1971)
- [17] FRANCK, U. F.: *Z. Naturforsch.*, **44**, 378 (1949)
- [18] WOJCIOWICZ, J.: *Oscillatory behaviour in electrochemical systems*, in J. O'M. BOCKRIS and B. E. CONWAY: *Modern Aspects of Electrochemistry*, Vol. **8**, Plenum Press, New York 1972
- [19] HORÁNYI, GY., INZELT, GY., SZETÉY, É.: *J. Electroanal. Chem.*, **81**, 395 (1977)
- [20] JEHRING, H., HUYEN, N. V., HORN, E.: *J. Electroanal. Chem.*, **88**, 265 (1978)
- [21] JEHRING, H., KUERSCHNER, U.: *J. Electroanal. Chem.*, **75**, 799 (1977)
- [22] FRAUNHOFER, J. A., BENKS, C. H.: *Potentiostats and their Applications*. Butterworth, London 1972
- [23] SCHROEDER, R. R., SHAIN, I.: *Chemical Instrumentation*, **1**, 233 (1969)
- [24] BOOMAN, G. L., HOLBROOK, W. B.: *Anal. Chem.*, **37**, 795 (1965)
- [25] BROWN, E. R., SMITH, D. E., BOOMAN, G. L.: *Anal. Chem.*, **40**, 1411 (1968)
- [26] LAMY, C., HERRMAN, C. C.: *J. Electroanal. Chem.*, **59**, 113 (1975)
- [27] GERREAU, D., SAVAENT, J. M.: *J. Electroanal. Chem.*, **86**, 63 (1978)
- [28] BRITZ, D.: *J. Electroanal. Chem.*, **88**, 309 (1978)
- [29] ARMSTRONG, R. D., FIRMAN, R. E.: *J. Electroanal. Chem.*, **34**, 391 (1972)
- [30] SALIE, G.: *Z. Phys. Chem., Leipzig*, **253**, 406 (1973)
- [31] BODE, H. W.: *Hálózatok és visszacsatolt erősítők tervezése; Műszaki Könyvkiadó, Budapest 1961*
- [32] SIMONYI, K.: *Villamosságtan*, Vol. **2**. Akadémiai Kiadó, Budapest 1957

Béla LENGYEL }  
Lajos MÉSZÁROS } H-1112 Budapest, Budaörsi út 45.



## CONTRIBUTIONS TO THE THEORY OF TOPOLOGICAL RESONANCE ENERGY

C. D. GODSIL<sup>1</sup> and I. GUTMAN<sup>2\*</sup>

(<sup>1</sup>Montanuniversität Leoben, Austria and <sup>2</sup>Faculty of Science, Kragujevac, Yugoslavia)

Received May 13, 1981

Accepted for publication September 18, 1981

The zeros of the matching polynomial of a molecular graph  $G$  are eigenvalues of an acyclic graph  $T(G, v)$ . The construction of  $T(G, v)$  and its basic properties are discussed.

A few years ago the topological resonance energy, TRE, was proposed as a novel theoretical index of aromaticity of conjugated compounds [1]. Although nowadays it is clear that the TRE method has a number of limitations [2], there have been several successful attempts to use it in various chemical problems [3–6] and one might expect that the TRE method (when cautiously applied) will be of some relevance also in the future.

The topological resonance energy is defined as [1]

$$\text{TRE} = \sum_{j=1}^n g_j(x_j - y_j) \quad (1)$$

where the  $x_j$ 's are the Hückel molecular orbital energy levels,  $g_j$  is the occupation number of the  $j$ -th molecular orbital and the  $y_j$ 's are the zeros of the matching polynomial  $\alpha(G)$  of the molecular graph  $G$ . Note that the  $x_j$ 's are the eigenvalues of the graph  $G$  [7].

Let  $G$  be a molecular graph with  $n$  vertices and  $m$  edges, let  $p(G, k)$  be the number of  $k$  matchings of  $G$ . Then the matching polynomial of  $G$  is defined as

$$\alpha(G) = \alpha(G, x) = \sum_{k=0}^m (-1)^k p(G, k) x^{n-2k}. \quad (2)$$

The basic mathematical properties of  $\alpha(G)$  have been reported elsewhere [8, 9]; for a review of the previous work in this field see [9].\*\* In particular, a number

\* To whom correspondence should be addressed

\*\* In the last two decades the matching polynomial (also named reference and acyclic polynomial) has been independently discovered several times and found applications in at least four different fields of science: statistical physics [10], chemical thermodynamics [11], graph theory of aromaticity [1–6] and pure mathematics [12]. One should also note that the rook polynomials, which have been extensively examined in combinatorial mathematics [13] are in fact special cases of matching polynomials [14]. Therefore the results exposed in the present paper may be of some relevance in all these fields.

of recurrence relations are known for  $\alpha(G)$ , among which we mention the following two [8, 12].

Let  $v$  be a vertex of  $G$  and let  $v$  be adjacent to the vertices  $w_1, w_2, \dots, w_d$ . Let the subgraph  $G-v$  be denoted by  $H$ . Then

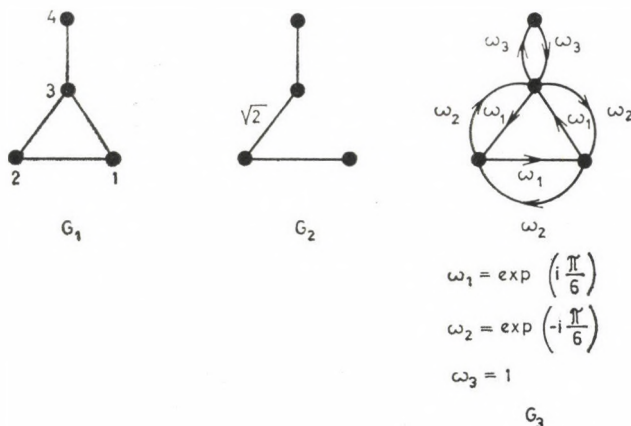
$$\alpha(G) = x \alpha(H) - \sum_{j=1}^d \alpha(H - w_j). \quad (3)$$

Let the graph  $G$  be composed of  $p$  disconnected parts  $G_1, G_2, \dots, G_p$ . Then

$$\alpha(G) = \alpha(G_1)\alpha(G_2) \dots \alpha(G_p). \quad (4)$$

A distinguished algebraic property of  $\alpha(G)$  is that all its zeros are real numbers [10, 15]. Consequently, TRE is also a real quantity.

In order to give a rational explanation of the above fact, there have been several attempts in the recent past to reduce the computation of  $y_j$ 's to the diagonalization of some Hermitian matrix. HERNDON and PÁRKÁNYI [16] noticed that because of symmetry the matching polynomial of a graph sometimes coincides with the characteristic polynomial of a certain acyclic graph with weighted edges. For example, the characteristic polynomial of  $G_2$  is equal to the matching polynomial of  $G_1$ ,  $\Phi(G_2) = \alpha(G_1)$ , and thus the eigenvalues of the graph  $G_2$  are at the same time the zeros of  $\alpha(G_1)$ .



AIHARA [17] and later also SCHAAD *et al.* [18] formulated a method by which a complex Hermitian matrix can be constructed, such that its characteristic polynomial is equal to  $\alpha(G)$ . For example, the digraph  $G_3$  represents the Hermitian matrix the characteristic polynomial of which coincides with  $\alpha(G_1)$ .

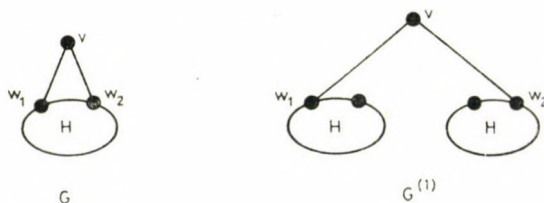
The method of HERNDON and PÁRKÁNYI can be applied to a limited class of symmetric mono- and bicyclic systems, whereas AIHARA's method works only for systems without condensed rings. Thus, for example, none of the methods described above can be applied to such simple molecules as azulene  $G_4$  or biphenylene  $G_5$  (which possess two and three condensed rings, respectively). Recently GRAOVAC [19] was able to extend AIHARA's method to a limited number of symmetric bicyclic conjugated systems with condensed rings (e.g. naphthalene, but not azulene).

In the present paper we shall describe a general graph theoretical result which connects the matching polynomial of an arbitrary molecular graph with the characteristic polynomial of an acyclic graph.

Let  $\Phi(G)$  be the characteristic polynomial of a graph  $G$  [7]. If  $G$  is acyclic, then [8, 9, 12]  $\alpha(G) = \Phi(G)$ , and so finding the zeros of the matching polynomial is simply equivalent to the graph eigenvalue problem. Therefore in the following we may assume that  $G$  possesses cycles and that the vertex  $v$  belongs to at least one cycle. We shall also assume that  $G$  is a connected graph.

**THEOREM 1.** For every graph  $G$  with a given vertex  $v$ , there exists an acyclic graph  $T(G, v)$  such that  $\alpha(G)$  is a divisor of  $\alpha[T(G, v)] = \Phi(T(G, v))$ .

*Proof.* We will use the same notation as in Eq. (3). Let us for simplicity assume that the vertex  $v$  of the graph  $G$  has degree two (i.e.  $v$  is connected with the vertices  $w_1$  and  $w_2$ ,  $d = 2$ ). We construct the graph  $G^{(1)}$  as follows.



Using Eqs (3) and (4) it is easy to see that

$$\alpha(G^{(1)}) = x\alpha(H)^2 - \alpha(H)[\alpha(H - w_1) + \alpha(H - w_2)],$$

i.e.

$$\alpha(G^{(1)}) = \alpha(G)\alpha(H). \quad (5a)$$

If the vertex  $v$  has degree  $d$ , then Eq. (5a) becomes

$$\alpha(G^{(1)}) = \alpha(G)\alpha(H)^{d-1}. \quad (5b)$$

Hence  $\alpha(G)$  is a divisor of  $\alpha(G^{(1)})$ .

Now, from the above construction is evident that in  $G^{(1)}$  the vertex  $v$  does not belong to any cycle and consequently, all cycles of  $G$  which contain the vertex  $v$  have been opened during the transformation  $G \rightarrow G^{(1)}$ .

If  $G^{(1)}$  is acyclic, then Theorem 1 is proved. If  $G^{(1)}$  is not acyclic, then we repeat our argument on the vertices  $w_1$  and  $w_2$  and construct the graph  $G^{(2)}$ . As an example we consider the case when  $w_1$  has degree three (and is adjacent to the vertices  $v_1, z_1$  and  $z_2$ ) and  $w_2$  has degree four (and is adjacent to the vertices  $v_1, z_3, z_4$  and  $z_5$ ).

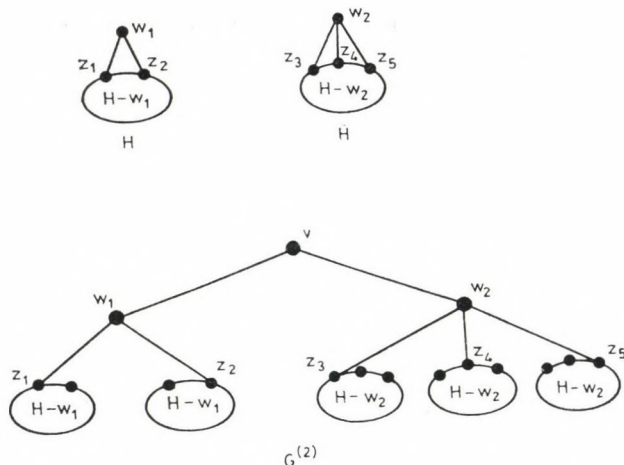
Using the same reasoning as before we conclude that  $\alpha(G^{(1)})$  is a divisor of  $\alpha(G^{(2)})$ , and thus  $\alpha(G)$  is a divisor of  $\alpha(G^{(2)})$ . In fact,

$$\begin{aligned}\alpha(G^{(2)}) &= \alpha(G^{(1)})\alpha(H - w_1)\alpha(H - w_2)^2 = \\ &= \alpha(G)\alpha(H)\alpha(H - w_1)\alpha(H - w_2)^2.\end{aligned}\quad (6a)$$

In the general case we obtain

$$\alpha(G^{(2)}) = \alpha(G)\alpha(H)^{d-1} \prod_{i=1}^d \alpha(H - w_j)^{d_j-1} \quad (6b)$$

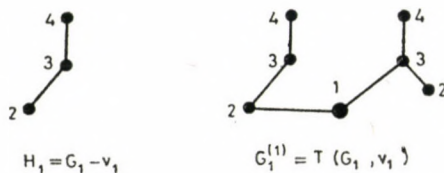
where  $d_j + 1$  is the degree of the vertex  $w_j$ .



If  $G^{(2)}$  is acyclic, then Theorem 1 follows. If  $G^{(2)}$  still possesses cycles, then we construct in the same manner the graph  $G^{(3)}$  etc. Finally, we must arrive at an acyclic graph  $G^{(t)}$  such that  $\alpha(G)$  is a divisor of  $\alpha(G^{(t)})$ . Then  $T(G, v) = G^{(t)}$ .  
Q. E. D.

A different proof of Theorem can be found in [20] where a number of consequences of this result are discussed.

In order to give an application of Theorem 1, consider the graph  $G_1$  and its vertex  $v_1$ . The  $T(G, v_1)$  is obtained in one step, i. e.  $T(G_1, v_1) = G_1^{(1)}$ .



Since  $\alpha(G_1^{(1)}) = \alpha(G_1)\alpha(H_1)$ , we have finally

$$\alpha(G_1) = \frac{\Phi(T(G_1, v_1))}{\Phi(H_1)} = \frac{x^7 - 6x^5 + 9x^3 - 2x}{x^3 - 2x} = x^4 - 4x^2 + 1.$$

Theorem 1 has two important consequences. Firstly, the zeros of  $\alpha(G)$  are eigenvalues of  $T(G, v)$ . Thus the entire theory of the matching polynomial and therefore also the theory of TRE turns out to be a special case of graph spectral theory. (Of course, not all eigenvalues of  $T(G, v)$  are zeros of  $\alpha(G)$ . The problem of the identification of those zeros of  $\Phi[T(G, v)]$  which are of interest for the TRE method will be examined later.)

Secondly, since the eigenvalues of all graphs are real numbers [7], all the zeros of  $\alpha(G)$  must also be real numbers and Theorem 1 provides an elementary and transparent demonstration of the reality of TRE. In particular, the calculation of the zeros of  $\alpha(G)$  is for all graphs shown to be equivalent with the diagonalization of a certain Hermitian matrix. Hence we obtained a general solution of the problem considered in papers [16–19].

The method for the construction of the graph  $T(G, v)$  is evident from the proof of Theorem 1. In order to formulate this procedure in a more precise manner, we need a few definitions. Let the vertices of the graph  $G$  be denoted by  $v_1, v_2, \dots, v_n$ .

A path of length  $p$  in the graph  $G$  is a sequence  $(v_{i_0}, v_{i_1}, \dots, v_{i_p})$  of  $p + 1$  mutually distinct vertices such that  $v_{i_{j-1}}$  is adjacent to  $v_{i_j}$ ,  $j = 1, 2, \dots, p$ . This path starts at the vertex  $v_{i_0}$  and ends at  $v_{i_p}$ . The sequence  $(v_i)$  will be understood as a path of length zero.

The path  $(v_{i_0}, v_{i_1}, \dots, v_{i_{p-1}})$  will be called the maximal proper subpath of the path  $(v_{i_0}, v_{i_1}, \dots, v_{i_{p-1}}, v_{i_p})$ .

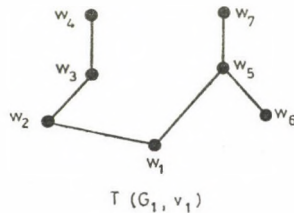
For example, there exist seven paths in the graph  $G_1$  which start at the vertex  $v_1$ . These are:  $W_1 = (v_1)$ ,  $W_2 = (v_1, v_2)$ ,  $W_3 = (v_1, v_2, v_3)$ ,  $W_4 = (v_1, v_2, v_3, v_4)$ ,  $W_5 = (v_1, v_3)$ ,  $W_6 = (v_1, v_3, v_2)$  and  $W_7 = (v_1, v_3, v_4)$ .  $W_1$  is a maximal proper subpath of  $W_2$  and  $W_5$ ,  $W_5$  is a maximal proper subpath of  $W_6$  and  $W_7$ , etc.  $W_4$ ,  $W_6$  and  $W_7$  are not maximal proper subpaths of any path in  $G_1$ .

**THEOREM 2.** Let  $G$  be a graph and  $v$  its vertex. Let  $W_1, W_2, \dots, W_N$  be the paths of  $G$  starting at  $v$ . Then  $T(G, v)$  is the graph whose vertices are

$W_1, W_2, \dots, W_N$  and two vertices  $W_i$  and  $W_j$  are adjacent in  $T(G, v)$  if  $W_i$  is a maximal proper subpath of  $W_j$  or *vice versa*.

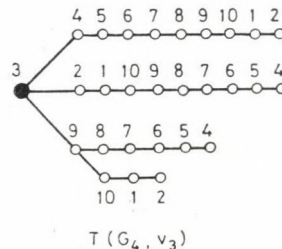
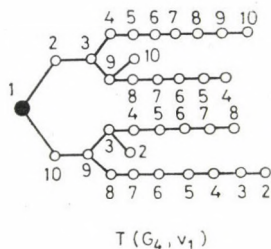
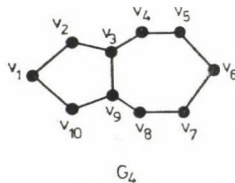
$T(G, v)$  is necessarily an acyclic graph.

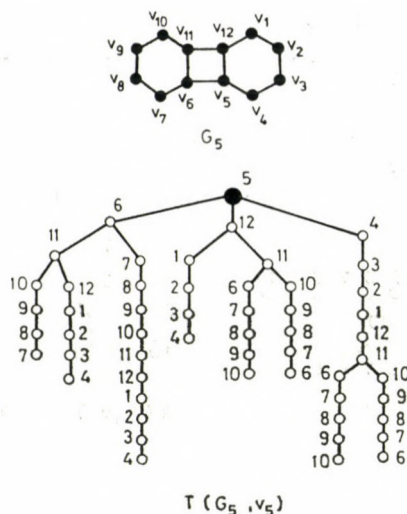
As an example we shall consider  $T(G_1, v_1)$  once again. The seven vertices of this graph correspond to the seven paths of  $G_1$  which start at  $v_1$ . Of course, the graph  $T(G_1, v_1)$  constructed according to Theorem 2 is the same as the graph  $G_1^{(1)}$  constructed following Theorem 1.



It is convenient to assign to the vertex  $W_j$  of  $T(G, v)$  the same label as that of the end vertex of the path  $W_j$ . The vertices of  $G_1^{(1)}$  in our previous example have been labelled according to this convention.

As further examples we present the graphs  $T(G_4, v_1)$ ,  $T(G_4, v_3)$  and  $T(G_5, v_5)$ .





After a little practice, the construction of  $T(G, v)$  becomes a routine task. We start with the vertex  $v$  and follow step-by-step the paths of  $G$ . For example from the vertex  $v_3$  of  $G_4$ , we can reach in one step the vertices  $v_4$ ,  $v_2$  and  $v_9$ . From  $v_4$  we must follow the path  $v_5, v_6, v_7, v_8, v_9, v_{10}, v_1, v_2$ . From  $v_9$  we can reach in one step either  $v_{10}$  or  $v_8$ . From  $v_{10}$  we can then continue only to  $v_1$  and there after to  $v_2$  where this path must be ended. *Etc.*

Every branch of  $T(G, v)$  is terminated when from a vertex we cannot pass to any other vertex (without repetition).

Some elementary properties of  $T(G, v)$  are the following.

(a) If  $G$  is acyclic, then  $T(G, v) = G$ .

(b) Let us denote by  $v$  the vertex of  $T(G, v)$  which corresponds to the path  $(v)$  of the graph  $G$ . Using the notation of Eq. (3) we have then

$$T(G, v) - v = \bigcup_{j=1}^d T(H, w_j) \quad (7)$$

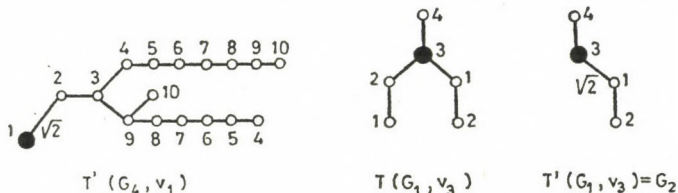
and

$$\Phi[T(G, v) - v] = \prod_{j=1}^d \Phi[T(H, w_j)]. \quad (8)$$

(c) If the vertex  $v$  is invariant under some symmetry operations on  $G$ , then it will be invariant under the same symmetry operations on  $T(G, v)$ . In particular, if  $G$  has a plane of symmetry which contains  $v$ , then  $T(G, v)$  also has such a plane of symmetry. This fact can be easily recognized on the example  $T(G_4, v_1)$ .

Since we are mainly interested in the solution of the eigenvalue problem of  $T(G, v)$  we can apply the well-known group theoretical arguments [7, 21] in order to reduce the dimension of the matrix which has to be diagonalized.

For example, instead of  $T(G_4, v_1)$  (which possesses 33 vertices) it is sufficient to solve the eigenvalue problem of the graph  $T'(G_4, v_1)$  (which has only 17 vertices).



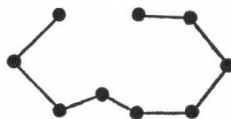
Similarly, instead of  $T(G_1, v_3)$  one may consider the eigenvalues of  $T'(G_1, v_3)$ , which on the other hand is just the previously mentioned graph  $G_2$ . This latter example illustrates the fact that the HERNDON'S method [16] for the calculation of  $\alpha(G)$  is a special case of our approach.

Therefore, whenever possible, one should choose the vertex  $v$  to be a symmetric one (like  $v_3$  in  $G_1$  or  $v_1$  in  $G_4$ ) and using group theory reduce the number of vertices of  $T(G, v)$ .

(d) In order to obtain a graph  $T(G, v)$  with as few vertices as possible, it is often convenient to choose  $v$  to be a vertex belonging to as many cycles of  $G$  as possible.

(e)  $T(G, v)$  reflects the path structure of the graph  $G$ . It is worth noting that recently  $T(G, v)$  has been independently considered in connection with the enumeration of certain types of paths in  $G$  [22].

From the spectrum of  $T(G, v)$  we can determine the zeros of  $\alpha(G)$ . For example, the set of the zeros of  $\alpha(G_4)$  is equal to the spectrum of  $T(G_4, v_3)$  minus twice the spectrum of  $P_9 = G_4 - v_3$ .



$P_9 = G_4 - v_3$

This conclusion follows from the application of Eq. (5), *viz.*,

$$\alpha[T(G_4, v_3)] = \alpha(G_4^{(1)}) = \alpha(G_4)\alpha(G_4 - v_3)^2,$$

*i.e.*

$$\alpha(G_4) = \Phi[T(G_4, v_3)]/\Phi(P_9)^2.$$

Applying Eqs (5), (6) and their generalizations for  $G^{(t)}$ ,  $t > 2$  we can in all cases eliminate those eigenvalues of  $T(G, v)$  which are not zeros of  $\alpha(G)$ . However, such a procedure may be quite tedious for large polycyclic molecular graphs. Fortunately, there exists a simpler criterion for deciding whether an eigenvalue of  $T(G, v)$  is a zero of  $\alpha(G)$ , based on the examination of the eigenvectors of  $T(G, v)$ .

Let the graph  $T(G, v)$  possess  $N$  vertices and let  $C_j = (C_{j1}, C_{j2}, \dots, C_{jN})$  be the eigenvector with the eigenvalue  $X_j$ ,  $j = 1, 2, \dots, N$ . Let the component of the vector  $C_j$  corresponding to the vertex  $v$  of  $T(G, v)$  be  $C_{jv}$ .

**THEOREM 3.** Suppose the polynomials  $\alpha(G - v)$  and  $\alpha(G)$  have no common zero. Then  $y$  is a zero of  $\alpha(G)$  if and only if for some  $j$ ,  $y = X_j$  and  $C_{jv}$  is not zero.

Before proving this Theorem it is worth noting that if the graph  $G$  has a Hamiltonian path, then the requirements of the Theorem are necessarily fulfilled [10].

*Proof.* From Theorem 2.5 of [20] we find that

$$\frac{\alpha(G - v)}{\alpha(G)} = \frac{\Phi [T(G, v) - v]}{\Phi [T(G, v)]} \quad (9)$$

From Eq. (3) in the proof of Theorem 5.2 in [20] we have further

$$\frac{\Phi [T(G, v) - v]}{\Phi [T(G, v)]} = \sum_{j=1}^N \frac{(C_{jv})^2}{x - X_j} \quad (10)$$

It follows from (10) that the poles of  $\Phi [T(G, v) - v] / \Phi [T(G, v)]$  are simple. Since  $\alpha(G - v)$  and  $\alpha(G)$  are assumed to have no common zero, it follows from (9) that there are exactly  $n$  such poles, where  $n$  is the number of vertices of  $G$ . Finally, it is clear from (10) that  $y$  is a pole if and only if  $C_{jv} \neq 0$  for some  $j$  such that  $X_j = y$ . Q.E.D.

According to Theorem 3, the zeros of  $\alpha(G)$  can be determined as follows. By solving the graph eigenvalue problem for  $T(G, v)$ , one automatically obtains the eigenvectors  $C_j$ . Those eigenvalues of  $T(G, v)$  for which  $C_{jv} \neq 0$  are necessarily zeros of  $\alpha(G)$ . Hence at least some zeros of  $\alpha(G)$  can be identified in this manner. If  $\alpha(G)$  and  $\alpha(G - v)$  have no common zero, then the above procedure yields all the zeros of  $\alpha(G)$ . It is a fortunate fact that for the great majority of chemically relevant graphs this condition is satisfied [23] and thus Theorem 3 is fully applicable.

\*

One of the authors (I. G.) would like to thank the Alexander von Humboldt Foundation for financial support of this research.

## REFERENCES

- [1] GUTMAN, I., TRINAJSTIĆ, N.: *Acta Chim. (Budapest)*, **91**, 203 (1976); AIHARA, J.: *J. Am. Chem. Soc.*, **98**, 2750 (1976)
- [2] GUTMAN, I.: *Theor. Chim. Acta* **56**, 89 (1980); AIHARA, J.: *Chem. Phys. Lett.*, **73**, 404 (1980); GUTMAN, I., MOHAR, B.: *Chem. Phys. Lett.*, **77**, 567 (1981)
- [3] AIHARA, J.: *J. Am. Chem. Soc.*, **99**, 2048 (1977), **101**, 558 (1979); *Bull. Chem. Soc. Japan*, **51**, 3540 (1978), **52**, 2202 (1979), **53**, 1163 (1980), **53**, 2689 (1980)
- [4] HERNDON, W. C.: *Tetrahedron Lett.*, **1979**, 3283; *Pure Appl. Chem.*, **52**, 1459 (1980)
- [5] ILIC, P., TRINAJSTIĆ, N.: *Pure Appl. Chem.*, **52**, 1459 (1980); *J. Org. Chem.*, **45**, 1738 (1980).
- [6] GUTMAN, I.: *Croat. Chem. Acta*, **53**, 581 (1980); *Z. Naturforsch.*, **36a**, 128 (1981)
- [7] CVETKOVIĆ, D., DOOB, M., SACHS, H.: *Spectra of Graphs — Theory and Application*, Academic Press, New York 1980
- [8] GUTMAN, I., HOSOYA, H.: *Theor. Chim. Acta*, **48**, 279 (1978)
- [9] GUTMAN, I.: *Match (Mülheim)*, **6**, 75 (1979); GODSIL, C. D., GUTMAN, I.: *J. Graph. Theory* **5**, 137 (1981)
- [10] HEILMANN, O. J.; LIEB, E. H.: *Commun. Math. Phys.*, **25**, 190 (1972)
- [11] HOSOYA, H.: *Bull. Chem. Soc. Japan*, **44**, 2332 (1971); NARUMI, H., HOSOYA, H.: *Bull. Chem. Soc. Japan*, **53**, 1228 (1980)
- [12] FARRELL, E. J.: *J. Comb. Theory*, **27B**, 75 (1979); *Ars Combinatoria*, **9**, 221 (1980)
- [13] RIORDAN, J.: *An Introduction to Combinatorial Analysis*, Wiley, New York 1958, Chs. 7 and 8
- [14] GODSIL, C. D., GUTMAN, I.: *Croat. Chem. Acta*, **54**, 53 (1981)
- [15] GODSIL, C. D., GUTMAN, I.: *Z. Naturforsch.*, **34a**, 776 (1979); GUTMAN, I.: *Croat. Chem. Acta*, **54**, 75 (1981)
- [16] HERNDON, W. C., PÁRKÁNYI, C.: *Tetrahedron*, **34**, 3419 (1978); HERNDON, W. C., ELLZEY, M. L.: *J. Chem. Inf. Comput. Sci.*, **19**, 260 (1979)
- [17] AIHARA, J.: *Bull. Chem. Soc. Japan*, **52**, 1529 (1979)
- [18] SCHAAD, L. J., HESS, B. A., NATION, J. B., TRINAJSTIĆ, N. (with an appendix by GUTMAN, I.): *Croat. Chem. Acta*, **52**, 233 (1979)
- [19] GRAOVAC, A.: *Chem. Phys. Lett* **82**, 248 (1981)
- [20] GODSIL, C. D.: *J. Graph Theory* **5**, 285 (1981)
- [21] HEILBRONNER, E.: *Helv. Chim. Acta*, **37**, 913 (1954); McCLELLAND, B. J.: *J.C.S. Faraday II*, **70**, 1453 (1974)
- [22] RANDIĆ, M., BRISSEY, G. M., SPENCER, R. B., WILKINS, C. L.: *Comput. Chem.*, **3**, 5 (1979)
- [23] GUTMAN, I.: unpublished computational results

Christopher D. GODSIL Ivan GUTMAN	}	Montanuniversität Leoben, A-8700 Leoben, Austria Faculty of Science, P.O. Box 60, 34000 Kragujevac, Yugoslavia
--------------------------------------	---	--

# THE INFLUENCE OF THE IONIC STRENGTH ON THE DISSOCIATION CONSTANT OF HYDROGEN CYANIDE

(SHORT COMMUNICATION)

V. GÁSPÁR and M. T. BECK\*

(Institute of Physical Chemistry, Kossuth Lajos University, Debrecen)

Received June 17, 1981

Accepted for publication September 18, 1981

For the study of the photoaquation of hexacyanoferrate(II) and octacyanomolybdate(IV) [1] the dissociation constant of hydrogen cyanide ( $K_d$ ) was determined at several ionic strengths in the range from 0.1 to 5.0 mol dm<sup>-3</sup> NaClO<sub>4</sub> ( $T = 298$  K).

Data in the literature are available only in the range of the Debye-Hückel theory and were extrapolated to zero ionic strength [2, 3, 4]. Different methods were used for the determination of  $K_d$ . BRITTON and ROBINSON calculated  $pK_d = 9.31$  by measuring the saturated vapor pressure of HCN, PANG determined  $pK_d = 9.22$  by spectrophotometric measurements and IZATT *et al.* got  $pK_d = 9.21$  by monitoring the pH with glass electrode [2].

In our study the dissociation constant was determined by a potentiometric titration method using cyanide selective and glass electrodes. A linearized form of titration curve was used for calculations [5].

## Experimental

0.1 mol dm<sup>-3</sup> sodium cyanide (Reanal product) stock solutions were freshly prepared and used only if no yellowish colouration occurred. The solutions were kept in plastic vessels in the dark and cold, under N<sub>2</sub> atmosphere.

1.0 mol dm<sup>-3</sup> perchloric acid stock solutions were prepared by diluting 60% (Merck product) perchloric acid. The concentration was determined by titration potassium hydrogencarbonate (Reanal product) using methylorange as an indicator.

For titration at different ionic strengths 0.1 mol dm<sup>-3</sup> perchloric acid and about 0.01 mol dm<sup>-3</sup> sodium cyanide solutions were diluted from the stock solutions.

The ionic strength of different samples was adjusted with 6.0 mol dm<sup>-3</sup> sodium perchlorate (Merck product) stock solution.

The cyanide concentration was determined with an OP-201 Universal Radelkis pH-meter using OP-711-D-IRadelkis ionselective electrode and K 401 Radiometer S.C.E. (filled with saturated sodium chloride to avoid the precipitation of potassium perchlorate).

The pH value of the same sample was determined with PHM-51 Radiometer pH meter using GK 2301 combined electrode (filled also with saturated sodium chloride).

The constant temperature was  $298 \pm 0.1$  K.

\* To whom correspondence should be addressed

### Calculations

A linearized form of the titration curve can be written as follows:

$$\frac{V + V_0}{C_{\text{HClO}_4}} [\text{CN}^-] = V_{\text{eq}} - \frac{1}{K_d} \frac{V + V_0}{C_{\text{HClO}_4}} [\text{CN}^-] [\text{H}^+] \quad (1)$$

where

$V_0$  volume of a titrated sodium cyanide solution (generally 50 mL),  
 $C_{\text{CN}^-}$  0.01 mol dm<sup>-3</sup>,  $I = 0.1, \dots, 5.0$  mol dm<sup>-3</sup> NaClO<sub>4</sub>.

$C_{\text{HClO}_4}$  concentration of perchloric acid solution used for titration (0.1 mol dm<sup>-3</sup>,  $I = 0.1, \dots, 5.0$  mol dm<sup>-3</sup> NaClO<sub>4</sub>),

$V$  volume of added acid (mL)

$V_{\text{eq}}$  equivalence volume of perchloric acid, defined as:  $V_{\text{eq}} = \frac{V_0 [C_{\text{CN}^-}]}{C_{\text{HClO}_4}}$  (mL),

$K_d$  the dissociation constant of HCN (mol dm<sup>-3</sup>).

The  $K_d$  values were calculated from the slope of (1) type lines by least squares method. The cyanide and hydrogen ion concentrations were calculated only in the first part of the titration curves, because of the well-known anomalous character of the cyanide selective electrode below pH = 8.5 [6].

### Results

Linearized titration curves at different ionic strengths are shown in Fig. 1.

The first part of the titration curves was linear in the whole range of the ionic strength from 0.1 to 5.0 mol dm<sup>-3</sup> NaClO<sub>4</sub>.

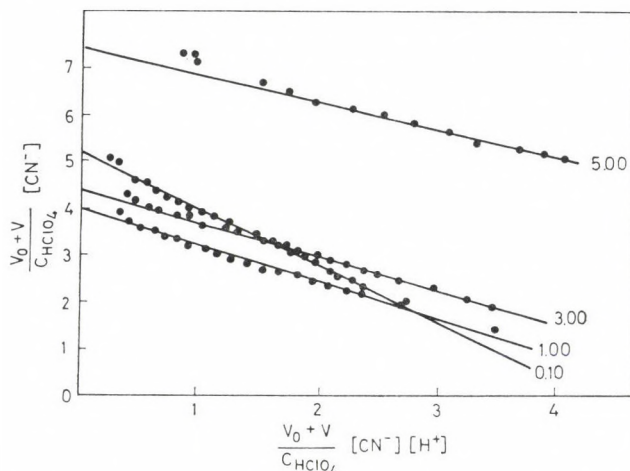


Fig. 1. Linearized titration curves at different ionic strengths

The results of the calculations are summarized as follows :

$I$ (mol dm <sup>-3</sup> NaClO <sub>4</sub> )	$\overline{pK_d}$
0.00	9.21 ± 0.01 (extrapolated)
0.10	9.06 ± 0.02
1.00	8.88 ± 0.02
3.00	8.81 ± 0.02
5.00	8.78 ± 0.02

The mean values were calculated from the results of three parallel measurements.

There is a good agreement between the DH theory and experimental results: the dissociation constant strongly increased with increasing the ionic strength.

#### REFERENCES

- [1] GÁSPÁR, V., BECK, M. T.: to be published
- [2] Stability Constants of Metal-Ion Complexes, London, The Chemical Society, Burlington House, W.1. 1964
- [3] BOUGHTON, J. H., KELLER, R. N.: J. Inorg. Nucl. Chem., **28**, 2851 (1966)
- [4] CHRISTENSEN, J. J., JOHNSTON, H. D., IZATT, R. M.: J. Chem. Soc(A), **1970**, 454
- [5] IVASKA, A.: Academic Dissertation, Abo Akademi, Abo, Finland 1975
- [6] GRATZL, M., RAKIÁS, F., HORVAI, G., TÓTH, K., PUNGOR, E.: Anal. Chim. Acta, **102**, 85 (1978)

Vilmos GÁSPÁR }  
Mihály T. BECK } H-4010 Debrecen



## STEROIDS, XXVIII\* NEIGHBOURING GROUP PARTICIPATION, V\*

(0<sup>-</sup>–4) NEIGHBOURING GROUP PARTICIPATION AND FRAGMENTATION  
IN THE 16-HYDROXYMETHYLANDROST-5-ENE-3,17-DIOL SERIES

Gy. SCHNEIDER\*\*, I. VINCZE, L. HACKLER, J. A. SZABÓ and Gy. DOMBI

(*Institute of Organic Chemistry, József Attila University, Szeged*)

Received May 15, 1981

Accepted for publication September 23, 1981

The four possible isomers of 16-hydroxymethylandrosta-5-ene-3 $\beta$ ,17-diol were transformed into the mixed *p*-toluenesulfonic acid–acetic acid esters (**1a**, **2a**, **3a**, **4a**), as well as into the C-17-tetrahydropyranyl acetals of the mixed esters (**1b**, **2b**, **3b**, **4b**). On alkaline methanolysis of the mixed esters, **1a** and **4a** yielded the  $\alpha$ - and  $\beta$ -oxetanes (**5a** and **6a**) condensed to the D ring of the sterane skeleton, while **2a** and **3a** gave a fragmentation product (**7a**). The mixed ester C-17-tetrahydropyranyl acetals (**1b**, **2b**, **3b**, **4b**) transformed into the 16-methoxymethyl derivatives (**1c**, **2c**, **3c**, **4c**) under similar experimental conditions.

Alkaline reactions of  $\alpha,\gamma$ -halohydrins or  $\alpha,\gamma$ -diol monosulfonates lead to the formation of four-membered oxetanes. The process is a neighbouring group participation characterized by the general symbol (0<sup>-</sup>–4). While three-, five- or six-membered cyclic ethers are formed rapidly and uniformly under similar conditions, the formation of oxetanes is often accompanied by substitution, elimination or fragmentation side-reactions. Oxetane formation takes place readily in compounds containing the reactive groups in favoured steric positions [1].

Steroids with their relatively rigid skeletons are suitable for the development of stable oxetane rings under solvolysis conditions or in a photochemical reaction.

In the literature mainly the formation of oxetanes condensed to rings A, B and D is reported, and spiro-oxetane derivatives have also been described. Alkaline solvolysis of the appropriate 5 $\alpha$ -hydroxy-3 $\beta$ -*p*-toluenesulfonate readily gives, 3 $\alpha$ ,5 $\alpha$ -epoxycholestane, since the groups taking part in the conversion are in favourable steric positions, furthermore, the 1,3-*diaxial* interaction of the C-19 methyl group and the hydrogen atoms is significantly reduced in the resulting cyclic system. The 5 $\beta$ ,3 $\alpha$ -isomer, however, yielded only a fragmentation product, 4,5-*sec*cholest-3-ene-5-one under similar experimental conditions, although the steric conditions of cyclization are satisfied

\* Parts XXVII and IV: Gy. SCHNEIDER, I. VINCZE, A. VASS, L. HACKLER, Gy. DOMBI: *Acta Chim. Acad. Sci. Hung.* **109**, 78 (1982)

\*\* To whom correspondence should be addressed

[2]. The  $6\beta$ -methyl [3] and  $6\beta$ -hydroxy [4] derivatives of  $3\alpha,5\alpha$ -epoxycholestan are also known. In the A-nor-cholestane series, both the  $2\alpha,5\alpha$ -epoxy and  $2\beta,5\beta$ -epoxy-A-nor-cholestane derivatives have been prepared by the solvolytic method. Formation of the latter compound was accompanied by fragmentation, since the C-19 methyl group exerts a strong hindrance on the ring system [5]. In the series of compounds with androstane skeleton,  $3\alpha,5\alpha$ -epoxyandrostane and its 1,17-dione derivative have been prepared [6]. The synthesis of the  $5\alpha,7\alpha$ - and  $5\beta,7\beta$ -epoxy derivatives condensed to the B ring of the cholestan skeleton has also been achieved in spite of the fact that the possibility of this synthesis was questioned earlier in the literature [7].  $\alpha$ -Oxetanes [8, 9] and  $\beta$ -oxetanes [10] condensed to the D ring are also known. Spiro-oxetane derivatives condensed to rings A and D, prepared by solvolysis, have also been reported [5, 11, 12].

Oxetane rings were developed at the A and B rings of cholestan and nor-cholestan photochemically [13, 14, 15, 16].

We reported earlier that reduction of 16-hydroxymethylandro-5-ene- $3\beta$ -ol-17-one with complex metal hydrides yielded a mixture of two 16-hydroxymethylandro-5-ene- $3\beta,17$ -diol isomers. Of these,  $16\alpha$ -*p*-toluenesulfonyloxymethylandro-5-ene- $3\beta,17\beta$ -diol 3,17-diacetate (**2a**) suffered partial fragmentation in alkaline media and formed partly an alkyl ether.  $16\beta$ -*p*-Toluenesulfonyloxymethylandro-5-ene- $3\beta,17\beta$ -diol 3,17-diacetate (**4a**) yielded the oxetane (**6a**) condensed to ring D [17]. The stereospecific cyclization reaction was suitable for the determination of the configuration of the isomers. This method of determining the configurations was developed earlier in our laboratory for the examination of the *cis* and *trans* modifications of 2-hydroxymethylcyclopentanol [18]. Conversion at the two isomers available of 16-hydroxymethylandro-5-ene- $3\beta,17$ -diol yielded the modifications  $16\beta,17\alpha$  (**3a**) [19] and  $16\alpha,17\alpha$  (**1a**) [20] which had been missing.

In the possession of the four isomers, the 16-*p*-toluenesulfonyl-oxy-methyl-17-acetoxy mixed esters (**1a**, **2a**, **3a**, **4a**) as well as the C-17-tetrahydropyranyl mixed ester acetals (**1b**, **2b**, **3b**, **4b**) were prepared and subjected to comparative solvolysis experiments.

### Solvolysis results

All the four possible isomers of 16-*p*-toluenesulfonyloxymethylandro-5-ene- $3\beta,17$ -diol diacetates (**1a**, **2a**, **3a**, **4a**) and 16-*p*-toluenesulfonyloxymethylandro-5-ene- $3\beta,17$ -diol 3-acetate-17-tetrahydropyranyl acetals (**1b**, **2b**, **3b**, **4b**) were subjected to methanolysis in the presence of four equivalents of sodium methoxide at the temperature of boiling.

The conversion was monitored by thin-layer chromatography.

After completion of the reaction the products were purified on a column packed with  $\text{Al}_2\text{O}_3$  of medium activity, by the suction chromatographic method.

Identification of the substances was based on the IR and  $^1\text{H-NMR}$  spectra (Table I).

Isomer  $16\alpha,17\alpha$  (**1a**) gave by rapid conversion an entirely uniform product (**5a**), which yielded the monoacetate (**5b**) with pyridine/acetic anhydride. In the IR spectrum, the band characteristic of oxetanes appeared at  $980\text{ cm}^{-1}$  [5, 18]. In the  $^1\text{H-NMR}$  spectrum, the AB spectrum fraction of the methylene protons in the oxetane ring is found at 3.9 and 4.75 ppm. The anisotropic shielding effect of the hetero atom in the resulting strained ring is shown by the strikingly high (0.52 ppm) diamagnetic shift of the C-18 angular methyl group. The presence of the four-membered hetero ring does not alter the coupling constant between  $16\beta\text{H},17\beta\text{H}$  (about 5 Hz) relative to  $\text{C}_{16},\text{C}_{17}$ -disubstituted steroids [21].

The formation of the oxetane ring in  $\alpha$ -position (**5a**) is particularly favourable, since the *quasi-axial* alkoxide group at C-17 exerts an  $\text{S}_{\text{N}}\text{i}$  attack at the C-16-*p*-toluenesulfonyloxymethyl, group being again in  $\alpha$ -position, on the opposite side relative to the C-18 methyl group, and this allows the development of a ring system relatively free of strain.

The  $16\beta,17\beta$  isomer (**4a**) also gave the earlier reported [17]  $16\beta,17\beta$ -oxetane derivative (**6a**) in a good yield (84%). The reaction is accompanied by some fragmentation, which can be explained by the relatively packed space in the  $\beta$ -oxetane with the C-18 methyl group in the same steric position.

The IR spectrum has the band characteristic of oxetanes at  $970\text{ cm}^{-1}$ . In the  $^1\text{H-NMR}$  spectrum the AB spectrum fragment of the methylene protons in the oxetane ring appears at 4.15 and 4.7 ppm. The anisotropic shielding effect of the hetero atom in the  $16\beta,17\beta$  fused ring gives rise to a paramagnetic shielding effect on the signal of the C-18 methyl protons (1.05 ppm), in contrast with the  $16\alpha,17\alpha$  fused ring. The  $16\alpha\text{H},17\alpha\text{H}$  coupling constant with a value of 9.5 Hz corresponds to experience obtained with C-16, C-17 disubstituted steroids [21].

The observation that in both steroid oxetanes (**5a**, **5b** and **6a**, **6b**) the coupling constants correspond to the C-16, C-17 disubstituted derivatives can be explained by the fact that the disubstituted D ring in steroids has such a stable conformation which cannot be altered significantly even the attachment of a four-membered ring.

The conversion of the two *trans* isomers (**2a**, **3a**) took place at a rate equal to that of the oxetane formation and led to the same fragmentation product (**7a**). Since the C-16-*p*-toluenesulfonyloxymethyl group has a distant steric position relative to the C-17 hydroxyl function, cyclization could not take place, however, this group could have taken part in nucleophilic ex-

**Table I**  
<sup>1</sup>H-NMR data

Compound	Substituent			Chemical shifts $\delta$				
	3	16	17	3	6	17	16 CH <sub>2</sub> O	18
<b>1c</b>	$\beta$ OH	$\alpha$ CH <sub>2</sub> -OCH <sub>3</sub>	$\alpha$ OH	3.4	5.45	3.8	3.52	0.75
<b>1d</b>	$\beta$ OAc	$\alpha$ CH <sub>2</sub> -OCH <sub>3</sub>	$\alpha$ OAc	4.6	5.45	5.08	3.4	0.85
<b>2c</b>	$\beta$ OH	$\alpha$ CH <sub>2</sub> -OCH <sub>3</sub>	$\beta$ OH	3.4	5.40	3.5	3.4	0.92
<b>2d</b>	$\beta$ OAc	$\alpha$ CH <sub>2</sub> -OCH <sub>3</sub>	$\beta$ OAc	4.6	5.50	4.6	3.4	0.81
<b>3c</b>	$\beta$ OH	$\beta$ CH <sub>2</sub> -OCH <sub>3</sub>	$\alpha$ OH	3.4	5.45	3.6	3.55	0.72
<b>3d</b>	$\beta$ OAc	$\beta$ CH <sub>2</sub> -OCH <sub>3</sub>	$\alpha$ OAc	4.6	4.5	4.65	3.5	0.82
<b>4c</b>	$\beta$ OH	$\beta$ CH <sub>2</sub> -OCH <sub>3</sub>	$\beta$ OH	3.4	5.4	3.8	3.55	0.80
<b>4d</b>	$\beta$ OAc	$\beta$ CH <sub>2</sub> -OCH <sub>3</sub>	$\beta$ OAc	4.6	5.45	4.85	3.4	0.84
<b>5a</b>	$\beta$ OH	16 $\alpha$ ,17 $\alpha$	oxetane	3.4	5.5	4.55	3.9; 4.75	0.52
<b>5b</b>	$\beta$ OAc	16 $\alpha$ ,17 $\alpha$	oxetane	4.6	5.5	4.6	3.9; 4.85	0.52
<b>6a</b>	$\beta$ OH	16 $\beta$ ,17 $\beta$	oxetane	3.5	5.4	4.48	4.15; 4.7	1.05
<b>6b</b>	$\beta$ OAc	16 $\beta$ ,17 $\beta$	oxetane	4.6	5.4	4.48	4.1; 4.7	1.05
<b>7a</b>	$\beta$ OH	Fragmentation		3.6	5.5	—	—	1.05
<b>7b</b>	$\beta$ OAc	Fragmentation		4.6	5.5	—	—	1.05
<b>8a</b>	$\beta$ OH	Fragmentation		3.5	5.5	—	—	0.80
<b>8b</b>	$\beta$ OAc	Fragmentation		4.6	5.4	—	—	0.85

\* Reaction with trichloroacetyl isocyanate (TAI) resulting in the formation of the

change or elimination reactions. Since the steric conditions of heterolytic fragmentation were given, this latter process occurred at a high rate and quantitatively (Fig. 1).

Fragmentation (Scheme B) followed the scheme observed for  $\alpha,\gamma$ -halohydrins by GROB and SCHIESS (Scheme A) (Fig. 2) [22]. Fragmentation can occur in all cases, where the nucleofugal group is located sterically distant from the alkoxide function developed in alkaline media and cyclization thus cannot take place. In several cases, it occurs simultaneously with the less favoured, oxetane formation [2], or instead of this reaction [22].

The structure of the fragmentation product (**7a**) was indicated by the signal of the aldehyde proton having a high chemical shift (9.6 ppm) in the <sup>1</sup>H-NMR spectrum; the environment of this aldehyde is aliphatic in nature and exhibits no coupling. The spectrum furthermore indicates the presence of three olefinic protons.

The aldehyde group of the fragment (**7a**) could be reduced with NaBH<sub>4</sub>

## of compounds 1-8

(ppm)		Other	Coupling constants $J$ (Hz)	Reaction with TAI* (Chemical shifts in ppm)
19	-OAc	Other		
1.02	—	OCH <sub>3</sub> : 3.36	$J_{16,17} = 5.5$ Hz	3 H: 4.8; 17H: 4.7; NH: 8.7
1.05	2.05:			—
	2.06	OCH <sub>2</sub> : 3.35	$J_{16,17} = 5.5$ Hz	
1.02	—	OCH <sub>3</sub> : 3.39	$J_{16,17} = 7.0$ Hz	3H: 4.7; 17H: 4.7; NH: 8.48
	2.03	OCH <sub>3</sub> : 3.35	$J_{16,17} = 7.0$ Hz	—
1.04	—	OCH <sub>3</sub> : 3.4	$J_{16,17} = 1.0$ Hz	3H: 4.7; 17H: 4.7; NH: 8.7
1.04	2.04	OCH <sub>3</sub> : 3.35	$J_{16,17} = 1.0$ Hz	—
1.03	—	OCH <sub>3</sub> : 3.38	$J_{16,17} = 10$ Hz	3H: 4.8; 17H: 5.0; NH: 8.55
1.04	2.04	OCH <sub>3</sub> : 3.35	$J_{16,17} = 10$ Hz	—
1.04	—	16H: 3.1	$J_{16,17} = 4.5$ Hz	3H: 4.7; NH: 8.4
1.06	2.05	16H: 3.2	$J_{16,17} = 5$ Hz	—
1.07	—	16H: 3.2	$J_{16,17} = 9$ Hz	3H: 4.6; NH: 8.4
1.06	2.02	16H: 3.2	$J_{16,17} = 9.5$ Hz	—
1.11	—	—CH= 5.05; =CH <sub>2</sub> : 4.1; 5.5 CHO: 9.5	—	3H: 4.6; NH: 8.8
1.10	2.05	—CH=: 5.1; =CH <sub>2</sub> : 4.1; 5.6 —CHO: 9.6	—	—
1.05	—	—CH=: 5.1; =CH <sub>2</sub> : 4.1; 5.6 —CH <sub>2</sub> OH: 3.2; 3.6	—	3H: 4.6; CH <sub>2</sub> OH: 3.6; 3.9; NH: 8.5
1.03	2.02	—CH=: 5.1; =CH <sub>2</sub> : 4.8; 5.6 —CH <sub>2</sub> OAc: 3.65; 3.95	—	—

trichloroacetylcarbamoyl derivative (TAC) [25]

and the resulting product (**8a**) was converted into the corresponding diacetate (**8b**) by treatment with a mixture of acetic anhydride and pyridine.

Both the oxetane formation and fragmentation processes fail to occur when the C-17 hydroxyl function is protected with a tetrahydropyranyl acetal linkage. Alkaline methanolysis of these derivatives (**1b**, **2b**, **3b**, **4b**) yielded the corresponding 16-methoxymethyl compounds (**1c**, **2c**, **3c**, **4c**) after acid hydrolysis of the protective group. The formation of these derivatives can be explained by S<sub>N</sub>2 S<sub>N</sub>-2 exchange of the 16-*p*-toluenesulfonyloxy group.

The absence of oxetane formation in the *cis* isomers (**1b**, **4b**) indicates that the (0<sup>-</sup>—4) neighbouring group participation takes place only in the presence of the alkoxide group. The absence of the fragmentation reaction in the two *trans* isomers (**2b**, **3b**) shows again that the  $\alpha,\gamma$  fragmentation takes place in the presence of an alkoxide group in *trans* position the nucleofugal group. The oxygen in acetal bond is not sufficiently nucleophilic to initiate either oxetane formation or fragmentation.

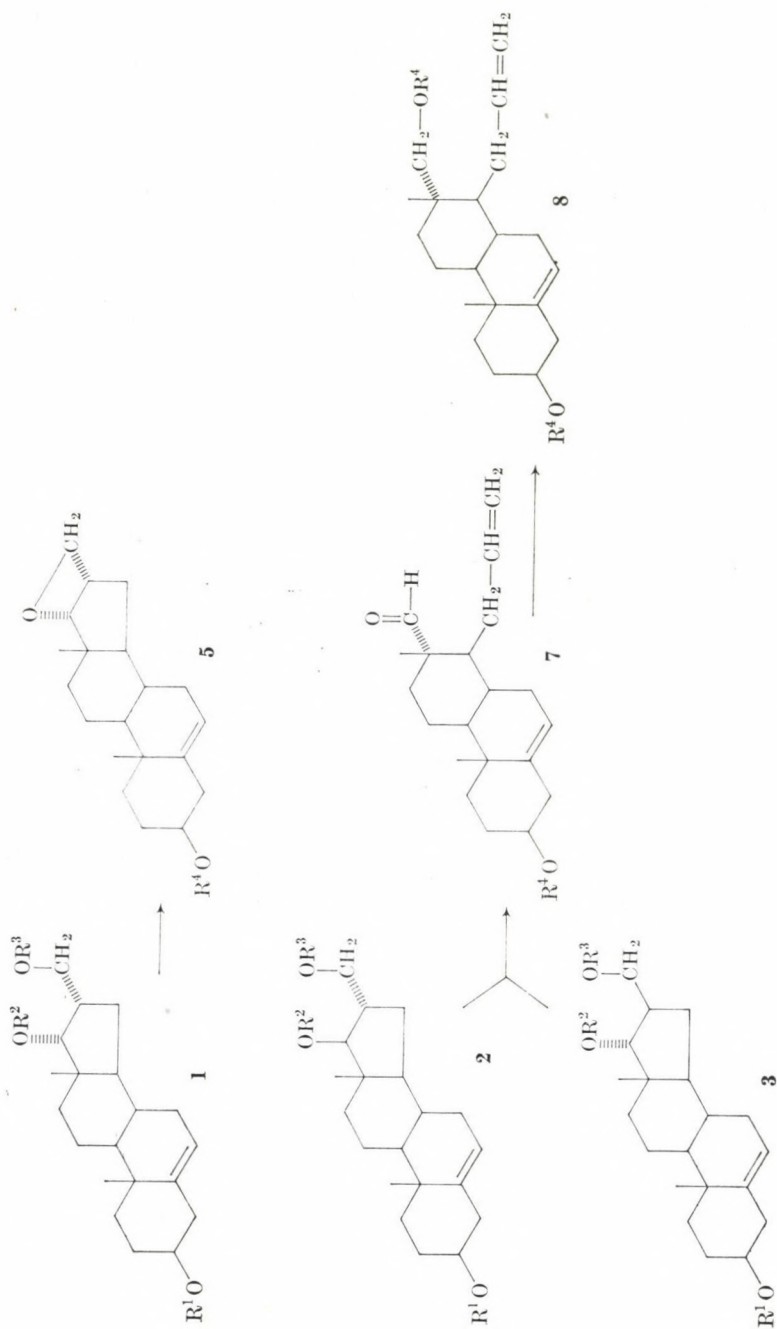


Fig. 1a

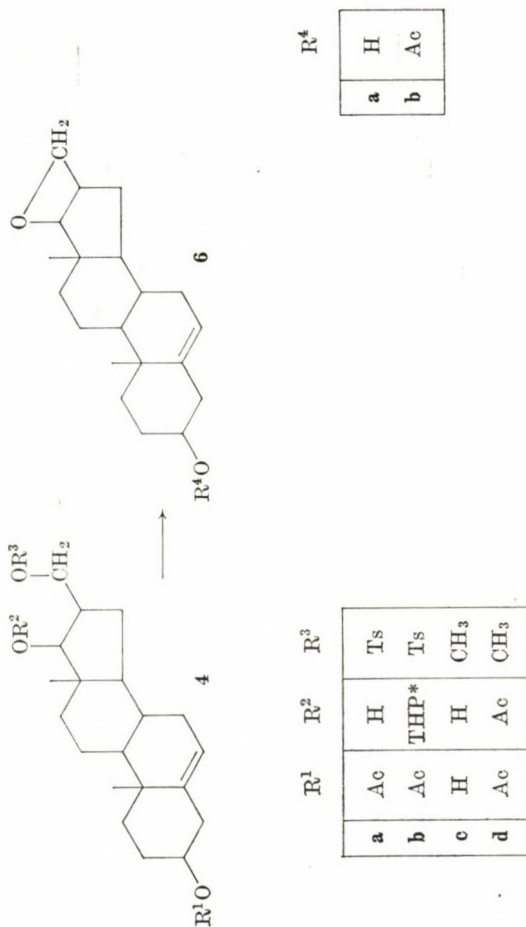


Fig. 1b



The IR spectra were recorded with a Unicam SP 200 instrument in KBr pellets.

The thin-layer chromatograms were obtained on Kieselgel-G (Merck) layers of 0.5 mm thickness. The developing solvent mixtures were the following: (I) methanol : benzene, 1 : 99; (II) methanol : benzene, 5 : 95; (III) acetone : benzene : petroleum ether, 30 : 35 : 35. The spots were detected by spraying with 50% aqueous phosphoric acid followed by heating at 100–120 °C for 15 min. The  $R_f$  values were measured for the spots observed in UV light of 365 nm wave length.

In the column chromatographic separation, the column was packed with  $Al_2O_3$  having an activity of III–IV standardized according to Brockmann. The dimensions of the chromatographic column were 25 × 2 cm. The weight of  $Al_2O_3$  packing was 50 g.

#### 16 $\alpha$ -*p*-Toluenesulfonyloxymethylandro-5-ene-3 $\beta$ ,17 $\alpha$ -diol 3-acetate (1a)

16 $\alpha$ -Hydroxymethylandro-5-ene-3 $\beta$ ,17 $\alpha$ -diol 24 (7.24 g; 0.02 mole) was dissolved in anhydrous pyridine (25 mL) and a solution of *p*-toluenesulfonyl chloride (7.5 g; 0.038 mole) in pyridine (25 mL) was added to it dropwise while cooling in ice. The reaction mixture was allowed to stand overnight, then added to an ice-cold solution of 20%  $H_2SO_4$  (100 mL). The crystals which separated were filtered off, washed until free from acid, and recrystallized from a mixture of benzene and petroleum ether (9.1 g; 88.1%).

The properties of this compound and the other products are listed in Table II.

#### 16 $\beta$ -*o*-Toluenesulfonyloxymethylandro-5-ene-3 $\beta$ ,17 $\alpha$ -diol 3-acetate (3a)

16 $\beta$ -Hydroxymethylandro-5-ene-3 $\beta$ ,17 $\alpha$ -diol (7.24 g; 0.02 mole) 20 was converted as described for 1a (8.7 g; 84.2%).

#### 16-*p*-Toluenesulfonyloxymethylandro-5-ene-3 $\beta$ ,17-diol 17-tetrahydropyranyl ether (1b, 2b, 3b, 4b)

(General procedure No. 1)

Compound 1a, 2a, 3a, 4a (2.58 g; 0.005 mole) was dissolved in dichloromethane (30 mL) and 3,4-dihydropyran (3 mL) and a catalytic amount of boron trifluoride etherate was added to the solution. It was allowed to stand for 24 h, neutralized with morpholine, washed with water, dried and evaporated to dryness. The oily-crystalline residue was subjected to chromatographic separation in a mixture of benzene and petroleum ether (50 : 50). This solvent mixture (8 × 100 mL) was used to elute the pure substance, which was finally recrystallized from a mixture of methanol and water.

#### 16-Methoxymethylandro-5-ene-3 $\beta$ ,17-diol (1c, 2c, 3c, 4c)

(General procedure No. 2)

Compound 1b, 2b, 3b, 4b (1.2 g; 0.002 mole) was dissolved in methanol (25 mL) and refluxed with  $NaOCH_3$  (0.45 g; 0.008 mole) for 48 h. The reaction mixture was acidified to pH 3 with aqueous hydrochloric acid, and boiled gently for 30 min. It was then diluted with water, the crystalline precipitate was filtered off, washed until neutral, and recrystallized from a mixture of ethanol and water.

#### 16-Methoxymethylandro-5-ene-3 $\beta$ ,17-diol 3,17-diacetate (1d, 2d, 3d, 4d)

(General procedure No. 3)

Compound 1c, 2c, 3c or 4c (0.334 g; 0.001 mole) was allowed to stand in a mixture of pyridine (2 mL) and acetic anhydride (2 mL) for 24 h. The reaction mixture was then diluted with water, the precipitate which separated was filtered off, washed with water, dried and recrystallized from methanol.

#### 16 $\alpha$ ,17 $\alpha$ -Epoxyethyleneandro-5-ene-3 $\beta$ -ol (5a)

Compound 1a (1.03 g; 0.002 mole) was dissolved in methanol (25 mL) and refluxed with  $NaOCH_3$  (0.45 g; 0.008 mole) for 6 h. The reaction mixture was then diluted with water, the precipitate was filtered off, washed with water, dried and recrystallized from benzene (0.560 g; 92.7%).

IR: 3500  $cm^{-1}$  (broad, OH), 980  $cm^{-1}$  (oxetane).

Table II

No.	Formula Molecular weight	M.p., °C solvent of crystallization	[ $\alpha$ ] <sub>D</sub>	$R_f$	Analysis, % Calcd./Found		Yield, %	Method No.
					C	H		
1a	C <sub>29</sub> H <sub>40</sub> O <sub>6</sub> S 516.70	136–137 benzene/petro- leum ether	–73°	0.80 (II)	67.42	7.80	88.1	
1b	C <sub>34</sub> H <sub>48</sub> O <sub>7</sub> S 600.82	173–176 methanol	–36°	0.95 (I)	67.55 67.97 67.80	7.90 8.05 8.25	85.7	1
1c	C <sub>21</sub> H <sub>34</sub> O <sub>3</sub> 334.50	208–210 ethanol/water	–64°	0.65 (III)	75.42 75.50	10.01 10.25	92.5	2
1d	C <sub>25</sub> H <sub>38</sub> O <sub>5</sub> 418.58	139–145 methanol	–53°	0.55 (I)	71.84 71.75	9.16 9.30	96.2	3
2b	C <sub>34</sub> H <sub>48</sub> O <sub>7</sub> S 600.82	153–155 methanol	–71°	0.85 (I)	67.97 67.85	8.05 8.30	91.3	1
2c	C <sub>21</sub> H <sub>34</sub> O <sub>3</sub> 334.50	182–183 ethanol/water	–93°	0.40 (III)	75.42 75.50	10.01 10.27	98.2	2
2d	C <sub>25</sub> H <sub>38</sub> O <sub>5</sub> 418.58	161–163 methanol	–114°	0.65 (I)	71.84 71.73	9.16 9.24	98.2	3
3a	C <sub>29</sub> H <sub>40</sub> O <sub>6</sub> S 516.70	152–155 benzene	–65°	0.70 (II)	67.42 67.57	7.80 7.71	84.2	
3b	C <sub>34</sub> H <sub>48</sub> O <sub>7</sub> S 600.82	165–167 methanol/water	–47°	0.85 (I)	67.97 67.83	8.05 8.21	88.3	1
3c	C <sub>21</sub> H <sub>34</sub> O <sub>3</sub> 334.50	194–197 methanol	–76°	0.35 (III)	75.42 75.54	10.01 10.21	92.7	2
3d	C <sub>25</sub> H <sub>38</sub> O <sub>5</sub> 418.58	142–144 methanol	–35°	0.60 (I)	71.84 71.70	9.16 9.31	96.5	3
4b	C <sub>34</sub> H <sub>48</sub> C <sub>7</sub> S 600.82	88–90 methanol	–34°	0.90 (I)	67.97 67.75	8.05 8.14	90.5	1
4c	C <sub>21</sub> H <sub>34</sub> O <sub>3</sub> 334.50	162–164° methanol	–53°	0.60 (III)	75.42 75.60	10.01 10.28	93.4	2
4d	C <sub>25</sub> H <sub>38</sub> O <sub>5</sub> 418.58	139–144 methanol	–44°	0.55 (I)	71.84 71.65	9.16 9.31	90.8	3
5a	C <sub>26</sub> H <sub>30</sub> O <sub>2</sub> 302.46	191–193 benzene	–49°	0.55 (II)	79.44 79.55	10.00 10.21	92.7	
5b	C <sub>22</sub> H <sub>32</sub> O <sub>3</sub> 344.49	118–122 methanol	–48°	0.65 (I)	76.72 76.80	9.36 9.50	94.4	
6a	C <sub>26</sub> H <sub>30</sub> O <sub>2</sub> 302.46	188–190 benzene	–66°	0.50 (II)	79.44 79.51	10.00 10.23	84.4	
6b	C <sub>22</sub> H <sub>32</sub> O <sub>3</sub> 344.49	122–125 methanol	–72°	0.60 (I)	76.72 76.65	9.36 9.41	96.1	
7a	C <sub>26</sub> H <sub>30</sub> O <sub>2</sub> 302.46	130–133 ethanol/water	–67°	0.60 (II)	79.44 79.58	10.00 9.95	95.0	
7b	C <sub>22</sub> H <sub>32</sub> O <sub>3</sub> 344.49	94–96 methanol	–62°	0.70 (I)	76.72 76.83	9.36 9.27	90.0	
8a	C <sub>20</sub> H <sub>32</sub> O <sub>2</sub> 304.47	138–140 ethanol	–67°	0.50 (II)	78.91 78.75	10.59 10.67	95.2	
8b	C <sub>24</sub> H <sub>36</sub> O <sub>4</sub> 388.54	75 methanol	–77°	0.50 (I)	74.20 74.30	9.34 9.47	90.9	

(I) methanol : benzene (1 : 99)

(II) methanol : benzene (5 : 99)

(III) acetone : benzene : petroleum ether (30 : 35 : 35)

**16 $\alpha$ ,17 $\alpha$ -Epoxyethyleneandrost-5-ene-3 $\beta$ -ol 3-acetate (5b)**

Compound **5a** (0.302 g; 0.001 mole) was acetylated according to General procedure No. 3, then crystallized from methanol (0.325 g; 94.4%).

IR: 1250, 1730 (OCO), 980  $\text{cm}^{-1}$  (oxetane)

**16 $\beta$ ,17 $\beta$ -Epoxyethyleneandrost-5-ene-3 $\beta$ -ol (6a)**

Compound **4a** (1.03 g; 0.002 mole) was transformed according to the procedure given for **5a**. The product obtained was subjected to chromatographic separation. With  $4 \times 100$  mL of benzene—petroleum ether (75 : 25) **7a** was eluted (0.012 g; 2%); with  $8 \times 100$  mL of benzene—petroleum ether (50 : 50) and  $2 \times 100$  mL of benzene **6a** was eluted (0.510 g; 84.4%).

IR: 3500 (broad, OH) 970  $\text{cm}^{-1}$  (oxetane).

**16 $\beta$ ,17 $\beta$ -Epoxyethyleneandrost-5-ene-3 $\beta$ -ol 3-acetate (6b)**

Compound **6a** (0.302 g; 0.001 mole) was acetylated according to General procedure No. 3, then crystallized from methanol (0.330 g, 96.1%).

IR: 1250, 1730 (OCO), 970  $\text{cm}^{-1}$  (oxetane)

**16,17-*seco*-5,15(16)-Androstadiene-13 $\alpha$ -formyl-3 $\beta$ -ol (7a)**

(General procedure No. 4)

Compound **2a**, **3a** (1.033 g; 0.002 mole) was dissolved in methanol (25 mL) and refluxed with  $\text{NaOCH}_3$  (0.45 g; 0.008 mole) for 6 h. The reaction mixture was neutralized with 10% ice-cold sulfuric acid, the precipitate which separated was filtered off, washed with water, dried and dissolved in benzene. The product was obtained by chromatographic separation in benzene—petroleum ether (50 : 50);  $8 \times 100$  mL of solvent mixture eluted the pure substance, which was crystallized from a mixture of ethanol and water.

**16,17-*seco*-Androsta-5,15-(16)-diene-13 $\alpha$ -formyl-3 $\beta$ -ol 3-acetate (7b)**

Compound **7a** (0.302 g; 0.001 mole) was acetylated according to General procedure No. 3, then crystallized from methanol (0.310 g, 90.0%).

IR: 1240, 1730 (OCO), 1690  $\text{cm}^{-1}$  (CO).

**16,17-*seco*-Androsta-5,15(16)-diene-13 $\alpha$ -hydroxymethyl-3 $\beta$ -ol (8a)**

Compound **7a** (0.604 g; 0.002 mole) was dissolved in methanol (50 mL) and  $\text{NaBH}_4$  (0.75 g; 0.02 mole) was added. The reduction mixture was diluted with ice-water then acidified with ice-cold 20% sulfuric acid. The precipitate was filtered off, washed until free from acid, and crystallized from ethanol (0.580 g; 95.2%).

**16,17-*seco*-Androsta-5,15(16)-diene-13 $\alpha$ -acetoxymethyl-3 $\beta$ -ol 3-acetate (8b)**

Compound **8a** (0.304 g, 0.001 mole) was acetylated according to General procedure No. 3, then crystallized from methanol (0.350 g; 90.9%).

IR: 1250, 1740 (OCO), 1690  $\text{cm}^{-1}$  (OC).

\*

The authors' thanks are due to Chemical Works of Richter Gedeon Ltd. (Budapest) for supporting this research. The authors are grateful to Dr. J. KISS and Mrs. É. G. GERGELY for the recording of IR spectra, to Dr. K. L. LÁNG and Dr. G. BARTÓK-BOZÓKI for the micro-analysis results and to Miss Cs. HORVÁTH for technical assistance.

## REFERENCES

- [1] CAPON, B., McMANUS, S. P.: Neighbouring Group Participation Vol. I, p. 125 Plenum Press, New York 1976  
 [2] CLAYTON, R. B., HENBEST, H. B., SMITH, M.: J. Chem. Soc., 1957, 1982

- [3] JULIA, S., DECOUVELAERE, B.: *Bull. Soc. Chim. France*, **1963**, 2476  
[4] TSUI, P., JUST, G.: *Canad. J. Chem.*, **51**, 3502 (1973)  
[5] HECKENDORN, R., TAMM, CH.: *Helv. Chim. Acta*, **51**, 1068 (1968)  
[6] HANSON, J. R., ORGAN, T. D.: *J. Chem. Soc. (C)*, **1970**, 1065  
[7] ROWLAND, A. T., DRAWBAUGH, R. S., DALTON, J. R.: *J. Org. Chem.*, **42**, 487 (1977)  
[8] KERB, U., WIECHERT, R.: *Ber.*, **95**, 2956 (1962)  
[9] PIKE, J. E.: *J. Org. Chem.*, **29**, 3476 (1964)  
[10] MATSUI, M., FUKUSHIMA, D. K.: *J. Org. Chem.*, **35**, 561 (1970)  
[11] ALLEN, W. S., BERNSTEIN, S., HELLER, M., LITTEL, R.: *J. Am. Chem. Soc.*, **77**, 4784 (1955)  
[12] BROWN, E. A.: *J. Medicinal Chem.*, **10**, 546 (1967)  
[13] FEIGENBAUM, A., PETE, J. P.: *Tetrahedron Letters*, **1972**, 2767  
[14] PETE, J. P., WOLFHUGEL, J. L.: *Tetrahedron Letters*, **1973**, 4637  
[15] KONDO, Y., WATERS, J. A., WITKOP, B., GUENARD, D., BEUGELMANS, R.: *Tetrahedron*, **28**, 797 (1972)  
[16] GUENARD, D., BEUGELMANS, R.: *Tetrahedron*, **32**, 781 (1976)  
[17] SCHNEIDER, GY., WEISZ-VINCZE, I.: *Chem. Commun.*, **1968**, 2030  
[18] KOVÁCS, Ö., SZILÁGYI, J., SCHNEIDER, GY.: *Magyar Kémiai Folyóirat*, **71**, 93 (1965)  
[19] SCHNEIDER, GY., VINCZE, I., VASS, A.: *Acta Chim. Acad. Sci. Hung.*, **95**, 321 (1977)  
[20] SCHNEIDER, GY., VINCZE, I., VASS, A., HACKLER, L., DOMBI, GY.: *Acta Chim. Acad. Sci. Hung.* **109**, 71 (1982)  
[21] SCHÖNECKER, B., TRESSELT, D., PONSOLD, K.: *Tetrahedron*, **31**, 2845 (1975)  
[22] GROB, C. A., SCHIESS, P. W.: *Angew. Chem.*, **79**, 1 (1967)  
[23] ADAM, G.: *Angew. Chem.*, **79**, 619 (1967)  
[24] SCHNEIDER, GY., WEISZ-VINCZE, I., VASS, A., KOVÁCS, K.: *Tetrahedron Letters*, **1972**, 3349  
[25] GOODLETT, V. W.: *Anal. Chem.*, **37**, 431 (1965)

Gyula SCHNEIDER  
Irén VINCZE  
László HACKLER  
József A. SZABÓ  
György DOMBI

H-6720 Szeged, Dóm tér 8.

## SYNTHESIS OF PEPTIDES CONTAINING D-GLUCOSAMINIC ACID, III\*

### SULFATION OF PEPTIDES

K. GÁLL-ISTÓK<sup>1</sup>, E. ZÁRA-KACZIÁN<sup>1</sup>, L. KISFALUDY<sup>2</sup> and GY. DEÁK<sup>1\*\*</sup>

(<sup>1</sup> *Research Institute of Experimental Medicine, Hungarian Academy of Sciences, Budapest, and* <sup>2</sup> *G. Richter Chemical Works, Budapest*)

Received December 3, 1980

In revised form August 17, 1981

Accepted for publication October 15, 1981

The sulfated derivatives of several oligopeptides containing 4,6-*O*-benzylidene-glucosaminic acid (H-BEGA-OH) were prepared using the adduct of pyridine and SO<sub>3</sub>.

In Part II of this series we reported that fragment condensation with azide had been found suitable for the preparation of the acetates of glycyalanyl-4,6-*O*-benzylidene-glucosaminic amide (H-Gly-Ala-BEGA-NH<sub>2</sub>), glycyal-4,6-*O*-benzylidene-glucosaminylalanine amide (H-Gly-BEGA-Ala-NH<sub>2</sub>) and 4,6-*O*-benzylidene-glucosaminylglycylalanine amide (H-BEGA-Gly-Ala-NH<sub>2</sub>), as well as the acetate of 4,6-*O*-benzylidene-glucosaminylglycylalanyl-4,6-*O*-benzylidene-glucosaminylglycylalanyl amide (H-BEGA-Gly-Ala-BEGA-Gly-Ala-NH<sub>2</sub>).

In continuation of this work, sulfated derivatives of peptides containing glucosaminic acid were to be prepared for the purpose of biological tests. The sulfation reaction may take place at the amino group of the amino acid in *N*-terminal position after removal of the protective group, and at the free hydroxyl groups in the molecule. As described earlier [1], the benzyloxycarbonyl group can be removed from the protected peptides by hydrogenolysis in alcoholic solutions containing acetic acid; in this case the acetal bonds in the 4,6-*O*-benzylidene group protecting the glucosaminic acid remain intact. In the following, methods suitable for the removal of the benzylidene group were examined, since in this way two further hydroxyl groups could be made accessible to the sulfation reaction.

There are only few data in the literature regarding the removal of the benzylidene group by hydrogenolysis, even if all manuals mention it; in the actual cases, usually acid hydrolysis is employed. BERGMANN *et al.* [2] applied it successfully in the case of *Z*-Gly-BEGA-OH and *N*-(benzyloxycarbonyl)-phenylalanyl-4,6-*O*-benzylidene-*D*-glucosaminic acid, using palladium black in methanolic solution containing a large excess of acetic acid; the hydrogenation was finished after the liberation of carbon dioxide had ceased. The mixture

\* Part II: *Acta Chim. Acad. Sci. Hung.*, **107**, 221 (1981)

\*\* To whom correspondence should be addressed

was then transferred into a closed system, and the reaction was continued there until the calculated amount of hydrogen gas had been absorbed. The substance obtained from the reaction contained neither Z, nor benzylidene group.

Precise repetition of this experiment in our laboratory failed to yield the expected product. The melting point of the material obtained by us was identical with that of the substance reported by BERGMANN *et al.*, but two spots were observed in the thin-layer chromatogram. In the IR spectrum, bands characteristic of monosubstituted benzene ring appeared at 705 and 750  $\text{cm}^{-1}$ , and the new band at 1780  $\text{cm}^{-1}$  indicated the formation of lactone or ester. Elemental analysis data of the product did not agree with the calculated values. Attempted purification of the mixture failed. The reaction was repeated with the acetates of Gly-BEGA-NH<sub>2</sub> and Ala-BEGA-NH<sub>2</sub>, but in both cases hygroscopic material was obtained which gave several spots in the TLC tests, and purification could not be achieved. In the IR spectra of the product mixtures from these experiments, the band indicating the presence of ester or lactone at about 1780  $\text{cm}^{-1}$  was absent. In the attempted reductive removal of the benzylidene group, the use of palladium-on-carbon instead of palladium black catalyst was also of no avail.

It was observed that benzaldehyde appeared in the reaction mixture when concentrated hydrochloric acid was used together with palladium-on-carbon in the hydrogenolytic experiments for removal of the benzyloxycarbonyl group. On the basis of observation and literature analogies it became evident that the removal of the protecting group should be effected by hydrolysis. Hence cleavage of the benzylidene group was attempted in methanol containing hydrochloric acid. The model compounds were Z-Gly-BEGA-NH<sub>2</sub> and Z-Ala-BEGA-NH<sub>2</sub>; these were refluxed for 30 min in 95% methanol containing 0.5% hydrochloric acid. Work-up of the reaction mixture gave a substance with definite melting point consisting of one spot on thin-layer. In the IR spectrum of the product, the intensity of the band characteristic of monosubstituted phenyl decreased. It was striking that the Amide I band at 1660  $\text{cm}^{-1}$ , characteristic of the peptide bond could not be found, however, new bands assignable to esters appeared at 1750 and 1230  $\text{cm}^{-1}$ . Consequently, the product is not, either on the basis of the IR spectrum, or the elemental analysis data, the substance expected.

Hydrolysis experiments in aqueous ethanol containing hydrochloric acid and in aqueous trifluoroacetic acid failed similarly. Although benzaldehyde always could be detected during processing, the products obtained were hygroscopic mixtures giving several spots in the thin-layer chromatograms, and their poor solubility in organic solvents of prevented purification.

Summing up the results of experiments, attempts at the removal of the 4,6-*O*-benzylidene group remained unsuccessful in both the hydrogenolysis

and the hydrolysis procedures. This can be attributed to the impossibility of purification of the resulting mixtures, in addition to the occurrence of side-reactions. The substances containing four hydroxyl groups, to be expected on the removal of the benzylidene group, are soluble only in water or short-chain alcohols, but in these solvents the components could not be separated. The results of column chromatographic experiments were also unsatisfactory, since these mixtures were so strongly bound to aluminium oxide or silica gel packing that they could not be eluted. Thus the initial project, sulfation, had to be realized with derivatives containing the benzylidene group.

According to the literature, glucoproteins are sulfated [3] in anhydrous pyridine with chlorosulfonic acid, oleum, or fuming sulfuric acid. These methods could not be employed in the present work, since these very active agents (mineral acids) would also cause the partial or total cleavage of the 4,6-*O*-benzylidene group, yielding thus a mixed end-product. For the sulfation of amino alcohols [4] the use of the pyridine-sulfur trioxide adduct ( $\text{Py}\cdot\text{SO}_3$ ) was reported. This basic reagent seemed to be suitable for the present purpose as it is recommended mainly for use with compounds sensitive to acids. Its application has frequently been described in the literature, though not in the field of glucoproteins.

The sulfated derivatives of the peptides were to be isolated in the form of the sodium salt, and to be characterized primarily by their sulfur to nitrogen ( $\text{S}\%/\text{N}\%$ ) ratio.

The reagent,  $\text{Py}\cdot\text{SO}_3$ , was prepared according to the literature method [5].

In order to determine the reaction conditions, the sulfuric acid semiester of *Z*-serinamide was prepared. The reaction was effected in pyridine solution with  $\text{Py}\cdot\text{SO}_3$  at 65 °C, whereupon the expected product was obtained in 77% yield. Further on, this reaction was used for determining the activity of the newly prepared batches of the  $\text{Py}\cdot\text{SO}_3$  reagent.

The next model compound was a dipeptide amide, H-Gly-BEGA-NH<sub>2</sub>. Under optimal conditions, the free hydroxyl group is converted into a sulfuric acid semiester, and the free amino group into sulfamidic acid. The best procedure was to use two mole-equivalents of  $\text{Py}\cdot\text{SO}_3$  calculated for one group to be sulfated, and the reagents were allowed to react in pyridine at 24 °C for 1 h. Increased temperature or extended reaction times resulted in decomposition of the mixture. Under such conditions,  $[\text{NaSO}_3(\text{Gly-BEGA})\text{SO}_3\text{Na}]\text{-NH}_2$  was isolated in 50% yield; this was the doubly sulfated derivative. The sulfur-nitrogen ration in the product was 1.60 (calcd.  $\text{S}\%/\text{N}\%$ : 1.53). The OH band at 3450  $\text{cm}^{-1}$  in the IR spectrum of the product indicates that one of the hydroxyl groups did not react. This assumption is confirmed by the OH  $\rightarrow$  OD exchange in heavy water (broad, deep band,  $\nu\text{OD}$ , 2300–2600  $\text{cm}^{-1}$ ).

On the basis of the former experience, the sulfation reactions of tripeptides containing glucosaminic acid were investigated. Under the conditions

used for the dipeptide amide H-Gly-BEGA-NH<sub>2</sub>, the corresponding derivatives of H-Gly-BEGA-Ala-NH<sub>2</sub> and H-Gly-Ala-BEGA-NH<sub>2</sub> were prepared in 50% yield. These compounds are now trebly sulfated derivatives. According to the TLC tests, the white, powder substances are homogeneous, and the IR spectra are identical with the spectra of the sodium salts of sulfated H-Gly-BEGA-NH<sub>2</sub> in the range of the characteristic bands. In the compounds, S%/N% = 1.67 (calculated value: 1.72).

In the case of H-BEGA-Gly-Ala-NH<sub>2</sub>, where the groups to be sulfated were located within one amino acid at the *N*-terminal part, the reaction period was extended to 24 h. Under these conditions, the expected product, (NaSO<sub>3</sub>)<sub>3</sub>-BEGA-Gly-Ala-NH<sub>2</sub> was obtained in 68% yield, being the trebly sulfated end-product.

In possession of the experience obtained in the sulfation of tripeptides, the sulfation of H-BEGA-Gly-Ala-BEGA-Gly-Ala-NH<sub>2</sub> was also successfully effected. In this case, too, a reaction time of 24 h and the reagent Py.SO<sub>3</sub> were used. The expected end-product, (NaSO<sub>3</sub>)<sub>3</sub>BEGA-Gly-Ala-BEGA-(NaSO<sub>3</sub>)<sub>2</sub>-Gly-Ala-NH<sub>2</sub> was obtained in 71% yield.

Biological studies on the peptides containing glucosaminic acid will be reported elsewhere.

### Experimental

M.p.'s were determined on a Büchi-Tottoli apparatus and are uncorrected. IR spectra were recorded in KBr pellets (Perkin Elmer Model 457). All compounds were analyzed for C, H, N with results of at least 0.4% accuracy. The *R<sub>f</sub>* values were determined using the ascending techniques of thin-layer chromatography in the following solvent systems:

- (1) EtOAc: AcOH: MeOH: H<sub>2</sub>O = 3:0.7:0.7:0.5;
- (2) *t*-BuOH: AcOH: H<sub>2</sub>O = 2:2:1;
- (3) EtOAc: *i*-PrOH: Py: H<sub>2</sub>O = 2.5:1:0.7:0.7.

For the detection of the spots ninhydrin or chlorotoluidin were used.

#### Sodium salt of the sulfuric acid semiester of *Z*-serine amide Z-Ser(SO<sub>3</sub>Na)-NH<sub>2</sub>

*Z*-Serine amide (0.95 g, 4 mmoles) was dissolved in anhydrous pyridine (15 mL), then the sulfur trioxide adduct [5] (in the following Py.SO<sub>3</sub>) (1.25 g; 8 mmoles) was added, and the reaction mixture was stirred at 65 °C for 1 h. The pyridine was then evaporated in vacuum (2.68 kPa) on a bath of 40 °C temperature, the residual yellow oil was dissolved in water (5 mL), made alkaline with 30% aqueous NaOH to pH 7.5, mixed with ethanol (30 mL) and cooled to 0 °C. The sodium sulfate which separated was filtered off and washed with ethanol (2 × 5 mL). The combined filtrate was evaporated to dryness in vacuum, water was removed by distillation with benzene (3 × 5 mL), then the residue was triturated with dry ether (4 × 10 mL), whereupon the oil turned into a white powder. A substance (1.1 g) decomposing at 170–175 °C was obtained. It was dissolved in methanol (27.5 mL), filtered, and ether (30 mL) was added in small portions while stirring and rubbing the walls of the vessel. The mixture was then cooled to 0 °C; the crystalline substance which separated was filtered off, washed with anhydrous ether (3 × 5 mL) and dried to obtain the analytically pure product (0.99 g; 73%), m.p. 168–177 °C (decompn).

C<sub>11</sub>H<sub>13</sub>N<sub>2</sub>NaO<sub>7</sub>S (340.291).

*R<sub>f</sub>*<sup>3</sup> 0.35.

IR; Amide I 1715, 1680 cm<sup>-1</sup>, Amide II 1540 cm<sup>-1</sup>, ν<sub>3</sub>SO<sub>2</sub> 1250 cm<sup>-1</sup>.

**[Sodium salt of the sulfuric acid semiesther of Z-serine  
Z-Ser(SO<sub>3</sub>Na)—ONa**

Z-Serine (0.96 g; 4 mmoles) was allowed to react with Py.<sub>2</sub>SO<sub>3</sub> as described above. The residue obtained on evaporation of the pyridine was dissolved in water (2 mL) and made alkaline to pH 8 with 30% NaOH (1.85 mL) while stirring at 0 °C. The jelly solution was mixed with ethanol (10 mL) and cooled to 0 °C. The crystals were filtered off with suction, washed with ethanol (2 × 3 mL), the washing liquor was combined with the filtrate, and this solution, now being free from sulfate, was mixed with ethanol (45 mL) while stirring and rubbing the walls of the vessel. The powdery material which separated on cooling was filtered off, washed with dry ether (10 × 5 mL) and dried to obtain 0.9 g (61%) of a product, m.p. 185–187 °C. It was dissolved in water (2 mL), clarified, mixed with ethanol (50 mL) and cooled to 0 °C. The white substance which separated was filtered off and washed with anhydrous ether (3 × 5 mL) to obtain a homogeneous substance (0.56 g; 38%) m.p. 178–181 °C (decompn.).

C<sub>11</sub>H<sub>11</sub>NNa<sub>2</sub>O<sub>8</sub>S (363.259).

R<sub>f</sub><sup>1</sup> = 0.4.

IR: Amide I 1715, Amide II 1530, ν<sub>as</sub>COO<sup>-</sup> 1625, ν<sub>s</sub>SO<sub>2</sub> 1250 cm<sup>-1</sup>.

**Sodium salt of the sulfated derivative of glycyI-4,6-O-benzylideneglucosaminic amide  
(NaSO<sub>3</sub>)<sub>3</sub>Gly-BEGA(SO<sub>3</sub>Na)—NH<sub>2</sub>**

H-Gly-BEGA-NH<sub>2</sub>.AcOH (10. g; 2.25 mmoles) was dissolved in anhydrous pyridine (15 mL), cooled to 15 °C, and Py.<sub>2</sub>SO<sub>3</sub> (2.4 g; 15.0 mmoles) was added to the mixture, with stirring. It was then stirred at room temperature for 1 h. The solvent was decanted from the syrup which separated, and the syrup was rubbed with dry benzene; the benzene was added to the pyridine solution. This resulted in the separation of a small amount of material on shaking. This procedure was repeated several times. The syrups were combined, dissolved in water (7 mL) and the benzene was removed in a vacuum desiccator. The residue was then made alkaline to pH 7.1 with 30% NaOH (about 2.8 mL) at 0 °C while stirring vigorously (the pH was checked potentiometrically). Ethanol (15 mL) was added to the jelly solution, it was cooled to 0 °C, the crystals were filtered off washed with ethanol (2 × 5 mL), the washing liquor was combined with the filtrate and this was mixed with ethanol (15 mL) added in small portions. A sticky material separated from which the liquid was decanted; the residue solidified on rubbing with ethanol (25 mL). After filtration it was washed with ethanol (2 × 5 mL) and with anhydrous ether (4 × 5 mL) and dried over paraffin chips and P<sub>2</sub>O<sub>5</sub> in a vacuum desiccator (0.43 g; m.p. 213–214 °C). The solution obtained from the crude product was mixed with ethanol (120 mL), cooled to -20 °C and processed as described above to obtain a second crop of the substance (0.4 g). The two products were found to be identical on the basis of the physical constants (0.83 g; 61%). S<sub>0</sub>%/N<sub>0</sub>%: 1.62; R<sub>f</sub><sup>1</sup> 0.38, developed twice.

IR: Amide I 1680, Amide II 1540, ν<sub>s</sub>SO<sub>2</sub> 1240, νOH 3450 cm<sup>-1</sup>.

**Sulfation of tripeptide amides containing 4-6-O-benzylideneglucosaminic acid**

The acetate of the appropriate tripeptide amide (2.2 g; 4.64 mmoles) was dissolved in anhydrous pyridine (33 mL), cooled to 15 °C and Py.<sub>2</sub>SO<sub>3</sub> (4.55 g; 28.6 mmoles) was added. The mixture was stirred at room temperature (24 °C) for 1 h (in the case of H-BEGA-Gly-Ala-NH<sub>2</sub>, for 24 h). The liquid was decanted from the syrup which separated, and the procedure was repeated as described for the sulfation of H-Gly-BEGA-NH<sub>2</sub>, using a total of 150 mL of benzene. The combined syrups were dissolved in water (7 mL), benzene was removed, and the solution was made alkaline to pH 7.2 at 0 °C. Ethanol (30 mL) was poured to the jelly solution, it was cooled to 0 °C, the inorganic crystals were filtered off, washed with ethanol (2 × 8 mL), then the combined sulfate-free filtrate was allowed to trickle through a filter bed made from clarifying carbon. The colourless solution was mixed with ethanol (250 mL), cooled to -20 °C, the powder-like substance which separated was filtered with suction, washed with ethanol (2 × 5 mL) and with ether (3 × 10 mL), then dried in a vacuum desiccator.

**Sodium salt of the sulfated derivative of H-Gly-BEGA-Ala-NH<sub>2</sub>  
(NaSO<sub>3</sub>)<sub>3</sub>Gly-BEGA(NaSO<sub>3</sub>)-Ala-NH<sub>2</sub>**

Yield 49%; S<sub>0</sub>%/N<sub>0</sub>%: 1.67 (calcd.: 1.72). M.p. 226–227 °C (decompn.); R<sub>f</sub><sup>1</sup> 0.42, developed twice.

IR: Amide I 1680, Amide II 1540, ν<sub>s</sub>SO<sub>2</sub> 1240 cm<sup>-1</sup>

**Sodium salt of the sulfated derivative of H-Gly-Ala-BEGA-NH<sub>2</sub>**  
 (NaSO<sub>3</sub>)Gly-Ala-BEGA(NaSO<sub>3</sub>)<sub>2</sub>NH<sub>2</sub>

Yield 49%; S<sub>0</sub>/N<sub>0</sub>: 1.62 M.p. 216 °C decompn.; R<sub>f</sub> 0.45, developed twice.  
 IR: Amide I 1680, Amide II 1540, ν<sub>s</sub>SO<sub>2</sub> 1240 cm<sup>-1</sup>.

**Sodium salt of the sulfated derivative of H-BEGA-Gly-Ala-NH<sub>2</sub>**  
 (NaSO<sub>3</sub>)<sub>3</sub>BEGA-Gly-Ala-NH<sub>2</sub>

Yield 68%; S<sub>0</sub>/N<sub>0</sub>: 1.68. M.p. 212° (decompn.); R<sub>f</sub> 0.3, developed twice.  
 IR: Amide I 1680, Amide II 1540, ν<sub>s</sub>SO<sub>2</sub> 1240 cm<sup>-1</sup>.

**Sodium salt of the sulfated derivative of 4,6-O-benzylideneglucosaminylglycylalanyl-  
 -4,6-O-benzylideneglucosaminylglycylalanine amide**  
 (NaSO<sub>3</sub>)<sub>3</sub>BEGA-Gly-Ala-BEGA(NaSO<sub>3</sub>)<sub>2</sub>-Gly-Ala-NH<sub>2</sub>

The acetic acid salt of H-BEGA-Gly-Ala BEGA-Gly-Ala-NH<sub>2</sub> (1.2 g; 1.4 mmole) was dissolved in anhydrous pyridine (18 mL), cooled to 10 °C, and Py.SO<sub>3</sub> (2.45 g; 15.4 mmoles) was added; the mixture was then stirred at room temperature for 24 h. The solution was mixed with benzene (400 mL) added in small portions, the sticky material which separated was rubbed with benzene, dried in a vacuum desiccator, and dissolved in water (13 mL). The clear, yellow solution was made alkaline to pH 7.5 with 30% NaOH (about 2.1 mL) at 0 °C, with vigorous stirring; the pH was checked potentiometrically, then anhydrous ethanol (3.3 mL) was added to the solution and it was cooled to 0 °C.

The jelly crystals which separated were filtered off with suction, washed with anhydrous ethanol (2 × 2 mL), then separately, with anhydrous ether (3 × 5 mL), and dried to obtain a white powder, Na<sub>2</sub>SO<sub>4</sub> (1.13 g).

The sulfate-free yellow filtrate was allowed to trickle through a filter bed made from activated carbon. The colourless solution yielded, on the addition of ethanol (200 mL), a white, well-sedimenting, powdery substance (1.3 g; 71%), which decomposed at 220–221 °C with the evolution of gas. R<sub>f</sub> 0.65. S<sub>0</sub>/N<sub>0</sub>: 1.52 (calcd. 1.64).

IR: Amide I 1675, Amide II 1540, ν<sub>s</sub>SO<sub>2</sub> 1240 cm<sup>-1</sup>.

\*

The authors express their thanks to Mrs. J. HASKÓ-BREUER for recording the infrared spectra and to Miss M. FODOR for the microanalyses.

The authors gratefully acknowledge the support of this work by the Chemical Works of Gedeon Richter Ltd., Budapest.

#### REFERENCES

- [1] GÁLL-ISTÓK, K., ZÁRA-KACZIÁN, E., KISFALUDY, L., DEÁK, GY.: *Acta Chim. Acad. Sci. Hung.*, **107**, 221 (1981)
- [2] BERGMANN, M., ZERVAS, L., RINKE, H., SCHEICH, H.: *Z. physiol. Chem.*, **224**, 23 (1934)
- [3] BERTELLINI, G., BUTTI, A., PIANTANIDA, BR., PRINO, G., RIVA, A., ROSSI, A., ROSSI, S.: *Arzneimittelforschung*, **21**, 247 (1971)
- [4] YUKO, INONE, KINZO NAGASAWA: *J. Org. Chem.*, **38**, 1810 (1973)
- [5] HOUBEN-WEYL: *Methoden der Organischen Chemie Band 11/2*, p. 657, Georg Thieme Verl. Stuttgart 1958

Klára GÁLL-ISTÓK

Erzsébet ZÁRA-KACZIÁN

Gyula DEÁK

H-1450 Budapest, P.O.Box 67.

Lajos KISFALUDY

H-1103 Budapest, Gyömrői u. 19/21.

## NMR RELAXATION STUDIES IN SOLUTION OF TRANSITION METAL COMPLEXES, VII PROTONATION OF THE VANADYL ION IN AQUEOUS SOLUTION

I. NAGYPÁL<sup>1\*</sup>, I. FÁBIÁN<sup>1</sup> and R. E. CONNICK<sup>2</sup>

<sup>1</sup> *Institute of Inorganic and Analytical Chemistry, Kossuth Lajos University, Debrecen and*

<sup>2</sup> *Department of Chemistry, University of California, Berkeley, California, USA)*

Received November 16, 1981

Accepted for publication December 11, 1981

The protonation of the vanadyl ion in aqueous solution has been detected and the equilibrium constant for the



reaction has been determined spectrophotometrically at 298 K, in 6 M (Na,H)ClO<sub>4</sub>. The transverse relaxation of water protons in acidic solutions of vanadyl ion has been studied at 2.5 and 100 MHz frequencies.

A model is given to interpret the relaxation measurements, which takes into account the presence of two paramagnetic sites and the coupling between them through the proton exchange reactions. The contradictory statements concerning to the relaxation behaviour of the system have been reinterpreted and reconciled by the use of the present model.

An electric circuit description of the coupled chemical exchange and paramagnetic relaxation processes is introduced and proved to be equivalent with that of the descriptions based on the BLOCH equations and on formal kinetic considerations. The interrelation of the proton exchange rate constants and the paramagnetic relaxation times are calculated and illustrated on a nomogram.

### Introduction

The NMR relaxation study of the ligand and proton exchange processes taking place in solution of paramagnetic transition metal complexes has received considerable attention since the laying of the foundation of the method by SWIFT and CONNICK [1]. Special attention has been directed to vanadyl complexes in order to understand the peculiar characteristics of vanadyl ion. In a program undertaken in our laboratory, a systematic equilibrium and NMR relaxation study of vanadyl complexes is in progress [2]. The survey of previous work in the literature revealed that there is a contradiction in the interpretation of the NMR relaxation results even in the simplest VO<sup>2+</sup> — H<sup>+</sup> system.

BALLHAUSEN and GRAY [3] described the VO(H<sub>2</sub>O)<sub>5</sub><sup>2+</sup> ion in terms of molecular orbitals. They stated that “the resistance of VO<sup>2+</sup> to protonation

\* To whom correspondence should be addressed

can be understood in terms of the MO bonding scheme. With the oxygen 2p orbitals used for  $\pi$ -bonding only the  $sp\sigma$  hybrid is left for protonation; it has considerable 2s character, and is energetically unsuited for bonding purposes."

RIVKIND [4] thoroughly studied the proton relaxation processes at 18.1 MHz frequency in aqueous vanadyl solutions in presence of oxalic, perchloric, nitric and sulphuric acids up to about 10 M. The considerable increase of the spin—spin relaxation rates with increasing acidity were interpreted as due to the formation and decomposition of  $VOH^{3+}$ , protonated vanadyl ion. For the protonation constant however, only a rough approximation was given, because the ionic strength was not held constant during the experiments. The  $[VOH^{3+}]/([VO^{2+}][H^+])$  protonation constants found are as follows:

$H_2C_2O_4$	$H_2SO_4$	$HNO_3$	$HClO_4$
$\sim 2.5$	$\sim 0.3$	$\sim 0.25$	$\sim 0.13$

The order of the protonation constants was interpreted as due to the interaction of the aquated vanadyl ion with the appropriate anions which increases the electron—density of the vanadyl oxygen.

COPENHAFFER and KENDING [5] studied the  $VO^{2+} - H_3PO_4$  system spectrophotometrically. The data from pH 0—2 could be interpreted by taking into account RIVKIND's results.

SWIFT, STEPHENSON and STEIN [6] also thoroughly studied the kinetics of the protonation of aquated vanadyl ion in aqueous solution, at 60 MHz frequency, in the presence of acetic, phosphoric, sulphuric and perchloric acids. Ionic strength was not held constant in their experiments, but the results were evaluated by taking into account the change of the activity coefficients. They stated, that the similarity of the activation parameters for the proton-catalyzed proton exchange of vanadyl ion and that of nickel(II) and chromium(III) ions is a strong argument against the RIVKIND's interpretation. REUBEN and FIAT [7] carefully studied the proton and deuteron relaxation in aqueous solution of vanadyl ion. They stated that  $T_{2B}$ , the paramagnetic relaxation time in the first hydration shell also plays a role in the overall relaxation. The role of the  $\tau_B$  and  $T_{2B}$  was separated through the comparative study of the proton and deuteron relaxation. The proton relaxation was studied at 60 MHz and the deuteron relaxation at 8.13 MHz frequencies. The assumed mechanism was the same in these two works [6—7], *i.e.* an encounter complex of  $VO(H_2O)_x^{2+}$  and  $H_3O^+$ , followed by the formation of a hydrogen-bonded complex between the  $H_3O^+$  and the waters on the  $VO(H_2O)_x^{2+}$ , and its dissociation.

None of the above interpretations is entirely satisfactory. Using the NMR relaxation method only, it is not possible to distinguish between the

second order proton-catalyzed proton exchange and the formation and decomposition of protonated vanadyl ion, as was done in a chemically completely different, but as an "exchange and relaxation model" very similar copper(II)-glycine system [8]. Thus an independent method of equilibrium analysis should be used to study the protonation of vanadyl ion. Having determined the protonation constant (stability constant of the hydrogen-bonded complex), the NMR relaxation data should be evaluated by taking into account both chemical environments and reaction pathways, in a similar manner as was done in the copper(II)-glycine system.

On the basis of the above, the aims of the present work are:

- to study the  $\text{VO}^{2+} + \text{H}^+ \rightleftharpoons \text{VOH}^{3+}$  equilibrium spectrophotometrically at constant  $\text{ClO}_4^-$  concentration,
- to interpret the NMR relaxation measurements at two different frequencies, taking into account both chemical environments and reaction pathways.

### Experimental

The  $\text{VO}(\text{ClO}_4)_2$  stock solution was prepared from  $\text{NH}_4\text{VO}_3$ . Ammonia was eliminated by heating in alkaline solution. The reduction was carried out mainly by HCl, and finished by KI in acidic solution.

The  $\text{I}_2$  formed was filtered off together with an appropriate amount of charcoal. The halide ions were precipitated with  $\text{AgClO}_4$  prepared from  $\text{Ag}_2\text{O}$  and  $\text{HClO}_4$ . The stock solution neither formed a precipitate with  $\text{AgClO}_4$  nor with HCl solution. The acidity of the stock solution was decreased by addition of sodium hydroxide. The  $\text{VO}^{2+}$  concentration was determined spectrophotometrically. For this, a standard solution was prepared from spectrally pure vanadium.  $\text{NaClO}_4$  was prepared from *p.a.* Merck NaOH and  $\text{HClO}_4$ . The ionic strength of all of the solutions studied was adjusted to 6 M ( $\text{Na}^+$ ,  $\text{H}^+$ ) $\text{ClO}_4^-$ .

A BECKMAN ACTA 3 spectrophotometer was used for the spectrophotometric measurements. Two spectra were recorded in the near IR region on a BECKMAN ACTA M4 instrument.

A NEWPORT N20 type instrument working at 2.5 MHz frequency was used to measure  $T_2$  proton relaxation times. In addition JEOL JNM MH-100 high resolution instrument was used to measure the half-width of the water protons, from which the relaxation times at 100 MHz were calculated in the usual way. All of the experiments were carried out as titrations, *i.e.* two solutions were prepared in which the vanadyl concentration was the same; one of them contained 6 M  $\text{NaClO}_4$  and the other 6 M  $\text{HClO}_4$ . The samples for the different measurements were prepared from these by appropriate mixing. The measurements of the density of some of the samples showed that the mixing did not cause more than 0.5% change in the vanadyl concentration. The density measurements were used to calculate the total proton concentration in the different samples.

### Results and Evaluation

Some of the spectra recorded between 550–800 nm are shown in Fig. 1. The isosbestic point at 756 nm indicates that two different species are in equilibrium in the solution. The same conclusion can be drawn from the COLEMAN–VARGA [9] plots, illustrated in Fig. 2. The two spectra recorded in the near IR region show a maximum 25% difference at 900 nm (see Fig. 3), which proves that the maximum of the equilibrium conversion is at least

25%, even if the molar absorption coefficient of the protonated complex is zero at this wave length. The change of the absorbancy as a function of  $\log [H^+]$  is seen in Fig. 4 at some wave lengths. It is seen in Fig. 4 that the "saturation"

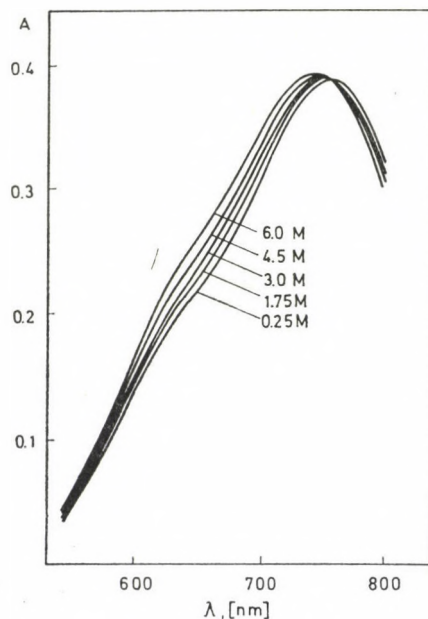


Fig. 1. The spectra of  $4.67 \cdot 10^{-3} M$   $VO(ClO_4)_2$  at different perchloric acid concentrations.  $I = 6 M (Na^+, H^+)ClO_4$ ,  $d = 5$  cm

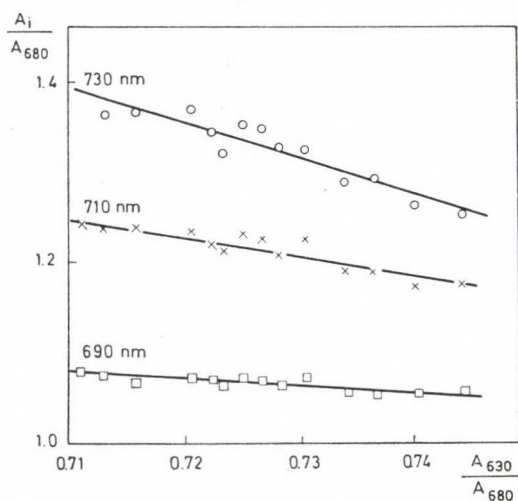


Fig. 2. COLEMAN-VARGA plots [9] of the spectra, indicating two species in equilibrium in the solution

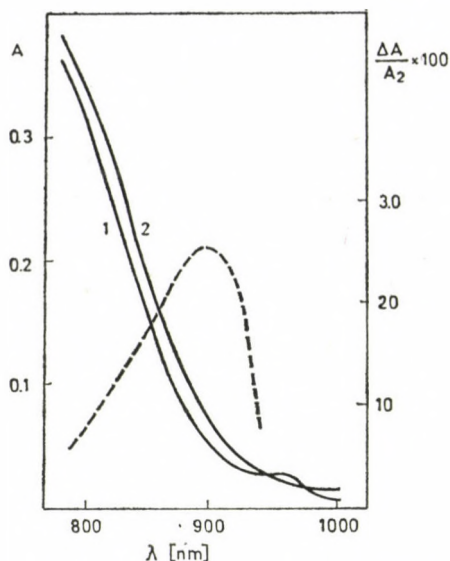


Fig. 3. The spectra of  $4.67 \cdot 10^{-3} M VO(VIO_4)_2$  in the near IR region. 1.  $[H^+] = 6.0 M$ ; 2.  $[H^+] = 0 M$ ;  $d = 5$  cm. The relative deviation of the spectra is shown by the dotted line

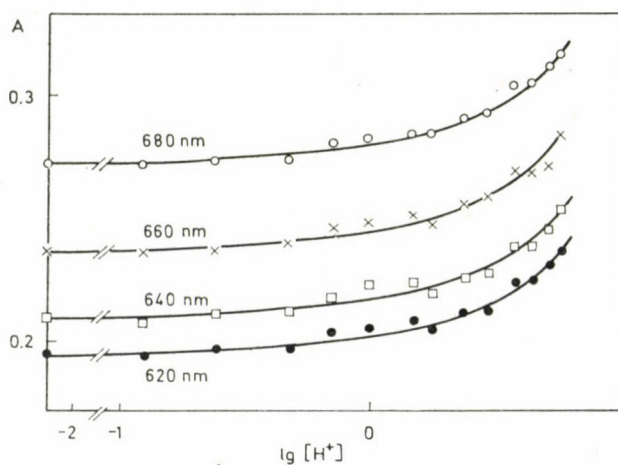


Fig. 4. The change of the absorbance of  $4.67 \cdot 10^{-3} M VO(ClO_4)_2$  as a function of  $\log [H^+]$  at different wave lengths. The full lines are calculated from the equilibrium constant

part of this type of plot is not reached even in  $6 M HClO_4$ , i.e. the maximum of the equilibrium conversion should be less than about 70%.

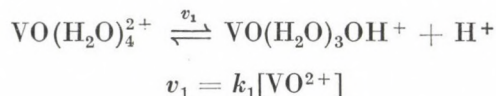
In accordance with the above considerations,

$$K = \frac{[VOH^{3+}]}{[VO^{2+}][H^+]} = 0.23 \pm 0.05$$

was found for the protonation constant of the vanadyl ion from the least squares analysis of the spectra. It means that about 50–60 percentage of the total vanadyl is found in protonated form in 6 M HClO<sub>4</sub>, i.e. the protonated species should be regarded as a separate chemical environment for the protons during the evaluation of the NMR relaxation measurements.

According to BALLHAUSEN and GRAY [3], the protonation of the vanadyl oxygen would result in a significant change of the charge transfer part of the spectrum. On the other hand, the charge transfer bands are — in general — much more sensitive to the change of the composition of the solvent. In spite of this, the difference between the two spectra recorded in the charge transfer region (250–210 nm) in 6 M HClO<sub>4</sub> and in 6 M NaClO<sub>4</sub> was less than 5%. It may be concluded therefore that the protonation site is not the vanadyl oxygen but one of the coordinated water molecules.

The relaxation rate, corrected for the relaxation of the water protons in the absence of vanadyl ion and normalized for the total vanadyl concentration, is shown in Fig. 5 as a function of the perchloric acid concentration. It is seen from the Figure that up to about 0.5 M HClO<sub>4</sub> the relaxation rate changes the same way at the two different frequencies. The extrapolated value of the ordinate in Fig. 5 gives  $k_1 = (1.3 \pm 0.2) \times 10^5 \text{ sec}^{-1}$ , the first order rate constant for the reaction



since the proton relaxation is chemical exchange controlled [6, 11]. The result is in good agreement with the earlier data when the same definition of  $k_1$

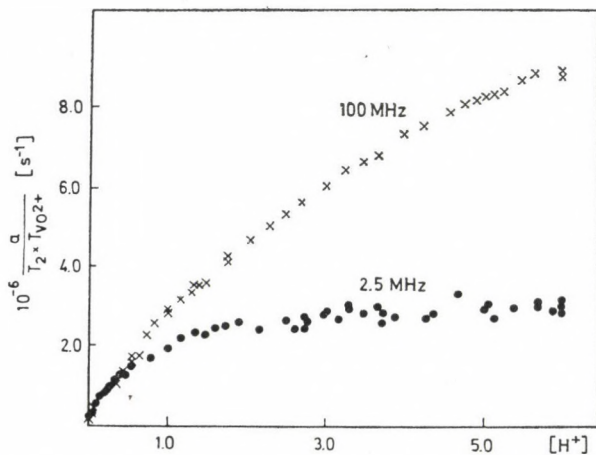
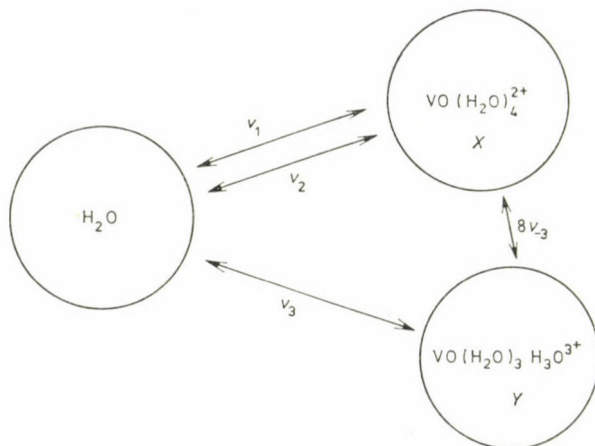


Fig. 5. Normalized relaxation rate of the water protons as a function of perchloric acid concentration at two different frequencies.  $T_{\text{VO}^{2+}}$  is the total vanadyl ion concentration and  $a$  is the total proton concentration

is used and the difference in ionic strengths is taken into account:  $6.2 \times 10^4$  [10],  $1.0 \times 10^5$  [6], and  $1.7 \times 10^5$  [11]  $\text{sec}^{-1}$ .

In accordance with the result of the spectrophotometric measurements, the evaluation of the data is based on the following scheme:



where:

$$v_1 = 1.28 \cdot 10^5 [\text{VO}^{2+}]$$

$$v_2 = k_2 [\text{VO}^{2+}] [\text{H}^+]$$



$$v_3 = k_3 [\text{VOH}^{3+}] = k_3 K [\text{VO}^{2+}] [\text{H}^+] = k_{-3} [\text{VO}^{2+}] [\text{H}^+]$$



$$X = 8[\text{VO}(\text{H}_2\text{O})_4^{2+}] / T_{2B}^{(1)}, \quad Y = 9[\text{VO}(\text{H}_2\text{O})_3\text{H}_3\text{O}^{3+}] / T_{2B}^{(2)}$$

Let us introduce the following denotions:  $a =$  total proton concentration  $= 2[\text{H}_2\text{O}] + [\text{H}^+]$ ;  $b = [\text{VO}^{2+}]$ ,  $c = [\text{VOH}^{3+}]$ . The ratio of the unrelaxed protons in the different sites are denoted by  $f_a$ ,  $f_b$  and  $f_c$ . With these the following equations may be written for the change of the concentration of the unrelaxed protons in the different sites, when the vanadyl concentration is much smaller than the water concentration:

$$\frac{d(a \cdot f_a)}{dt} = (v_1 + v_2)f_b + v_3f_c - (v_1 + v_2 + v_3)f_a = -\frac{a \cdot f_a}{T_{2p}} \quad (4a)$$

$$\frac{d(8b \cdot f_b)}{dt} = (v_1 + v_2)f_a + 8v_3f_c - (v_1 + v_2 + 8v_3 + X)f_b = 0 \quad (4b)$$

$$\frac{d(9c \cdot f_c)}{dt} = v_3f_a + 8v_3f_b - (9v_3 + Y)f_c = 0 \quad (4c)$$

Dividing all three equations by  $f_a$ , yields after rearrangement :

$$\frac{a}{T_{2p}} = (v_1 + v_2)(1 - f_b/f_a) + v_3(1 - f_c/f_a) \quad (5a)$$

$$(v_1 + v_2) = (v_1 + v_2 + 8v_3 + X)f_b/f_a - 8v_3f_c/f_a \quad (5b)$$

$$v_3 = -8v_3f_b/f_a + (9v_3 + Y)f_c/f_a \quad (5c)$$

$f_b/f_a$  and  $f_c/f_a$  may be expressed from equations (5b) and (5c). Substituting these into equation (5a) :

$$\frac{a}{T_{2p}} = \frac{(v_1 + v_2)(9v_3X + 9v_3Y + XY) + v_3(8v_3X + 8v_3Y + XY)}{9v_1v_3 + 9v_2v_3 + 8v_3^2 + 9v_3X + 8v_3Y + v_1Y + v_2Y + XY} \quad (6)$$

There are three different methods for the derivation of equation (6). The method illustrated above was used first by GENSER and CONNICK [12]. Two other methods, based on probability considerations [13] and on the matrix formulation of the BLOCH equations [14] were published by us earlier.

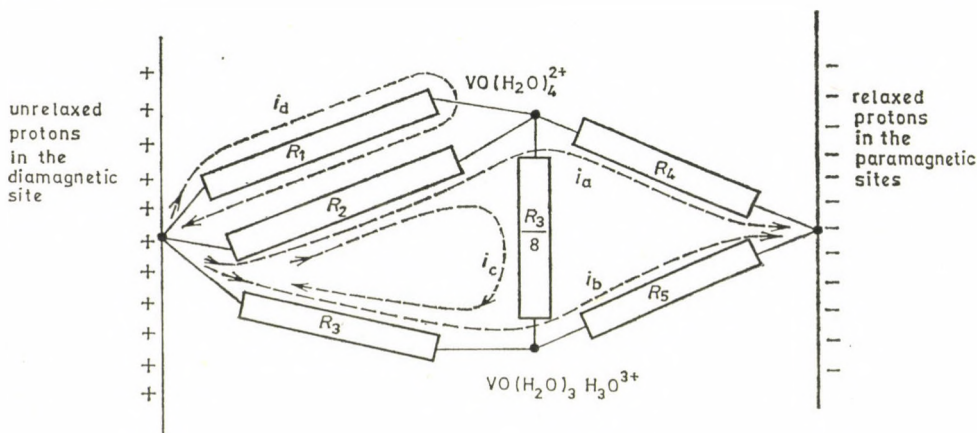
Here we introduce a new method to calculate the exchange contribution of the paramagnetic  $T_2$  relaxation, which seems to be the most concise, and conceptually it is closest to the processes actually taking place in the system when the pulse methods are used to measure the  $T_2$  relaxation time. The system may be regarded as a condenser, which is suddenly filled up, then discharged through differently coupled resistances. The different quantities representing the condenser and the system studied correspond to each other as follows :

Condenser	Paramagnetic system
Capacity, $C$	Total proton concentration, $a$
Voltage, $U$	Ratio of unrelaxed protons, $f_a$
Charge, $Q = C \cdot U$	Concentration of unrelaxed protons, $a \cdot f_a$
Change of the charge	
$\frac{dQ}{dt} = i = -\frac{Q}{C \cdot R}$	$\frac{d(a \cdot f_a)}{dt} = -\frac{a \cdot f_a}{T_{2p}}$
Conductance = $1/R$	$a/T_{2p}$
Current between two points of the circuit	Flow rate of the unrelaxed protons between two sites
$i_{a,b} = \kappa_{a,b}(U_a - U_b)$	$v_{a,b}(f_a - f_b)$
Conductance between two points of the circuit	Rate of chemical exchange between sites $a$ and $b$ or the rate of paramagnetic relaxation
$\kappa_{a,b}$	$v_{a,b}, X, Y$

(For  $CW$  NMR an analogous network of coupled resistances and a voltage source would be the appropriate model)

The pulsed NMR method may be visualized in terms of the above scheme. After a sudden filling of the condenser it is discharged through the appropriate resistances, *i.e.* through the different chemical exchange and paramagnetic relaxation processes. The time necessary to reduce the initial charge to its *e*-th part is  $CR$ , *i.e.*  $T_{2p}$ . Thus the aim of the derivation of the paramagnetic exchange-contribution is to express the resultant conductance of the appropriate circuit in terms of the individual resistances (conductances).

The electric circuit which may be drawn for the  $VO^{2+} - H^+$  system is as follows:



where:  $R_1 = 1/v_1$ ,  $R_2 = 1/v_2$ ,  $R_3 = 1/v_3$ ,  $R_4 = 1/X$ ,  $R_5 = 1/Y$ . The starting equations — based on the KIRCHOFF's rule — are as follows:

$$\begin{aligned} i_d R_1 + (i_d - i_a - i_c) R_2 &= 0 \\ (i_a + i_c - i_d) R_2 + i_a R_4 &= U \\ (i_a + i_c - i_d) R_2 + i_c R_3 \cdot 8 + (i_c - i_b) R_3 &= 0 \\ (i_b - i_c) R_3 + i_b R_5 &= U \end{aligned}$$

These equations are linear for  $i_b$ ,  $i_c$ ,  $i_d$  and  $i_a$ . Thus the resultant conductance  $(i_a + i_b)/U$  ( $= a/T_{2p}$ ) may be expressed as follows from the appropriate determinants:

$$\frac{a}{T_{2p}} = \frac{\frac{1}{R_2 R_4 R_5} + \frac{1}{R_1 R_4 R_5} + \frac{1}{R_3 R_4 R_5} + \frac{8}{R_3^2 R_4} + \frac{8}{R_3^2 R_5} + \frac{9}{R_2 R_3 R_4} + \frac{9}{R_1 R_3 R_4} + \frac{9}{R_2 R_3 R_5} + \frac{9}{R_1 R_3 R_5}}{\frac{1}{R_4 R_5} + \frac{1}{R_2 R_5} + \frac{1}{R_1 R_5} + \frac{8}{R_3 R_5} + \frac{8}{R_3^2} + \frac{9}{R_3 R_4} + \frac{9}{R_2 R_3} + \frac{9}{R_1 R_3}} \quad (8)$$

It is easy to show that equations (6) and (8) are the same; they are equally appropriate for expressing the chemical exchange and paramagnetic relaxation contribution to the measured relaxation time. All of these methods are applicable only when the  $\Delta\omega$  transverse relaxation [1] is unimportant, as is the case here.

Figure 5 shows that the effect of  $v_1$  is negligible compared to that of  $v_2, v_3$  and  $8b/T_{2B}^{(1)}$ ; therefore its contribution to the measured relaxation rate may be regarded as an additive term. With this assumption equation (6) may be rearranged into the following form, which describes the dependence of the relaxation rate — normalized for  $[\text{VO}^{2+}]$  — on the hydrogen ion concentration.

$$S = [\text{H}^+] \frac{Z + \frac{W}{9} + \frac{9ZW}{P} [\text{H}^+]}{1 + \left( Z + \frac{64W}{9} \right) [\text{H}^+]} \quad (9)$$

where

$$S = \frac{a}{T_{2p} [\text{VO}^{2+}]} - k_1$$

$$P = \frac{8}{T_{2B}^{(1)}}$$

$$Z = \left( k_2 + \frac{8}{9} K k_3 \right)$$

$$W = \frac{K}{T_{2B}^{(2)} + k_3^{-1}}$$

The  $S$  values may be calculated directly from the measured data. These are plotted as a functions of  $[\text{H}^+]$  in Figures 6 and 7. It is seen from the Figures that the normalized relaxation rate changes the same way at the two frequencies up to about 0.3  $M$   $\text{HClO}_4$  only. The straight line describing the data at 100 MHz frequency clearly shows that the  $T_{2B}$  in the first hydration sphere of aquated vanadyl ion has no role in the measured data, while it is an important factor in governing the relaxation rate at 2.5 MHz frequency.

The mathematical analysis of equation (9) shows that the slope of the straight line at 100 MHz frequency may be given as follows:

$$\text{slope} = Z + \frac{1}{9} W = (3.6 \pm 0.4) 10^6 M^{-1} \text{sec}^{-1}.$$

Thus, assuming that the paramagnetic relaxation time in the protonated vanadyl ion is negligible compared to  $k_3^{-1}$ , then:

$$k_2 + K \cdot k_3 = k_2 + k_{-3} = (3.6 \pm 0.4) 10^6 M^{-1} \text{sec}^{-1}.$$

The most important conclusion of this result is that the effects of the proton-catalyzed proton exchange and the formation and dissociation of the protonated vanadyl ion can not be separated, even when the equilibrium constant is known from independent measurements.

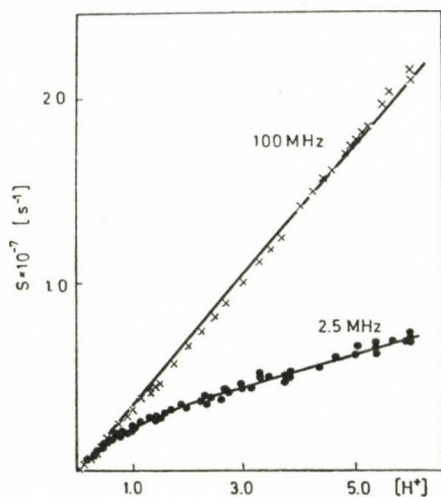


Fig. 6. The  $S = f([H^+])$  function at two different frequencies up to  $t_0^*[H^+] = 6.0 M$  (see: text)

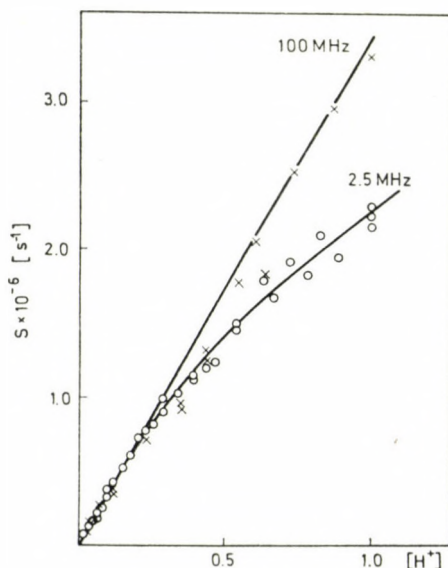


Fig. 7. The  $S = f([H^+])$  function at two different frequencies up to  $[H^+] = 1.0 M$

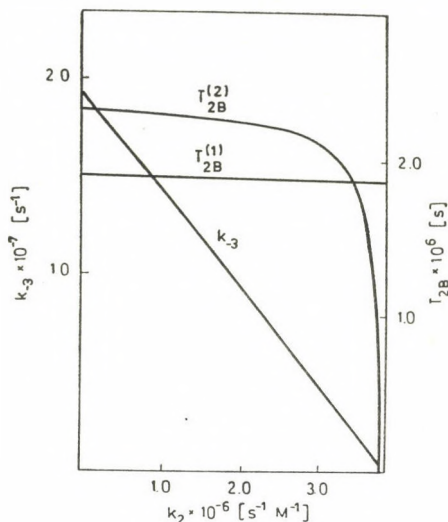


Fig. 8. The inter-relationship of the parameters representing the exchange processes and the paramagnetic relaxation in the  $\text{VO}^{2+}-\text{H}^+$  system

The least squares fit of the  $S = f[\text{H}^+]$  function at 2.5 MHz for  $P$ ,  $Z$  and  $W$  leads to the following results:

$$P = (4.2 \pm 0.4) 10^6 \text{ sec}^{-1}$$

$$Z = (3.9 \pm 0.4) 10^6 \text{ M}^{-1}\text{sec}^{-1}$$

$$W = (9.8 \pm 0.8) 10^4 \text{ M}^{-1}\text{sec}^{-1}$$

From these data only  $T_{2B}^{(1)}$  can be given; the other parameters,  $k_2$ ,  $k_3$  and  $T_{2B}^{(2)}$  are inter-related.

$$T_{2B}^{(1)} = (1.9 \pm 0.2) 10^{-6} \text{ sec (2.5 MHz)}$$

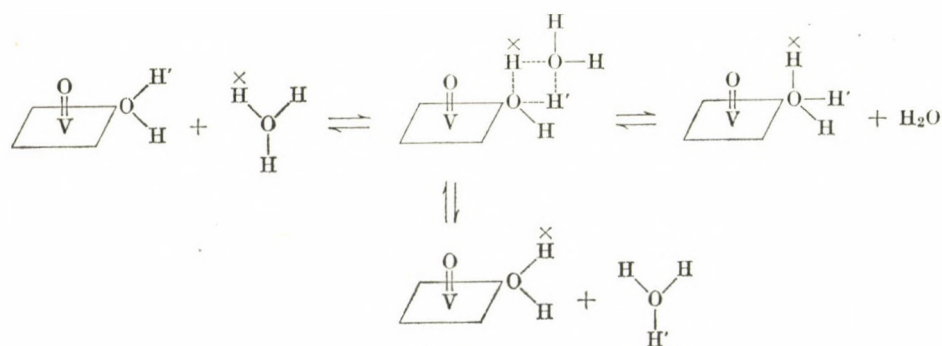
The inter-relationship of the parameters is illustrated in Fig. 8. It is a reasonable assumption, that  $T_{2B}^{(1)} \leq T_{2B}^{(2)}$ , thus the following range of the parameters may be read from the Figure:

$$1.9 10^{-6} \text{ sec} < T_{2B}^{(2)} < 2.4 10^{-6} \text{ sec}$$

$$k_2 < 3.9 10^{-6} \text{ M}^{-1} \text{ sec}^{-1}$$

$$1.9 10^7 \text{ sec}^{-1} > k_3 > 2 10^6 \text{ sec}^{-1}$$

It should be mentioned, that different protons may be distinguished in the  $\text{VO}(\text{H}_2\text{O})_3\text{H}_3\text{O}^{3+}$  site. In this derivation, however, the nine protons are regarded, as equivalent. It means, that the  $T_{2B}^{(2)}$ -range given from this consideration is an "average" of the different paramagnetic relaxation times characterizing the different protons in the protonated vanadyl ion. In principle, it would be possible to distinguish between the different protons of  $\text{VO}(\text{H}_2\text{O})_3\text{H}_3\text{O}^{3+}$ , but the resulting equations are much more complicated, or they contain more than three parameters to be fitted. The present experimental data, however, can be fitted within the experimental error with a one-parameter equation at 100 MHz and with a three-parameter equation at 2.5 MHz, thus the use of a more complicated model is not justified. It is seen in Fig. 8. That the  $k_2 \cong 0$  case would agree with RIVKIND's [4], the  $k_3 \cong 0$  case would agree with SWIFT's [6] interpretation. The most probable situation is, however, that both processes are taking place: protonated vanadyl ion is formed at sufficiently high hydrogen ion concentration, but the proton-catalyzed proton-exchange without the stabilization of the  $\text{VOH}^{3+}$  hydrogen-bonded complex is also an important reaction pathway. The mechanism of the proton exchange in the light of the above is probably as follows:



Contrary to RIVKIND's interpretation however, the protonation site of the vanadyl ion is not the  $\text{VO}^{2+}$  oxygen, but one of the coordinated water molecules. Quantum chemical calculations are in progress to predict the most probable structure of the protonated vanadyl ion.

#### REFERENCES

- [1] SWIFT, T. J., CONNICK, R. E.: *J. Chem. Phys.*, **37**, 307 (1962)
- [2] NAGYPÁL, I., FÁBLIÁN, I.: part V, part VI, *Inorg. Chim. Acta* **61**, 109 (1982), **62**, 193 (1982)
- [3] BALLHAUSEN, C. J., GRAY, H. B.: *Inorg. Chem.*, **1**, 111 (1962)

- [4] RIVKIND, A. J.: Dokl. Acad. Nauk USSR, **142**, 137 (1962)  
[5] COPENHAFFER, W. C., KENDING, M. W.: Inorg. Chim. Acta, **17**, 175 (1976)  
[6] SWIFT, T. J., STEPHENSON, T. A., STEIN, G. R.: J. Am. Chem. Soc., **89**, 1611 (1967)  
[7] REUBEN, J., FIAT, D.: Inorg. Chem., **6**, 579 (1967); **8**, 1821 (1969)  
[8] NAGYPÁL, I., DEBRECZENI, F., CONNICK, R. E.: Inorg. Chim. Acta, **48**, 225 (1981)  
[9] COLEMAN, I. S., VARGA, L. P.: Inorg. Chem., **9**, 1015 (1970)  
[10] REUBEN, J., FIAT, D.: J. Am. Chem. Soc., **91**, 4652 (1968)  
[11] WÜTHRICH, K., CONNICK, R. E.: Inorg. Chem., **7**, 1377 (1968)  
[12] GENSER, E. E., CONNICK, R. E.: J. Chem. Phys., **58**, 990 (1973)  
[13] NAGYPÁL, I., FARKAS, E., DEBRECZENI, F., GERGELY, A.: J. Phys. Chem., **82**, 1548 (1978)  
[14] DEBRECZENI, F., NAGYPÁL, I.: J. Magn. Res., **37**, 363 (1980)

István NAGYPÁL	}	H-4010 Debrecen
István FÁBIÁN		
Robert E. CONNICK		Berkeley, California, 94720, USA

## MECHANISTIC FEATURES OF COBALOXIME(II) CATALYZED OXIDATIONS WITH DIOXYGEN

S. NÉMETH, A. FÜLEP-POSZMIK and L. I. SIMÁNDI\*

(Central Research Institute for Chemistry, Hungarian Academy of Sciences, Budapest)

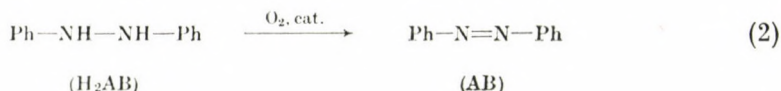
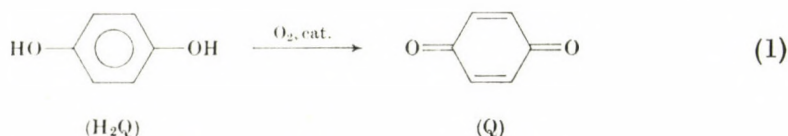
Received December 12, 1981

Accepted for publication December 16, 1981

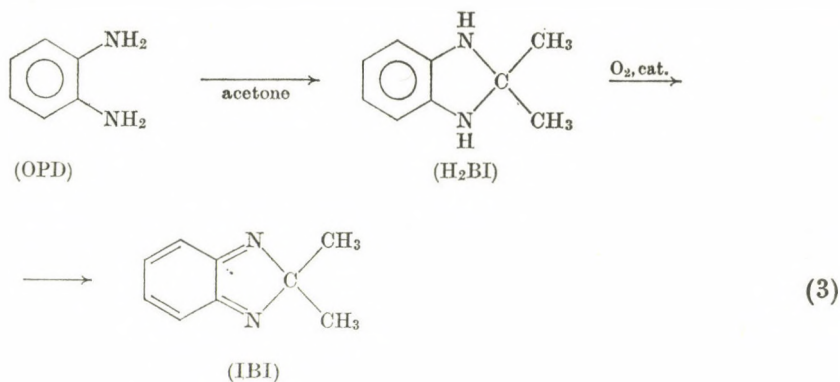
Cobaloxime(II) derivatives of the formula  $\text{Co}(\text{Hdmg})_2\text{L}_n$ , where  $\text{Hdmg}^-$  is the monoanion of dimethylglyoxime, L is  $\text{Ph}_3\text{P}$ , py and  $\text{Et}_3\text{N}$  and  $n = 1$  or 2, are active catalysts of dehydrogenation and oxygen insertion reactions at room temperature and atmospheric  $\text{O}_2$  pressure. Hydrogen peroxide is not an intermediate and inactive cobaloxime(III) derivatives are not formed during the reactions. ESR, UV-Vis and polarography data point to successive O-atom transfer from superoxocobaloxime(III) and  $\mu$ -peroxodicobaloxime(III) to the substrates *via* a cobalyl ion type oxenoid reagent.

We have recently reported that cobaloxime(II) complexes of the general formula  $\text{Co}(\text{Hdmg})_2\text{L}_n$ , where L is  $\text{Ph}_3\text{P}$ , py and  $\text{NEt}_3$ ,  $\text{Hdmg}^-$  is the monoanion of dimethylglyoxime, and  $n = 1$  or 2, show a remarkable catalytic activity in the oxidation of certain organic compounds by molecular oxygen under mild conditions [1–3]. The catalytic oxidations observed thus far include both **dehydrogenations** and **oxygen insertions**, as exemplified by the following equations :

### Dehydrogenations



\* To whom correspondence should be addressed



### Oxygen insertions



where

H<sub>2</sub>Q -- hydroquinone, Q — *p*-benzoquinone,

H<sub>2</sub>AB -- hydrazobenzene, AB — azobenzene

OPD -- *o*-phenylenediamine,

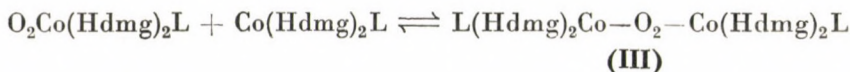
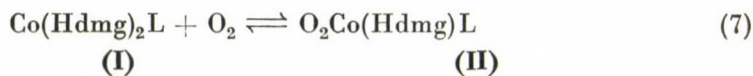
H<sub>2</sub>BI -- 2,2-dimethyldihydrobenzimidazole

IBI -- 2,2-dimethyl-2*H*-benzimidazole

Apparently, the catalyst system contains an active species which is capable of abstracting hydrogen atom(s) and/or transferring oxygen atom(s). This behaviour indicates that the cobaloxime(II) — dioxygen catalytic systems may be regarded as models for biological oxidoreductases and their study might provide mechanistic information on the type of species responsible for catalytic oxidation in living organisms. Of particular interest are the systems in which a species capable of transferring an oxygen atom to a substrate might form, especially if it is derived from dioxygen. The reactions of Eqs (4)–(6) take place in acetone but other nonprotic solvents can also be applied (benzene, THF). In these media formation of the observed products strongly indicates direct transfer of an O-atom from some “oxenoid” species present in the cobaloxime (II)–dioxygen system.

Relevant to this work is the nature of oxygen complexes formed upon contact of the various cobaloxime(II) derivatives with dioxygen or air. According to ESR investigations, cobaloxime(II) reacts with O<sub>2</sub> in nonprotic solvents

to yield mononuclear superoxo and dinuclear  $\mu$ -peroxo complexes [4]:



A subsequent slower process provides a dinuclear  $\mu$ -superoxodicobaloxime and a  $\text{Co(Hdmg)}_2(\text{OH})\text{L}$  type cobaloxime (III) complex. Both superoxo complexes can be readily detected *via* their 8 and 15 line ESR spectra, respectively, while the  $\mu$ -peroxo complexes III have typical UV-Vis spectra depending on the type of ligand L. Thus the presence or absence, and the changes in concentration of these oxygen complexes can be conveniently detected during any catalytic reaction.

### Results and Discussion

A basic fact relating to the oxidation mechanisms operating in the cobaloxime(II) systems is that cobaloxime(III) derivatives of the general formula  $\text{Co(Hdmg)}_2(\text{X})\text{L}$  (where X is  $\text{OH}^-$  or Cl) do **not** catalyze reactions (1)–(6). The addition of such complexes to a catalytic system either prior to or during the reaction has no effect whatsoever on the process.

The addition of free-radical acceptors to the reacting mixtures did not affect the rate of the reactions (quinone, 2,6-disubstituted quinones, hydroquinone, 2,6-disubstituted hydroquinones). The ESR spectra recorded during reaction did not reveal the presence of any organic radicals.

The above observations strongly favour non-radical (molecular) mechanisms for the cobaloxime(II) catalyzed oxidations studied.

#### *Catalytic dehydrogenations*

Catalytic reactions (1)–(3) were performed at 1 atm of  $\text{O}_2$  pressure and at room temperature in acetone. The substrate to catalyst ratio was varied between 200 and 5. The concentration of the organic reactants and products was followed by gas chromatography and UV-Vis spectrophotometry (azobenzene). The initial rates of  $\text{O}_2$  uptake listed in Table I reveal the following reactivity order for the three substrates



The stoichiometries are correctly represented by Eqs (1)–(3) as the amount of product at any instant is equivalent to the amount of  $\text{O}_2$  consumed up to

Table I

Substrates	$C_{\text{subs.}}$ [mol/L]	$C_{\text{cat.}}$ [mol/L]	Initial rate of $O_2$ uptake [n mL/min]
H <sub>2</sub> AB	0.1	$2 \times 10^{-3}$	22
H <sub>2</sub> O	0.1	$1 \times 10^{-2}$	1.7
H <sub>2</sub> BI	0.1	$1 \times 10^{-2}$	0.9
Ph <sub>3</sub> P	0.1	$1 \times 10^{-2}$	0.27
Bu-NC	0.1	$1 \times 10^{-2}$	0.08

Solvent 50 mL acetone,  $T = 25^\circ\text{C}$ ,  $p_{O_2} = 1$  atm in every reaction

that time, within the error of the analytical methods used (gas volumetry and gas chromatography).

The reactivity of the cobaloxime oxygen complexes towards the substrates has been demonstrated by adding solutions of H<sub>2</sub>AB, H<sub>2</sub>Q and H<sub>2</sub>BI to freshly oxygenated cobaloxime(II) solutions ( $L = \text{Ph}_3\text{P}$ ) in acetone, where rapid formation of II and III is known to take place. Complete disappearance of these oxygen complexes was observed with H<sub>2</sub>AB; their concentration was strongly decreased in the presence of H<sub>2</sub>Q and H<sub>2</sub>BI. When these solutions are cooled to  $-40^\circ\text{C}$  the colour of the oxygen complexes reappears, catalytic oxidation being apparently slowed down.

A question of importance is whether or not hydrogen peroxide is formed as an intermediate in these dehydrogenations. The formation of H<sub>2</sub>O<sub>2</sub> is a reasonable possibility, which can be realized *via* successive or simultaneous H atom transfer from the substrate to coordinated dioxygen. The intermediacy of H<sub>2</sub>O<sub>2</sub> has been demonstrated by HALPERN and SENN [5] in the oxidation of Ph<sub>3</sub>P catalyzed by Pt(Ph<sub>3</sub>P)<sub>3</sub>. Although, no H<sub>2</sub>O<sub>2</sub> is formed in reactions (1)–(3), it still may be present as an intermediate, which would subsequently react with a second molecule of the substrate to complete the catalytic cycle. Both polarography and conventional chemical analysis failed to detect H<sub>2</sub>O<sub>2</sub> during dehydrogenations (1)–(3). It has been shown that H<sub>2</sub>O<sub>2</sub> reacts but very slowly with the substrates used, thus, if formed, it should have been accumulated in the reacting systems. Cobaloxime(II) compounds react with H<sub>2</sub>O<sub>2</sub> only slowly and the products are catalytically inactive cobaloxime(III) derivatives. These facts strongly disfavour the intermediate formation of hydrogen peroxide in these systems.

As concerns the type of cobaloxime species present during catalytic oxidation, the following has been established. In the case of the most rapidly oxidized substrate, H<sub>2</sub>AB, ESR experiments have shown that only the unchanged cobaloxime(II) catalyst, Co(Hdmg)<sub>2</sub>L, is present during the fastest

stage of the reaction: its signal intensity was equal, within the experimental error, to that of a solution prepared under  $N_2$  without added substrate. None of the oxygen complexes or cobaloxime(III) derivatives could be observed by polarography during the reaction. At later stages, however, when the product azobenzene reaches appreciable concentrations, the ESR signal due to  $Co(Hdmg)_2L$  decreases owing to complex formation between catalyst and product (*cf.* later).

During the catalytic oxidation of  $H_2Q$  and  $H_2BI$ , *i.e.* the less reactive substrates, the picture is slightly different inasmuch as at the first stage all 3 components of equilibria [7], *i.e.* **I**, **II** and **III** are present at readily detectable levels as witnessed by ESR and UV-Vis spectra. Later, however, **III** slowly disappears and  $Co(Hdmg)_2(OH)L$  begins to accumulate, as shown by the polarograms recorded. This is accompanied by the decrease of the catalytic activity (slower  $O_2$  uptake).

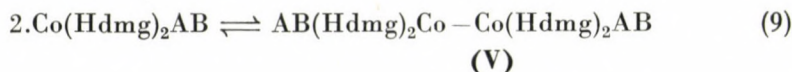
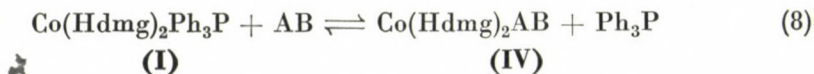
From these observations it is evident that the faster the catalytic reaction, the lower the concentrations of the oxygen complexes **II** and **III** are at a given extent of reaction.

#### *Effect of product on hydrazobenzene oxidation*

The decrease of the ESR signal intensity due to  $Co(Hdmg)_2L$  at later stages of  $H_2AB$  oxidation without observable formation of **II** and/or **III**, or any cobaloxime(III) complexes deserves special attention. Such a situation is expected to prevail if a cobaloxime(II) dimer forms, which would have no ESR signal.

The volumetric  $O_2$  uptake curves shown in Fig. 1 illustrate the observed phenomena with respect to the effect of azobenzene. Curve 1 corresponds to a typical catalytic oxidation: the system contains only the catalyst and hydrazobenzene. The remarkably fast reaction comes to a rather abrupt stop after about 70% of the  $O_2$  required has been consumed. Similar curves but with smaller final  $O_2$  uptake are observed if the system contains added product (AB, curves 2 and 3). In the presence of excess  $Ph_3P$ , the  $O_2$  consumption becomes greater than without additives (curves 4 and 5).

The observed behaviour can be rationalized in terms of complex formation between cobaloxime(II) and azobenzene, followed by dimerization to an ESR-inactive species:



If dimer V is catalytically inactive, *i.e.* does not react with  $O_2$ , it will gradually tie up the active catalyst I, reducing both the rate and conversion. Added product will enhance these phenomena. According to Eq. (8), excess  $Ph_3P$

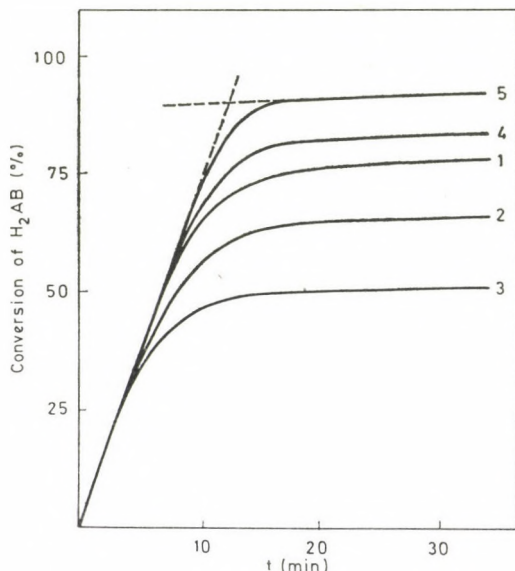


Fig. 1. Effect of additives on kinetic curves of  $H_2AB$  oxidation catalyzed by  $(Ph_3P)_2Co(Hdmg)_2$ . Solvent acetone,  $T = 25^\circ C$ ,  $p_{O_2} \approx 1$  atm,  $C_{H_2AB} = 0.1$  mol/L.

1.  $3 \times 10^{-4}$  mol/L  $(Ph_3P)_2Co(Hdmg)_2$ ;
2.  $3 \times 10^{-4}$  mol/L  $(Ph_3P)_2Co(Hdmg)_2$  + 0.05 mol/L AB;
3.  $3 \times 10^{-4}$  mol/L  $(Ph_3P)_2Co(Hdmg)_2$  + 0.1 mol/L AB;
4.  $3 \times 10^{-4}$  mol/L  $(Ph_3P)_2Co(Hdmg)_2$  + 0.05 mol/L  $Ph_3P$ ;
5.  $3 \times 10^{-4}$  mol/L  $(Ph_3P)_2Co(Hdmg)_2$  + 0.1 mol/L  $Ph_3P$

suppresses complex formation with AB, leading to a longer life of the catalyst and, consequently, to a higher conversion.

To support these assumptions we have prepared dimer V under  $N_2$ . Its elemental analysis, infrared spectra and gas chromatographic behaviour were consistent with the proposed composition. Acetone solutions of the solid prepared give no ESR signals. Methanol solutions of the solid show a polarographic half-wave potential at about 1.25 V (*vs.* S.C.E. under  $N_2$ ), indicating that cobalt is in the +2 oxidation state. Its acetone solutions react with dioxygen extremely slowly, and do not catalyze the oxidation of hydrazobenzene. However, the addition of excess  $Ph_3P$  starts and sustains the catalytic reaction.

It is interesting that  $Co(Hdmg)_2(Ph_3P)$  is quite stable against dimerization in acetone solution [6], however, replacement of the *axial*  $Ph_3P$  ligand strongly enhances the formation of a diamagnetic cobaloxime(II) dimer.

### Oxygen insertions

Reactions (4)–(6) resulting in a net O-atom insertion occur at room temperature and atmospheric O<sub>2</sub> pressure. The volumetric O<sub>2</sub>-uptake rates are much lower than for dehydrogenations with the same cobaloxime(II) catalysts. Reaction (4) was tested for H<sub>2</sub>O<sub>2</sub>; it was not found to appear at any stages of the process.

The substrates of reactions (4) and (5) are also good ligands. If catalysts Co(Hdmg)<sub>2</sub>L with L other than Ph<sub>3</sub>P (*e.g.* pyridine, Et<sub>3</sub>N) are used for the oxidation of Ph<sub>3</sub>P as substrate at substrate to catalyst ratios of 5–20, then the catalyst is first converted to Co(Hdmg)<sub>2</sub>Ph<sub>3</sub>P. Already at the early stages of the reaction, the oxygen complexes of types II and III (with L = Ph<sub>3</sub>P) can be readily detected by ESR and UV-Vis spectroscopy, respectively.

Similarly, *n*-butyl and *n*-octyl isocyanide substrates first displace the *axial* ligand L and the resulting isocyano complexes will act as catalysts. The rate of isocyanide oxidation is independent of the nature of L in the complex used as the source of cobaloxime(II). The UV-Vis spectra are practically the same during oxidation with any initial Co(Hdmg)<sub>2</sub>L.

### Conclusions

The cobaloxime(II) catalyst systems described are capable of effecting both dehydrogenation and oxygen insertion processes. The results presented indicate the involvement of an "oxenoid" reagent, which can transfer two oxygen atoms in succession to suitable acceptors or can abstract 2 × 2 hydrogen atoms from suitable H atom donors. These rather remarkable features are required by the facts that

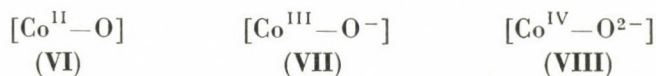
- (i) H<sub>2</sub>O<sub>2</sub> is not involved as an intermediate, and
- (ii) there is no loss of cobaloxime in the form of cobaloxime(III), which is known to lack catalytic activity.

Let us illustrate the requirements on an example. Suppose that the superoxo complex II is responsible for the dehydrogenation of hydrazobenzene, leading to the formation of either H<sub>2</sub>O<sub>2</sub> or H<sub>2</sub>O:

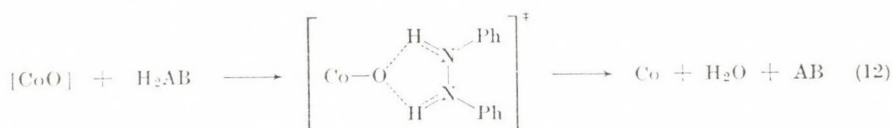


(for clarity, Co now stands for Co(Hdmg)<sub>2</sub>L). Formally, reaction (10) reproduces Co, which is necessary for repeated catalytic cycles to occur. However, the failure to detect H<sub>2</sub>O<sub>2</sub> during the reaction eliminates process (10) as a possibility. On the other hand, reaction (11) conforms to the observations,

but it is hard to visualize the identity of the species [CoO]. Formally, it is a cobaltyl ion and may be represented by one of the following structures :



or more probably, by a resonance hybrid of the three structures. The transfer of one H atom to [CoO] would produce the highly stable hydroxocobaloxime(III) moiety,  $\text{Co}^{\text{III}}-\text{OH}$ , *i.e.*  $\text{Co}(\text{Hdmg})_2(\text{OH})\text{L}$ , which is catalytically inactive. Consequently, the transfer of each H atom would lead to the loss of a catalyst molecule, which is clearly not the case. One must, therefore, conclude that 2 H atoms are abstracted by [CoO] in a concerted process, *via* a possible transition state as depicted by Eq. (12) :



In summary, the absence of  $\text{H}_2\text{O}_2$  and the lack of cobaloxime(III) formation require the presence of a "double" oxenoid reagent capable of releasing 2 oxygen atoms successively. This function can be performed presumably by both the superoxocobaloxime  $\text{CoO}_2$  and the  $\mu$ -peroxocobaloxime  $\text{Co}-\text{O}_2-\text{Co}$  (II and III). In the latter case, Eq. (11) should be replaced by



In both cases the second O atom is transferred (abstracted) from [CoO], a species whose nature requires further exploration.

Oxygen insertions (4)–(6) can also be readily interpreted in terms of II, III and the hypothetical new oxenoid reagent [CoO]. For example,



A species analogous to [CoO] has been assumed by GROVES and VAN DER PUY [7] to be the oxenoid reagent in cyclohexanol oxidation by hydrogen peroxide in the presence of iron(II) salts, *viz.* the ferryl ion,  $\text{FeO}^{2+}$ . The same iron oxo intermediate has been invoked to explain selective *cis*-1,2-diol for-

mation from cyclohexanol when hydroxylated with iron(II)-peroxy acid systems [8, 9]. A porphyrin-bound iron oxo species was suggested to be responsible for the regioselectivity observed in the iron-porphine catalyzed oxygen transfer from iodosylbenzene to hydrocarbons [10]. Reactive oxometallo species are not restricted to iron. An oxoporphinatochromium(V) complex has been generated, which is capable of hydroxylating and epoxidizing hydrocarbons under catalytic and stoichiometric conditions, the oxygen source being iodosylbenzene [11].

Work is in progress to obtain a deeper insight into the mechanisms of these catalytic oxidations.

### Experimental

All chemicals used were of reagent grade.  $\text{Co}(\text{Hdmg})_2\text{L}_n$  complexes were prepared according to standard methods [4]. All reactions were followed by gas volumetry and quantitative GC analysis. UV-Vis spectra were recorded on a Beckman Acta MIV, IR spectra on a Hitachi Model EPI-G3, and ESR spectra on a JES-ME-3X type spectrometer.

Preparation and characterization of  $[\text{ABCo}^{\text{II}}(\text{Hdmg})_2]_2$  (V). The complex itself was prepared similarly to the usual cobaloxime(II) compounds [4] under  $\text{N}_2$ . UV-Vis spectrum under  $\text{N}_2$  does not show any band around 470 nm. The acetone solution of V does not give any ESR signal even under  $\text{N}_2$ . The IR spectrum supports the presence of AB in the coordination sphere. From the solution of V in different solvents the expected amount of AB can be detected by GLC, corresponding to 1:1 AB/Co ratio. Quantitative decomposition of  $\text{Co}(\text{Hdmg})_2\text{X}_{2-n}\text{L}_n$  complexes at the temperature of the injector (250 °C) of the GLC gives free L.  $\text{Ph}_3\text{P}$ , py or  $\text{NR}_3$  can be measured by GLC in such a way.

\*

We thank Mr. J. BODNÁR for recording the IR spectra.

### REFERENCES

- [1] NÉMETH, S., SZEVEÉNYI, Z., SIMÁNDI, L. I.: *Inorg. Chim. Acta*, **44**, L107 (1980)
- [2] NÉMETH, S., SIMÁNDI, L. I.: *J. Mol. Catal.*, **14**, 69 (1982)
- [3] NÉMETH, S., SIMÁNDI, L. I.: *Inorg. Chim. Acta*, **64**, L21 (1982)
- [4] SCHRAUZER, G. N., LIAN, PIN LEE: *J. Am. Chem. Soc.*, **92**, 1551 (1970)
- [5] SENN, A., HALPERN, J.: *J. Am. Chem. Soc.*, **99**, 8337 (1977)
- [6] SCHNEIDER, P. W., PHELAN, P. F., HALPERN, J.: *J. Am. Chem. Soc.*, **91**, 77 (1969)
- [7] GROVES, J. T., VAN DER PUY, M.: *J. Am. Chem. Soc.*, **96**, 5274 (1974); **98**, 5290 (1976)
- [8] GROVES, J. T., McCLUSKY, G. A.: *J. Am. Chem. Soc.*, **98**, 859 (1976)
- [9] GROVES, J. T.: Mechanisms of metal-catalyzed oxygen insertion, in "Metal Ion Activation of Dioxygen", T.G. SPIRO, Ed., pp. 125-162. John Wiley and Sons, New York Chichester, Brisbane, Toronto 1980
- [10] GROVES, J. T., NEMO, T. E., MYERS, R. S.: *J. Am. Chem. Soc.*, **101**, 1032 (1979)
- [11] GROVES, J. T., KRUPER, W. J.: Jr.: *J. Am. Chem. Soc.*, **101**, 7613 (1979)

Sándor NÉMETH

Annamária FÜLEP-POSZMIK

László I. SIMÁNDI

H-1525 Budapest, P.O. Box 17.



## ON THE TORSIONAL INTERNAL COORDINATE IN MOLECULAR VIBRATIONS

R. AROCA<sup>1\*</sup>, E. A. ROBINSON<sup>1</sup>, Yu. N. PANCHENKO<sup>2</sup> and V. J. PUPYSHEV<sup>2</sup>

(<sup>1</sup> *Department of Chemistry and Erindale College, University of Toronto, Mississauga, Ontario, Canada* and <sup>2</sup> *Molecular Spectroscopy Laboratory, Department of Chemistry, M. V. Lomonosov Moscow State University, Moscow, USSR*)

Received September 8, 1981

In revised form December 22, 1981

Accepted for publication December 24, 1981

A definition of a torsional internal coordinate is discussed under maximal separation from other vibrational coordinates. The arbitrariness and symmetry restrictions present in the problem are disclosed. It is also shown that ECKART vectors provide a method to define and normalize the dihedral angle change.

### Introduction

A torsional motion in polyatomic molecules has been defined as the rotation of one part of a molecule with respect to the remainder. When hindrance is large, the torsional motion becomes a torsional oscillation with a vibrational frequency

$$\omega = \frac{1}{2\pi} \sqrt{\frac{kI}{I_A I_B}}$$

where  $k$  is the force constant of the oscillator,  $I_A$  and  $I_B$  are the moments of inertia of groups A and B respectively (see Fig. 1) about the rotational axis, and  $I = I_A + I_B$ . Internal rotation is bounded by two limiting cases, the free rotor ( $k = 0$ ) and a rigid structure ( $k = \infty$ ). Torsional oscillation frequencies are normally observed in the far infrared region of the spectrum. Correspondingly, force constants are about an order of magnitude smaller than a normal bending force constant. This represents, in a pseudo-diatom-like picture, a very shallow potential well which corresponds to a large amplitude motion. Theoretically an internal motion with a large amplitude cannot be properly treated within the approach of infinitesimal vibrations, which is the standard semi-rigid procedure [1] and therefore a suitable theoretical extension is required to include this particular coordinate. Experimentally it is observed that internal rotations strongly couple with molecular rotation and are responsible for the patterns of change that occur in the rotational

\* To whom correspondence should be addressed

spectra of rigid models which can be analyzed to yield information about the torsional potential well. There is also evidence [2] of internal rotation—vibrational coupling, thus casting doubt on the common assumption in which the internal rotation may be considered separable from other vibrations. The separation of the torsion from other vibrations becomes more valid the lower

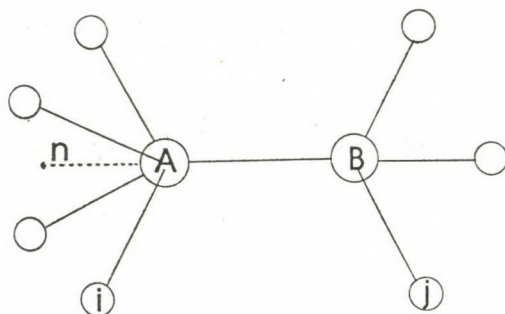


Fig. 1. Molecular model for internal rotation

the force constant value. For a large number of molecules, however, torsional frequencies are comparable in value to some bending (skeletal) vibrational frequencies and, thus, their treatment within the vibrational problem seems necessary.

The definition of an internal coordinate for the torsional oscillation has been a controversial issue in the literature. For instance, it has been argued by MAYANTZ and SHALTUPER [3] that an independent internal vibrational coordinate for the torsional motion cannot be worked out, while WILLIAMS [4] has recently summarized most of the previous results on torsional internal coordinates and has given generalized expressions for the WILSON's vectors [1] of oscillating atoms. These generalized expressions should be "applicable to molecules of any geometry and symmetry" [4]. These results, however, seem to be restricted to the molecular model of *coaxial* symmetry-top groups. The general case of two asymmetric rotors does not allow a maximal separation of torsion from rotation, thereby preventing the definition of an internal torsional coordinate.

A definition of the internal torsional coordinate is attempted here using a minimization technique, *i.e.* minimizing the contribution of other vibrations to the torsion and thereby defining the coordinate under maximal separation from remaining vibrational coordinates. It is also shown for the particular case of two *coaxial* symmetric rotors that ECKART vectors as defined by LOUCK and GALBRAITH [5] provide a suitable and convenient framework for the discussion of the torsion coordinate. WILLIAMS' notation will be followed as closely as possible.

### Derivation of the torsional coordinate expressions

According to MALHIOT and FERIGLE [6] an internal coordinate may be defined as the difference between a scalar function  $f(r_i)$  of instantaneous position vectors relative to some fixed point and the same function at the equilibrium configuration. Therefore the torsional internal coordinate is defined as

$$\Delta\tau = f(r_i) - f(r_i^0) \quad (1)$$

( $i = 1, 2, \dots, N$ , where  $N$  is the total number of atoms in the molecule).

Considering infinitesimal deviations from the equilibrium configuration, which is the basic assumption in the theory of infinitesimal vibrations, if  $f(r_i)$  is expanded in a Taylor series and terms higher than first order in the expansion are neglected, it is found that

$$\Delta\tau = \sum_i (\nabla_i f)_0 (r_i - r_i^0) = \sum_i s_i \cdot \Delta r_i \quad (2)$$

where the symbol  $( )_0$  is used for the gradient at equilibrium. It is known from ECKART conditions [1, 5] that  $s_i$  vectors must satisfy the equations

$$\sum_{i=1}^N s_i = 0 \quad (3)$$

$$\sum_{i=1}^N s_i \times r_i = 0 \quad (4)$$

and since  $s_i$  are three-dimensional vectors, there is a total of  $3N$  coordinates. Equations (3) and (4) provide a total of six relationships between them and one equation for normalization. There exists then an arbitrariness in the selection of  $s_i$  coordinates of the order of  $3N - 7$ , and therefore a general expression for these coefficients is given by

$$s'_i = \sum_{a=1}^{3N-7} c_a s_i^a \quad (5)$$

Equation (5) certainly supports the argument [3] that a definite value of a torsional coordinate (2) does not uniquely determine every dihedral change in the linear combination defining the internal coordinate. This indeterminacy does not, however, question the internal coordinate definition.

Let us consider initially a group of atoms  $i = 1, \dots, m$  attached to a fixed, nonterminal atom A, and if  $r_i$  is the equilibrium position vector of the  $i$ th atom from the centre of mass of the molecule,  $\rho_i$  the equilibrium bond

length between A and the  $i$ th atom, and  $e_i$  a unit vector directed along the bond, then  $p_i = \rho_i e_i$  is the bond vector.

All changes of  $p_i$  vectors then represent the displacement from the reference geometry in terms of molecule fixed coordinates and can be due to internal motions (vibrations) or internal rotation about an axis  $n$ .

The total change  $dp_i$  due to internal motion can thus be written

$$dp_i = dp_i^v + (p_i \times n) d\Phi$$

where  $(p_i \times n) d\Phi$  is the contribution to the atomic displacements due to an internal clockwise rotation  $d\Phi$  of the group of terminal atoms with respect to an axis  $n$  which coincide with the chemical bond A—B. In order to separate both contributions the sum of the squares of  $dp_i^v$  is minimized. Internal torsional contributions are therefore maximally separated from other internal motions,

$$\sum_i \|dp_i^v\|^2 = \sum_i \|dp_i - (p_i \times n) d\Phi\|^2 \quad (7)$$

or

$$\sum_i \|dp_i^v\|^2 = \sum_i \|dp_i\|^2 + d^2\Phi \sum_i \|(p_i \times n)\|^2 - 2 \sum_i (dp_i, (p_i \times n)) d\Phi \quad (8)$$

Taking the derivative with respect to  $d\Phi$ , and setting it equal to zero, we have

$$2d\Phi \sum_i \|(p_i \times n)\|^2 - 2 \sum_i (dp_i, (p_i \times n)) = 0 \quad (9)$$

and

$$d\Phi = \frac{\sum_i (dp_i, (p_i \times n))}{\sum_i (p_i \times n)(p_i \times n)} = \frac{(p_i \times n) \cdot (p_i \times n)}{\sum_j (p_j \times n)(p_j \times n)} \quad (10)$$

Equation (6) can be rewritten using mass-weighted vectors defined [1] as  $p_i = \sqrt{m_i} p_i$ . The expression obtained by the minimization procedure is then given by

$$d\Phi = \frac{\sum_i (dp_i, (p_i \times n))}{\sum_i (p_i \times n) \cdot (p_i \times n)} = \frac{\sum_i m_i a_i^2}{\sum_i m_i a_i^2} \quad (11)$$

where  $a_i^2$  is the square of the distance of the  $i$ th atom from the  $n$  axis. It should be noted that

$$K_i = \frac{m_i a_i^2}{I_A} \text{ and } \sum_i K_i = 1. \quad (12)$$

The first terms in (10) and (11) represent the projection of a displacement  $dp_i$  on the axis perpendicular to the plane formed by  $p_i$  and  $n$ , and is termed  $d\Phi_i$ . When all  $m$  terminal atoms are equivalent (same distance  $a_i$  and mass), then  $K_i = \frac{1}{m}$  and  $d\Phi = \frac{1}{m} \sum_i d\Phi_i$ , which is the classical formula for molecules in which a symmetric-top group is attached to the frame.

If we define  $\Delta\tau_i = K_i \Delta\Phi$ ,  $\Delta\tau_i$  is clearly the change in the dihedral angle due to the rotation of the atom  $i$  by the angle  $\Delta\Phi$ . The actual change in a vector  $r_i$  upon rotation through  $\Delta\Phi$  about the  $n$  axis is given by

$$\Delta r_i = (r_i \times n) \Delta\Phi. \quad (13)$$

Equilibrium position vectors  $r_i$  can be written in terms of bond vectors and  $r_A$ , the equilibrium position vector for the atom A.

$$r_i = r_A + \varrho_i e_i; \quad r_j = r_B + \varrho_j e_j; \quad r_B = r_A + \varrho_{AB} e_{AB} \quad (14)$$

For systems where the centre of mass lies on the axis of rotation ( $r_A \times n = 0$ ) and (13) gives

$$\Delta r_i = -\varrho_i \sin \alpha_i h_i \Delta\Phi \quad (15)$$

where

$$h_i = (e_i \times e_{AB}) (\sin \alpha_i)^{-1}. \quad (16)$$

Combining previous results the explicit value of  $\Delta\tau_i$  is found:

$$\Delta\tau_i = -\frac{K_i}{\varrho_i \sin \alpha_i} h_i \cdot \Delta r_i. \quad (17)$$

Hence

$$s_i = -\frac{K_i}{\varrho_i \sin \alpha_i} h_i. \quad (18)$$

The so-called general expression [4] for a torsional coordinate of a molecular model in which the axis of internal rotation is the A-B chemical bond can now be written using ECKART's conditions (4).

$$\sum_{i=1}^m \varrho_i (s_i \times e_i) + \sum_{j=1}^l s_j \times (e_{AB} \varrho_{AB} + e_j \varrho_j) + (s_B \times e_{AB}) \varrho_{AB} = 0. \quad (19)$$

Taking the vector product of  $e_{AB}$  with each side, and with the aid of the properties of the triple vector product, equation (19) gives

$$\sum_{i=1}^m \varrho_i (e_{AB} \cdot e_i) s_i + \sum_{j=1}^l \varrho_j (e_{AB} \cdot e_j) s_j + \sum_{j=1}^l s_j \varrho_{AB} + s_B \varrho_{AB} = 0, \quad (20)$$

$$(e_{AB} \cdot e_i) = \cos \alpha_{iAB}, \quad (e_{AB} \cdot e_j) = -\cos \alpha_{jBA}.$$

Hence, (2) finally produces

$$s_B = - \sum_{j=1}^l s_j - \sum_{i=1}^m \frac{\rho_i \cos \alpha_i}{\rho_{AB}} s_i + \sum_{j=1}^l \frac{\rho_j \cos \alpha_j}{\rho_{AB}} s_j. \quad (21)$$

A similar expression can be obtained for  $s_A$ :

$$s_A = - \sum_{i=1}^m s_i - \sum_{i=1}^l \frac{\rho_j \cos \alpha_j}{\rho_{AB}} s_j + \sum_{i=1}^m \frac{\rho_i \cos \alpha_i}{\rho_{AB}} s_i. \quad (22)$$

Combining  $\Delta\tau = \sum_i \Delta\tau_i$ , with (17), (21) and (22), the general expression (2) is obtained:

$$\begin{aligned} \Delta\tau = & \sum_{i=1}^m K_i [(\rho_i \sin \alpha_i)^{-1} - (\rho_{AB} \operatorname{tg} \alpha_i)^{-1}] h_i \cdot \Delta r_A + \\ & + \sum_{j=1}^l K_j (\rho_{AB} \operatorname{tg} \alpha_j)^{-1} h_j \cdot \Delta r_A + \sum_{j=1}^l K_j [(\rho_j \sin \alpha_j)^{-1} - \\ & - (\rho_{AB} \operatorname{tg} \alpha_j)^{-1}] h_j \cdot \Delta r_B + \sum_{i=1}^m K_i (\rho_{AB} \operatorname{tg} \alpha_i)^{-1} h_i \cdot \Delta r_B - \\ & - \sum_{i=1}^m K_i (\rho_i \sin \alpha_i)^{-1} h_i \cdot \Delta r_i - \sum_{j=1}^l K_j (\rho_j \sin \alpha_j)^{-1} h_j \cdot \Delta r_j. \end{aligned} \quad (23)$$

It was previously pointed out that for internal symmetric rotors  $K_i = m^{-1}$  and  $K_i = l^{-1}$ . Therefore, for molecules in which the axis of internal rotation is the axis of local symmetry, expressions (23) in the present work and (32) in WILLIAMS' paper are equivalent. It is thus concluded that this formula is in fact restricted to the torsion of *coaxial* symmetric rotors.

### Torsional motion and the Eckart frame

The results of the previous section can be obtained independently using ECKART vectors and ECKART frames, and the symmetry restrictions clearly visualized from the geometry of the problem.

LOUCK and GALBRAITH [5] have defined three ECKART vectors  $\vec{E}_i$  ( $i = 1, 2, 3$ ) in terms of the equilibrium position vectors, the masses of the particles and the instantaneous position vectors. They have also defined an ECKART frame as a right-handed triad of unit vectors  $\vec{f}_i$  ( $i = 1, 2, 3$ ) in terms of the vectors  $\vec{E}_i$ . The equilibrium (static molecular model) ECKART frame and the equilibrium principal axis frame coincide. Therefore, in matrix notation

ECKART vector matrix at equilibrium can be written as [7]

$$F_0 = AM\tilde{A} \quad (24)$$

where  $F_0$  is a  $3 \times 3$  matrix whose columns contain the components of the 3 vectors  $\tilde{E}_i$ ,  $M$  is the  $N \times N$  diagonal mass matrix, and  $\tilde{A}$  is the transpose of  $A$  containing the component of the equilibrium vectors  $r_i^0$ . Thus  $F_0$  is a diagonal matrix in the equilibrium inertial principal axis frame.

For the study of torsional motion, local ECKART frames can be defined from the position vectors of the rotors A and B as well as ECKART vector matrices  $F_A$  and  $F_B$ . Assuming two coaxial symmetric rotors with a common  $z$  axis, the principal axis frames are linked to the ECKART frames locally, and the  $F$  matrices are diagonal. Infinitesimal rotations  $d\Phi_A$  of the rotor A and  $d\Phi_B$  of the rotor B are equivalent to considering infinitesimal rotations of the rotor-fixed axis system. MEYER and REDDING [7] have recently shown that a simple rotation of the molecular groups produces a rotation of the ECKART frame, and that the change in  $F$  can simply be written as

$$dF = dRF. \quad (25)$$

The antisymmetric matrix  $dR$  of a rotation  $d\Phi$  about the  $z$  axis is given by

$$dR = \begin{bmatrix} 0 & d\Phi & 0 \\ -d\Phi & 0 & 0 \\ 0 & 0 & 0 \end{bmatrix}$$

Considering that for the unmixed torsional motion  $dF_A + dF_B = 0$ , two equations are obtained:

$$F_1^A d\Phi_A + F_1^B d\Phi_B = 0, \quad (26)$$

$$F_2^A d\Phi_A + F_2^B d\Phi_B = 0. \quad (27)$$

Subtracting (27) from (26) produces the trivial result  $F_1^A = F_2^A$ , confirming that A and B are symmetric rotors. Adding these two equations, it is found that

$$I_A d\Phi_A + I_B d\Phi_B = 0, \quad (28)$$

meaning that the contribution of the angular momentum about the axis of internal rotation to the total angular momentum is zero.

The first term in (28) for a small change  $\Delta\Phi$  represents

$$I_A \Delta\Phi_A = \sum_i m_i a_i^2 \Delta\Phi_A \quad (29)$$

or

$$\Delta\Phi_A = \sum_i K_i \Delta\phi_A = \sum_{i=1}^m \Delta\tau_i \quad (30)$$

where  $K_i$  are the same coefficients defined by (12). The total rotation  $\Delta\Phi_A$  is the addition of atomic normalized contributions  $\Delta\tau_i$  defined by (17). The angle of torsion within the molecule is defined by

$$\Delta\tau = \Delta\Phi_A - \Delta\Phi_B = \sum_i^{m+l} \Delta\tau_i = \sum_i^{m+l} s_i \cdot \Delta r_i. \quad (31)$$

Equation (31) can now be rewritten for two particular cases.

i) *Coaxial-equivalent symmetric rotors*: in this case  $\Delta\Phi_A = -\Delta\Phi_B$ :

$$\Delta\tau = \sum_i K_i \Delta\phi_A - \sum_j K_j \Delta\phi_B \quad (32)$$

$$\Delta\tau = 2 \sum_i K_i \Delta\phi_A = -2 \sum_i K_i ((\rho_i \sin \alpha_i)^{-1} h_i \cdot \Delta r_i) \quad (33)$$

ii) *Non-equivalent coaxial symmetric rotors*:

$$\Delta\tau = \sum_i K_i \Delta\phi_A - \sum_j K_j \Delta\phi_B \quad (34)$$

$$\Delta\tau = - \sum_i K_i (\sin \alpha_i)^{-1} h_i \cdot \Delta r_i - \sum_j K_j (\rho_j \sin \alpha_j)^{-1} h_j \cdot \Delta r_j. \quad (35)$$

In all previous cases the value  $\Delta\Phi$  has been taken from (15).

### Discussion and Conclusions

The molecular model considered in this particular discussion of the torsional vibrational coordinate consists of two semi-rigid parts connected by a chemical bond A—B about which the two parts may rotate with respect to each other. For all previous derivations it has been assumed that the axis of rotation coincides with the bond A—B and contains the centre of mass of the entire molecule. Under these conditions equations (15) to (23) are valid. For the particular case in which the centre of mass of the respective rotor lies also on the axis of rotation, equation (23) is reduced to the case of two equivalent *coaxial* symmetric rotors (33) or two non-equivalent *coaxial* symmetric rotors (35). This simplification of (23) could have been inferred from the model itself where null  $s$  vectors should be assigned to the atoms

forming the bond about which the torsion occurs. Therefore equation (23) does not represent a general case and it is restricted to *coaxial* symmetric rotors.

The general case is a molecular model of two asymmetric-top groups joined by a chemical bond A—B about which the two parts may rotate with respect to each other. In this case the centre of mass of the asymmetric-top group does not lie on the axis of rotation. The translation of the molecule as a whole is neglected; *i.e.*, ECKART's condition (3) is fulfilled. There exists, however, a net contribution of the torsion to the total rotational energy [8] given by the kinetic energy of a mass  $M_1$  at the centre of mass of the top-1 and a mass  $M_2$  at the centre of mass of the top-2 relative to an axis system whose origin is at the centre of mass of the whole molecule. Therefore, the  $s$  vectors for the internal torsional coordinate of two asymmetric rotors will not satisfy the ECKART condition (4), *i.e.*, vibration and rotation cannot be separated for this particular internal coordinate. It is thereby concluded that a torsional internal coordinate for the model of two asymmetric rotors oscillating about an A—B bond cannot be defined. Finally, it should be noted that ECKART's condition (4) was used in the derivation of (23) which explains the restriction of this formula to *coaxial* symmetric rotors.

\*

The authors wish to thank Professor F. TÖRÖK and Dr. N. F. STEPANOV for helpful discussions.

## REFERENCES

- [1] WILSON, E. B., DECIUS, J. C., CROSS, P.: "Molecular Vibrations", McGraw-Hill, New York 1955
- [2] DREIZLER, H.: in Molecular Spectroscopy Modern Research, Academic Press, K. H. RAO, C. W. MATHEWS (editors), 1972
- [3] MAYANTZ, L. S., SHALTUPER, G. B.: J. Mol. Struct., **24**, 409 (1975)
- [4] WILLIAMS, I. H.: J. Mol. Spectrosc., **66**, 288 (1977)
- [5] LOUCK, D. J., GALBRAITH, H. W.: Rev. Mod. Phys., **48**, 69 (1976)
- [6] MALHIOT, R. J., FERIGLE, S. M.: J. Chem. Phys., **22**, 717 (1954)
- [7] MEYER, F. O., REDDING, R. W.: J. Mol. Spectrosc., **70**, 410 (1978)
- [8] MEAKIN, P., HARRIS, D. O., HIROTA, E.: J. Chem. Phys., **51**, 3775 (1969)

Ricardo AROCA

Edward A. ROBINSON

Mississauga, Ontario L5L 1C6, Canada

Yu. N. PANCHENKO

V. J. PUPYSHEV

Moscow 117234 USSR



## RECENSIONES

### Joachim BUDDRUS: *Grundlagen der Organischen Chemie*

Walter de Gruyter, Berlin—New York 1980, 754 Seiten

Wer sich die Aufgabe stellt, ein Lehrbuch der organischen Chemie für Grundkurse an Hochschulen zu schreiben, ist in einer schwierigen Lage. Das Gebiet der organischen Chemie ist gewaltig, der Verfasser ist jedoch durch die gegebene — und meist geringe — Stundenzahl und durch den fundierenden, einführenden Charakter des Buches gebunden. Die vielleicht wichtigste Frage der Strategie des Buchschreibens ist dabei, was aus dem hoffnungslos riesigen aber aus diesem oder jenem Grund gleich wesentlich erscheinenden Material im Buch enthalten und mit welchem Gewicht behandelt sein soll. Im großen und ganzen sind die Prinzipien für die Abfassung gegeben: neben der herkömmlichen, mehr oder minder kurzgefaßten, auf den Typen des Kohlenstoffgerüsts und der funktionellen Gruppen beruhenden Behandlungsweise hat sich in letzterer Zeit ein moderneres System durchgesetzt, das sich auf Begriffe, Prinzipien und vor allem auf Reaktionstypen stützt. Es erwies sich, daß beide Selektionsprinzipien geeignet sind, ein gutes Lehrbuch der organischen Chemie zu schreiben. Beide Näherungen besitzen ihre Vor- und Nachteile: die erste gibt einen besseren Überblick über die Gesamtheit der organischen Chemie, jedoch verliert sich der Studierende dabei leicht in den Einzelheiten, er sieht den Wald vor Bäumen nicht. Die zweite ist kaum geeignet, das Stoffwissen zu erweitern, gibt aber dafür solche theoretische Grundlagen, die die Studenten befähigen, ein beliebiges Gebiet der organischen Chemie in ausreichender Tiefe zu verstehen und sein Wissen auf dem gegebenen Gebiet zu nutzen.

Dem Aufbau nach folgt das vorliegende Buch eher dem traditionellen Weg. Der einleitende Abschnitt, worin die Grundbegriffe, die allgemeinen Fragen der Bindungstheorie und der chemischen Reaktionen behandelt sind, ist auffallend kurz (29 Seiten), so daß zum Verständnis des Buches früher erworbene, gründliche theoretische Kenntnisse erforderlich sind. Der Verfasser verschweigt nicht, daß er bei der Behandlung der wichtigen Erscheinungen der organischen Chemie (Konformationsgleichgewichte, Aromatizität, Tautomerie usw.) auf spektroskopische Methoden, vor allem auf die Kernmagnetische Resonanz-Spektroskopie basieren wird. Diese Konzeption ist nicht neu, gehört aber dennoch zu den Vorzügen des Buches: durch ihre konsequente Anwendung erreicht der Verfasser, daß die anregenden theoretischen und praktischen Probleme und ihre Lösungen untrennbar mit den gegenwärtig am allgemeinsten angewendeten Methoden der Strukturuntersuchung verbunden bleiben.

Nach dem einleitenden Teil folgen die Kapitel über gesättigte Kohlenwasserstoffe, Olefine, Acetylen-Kohlenwasserstoffe und mehrfach ungesättigte Kohlenwasserstoffe. Nach der Vorführung der Cycloparaffine und der benzoiden Kohlenwasserstoffe werden die Halogenverbindungen, die metallorganischen Verbindungen, die Alkohole und Phenole, Äther, Oxoverbindungen und schließlich die Carbonsäuren und ihre funktionellen Derivate in der gewohnten Reihenfolge behandelt. Das Kapitel über Amine bildet den Übergang zum Thema Aminosäuren, Peptide und Proteine. Abschließend folgen die Kapitel über heterocyclische Verbindungen und kurz die im vorangegangenen nicht berührten Naturstoffe.

Dieser klassische Aufbau wird vorteilhaft ergänzt durch Teile über Polymerisationsreaktionen (Kapitel 6), pericyclische Reaktionen (Kapitel 7), nichtbenzoide aromatische und antiaromatische Verbindungen (Kapitel 10), Enantiomerie (Kapitel 11) sowie nukleophile Substitutions- und Eliminationsreaktionen (Kapitel 12 bzw. 13).

Der Wert des Buches wird gesteigert durch die Behandlung moderner Synthesemethoden (z. B. die Wittig-Synthese), mehrstufiger und technischer Synthesen, Metall-Alken-Komplexe

und im allgemeinen die Vorführung der Bedeutung von elementarorganischen Verbindungen in der organischen Chemie. Die kurze Behandlung der Kohlenhydrate am Ende des Kapitels über Oxoverbindungen ist auch gut gelungen.

Die Behandlungsart des Stoffes ist durchaus von hohem Niveau und wohl fundiert, obwohl äußerst knappgefaßt und stellenweise sogar lakonisch. Dadurch konnte der Verfasser nahezu das gesamte Gebiet der organischen Chemie auf 754 Seiten erörtern. Demgemäß ist jedes einzelne Wort von Gewicht, wobei der Mangel an erklärenden, lockerer verfaßten Teilen das Buch zu einer trockenen Lektüre macht und das Verständnis des Stoffes erschwert. Die Vertiefung in die Theorie der organischen Chemie ist keineswegs im Text vorhanden, jedoch strebt der Verfasser dies offensichtlich nicht an. Die einfachen Aufgaben am Schluß der einzelnen Kapitel passen gut zum behandelten Stoff; ihre Lösung ist im Anhang zu finden. Die Formeln und Abbildungen zur Illustration des Textes sind zwar nicht besonders augenfällig, doch klar und anschaulich.

Nach der Meinung des Rezensenten kann dieses Lehrbuch — wegen der außerordentlich gedrängten Fassung — für den Grundstufenunterricht nur zusammen mit erklärenden Vorlesungen oder bei eingehender Behandlung in Seminaren mit Erfolg verwendet werden.

Ein wesentlicher Mangel ist die nahezu unbegreifliche Kürze des Kapitels über heterocyclische Verbindungen: insgesamt 21 Seiten! Der Titel des Kapitels 11 („Enantiomerie“) ist ungewöhnlich, noch mehr aber die auffallend geringe Anzahl der Beispiele sowie das Fehlen von geschichtlichen Hinweisen.

Die „Grundlagen der Organischen Chemie“ von Joachim BUDDRUS ist ein wertvolles Lehrbuch, eigenartiges und gedankenerregendes Produkt der jetzigen, nach der sprunghaften theoretischen Entwicklung folgenden Epoche der organischen Chemie.

Á. KUCSMAN

Department of Organic Chemistry, Eötvös Loránd University, Budapest

### Jaroslav BENES: *Radioaktive Kontamination der Biosphäre*

VEB Gustav Fischer Verlag Jena, 1981, 206 pp.

In der Verunreinigung der Umwelt spielt die Kontamination der Biosphäre mit radioaktiven Stoffen eine zunehmende Rolle. Die Energieerzeugung durch Atomkraftwerke sowie die Verbreitung der friedlichen Anwendung von radioaktiven Isotopen erhöhen die Gefahr der Umweltverschmutzung. Deswegen kommt dem Buch, das für einen breiten Kreis von Lesern bestimmt ist, eine große Bedeutung zu.

Gliederung und Wahl der einzelnen Kapitel erfolgte nach didaktischen Gesichtspunkten, um Physikern, Ärzten, Chemikern und Biologen Überblick zu geben.

Die erste tschechische Auflage erschien im Jahre 1974 und war hauptsächlich für tschechische Leser bestimmt. Für die deutschsprachige Ausgabe wurde das Buch umgearbeitet und einiges Bild- und Tabellenmaterial ausgewechselt, um es für einen allgemeinen Leserkreis geeignet zu machen. Unter diesem Gesichtspunkt wurde die Gliederung der Kapitel vorgenommen:

Kapitel 1. befaßt sich mit der Bestimmung der „Biosphäre“, unterteilt in Definition und Struktur der Ökosysteme (20 Seiten). Kapitel 2 - 6 vermitteln die Grundkenntnisse über die Radioaktivität und über die verschiedenen Quellen der ionisierenden Strahlung in der Biosphäre, wie natürliche, kosmische und von den künstlichen Radionukliden herrührende Strahlung. Diese Problematik nimmt in dem Buch insgesamt 50 Seiten ein. Die Kapitel 7 und 8 (30 Seiten) geben einen Überblick über die von radioaktiven Abfällen verursachten Umweltschmutzungen. Die Radioaktivität der Atmosphäre, des Wassers, des Bodens und der Pflanzen wird in den nächsten Kapiteln (9-13) auf 65 Seiten detailliert behandelt. Von besonderem Interesse sind die „Bewegung der radioaktiven Stoffe in der Biosphäre“ (Kapitel 14) und die „Kontamination des Organismus durch radioaktive Stoffe“ (Kapitel 15; 14 Seiten).

Der Verfasser rundet das dargelegte Material mit Ausführungen über den Strahlenschutz und über die Dosimetrie ab, wobei auch auf die internationalen Empfehlungen und auf nationalen Strahlenschutzvorschriften eingegangen wird. Das Buch wird mit dem Kapitel:

„Perspektiven der Strahlen-genetik und künftige Quellen der Kontamination der Biosphäre“ abgeschlossen.

Das Buch enthält 137 Literaturhinweise, 34 Abbildungen und 25 Tabellen. Die Einheiten sind dem SI-System (Systeme Internationale) entsprechend angegeben.

Das Werk vermittelt ein umfassendes Bild über das bisher in dieser Hinsicht nicht behandelte Gebiet des Umweltschutzes und wird durch die gute Zusammenstellung auf verschiedenen Fachgebieten der Isotopenanwendung tätigen Forschern viel Hilfe bieten. Das Buch ist in einem leicht verständlichen Stil geschrieben und fesselt die Aufmerksamkeit des Lesers.

I. BÁLINT-AMBRÓ

Research Institute for Heavy Chemical Industries, Veszprém

### L. NEMES: *Determination of molecular geometry by rotational spectroscopy*

Akadémiai Kiadó, Budapest, 1981.

256 pages, 291 references, 18 figures and 27 tables

This book is published as Volume 51 of the series "New results in chemistry" in Hungarian, (editor: B. CSÁKYÁRI). The calculation of bond lengths and bond angles in molecules from high resolution rotational spectra and its practical and theoretical problems are discussed. For the determination of molecular structures in the gaseous phase microwave spectroscopy and, recently, laser spectroscopy are extensively used. The high resolution of these methods makes the study of the rotational structure of spectra possible both in the ground and in the excited vibrational states. The author proves through numerous examples that certain molecular structural problems, e.g. the planarity or linearity of molecules, the sequence of atoms in the molecule, etc., can be decided only in the accurate knowledge of the molecular geometry. The determination of molecular geometry with high precision is a difficult task, in spite of the fact that the rotational transitions are accurately known from the spectrum. The difficulty originates from the dependence of the accurate effective rotational constants that can be calculated from the experimental transitions, on the vibrational-rotational state of the molecule. Thus the structure  $r_0$  — or in the excited state  $r_v$  — calculated from them differs from structure  $r_e$  belonging to the potential minimum of the molecule, which is considered as the real molecular geometry.

The author discusses in detail the structures  $r_z$ ,  $r_s$ , and  $r_m$  approximating  $r_e$  which are calculated from structure  $r_0$ , in the knowledge of the molecular force field, the Coriolis zeta constants and the spectra of the isotope substituted derivatives. These are compared and discussed on the basis of data published in the literature, their physical meaning is given, as well as the method of their corrections, and the calculation methods known so far. A separate chapter is devoted the problems concerning the regression calculations.

Similar problems arise in the determination of the molecular geometry by electron diffraction. The author discusses the electron diffraction structures  $r_e$  and  $r_e^0$  as well, of which  $r_e^0$  corresponds to  $r_z$ . This is the basis for the determination of the molecular geometry from combined electron diffraction and microwave data. Corresponding to the importance of this problem, a separate chapter deals with this question.

The author uses the SI units, but the conversion of spectroscopic data into other units, e.g. into cgs units is also provided.

The book fills a gap both in the Hungarian and international literature on spectroscopy.

Numerous works are published on microwave spectroscopy and rotational spectra, but a book was missing that systematically surveys all the problems of the determination of geometry and which strives for completeness.

This work is useful mainly for experts, but can be successfully applied also by those who only want to clear up some basic concepts, or to look after a given method.

L. SZTRAKA

Department of Physical Chemistry, Technical University, Budapest

W. J. CRIDDLE and G. P. ELLIS: *Spectral and Chemical Characterization of Organic Compounds: A Laboratory Handbook* (2nd ed).

John Wiley and Sons, Chichester—New York—Brisbane—Toronto 1980, IX + 115 pages

A practical guide to the qualitative analysis and identification of organic and pharmaceutical substances — this might be another version of the title of this book; indeed, students of organic chemistry or pharmacy will find clear-cut guidance and a surprisingly great amount of information in this short laboratory manual on the classic and modern techniques of identifying organic compounds.

Chapter 1 (6 pages) deals with preliminary tests of characterization: qualitative elemental analysis, ignition, colour and odour, determination of the melting and boiling points, the important solubility characteristics.

In Chapter 2 (28 pages) the chemical and spectroscopic characterization methods are given, well grouped in tables according to functional groups. Basic knowledge of the principles of the spectroscopic methods (IR, UV,  $^1\text{H-NMR}$ , MS) is assumed, and here the techniques of preparing the samples and the rudiments of interpretation of the spectra are discussed, with hints where one or the other kind of spectroscopy may prove most expedient. Ample notes explain the reactions on which the chemical tests for functional groups are based, or the notes call attention to possible exceptions and pitfalls.

Chapter 3 (3 pages) briefly describes the separation of organic mixtures, based mainly on the different solubilities of the components in water, ether, dilute acid or alkali.

Next (Chapter 4; 21 pages), procedures for the preparation of characteristic crystalline derivatives are given, to confirm the identity of compounds such as alcohols, aldehydes, amides, amines, esters, organic halides, hydrocarbons, phenols, organic sulfur compounds, etc.

Chapter 5 (50 pages) consists of 35 tables excellently arranged according to types of organic compounds (e.g. acetals, alcohols, etc.); the laboratory worker can find here the boiling or melting points of a host of the most common organic chemicals, the m.p.'s of their characteristic derivatives, and special notes which may assist final identification.

The last chapter (3 pages) is designed for students of pharmacy and completes the previous material with six tables listing the physical constants of about 170 pharmaceutical compounds which are mostly in common use.

The authors' vast experience in the research and teaching of organic chemistry, together with the ability of lucid and concise writing is reflected in the excellence of this small volume: in the selection of the material, in its arrangement and presentation. The second edition made use of all the experience obtained through the warm reception and responses to the first publication. When the book comes to a third edition, the authors may perhaps consider the reviewer's suggestion to include brief mention of the potentialities also of  $^{13}\text{C-NMR}$  spectroscopy.

The book is primarily intended and recommended to students and lecturers of organic chemistry, but with the many excellently arranged data it may also serve as a convenient source of rapid information to any chemist working in an organic laboratory.

F. KÁLLAY

Research Institute for Organic Chemical Industry, Budapest

## INDEX

### PHYSICAL AND INORGANIC CHEMISTRY

Thermal Decomposition of Oxetane and Oxetane- $d_2$ in the Pressure Independent Range, Zs. HUNYADI-ZOLTÁN, L. ZALOTAI, T. BÉRCES, F. MÁRTA.....	371
Effect of Dispersion Interactions on NMR Shielding Constants, U. POHLE, G. GROSSMANN (in German) .....	381
Simulation of the Instabilities Observed in Potentiostatic Studies of Active—Passive Transition, B. LENGYEL, L. MÉSZÁROS .....	397
Contributions to the Theory of Topological Resonance Energy, C. D. GODSIL, I. GUTMAN	415
The Influence of the Ionic Strength on the Dissociation Constant of Hydrogen Cyanide (Short Communication), V. GÁSPÁR, M. T. BECK.....	425
NMR Relaxation Studies in Solution of Transition Metal Complexes, VII. Protonation of the Vanadyl Ion in Aqueous Solution, I. NAGYPÁL, I. FÁBIÁN, R. E. CONNICK	447
Mechanistic Features of Cobaloxime(II) Catalyzed Oxidations with Dioxygen, S. NÉMETH, A. FÜLEP-POSZMIK, L. I. SIMÁNDI .....	461
On the Torsional Internal Coordinate in Molecular Vibrations, R. AROCA, E. A. ROBINSON, YU. N. PANCHENKO, V. I. PUPYSHEV.....	471

### ORGANIC CHEMISTRY

Liquid Crystals, IV. Correlation between the Thermal Stability and Molecular Structure in Cholesteryl 2-Ethoxyethyl-carbonate and its Sulfur-Containing Analogues, P. M. AGÓCS, G. MOTIKA, P. ZSÉDENYI.....	357
A New Route for the Preparation of <i>N</i> -Substituted <i>N</i> -Demethylapocodeine Derivatives, S. BERÉNYI, S. HOSZTAFI, S. MAKLEIT, I. SZEIFERT.....	363
Steroids, XXVIII. Neighbouring Group Participation, V. (0 <sup>-</sup> —4)-Neighbouring Group Participation and Fragmentation in the 16-Hydroxymethylandroster-5-ene-3,17-diol Series, Gy. SCHNEIDER, I. VINCZE, L. HACKLER, J. A. SZABÓ, Gy. DOMBI.....	429
Synthesis of Peptides Containing D-Glucosaminic Acid, III. Sulfation of Peptides, K. GÁLL-ISTÓK, E. ZÁRA-KACZIÁN, L. KISFALUDY, Gy. DEÁK.....	441
RECENSIONES .....	481



PRINTED IN HUNGARY

Akadémiai Nyomda, Budapest



Les Acta Chimica paraissent en français, allemand, anglais et russe et publient des mémoires du domaine des sciences chimiques.

Les Acta Chimica sont publiés sous forme de fascicules. Quatre fascicules seront réunis en un volume (3 volumes par an).

On est prié d'envoyer les manuscrits destinés à la rédaction à l'adresse suivante:

*Acta Chimica*  
*Budapest, P.O. Box 67, H-1450, Hongrie*

Toute correspondance doit être envoyée à cette même adresse.

La rédaction ne rend pas de manuscrit.

Abonnement en Hongrie à l'Akadémiái Kiadó (1363 Budapest, P. O. B. 24, C. C. B. 215 11488), à l'étranger à l'Entreprise du Commerce Extérieur «Kultura» (H-1389 Budapest 62, P.O.B. 149 Compte-courant No. 218 10990) ou chez représentants à l'étranger.

---

Die Acta Chimica veröffentlichen Abhandlungen aus dem Bereich der chemischen Wissenschaften in deutscher, englischer, französischer und russischer Sprache.

Die Acta Chimica erscheinen in Heften wechselnden Umfangs. Vier Hefte bilden einen Band. Jährlich erscheinen 3 Bände.

Die zur Veröffentlichung bestimmten Manuskripte sind an folgende Adresse zu senden

*Acta Chimica*  
*Budapest, Postfach 67, H-1450, Ungarn*

An die gleiche Anschrift ist jede für die Redaktion bestimmte Korrespondenz zu richten. Manuskripte werden nicht zurückerstattet.

Bestellbar für das Inland bei Akadémiái Kiadó (1363 Budapest, Postfach 24, Bankkonto Nr. 215 11488), für das Ausland bei »Kultura« Außenhandelsunternehmen (H-1389 Budapest 62, P.O.B. 149. Bankkonto Nr. 218 10990) oder seinen Auslandsvertretungen.

---

«Acta Chimica» издают статьи по химии на русском, английском, французском и немецком языках.

«Acta Chimica» выходит отдельными выпусками разного объема, 4 выпуска составляют один том и за год выходят 3 тома.

Предназначенные для публикации рукописи следует направлять по адресу:

*Acta Chimica*  
*Budapest, P.O. Box 67, H-1450, ВНР*

Всякую корреспонденцию в редакцию направляйте по этому же адресу.

Редакция рукописей не возвращает.

Отечественные подписчики направляйте свои заявки по адресу Издательства Академии Наук (1363 Budapest, P.O.B. 24, Текущий счет 215 11488), а иностранные подписчики через организацию по внешней торговле «Kultura» (H-1389 Budapest 62, P.O.B. 149. Текущий счет 218 10990) или через ее заграничные представительства и уполномоченных.

Periodicals of the Hungarian Academy of Sciences are obtainable  
at the following addresses:

**AUSTRALIA**

C.B.D. LIBRARY AND SUBSCRIPTION SERVICE  
Box 4886, G.P.O., Sydney N.S.W. 2001  
COSMOS BOOKSHOP, 145 Ackland Street  
St. Kilda (Melbourne), Victoria 3182

**AUSTRIA**

GLOBUS, Höchstädtplatz 3, 1206 Wien XX

**BELGIUM**

OFFICE INTERNATIONAL DE LIBRAIRIE  
30 Avenue Marnix, 1050 Bruxelles  
LIBRAIRIE DU MONDE ENTIER  
162 rue du Midi, 1000 Bruxelles

**BULGARIA**

HEMUS, Bulvar Ruszki 6, Sofia

**CANADA**

PANNONIA BOOKS, P.O. Box 1017  
Postal Station "B", Toronto, Ontario M5T 2T8

**CHINA**

CNPICOR, Periodical Department, P.O. Box 50  
Peking

**CZECHOSLOVAKIA**

MAD'ARSKÁ KULTURA, Národní třída 22  
115 66 Praha  
PNS DOVOZ TISKU, Vinohradská 46, Praha 2  
PNS DOVOZ TLAČE, Bratislava 2

**DENMARK**

EJNAR MUNKSGAARD, Norregade 6  
1165 Copenhagen K

**FEDERAL REPUBLIC OF GERMANY**

KUNST UND WISSEN ERICH BIBER  
Postfach 46, 7000 Stuttgart 1

**FINLAND**

AKATEEMINEN KIRJAKAUPPA, P.O. Box 128  
SF-00101 Helsinki 10

**FRANCE**

DAWSON-FRANCE S. A., B. P. 40, 91121 Palaiseau  
EUROPÉRIODIQUES S. A., 31 Avenue de Ver-  
sailles, 78170 La Celle St. Cloud  
OFFICE INTERNATIONAL DE DOCUMENTA-  
TION ET LIBRAIRIE, 48 rue Gay-Lussac  
75240 Paris Cedex 05

**GERMAN DEMOCRATIC REPUBLIC**

HAUS DER UNGARISCHEN KULTUR  
Karl Liebknecht-Straße 9, DDR-102 Berlin  
DEUTSCHE POST ZEITUNGSVERTRIEBSAMT  
Straße der Pariser Kommüne 3-4, DDR-104 Berlin

**GREAT BRITAIN**

BLACKWELL'S PERIODICALS DIVISION  
Hythe Bridge Street, Oxford OX1 2ET  
BUMPUS, HALDANE AND MAXWELL LTD.  
Cowper Works, Olney, Bucks MK46 4BN  
COLLET'S HOLDINGS LTD., Denington Estate  
Wellingborough, Northants NN8 2QT  
WM. DAWSON AND SONS LTD., Cannon House  
Folkestone, Kent CT19 5EE  
H. K. LEWIS AND CO., 136 Gower Street  
London WC1E 6BS

**GREECE**

KOSTARAKIS BROTHERS INTERNATIONAL  
BOOKSELLERS, 2 Hippokratous Street, Athens-143

**HOLLAND**

MEULENHOF-BRUNA B.V., Beulingstraat 2,  
Amsterdam  
MARTINUS NIJHOFF B.V.  
Lange Voorhout 9-11, Den Haag

**SWETS SUBSCRIPTION SERVICE**

347b Heereweg, Lisse

**INDIA**

ALLIED PUBLISHING PRIVATE LTD., 13/14  
Asaf Ali Road, New Delhi 110001  
150 B-6 Mount Road, Madras 600002  
INTERNATIONAL BOOK HOUSE PVT. LTD.  
Madame Cama Road, Bombay 400039  
THE STATE TRADING CORPORATION OF  
INDIA LTD., Books Import Division, Chandralok  
36 Janpath, New Delhi 110001

**ITALY**

INTERSCIENTIA, Via Mazzè 28, 10149 Torino  
LIBRERIA COMMISSIONARIA SANSONI, Via  
Lamarmora 45, 50121 Firenze  
SANTO VANASIA, Via M. Macchi 58  
20124 Milano  
D. E. A., Via Lima 28, 00198 Roma

**JAPAN**

KINOKUNIYA BOOK-STORE CO. LTD.  
17-7 Shinjuku 3 chome, Shinjuku-ku, Tokyo 160-91  
MARUZEN COMPANY LTD., Book Department,  
P.O. Box 5050 Tokyo International, Tokyo 100-31  
NAUKA LTD. IMPORT DEPARTMENT  
2-30-19 Minami Ikebukuro, Toshima-ku, Tokyo 171

**KOREA**

CHULPANMUL, Phenjan

**NORWAY**

TANUM-TIDSKRIFT-SENTRALEN A.S., Karl  
Johansgatan 41-43, 1000 Oslo

**POLAND**

WĘGIERSKI INSTYTUT KULTURY, Marszał-  
kowska 80, 00-517 Warszawa  
CKP I W, ul. Towarowa 28, 00-958 Warszawa

**ROUMANIA**

D. E. P., Bucureşti  
ILEXIM, Calea Grivitei 64-66, Bucureşti

**SOVIET UNION**

SOJUZPECHAT - IMPORT, Moscow  
and the post offices in each town  
MEZHDUNARODNAYA KNIGA, Moscow G-200

**SPAIN**

DIAZ DE SANTOS, Lagasca 95, Madrid 6

**SWEDEN**

ALMQVIST AND WIKSELL, Gamla Brogatan 26  
101 20 Stockholm  
GUMPERS UNIVERSITETSBOOKHANDEL AB  
Box 346, 401 25 Göteborg 1

**SWITZERLAND**

KARGER LIBRI AG, Petersgraben 31, 4011 Basel

**USA**

EBSO SUBSCRIPTION SERVICES  
P.O. Box 1943, Birmingham, Alabama 35201  
F. W. FAXON COMPANY, INC.  
15 Southwest Park, Westwood Mass. 02090  
THE MOORE-COTTRELL SUBSCRIPTION  
AGENCIES, North Cohocton, N. Y. 14868  
READ-MORE PUBLICATIONS, INC.  
140 Cedar Street, New York, N. Y. 10006  
STECHELT-MACMILLAN, INC.  
7250 Westfield Avenue, Pennsauken N. J. 08110

**YUGOSLAVIA**

JUGOSLOVENSKA KNJIGA, Terazije 27, Beograd  
FORUM, Vojvode Mišića 1, 21000 Novi Sad